Targeting Reader Domains of the Epigenetic Code

Dissertation

zur Erlangung des Doktorgrades der Naturwissenschaften

vorgelegt beim Fachbereich 14 | Biochemie, Chemie und Pharmazie

der Johann Wolfgang Goethe-Universität

in Frankfurt am Main

von

Nicolas Bauer

aus Offenbach am Main

Frankfurt am Main

2023

(D30)

vom Fachbereich 14 | Biochemie, Chemie und Pharmazie der

Johann Wolfgang Goethe-Universität Frankfurt als Dissertation angenommen

Dekan: Prof. Dr. Clemens Glaubitz

Gutachter: Prof. Dr. Stefan Knapp

                  Prof. Dr. Eugen Proschak

Datum der Disputation: 13.03.2024

Table of Contents

1 Introduction

1.1 The Epigenetic Code

According to the central dogma of molecular biology, formulated by Francis Crick in 1958, genes are expressed from DNA by two processes known as transcription and translation.[1–3] The genetic information of a cell is stored in the form of a DNA nucleotide sequence. During transcription, a part of this sequence is copied into messenger RNA (mRNA) by RNA polymerase (**Figure 1**). After exiting the nucleus, the mRNA provides the coding information to the ribosome, where its nucleotide triplet, or codon, sequence is translated into specific amino acids by pairing complementary transfer RNA (tRNA). The tRNAs each carry specific amino acids that are connected to form a polypeptide which later folds into an active protein. The genetic code therefore is the basis for the primary structure of the proteome and mutations of the DNA code have been implicated in many diseases.[4]
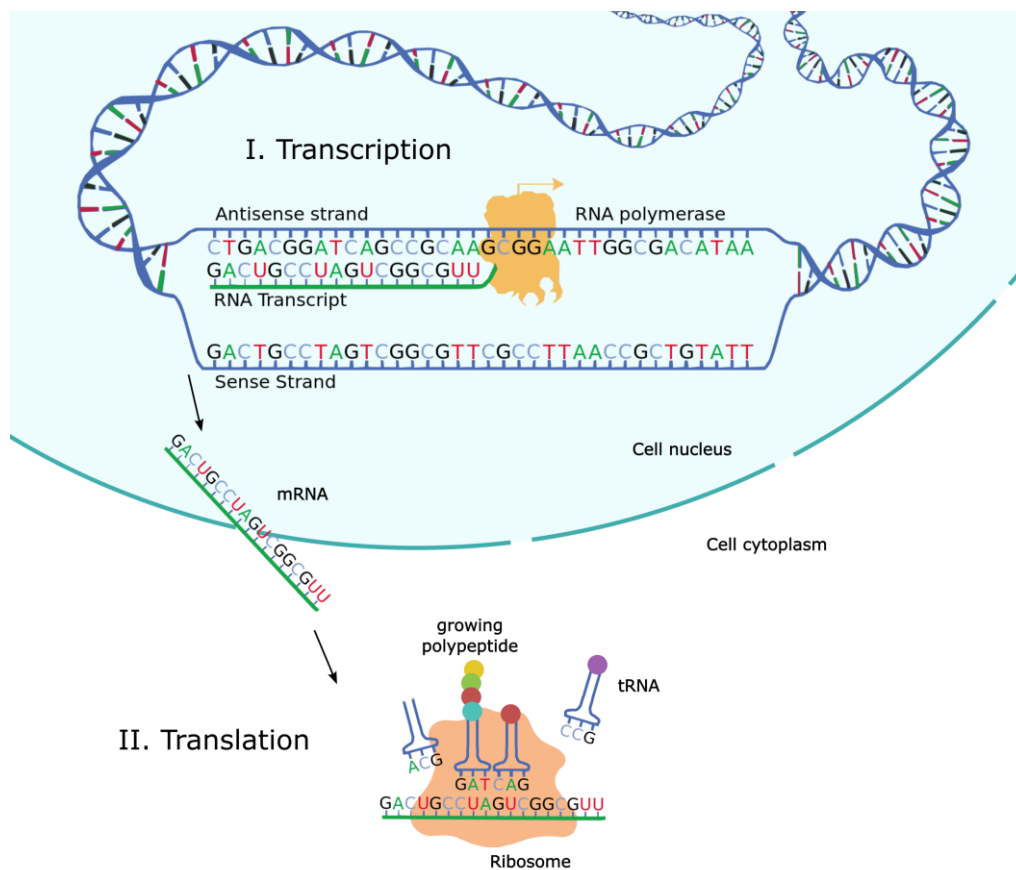

Figure 1: Gene expression from DNA *via* transcription and translation (adapted from the National Human Genome Research Institute).[5] The genetic information is stored in the form of nucleotide triplets (codons). I) During transcription, RNA polymerase copies information from the DNA sequence into an RNA transcript, creating mRNA which then exits the nucleus through the nuclear pore complex. II) To initiate translation, the ribosome assembles around the mRNA and facilitates binding of the first complementary tRNA. During elongation, the last tRNA transfers its attached amino acid to the previous tRNA, creating a growing peptide chain. The polypeptide is released when the ribosome reaches a stop codon in the mRNA.

In addition to the unidimensional information encoded in the genome, a more complex mechanism is involved, regulating which gene is actively transcribed. "The study of mitotically and/or meiotically

heritable changes in gene function that cannot be explained by changes in DNA sequence" has been termed epigenetics.[6] In contrast to genetic information, epigenetic information can be stored in a number of ways, including modification of DNA, RNA or proteins.[7] While alterations in the genetic code rely on mutations to change the nucleotide sequence, changes to the epigenetic code can happen much more readily. Even though epigenetic marks are also "mitotically stable", meaning all cells that result from division or proliferation will have the same epigenome, epigenetic modifications can also occur due to environmental signals.[8] Additionally, while all cells in one organism share the same genetic code, the epigenetic code is tissue specific.

1.1.1 DNA Methylation

One of the possible epigenetic modifications is the methylation of DNA by DNA methyltransferases (DNMTs). In mammals, DNA methylation can almost exclusively be found at CpG sites[9], regions where a guanine nucleotide follows a cytosine nucleotide (**Scheme 1**). The methylation results in 5-methylcytosine (5mC) and usually takes places on the cytosine of both strands. In the human genome, CpG nucleotides occur at only 21% of the frequency that would be expected from random distribution.[10] This under-representation might be attributed to the tendency of methylated cytosines to deaminate over time, forming thymine and resulting in a mismatched guanine-thymine base pair.[11] If the thymine is then complemented with adenine during DNA replication or by repair mechanisms, this introduces a permanent mutation.
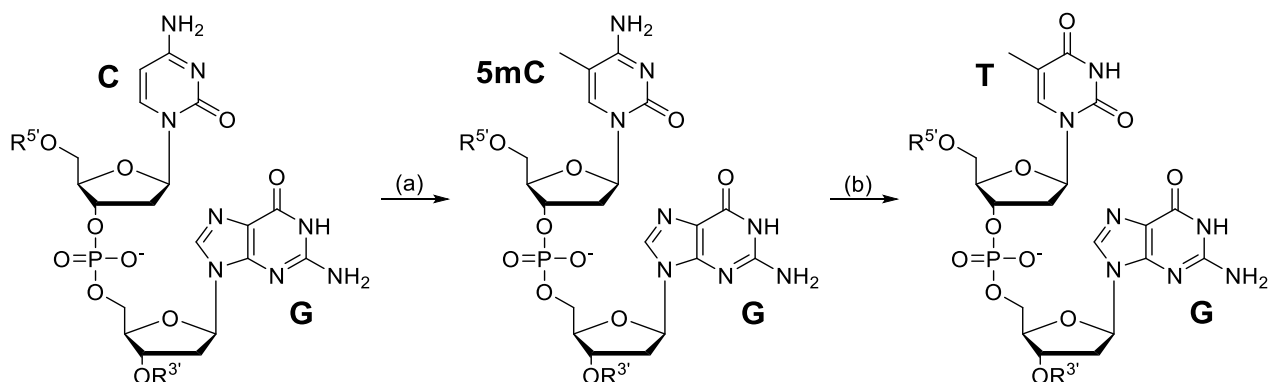
Scheme 1: Loss of CpG sites through methylation. (a) Methylation of cytosine (C) to form 5-methylcytosine (5mC) catalyzed by a DNA methyltransferase (DNMT). (b) Spontaneous deamination of 5-methylcytosine, resulting in thymine (T) and consequently a mismatched base pair with the complementary strand.

While DNMTs have been found to be responsible for DNA methylation, no direct DNA demethylase has been identified so far. Instead, demethylation seems to appear *via* passive dilution or through indirect pathways that involve deamination or oxidation of 5mC together with base excision repair (BER).[12] Even though most CpG sites are methylated, about five percent cluster into so-called CpG islands (CGIs), where this sequence is mostly unmethylated.[13] In humans, the majority of promotor regions are embedded in GCIs[14,15], where methylation is generally associated with the silencing of genes.[16] Accordingly, abnormal methylation in promotor regions has been frequently found in

different types of cancer.[17–19] Especially DNA repair genes are often repressed due to hypermethylation of CGIs in their promotor regions[20]. At the same time, global hypomethylation can be observed in tumor cells, causing genetic instability and activation of oncogenes.[21]

1.1.2   Histone Modifications

Another important epigenetic mechanism is the modification of histones, structural proteins the DNA wraps around to form chromatin (**Figure 2**). Those modifications include methylation, acetylation, phosphorylation, ubiquitinylation, sumoylation, biotinylation and ADP-ribosylation[22] and predominantly occur on the *N*-terminal tails of histone proteins. By modifying the histone tails, these chemical groups serve as dynamic marks that influence DNA accessibility and the recruitment of protein complexes involved in gene regulation.[23]
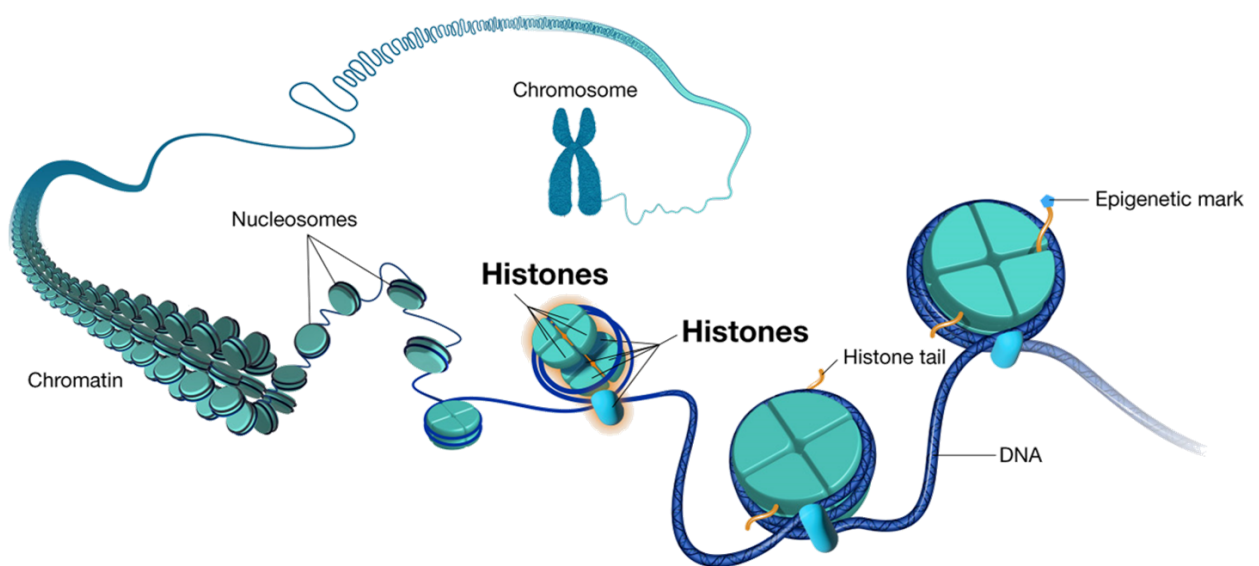

Figure 2: Structure of chromatin, a complex of DNA and histone proteins (adapted from the National Human Genome Research Institute).**[24]** The DNA double helix is wrapped around core histone octamers (two copies of H2A, H2B, H3 and H4), forming nucleosomes. This structure then further coils around linker histones (H1), eventually resulting in chromosomes. Epigenetic marks occur mainly on the *N*-terminal histone tails.

One of the most investigated histone modifications is the acetylation of histones. It mainly occurs on the lysine residues of histone tails and is regulated by histone acetyl transferases (HATs) and histone deacetylases (HDACs).[25] Under physiological conditions, the lysine's ε-amino group is protonated, creating a strong interaction with the negatively charged phosphate backbone of DNA. Acetylation removes the positive charge, resulting in a weaker interaction and therefore more open chromatin structure (**Figure 3**).[26] This causes the DNA to be more accessible, facilitating the binding of transcription factors and other regulatory proteins.
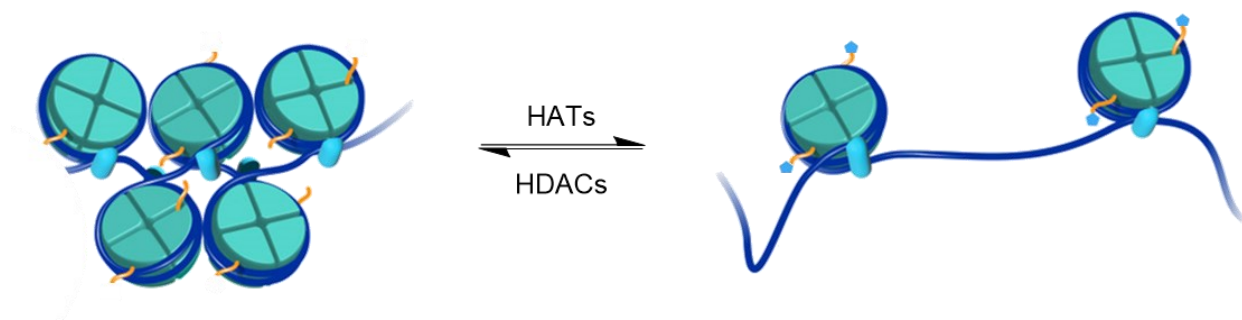
Figure 3: Chromatin structure depending on the acetylation state. Histone acetyl transferases (HATs) add acetyl groups (light blue) to histone tails (orange) (adapted from the National Human Genome Research Institute).[24] This removes the positive charge from lysine residues, causing weaker binding to DNA and therefore a more open chromatin structure. Histone deacetylases remove this acetyl group, resulting in chromatin that is less accessible for transcription.

Histone phosphorylation takes place on serine, threonine or tyrosine residues. The highly dynamic phosphorylation state is controlled by kinases and phosphatases and is believed to influence mitosis, cell death, repair, replication and recombination. While the phosphate's added negative charge clearly influences the chromatin structure, its precise function remains to be fully understood.[27]

In contrast to acetylation and phosphorylation, methylation does not directly alter the chromatin structure by adding or removing a charge. Instead, gene expression is regulated through recruiting chromatin remodelers or transcription factors that bind depending on the methylation state.[28] Histone methylation can occur on lysine or arginine residues, where lysines can be mono-, di- or tri-methylated and arginines can be mono- or dimethylated.[26] Are large number of different methyltransferases have been identified, each having specific substrates and reaction products.[29,30] SET7/9 for example is only able to mono-methylate H3K4.[31] Depending on the residue and the number of methyl groups, methylation can either enhance or suppress gene expression. Mono-methylated H3K9 and H3K27 correlate with gene activation, while di- and tri-methylation of those residues is associated with repression.[32,33]

In addition to the previously mentioned modifications, histones can also be modified through the attachment of small proteins, for example ubiquitin or small ubiquitin-related modifier (SUMO). The first protein that was found to be ubiquitinylated is histone H2A, with H2A and H2B being the most abundant ubiquitinylated proteins in the nucleus.[34,35] Ubiquitin attachment occurs at lysine residues, primarily at H2AK119 and H2BK120.[34,36] Besides monoubiquitinylation, histones can also be polyubiquitinylated, often as a response to DNA damage.[37,38] While the addition or removal of ubiquitin definitely influences transcription, ubiquitinylation is probably the most complex and least understood type of modification to histones.[39,40] Importantly, research also suggests "crosstalk" between different histone modifications, such as H2B ubiquitinylation influencing H3 methylation.[41,42]

1.1.3 RNA Epigenetics

In addition to the modifications of DNA and proteins, RNA also plays a significant role in the epigenetic gene regulation. Among those three components, RNA stands out as the most versatile. While most of the human genome is transcribed into RNA, only a small fraction of transcribed RNA is responsible for encoding proteins.[43] Along with the previously mentioned mRNA, there is also non-coding RNA which can exhibit a variety of functions. One example for this is microRNA (miRNA), which selectively silences genes by binding to complementary mRNA.[44] Additionally, some types of RNA, including long non-coding RNA (lncRNA), also play a role in gene regulation by influencing chromatin organization through architectural roles.[45] In analogy to DNA methylation, RNA nucleotides can also carry modifications. The most common RNA modification is N^6-methyl adenosine (m^{6}A), followed by 5-methylcytosine.[46,47] Other possible modifications include the 2'-*O*-methylation of the ribose unit and the conversion of uridines to pseudouridines.[48] *N*-methylation of adenosine is reversible and has been observed to occur through two different processes. M^{6}A can be demethylated through successive oxidation by FTO (fat mass and obesity-associated protein).[49,50] Additionally, direct demethylation mediated by ALKBH5 was also found.[51] Diseases associated with m^{6}A-binding proteins include a variety of different cancers.[46,52]

1.2 Histone Deacetylases (HDACs)

While its complexity makes it difficult, if not impossible, to fully understand the epigenetic code and its implications in gene expression in its entirety, some of its components have been investigated quite thoroughly. Especially histone acetylation is an epigenetic mark that has been extensively researched. Among the different kinds of acylation, including propionylation, butyrylation[53], crotonylation[54] and other types, that are associated with activating transcription[55], acetylation is the most abundant. Acetylation marks are added to lysine residues of *N*-terminal histone tails by HATs and removed by HDACs. The acetyl moiety is transferred from acetyl-coenzyme A (CoA), cleaving a reactive thioester (**Scheme 2**).[56] In cellular environments, the basic ε-amino group of lysine exists in a protonated state, creating positively charged histone tails. This enhances the affinity to the negatively charged phosphate backbone of DNA, resulting in a condensed form of chromatin, called heterochromatin. After acetylation by HATs, this charge is neutralized, weakening the interaction to DNA, generating uncondensed euchromatin and promoting binding of transcription factors.[57] Histone deacetylation by HDACs is therefore associated with repressed transcriptional activity. Importantly, HDACs cannot only acetylate histones, but have a variety of additional substrates that are associated with tumor progression, cell cycle control and apoptosis.[58] Noteworthy is, that the evolution of HDACs precedes the evolution of histones, which supports the idea that the primary targets may have not been histones.[59]
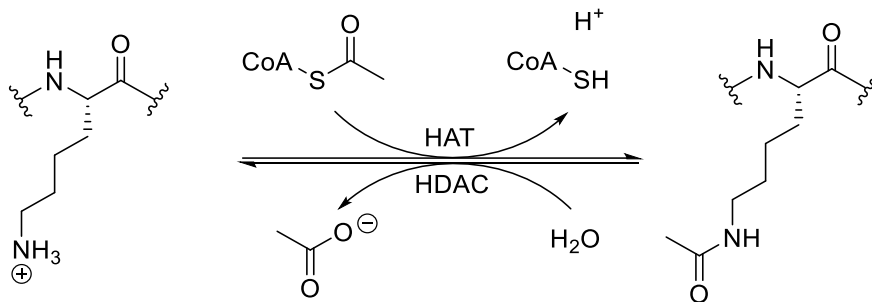
Scheme 2: Mechanism of histone lysine acetylation and deacetylation. The acetyl moiety is transferred by histone acetyl transferase (HAT) from coenzyme A (CoA), reacting with a thioester, and cleaved by histone deacetylase (HDAC) in the presence of water. Deacetylation regenerates a positive charge that attracts the negatively charged DNA backbone, causing a less accessible chromatin structure.

1.2.1 HDAC Classification and Function

HDAC proteins are grouped into four classes, based on their structure, function and cellular localization (**Figure 1**).[60] The "classical" HDACs, Class I, II (a and b) and IV, comprise HDAC1 to HDAC11, exhibit a zinc-dependent catalytic site and are consequently affected by zinc-chelating inhibitors, hydroxamic acids being the most common example.[61] Distinguished from those are class III HDACs, consisting of SIRT1 to SIRT7, which belong to the sirtuin family. They are NAD^+-dependent and therefore not affected by zinc-chelating compounds.[62]
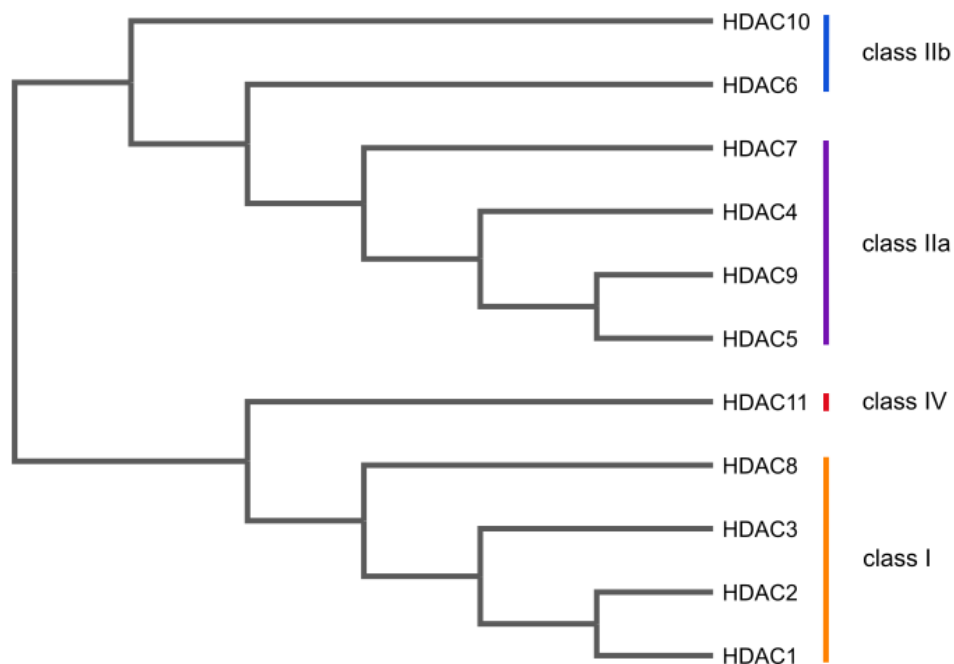

Figure 4: Phylogenetic tree and classification of the HDAC family based on full-length sequence alignment (created using ClustalW). Class III HDACs, or sirtuins, consist of SIRT1-7 (not included in the figure).

The Class I family includes HDAC1, 2, 3 and 8. HDAC1-3 are ubiquitously expressed, primarily localized in the nucleus and involved in many cellular processes, including regulation of proliferation, apoptosis and DNA damage response. HDAC1 and HDAC2 are quite similar and can often be found together in primarily repressive complexes such as Sin3, the nucleosome remodeling and deacetylase complex (NuRD) and the corepressor of REST (CoREST).[63,64] Additionally, HDAC1 and 2 are also part of the mitotic deacetylase complex (MiDAC), which has been shown to be important for chromosome alignment during mitosis in cancer cell lines.[65] HDAC2 inhibition was also shown to cause chromatin decondensation and sensitization of tumor cells to chemotherapy.[66] Apart from transcriptional regulation through deacetylation of histones, HDAC1 and 2 also mediate the deacetylation of the tumor suppressor p53, thereby deactivating it.[67–69] HDAC3 has been found to be recruited to the corepressor complexes SMRT (silencing mediator of retinoic acid and thyroid hormone receptor) and NCoR (nuclear receptor corepressor), where the enzymatic activity of HDAC3 is enhanced through

recruitment to these complexes.[70–72] In contrast to the other members of class I, HDAC8 was not found to be involved in similar multiprotein complexes.[73] In summary, class I HDACs appear to be crucial for cell survival and proliferation through transcriptional regulation.[74]

Class II HDACs occur in the cytoplasm, as well as the nucleus and are subdivided into class IIa and IIb. Unlike the members of class I, their function is usually tissue specific.[58] The class IIa family comprises HDAC4, 5, 7 and 9 which regulate nuclear-cytoplasmic shuttling.[75] They are also recruited to the SMRT/NCoR-HDAC3 transcriptional repression complex.[76] In contrast to other members of the HDAC family, class IIa HDACs exhibit a very low enzymatic activity.[77] HDAC6, a member of class IIb, is the only deacetylase that contains two deacetylase domains.[78] Among other things, it has been shown to regulate the deacetylation of α-tubulin.[79,80] Another member of this class, HDAC10, has independently been discovered by four different groups, but very little is currently known about its function.[81–84] Its substrates have been shown to include ubiquitous acetylated polyamines, such as putrescine, spermidine and spermine.[85]

HDAC11 is the sole member of class IV. In contrast to the other deacetylases, it seems to primarily deacylate fatty acids from lysines and its ability to directly deacetylate histones has not yet been confirmed.[86] Consisting of 347 amino acids, it is the smallest known HDAC, with the catalytic domain including over 80% of the protein sequence.[87] It is the most recently discovered and probably least understood type of histone deacetylase.

1.2.2 HDAC Structure and Inhibitors

Class I and II HDACs share a highly conserved catalytic site of about 390 amino acids.[88] This deacetylase domain consists of a tubular hydrophobic channel with a depth of 11 Å and a Zn^{2+} ion near its bottom (**Figure 5**).[89] This channel facilitates binding of an acetyl lysine residue and the zinc catalyzes the hydrolysis of its acetyl group. The existence of this zinc ion in the catalytic site of the classical HDACs is exploited by most HDAC inhibitors through employing a zinc-binding moiety.
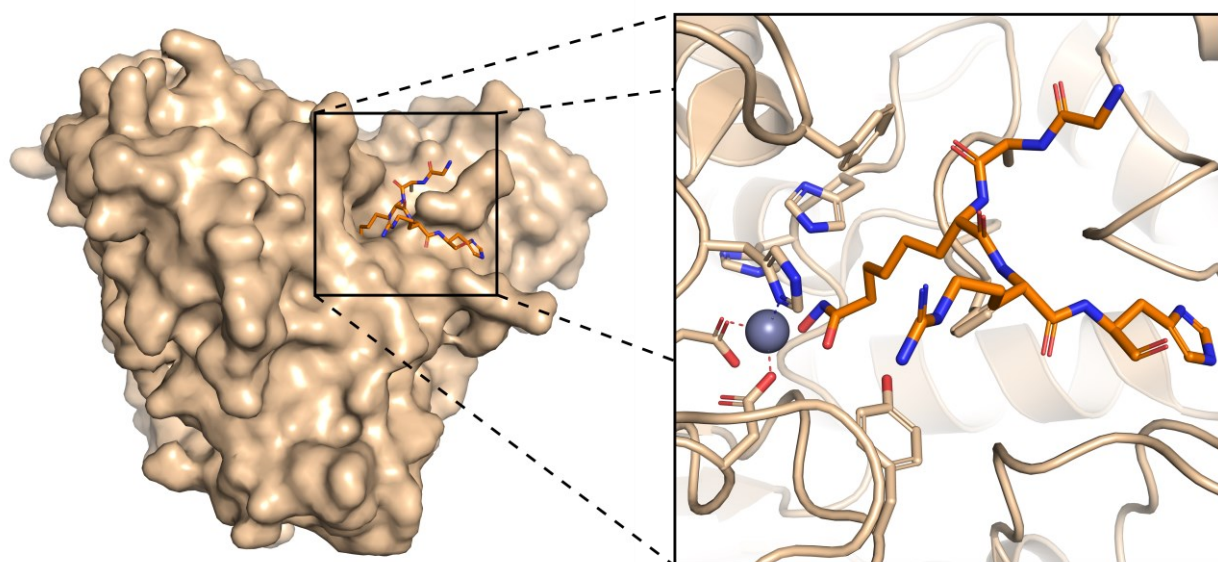
Figure 5: Co-crystal structure of HDAC1 and peptide-based inhibitor H4K16Hx (orange)**.** The inhibitor mimics a histone lysine residue but employs a hydroxamic acid to increase affinity to the zinc ion (grey) (PDB: 5ICN).[90]

Some fatty acids, such as valproic and phenylbutyric acid have been found to be weak inhibitors of deacetylases.[91,92] Much more potent binders than those, however, are hydroxamic acids. One of the first natural products found to inhibit HDACs is trichostatin A (**1**) (**Figure 6**), which exhibits a low nanomolar affinity to the zinc-dependent HDACs.[93] The first HDAC inhibitor that has been approved by the United States Food and Drug Administration (FDA) for the treatment of cutaneous T-cell lymphoma (CTCL) is suberanilohydroxamic acid (SAHA) (**2**).[94] The rather minimalistic structure of this pan-HDAC inhibitor illustrates a common design strategy for HDAC inhibitors, consisting of a zinc-binding group (ZBG), a hydrophobic linker and a capping group. Other representatives of approved hydroxamic acid-based drugs are belinostat (**3**), approved by the FDA for peripheral T-cell lymphoma (PTCL), and panobinostat (**4**), approved by the FDA and European Medicines Agency (EMA) for multiple myeloma (MM). The potency of the hydroxamic acid warhead resulted in many additional inhibitors with similar structures to emerge as clinical candidates.[95]
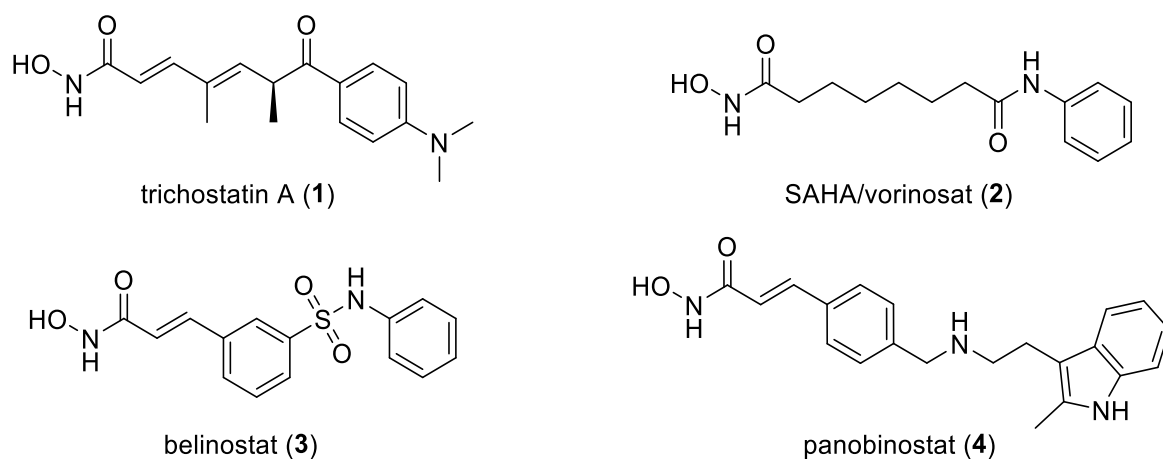
trichostatin A (**1**)

SAHA/vorinosat (**2**)

belinostat (**3**)

panobinostat (**4**)

Figure 6: Hydroxamic acid pan-HDAC inhibitors. Compounds **2-4** are approved for the treatment of hematological neoplasms (represented by T-cell lymphomas and multiple myeloma).

Another natural product that was later discovered to be an inhibitor of histone deacetylases is the depsipeptide romidepsin (**5**), which acts as a prodrug.[96] In cells, the disulfide bond is reduced, releasing the active compound **6**, which again matches the typical design of HDAC inhibitors, containing a zinc-binding thiol, a hydrophobic linker and a cyclic peptide which acts as a capping group (**Figure 7**). It exhibits a potent activity for HDAC1-3, 10 and 11 and is approved for the treatment of CTCL and PTCL.[95]

romidepsin (**5**)

6
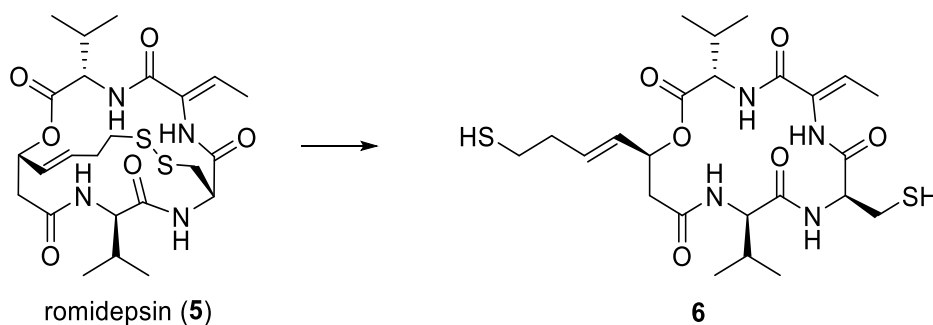
Figure 7: Mechanism of activation of romidepsin (5). In cells, the disulfide is reduced, releasing thiol **6**, which potently binds the zinc ion of many HDACs.

Despite their on-target effect, the currently FDA-approved HDAC inhibitors still have some major disadvantages. They cause a number of significant side effects, such as cardiotoxicity,[97,98] and compounds **2** and **5** were therefore not approved by the EMA.[99,100] The hydroxamic acid warhead is intrinsically prone to hydrolysis and a pharmacokinetics study of inhibitor **2** found 4-anilino-4-oxobutanoic acid and 6-anilino-6-oxohexanoic acid to be the major metabolites *in vivo*. Additionally, glucuronidation was found to be a substantial pathway of elimination. The low metabolic stability results in a short half-life of approximately 2 h.[97] Another significant downside to the previously mentioned HDAC inhibitors is that they only seem to be efficacious against hematological malignancies. They were not effective against multiple tested solid tumors, potentially due to bad tissue penetration.[98] In addition to the hydroxamic acids, which usually bind to all HDACs, some more selective warheads have been discovered. One of the first discovered alternative HDAC inhibitors is

the benzamide CI-994 (**7**), which has shown activity against different solid tumors (**Figure 8**).[101–103] This has prompted the development of a new class of inhibitors that are selective for HDAC1-3 and bind by chelating the zinc ion with the amide oxygen and the aromatic nitrogen (**Figure 9**).[104-108] The increased steric demand of this ZBG compared to hydroxamic acids or thiols is accepted by a lateral cavity that is only present in class I HDACs. While HDAC8 also possesses this cavity, the substitution of a tryptophan for a leucine residue results in not enough space for binding the phenyl moiety.[95] The fluorinated derivative chidamide (**8**) has been approved by China's National Medical Products Administration (NMPA) for the treatment of PTCL and in Japan for the treatment of relapsed or refractory adult T-cell leukemia-lymphoma (ATLL).[109–111]
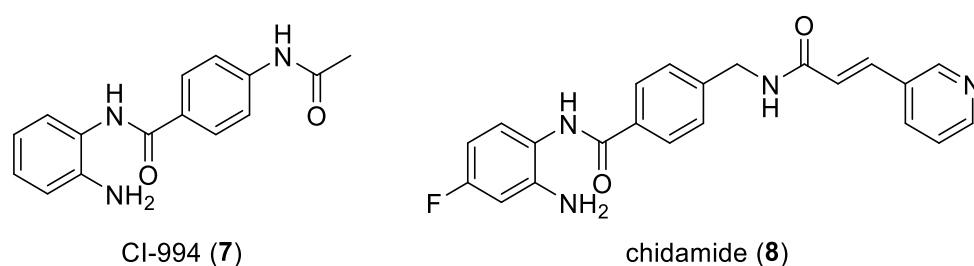
Figure 8: Benzamide-based HDAC inhibitors CI-994/tacedinaline (7) and chidamide/tucidinostat (8).

Since HDAC1 and 2 contain a 14 Å long cavity adjacent to the catalytic site, further efforts were made to target that "foot pocket" and create more potent and selective inhibitors (**Figure 9**). Derivatization with additional aromatic residues resulted in different nanomolar inhibitors for HDAC1/2, such as BRD6929 (**9**), and decreased affinity for HDAC3, which possesses a smaller foot pocket due to the substitution of a tyrosine for a serine residue.[112–116] Owing to a sequence similarity of the catalytic domains of 94%, the development of an inhibitor that discriminates between HDAC1 and 2 appears to be rather difficult. Some inhibitors have been found to differ in binding kinetics between the two isoforms, thereby achieving a longer residence time and thus kinetic selectivity for HDAC2.[117]
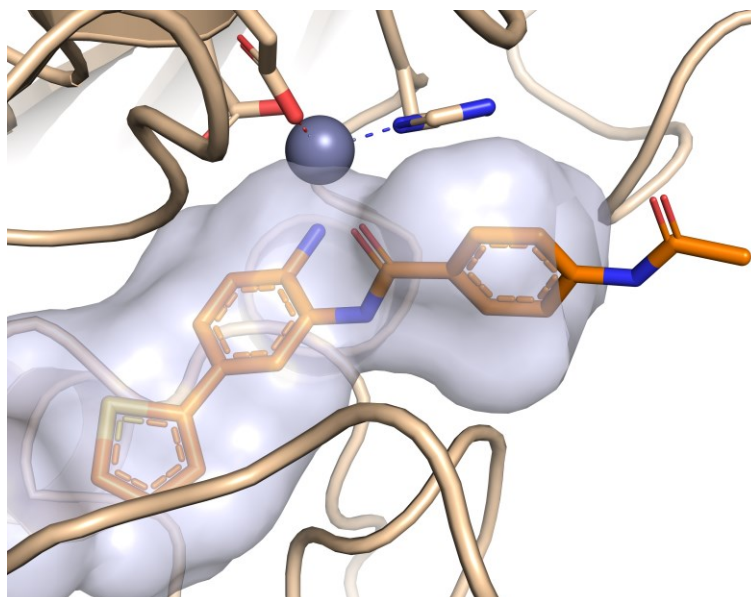
Figure 9: Co-crystal structure of HDAC2 and inhibitor BRD6929 (**9**, orange)**.** The thiophene reaches into a pocket present in HDAC1 and 2 (PDB: 4LY1).

Apart from the mentioned types of HDAC inhibitors, researchers have discovered new inhibitors with different ZBGs, such as ethyl ketone **10**[118] and isoxazole **11**[119] (**Figure 10**). Both compounds potently bind class I HDACs in the low nanomolar range. When bound to the protein, ketone **10** exists as the hydrate, forming a bivalent interaction to the zinc ion. Additionally, inhibitors with a 2-methylthiobenzamide warhead were found to be potent and selective for HDAC3.[120]
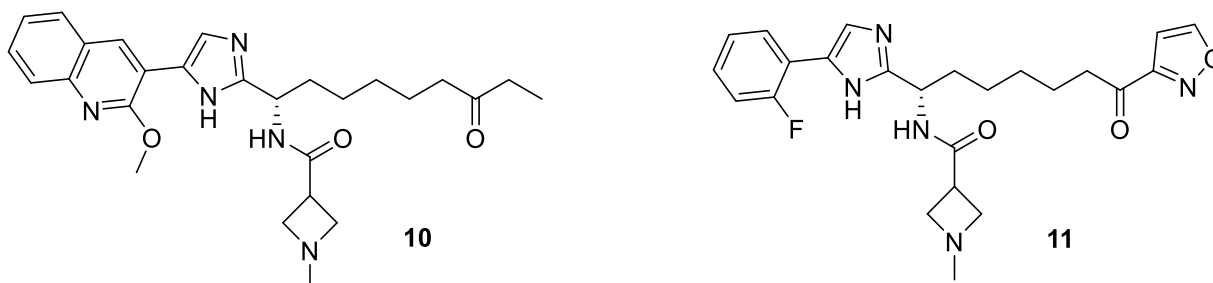
Figure 10: Ethyl ketone 10 and isoxazole 11 are potent inhibitors of class I HDACs.

As previously mentioned, HDAC1-3 form the catalytic subunit of a number of regulatory complexes. Being part of such a complex increases the enzymatic activity and importantly results in the same enzyme having different biological functions depending on the type of complex.[121] Interestingly, HDAC inhibitors have been found to show selectivity for different complexes and not just isoforms.[122,123] This aspect should be considered when developing HDAC inhibitors targeted at specific biological activities, as it might give additional means of achieving selectivity.

1.3 Bromodomains

While certain enzymes, such as HDACs, add epigenetic modifications, there are other enzymes which can "read" or bind to those modifications. Acetylated lysine residues of histone tails are recognized by bromodomains (BDs), small evolutionarily conserved protein substructures that can be found in 46 different BD-containing proteins (BCPs).[124] These BCPs contain between one to six BDs and facilitate the recruitment of proteins to the transcriptional machinery or chromatin remodeling complexes, thereby serving an essential role in transcriptional regulation, DNA damage repair and cell proliferation. In humans, 61 distinct BDs have been identified and classified into eight subfamilies (**Figure 11**). The different families of BCPs include HATs, such as PCAF, GCN5L2 and EP300,[125–128] histone methyl transferases, such as ASH1L and MLL,[129,130] ATP-dependent chromatin remodeling complexes, such as BAZ1B,[131] helicases, such as SMARCA2,[132] and transcriptional coactivators, such as TRIMs that may also act as ubiquitin ligases.[133]
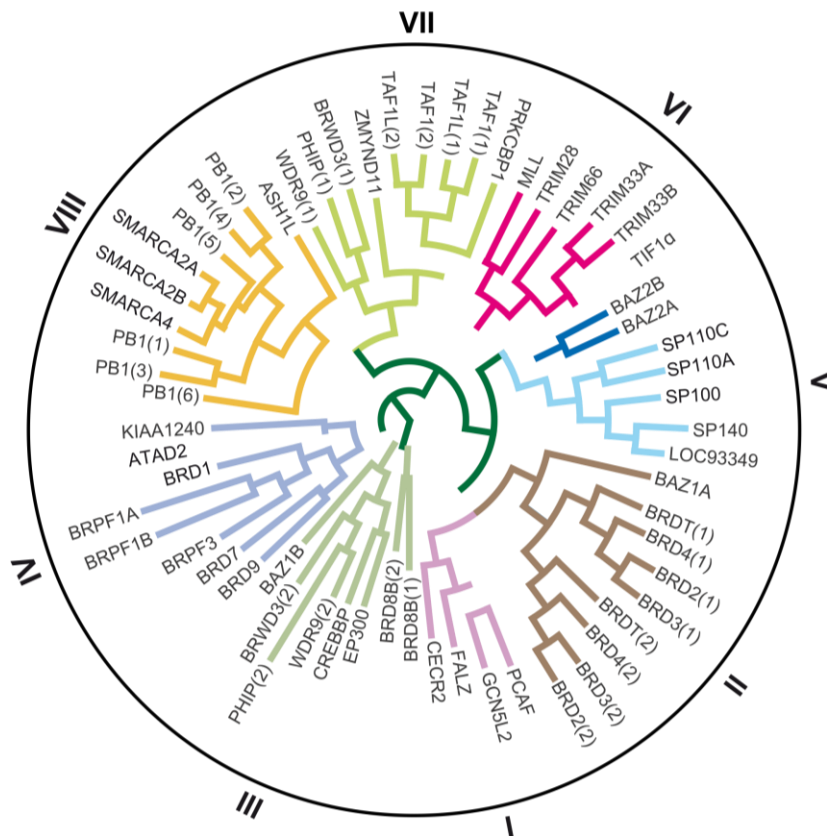
Figure 11: Classification of the 61 different bromodomains into eight subtypes, according to the domain architecture and homology.[134]

All BDs share a conserved structure that contains a bundle of four α-helices (αA, αB, αC and αZ), which are connected by variable loops (ZA- and BC-loop). The loops line a deep hydrophobic pocket that serves as the binding site for acetylated lysine residues. The acetyl lysine binds to an asparagine residue which is present in most bromodomains (**Figure 12**). In the binding site, four highly conserved water molecules are present, with one of them being in direct contact to the acetyl lysine.[135] Large sequence

variations between different BDs are responsible for substrate binding specificity. In contrast to the conserved catalytic site, the surface properties vary a lot between different BDs, ranging from predominantly positively to negatively charged. Additionally, the C and N termini might differ a lot, sometimes containing additional helices.[136]
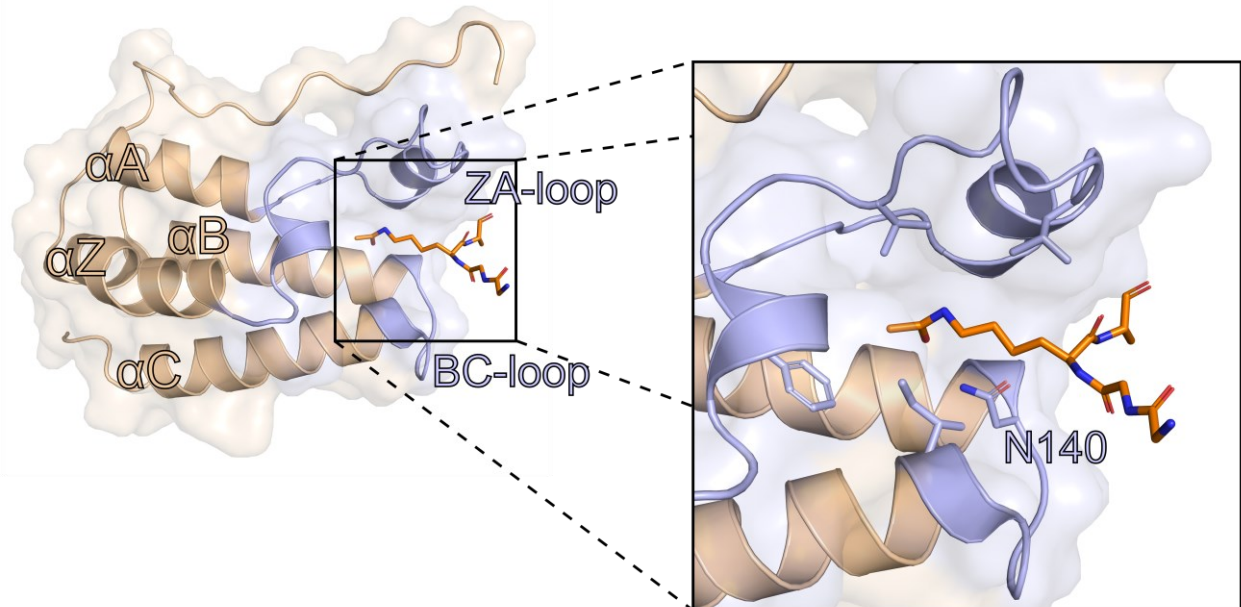

Figure 12: Crystal structure of BRD4 BD1 with an acetylated peptide (H3K14ac, orange)**.** The four helices (αA, αB, αC and αZ) are connected by two loops (ZA-loop and BC-loop, light blue), which form a hydrophobic pocket that serves as the acetyl lysine binding site (PDB: 3JVK).[137]

1.3.1   The Bromodomain and Extra-Terminal (BET) Family

BCPs that have gained significant attention in recent years are the bromodomain and extra-terminal (BET) proteins. The BET family comprises BRD2, 3, 4 and BRDT, with each member containing two N-terminal BDs and one extra-terminal (ET) domain (**Figure 13**). While the BDs bind to acetylated histones, the more diverse C-terminal end of the protein is responsible for interacting with transcription factors, chromatin modifying factors and other proteins. Research suggests that the differences in biological activities between BET proteins result mainly from the different enzymes which interact with the ET domain and the C-terminal domain (CTD), which is present in BRD4 and BRDT.[138,139] The respective first and second BDs (BD1 and BD2) in different BET proteins are more closely related to each other than BD1 and BD2 in the same protein.

Figure 13: Domain organization of the BET family members (adapted from literature[140])**.** All four BET proteins contain two bromodomains (BD1 and BD2) and one extra-terminal domain (ET). BRD4 and BRDT also contain a C-terminal domain (CTD).

BET proteins are involved in a variety of diverse cellular processes, including transcriptional regulation,[141] hematopoiesis,[142] adipogenesis,[143] and spermatogenesis.[144] BRD4, for example, is a key mediator in transcription by interacting with the positive transcription elongation factor b complex (p-TEFb) through its CTD. P-TEFb, which comprises cyclin-dependent kinase 9 (CDK9) and its activator cyclin T1, is activated and recruited to chromatin by BRD4. The heterodimer afterwards phosphorylates and thus activates RNA polymerase II (RNAP II), thereby initiating transcriptional elongation (**Figure 14**).[145–147]
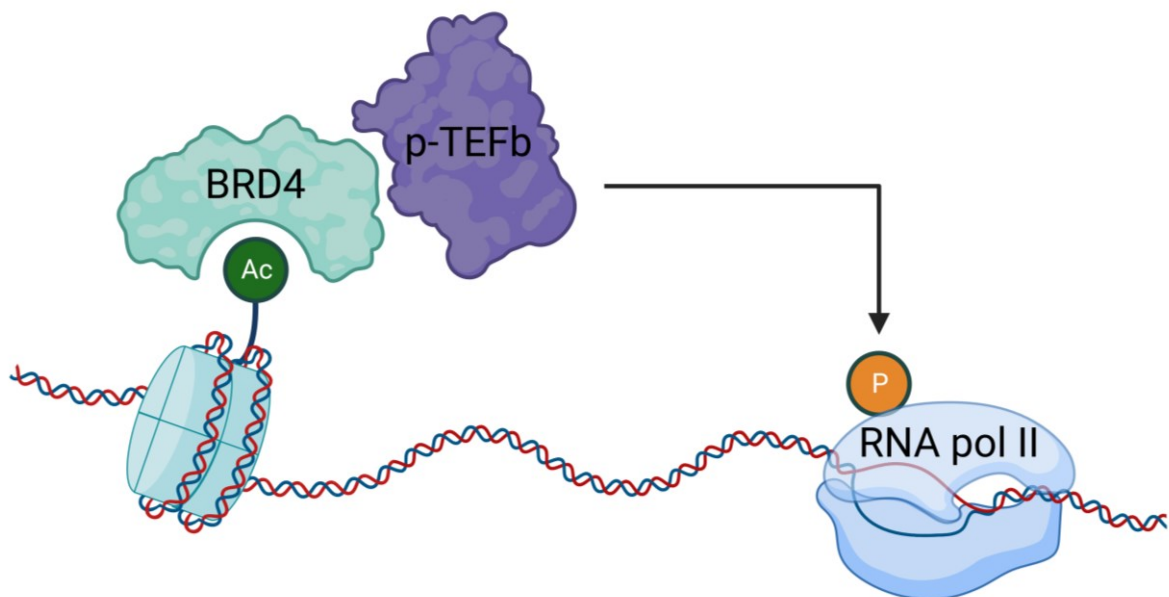
Figure 14: Transcriptional activation by BRD4 (adapted from literature[148], created using BioRender)**.** BRD4 binds to acetylated histones and recruits the positive transcription elongation factor b (p-TEFb) to chromatin. P-TEFb is activated by BRD4 and phosphorylates RNA polymerase II (RNAP II) to initiate gene transcription.

BRD4 and BRD2 have also been found to regulate transcription by occupying (super) enhancers, regions located distantly to gene promoters.[149–151] By forming loops, DNA can bring enhancers and promoters in proximity, thereby facilitating the expression of certain genes (**Figure 15**).[152] BRD4 appears to be particularly enriched at enhancer regions, some of which are associated with oncogenes

such as MYC. Inhibition of BET proteins leads to a preferential loss of BRD4 at enhancers, thereby targeting different oncogenic drivers and primarily affecting tumor cells.[153]
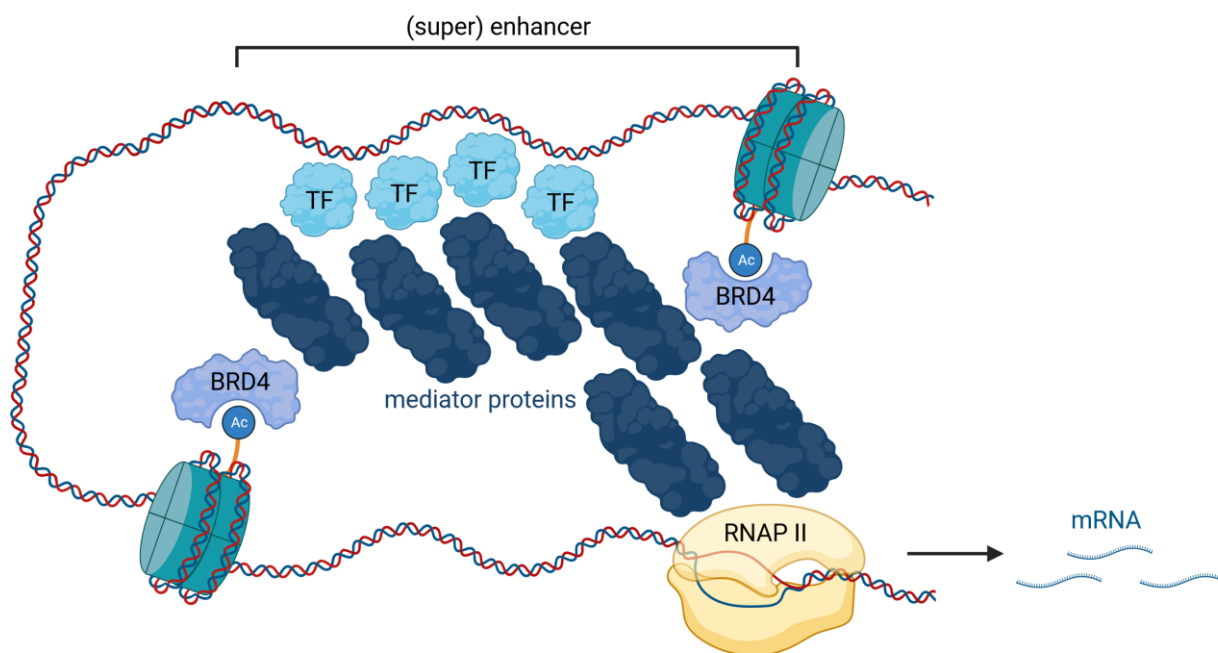

Figure 15: Mechanism of (super) enhancer regions (adapted from literature[154], created using BioRender). Transcription factors bind to the enhancer and increase the activity of distantly located gene promoters. BRD4 binds preferentially to enhancers and interacts with the mediator complex, enhancing the expression of many oncogenes.

By facilitating the expression of growth-promoting oncogenes like MYC and BCL-2, BET proteins play an important role in different types of cancer.[155,156] While BRD4, which is often overexpressed or dysregulated in tumor cells, suppresses apoptosis, inhibition of BRD4 seems to induce the programmed cell death in a variety of cancers.[157] BRD4 and other BET proteins have been shown to be crucial for the development of hard-to-treat pancreatic cancer.[158–160] Another aggressive type of cancer is the NUT (nuclear protein in testis) midline carcinoma (NMC), which features a fusion of the NUT protein with BRD4.[161] The BRD4-NUT oncogene recruits CBP/p300, eventually leading to hyperacetylated chromatin domains and inactivation of p53.[162] Research has shown that BET proteins are involved in many additional types of cancer[163–171] and inflammation[172–174].

1.3.2 BET Inhibitors

Enthusiasm for the anti-proliferative effects in cancer cells and the prospect of targeting undruggable oncogenes such as MYC, has resulted in the development of a variety of different BET inhibitors and a large number of clinical trials.[175,176] The first potent and selective inhibitors for the BET family were the triazolodiazepines and I-BET762 (**12**) and JQ1 (**13**) (**Figure 16A**).[172,177] The triazole moiety mimics acetyl lysine and forms hydrogen bonds to the conserved asparagine residue and to a conserved water molecule. A common feature of BET inhibitors are aromatic moieties that target the hydrophobic WFP shelf unique to BET proteins to increase potency and selectivity (**Figure 16B**). In preclinical studies, JQ1

proved to be effective against prostate,[170] liver,[178] breast,[179,180] lung[181,182] and pancreatic cancer,[183,184] as well as leukemia.[169,185] Its short half-life, however, limits its use in a clinical setup.[186]
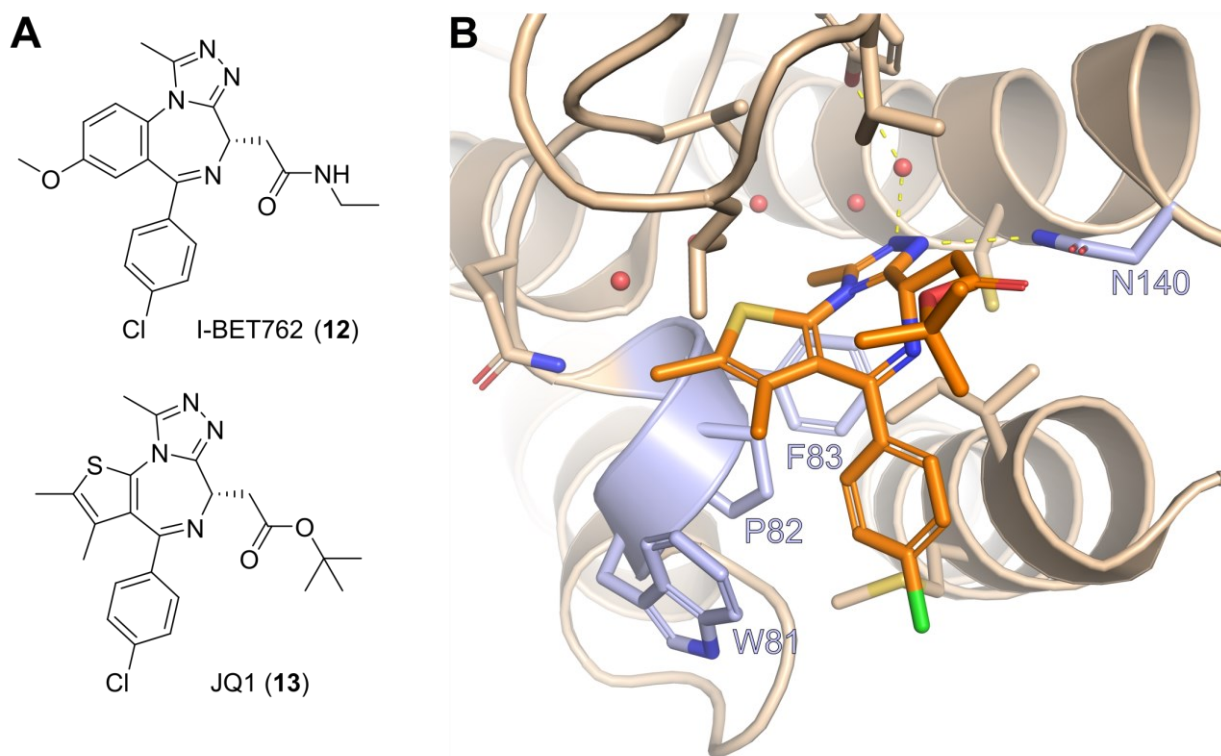

Figure 16: The first potent and selective triazolodiazepine-based BET inhibitors. (**A**) Benzodiazepine I-BET762 (**12**) and thienodiazepine JQ1 (**13**). (**B**) Crystal structure of BRD4 BD1 with JQ1 (**13**) (orange). The triazole acts as an acetyl lysine mimetic and forms hydrogen bonds to a conserved asparagine residue (light blue) and to a conserved water molecule. The phenyl moiety interacts with the hydrophobic WPF shelf (light blue) (PDB: 3MXF).

The promising initial results from inhibiting BET proteins have encouraged researchers to further develop BET inhibitors with the goal of designing more potent and selective compounds. By employing a pyrrolopyridone moiety as an acetyl lysine mimetic, ABBV-075 (**14**) was discovered (**Figure 17A**).[187] Low nanomolar affinity could be achieved through using a bidentate interaction to the conserved asparagine. Modification of this scaffold later yielded BD2-selective ABBV-744 (**15**).[188] By examination of the respective crystal structures of the first and second BDs with ligand **15**, three key differences can be spotted to explain the selectivity (**Figure 17B**). The ethyl amide fills a cleft between H437 and P434 and shows a hydrophobic interaction with the histidine in BD2, which is not happening with the aspartate in BD1. Since BD2 employs V439 instead of I146, it allows binding of slightly larger residues, explaining the better selectivity of the xylyl moiety. The substituent also makes an edge to face interaction with H437. The tertiary dimethyl alcohol further increases the selectivity for BD2, possibly due to BD1 not providing enough space for binding this moiety. Research suggests that the two BDs in BET proteins have different functions and different phenotypes have been observed if one or both BDs were inhibited. In prostate cancer cell lines, BD2-selective inhibitor **15** was shown to selectively replace

BRD4 from androgen receptor (AR) containing super-enhancers, while having less impact on global transcription compared to pan-BET inhibitor **14**.[189]
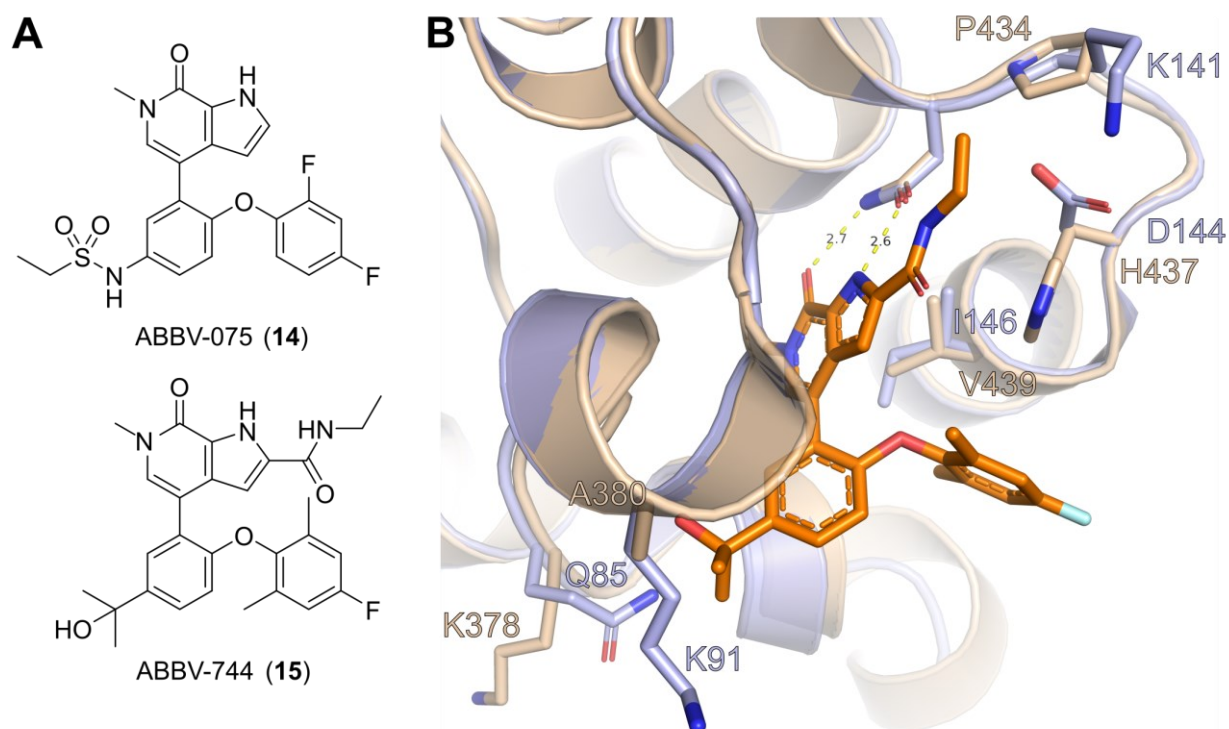

Figure 17: Potent pyrrolopyridone-based BET inhibitors. (**A**) Pan-BET inhibitor ABBV-075 (**14**) and BD2-selective ABBV-744 (**15**). (**B**) Crystal structure of ABBV-744 (**15**) (orange) with BRD4 BD1 (wheat, PDB: 6ONY) and BRD4 BD2 (light blue, PDB: 6E6J). Important residues for binding and selectivity are shown and labeled.

In contrast to the already stated compounds, the BD1-selective inhibitor GSK789 exploits an interaction of a tertiary amine to the aforementioned D144 (PDB: 6Z7L).[190] Inhibitor CDD-956 achieves selectivity for the first bromodomain by binding to a hydrophobic groove on the surface of the protein (PDB:7UBO).[191] Studies indicate that BD1 is primarily responsible for chromatin binding and inhibition of BD1 seems to match the anti-proliferative effects for the unselective inhibition of BET proteins.[192,193]

The existence of the tandem BDs in BET proteins has been taken advantage of by many inhibitors in the recent years. By binding to both BDs at the same time, quite potent inhibitors were developed, sometimes reaching sub-nanomolar affinity.[194–203] Since these inhibitors usually consist of two ligands like JQ1 connected by a linker, they reach quite high molecular weights, potentially limiting their usability in a clinical setting. Nevertheless, first studies show promising results for tumor growth inhibition *in vivo* for the bivalent inhibitor AZD5153, which was developed by fusing two acetyl lysine mimetics.[196]

1.4 Combined Inhibition

Inhibition of BET proteins has shown to be promising when combined with additional therapeutics.[204,205] Especially complex diseases like cancer may require complex treatment in the form of a polypharmacy approach.[206] This combination therapy is a common strategy to prevent compensatory mechanisms, such as resistance to single drugs.[207] Apart from different kinase inhibitors,[208–211] BET inhibitors are frequently used in combination with epigenetic drugs, such as HDAC inhibitors.[212–218] The combination of HDAC inhibitors together with other classes of protein inhibitors has been frequently employed as well.[219–221] At first, the combined inhibition of BET proteins and HDACs might seem counterintuitive, since HDACs remove the acetyl lysine marks, which are recognized by bromodomains. However, BET proteins and HDACs seem to induce similar genes and their combined inhibition appears to shift the ratio of pro- and anti-apoptotic proteins in cancer cells towards apoptosis.[218] Simultaneous inhibition of both classes of proteins was shown to attenuate levels of the oncogenes MYC and BCL-2.[212] In pancreatic ductal adenocarcinoma (PDAC) cells, which is one of the most lethal human cancers that is resistant to virtually all therapeutic approaches,[222] the tumor suppressor p57 was de-repressed upon combined inhibition.[223] A possible explanation for the observed synergy is that the hyperacetylation caused by HDAC inhibition results in a redistribution of BRD4 throughout the genome, delocalizing it from previous acetylation sites.[224] This effect is then enhanced through inhibition of BET proteins, further decreasing BRD4 concentration at specific regions.

Since drug-drug interactions can be rather unpredictable and multiple therapeutics can exhibit a different pharmacokinetic behavior or biodistribution, it is advantageous to keep the number of medications to a minimum.[225] Those issues can be circumvented by employing multi-target drugs. Many successful drugs exploit this polypharmacology, producing additive or even synergistic effects. While a number of medications, such as aspirin, reveal many of their interactions at a late stage, often including favorable off-target effects, multi-target drugs can also be intentionally designed.[226,227]

Using BET inhibitors **12**[228], **13**,[229–231] **15**[232] and other scaffolds,[233–240] several inhibitors with dual BET/HDAC activity were developed in recent years. Most of these compounds are fused with HDAC inhibitor **2** by adding a simple short linker with a hydroxamic acid to the BET inhibiting moiety, resulting, among others, in compounds **16**, **17** and **18** (Figure 18). The dual inhibitors could demonstrate promising results against different cancer cell lines, including NMC,[230,234] PDAC,[229,230] and leukemia.[233,235,237]

The BET/HDAC inhibitor TW9 (**19**) was designed by combining JQ1 (**13**) with the benzamide CI-994 (**7**). It was significantly more potent in inhibiting proliferation of PDAC cells compared to its parent compounds or a combination of both inhibitors. Compound **19** was shown to block cell-cycle progression by targeting the super-enhancer-associated transcription factor FOSL1. Additionally, synergy could be observed, when the dual inhibitor was used together with the chemotherapy drug gemcitabine.[230] Unfortunately, those promising first results could not be reproduced *in vivo*, since the compound did not permeate into the tumor tissue of the treated mice.
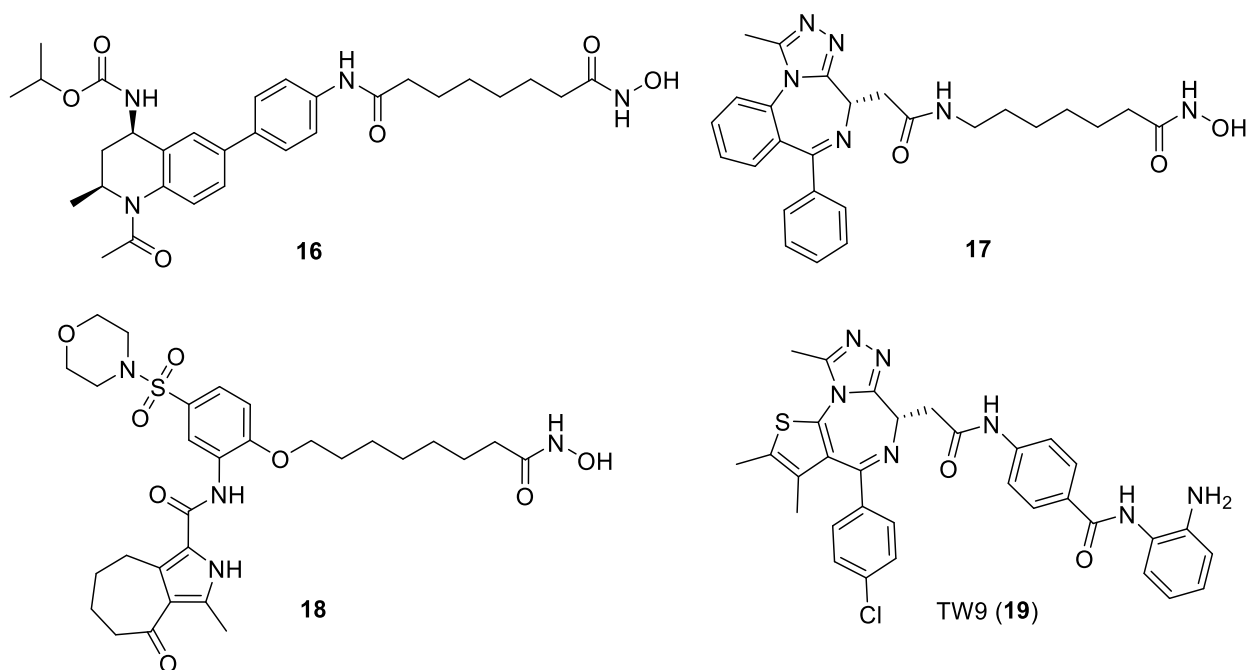
Figure 18: Selected dual BET/HDAC inhibitors. Inhibitors **16**,[234] **17**[228] and **18**[237] consist of different BET-inhibiting moieties and the HDAC inhibitor SAHA (**2**). Dual inhibitor TW9 (**19**) was designed by combining JQ1 (**13**) and CI-994 (**7**).[230]

A potential issue that many published dual inhibitors have, is that the combination of two pharmacophores inevitably results in a compound with higher molecular weight than its predecessors. Since larger molecules have been associated with poorer pharmacokinetic profiles, it should be desirable to keep the final inhibitor's size as small as possible while retaining the dual activities.[241,242]

2 Objective

The simultaneous inhibition of HDACs and BET proteins has shown promising anti-proliferative effects against different cancer cell lines. Reflecting the attractiveness of combined inhibition, many dual BET/HDAC inhibitors have been developed in recent years.[243] Most dual inhibitors contain a hydroxamic acid warhead. The hydroxamic acid-based inhibitors are pan-HDAC inhibitors and are generally not metabolically stable.[97] While a few published dual inhibitors contain the class I selective benzamide moiety,[230,232] their molecular weight exceeds 600 Da, limiting their application *in vivo*.[241,242] Inhibitor TW9 (**19**), which was developed by T. Weiser, showed promising *in vitro* results for the treatment of pancreatic cancer.[230] Those results could unfortunately not be translated to *in vivo* mouse models, probably due to unfavorable pharmacokinetic characteristics. While the so far published dual BET/HDAC inhibitors can be described as simple adducts of a BET and HDAC inhibitor, it was hypothesized that the merging of two pharmacophores, creating a highly integrated dual inhibitor with a minimized molecular weight, might yield a better outcome.[244]

For this approach, the first important step was to find respective BET and HDAC ligands with a considerable structural similarity. As the class I selective HDAC inhibitor CI-994 (**7**) was chosen, BET inhibitors with good compatibility and structural overlap had to be selected. Compounds ABBV-075 (**14**) and the slightly more potent (0.6 nM) cyclic derivative **20**[245] (**Figure 19**) were chosen for their high potency and good pharmacokinetic profiles. Inhibitor **21** was also determined to be a good starting point due to its high potency for BRD4.[246] For the dual inhibitors based on compounds **14** and **20**, multiple attachment points for the HDAC-binding moiety were to be explored.
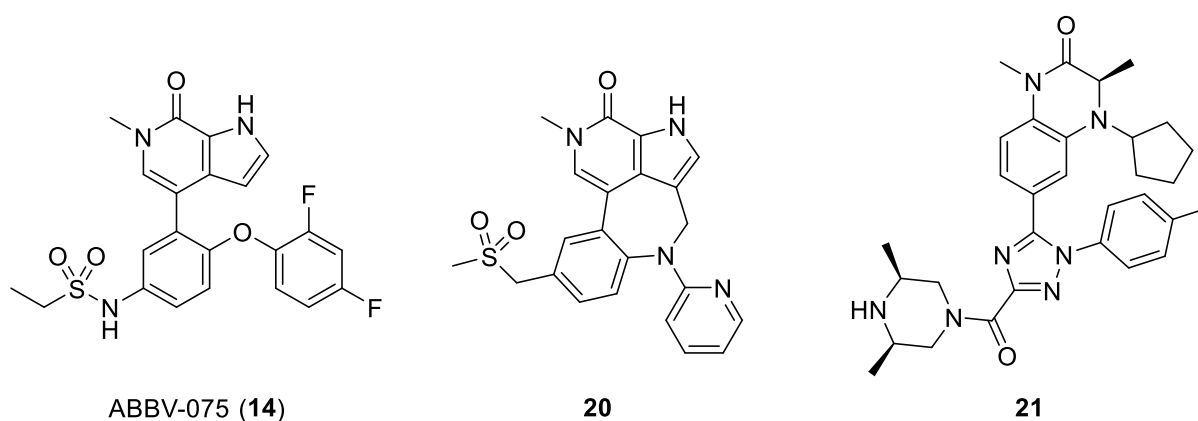
ABBV-075 (**14**)   **20**   **21**

Figure 19: Selected BET inhibitors for the development of dual BET/HDAC inhibitors. Inhibitors ABBV-075 (**14**), **20** and **21** were used as starting points due to their high potency.

For a slightly differing approach, the azobenzene MS436 (**22**) was selected as a BET ligand because of its low starting molecular weight and significant structural similarity to **7** (**Figure 20**).[247] This was thought to be ideal for merging the two pharmacophores, resulting in a dual inhibitor with a good balance between size and potency.
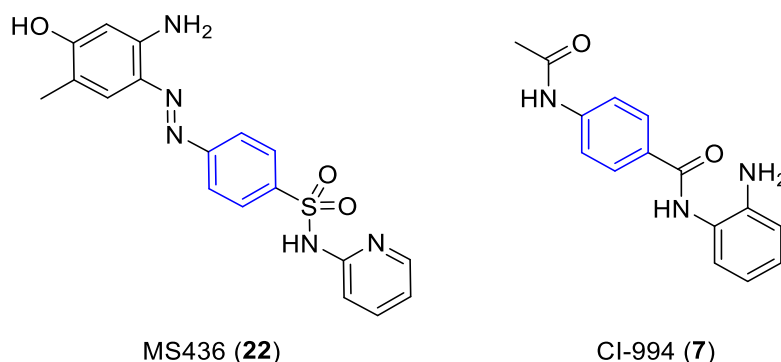
MS436 (**22**)   CI-994 (**7**)

Figure 20: BET inhibitor MS436 (22) and HDAC inhibitor CI-994 (7). Both molecules show a good structural overlap, and the central phenyl moiety (blue) can be fused to become the center of the dual inhibitor.

As previously discussed, most published BET/HDAC inhibitors contain a pan-HDAC-binding warhead. While benzamide **7** only binds proteins of class I, it would be ideal to develop an inhibitor that is selective for HDAC1 and 2. This can likely be achieved through the addition of an aromatic substituent that targets the foot pocket, as seen for BRD6929 (**9**).

Another strategy that has been frequently employed in recent years, is to hijack the ubiquitin-proteasome system (UPS) through so-called proteolysis targeting chimeras (PROTACs). By linking an inhibitor of the protein of interest (POI) to a ligand for an E3 ubiquitin ligase, a ternary complex between the POI, the PROTAC and the E3 ligase is created. The POI is then polyubiquitinylated and therefore tagged for proteasomal degradation.[248] Advantages of this approach are the catalytic mechanism of the PROTAC and a potential better selectivity compared to the used POI inhibitor. Numerous groups could show the possible degradation of BRD4 using PROTACs that target the E3 ligase cereblon (CBRN) through employing thalidomide or related ligands.[249–256] Additionally, by targeting the von Hippel-Lindau (VHL) E3 ligase, many potent and sometimes selective BRD4 degraders were developed.[257–262]

HDACs were also repeatedly shown to be possible targets for PROTAC-induced degradation.[263] Working PROTACs were, for example, reported for HDAC3[264] and HDAC6[265–267]. Benzamide-based PROTACs targeting class I HDACs were also published[268,269], but compared to BRD4 there are significantly less reported degraders for HDACs.

Fischer *et al*. reported several PROTACs that were based on BET inhibitor **13**, using different linker lengths and attachment points. They could show that some of those compounds induced degradation and were also able to crystallize the ternary complexes with CRBN for a few of the degraders.[270] The crystal structure of dBET23, for example, suggests that adding an HDAC-binding moiety to the degrader should not interfere with ternary complex formation of BRD4 (**Figure 21**). Therefore, another strategy that was pursued was to develop PROTACs that simultaneously target BRD4 and HDAC class I. The degraders were designed based on dual inhibitor **19** and the developed novel inhibitors.
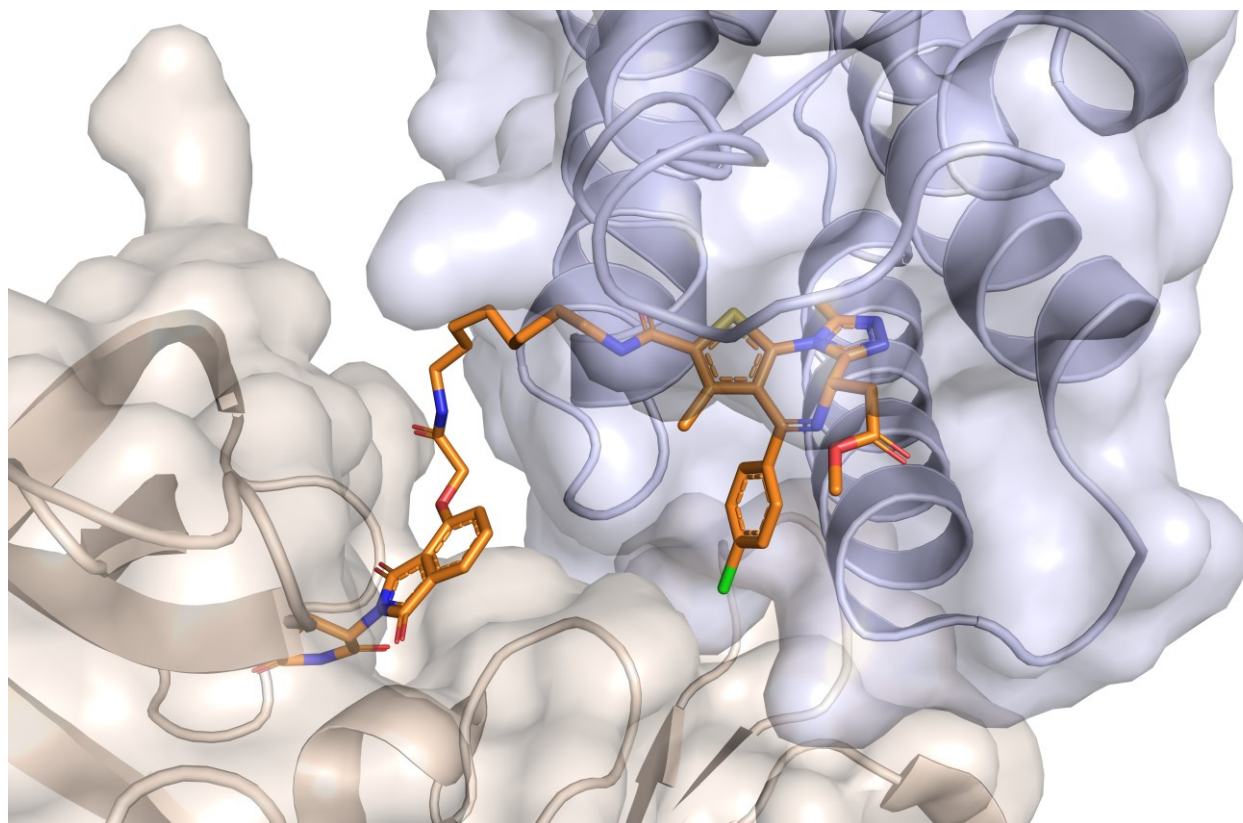
Figure 21: Co-crystal structure of a ternary complex of the first bromodomain of BRD4 BD1 (lightblue) and CRBN (beige) bound to PROTAC dBET23 (orange) (PDB: 6BN7).

3 Results

3.1 Increasing HDAC Selectivity

In an attempt to get a BET/HDAC inhibitor that is selective for HDAC1/2 while simultaneously improving potency, dual inhibitor **19** was used as a template, to which aromatic substituents were added. For the synthesis of the substituted dual inhibitors, commercially available 4-bromo-2-nitroaniline (**23**) was first *Boc*-protected, yielding intermediate **24** and Suzuki coupling with different arylboronic acids provided the respective biaryls **25a-d** (**Scheme 3**). Iron and ammonium chloride were used for a mild reduction of the nitro group to the anilines **26a-d**. Afterwards, amide coupling with *Fmoc*-protected *p*-aminobenzoic acid yielded intermediates **28a-d** which were then deprotected with morpholine to give anilines **29a-d**. Amide coupling with the acid derivative of JQ1 (**30**), followed by *Boc*-deprotection with TFA, finally provided inhibitors **31a-c**.
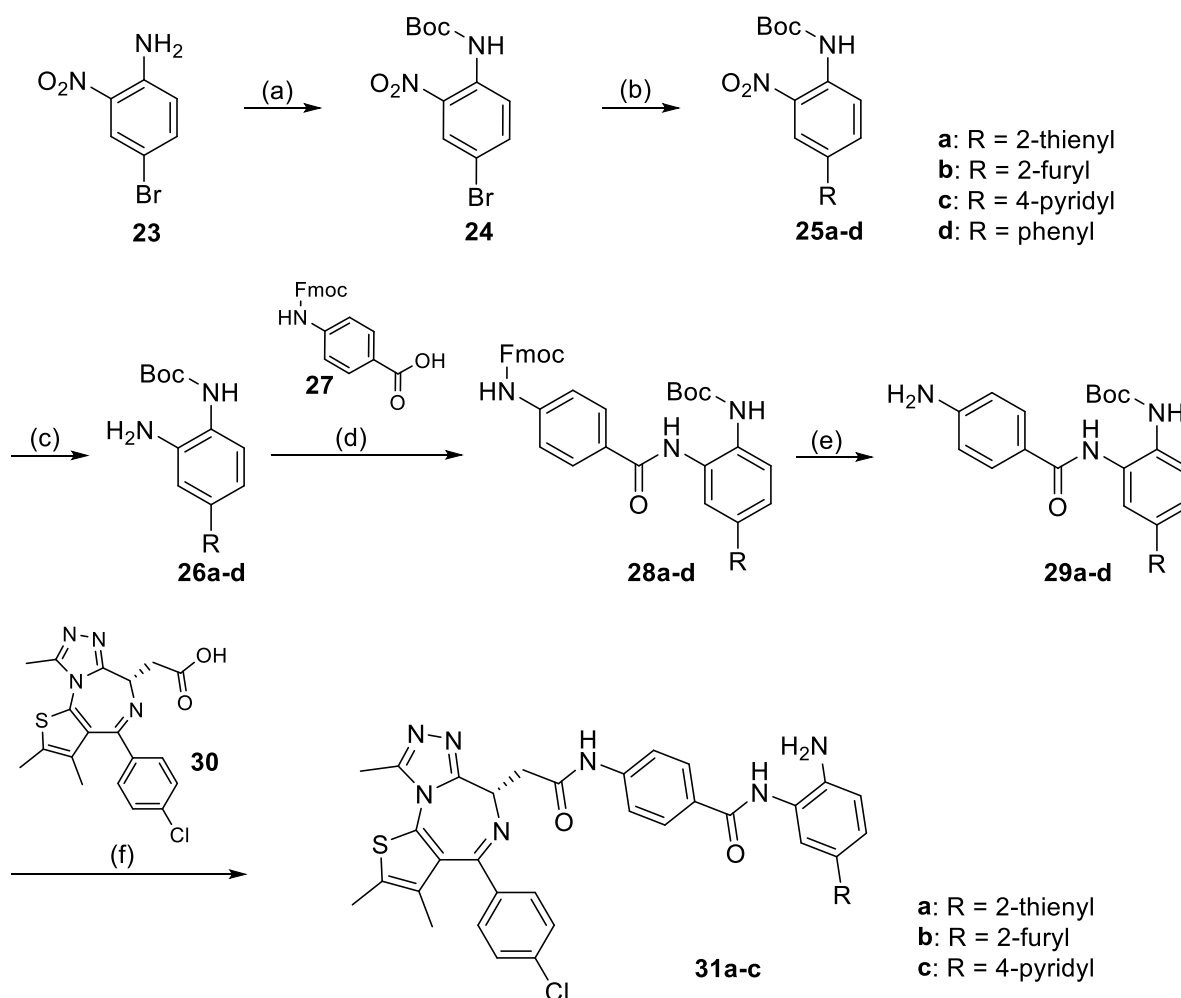
Scheme 3: Synthesis of substituted dual inhibitors 31a-c. Reagents and conditions: (a) NaH, Boc$_2$O, THF, -10 °C to rt, 4 h; (b) arylboronic acid, K$_2$CO$_3$, Pd XPhos G2, XPhos, DMF/H$_2$O, 100 °C, 2 h; (c) Fe, NH$_4$Cl, MeOH/H$_2$O, 85 °C, 3 h; (d) PyAOP, DIPEA, DMF, rt, 16 h; (e) morpholine/ACN, rt, 2 h; (f) (1) HATU, DIPEA, DMF, rt, 16 h; (2) TFA/DCM, rt, 1 h.

The activity of compounds **31a-c** was assessed by a thermal shift assay using differential scanning fluorimetry (DSF), which measures the increase in the melting temperature (T_m) of the protein upon

ligand binding, which for a given protein domain correlates with the affinity of the ligand. The compounds were tested against both bromodomains of the four BET proteins with JQ1 (**13**) and TW9 (**19**) as controls (**Table 1**). Surprisingly, all three inhibitors showed significantly reduced binding compared with the control compounds. The low thermal shift was difficult to explain since the HDAC-binding part of inhibitor **19**, which was modified, protrudes outside of the bromodomain binding pocket[230] and compounds **31a-c** could not successfully be crystallized with BRD4.

Table 1: Modification of the initial dual inhibitor
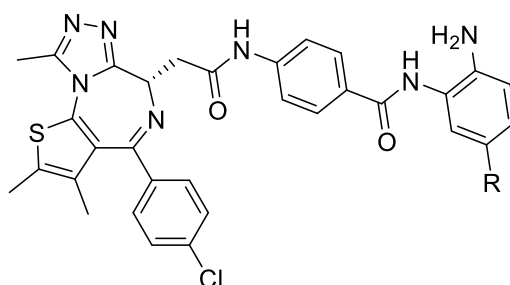
	R	DSF ΔT_m (K)[1]							
		BRD4-BD1	BRD4-BD2	BRD3-BD1	BRD3-BD2	BRD2-BD1	BRD2-BD2	BRDT-BD1	BRDT-BD2
13	-	11.6 ± 0.8	14.2 ± 0.1	9.1 ± 0.1	10.6 ± 0.1	9.4 ± 0.1	11.2 ± 0.1	7.9 ± 0.1	6.5 ± 0.1
19	H	7.0 ± 0.7	12.6 ± 0.2	4.4 ± 0.2	4.7 ± 0.2	4.6 ± 0.1	n.d.	3.0 ± 0.1	5.5 ± 0.1
31a	2-thienyl	0.0 ± 0.1	3.0 ± 0.1	-0.1 ± 0.1	-0.3 ± 0.1	-0.2 ± 0.4	-1.0 ± 0.4	-0.7 ± 0.2	0.5 ± 0.4
31b	2-furyl	-0.3 ± 0.1	2.9 ± 0.4	-0.4 ± 0.1	0.1 ± 0.2	0.4 ± 0.1	0.1 ± 0.3	-0.6 ± 0.1	1.1 ± 0.3
31c	2-pyridyl	2.7 ± 1.4	3.3 ± 2.3	0.6 ± 0.8	2.2 ± 0.3	2.2 ± 0.3	4.0 ± 0.4	0.7 ± 0.5	3.3 ± 0.5

[1] Mean and standard error of the mean (SEM) of two independent experiments that were themselves performed in technical triplicates.

To assess the inhibition of HDACs, a fluorogenic HDAC assay, with CI994 (**7**) and TW9 (**19**) as controls, was performed (**Table 2**). While the substitution does not appear to increase HDAC1 inhibition, selectivity against HDAC3 seems to improve, especially for inhibitors **31a** and **b**.

Table 2: Influence of substitution on HDAC inhibition

Compounds	R	Fluorogenic HDAC assay - IC$_{50}$ (μM)	
		HDAC1	HDAC3
CI994 (**7**)	-	6.4	2.5
19	H	2.5	4.0
31a	2-thienyl	25.3	589.4
31b	2-furyl	4.5	622.8
31c	2-pyridyl	8.6	36.6

3.2 Novel Adducts

Since the substituted derivatives **31a-c** essentially lost their binding affinity to BET proteins, novel compounds had to be designed. For the development of a dual inhibitor based on BET inhibitor **21**, the synthesis of the dihydroquinoxalinone scaffold was adapted from literature.[246] In analogy to **Scheme 3**, *Boc*-protected phenylenediamine **32** was first coupled to carboxylic acid **27** and the resulting *Fmoc*-protected intermediate **33** was then deprotected with morpholine to provide aniline **34** (**Scheme 4**). According to a published protocol, ethyl isocyanoacetate **35** was reacted with previously diazotized *p*-toluidine **36** to create triazole **37** in a cycloaddition.[271] Afterwards, reaction with sodium hydride and *N*-bromosuccinimide (NBS) provided intermediate **38**.
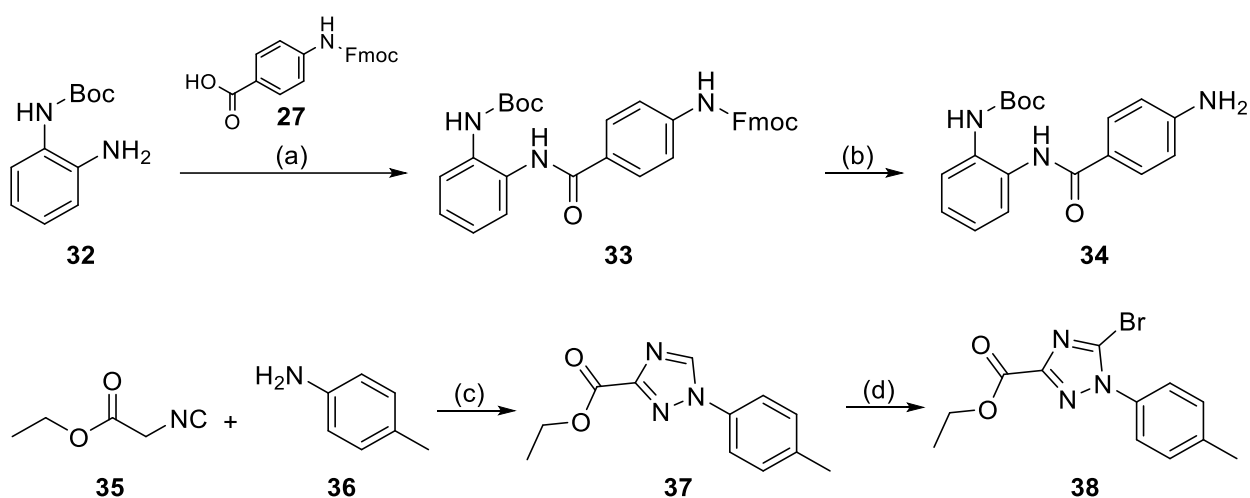
Scheme 4: Synthesis of intermediates 34 and 38. Reagents and conditions: (a) PyAOP, DIPEA, DMF, rt, 16 h; (b) morpholine/ACN, rt, 2 h; (c) (1) HCl, NaNO$_2$, H$_2$O, 0 °C, 10 min; (2) NaOAc · 3 H$_2$O, MeOH/H$_2$O, 0 °C to rt, 4 h; (d) NaH, NBS, THF, rt, 24 h.

For the synthesis of the dihydroquinoxalinone core, 4-bromo-2-fluoro-1-nitrobenzene (**39**) was first reacted with D-alanine to receive the enantiopure intermediate **40** (**Scheme 5**). Reduction with sodium dithionite, followed by cyclization, provided dihydroquinoxalinone **41**. Reductive amination with cyclopentanone gave substituted analogue **42** with was afterwards methylated to finish the asparagine binding scaffold **43**. Miyaura borylation gave intermediate **44** which was afterwards reacted in a Suzuki coupling with compound **38** to yield diaryl triazole **45**. Saponification with lithium hydroxide gave carboxylic acid **46** and amide coupling with aniline **34**, followed by *Boc*-deprotection with TFA, provided dual inhibitor **47**.
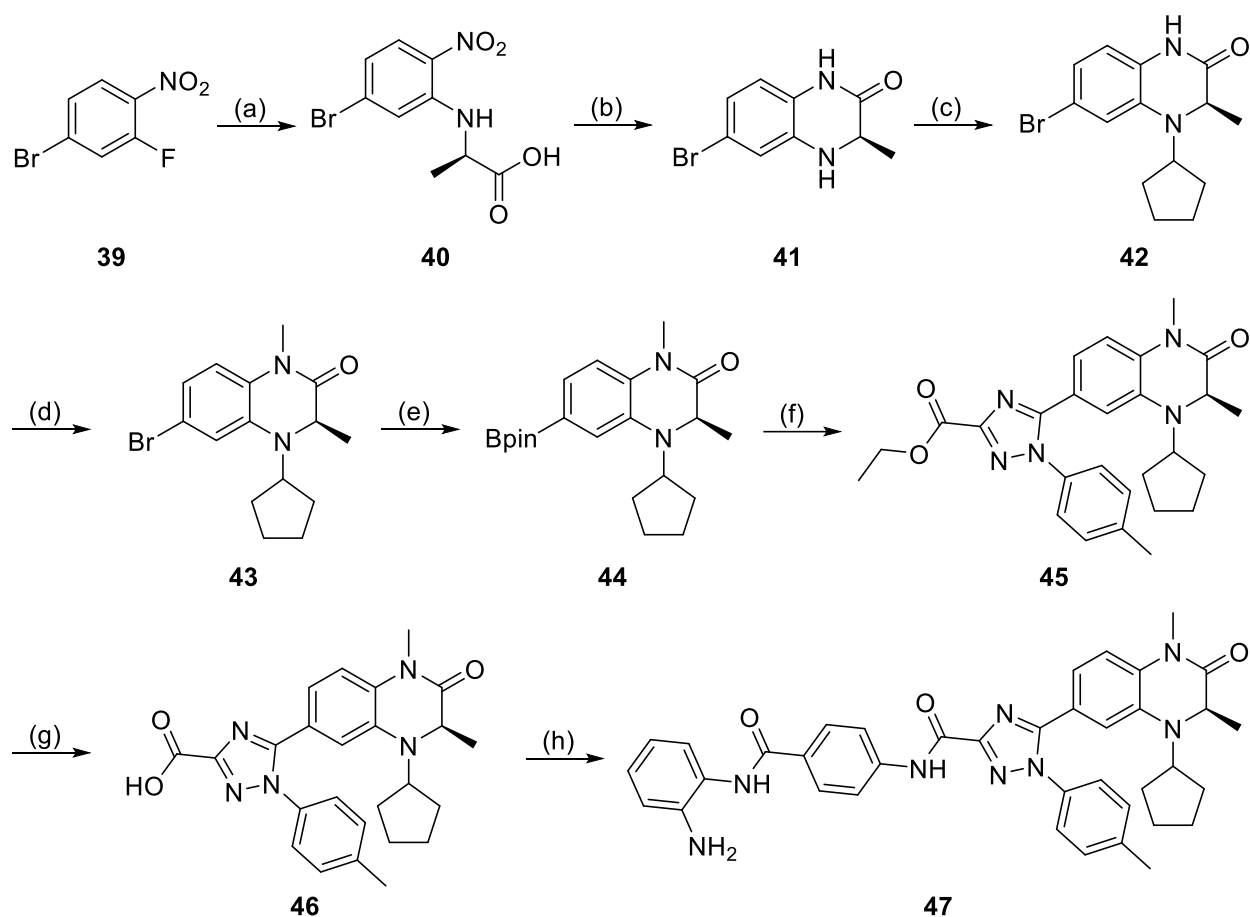
Scheme 5: Synthesis of dual inhibitor 47. Reagents and conditions: (a) D-alanine, K_2CO_3, EtOH/H_2O, 80 °C, 3 h; (b) K_2CO_3, $Na_2S_2O_4$, H_2O, 60 °C, 16 h; (c) phenylsilane, cyclopentanone, dibutyltin dichloride, THF, rt, 10 h; (d) NaH, iodomethane, 0 °C to rt, 2 h; (e) Pd(dppf)Cl_2, B_2pin_2, KOAc, DMSO, 80 °C, 16 h; (f) **38**, Pd(dppf)Cl_2, $NaHCO_3$, THF/H_2O, 80 °C, 16 h; (g) LiOH · H_2O, THF/H_2O, rt, 16 h; (h) (1) **34**, HATU, DIPEA, DMF, rt, 16 h; (2) TFA/DCM, rt, 1 h.

The activity of the dihydroquinoxalinone based inhibitors was again assessed by a thermal shift assay (**Table 3**). While especially carboxylic acid **46** shows a significant thermal shift, the introduction of the HDAC-binding moiety in compound **47** appears to notably reduce binding. The balance between potency and molecular size was determined to be not ideal and for this reason, this scaffold was not further investigated.

Table 3: SAR of the dihydroquinoxalinone scaffold

Compounds	DSF ΔT_m (K)[1]	
	BRD4-BD1	BRD4-BD2
JQ1 (**13**)	11.6 ± 0.8	14.2 ± 0.1
TW9 (**19**)	7.0 ± 0.7	12.6 ± 0.2
45	9.5 ± 0.1	8.2 ± 0.8
46	12.6 ± 0.1	9.3 ± 0.2
47	7.4 ± 0.1	6 ± 3

[1] Mean and SEM of two independent experiments that were themselves performed in technical triplicates.

For another approach, the pyrrolopyridone based BET inhibitors **14** and **20** were used for the development of different dual inhibitors. The synthesis of the pyrrolopyridone core was adapted from published protocols.[187,272] 2-chloro-4-methyl-3-nitropyridine **48** was reacted with sodium methoxide to give methoxypyridine **49** which was afterwards brominated to yield intermediate **50** (**Scheme 6**). Reaction with *N,N*-dimethylformamide dimethyl acetal (DMF-DMA) provided compound **51** which after reductive cyclization with iron gave pyrrolopyridone **52**. Protection with a tosyl group (Ts) provided compound **53** and acidic ether cleavage, followed by isomerization, yielded pyrrolopyridone **54**. Methylation gave the finished asparagine binding scaffold **55** and Miyaura borylation provided boronate **56**. If detosylation was performed under basic hydrolysis before the borylation, boronate **57** was received.
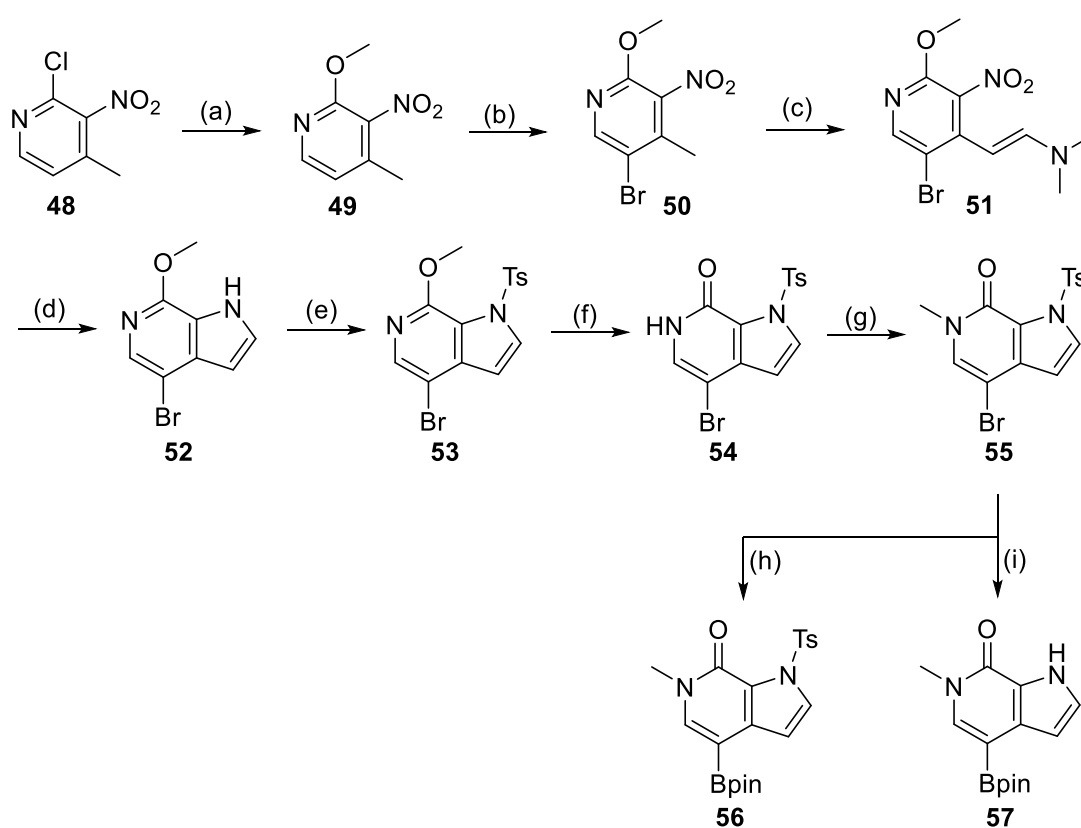
Scheme 6: Synthesis of the pyrrolopyridone scaffold. Reagents and conditions: (a) NaOMe, MeOH, reflux, 16 h; (b) Br_2, NaOAc, AcOH, 80 °C, 16 h; (c) DMF-DMA, DMF, 90 °C, 16 h; (d) Fe, AcOH/MeOH/H_2O, reflux, 2 h; (e) NaH, TsCl, THF, 0 °C to rt, 2 h; (f) HCl in dioxane, 50 °C, 2 h; (g) NaH, MeI, DMF, 0 °C to rt, 2 h; (h) B_2pin_2, KOAc, Pd XPhos G2, XPhos, dioxane, 80 °C, 2 h; (i) (1) LiOH · H_2O, dioxane/H_2O, 85 °C, 2.5 h; (2) B_2pin_2, KOAc, Pd XPhos G2, XPhos, dioxane, 80 °C, 4 h.

For the pyrrolopyridone based dual inhibitors the right attachment point of the HDAC-binding moiety had to be found. Based on the crystal structure (**Figure 17**), different exit vectors and attachment points were deemed possible and dual inhibitors were designed.
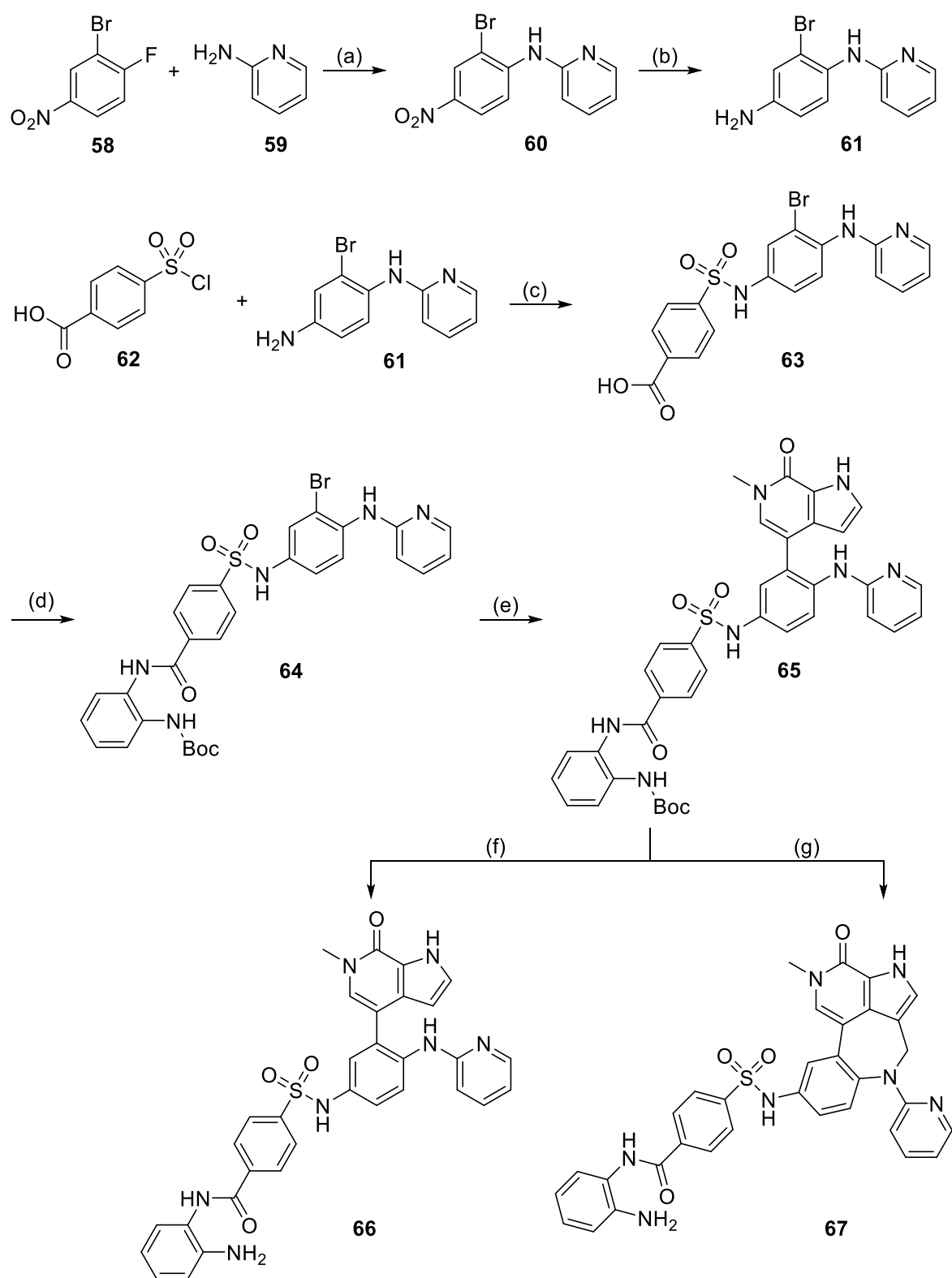
Scheme 7: Synthesis of dual inhibitors 66 and 67. Reagents and conditions: (a) NaH, DMF, -10 °C to rt, 16 h, (b) Na$_2$S$_2$O$_4$, EtOH/H$_2$O, reflux, 1 h; (c) pyridine, THF, rt, 16 h; (d) **32**, HATU, DIPEA, DMF, rt, 16 h; (e) **57**, K$_3$PO$_4$, Pd XPhos G2, XPhos, dioxane/H$_2$O, 60 °C, 16 h; (f) TFA/DCM, rt, 1 h; (g) (1) paraformaldehyde, AcOH, 80 °C, 1 h; (2) TFA/DCM, rt, 1 h.

The reaction of 2-bromo-1-fluoro-4-nitrobenzene (**58**) with 2-aminopyridine (**59**) produced the highest yield for compound **60** (**Scheme 7**) when sodium hydride was used as a base. Reduction with sodium dithionite provided aniline **61** and subsequent reaction with sulfonyl chloride **62** gave compound **63**.

Amide coupling with aniline **32** yielded intermediate **64** and subsequent Suzuki coupling with boronate **57** provided *Boc*-protected inhibitor **65**. Reaction with TFA gave deprotected inhibitor **66**, while Pictet-
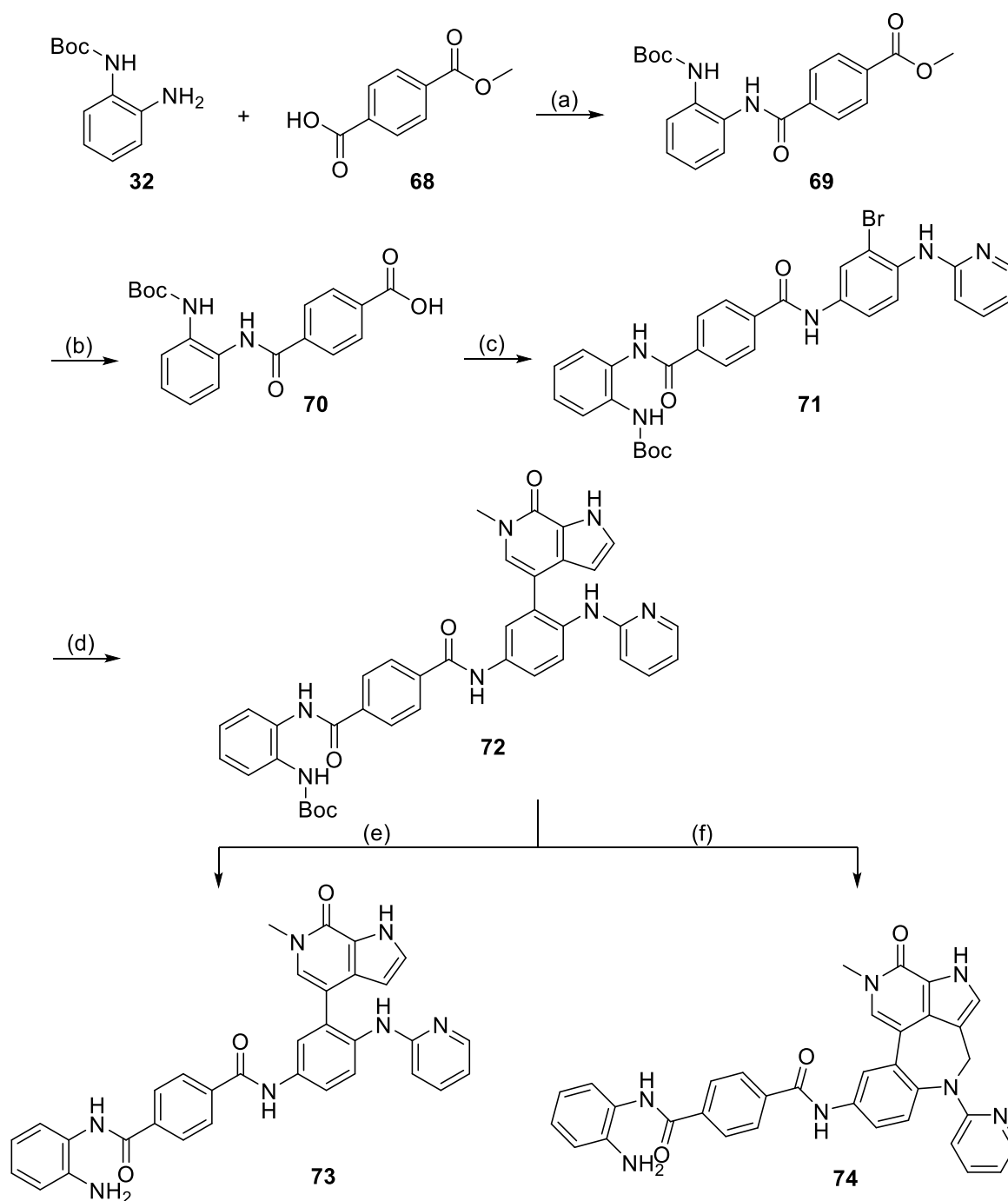
Scheme 8: Synthesis of dual inhibitors 73 and 74. Reagents and conditions: (a) HATU, DIPEA, DMF, rt, 16 h; (b) LiOH · H$_2$O, THF/MeOH/H$_2$O, rt, 16 h; (c) **61**, HATU, DIPEA, DMF, rt, 16 h; (d) **57**, K$_3$PO$_4$, Pd XPhos G2, XPhos, dioxane/H$_2$O, 65 °C, 16 h; (e) TFA/DCM, rt, 1 h; (f) (1) paraformaldehyde, AcOH, 80 °C, 1 h; (2) TFA/DCM, rt, 1 h.

Spengler reaction with paraformaldehyde, followed by deprotection with TFA, provided cyclic inhibitor **67**. To investigate the influence of an amide connection in comparison to the sulfonamide of compounds **66** and **67**, another set of inhibitors was designed (**Scheme 8**). Aniline **32** was reacted with methyl terephthalate (**68**) to yield intermediate **69** and saponification provided carboxylic acid **70**. Afterwards, amide coupling with aniline **61** gave compound **71** and subsequent Suzuki coupling with

boronate **57** yielded compound **72**. Similar to **Scheme 7**, deprotection with TFA gave open inhibitor **73**, while ring closure, followed by deprotection, provided cyclic inhibitor **74**.

Since the introduction of the pyridine substituent in inhibitor **20** could not be achieved with a satisfying yield, it was tested if the synthetically more accessible cyclohexane derivative would show a similar potency. For the synthesis of this new BET inhibitor, nitrobenzene **75** was reduced with hydrogen and palladium on carbon to provide aniline **76** (**Scheme 9**). Iodination with *N*-iodosuccinimide (NIS) gave aryl iodide **77** and reductive amination yielded intermediate **78**. Subsequent Suzuki coupling resulted in inhibitor **79** and after ring closure with paraformaldehyde, cyclic inhibitor **80** was obtained.
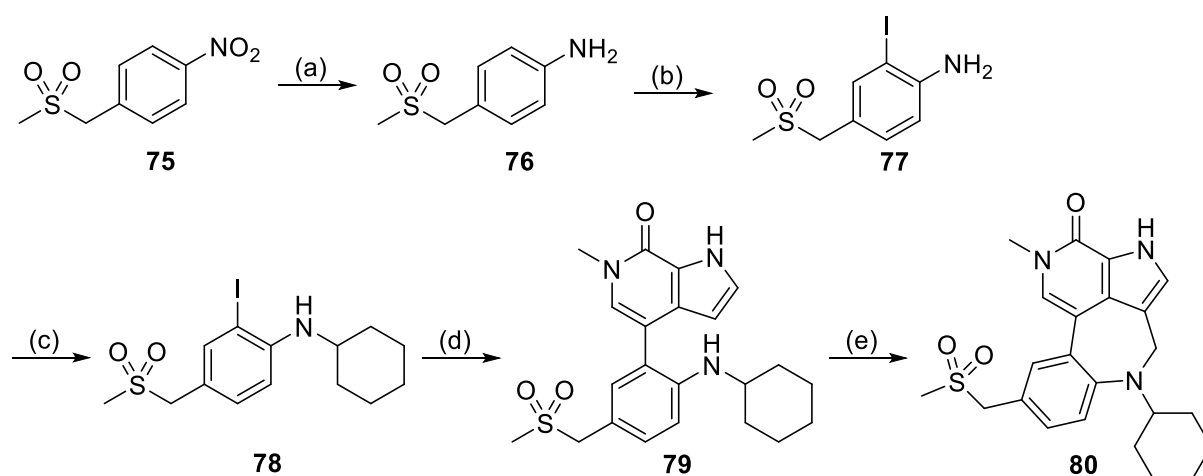
Scheme 9: Synthesis of BET inhibitors 79 and 80. Reagents and conditions: (a) H_2, Pd/C, THF, rt, 90 min; (b) NIS, DMF, rt, 1 h; (c) cyclohexanone, NaBH(OAc)$_3$, AcOH/MeOH, rt, 2 h; (d) **56**, K$_3$PO$_4$, Pd XPhos G2, XPhos, dioxane/H$_2$O, 60 °C, 16 h; (e) paraformaldehyde, AcOH, 80 °C, 1 h.

For the attachment of the HDAC-binding moiety directly on the pyrrolopyridone core, compound **53** was reacted with lithium diisopropylamide (LDA) and ethyl chloroformate to obtain carbonyl functionalized intermediate **81**, as described in the literature (**Scheme 10**).[188] Ether cleavage produced pyrrolopyridone **82** and methylation gave compound **83**. Basic hydrolysis was performed to remove the tosyl group and the resulting carboxylic acid **84** was re-esterified with thionyl chloride in ethanol, providing intermediate **85**. Since conversion under standard Miyaura borylation conditions using potassium acetate proved to be difficult for this substrate, potassium ethyl hexanoate was instead used as a base, as described by Barroso *et al.*,[273] yielding boronate **86**.
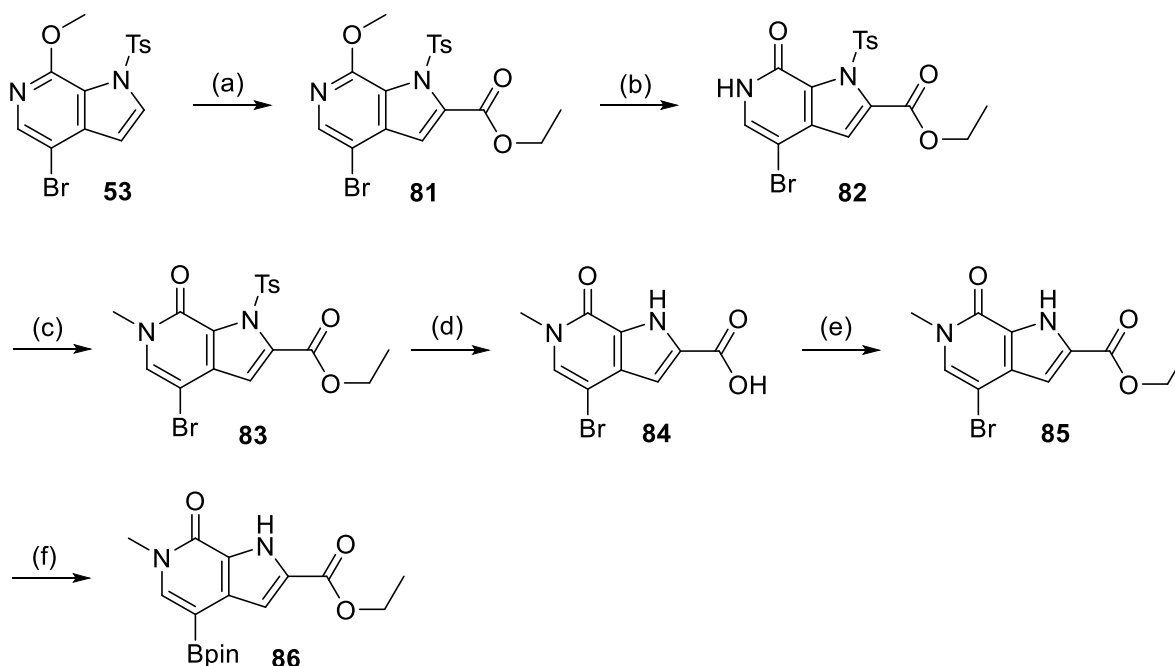
Scheme 10: Synthesis of intermediate 86. Reagents and conditions: (a) (1) LDA, THF, -78 °C, 1 h; (2) ethyl chloroformate, 78 °C to rt, 16 h; (b) (1) NaI, TMSCl, ACN, rt, 1 h (2) H_2O, 65 °C, 2 h; (c) Cs_2CO_3, MeI, DMF, rt, 16 h; (d) LiOH·H_2O, dioxane/H_2O, 90 °C, 2 h; (e) $SOCl_2$, EtOH, 75 °C, 16 h; (f) B_2pin_2, potassium ethyl hexanoate, Pd XPhos G2, XPhos, MeTHF, 50 °C, 16 h.

Reaction of carboxylic acid **84** with aniline **34** provided intermediate **87** (**Scheme 11**). Since borylation of aryl iodide **78** did not produce the desired product, aryl bromide **87** was instead borylated, yielding boronate **88**. Subsequent Suzuki coupling with aryl iodide **78** then gave *Boc*-protected compound **89**. And, similar to the previously described compounds, deprotection provided inhibitor **90** while after ring closure and subsequent deprotection, inhibitor **91** was obtained.
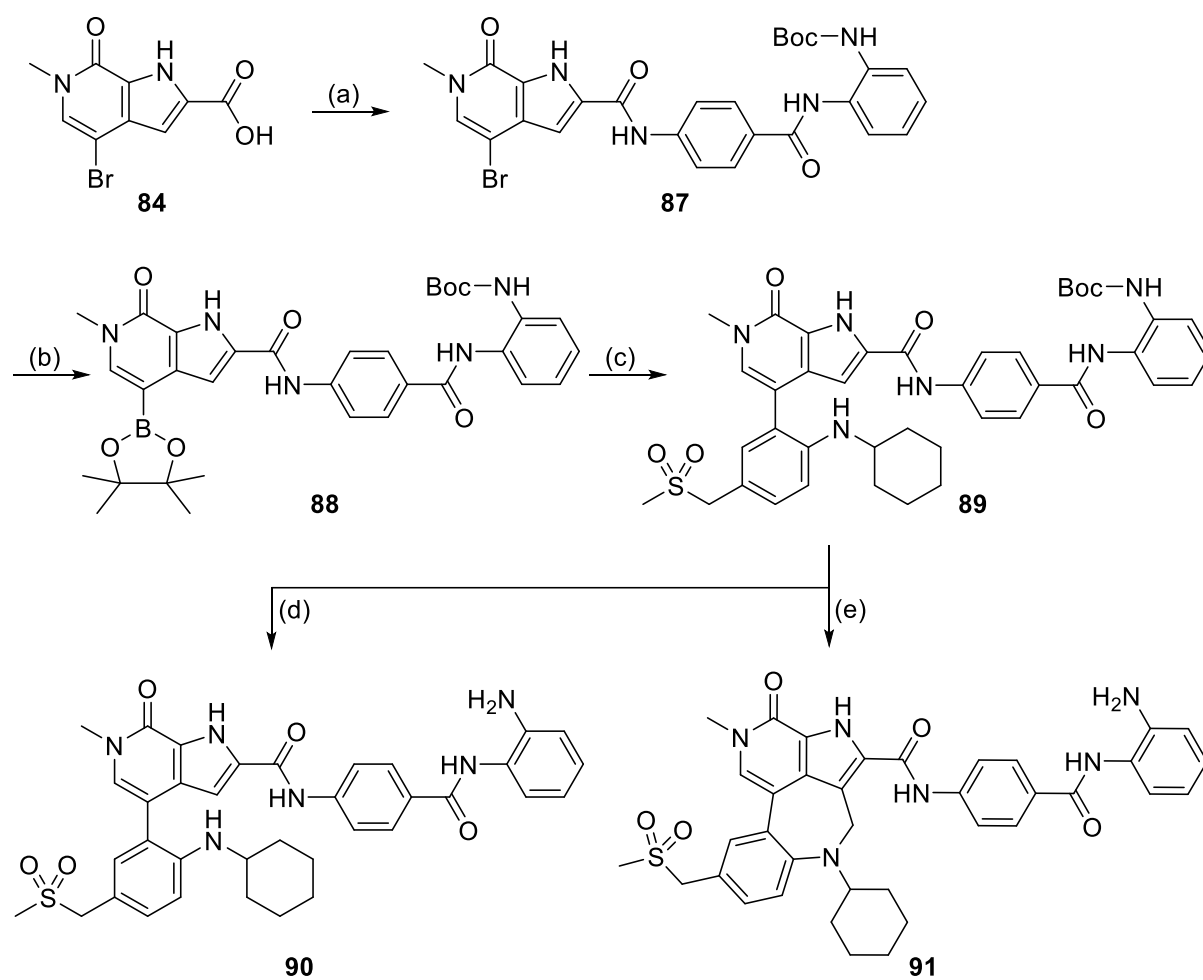
Scheme 11: Synthesis of dual inhibitors 90 and 91. Reagents and conditions: (a) **34**, HATU, DIPEA, DMF, rt, 16 h; (b) B_2pin_2, KOAc, Pd XPhos G2, XPhos, dioxane, 80 °C, 4 h; (c) **78**, K_3PO_4, Pd XPhos G2, XPhos, dioxane/H_2O, 60 °C, 16 h; (d) TFA/DCM, rt, 1 h; (e) (1) paraformaldehyde, AcOH, 80 °C, 1 h; (2) TFA/DCM, rt, 1 h.

As for the previous compounds, binding of the described pyrrolopyridone-based inhibitors, together with compounds **92-95** (**Figure 22**) against BRD4 was assessed by a thermal shift assay, while inhibition of HDACs was determined by a fluorogenic HDAC assay (**Table 4**). When comparing thermal shifts of the BET inhibitors **20** and **80**, the cyclohexyl residue seems to slightly reduced binding compared to the pyridyl residue (ΔT_m = 15.9 *vs.* 17.1 K for BD1). The non-cyclic derivative **79** shows further reduced binding (ΔT_m = 12.6 K) compared to the cyclic inhibitor. The same trend can be observed for the dual inhibitor pairs **66/67** and **73/74**, where the cyclic derivative is significantly more potent than the open compound. In the case of inhibitor **91**, however, cyclization appears to almost completely remove binding affinity to BRD4. As expected, inhibitors **94** and **95** show a preference for the second BD due to their similarity to ABBV-744 (**14**). Generally, the introduction of the HDAC-binding moiety in the dual inhibitors does not seem to significantly reduce the thermal shift compared with the BET inhibitors. The ΔT_m values should not be seen as a real indication of binding affinity, as larger and more lipophilic compounds generally tend to have higher thermal shifts. The observed stabilization can, however, be used as a first qualitative assessment of inhibitor binding. When comparing HDAC1 inhibition,

sulfonamides **66** and **67** and diaryl ether **92** show the best activity in the new series. The other compounds exhibit a rather weak inhibition of HDAC1 and 3.

A

ABBV-075 (**14**)   ABBV-744 (**15**)   **20**   **79**   **80**

B

66   **73**   **90**

67   **74**   **91**

92[1]   **93**[1]   **94**[2]

95[3]
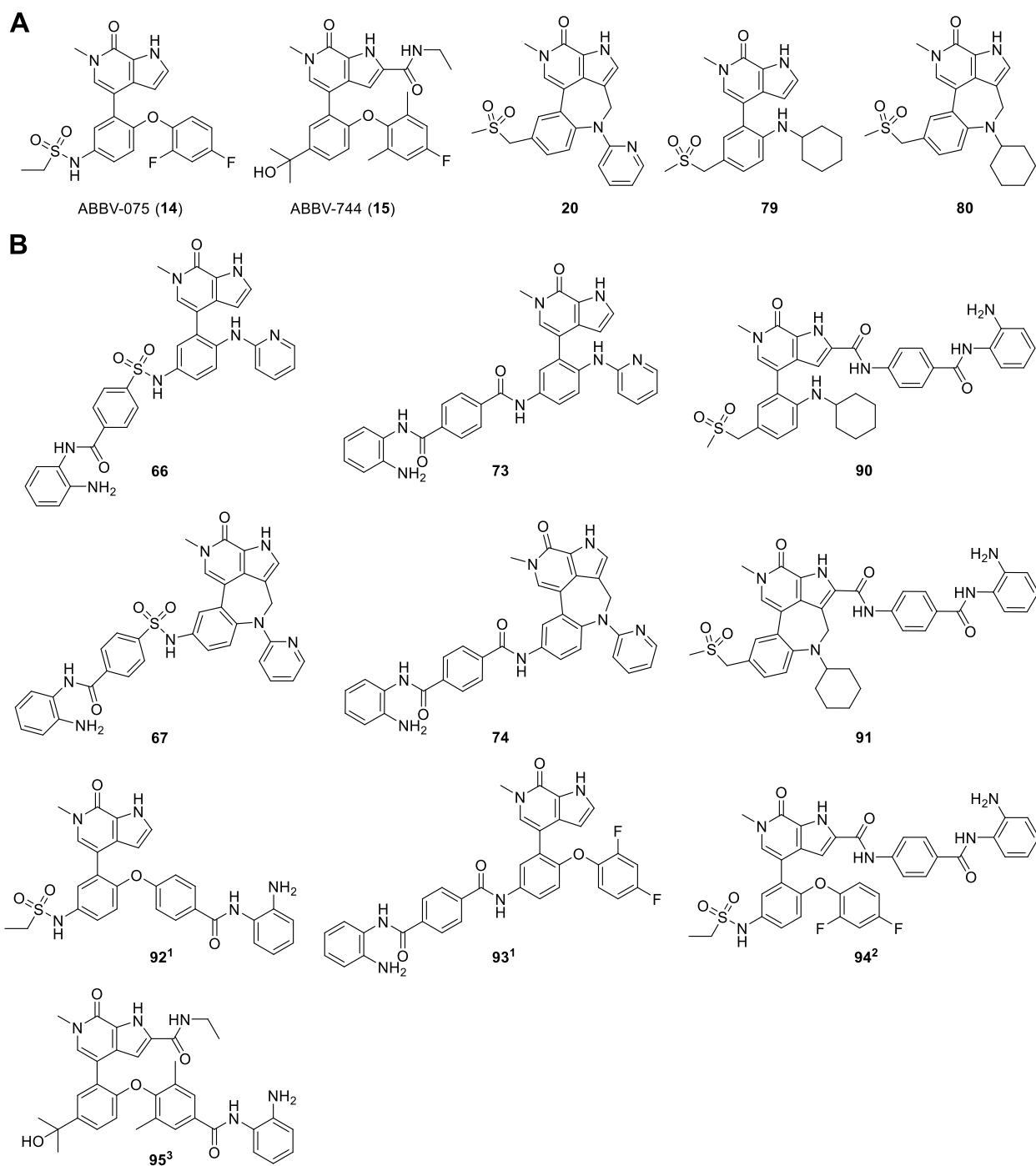
Figure 22: Pyrrolopyridone-based BET inhibitors (A) and dual BET/HDAC inhibitors (B). [1]Synthesis can be found in the master's thesis of Nicolas Bauer; [2]Synthesis can be found in the master's thesis of Julian Breidenbach; [3]Synthesis can be found in the master's thesis of Dennis Keller.

Table 4: Activity of the pyrrolopyridone-based inhibitors

Compounds	DSF ΔT_m (K)[1]		Fluorogenic HDAC assay - IC$_{50}$ (µM)	
	BRD4-BD1	BRD4-BD2	HDAC1	HDAC3
JQ1 (**13**)	11.6 ± 0.8	14.2 ± 0.1	-	-
CI-994 (**7**)	-	-	6.4	2.5
TW9 (**19**)	7.0 ± 0.7	12.6 ± 0.2	2.5	4.0
ABBV-075 (**14**)	17.9 ± 0.1	22.3 ± 0.2	-	-
ABBV-744 (**15**)	8.4 ± 0.2	20.4 ± 0.2	-	-
20	17.1 ± 0.1	15.4 ± 0.1	-	-
79	12.6 ± 0.2	10.0 ± 0.3	-	-
80	15.9 ± 0.3	10.8 ± 1.2	-	-
66	9.5 ± 0.2	-	9.7	17.5
67	19.0 ± 0.2	21.1 ± 0.2	5.0	4.5
73	8.3 ± 0.2	9.7 ± 0.2	47.7	5.4
74	15.1 ± 0.1	14.7 ± 0.2	21.3	10.6
90	10.1 ± 0.2	2.0 ± 0.3	37.2	27.9
91	2.3 ± 0.3	1.8 ± 0.4	-	77.9
92	14.5 ± 0.2	18.1 ± 0.2	8.9	7.9
93	8.5 ± 0.4	10.6 ± 0.5	29.3	41.3
94	13.7 ± 0.2	21.6 ± 0.3	100.8	376.1
95	6.8 ± 0.1	20.9 ± 0.2	18.4	29.9

[1] Mean and SEM of two independent experiments that were themselves performed in technical triplicates.

Many inhibitors could be co-crystallized together with BRD4 to analyze their binding mode. Compound **80** binds similar to the published pyrrolopyridone-based inhibitors and the cyclohexyl moiety sits on top of the WPF shelf (**Figure 23**). The slightly reduced binding might be explained by the lost π-π interaction to the tryptophan residue.
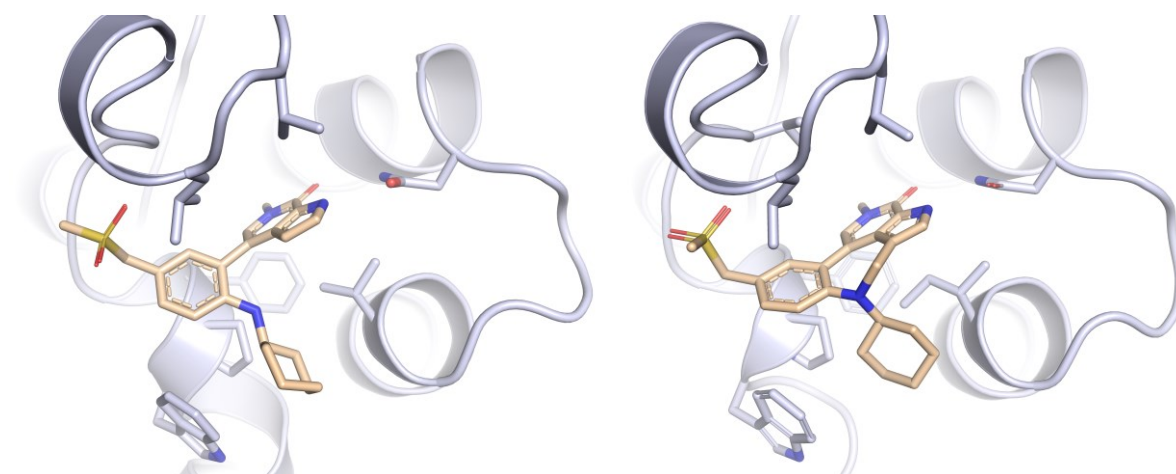
Figure 23: Co-crystal structures of BRD4 BD2 with 79 (left) and BD1 with 80 (right).

In the co-crystal structure of dual inhibitor **92**, it can be observed that the HDAC-binding moiety exits into the solvent without interfering with binding to BRD4. The central phenyl ring interacts with the WPF shelf in a similar way to the parent BET inhibitors (**Figure 24**).
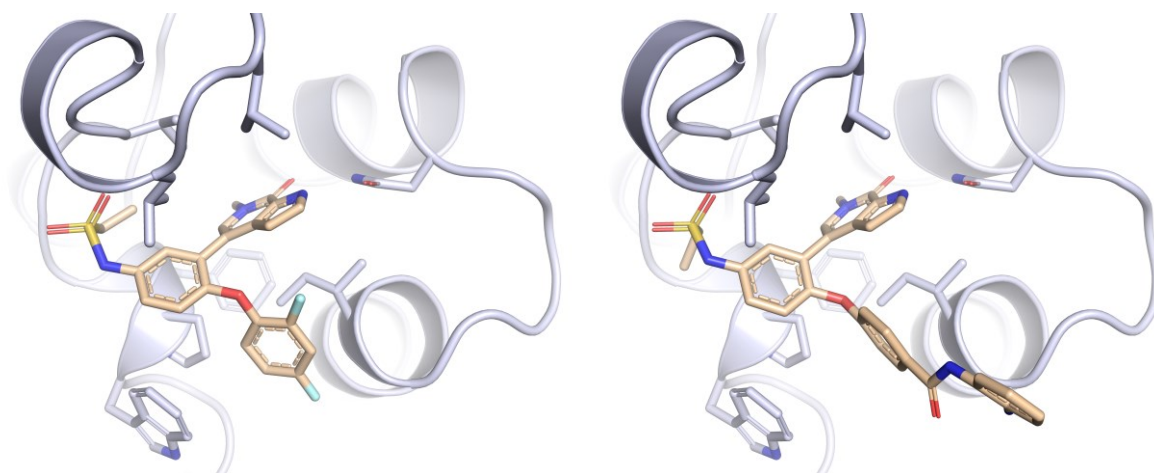
Figure 24: Co-crystal structures of BRD4 BD1 with ABBV-075 (14) (left) and dual inhibitor 92 (right). The dual inhibitor has a similar binding mode to the BET inhibitor and the HDAC-binding moiety points towards the solvent.

To further assess the activity of selected dual inhibitors, they were tested in the pancreatic cancer cell line Patu8988T. HDAC activity was evaluated by comparing histone H3 acetylation after treatment with 1 µM inhibitor (**Figure 25A**). Unfortunately, most dual inhibitors did not show a strong effect on acetylation. The highest acetylation levels of the new series can be observed for compound **93**. Interestingly, acetylation results do not strongly correlate with the previous inhibition results (**Table 5**). The BET-inhibiting effect of the synthesized compounds was assessed by analyzing expression levels of the BET-inhibition biomarkers *HEXIM1*, *p57* and *CDKN1C* (**Figure 25B** and **C**) after treatment with the inhibitors. Most compounds show a strong increase in the mRNA levels of the selected biomarkers, but, in accordance with the DSF results, (**Table 4**) the dual compounds appear to lose some BET activity compared to the parent inhibitor. Next, the viability of pancreatic cancer cells (Patu8988T) after inhibitor treatment was evaluated (**Figure 25D**). From those results, BET inhibition seems to have a strong effect on cell viability. Interestingly, dual inhibitors **19** and **93** were the most potent in reducing the viability of PatuT cells. Isothermal titration calorimetry (ITC) measurements further showed that dual inhibitor **92** binds to BRD4 BD1/BD2 with a K_D value of 12 nM/16 nM, respectively (**Figure 25E**). Its attenuated effect in cells might be attributed to bad cell permeability compared to the parent BET inhibitor.
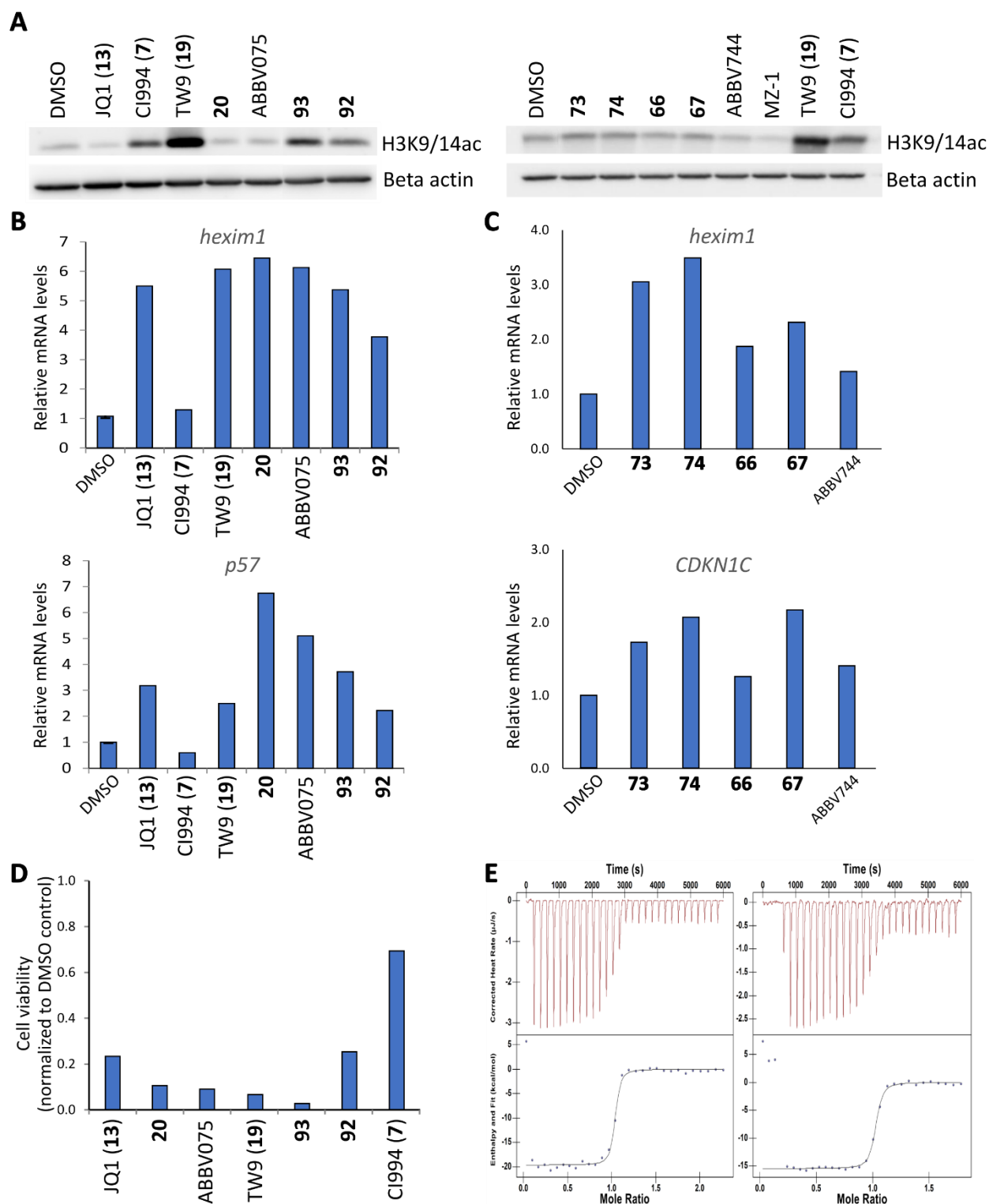
Figure 25: Biological effects of the dual BET/HDAC inhibitors. (A) Effect on histone H3 K9/K14 acetylation in pancreatic cancer cells (Patu8988T) 48 h after incubation with 1 μM compound monitored by Western blot (WB) (two sets of inhibitors). (B) Upregulation of mRNA levels of BET-inhibition biomarkers *HEXIM1* and *CDKN1C* in Patu8988T cells 6 h after treatment with 1 μM compound. (C) Upregulation of mRNA levels of BET-inhibition biomarkers *HEXIM1* and *p57* in Patu8988T cells 6 h after treatment with 1 μM compound for a second set of inhibitors. (D) Cell viability of Patu8988T cells 3 d after treatment with 10 μM inhibitor. (E) ITC data of **92** binding to BRD4 BD1 (left) and BD2 (right).

3.3 Pharmacophore Merging

3.3.1 Dual inhibitor Development

While the previously discussed dual inhibitors generally exhibit good activity in inhibiting BET bromodomains and HDACs, the resulting molecules are also quite large, potentially limiting their biological application. For this reason, a novel series of inhibitors was designed. The BET inhibitor MS436 (**22**) was
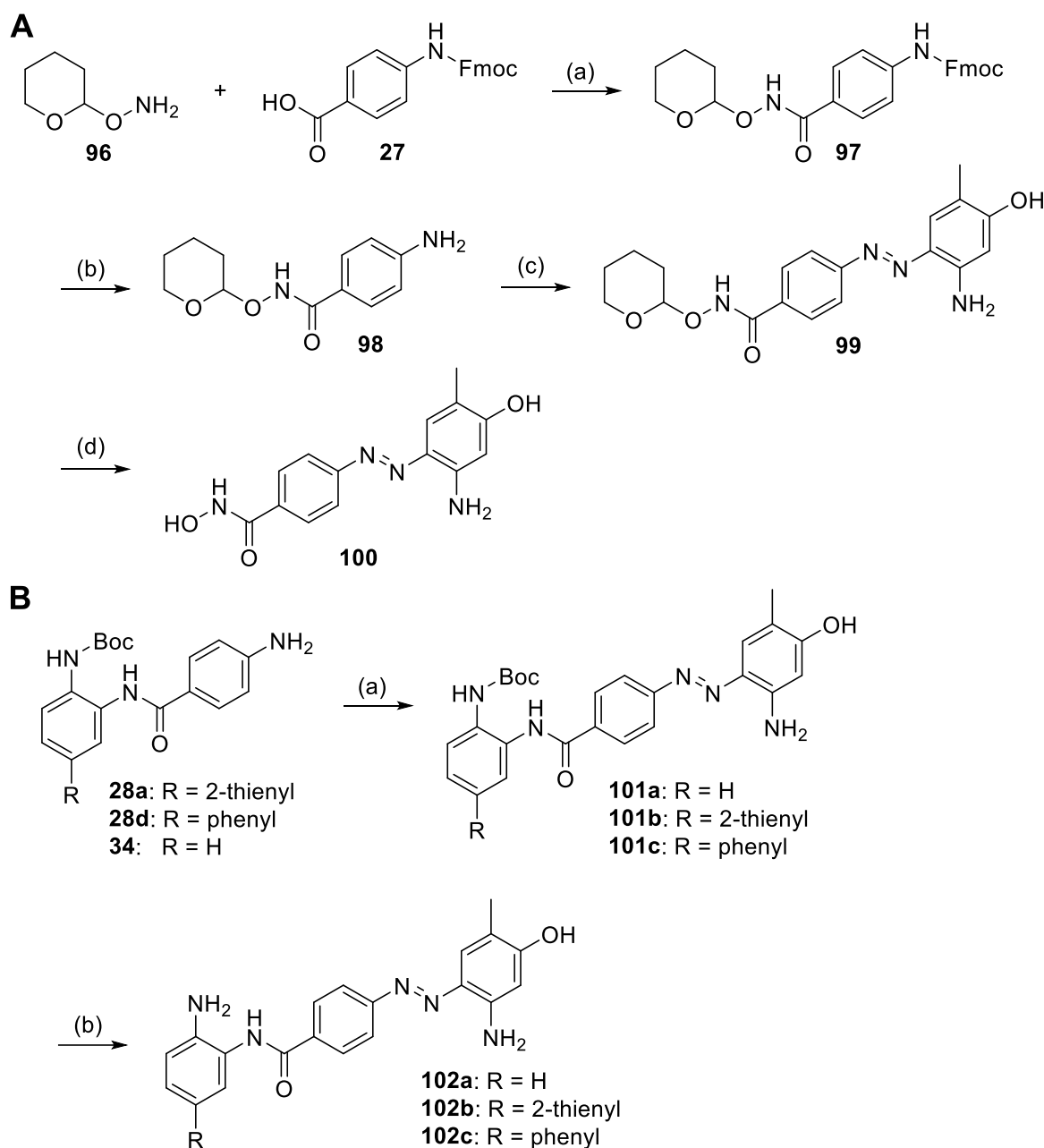
Scheme 12: (A) Synthesis of diazobenzene-based inhibitor 100. Reagents and conditions: (a) PyAOP, DIPEA, DMF, rt, 16 h; (b) morpholine/ACN, rt, 3 h; (c) (1) conc. HCl, isoamyl nitrite, MeOH/ACN, -10 °C, 1 h; (2) 5-amino-2-methylphenol, K_2CO_3, MeOH/H_2O/ACN, -10 C to rt, 2 h; (d) TFA/DCM, rt, 1 h. **(B) Synthesis of diazobenzene-based inhibitors 102a-c.** Reagents and conditions: (a) (1) conc. HCl, isoamyl nitrite, MeOH/ACN, -10 °C, 1 h; (2) 5-amino-2-methylphenol, K_2CO_3, MeOH/H_2O/ACN, -10 C to rt, 2 h; (b) TFA/DCM, rt, 1 h.

used as a starting scaffold due to its structure and low molecular weight. A series of diazobenzene-based inhibitors with different HDAC-binding moieties was therefore synthesized.

The synthesis of the hydroxamic acid-based inhibitor started by reacting tetrahydropyranyl (THP)-protected hydroxylamine **96** with carboxylic acid **27** (**Scheme 12A**), providing compound **97**. After *Fmoc*-deprotection with morpholine, aniline **98** was obtained. Diazotization and subsequent azo coupling gave diazobenzene **99** and after deprotection with TFA, inhibitor **100** was obtained. To synthesize the benzamide-based inhibitors, the respective aniline was reacted in a diazotization and subsequent azo coupling, as previously described, yielding compounds **101a-c** (**Scheme 12**). After *Boc*-deprotection with TFA, inhibitors **102a-c** were obtained.

Inhibitor **100** showed the same T_m shift as the parent BET inhibitor **22** and for benzamide-based dual inhibitors **102a-c** the ΔT_m was actually slightly increased (**Table 5**). An SAR (structure-activity relationship) investigation with different phenols **100a-g** revealed that most additional substituents were not tolerated and that the original ASN binding group showed the highest stabilization of BRD4 (**Supporting Table S 1**). The cellular binding was measured *via* a NanoBRET target engagement assay. Here, inhibitors **100** and **102a** showed a micromolar EC_{50} for HDAC1 and 2, while substituted analogues **102b** and **102c** bound in the nanomolar range, likely by targeting the previously discussed foot pocket.

Table 5: Merged dual inhibitors

Compounds	DSF ΔT_m (K)[1]		NanoBRET EC_{50} (µM)[2] intact cells			
	BRD4-BD1	BRD4-BD2	BRD4-BD1	BRD4-BD2	HDAC1	HDAC2
MS436 (**22**)	4.0 ± 0.4	2.9 ± 0.1	2.85 ± 0.4	62 ± 15	18.8 ± 1.0	> 50
100	4.1 ± 0.6	3.4 ± 0.1	n.d.	n.d.	31 ± 13	16.2 ± 0.8
102a	5.2 ± 0.3	3.0 ± 0.2	n.d.	n.d.	10.8 ± 5.1	> 50
102b	5.1 ± 0.4	2.4 ± 0.1	n.d.	n.d.	0.17 ± 0.02[3]	0.26[4]
102c	5.1 ± 0.8	3.7 ± 0.4	n.d.	n.d.	0.13 ± 0.02[3]	0.19[4]
106	4.0 ± 0.1	2.0 ± 0.9	n.d.	n.d.	2.1[4]	n.d.
107a	4.2± 0.2	4.8± 0.2	n.d.	n.d.	2.9[4]	n.d.
107b	7.5 ± 0.2	5.2 ± 0.2	0.19 ± 0.03	0.05 ± 0.01	2.1 ± 0.7	1.3 ± 0.9
114a	4.0 ± 0.2	4.8 ± 0.2	0.18 ± 0.03	0.20 ± 0.03	23 ± 11	25 ± 12
114b	4.7 ± 0.2	5.6 ± 0.5	n.d.	n.d.	58[4]	n.d.
119	1.9 ± 0.2	1.9 ± 0.3	2.55 ± 0.08	2.94 ± 0.18	2.3 ± 0.6	3.7 ± 2.4
123a	3.9 ± 0.4	4.5 ± 0.1	0.25 ± 0.02	0.19 ± 0.02	2.6 ± 1.1	1.6 ± 0.7
128	2.0 ± 0.3	4.6 ± 0.3	n.d.	n.d.	n.d.	n.d.
130	3.5 ± 0.2	5.1 ± 0.9	0.30[4]	0.13[4]	17.8 ± 0.7[3]	30.0[4]
(+)-JQ1 (**13**)	6.7 ± 0.1	5.8 ± 0.6	0.06 ± 0.01	0.11 ± 0.01	n.d.	n.d.
CI-944 (**7**)	n.d.	n.d.	n.d.	n.d.	5.0 ± 0.8	2.0 ± 0.7

[1]n=6; [2] Mean and SEM of at least three independent experiments that were themselves performed in technical duplicates. [3]n=2; [4]n=1

When comparing the co-crystal structures of dual inhibitor **102a** with BET inhibitor **22**, a similar but slightly shifted binding mode can be observed (**Figure 26**). In both cases, the phenol binds to the

conserved asparagine residue and the central phenyl moiety is sandwiched between the WPF shelf and a leucine residue.
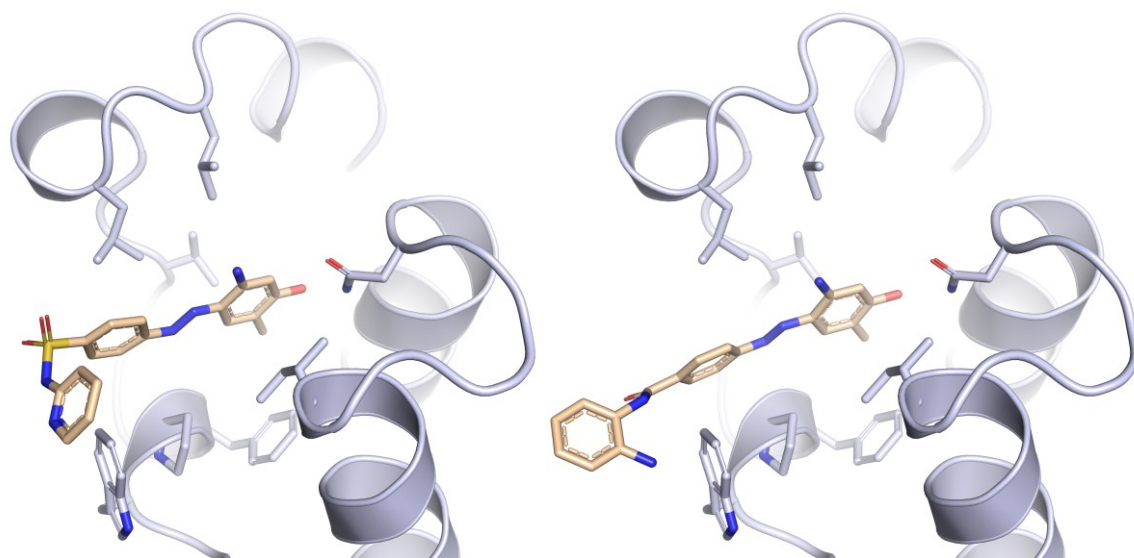
Figure 26: Co-crystal structures of BRD4 BD1 with MS436 (22) (left, PDB: 4NUD) and 102a (right, PDB: 8P9F). The dual inhibitor possesses a similar binding mode to the parent BET inhibitor.

3.3.2 Structure-Guided Optimization of the BET-Binding Moiety and Linker Replacement

In an effort to improve binding to the critical asparagine, the phenol was replaced with a hydroxyindole. For the synthesis, the respective chloro- or methylindole **103a/b** was reacted with pivaloyl (Piv) chloride giving intermediate **104a/b**, which was afterwards borylated with boron tribromide and then hydroxylated using sodium perborate as described by Lv *et al.*[274,275] to provide the respective hydroxyindole **105a/b** (**Scheme 13**). As described before, azo coupling of the respective anilines **98** or **34**, followed by *Boc*-deprotection with TFA, gave hydroxamic acid **106** and inhibitor **107a/b**.
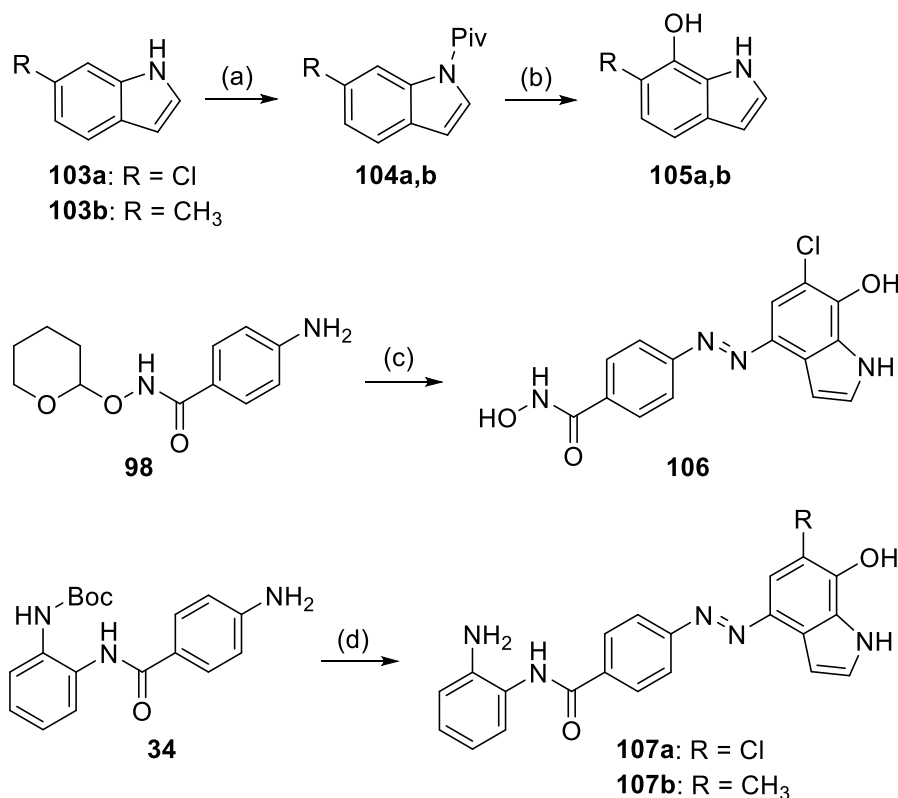
Scheme 13: Synthesis of hydroxyindole-based inhibitors 106 and 107a,b. Reagents and conditions: (a) PivCl, TEA, DMAP, DCM, 0 °C to rt, 16 h; (b) (1) BBr$_3$, DCM, rt, 1 h; (2) K$_2$CO$_3$, sodium perborate, THF/H$_2$O; (c) (1) conc. HCl, isoamyl nitrite, MeOH/ACN, -10 °C, 1 h; (2) **105a**, K$_2$CO$_3$, MeOH/H$_2$O/ACN, -10 °C to rt, 2 h; (3) TFA/DCM, rt, 1 h; (d) (1) conc. HCl, isoamyl nitrite, MeOH/ACN, -10 °C, 1 h; (2) **105a** or **b**, K$_2$CO$_3$, MeOH/H$_2$O/ACN, -10 °C to rt, 2 h; (3) TFA/DCM, rt, 1 h.

While inhibitor **106** had a similar thermal shift to phenol **100**, the introduction of the hydroxyindole moiety showed a significant improvement for inhibitor **107b** (7.5 K *vs.* 5.2 K for **102a**, **Table 5**). By substituting a chloride for the methyl substituent, as in compound **107a**, the ΔT_m was impaired (4.2 K). It should be noted that all thermal shifts for the azo compounds should be evaluated carefully, since their red color might interfere with the DSF assay. Interestingly, the hydroxyindole-based inhibitors also showed improved cellular binding to HDAC1 (EC$_{50} \approx 2$ µM).

In the next step, the azo-moiety was replaced, while at the same time substituting the 7-hydroxyindole moiety with the more stable pyrrolopyridone. This also facilitated compound synthesis. To test, which linking moiety would be accepted, different scaffolds were synthesized. First, quinoline **108** was oxidized to the *N*-oxide **109** with *meta*-chloroperoxybenzoic acid (*m*CPBA) (**Scheme 14**). Reaction with mesyl chloride and water then provided 2-hydroxyquinoline **110** which was afterwards chlorinated to intermediate **111**. After Suzuki coupling with boronate **56**, compound **112** was received. Basic hydrolysis provided carboxylic acid **113** which was then coupled to the respective amine, providing inhibitor **114a/b**.
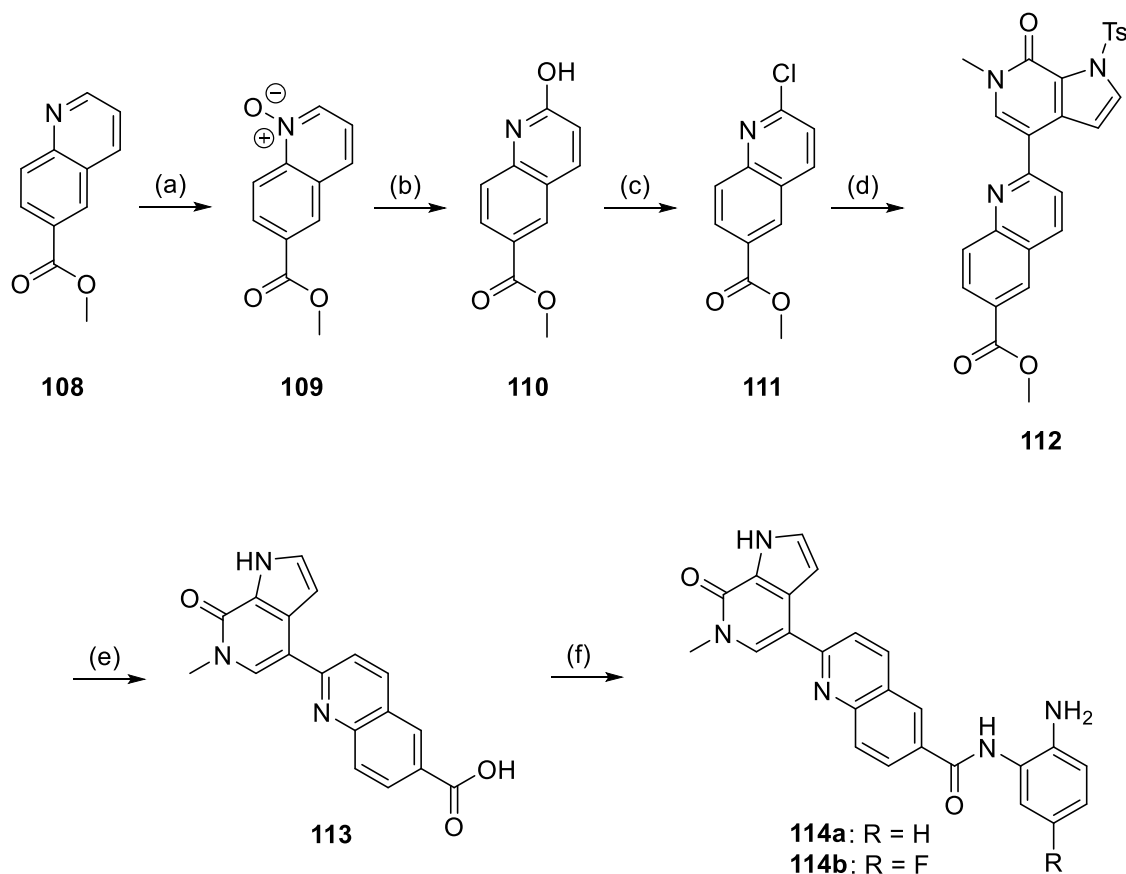
Scheme 14: Synthesis of inhibitors 114a and b. Reagents and conditions: (a) *m*CPBA, DCM, 0 C to rt, 3 h; (b) MsCl, H_2O/ACN, rt, 45 min; (c) SOCl$_2$, DMF, DCM, 0°C to rt, 16 h; (d) **56**, K$_3$PO$_4$, Pd XPhos G2, XPhos, dioxane/H_2O, 70 °C, 1 h; (e) LiOH · H_2O, dioxane/H_2O, 80°C, 2 h; (f) (1) **32** or 4-fluorobenzene-1,2-diamine, PyAOP, DIPEA, DMF, rt, 16 h; (2) TFA/DCM, rt, 1 h.

The quinoline-based inhibitors had a similar thermal shift to the initial compounds and **114a** had a cellular EC_{50} for BRD4 BD1 of 180 nM (**Table 5**). In the co-crystal structures of BRD4 with azobenzene **107b** and quinoline **114a**, a similar binding mode can be observed (**Figure 27**). Both scaffolds employ a bivalent interaction to the catalytic asparagine residue which likely improves their potency. The introduction of the central quinoline moiety seems to impair binding to HDAC1, however, with a tenfold decrease for inhibitor **114a**, compared to compound **107b**.
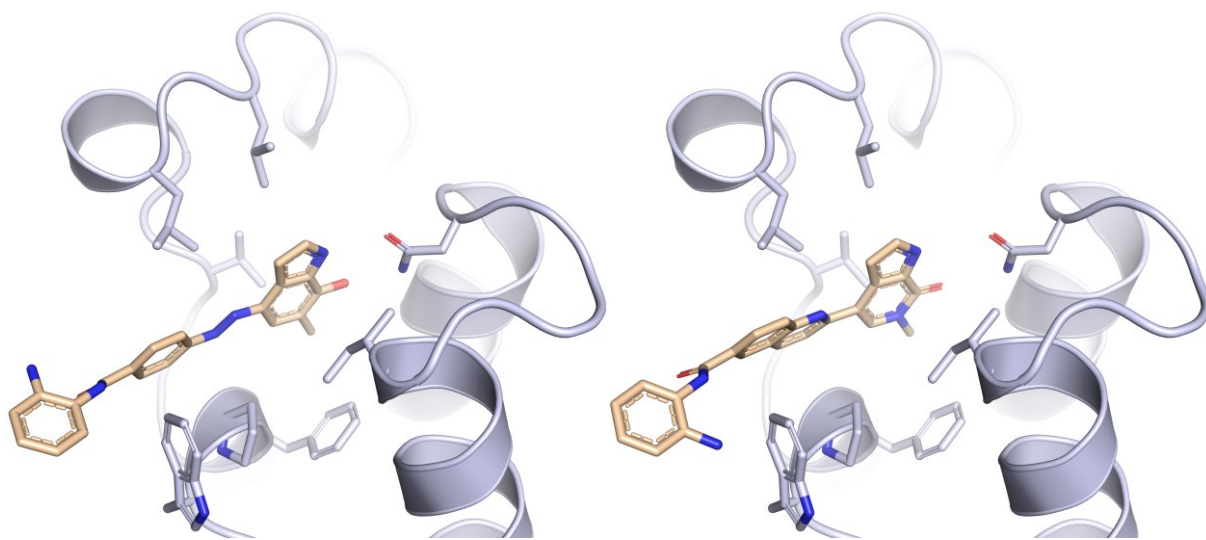
Figure 27: Co-crystal structure of BRD BD1 with 107b (left, PDB: 8P9G) and 114a (right, 8P9H). Both ligands employ a bivalent interaction to the catalytic asparagine. Inhibitor **114a** binds similar to azobenzene **107b**.

For the next derivative, transmetallation of compound **55** with isopropyl magnesium chloride, followed by reaction with dry ice, provided carboxylic acid **115** and after basic detosylation, intermediate **116** was obtained (**Figure 15**). The intermediate was first converted to the acyl chloride and then reacted with methyl 4-aminobenzoate to provide compound **117**. Saponification gave carboxylic acid **118**, which was afterwards coupled to phenylenediamine to give inhibitor **119**.
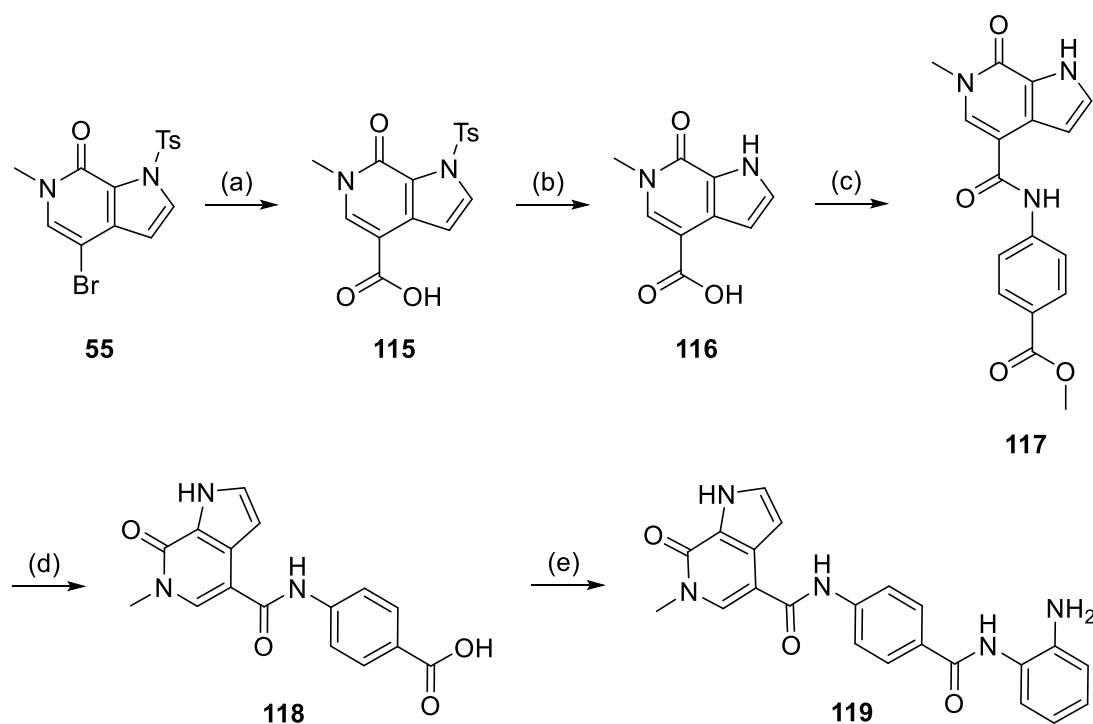
Scheme 15: Synthesis of inhibitor 119. Reagents and conditions: (a) (1) *i*PrMgCl · LiCl, THF, -40 C, 2 h; (2) CO₂ (s), 0.5 h; (b) LiOH · H₂O, dioxane/H₂O, 90 C, 1 h; (c) (1) SOCl₂, dioxane, 80 C, 16 h; (2) methyl 4-aminobenzoate, DIPEA, DMA, rt, 1 h; (d) LiOH · H₂O, THF/MeOH/H₂O, 60 °C, 1 h; (e) *o*-phenylenediamine, PyAOP, DIPEA, DMF, rt, 16 h.

In cells, the amide-based inhibitor showed good potency for binding to HDAC1/2 but lost most of its potency for binding to BRD4 (**Table 5**).

For another approach, the HDAC-binding moiety was directly connected to the pyrrolopyridone scaffold. Suzuki coupling of the respective halobenzene **120a-f** with boronate **56** provided methyl esters **121a-f** (**Scheme 16**). Saponification gave carboxylic acids **122a-f** and after subsequent amide coupling, inhibitors **123a-f** were obtained.

123a: X=CH, Y=CH, R=H
123b: X=CH, Y=CH, R=NH$_2$
123c: X=CH, Y=CH, R=OMe
123d: X=N, Y=CH, R=H
123e: X=N, Y=N, R=H
123f: X=CH, Y=N, R=H
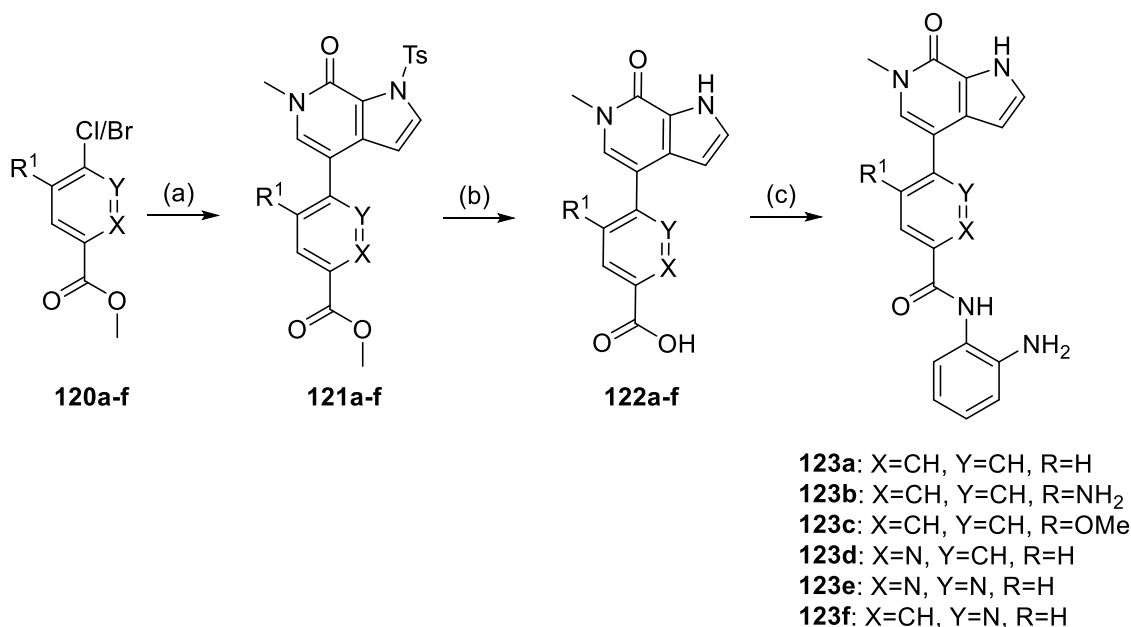
Scheme 16: Synthesis of inhibitors 123a-f. Reagents and conditions: (a) **56**, K$_3$PO$_4$, Pd XPhos G2, XPhos, dioxane/H$_2$O, 70 C, 1 h; (b) LiOH · H$_2$O, dioxane/H$_2$O, 80 C, 2 h; (c) *o*-phenylenediamine, PyAOP, DIPEA, DMF, rt, 16 h.

Compared to inhibitors **114a** and **119**, compound **123a** showed the best balance between binding BRD4 and HDAC 1/2. In the cellular NanoBRET assay, the dual inhibitor bound to BRD4 in the nanomolar and to HDAC1 and 2 in the low micromolar range (**Table 5**).

To test the effects of an ethylamide substituent, additional analogues were synthesized. First, ethyl ester **83** was reacted with magnesium methoxide and ethylamine to provide ethylamide **124** (**Scheme 17A**). After Miyaura borylation, boronate **125** was obtained. Suzuki coupling of chloroquinoline **111** with boronate **125** then gave intermediate **126** (**Scheme 17B**). Saponification yielded carboxylic acid **127** and subsequent amide coupling provided inhibitor **128**. Coupling of chloropicolinate **120d** with boronate and subsequent saponification gave carboxylic acid (**Scheme 17C**). After reaction with phenylenediamine, inhibitor **130** was obtained.
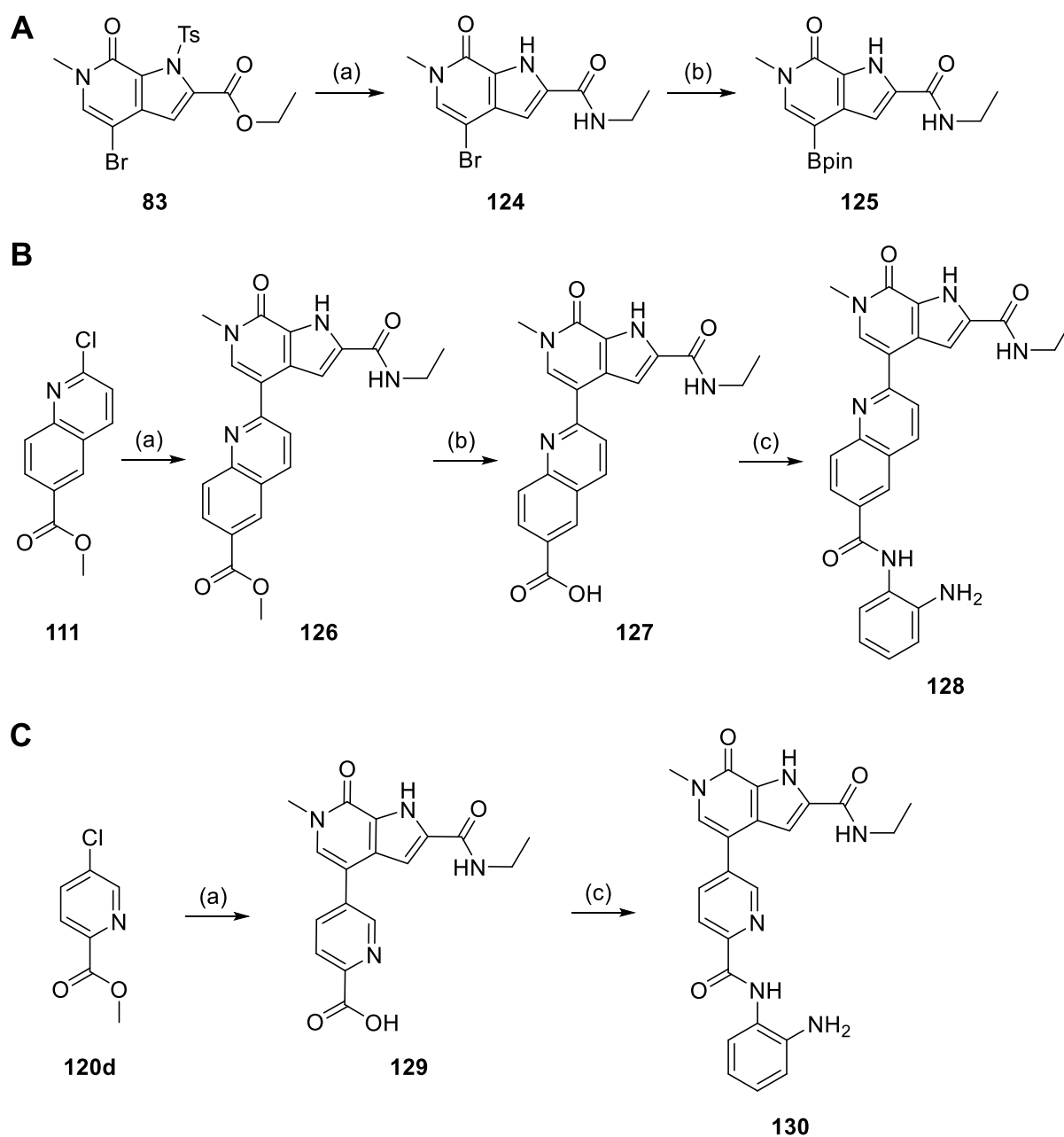
Scheme 17: (A) Synthesis of boronate 125. Reagents and conditions: (a) ethylamine, Mg(OMe)$_2$, THF/MeOH, 55 °C, 16 h; (b) B$_2$pin$_2$, potassium ethyl hexanoate, Pd XPhos G2, XPhos, MeTHF, 55 °C, 16 h. **(B) Synthesis of inhibitor 128.** Reagents and conditions: (a) **125**, K$_3$PO$_4$, Pd XPhos G2, XPhos, dioxane/H$_2$O, 60 °C, 2 h; (b) LiOH · H$_2$O, dioxane/MeOH/H$_2$O, rt, 16 h; (c) o-phenylenediamine, PyAOP, DIPEA, DMF, rt, 16 h. **(C) Synthesis of inhibitor 130.** Reagents and conditions: (a) (1) **125**, K$_3$PO$_4$, Pd XPhos G2, XPhos, dioxane/H$_2$O, 75 °C, 90 min; (2) LiOH · H$_2$O, rt, 1 h; (b) o-phenylenediamine, PyAOP, DIPEA, DMF, rt, 16 h.

As expected, inhibitors **128** and **130**, showed a slight preference for the second bromodomain of BRD4 (**Table 5**), but both compounds exhibited really low solubility, likely due to strong intermolecular hydrogen bonding of the substituted pyrrolopyridone scaffold.

The SAR of compound **123a** was further explored, testing the effect of additional substituents or heteroatoms in the central aromatic ring (**Table 6**). Replacing the phenyl group by a pyridine moiety in inhibitor **123d** resulted in almost identical binding to BRD4, while slightly attenuating HDAC binding. Adding exocyclic substituents, as in compounds **123b** and **123c**, drastically impaired both BET and HDAC binding in cells. Also, the position of the endocyclic nitrogen appears to be critical because nicotinamide-containing **123e** and pyridazine-containing **123f** showed an about two-fold reduced binding affinity to BRD4 compared with inhibitor **123d**.

Table 6: Modification of the central ring
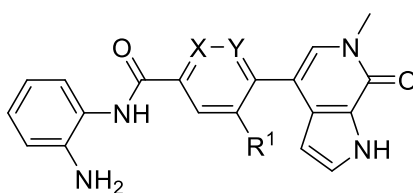
Compounds	X	Y	R^1	DSF ΔT_m (K)[1]		NanoBRET EC_{50} (µM) intact cells[2]			
				BRD4-BD1	BRD4-BD2	BRD4-BD1	BRD4-BD2	HDAC1	HDAC2
123a	CH	CH	H	3.9 ± 0.4	4.5 ± 0.1	0.25 ± 0.02	0.19 ± 0.02	2.6 ± 1.1	1.55 ± 0.73
123b	CH	CH	NH_2	0.9 ± 0.2	1.7 ± 0.3	3.7 ± 0.5	2.05 ± 0.37	34.4 ± 5.8	39.7 ± 9.0
123c	CH	CH	OMe	3.8 ± 0.1	4.3 ± 0.3	0.39 ± 0.06	0.23 ± 0.07	> 50	> 50
123d	N	CH	H	4.2 ± 0.4	4.7 ± 0.4	0.24 ± 0.02	0.16 ± 0.04	4.8 ± 2.3	2.48 ± 0.66
123e	CH	N	H	2.9 ± 0.3	3.6 ± 0.2	0.39 ± 0.02	0.29 ± 0.12	16.8 ± 6.7	4.56 ± 0.57
123f	N	N	H	2.6 ± 0.0	3.4 ± 0.2	0.48 ± 0.14	0.32 ± 0.13	6.1 ± 1.0	3.09 ± 0.13
(+)-JQ1 (**13**)	-	-	-	6.7 ± 0.1	5.8 ± 0.6	0.06 ± 0.01	0.11 ± 0.01	n.d.	n.d.
CI-944 (**7**)	-	-	-	n.d.	n.d.	n.d.	n.d.	5.0 ± 0.8	2.0 ± 0.7

[1]Mean and SEM of three independent repeats performed in technical triplicates.
[2] Mean and SEM of at least three independent experiments that were themselves performed in technical duplicates.

3.3.3 Optimization of the HDAC-Binding Moiety

In an effort to target the foot pocket of HDAC1 and 2 and further improve binding, additional aromatic substituents were introduced to the inhibitors. By reacting the carboxylic acids **122a** or **122d** with anilines **26a,b** or **d**, compounds **131a-d** were generated (**Scheme 18**). After deprotection with TFA, inhibitors **132a-d** could be obtained.

122a: X=CH
122d: X=N

131a: X=CH, R=phenyl
131b: X=N, R=phenyl
131c: X=N, R=2-furyl
131d: X=N, R=2-thienyl

132a: X=CH, R=phenyl
132b: X=N, R=phenyl
132c: X=N, R=2-furyl
132d: X=N, R=2-thienyl
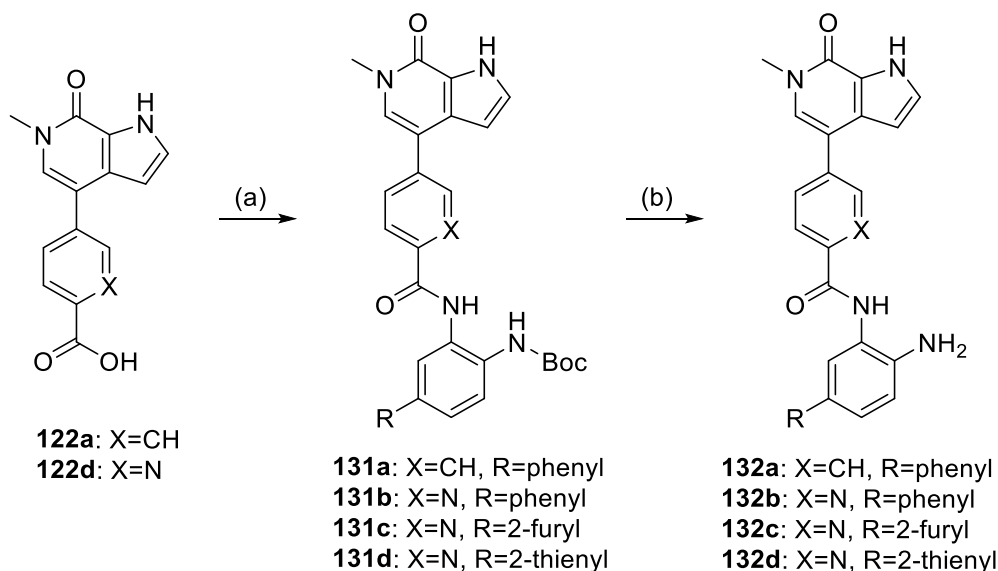
Scheme 18: Synthesis of substituted inhibitors 132a-d. Reagents and conditions: (a) **26a,b,d**, PyAOP, DIPEA, DMF, rt, 16 h; (b) TFA/DCM, rt, 1 h.

Through reacting carboxylic acid **122d** with 4-fluorobenzene-1,2-diamine, compound **133** was obtained, serving as a negative control for HDAC1/2 inhibition (**Scheme 19**).

122d

133
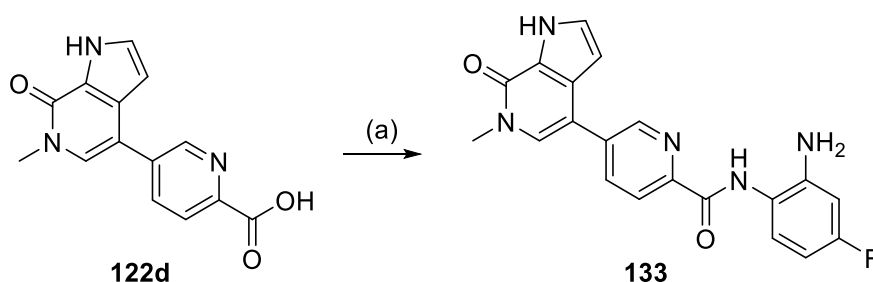
Scheme 19: Synthesis of inhibitor 133. Reagents and conditions: (a) 4-fluorobenzene-1,2-diamine, PyAOP, DIPEA, DMF, rt, 16 h.

By introducing a phenyl or 2-thienyl moiety, the cellular affinity for HDAC1 and 2 could be significantly improved, resulting in nanomolar EC_{50} values (**Table 7**, **Figure 29B**), with phenyl-substituted **132b** showing the strongest binding to HDAC1 (EC_{50} = 110 nM) and thienyl-substituted **132d** the strongest binding to HDAC2 (EC_{50} = 60 nM), while only weakly binding to HDAC3 (**Supporting Figure S 1**). Binding to BRD4 did not significantly change through the addition of an additional substituent. This was consistent with the co-crystal structure of BRD4 with **132b**, which shows that the phenyl group of the HDAC warhead protrudes into the solvent, only weakly interacting with a tryptophan residue (**Figure**

28). As expected based on the literature,[276] 4-fluorination led to a decreased HDAC1/2 binding affinity in the case of compound **133**.

Table 7: Optimization of the HDAC warhead
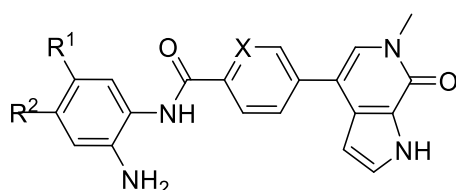
Compounds	X	R[1]	R[2]	NanoBRET EC$_{50}$ (µM) intact cells[1]				
				BRD4-BD1	BRD4-BD2	HDAC1	HDAC2	HDAC3
123a	CH	H	H	0.25 ± 0.02	0.19 ± 0.02	2.6 ± 1.1	1.55 ± 0.73	32 ± 16
123d	N	H	H	0.24 ± 0.02	0.16 ± 0.04	4.8 ± 2.2	2.48 ± 0.66	> 50
132a	CH	phenyl	H	0.42 ± 0.11	0.52 ± 0.18	0.19 ± 0.03	0.36 ± 0.12	6.5 ± 2.8
132b	N	phenyl	H	0.36 ± 0.13	0.25 ± 0.12	0.11 ± 0.03	0.10 ± 0.02	13.6 ± 4.8
132c	N	2-furyl	H	0.37 ± 0.05	0.31 ± 0.05	1.32 ± 0.98	2.9 ± 1.7	n.d.
132d	N	2-thienyl	H	0.29 ± 0.05	0.18 ± 0.04	0.14 ± 0.05	0.06 ± 0.01	11.4 ± 6.9
133	CH	H	F	0.34 ± 0.10	0.10 ± 0.01	36 ± 12	14.2 ± 4.5	> 50
CI-944 (**7**)	-	-	-	n.d.	n.d.	5.0 ± 0.8	2.0 ± 0.7	11.1 ± 6.2

[1] Mean and SEM of at least three independent experiments performed in technical duplicates.
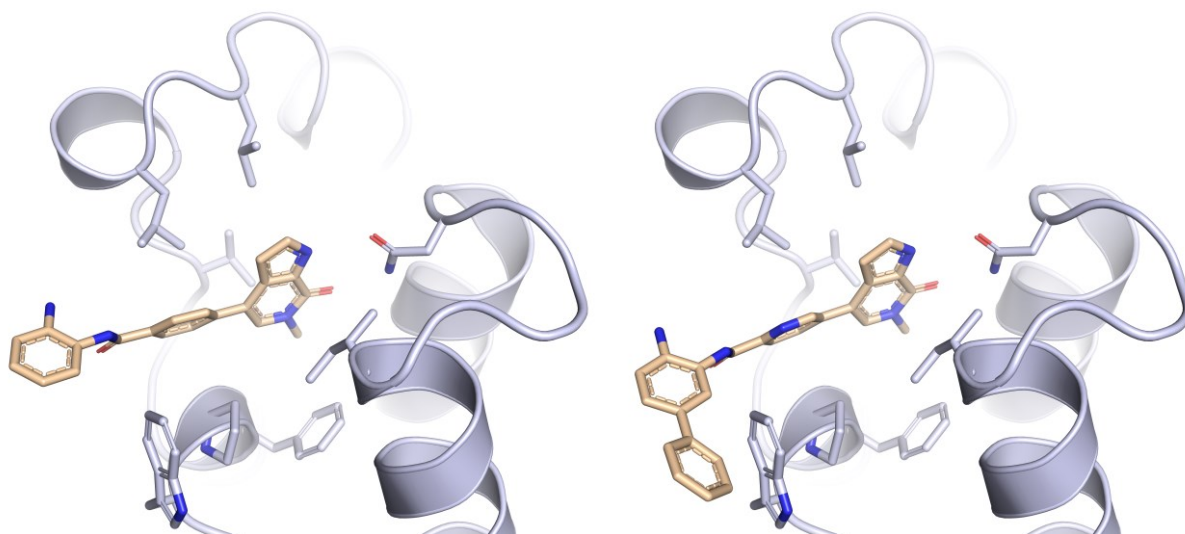
Figure 28: Co-crystal structure of BRD4 BD1 with 123a (left, PDB: 8P9I) and 132b (right, PDB: 8P9L).

For inhibitor **132b**, an inhibition assay for HDAC1-11 was performed by Reaction Biology. The data was consistent with the NanoBRET data and showed high selectivity for HDAC1 and 2 (**Figure 29D** and **Supporting Table S 5**). At a concentration of 1 µM, only HDAC1 and 2 were significantly inhibited, with a residual activity of 20.5% and 50.3%, respectively. When measuring a DSF selectivity panel against 32 bromodomains, inhibitor **132a** proved to be highly selective for the BET family (**Figure 29A**). While inhibitor **123a** still showed binding to BRD7 and 9, this off-target activity was, interestingly, removed through addition of the additional substituent in compound **132a** (**Supporting Table S 6**).
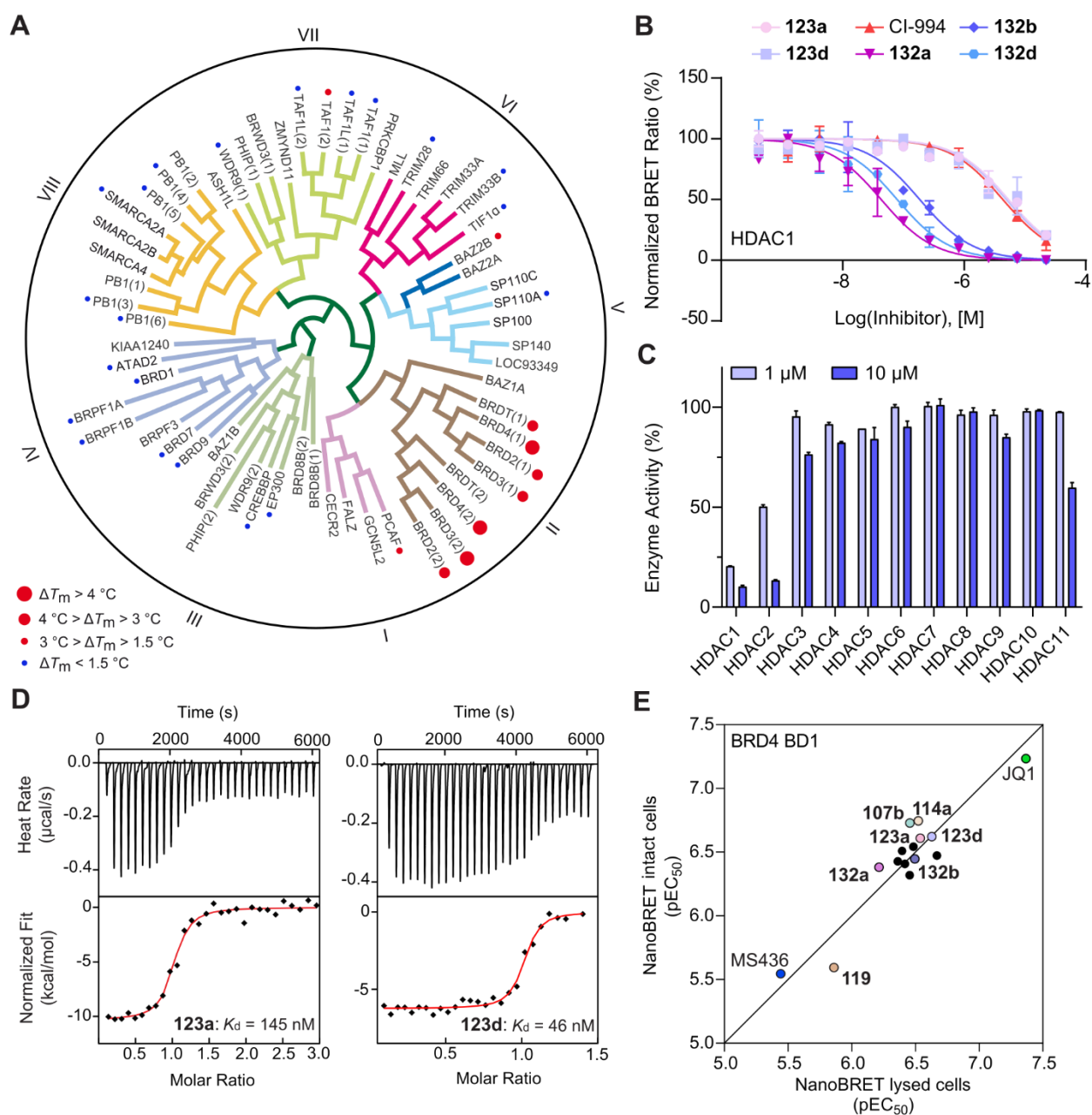
Figure 29: Biophysical data of the dual inhibitors. (A) DSF bromodomain selectivity panel for inhibitor **132a** measured at a compound concentration of 10 µM showing high selectivity for the BET family domains. (B) NanoBRET data for inhibitor binding to HDAC1 measured in intact cells. (C) Zinc-dependent HDACs selectivity panel. Residual enzyme activity of HDAC1-11 after inhibition with different concentrations of **132b** compared with the uninhibited control reaction, showing high selectivity for HDAC1/2. Experiments were performed by Reaction Biology. Mean of duplicate measurements. (D) ITC data of **123a** and **123b** binding to BRD4 BD1. (E) Correlation of NanoBRET data for inhibitor binding to BRD4-BD1 in intact *vs.* lysed cells. The pEC_{50} is defined as the negative logarithm of the EC_{50}.[277]

ITC experiments showed a binding affinity to BRD4 BD1 of 145 nM for inhibitor **123a** and 46 nM for inhibitor **123d** (**Figure 29 D** and **Supporting Table S 4**). The additional aromatic substituent of inhibitors **132a-d** reduced their solubility and for this reason, ITC could not be measured for those compounds. For BRD4, NanoBRET data for lysed and intact cells showed a good correlation for the tested compounds, not differing by more than a factor of two, suggesting good cell permeability (**Figure 29 E** and **Supporting Table S 2**). For HDAC1 and 2, compounds were up to 5 times more potent in lysed

mode, with inhibitor **132b** showing an EC_{50} value of 27 nM (**Supporting Table S 3**). This might be attributed to HDAC1/2 being localized in the nucleus, whereas the isolated BRD4 bromodomains are expected to be found in the cytosol.

3.3.4   Biological Evaluation

The dual inhibitors were tested for their HDAC activity in pancreatic cancer cells by Western blot (WB) (**Figure 30A**). Most potent in inhibiting histone deacetylation were substituted inhibitors **132a**-**d**, showing similar results to reference compound **9**. Interestingly, inhibitor **123a** also caused high acetylation levels and appeared to be more potent than parent HDAC inhibitor **7**. A concentration-dependent effect could be shown for compounds **132a** and **132b** (**Figure 30B**), with inhibitor **132b** appearing slightly more potent, consistent with its EC_{50} values in the NanoBRET assay.

To assess the effect of BET inhibition, we analyzed the mRNA levels of *HEXIM1* and *p57* by quantitative RT-PCR (**Figure 30C**). All dual inhibitors showed an increase in expression levels, with inhibitors **132a**-**d** again showing the strongest effect. Next, expression levels of the transcription factors *MYC* and *TP63* in NMC HCC2429 cells were tested (**Figure 30D**). Both are oncogenes which are upregulated in NMC through the formation of hyperacetylated megadomains.[278] All tested dual inhibitors caused a significant decrease in mRNA levels and were potent than the parent BET inhibitor **22**, which correlates nicely with the BRD4 binding data.

The biological effect of the dual inhibitors was tested in pancreatic Patu8988T cells as well as NMC HCC2429 cells (**Figure 30E** and **Supporting Table S 7**). In PatuT cells, the combination of starting scaffolds **7** and **22** showed a synergistic effect at reducing cell viability. Intriguingly, the tested dual inhibitors were even more potent at reducing viability of the pancreatic cancer cells, having IC_{50} values in the low micromolar range. Interestingly, all inhibitors were more potent in reducing the viability of HCC2429 cells. No synergism could be observed for the combination of compounds **7** and **20** in the NMC cell line, which appears to be particularly sensitive to BET inhibition. The synthesized dual inhibitors were, however, still the most potent of the tested compounds.
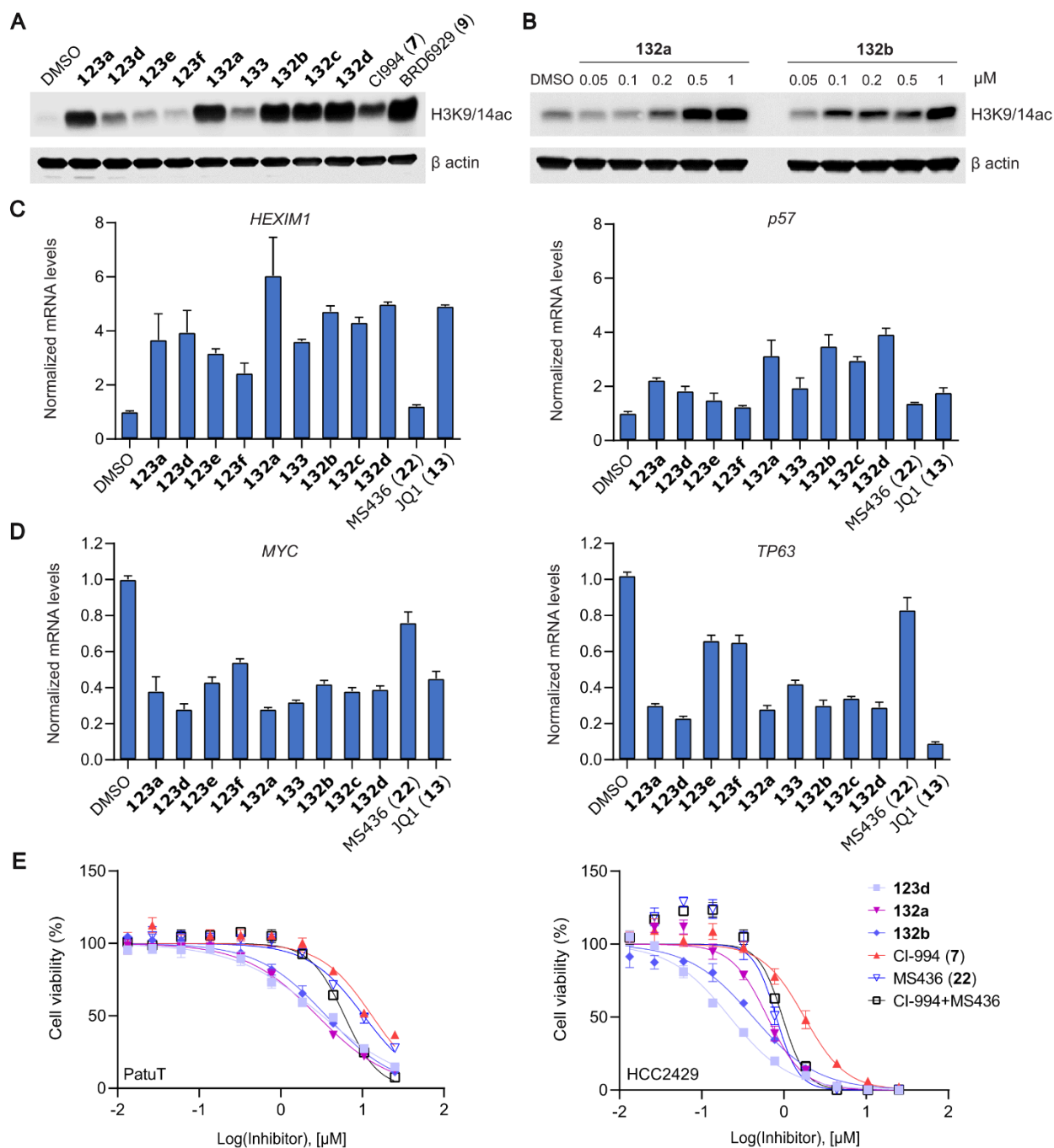
Figure 30: Biological effects of the optimized dual BET/HDAC inhibitors. (A) Effect on histone H3 K9/K14 acetylation in Patu8988T cells 48 h after incubation with 1 µM compound monitored by Western blot. (B) WB showing the concentration-dependent inhibition of histone H3 K9/K14 deacetylation in Patu8988T cells 48 h after treatment with **132a** and **132b**. (C) Upregulation of mRNA levels of BET-inhibition biomarkers *HEXIM1* and *p57* in Patu8988T cells 6 h after treatment with 1 µM compound. (D) mRNA levels of oncogenic drivers *MYC* and *TP63* in NMC cells 6 h after treatment with 1 µM compound, showing that the optimized dual inhibitors significantly downregulated both transcription factors. (E) Cell viability of pancreatic cancer cell line PatuT (left) and NMC cell line HCC2429 (right) after 3d-treatment with different concentrations of inhibitors.[277]

The most promising inhibitor, **132b**, was further evaluated in a pharmacokinetics (PK) study (**Figure 31** and **Supporting Table S 8**). After oral (po), intravenous (iv) or intraperitoneal (ip) administration, plasma samples were taken from the treated mice to determine the plasma concentration of the administered compound. The observed area under the curve (AUC), indicative of total drug exposure, was highest for intraperitoneal injection (4807 ng·h/mL), followed by oral (3168 ng·h/mL) and intravenous administration (917 ng·h/mL) (**Supporting Table S 9**). Unfortunately, the tested inhibitor exhibited a rather short half-life of 1.4 h (ip) up to 6.1 h (po).
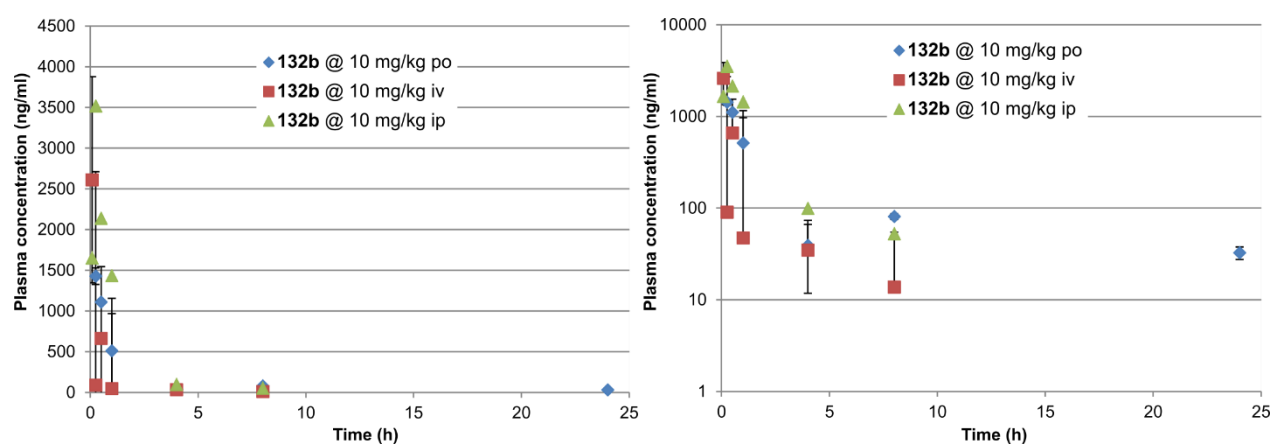
Figure 31: PK study results for inhibitor 132b. For each administration, 6 mice were treated with 10 mg/kg of inhibitor **132b**. po: oral administration; iv: intravenous administration; ip: intraperitoneal administration. Samples were taken from the retrobulbar venous plexus. The study was performed by Pharmacelsus.

The optimized dual inhibitors could achieve satisfying binding affinities for BRD4 and HDAC1/2 and good cell permeability, which also translated into promising biological effects in pancreatic cancer cells. Some compound properties were, however, still leaving room for improvement. The developed compounds did not exhibit great solubility, likely owing to a large percentage of aromatic moieties. Pharmacokinetic investigation further suggested suboptimal metabolic stability and high clearance in the treated mice. Those results did therefore not encourage further *in vivo* studies without additional optimization of the inhibitors. Since the inhibitors already show good binding affinities, a promising strategy might be the application of bioisosteres to improve the pharmacokinetic characteristics.

3.3.5 Bioisosteric Replacement

Introduced by Philip E. Eaton,[279–281] the cubane scaffold was suggested as a bioisostere of the phenyl ring, due to having virtually identical dimensions, apart from the obvious non-planarity. Reflecting its attractiveness as a potential replacement for the phenyl moiety, cubanes have often been used in medicinal chemistry.[282–286] Additionally, indicative of its interesting chemical properties, a lot of research about cubane synthesis has been published in recent years, focusing on more efficient synthesis or novel functionalization of the cubane scaffold.[287–303]

It was hypothesized that a replacement of the central phenyl moiety in the developed dual BET/HDAC inhibitors with a cubane might improve their metabolic stability and possibly also their solubility by preventing excessive π-π-stacking between molecules. Docking of the cubane analogue with BRD4 gave promising results by suggesting enough space in the binding site and similar binding affinity to the phenyl-based inhibitor (**Figure 32**).
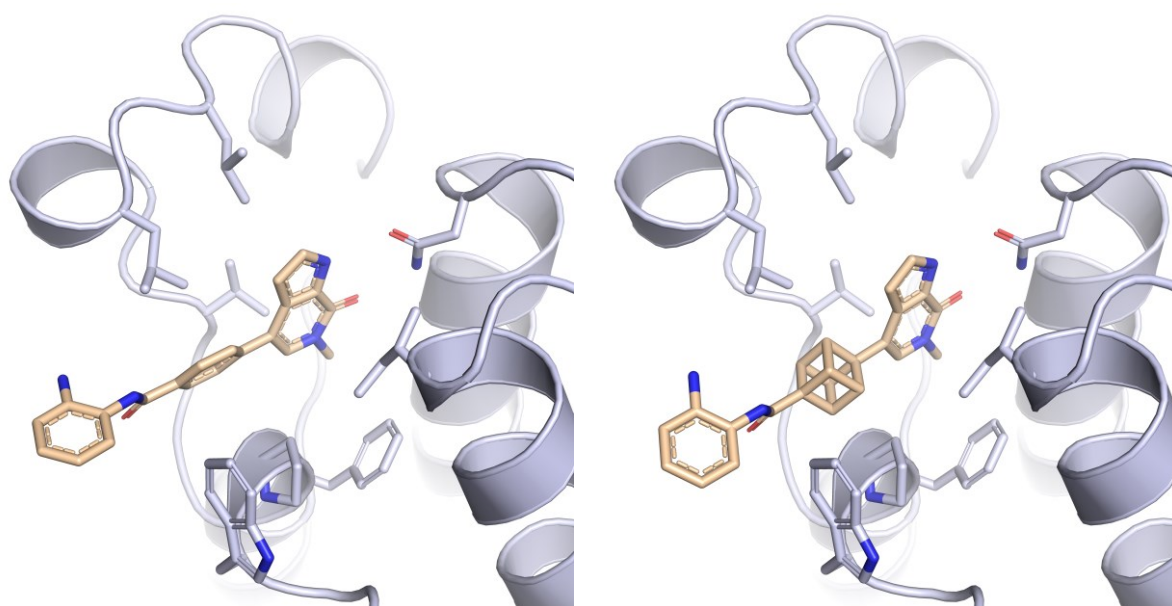
Figure 32: Comparison of phenyl- and cubane-containing inhibitors. Co-crystal structure of BRD4 BD1 with **123a** (left) and model of the cubane-containing inhibitor with BRD4 BD1 (right). Docking was performed using SeeSAR.

The synthesis of the cubane scaffold was adapted from a published procedure.[295] Initially, cyclopentanone **134** was protected with ethylene glycol, providing ketal **135** (**Scheme 20**). Bromination gave intermediate **136**, which was directly reacted with sodium hydroxide in methanol without previous isolation. Elimination gave diene **137**, which spontaneously underwent Diels-Alder reaction, yielding compound **138**. Deprotection in concentrated sulfuric acid provided diketone **139**. Next, the most critical step in the synthesis was the photocyclization of compound **139**. Unfortunately, no suitable photoreactor was available, which needed to produce emission in the region of 300 to 350 nm. Additionally, diketone **139** was produced on a scale of approximately 100 g, requiring high light

intensity or excessive reaction times from common laboratory light sources to achieve full conversion. Since UV light was necessary for the cyclization, it was speculated that exposing the reaction mixture to sunlight should also yield the desired product. Intriguingly, after simply leaving the reaction mixture outside, monitoring by ^{1}H NMR indicated full conversion without showing significant side reactions after about 3 weeks. This reaction could successfully and reproducibly be carried out on a 20 g scale to provide cyclized intermediate **140**. Subsequent Favorskii rearrangement through reflux in aqueous sodium hydroxide solution, followed by acidification, finally yielded cubanedicarboxylic acid **141**.
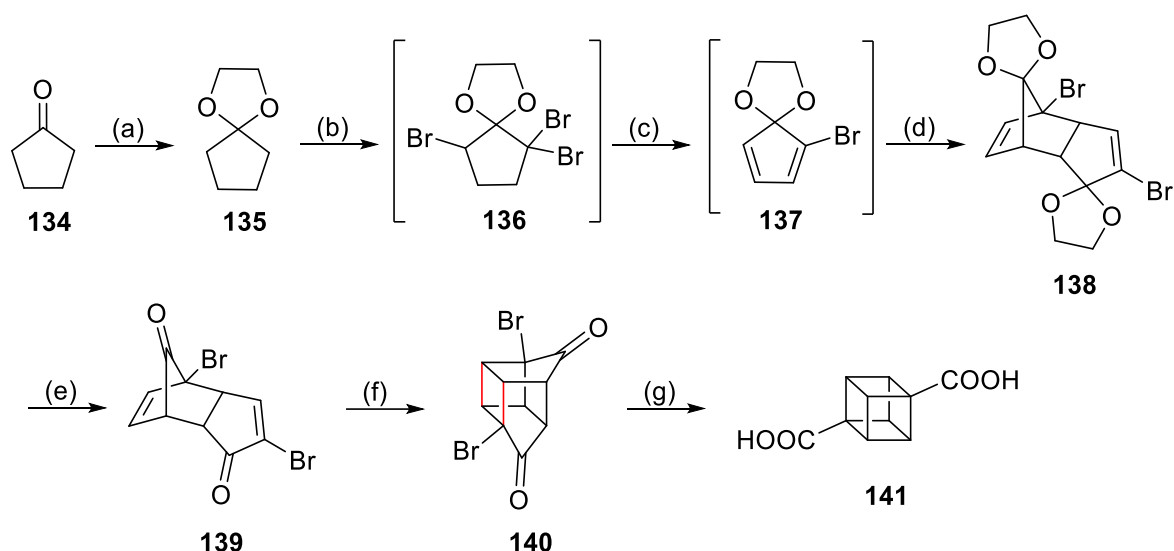
Scheme 20: Synthesis of cubane-1,4-dicarboxylic acid (141). Reagents and conditions: (a) ethylene glycol, DOWEX 50W X8, benzene, reflux, 2 d; (b) Br$_2$, dioxane, 0 °C to rt, 16 h; (c) NaOH, MeOH, 0 °C to reflux, 16 h; (d) *in situ*; (e) conc. H$_2$SO$_4$, rt, 30 h; (f) hv (sunlight), cat. H$_2$SO$_4$, H$_2$O/MeOH, 21 d, the newly formed bonds are highlighted in red; (g) (1) NaOH, H$_2$O, reflux, 3 h; (2) aq. HCl.

Since traditional Pd-catalyzed cross-coupling reactions have not been reported to be successful for the cubane scaffold, possibly due to isomerization,[304–306] arylation of compound **141** was not straightforward. In 2016, the Baran group published the Fe-catalysed C-C coupling of a redox-active ester of cubane, but a rather limited scope was demonstrated.[307] Recently, the MacMillan group reported the Cu-photoredox-catalyzed arylation, amination and alkylation of cubanes, employing redox-active esters, as well.[293] To synthesize the redox-active ester of cubane, at first, dicarboxylic acid **141** was esterified, providing dimethylester **142** (**Scheme 21**). Through saponification, monomethylester **143** was accessible, which could afterwards be coupled to tetrachlorophthalimide to yield redox-active ester **144**.
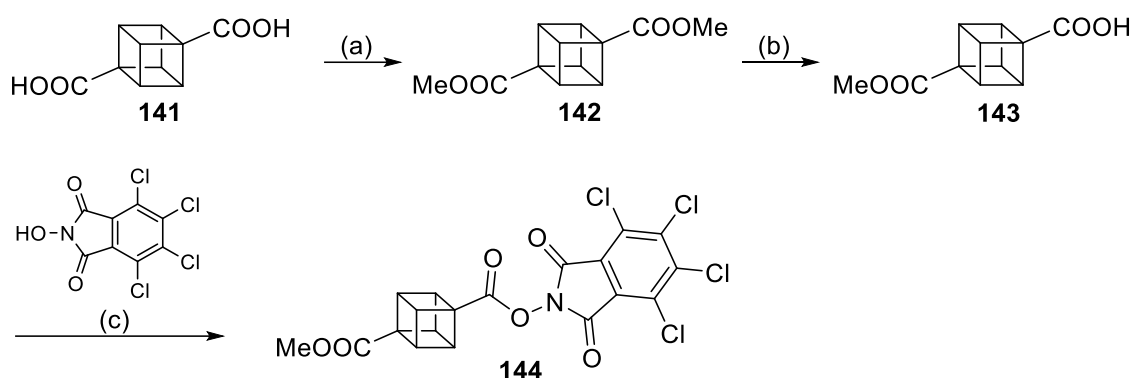
Scheme 21: Synthesis of redox-active ester 144. Reagents and conditions: (a) DOWEX 50W X8, MeOH, reflux, 18 h; (b) (1) NaOH, MeOH/THF, rt, 16 h; (2) aq. HCl; (c) EDC · HCl, DIPEA, DMAP, DCM, rt, 16 h.

Similar to other coupling reactions from the MacMillan group,[308,309] the proposed reaction mechanism utilized silyl radicals. For this, the appropriate aminosilane had to be synthesized by subsequently reacting supersilane **145** with triflic acid and *tert*-butylmethylamine, providing compound **146** (**Scheme 22A**). Using an Ir photocatalyst and different sources of blue light, the coupling of ester **144** with aryl bromide **55** was attempted. Unfortunately, none of the tested conditions could provide the desired product **147**, possibly due to not using a light source with the exactly right emission wavelength or intensity. Usually, only degradation of the starting material **144** was observed.
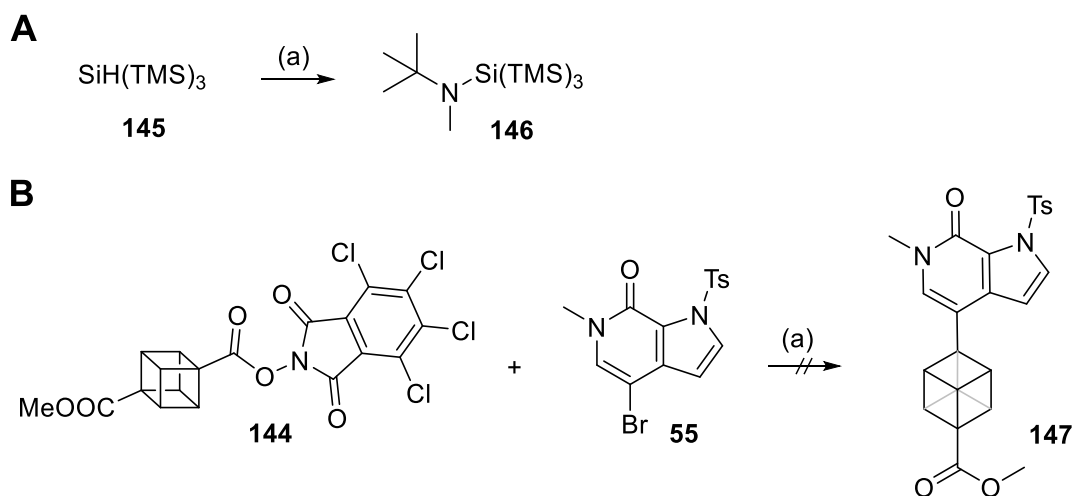
Scheme 22: (A) Synthesis of aminosilane 146. Reagents and conditions: (a) (1) CF$_3$SO$_3$H, DCM, 0 °C to rt, 1 h; (2) *t*BuMeNH, DIPEA, 0 °C to rt, 16 h; **(B) Attempted arylation of cubane 144 through copper-mediated cross-coupling.** Reagents and conditions: (a) *t*BuMeNSi(TMS)$_3$ (**146**), NaOAc, [Ir(dFCF$_3$bpy)$_2$(4,4'-d(CF$_3$)bpy)]PF$_6$, Cu(acac)$_2$, hv (blue light), acetone, rt, 2 h.

Further developing the Baran-type coupling, Bernhard *et al*. published the Ni-catalyzed arylation of cubane.[292] To test the published coupling conditions, aryl bromide was metallated with isopropylmagnesium chloride, followed by transmetallation, to provide the organozinc intermediate **148** (**Scheme 23**). Reaction with cubane **144** under nickel catalysis could successfully produce a small amount of compound **147**, as indicated by HPLC-MS. Saponification yielded carboxylic acid **149**, which

after coupling to phenylene diamine gave intermediate **150**. Detosylation, followed by purification *via* preparative HPLC, finally provided cubane-based inhibitor **151**.
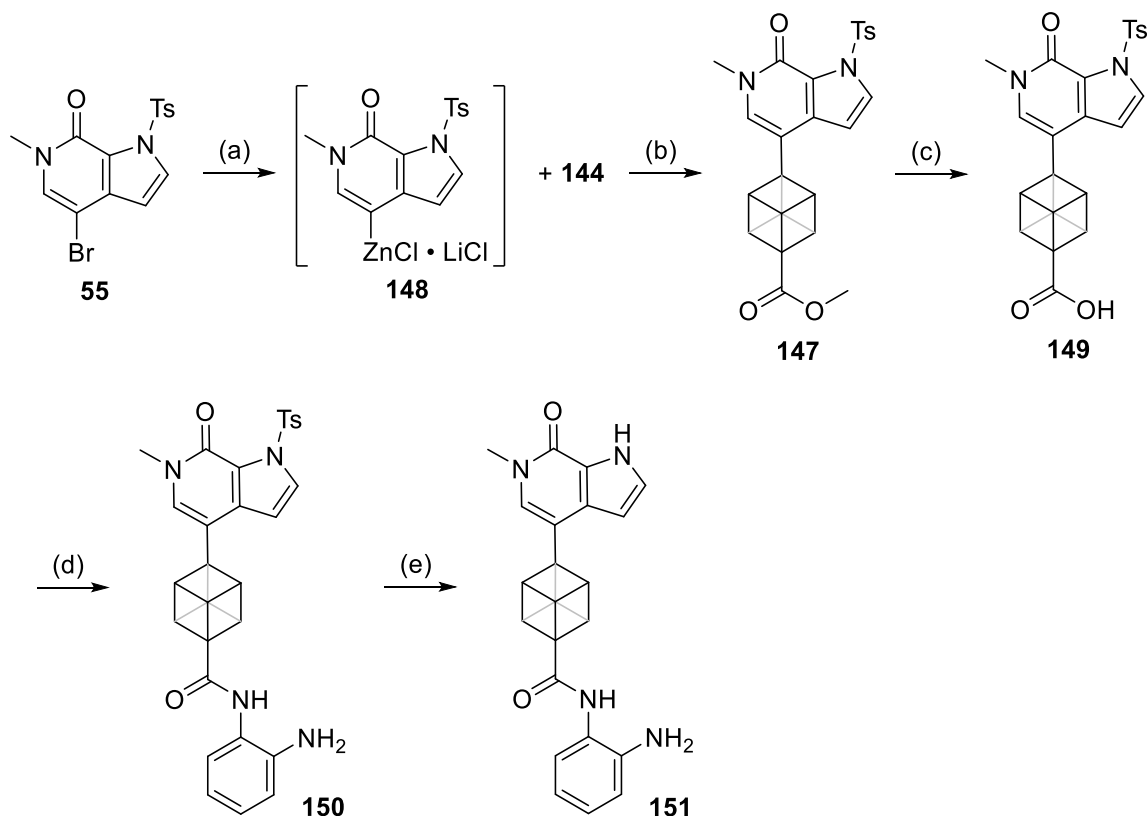
Scheme 23: Synthesis of cubane-containing inhibitor 151 through nickel-catalyzed cross-coupling. Reagents and conditions: (a) (1) iPrMgCl · LiCl, THF, -10 °C, 30 min; (2) ZnCl$_2$, 10 min; (b) (4,4'-dtbbpy)NiCl$_2$, DMF/THF, rt, 2 h; (c) LiOH · H$_2$O, MeOH/H$_2$O, rt, 16 h; (d) phenylenediamine, PyAOP, DIPEA, DMF, rt, 1 h; (e) LiOH · H$_2$O, dioxane/ H$_2$O, 70 °C, 16 h.

To test the activity of the synthesized compound, a thermal shift assay with BRD4 and 7 was performed (**Table 8**). Unfortunately, substitution for the cubane moiety seemed to almost completely diminish binding to BRD4 and 7. Possible explanations for the reduced affinity might be the lost π- π interaction or not enough space in the binding site to accommodate the bulkier substituent. Another suitable bioisostere might be the recently published oxabicyclooctane,[310] but the same issues be could present there.

Table 8: Binding data for cubane-based inhibitor 151

Concentration	DSF ΔT_m (K)[1]	
	BRD4-BD1	BRD7
10 µM	0.6 ± 0.1	0.8 ± 0.1
20 µM	0.7 ± 0.1	0.9 ± 0.2
30 µM	0.6 ± 0.1	1.4 ± 0.4

[1] The experiments were performed in technical triplicates.

3.4 BET/HDAC PROTACs

For another approach, it was tested if the PROTAC strategy would be suitable for the degradation of two different protein classes, using only one molecule. First, linker conjugates with the common CRBN ligand thalidomide had to be synthesized. By reacting linker **152** with hydroxy-thalidomide **153** in a Mitsunobu reaction, compound **154a** could be provided (**Scheme 24**). Alternatively, thalidomide **153** could be reacted in a Williamson ether synthesis by alkylation with bromide linkers **155a/b**, yielding conjugates **154b/c**. And lastly, through nucleophilic aromatic substitution with amines **156a/b** and fluoro-thalidomide **157**, compounds **154d** and **154e** were accessible.
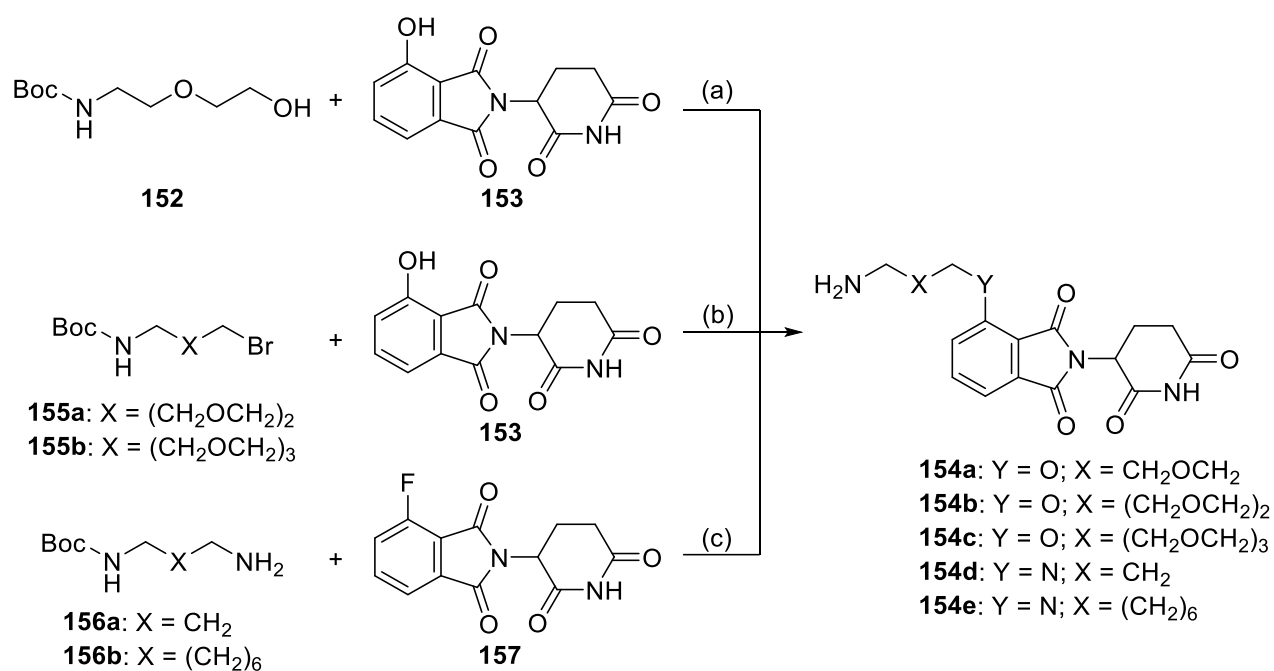
Scheme 24: Synthesis of thalidomide-based conjugates 154a-e. Reagents and conditions: (a) (1) PPh₃, DIAD, THF/DMF, rt, 16 h; (2) TFA/DCM, rt, 1 h; (b) (1) NaHCO₃, NaI, DMF, 80 °C, 3 d; (2) TFA/DCM, rt, 1 h; (c) (1) DIPEA, DMSO, 130 °C, 16 h; (2) TFA/DCM, rt, 1 h.

3.4.1   Pyrrolopyridone-Based PROTACs

One issue with developing PROTACs that target two different protein classes lies in that fact the necessary linker attachment must not interfere with binding to either protein. Fortunately, the binding data for inhibitor **130** indicated a possible attachment point that retains binding activity to BRD4 and HDAC1/2 (**Table 5**). Due to the improved binding affinity, a phenyl substituent as in inhibitor **132a** was introduced. The synthesis started by reacting aniline **26d** with bromobenzoyl chloride, yielding compound **158** (**Scheme 25**). Suzuki coupling with boronate **86** provided intermediate **159** and subsequent saponification gave carboxylic acid **160**. Afterwards, amide coupling with different thalidomide-linker conjugates, followed by *Boc*-deprotection with TFA, provided the different CRBN-based PROTACs **161a-c**.
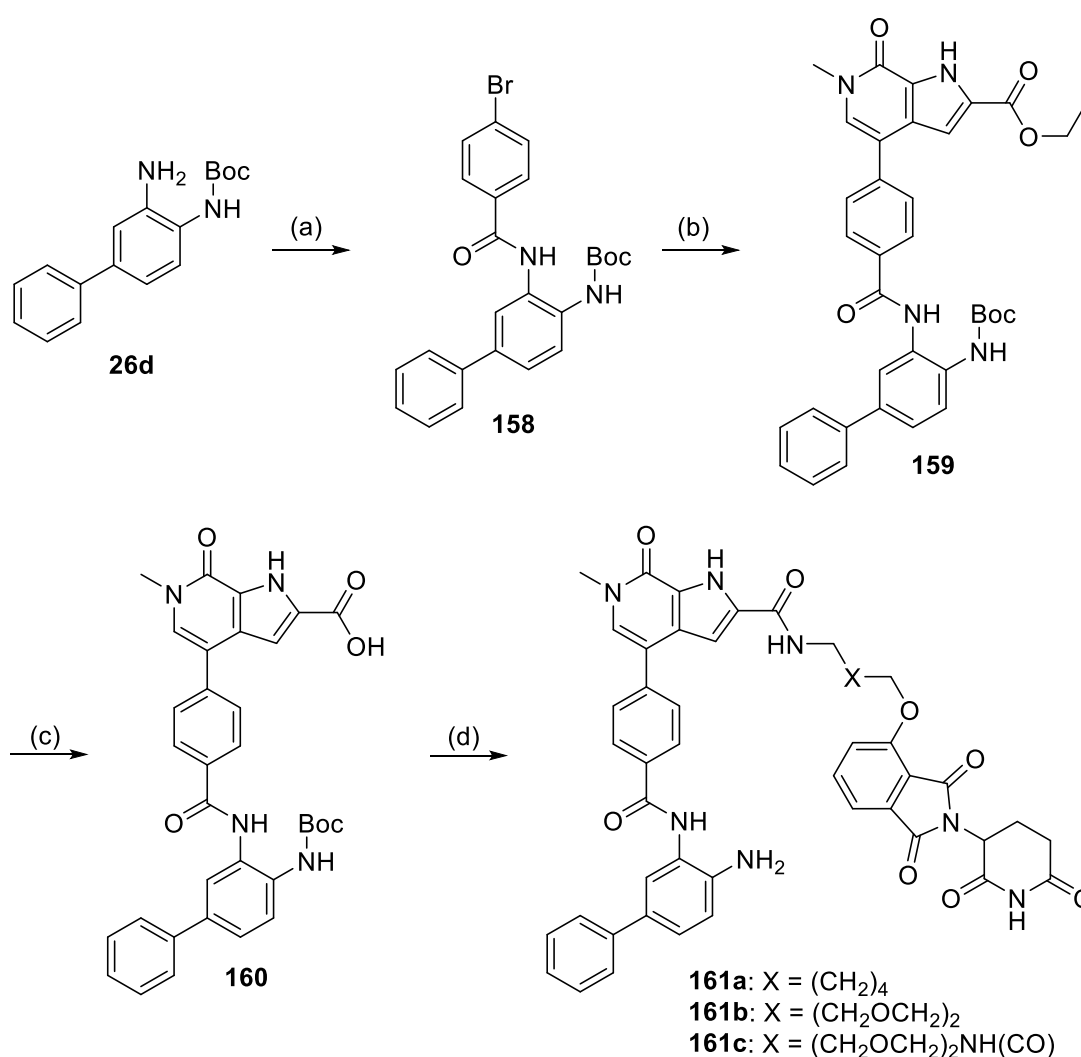
Scheme 25: Synthesis of PROTACs 161a-c. Reagents and conditions: (a) 4-bromobenzoyl chloride, DIPEA, DCM, rt, 2 h; (b) **86**, K_3PO_4, Pd XPhos G2, XPhos, dioxane, 70 °C, 2 h; (c) LiOH·H_2O, MeOH/THF/H_2O, 40 °C, 4 h; (d) (1) thalidomide-linker conjugate, PyAOP, DIPEA, DMF, rt, 16 h; (2) TFA/DCM, rt, 30 min.

By coupling compound **160** with linkers **162a-c**, followed by ester deprotection with TFA, carboxylic acids **163a-c** could be received (**Scheme 26**). After reaction with the VHL ligand and subsequent *Boc*-deprotection, VHL-based PROTACs **164a-c** were isolated.
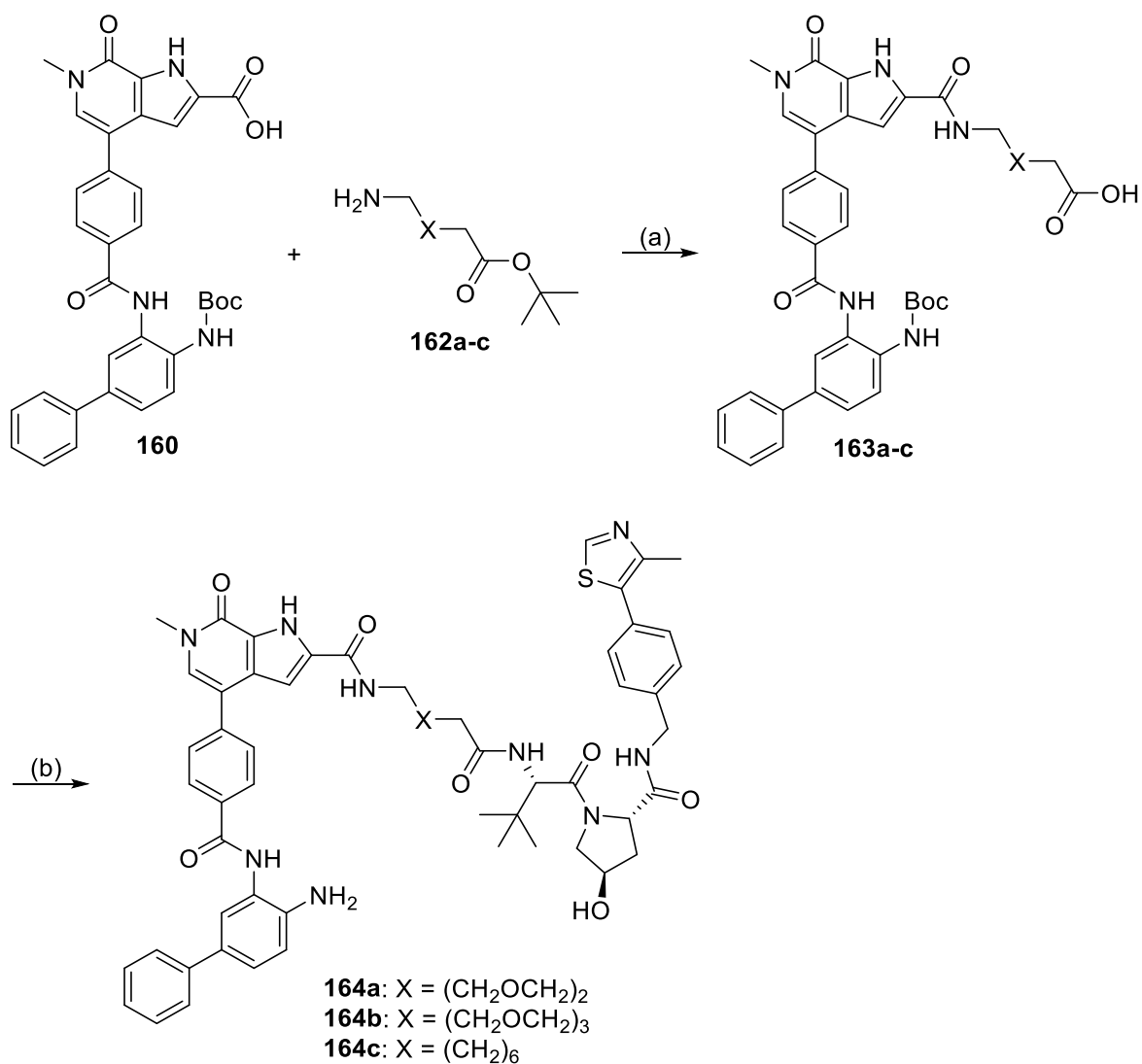
Scheme 26: Synthesis of PROTACs 164a-c. Reagents and conditions: (a) (1) PyAOP, DIPEA, DMF, rt, 2 h; (2) LiOH·H_2O, MeOH/THF/H_2O, rt, 24 h; (b) (1) VHL ligand 1 (HCl), PyAOP, DIPEA, DMF, rt, 2 h; (2) TFA/DCM, rt, 30 min.

To assess, whether the attached E3 ligand would interfere with binding to BRD4 and HDAC1/2, the synthesized PROTACs were measured *via* a cellular NanoBRET target engagement assay (**Table 9**). In cells, all tested compounds retained most of their binding to HDAC1 and 2, with EC_{50} values in the high nanomolar range, also indicating sufficient cell permeability. For BRD4, binding appeared to be significantly impaired through the addition of the E3 ligand. For all dual PROTACs, EC_{50} values were reduced by a factor of approximately 10, now binding to the first bromodomain in the micromolar range.

Table 9: Target engagement assay for PROTACs

Compounds	E3-Ligase	X	NanoBRET EC$_{50}$ (µM) intact cells[1]		
			BRD4-BD1	HDAC1	HDAC2
130	-	-	0.3	17.8 ± 0.7[2]	30.0
132a	-	-	0.42 ± 0.11[3]	0.19 ± 0.03[3]	0.36 ± 0.12[3]
161a	CRBN	$(CH_2)_4$	2.4	0.83	0.63
161b	CRBN	$(CH_2OCH_2)_2$	4.1	0.89	0.16
161c	CRBN	$(CH_2OCH_2)_2NH(CO)$	2.0	0.89	0.18
164a	VHL	$(CH_2OCH_2)_2$	3.1	0.39	0.22
164b	VHL	$(CH_2OCH_2)_3$	5.2	0.52	0.19
164c	VHL	$(CH_2)_6$	8.4	0.93	0.55

[1] Experiments performed in technical duplicates (n=1). [2] n=2; [3] n=3

To assess, whether the synthesized PROTACs were actually capable of degrading BRD4, a HiBiT assay was performed. In this fluorescence-based assay, the HiBiT tag is fused to the POI. When bound to its complementation partner, the LgBiT, the NanoLuc luciferase is reconstituted and a bioluminescent signal is generated.[248] Through a decrease of the fluorescence signal, a time and dose-dependent degradation of the POI can be measured. Unfortunately, none of the tested compounds could show significant degradation of BRD4, possibly owing to a weak binding affinity.

3.4.2   Diazepine-Based PROTACs

Since the pyrrolopyridone-based PROTACs were not able to degrade BRD4, another approach that was thought to be promising was to develop degraders based on the initial diazepine-based dual inhibitor **19**. As one side of the core scaffold was already used for attachment of the HDAC-binding moiety, a new attachment point for the linker had to be created. According to a published procedure, BET inhibitor **7** could be further functionalized by adding a second carboxylic acid moiety.[270]

In the first step, the acid labile *tert*-butyl ester of starting material **7** had to be transformed into the methyl ester, providing compound **165** (**Scheme 27**). Selective oxidation of one methyl group with manganese(III) acetate in a mixture of acetic acid and acetic anhydride yielded acetylated intermediate **166**. After deacetylation, alcohol **167** was isolated, which was afterwards oxidized with Dess-Martin periodinane (DMP), providing aldehyde **168**. In the following Pinnick oxidation, carboxylic acid **169** was produced. The synthesis could be optimized, increasing the overall yield from the published 23% to 62%, while at the same time being scaled up, generating several grams of functionalized inhibitor **169**. Since two orthogonal protecting groups were needed for both carboxylic acid functionalities, the first idea was to install a *tert*-butyl ester on the newly generated acid moiety, producing ester **170**. This was, however, not successful under various tested reactions conditions. Typical conditions, such as the Steglich esterification, using different activating agents or reaction of the acyl chloride did not produce any product, likely due to the low nucleophilicity of *tert*-butanol.
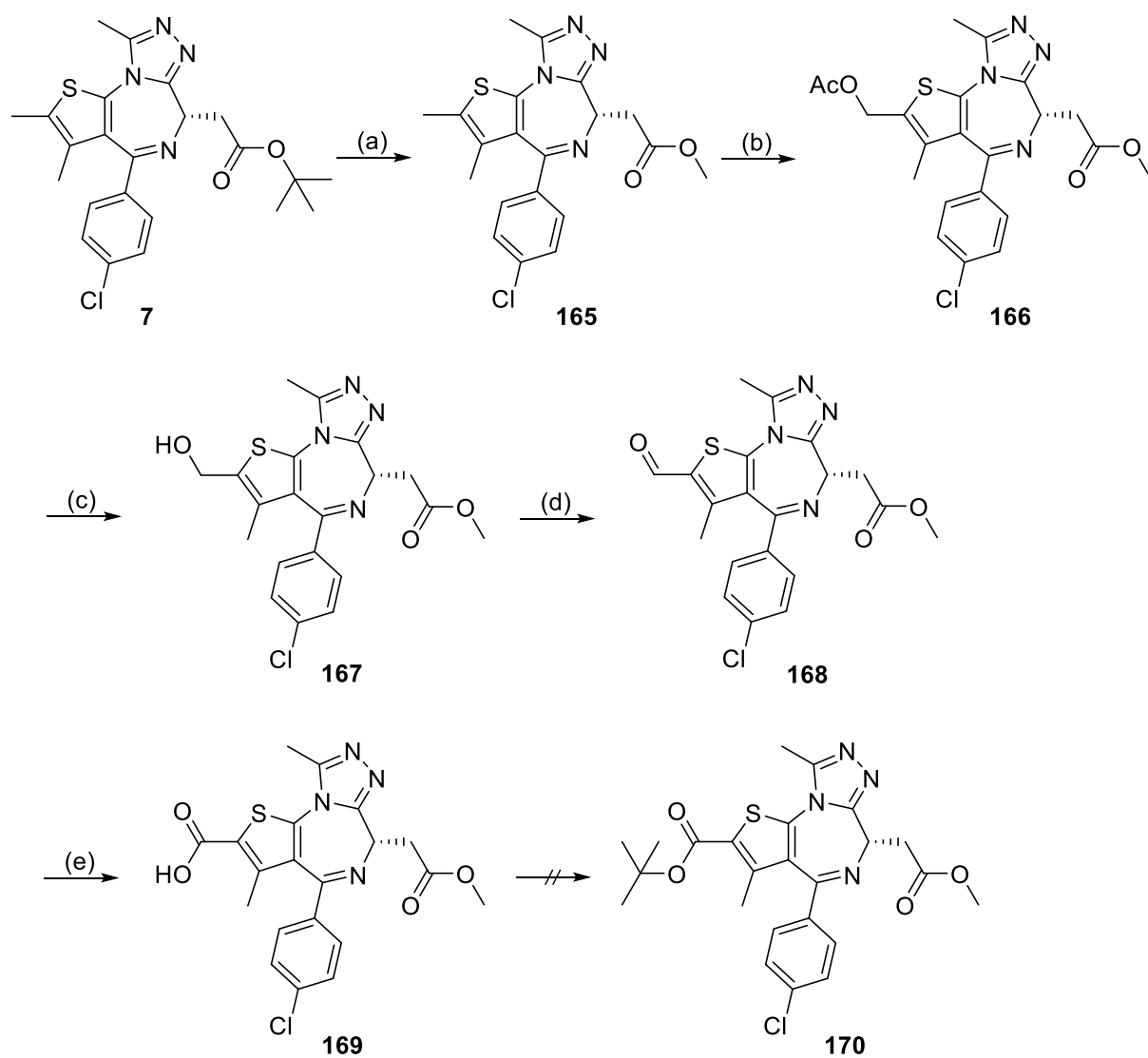
Scheme 27: Functionalization of inhibitor 7. Reagents and conditions: (a) MeOH, H_2SO_4, reflux, 20 h; (b) $Mn(OAc)_3 \cdot 2\,H_2O$, Ac_2O, H_2SO_4, AcOH, rt, 3 d, then 50 °C, 3 d; (c) K_2CO_3, MeOH, rt, 2 h; (d) DMP, DCM, rt, 2 h; (e) $NaClO_2$, H_2O_2, NaH_2PO_4, ACN/H_2O, rt, 30 min.

By using isopropanol instead, isopropyl ester **171** could successfully be synthesized (**Scheme 28**). Following a protocol published by K. C. Nicolaou,[311] the methyl ester could afterwards selectively be cleaved with trimethyltin hydroxide, yielding carboxylic acid **172**. Amide coupling with aniline **34** and propanephosphonic acid anhydride (T3P) as an activating agent then gave compound **173**. After subsequent saponification, acid-functionalized inhibitor **174** could be isolated.
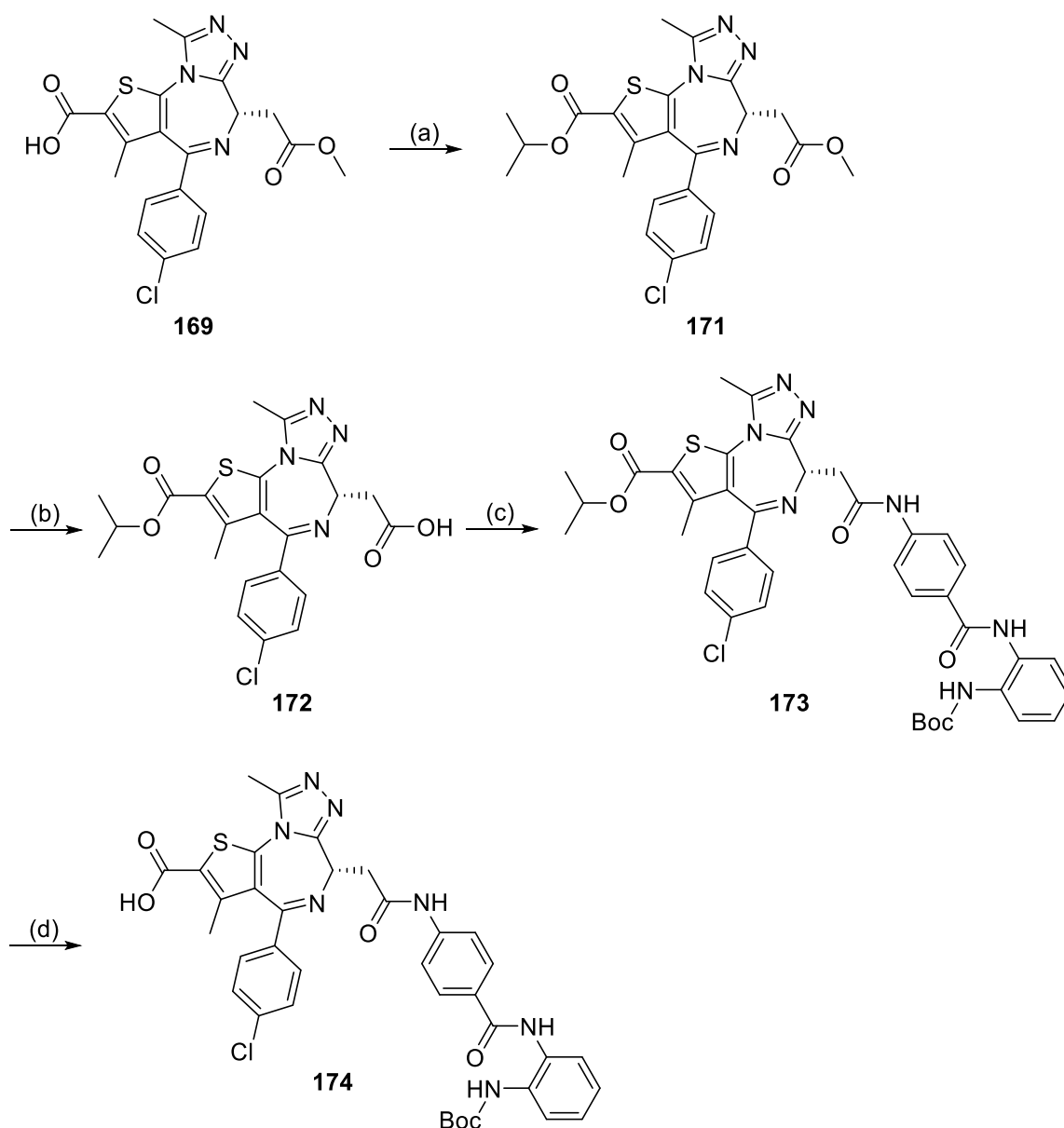
Scheme 28: Synthesis of functionalized inhibitor 174. Reagents and conditions: (a) PyAOP, DMAP, DIPEA, *i*PrOH, DMF, rt, 16 h; (b) Me₃SnOH, DCE, 80 °C, 5 d; (c) **34**, T3P, pyridine, ACN, rt, 2 h; (d) LiOH·H₂O, MeOH/H₂O, rt, 3 h.

By reacting compound **174** with the different thalidomide-linker conjugates **154a-f**, followed by *Boc*-deprotection with TFA, the PROTACs **175a-f** were provided (**Scheme 29**).

154a: Y = O; X = CH$_2$OCH$_2$
154b: Y = O; X = (CH$_2$OCH$_2$)$_2$
154c: Y = O; X = (CH$_2$OCH$_2$)$_3$
154d: Y = N; X = CH$_2$
154e: Y = N; X = (CH$_2$)$_6$
154f: Y = N; X = (CH$_2$)$_4$

174

175a: Y = O; X = CH$_2$OCH$_2$
175b: Y = O; X = (CH$_2$OCH$_2$)$_2$
175c: Y = O; X = (CH$_2$OCH$_2$)$_3$
175d: Y = N; X = CH$_2$
175e: Y = N; X = (CH$_2$)$_6$
175f: Y = N; X = (CH$_2$)$_4$
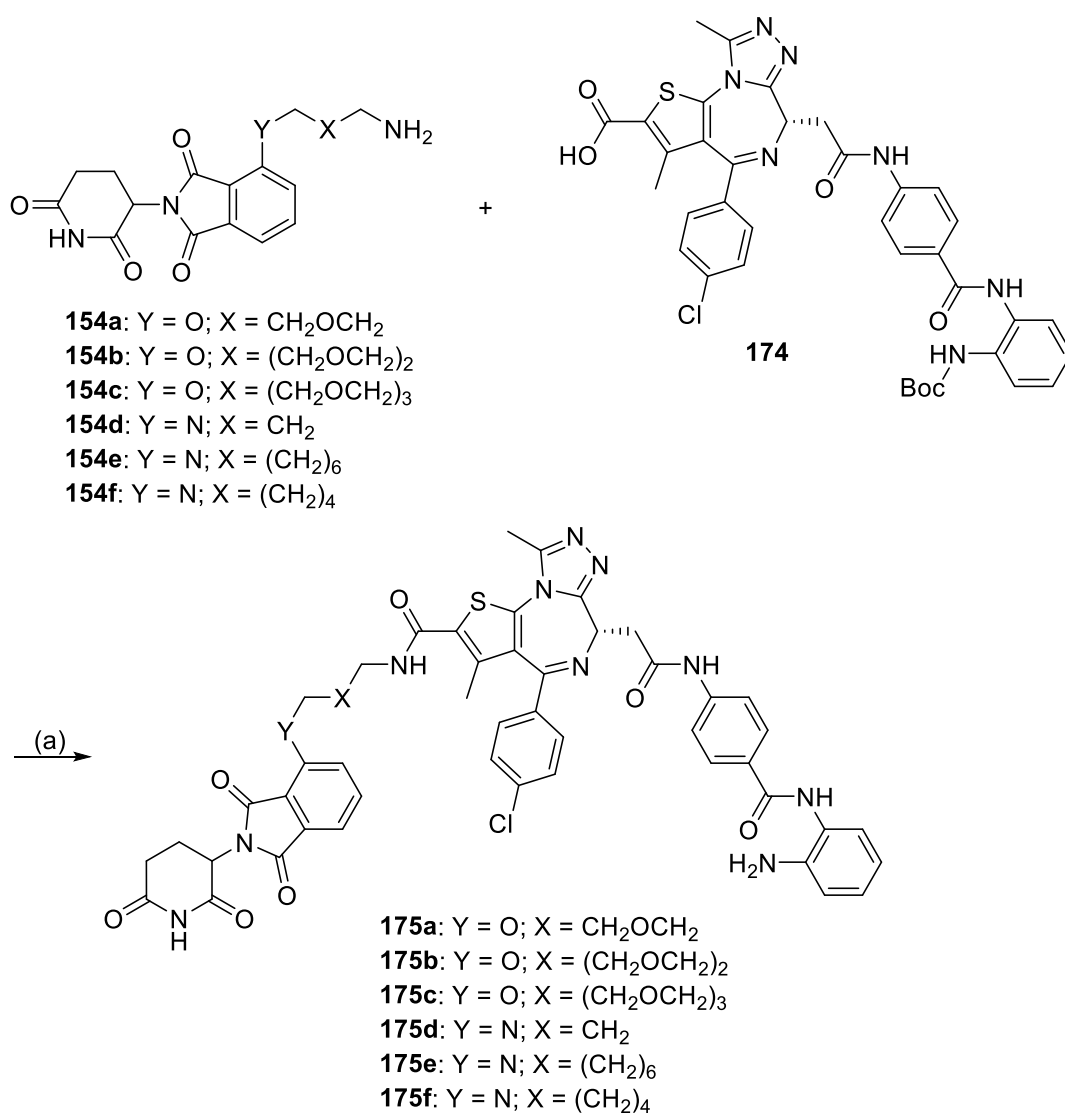
Scheme 29: Synthesis of CRBN-based PROTACs 175-f. Reagents and conditions: (a) (1) PyAOP, DMAP, DIPEA, DMF, rt, 16 h; (2) TFA/DCM, rt, 1 h.

Additionally, carboxylic acid **174** was coupled to the VHL-based linker conjugates **176a-e** (**Scheme 30**). After *Boc*-deprotection with TFA, PROTACs **177a-e** were provided. In the acidic deprotection conditions the HDAC-binding moiety partially underwent condensation, creating the respective benzimidazole (**Supporting Figure S 2**). This issue was present for all PROTACs **175a-f** and **177a-e** and was the cause of a difficult chromatographic purification. Interestingly, this reaction did not occur for all previously synthesized HDAC inhibitors which were subjected to identical deprotection conditions.

176a: X=O
176b: X=OCH$_2$CH$_2$O
176c: X=(CH$_2$OCH$_2$)$_2$CH$_2$O
176d: X=(CH$_2$)$_3$
176e: X=(CH$_2$)$_4$

174

177a: X=O
177b: X=OCH$_2$CH$_2$O
177c: X=(CH$_2$OCH$_2$)$_2$CH$_2$O
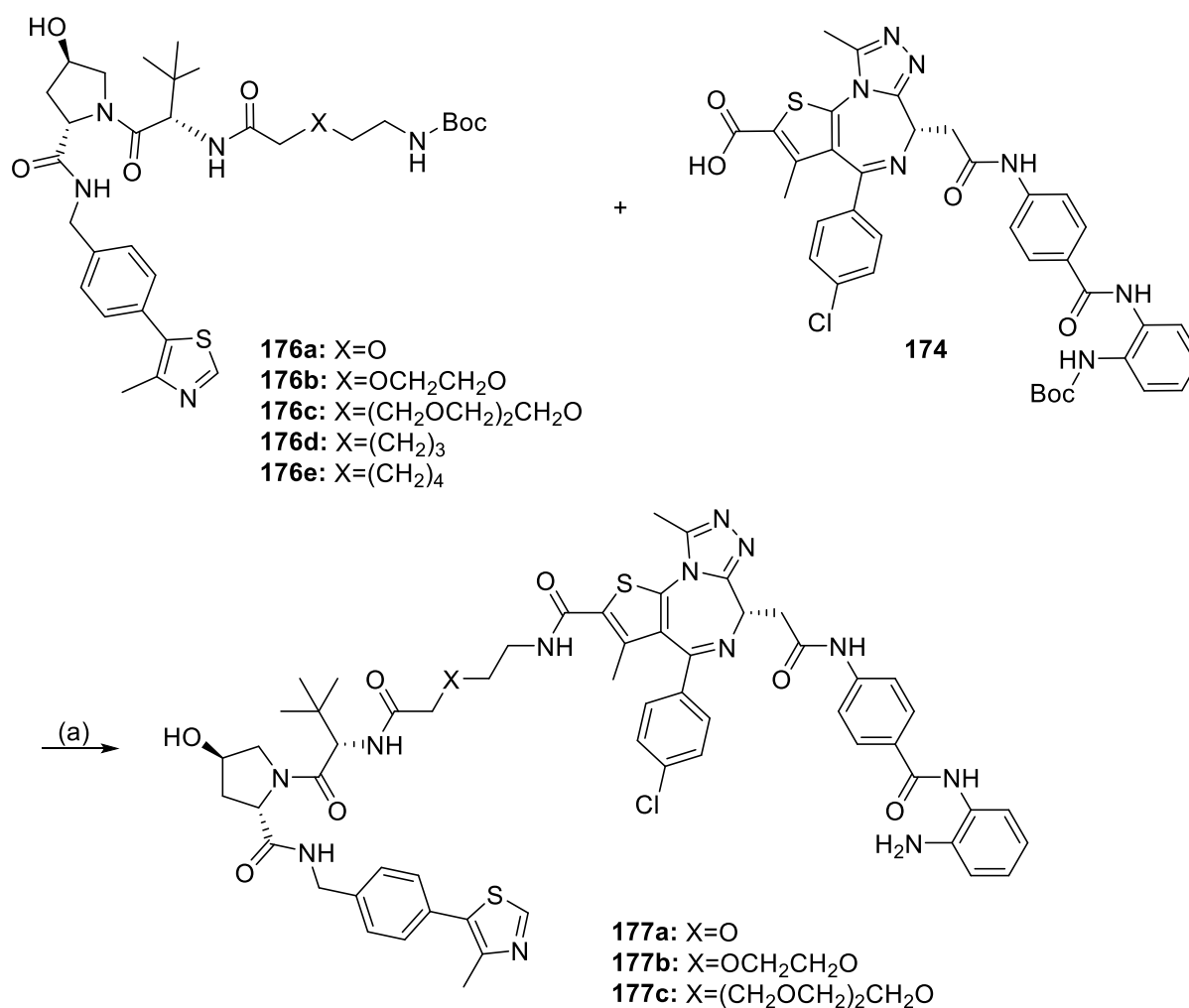
Scheme 30: Synthesis of VHL-based PROTACs 176a-e. Reagents and conditions: (a) (1) PyAOP, DMAP, DIPEA, DMF, rt, 16 h; (2) TFA/DCM, rt, 1 h.

The synthesized diazepine-based PROTACs were evaluated *via* a HiBiT assay to measure the concentration-dependent-degradation (**Figure 33A**). For the tested compounds, significant degradation of BRD2 and 4 could only be observed for PROTACs **175b**, **c** and **e**. When comparing potency to the published BET degraders MZ1 and dBET6, a significantly higher dose of the dual PROTACs was needed to achieve degradation, with a DC_{50} in the micromolar range. Interestingly, protein levels did not reach zero with compounds **175b**, **c** and **e** but instead appeared to plateau at approximately 30%. Additionally, kinetics were measured to look at the time-dependent degradation of BRD2 and 4 (**Figure 33B** and **C**). The data shows that for compound **175e** and **b**, degradation was basically maximized after a few hours. In contrast to the references MZ1 and dBET6, no complete reduction of protein levels to zero was measured again (**Supporting Figure S 3**).
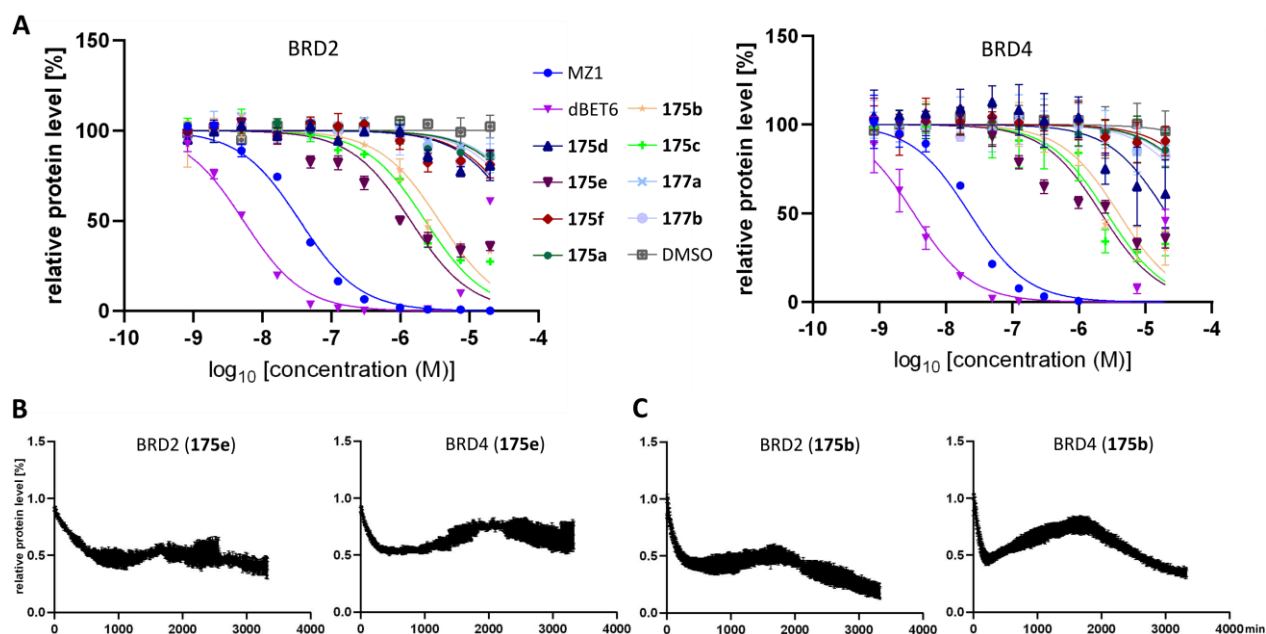
Figure 33: Effects on the degradation of BRD2/4. (A) Concentration-dependent levels of BRD2 (left) and BRD4 (right) 5 h after treatment with PROTACs measured *via* HiBiT. (B) Time-dependent proteins levels after treatment with 10 µM **175e** measured *via* HiBiT. (C) Time-dependent protein levels after treatment with 10 µM **175b**.

For further evaluation of the dual PROTACs, HDAC1 levels were monitored by WB in pancreatic PatuT cells (**Figure 34A**). After 24 h, no effect could be seen, while after 48 h, reduced HDAC1 levels could be detected for compound **175b**, **c** and **e**. Increased histone acetylation, consistent with lower levels of HDAC1, could be observed for PROTAC **175e**. Additionally, BRD2 and 4 levels in the pancreatic PSN1 and PatuT cells were monitored by WB (**Figure 34B**). In agreement with the HiBiT data, PROTACs **175b** and **e**, and, to a lesser extent, **177a**, did show significantly reduced levels of BRD4 in both cell lines. Interestingly, and in contrast to the control MZ-1, the novel compounds appear to have a stronger effect on BRD4 than on BRD2.
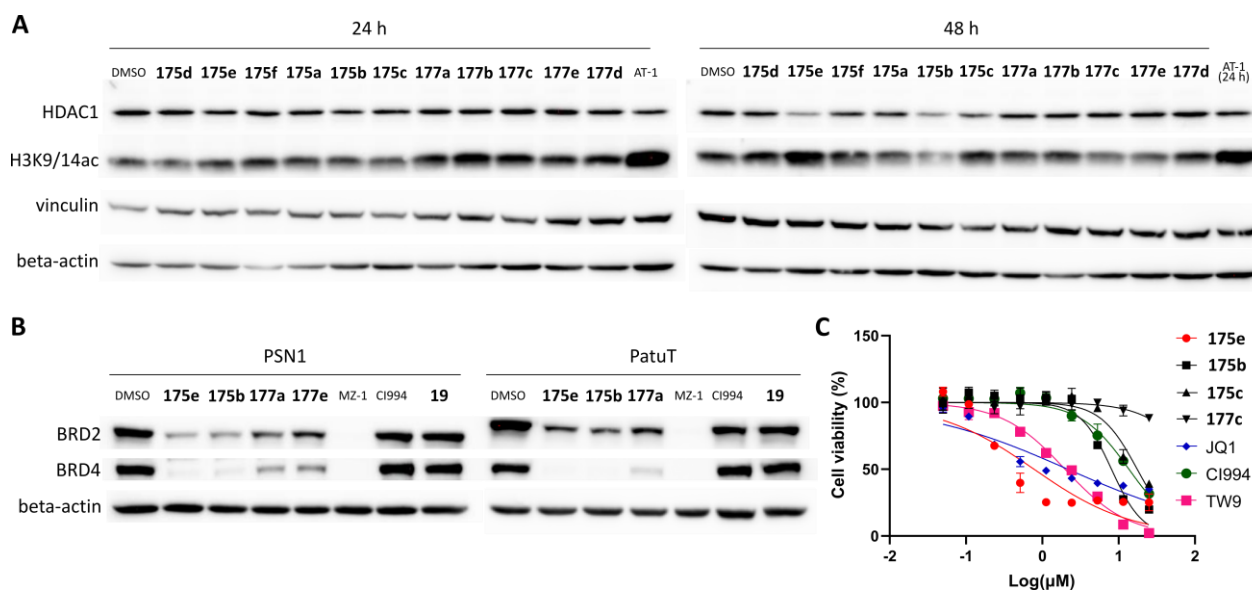
Figure 34: Biological effects of the dual BET/HDAC PROTACs. (A) Effect on HDAC1 degradation and histone H3 K9/K14 acetylation in Patu8988T cells after incubation with 10 µM compound monitored by Western blot. (B) Effect on BRD2 and 4 degradation in pancreatic cancer cell lines PSN1 and Patu8988T 24 h after incubation with 10 µM compound. (C) Viability of Patu8988T cells 3 d after treatment with different concentrations.

Lastly, some of the dual BET/HDAC PROTACs were evaluated for their effect on the viability of pancreatic cancer cells (**Figure 34C**). Compound **175e**, which also showed the strongest effect on reducing HDAC1 levels, reduced cell viability the most of all tested compounds. Intriguingly, dual PROTAC **175e** was also more potent than the parent inhibitor **19** (IC_{50} = 0.8 µM *vs.* 2.0 µM, **Supporting Table S 10**). As with the HiBiT measurement, the curve seems to reach a plateau when the compound concentration exceeds approximately 1 µM. This might be due to this being the maximum solubility of PROTAC **175e** under the assay conditions.

4 Summary and Discussion

The term epigenetics describes stable heritable traits which cannot be explained by the DNA sequence and the sum of all epigenetic marks that influence the phenotype of a cell can be described as the epigenetic code. An important epigenetic mechanism is the modification of histones, structural proteins the DNA wraps around to form chromatin. Those modifications include methylation, acetylation, phosphorylation, ubiquitinylation, sumoylation, biotinylation and ADP-ribosylation[22] and predominantly occur on the *N*-terminal tails of histone proteins. By modifying the histone tails, these chemical groups serve as dynamic marks that influence DNA accessibility and the recruitment of protein complexes responsible for gene regulation. The acetylation of histones is one of the most widely studied types of histone modification and by affecting the charge of histones, and therefore their binding to DNA, it is heavily involved in transcriptional regulation. Histone deacetylases (HDACs) remove those acetylation marks and bromodomain and extra-terminal domain (BET) proteins bind to acetylated histones, thereby initiating transcription. Due to their impact on the regulation of genes, including different oncogenes and tumor suppressors, both classes of proteins have sparked interest for the treatment of diverse diseases, such as cancer.

The simultaneous inhibition of HDACs and BET proteins has shown promising anti-proliferative effects against different cancer types, including the difficult to treat pancreatic cancer.[229,230] Reflecting the attractiveness of combined inhibition, many dual BET/HDAC inhibitors have been developed in recent years.[228–240,243] As an HDAC-binding moiety, most dual inhibitors contain a hydroxamic acid warhead, which is unselective and generally not metabolically stable.[97] While some published dual inhibitors, such as inhibitor TW9 (**19**), contain the class I selective benzamide moiety[232] and show promising *in vitro* results for the treatment of pancreatic cancer,[230] their molecular weight exceeds 600 Da, limiting their application *in vivo* due to unfavorable pharmacokinetic characteristics.[241,242]

In this work, the strategy of concurrently targeting HDACs and BET proteins was further pursued by developing different types of dual inhibitors. As a way to improve potency and selectivity for HDAC1/2, dual inhibitor **19** was decorated with different aromatic substituents, to target the so-called "foot pocket" of those two enzymes. The resulting inhibitors **31a-c** (**Figure 35**) unfortunately lost their binding affinity to BET proteins. This result was difficult to explain as the co-crystal structure of compound **19** with BRD4 showed the HDAC-binding moiety to protrude out of the binding site and into the solvent.[230]
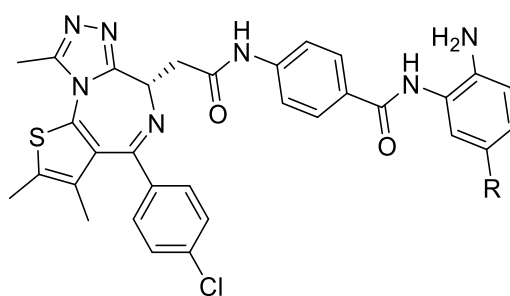
19: R = H
31a: R = 2-thienyl
31b: R = 2-furyl
31c: R = 4-pyridyl

Figure 35: Diazepine-based dual inhibitors. The substituted inhibitors **31a-c** unfortunately lost their affinity to BRD4.

Dihydroquinoxalinone **21** and pyrrolopyridone **14** were chosen as alternative starting points for the development of dual inhibitors due to their high potency for BRD4. While dihydroquinoxalinone-based dual inhibitor **47** lost some affinity to BRD4 through addition of the HDAC-binding moiety, the different pyrrolopyridone-based inhibitors generally retained most of their potency (**Figure 36**). In a thermal shift assay, the dual inhibitors caused a high stabilization of BRD4, surpassing the reference BET inhibitor JQ1 (**13**). All three tested attachment points for the HDAC-binding moiety on the core scaffold seemed to be tolerated by the binding site. Those dual inhibitors were further investigated for their biological effect in pancreatic cancer cells. Analysis of the BET-inhibition biomarkers *HEXIM1*, *p57* and *CDKN1C* showed a strong upregulation from some dual inhibitors. When comparing the BET and dual BET/HDAC inhibitors, the dual inhibitors showed more attenuated effect in cells, which might be attributed to worse cell permeability.

47

X: O or NH
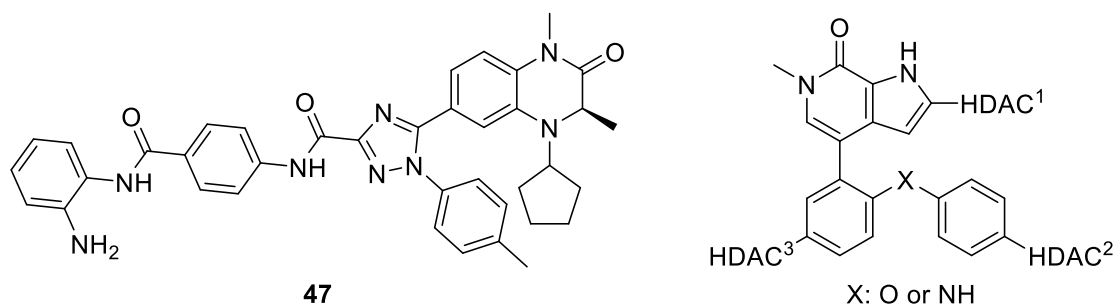
Figure 36: Dihydroquinoxalinone-based dual inhibitor 47 and pyrrolopyridone-based inhibitors. The HDAC-binding moiety was attached to one of three different positions on the pyrrolopyridone core scaffold.

The effect on histone acetylation, however, appeared to be not exceptional. This was in accordance with HDAC1 inhibition data, where the dual inhibitors exhibited IC_{50} values in the micromolar range. Among the tested compounds, dual inhibitor **93** reduced the viability of pancreatic cancer cells the most, which was likely primarily a result of its potent BRD4 inhibition.

The dual BET/HDAC inhibitors described above are essentially simple adducts of a BET and HDAC inhibitor. It was hypothesized that the merging of two pharmacophores, creating a highly integrated dual inhibitor with a minimized molecular weight, might yield a better outcome. With the aim of creating a good balance between potency and molecular size, the BET inhibitor MS436 (**22**) was chosen as a starting scaffold due to its small size and structural similarity with HDAC inhibitor CI-994 (**7**). The merged dual inhibitor **102a** (**Figure 37**) actually exhibited higher stabilization of BRD4 than its parent inhibitor, while additionally showing binding to HDAC1.
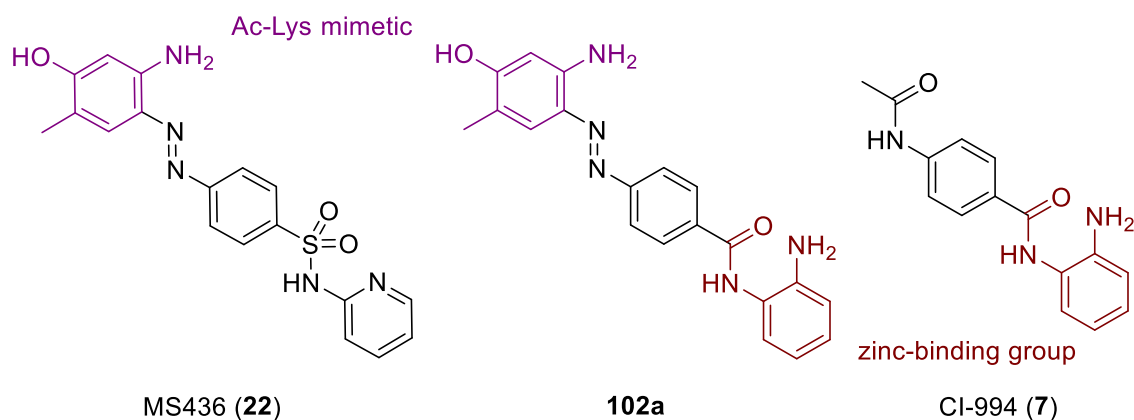
Figure 37: Strategy for the merging of BET and HDAC pharmacophores. The dual inhibitor **102a** contains the acetyl lysine mimetic of BET inhibitor **22** and the zinc-binding group of HDAC inhibitor **7**, while retaining a minimal size.

By exploiting a bivalent interaction to a conserved asparagine, the binding to BRD4 could be further improved, resulting in inhibitor **107b** (**Figure 38**). For the sake of better stability and to facilitate compound synthesis, further optimization was needed. The best balance between BET and HDAC binding was achieved with compound **123a**, which exhibited cellular target engagement to BRD4 in the nanomolar and

132a: X=CH, R=phenyl
132b: X=N, R=phenyl
132c: X=N, R=2-furyl
132d: X=N, R=2-thienyl
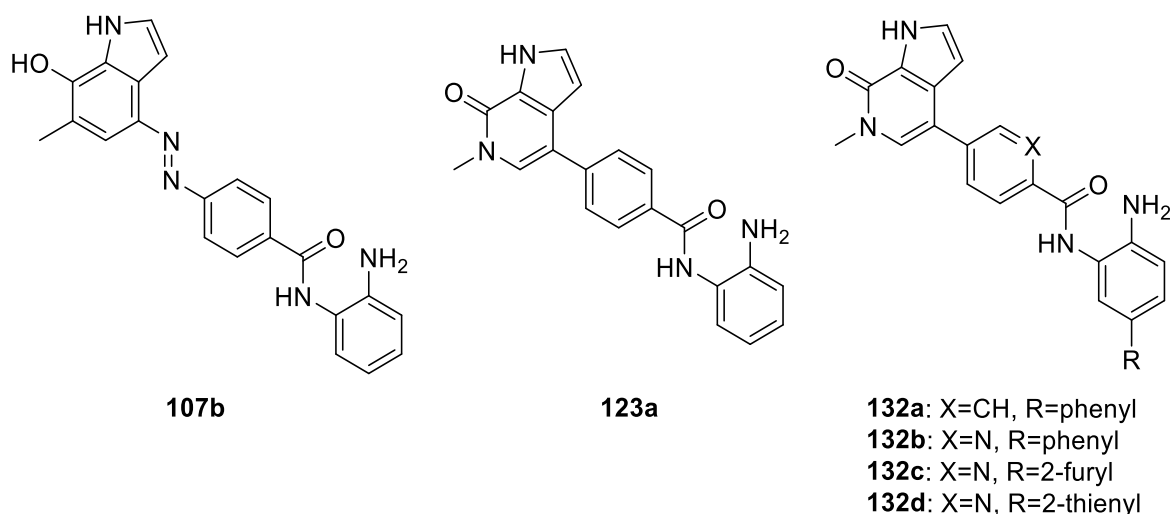
Figure 38: Stepwise optimization of the merged dual inhibitor. Replacement of the hydroxyindole improved stability and facilitated compound synthesis. The addition of aromatic substituents enhanced binding to HDAC1/2.

to HDAC1/2 in the low micromolar range. By introducing aromatic substituents, the HDAC binding could be significantly improved, with the best inhibitor **132b** binding to HDAC1/2 with EC_{50} values of 110 nM and 100 nM, respectively, in a cellular target engagement assay. A selectivity panel further revealed compound **132b** to be selective for HDAC1/2 over all other zinc-dependent HDACs. In pancreatic cancer cells, histone deacetylation was effectively blocked by the substituted inhibitors **132a-d**. Additionally, the tumor suppressors and markers of BET inhibition *HEXIM1* and *p57* were significantly upregulated. In NUT midline carcinoma (NMC) cells, the oncogenic drivers *MYC* and *TP63* were downregulated. When investigating the viability of pancreatic cancer cells, the synergy of combined BET and HDAC inhibition could be confirmed. The dual inhibitors, however, were even more potent in reducing the cell viability with IC_{50} values of approximately 3 µM. In NMC cells, no synergistic effect could be observed for the combination of a BET and HDAC inhibitor, but dual inhibitor **132b** still was the most potent in reducing cell viability (IC_{50} = 220 nM).[277] Overall, the promising *in vitro* results provide a basis for future studies of dual BET/HDAC inhibitors in pancreatic and other types of cancer. Since a pharmacokinetics study suggested suboptimal metabolic stability and high clearance for compound **132b**, additional optimization of the inhibitors would be needed to encourage further *in vivo* studies.

In another approach, the emerging PROTAC strategy, with the aim of degrading the proteins of interest instead of simply inhibiting them, was pursued for the combined targeting of HDACs and BET proteins. Using the above-described dual inhibitor scaffold, ligands for the E3 ligases CBRN and VHL were attached, creating dual PROTACs **161a-c** and **164a-c** (**Figure 39**). In a cellular target engagement assay, the PROTACs

161a: X = (CH$_2$)$_4$
161b: X = (CH$_2$OCH$_2$)$_2$
161c: X = (CH$_2$OCH$_2$)$_2$NH(CO)

164a: X = (CH$_2$OCH$_2$)$_2$
164b: X = (CH$_2$OCH$_2$)$_3$
164c: X = (CH$_2$)$_6$
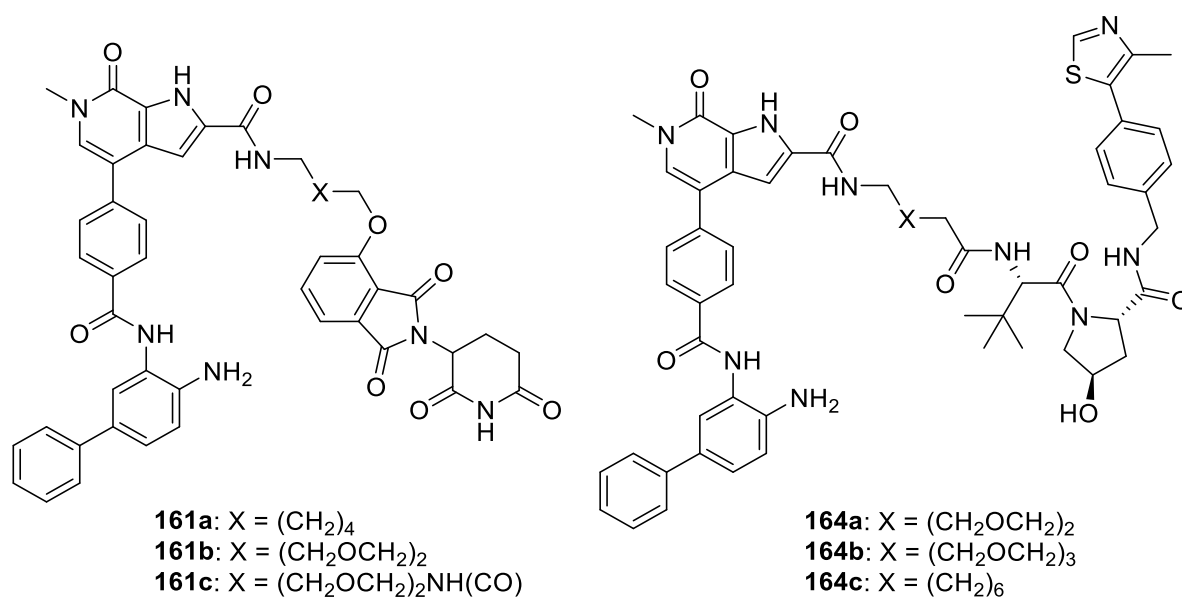
Figure 39: Pyrrolopyridone-based dual BET/HDAC PROTACs. The synthesized compounds exhibited cellular binding to BRD4 and HDAC1/2 but did not show degradation of BRD4.

bound weaker than the dual inhibitors, but still showed EC$_{50}$ values in the low micromolar range for BRD4 and in the nanomolar range for HDAC1/2. Evaluation *via* a fluorescence-based HiBiT assay, however, indicated no degradation of BRD4. For this reason, another series of PROTACs, based on diazepine **19**, was designed and synthesized, yielding compounds **175a-f** and **177a-e** (**Figure 40**). In the HiBiT assay, some of the tested degraders were able to decrease BRD4 levels. Monitoring *via* Western blot also showed reduced BRD4 levels after treatment in two different pancreatic cancer cell lines, with the strongest effect from thalidomide-based PROTACs **175b** and **e**. Interestingly, a slight selectivity for BRD4 could be seen, with only a small reduction of BRD2 levels being observed. Monitoring of HDAC1 levels showed an effect after treatment with compound **175e** after 48 h. This was the only PROTAC for which reduced levels of HDAC1

175a: Y = O; X = CH$_2$OCH$_2$
175b: Y = O; X = (CH$_2$OCH$_2$)$_2$
175c: Y = O; X = (CH$_2$OCH$_2$)$_3$
175d: Y = N; X = CH$_2$
175e: Y = N; X = (CH$_2$)$_6$
175f: Y = N; X = (CH$_2$)$_4$

177a: X=O
177b: X=OCH$_2$CH$_2$O
177c: X=(CH$_2$OCH$_2$)$_2$CH$_2$O
177d: X=(CH$_2$)$_3$
177e: X=(CH$_2$)$_4$
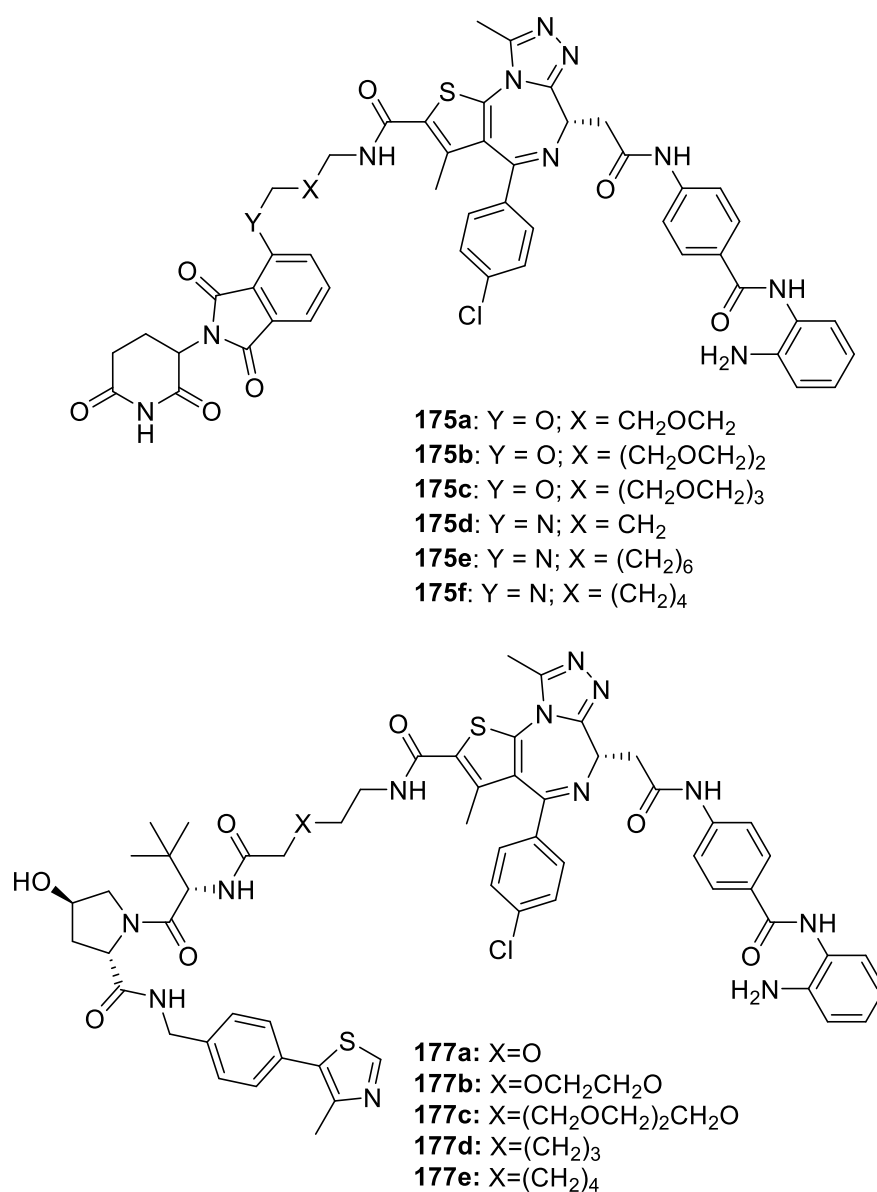
Figure 40: Diazepine-based dual BET/HDAC PROTACs. Compound **175e** was shown to decrease levels of BRD4 and HDAC1 and to potently decrease the viability of pancreatic cancer cells.

could be seen together with increased histone acetylation. Additionally, PROTAC **175e** potently decreased the viability of pancreatic PatuT cells with an IC_{50} value of 800 nM. This was more potent than all previously investigated dual BET/HDAC inhibitors and therefore encourages further biological investigation. The experiments should be repeated with the use of a proteasome inhibitor to determine whether the observed effects are truly a result of protein degradation. Additionally, the use of mass spectrometry-based proteomics profiling would be interesting to evaluate the selectivity of compound **175e**. Overall, the application of PROTACs for the simultaneous targeting of two different classes of proteins appears to be a viable alternative strategy that needs to be further investigated.

In summary, this work has produced different approaches for simultaneously targeting epigenetic reader and modifier proteins. By developing a novel scaffold that selectively inhibits HDAC1/2 together with BET proteins in cells, an effective tool for the investigation of pancreatic cancer, and other diseases which are sensitive to epigenetic processes, was created. The compound's small size further gives the opportunity to further develop the inhibitor towards optimized pharmacokinetic properties, potentially resulting in a drug for cancer treatment.

A second novel approach that was pursued, was the development of a small-molecule degrader, targeting HDACs and BET proteins. Through synthesizing a variety of different molecules, a compound that was capable of lowering BRD4 levels and, at the same time, increasing histone acetylation was developed. While additional mechanistic investigations are needed to verify the degradation, the potent antiproliferative effects in pancreatic cancer cells encourage further studies following this alternative new strategy.

5 Zusammenfassung

Der Begriff Epigenetik beschreibt stabile vererbbare Merkmale, die sich nicht durch die DNA-Sequenz erklären lassen, und die Summe aller epigenetischen Markierungen, die den Phänotyp einer Zelle beeinflussen, kann als epigenetischer Code bezeichnet werden. Ein wichtiger epigenetischer Mechanismus ist die Modifikation von Histonen, Strukturproteinen, um die sich die DNA zur Bildung von Chromatin wickelt. Zu diesen Modifikationen gehören Methylierung, Acetylierung, Phosphorylierung, Ubiquitinylierung, Sumoylierung, Biotinylierung und ADP-Ribosylierung, die vor allem an den *N*-terminalen Schwänzen der Histonproteine auftreten. Durch die Veränderung der Histonschwänze dienen diese chemischen Gruppen als dynamische Markierungen, die die Zugänglichkeit der DNA und die Rekrutierung von Proteinkomplexen, die für die Genregulation verantwortlich sind, beeinflussen. Die Acetylierung von Histonen ist eine der am besten untersuchten Arten der Histonmodifikation und ist durch die Beeinflussung der Ladung von Histonen, und damit ihrer Bindung an die DNA, stark an der Transkriptionsregulation beteiligt. Histondeacetylasen (HDACs) entfernen diese Acetylierungsmarkierungen und *Bromodomain and Extra-Terminal Domain* (BET)-Proteine binden an acetylierte Histone und leiten so die Transkription ein. Aufgrund ihres Einflusses auf die Regulierung von Genen, darunter verschiedene Onkogene und Tumorsuppressoren, haben beide Proteinklassen das Interesse an der Behandlung verschiedener Krankheiten, wie etwa Krebs, geweckt.

Die gleichzeitige Hemmung von HDACs und BET-Proteinen hat vielversprechende proliferationshemmende Wirkungen bei verschiedenen Krebsarten gezeigt, darunter auch beim schwer zu behandelnden Bauchspeicheldrüsenkrebs. Angesichts der Attraktivität der kombinierten Inhibierung beider Proteine wurden in den letzten Jahren zahlreiche duale BET/HDAC-Inhibitoren entwickelt. Die meisten dualen Inhibitoren enthalten als HDAC-bindenden Teil ein Hydroxamsäuremotiv, welches unselektiv und im Allgemeinen nicht metabolisch stabil ist. Einige veröffentlichte duale Inhibitoren, wie der Inhibitor TW9 (**19**), enthalten zwar das Klasse-I-selektive Benzamidmotiv und zeigen vielversprechende *in-vitro*-Ergebnisse für die Behandlung von Bauchspeicheldrüsenkrebs, ihr Molekulargewicht übersteigt jedoch 600 Da, was ihre Anwendung *in vivo* aufgrund ungünstiger pharmakokinetischer Eigenschaften einschränkt.

In dieser Arbeit wurde die Strategie, gleichzeitig HDACs und BET-Proteine zu beeinflussen, durch die Entwicklung verschiedener Arten von dualen Inhibitoren weiterverfolgt. Um die Wirksamkeit und Selektivität für HDAC1/2 zu verbessern, wurde der duale Inhibitor **19** mit verschiedenen aromatischen Substituenten versehen, die in die sogenannte "Fußtasche" dieser beiden Enzyme passen sollten. Die resultierenden Inhibitoren **31a**-**c** (**Abbildung 1**) verloren leider ihre Bindungsaffinität zu den BET-Proteinen. Dieses Ergebnis war schwer zu erklären, da die Kristallstruktur von Verbindung **19** mit BRD4

zeigte, dass der HDAC-bindende Teil aus der Bindungsstelle heraus und in das Lösungsmittel hineinragt.
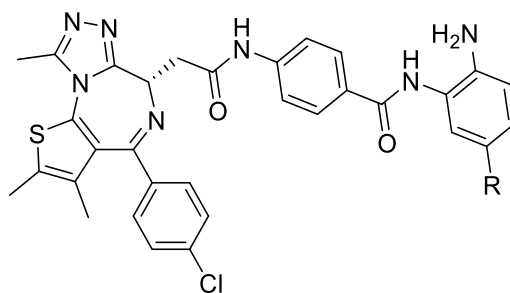
19: R = H
31a: R = 2-thienyl
31b: R = 2-furyl
31c: R = 4-pyridyl

Abbildung 1: Diazepin-basierte duale Inhibitoren. Die substituierten Inhibitoren **31a-c** zeigten leider keine Affinität zu BRD4.

Dihydrochinoxalinon **21** und Pyrrolopyridon **14** wurden aufgrund ihrer hohen Potenz für BRD4 als alternative Ausgangspunkte für die Entwicklung von dualen Inhibitoren gewählt. Während der auf Dihydrochinoxalinon basierende duale Inhibitor **47** durch die Ergänzung des HDAC-bindenden Teils etwas an Affinität zu BRD4 verlor, behielten die verschiedenen Pyrrolopyridon-basierten Inhibitoren im Allgemeinen den Großteil ihrer Potenz bei (**Abbildung 2**). In einem *Thermal Shift Assay* bewirkten die dualen Inhibitoren eine hohe Stabilisierung von BRD4 und übertrafen den BET-Referenzinhibitor JQ1 (**13**). Alle drei getesteten Anknüpfungspunkte für das HDAC-bindende Motiv am Grundgerüst schienen von der Bindungsstelle toleriert zu werden. Diese dualen Inhibitoren wurden anschließend auf ihre biologische Wirkung in Bauchspeicheldrüsenkrebszellen untersucht. Die Analyse der BET-Inhibitions-Biomarker *HEXIM1*, *p57* und *CDKN1C* zeigte eine starke Hochregulierung durch einige duale Inhibitoren. Beim Vergleich der BET- und dualen BET/HDAC-Inhibitoren zeigten die dualen Inhibitoren eine schwächere Wirkung in den Zellen, was auf eine schlechtere Zellpermeabilität zurückzuführen sein könnte.

47

X: O or NH
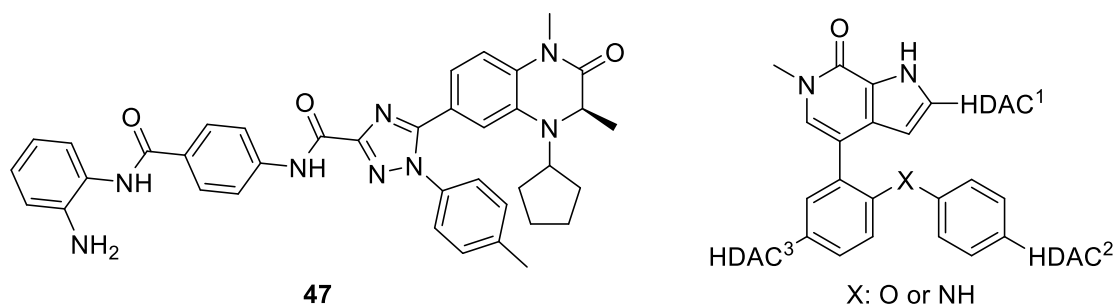
Abbildung 2: Dihydrochinoxalinon-basierter dualer Inhibitor 47 und Pyrrolopyridon-basierte Inhibitoren. Der HDAC-bindende Teil wurde an einer von drei verschiedenen Positionen des Pyrrolopyridongerüsts angebracht.

Die Wirkung auf die Histon-Acetylierung schien jedoch nicht außergewöhnlich zu sein. Dies stand im Einklang mit den Daten zur HDAC1-Inhibition, bei denen die dualen Inhibitoren IC_{50}-Werte im mikromolaren Bereich aufwiesen. Von den getesteten Verbindungen verringerte der duale Inhibitor **93** jedoch die Viabilität von Bauchspeicheldrüsenkrebszellen am stärksten, was wahrscheinlich in erster Linie auf seine starke BRD4-Inhibition zurückzuführen ist.

Während die bisher beschriebenen dualen BET/HDAC-Inhibitoren als Addukte eines BET- und eines HDAC-Inhibitors beschrieben werden können, wurde angenommen, dass die Verschmelzung von zwei Pharmakophoren zu einem hochintegrierten dualen Inhibitor mit einem minimalen Molekulargewicht ein besseres Ergebnis liefern könnte. Mit dem Ziel, ein ausgewogenes Verhältnis zwischen Wirksamkeit und Molekülgröße zu erreichen, wurde der BET-Inhibitor MS436 (**22**) aufgrund seiner geringen Größe und strukturellen Ähnlichkeit mit dem HDAC-Inhibitor CI-994 (**7**) als Ausgangsgerüst gewählt. Der fusionierte duale Inhibitor **102a** (**Abbildung 3**) zeigte tatsächlich eine stärkere Stabilisierung von BRD4 als sein Ausgangsinhibitor, während er zusätzlich eine Bindung an HDAC1 zeigte.
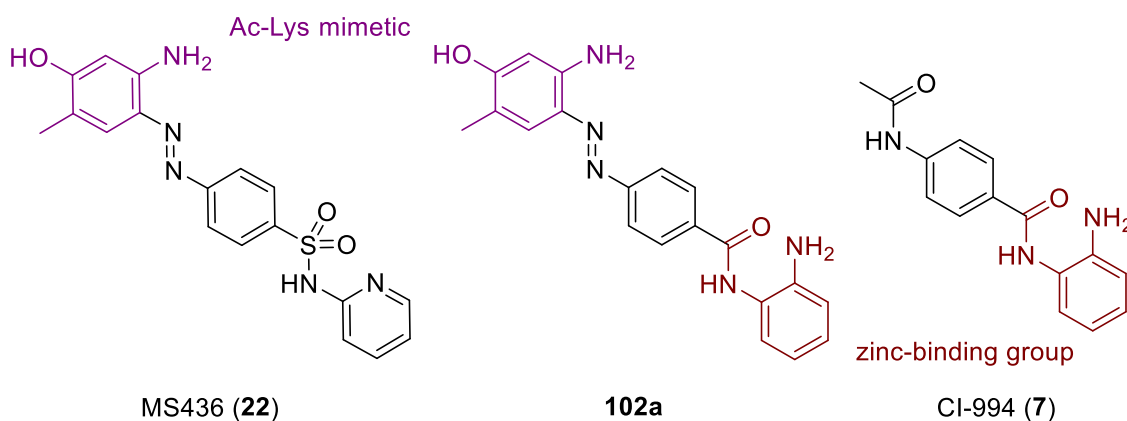
Abbildung 3: Strategie für die Verschmelzung der BET- und HDAC-Pharmakophore. Der duale Inhibitor **102a** vereint das Acetyllysin-Mimetikum des BET-Inhibitors **22** und die zinkbindende Gruppe des HDAC-Inhibitors **7**, wobei er eine minimale Größe aufweist.

Durch die Ausnutzung einer bivalenten Wechselwirkung mit einem konservierten Asparagin konnte die Bindung an BRD4 weiter verbessert werden, was zu dem Inhibitor **107b** führte (**Abbildung 4**). Im Hinblick auf eine bessere Stabilität und zur Erleichterung der Synthese war eine weitere Optimierung erforderlich. Das beste Verhältnis zwischen BET- und HDAC-Bindung wurde mit Verbindung **123a** erreicht, die eine zelluläre Zielbindung an BRD4 im nanomolaren und an HDAC1/2 im niedrigen mikromolaren Bereich aufwies. Durch die Einführung aromatischer Reste konnte die HDAC-Bindung deutlich verbessert werden, wobei der beste Inhibitor **132b** mit EC_{50}-Werten von 110 nM bzw. 100 nM in einem zellulären Target-Engagement-Assay an HDAC1/2 band. Ein Selektivitätspanel zeigte außerdem, dass die Verbindung **132b** selektiv für HDAC 1/2 gegenüber allen anderen zinkabhängigen HDACs ist.

107b

123a

132a: X=CH, R=phenyl
132b: X=N, R=phenyl
132c: X=N, R=2-furyl
132d: X=N, R=2-thienyl
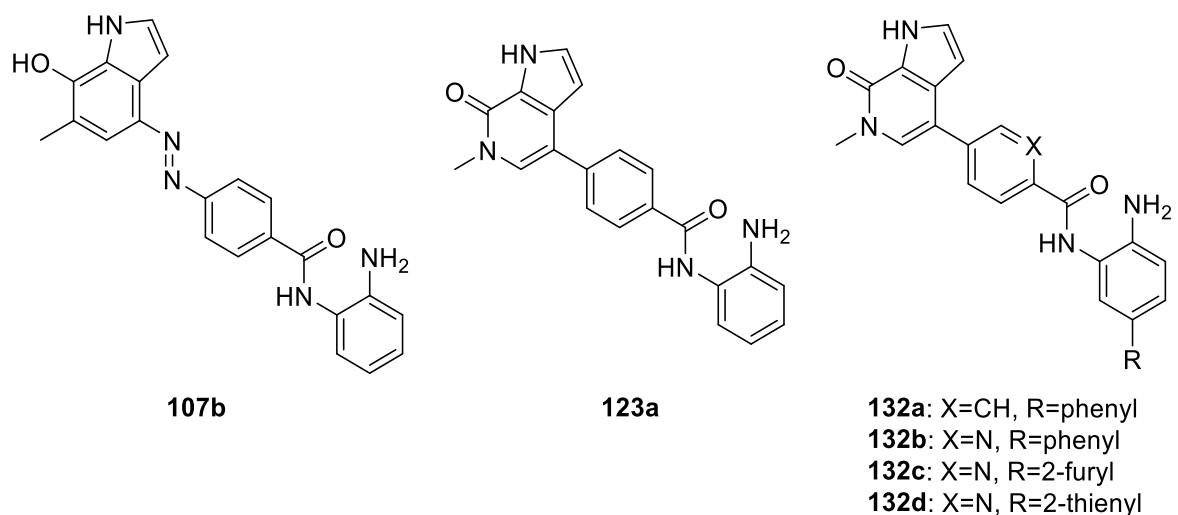
Abbildung 4: Schrittweise Optimierung des fusionierten dualen Inhibitors. Die Substitution des Hydroxyindols verbesserte die Stabilität und erleichterte die Synthese. Die Ergänzung aromatischer Substituenten verbesserte die Bindung an HDAC1/2.

In Bauchspeicheldrüsenkrebszellen wurde die Histondeacetylierung durch die substituierten Inhibitoren **132a-d** wirksam blockiert. Außerdem wurden die Tumorsuppressoren und BET-Inhibitions-Biomarker *HEXIM1* und *p57* signifikant hochreguliert. In *NUT-Midline Carcinoma* (NMC)-Zellen wurden die Onkogene *MYC* und *TP63* herunterreguliert. Bei der Untersuchung der Viabilität von Bauchspeicheldrüsenkrebszellen konnte die Synergie der kombinierten Hemmung von BET-Proteinen und HDACs bestätigt werden. Die dualen Inhibitoren waren bei der Verringerung der Zellviabilität mit IC_{50}-Werten von etwa 3 µM jedoch noch wirksamer. Bei NMC-Zellen konnte kein synergistischer Effekt für die Kombination von BET- und HDAC-Inhibitoren beobachtet werden, aber der duale Inhibitor **132b** war immer noch am effektivsten in der Verringerung der Zelllviabilität (IC_{50} = 220 nM). Insgesamt bilden die vielversprechenden *in-vitro*-Ergebnisse eine Grundlage für künftige Studien mit dualen BET/HDAC-Inhibitoren bei Bauchspeicheldrüsenkrebs und anderen Krebsarten. Da eine pharmakokinetische Studie auf eine suboptimale metabolische Stabilität und eine hohe Clearance der Verbindung **132b** hindeutet, wäre eine zusätzliche Optimierung der Inhibitoren erforderlich, um weitere *in-vivo*-Studien zu fördern.

Bei einem anderen Ansatz wurde die aufkommende PROTAC-Strategie, die darauf abzielt, die relevanten Proteine abzubauen, anstatt sie einfach zu hemmen, für das kombinierte *Targeting* von HDACs und BET-Proteinen verfolgt. Unter Verwendung des oben beschriebenen dualen Inhibitorgerüsts wurden Liganden für die E3-Ligasen CBRN und VHL angebracht, wodurch die dualen PROTACs **161a-c** und **164a-c** entstanden (**Abbildung 5**). In einem zellulären Target-Engagement-Assay banden die PROTACs schwächer als die dualen Inhibitoren, zeigten aber dennoch EC_{50}-Werte im

niedrigen mikromolaren Bereich für BRD4 und im nanomolaren Bereich für HDAC1/2. Die Auswertung mittels eines fluoreszenzbasierten HiBiT-Assays zeigte jedoch keinen Abbau von BRD4.

161a: X = (CH$_2$)$_4$
161b: X = (CH$_2$OCH$_2$)$_2$
161c: X = (CH$_2$OCH$_2$)$_2$NH(CO)

164a: X = (CH$_2$OCH$_2$)$_2$
164b: X = (CH$_2$OCH$_2$)$_3$
164c: X = (CH$_2$)$_6$
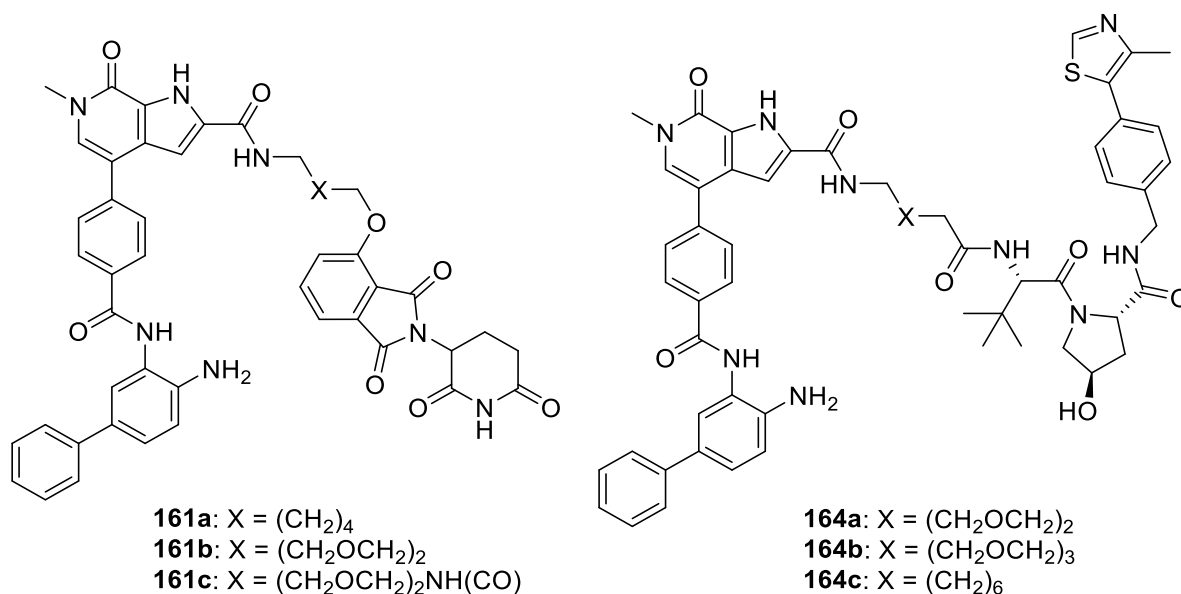
Abbildung 5: Pyrrolopyridon-basierte duale BET/HDAC PROTACs. Die synthetisierten Verbindungen zeigten eine zelluläre Bindung an BRD4 und HDAC1/2, aber keinen Abbau von BRD4

Aus diesem Grund wurde eine weitere Reihe von PROTACs auf der Basis von Diazepin **19** entwickelt und synthetisiert, woraus die Verbindungen **175a**-**f** und **177a**-**e** hervorgingen (**Abbildung 6**). Im HiBiT-Assay konnten einige der getesteten *Degrader* die BRD4-Werte senken. Die Analyse mittels Western Blot zeigte ebenfalls eine Verringerung der BRD4-Werte nach der Anwendung in zwei verschiedenen Bauchspeicheldrüsenkrebs-Zelllinien, wobei die stärkste Wirkung von den Thalidomid-basierten PROTACs **175b** und **e** ausging. Interessanterweise konnte eine leichte Selektivität für BRD4 festgestellt werden, wobei nur eine geringe Verringerung der BRD2-Werte zu beobachten war. Die Untersuchung der HDAC1-Werte zeigte eine Wirkung nach der Anwendung von Substanz **175e** nach 48 Stunden. Dies war der einzige PROTAC, bei dem eine Verringerung der HDAC1-Werte zusammen mit einer erhöhten Histonacetylierung festgestellt werden konnte. Darüber hinaus verringerte PROTAC **175e** die Viabilität von PatuT-Zellen der Bauchspeicheldrüse mit einem IC$_{50}$-Wert von 800 nM stark. Dies war wirksamer als alle zuvor untersuchten dualen BET/HDAC-Inhibitoren und spricht daher für weitergehende biologische Untersuchungen.

Die Experimente sollten unter Verwendung eines Proteasominhibitors wiederholt werden, um festzustellen, ob die beobachteten Wirkungen tatsächlich auf den Proteinabbau zurückzuführen sind. Darüber hinaus wäre der Einsatz von massenspektrometriebasierten *Proteomics*-Untersuchungen interessant, um die Selektivität von Verbindung **175e** zu bewerten. Insgesamt scheint die Anwendung

von PROTACs für die gleichzeitige Anwendung auf zwei verschiedenen Klassen von Proteinen eine umsetzbare alternative Strategie zu sein, die weiter untersucht werden sollte.

175a: Y = O; X = CH₂OCH₂
175b: Y = O; X = (CH₂OCH₂)₂
175c: Y = O; X = (CH₂OCH₂)₃
175d: Y = N; X = CH₂
175e: Y = N; X = (CH₂)₆
175f: Y = N; X = (CH₂)₄

177a: X=O
177b: X=OCH₂CH₂O
177c: X=(CH₂OCH₂)₂CH₂O
177d: X=(CH₂)₃
177e: X=(CH₂)₄
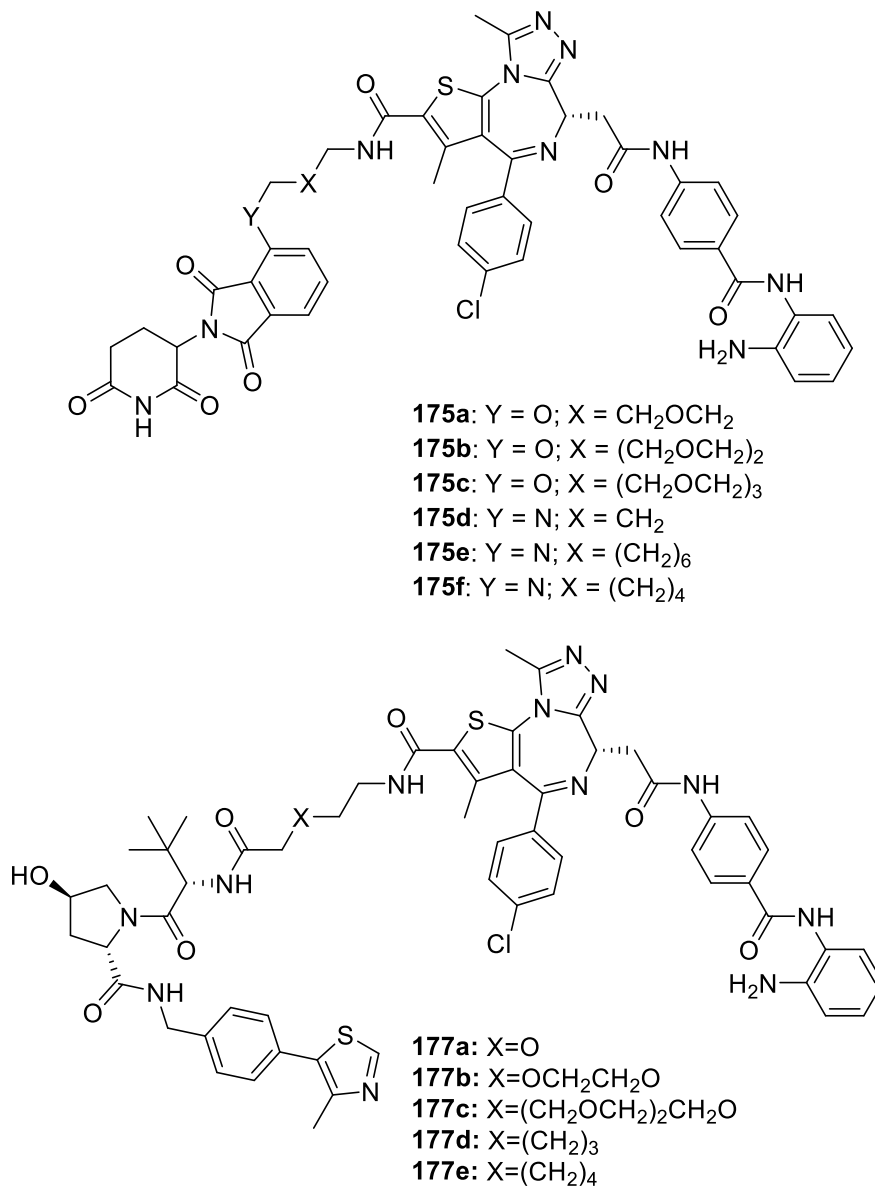
Abbildung 6: Diazepin-basierte duale BET/HDAC PROTACs. Substanz **175e** gelang es, die Werte von BRD4 und HDAC1 zu verringern und die Lebensfähigkeit von Bauchspeicheldrüsenkrebszellen wirksam zu reduzieren.

Zusammenfassend lässt sich sagen, dass diese Arbeit verschiedene Ansätze für das gleichzeitige Adressieren von epigenetischen Leser- und Modifikationsproteinen hervorgebracht hat. Durch die Entwicklung eines neuartigen Gerüsts, das selektiv HDAC1/2 zusammen mit BET-Proteinen in Zellen hemmt, wurde ein wirksames Instrument für die Untersuchung von Bauchspeicheldrüsenkrebs und anderen Krankheiten, die auf epigenetische Prozesse ansprechen, geschaffen. Die geringe Größe der Verbindung bietet zudem die Möglichkeit, den Inhibitor in Richtung optimierter pharmakokinetischer Eigenschaften weiterzuentwickeln, was zu einem Medikament für die Krebsbehandlung führen könnte.

Ein zweiter neuer Ansatz, der verfolgt wurde, war die Entwicklung eines *Degraders*, der auf HDACs und BET-Proteine abzielt. Durch die Synthese einer Vielzahl verschiedener Moleküle wurde eine Verbindung entwickelt, die in der Lage ist, den BRD4-Wert zu senken und gleichzeitig die Histon-Acetylierung zu erhöhen. Obwohl weitere mechanistische Untersuchungen erforderlich sind, um den Abbau zu verifizieren, ermutigen die starken antiproliferativen Wirkungen in Bauchspeicheldrüsenkrebszellen zu weiteren Studien zu dieser neuen alternativen Strategie.

6   Methods

6.1 Biophysical Characterization

Differential scanning fluorimetry (DSF)

The effects of inhibitor binding on the apparent melting temperature of recombinant bromodomains were determined by DSF in a 96-well plate (Starlab) at a protein concentration of 2 µM with 10 µM compound in buffer containing 25 mM HEPES, pH 7.5, 150 mM NaCl, and 0.5 mM TCEP. SYPRO Orange (5000×, Invitrogen), a dye that shows strong fluorescence upon binding to hydrophobic regions of unfolded proteins, was added at a dilution of 1:1000 (final concentration of 5x). Protein unfolding profiles were recorded using an MX3005P real-time qPCR instrument (Agilent; excitation/emission filters = 492/610 nm) while increasing the temperature from 25 to 95 °C at a heating rate of 3 °C/min. T_m values were calculated after fitting the fluorescence curves to the Boltzmann equation. Differences in melting temperature upon compound binding are given as $\Delta T_m = T_m$ (protein with inhibitor) - T_m (protein without inhibitor). Measurements were performed in triplicates.

Crystallization and structure determination.

Protein crystallization and structure solution was performed by Dimitrios-Ilias Balourdas. Crystals of BRD4 in complex with dual inhibitors were grown using the sitting-drop vapor-diffusion technique at 277 K utilizing a mosquito crystallization robot (TTP Labtech, Royston, UK). BRD4 BD1 protein (10 mg/mL in 25 mM HEPES pH 7.5, 150 mM NaCl, 0.5 mM TCEP, 5% glycerol) was incubated with inhibitors at a final concentration of 1 mM prior to setting up crystallization trials. Crystals were cryo-protected with mother liquor supplemented with 23% ethylene glycol and flash-frozen in liquid nitrogen. X-ray diffraction data sets were collected at 100 K at beamline X06SA of the Swiss Light Source, Villigen, Switzerland. The obtained diffraction data were integrated with the program XDS and scaled with AIMLESS, which is part of the CCP4 package. The structures were then solved by molecular replacement using PHASER or by difference Fourier analysis using PHENIX with PDB entry 6YQN as a starting model. Structure refinement was performed using iterative cycles of manual model building in COOT and refinement in PHENIX. Dictionary files for the compounds were generated using the Grade Web Server (http://grade.globalphasing.org).

Isothermal titration calorimetry (ITC)

ITC measurements were performed by Dimitrios-Ilias Balourdas. Measurements were performed using a Nano ITC micro-calorimeter (TA Instruments, New Castle, Pennsylvania). For all experiments, reverse titration was performed (syringe containing the protein solution; cell containing the ligand) in ITC buffer containing 25 mM HEPES, pH 7.5, 150 mM NaCl, 0.5 mM TCEP, and 5% glycerol. All compounds were diluted from 50 mM DMSO stocks to 20 µM in ITC buffer and BRD4-BD1 was diluted to 120 µM in

a DMSO-adjusted ITC buffer. BRD4-BD1 (120 µM) was titrated into the compound solution (20 µM) with an initial injection (4 µL) followed by 29 identical injections (8 µL), at a rate of 0.5 µL/s and with 150 or 200 s intervals. All experiments were performed at 15 °C whilst stirring at 350 rpm. The heat of dilution was determined by independent titrations (protein into buffer) and was subtracted from the experimental raw data. Data were processed using the NanoAnalyze software (version 3.10.0) provided by the instrument manufacturer. The first injection was excluded from the analysis, and fitted curves were generated by applying the independent model (single binding site) to the raw data.

NanoBRET assay

The NanoBRET assays were performed by Lena Marie Berger and Benedict-Tilman Berger. The assay was performed as described by Machleidt *et al.*[312] In brief: BRD4 bromodomains and full-length HDACs were obtained as plasmids cloned in frame with a terminal NanoLuc fusion (Promega). Plasmids were transfected into HEK293T cells using FuGENE HD (Promega, E2312), and proteins were allowed to express for 20 h. Serially diluted inhibitor and the corresponding NanoBRET Tracer (Promega) at a concentration determined previously as the tracer $K_{D,app}$ were pipetted into white 384-well plates (Greiner #781207) for BRD assays or white 96-well plates (Corning #3600) for HDAC using an Echo acoustic dispenser (Labcyte). The corresponding protein-transfected cells were added and reseeded at a density of 2x 10^5 cells/mL after trypsinization and resuspending in Opti-MEM without phenol red (Life Technologies). The system was allowed to equilibrate for 2 hours at 37 °C/5% CO_2 prior to BRET measurements. To measure BRET, NanoBRET NanoGlo substrate + Extracellular NanoLuc Inhibitor (Promega, N2540) was added as per the manufacturer's protocol, and filtered luminescence was measured on a PHERAstar plate reader (BMG Labtech) equipped with a luminescence filter pair (450 nm BP filter (donor) and 610 nm LP filter (acceptor)). For lysed-mode NanoBRET experiments, digitonin (Promega, #G9441) was added as per the manufacturer's instructions to a final concentration of 50 ng/mL. Competitive displacement data were then graphed using a normalized 3-parameter curve fit with the following equation: Y=100/(1+10^(X-LogIC_{50})).

HDAC selectivity profile

Selectivity and inhibition of HDAC enzymatic activity was tested for compound **132b** at a concentration of 1 µM and 10 µM against all zinc-dependent human HDACs (HDAC1-11). The reactions were performed by Reaction Biology using a protease-coupled assay with fluorogenic substrates where, after deacetylation by the HDAC and subsequent proteolytic digest, the free fluorophore 7-amino-4-methyl coumarin (AMC) can be quantified.[313] The following substrates were used for the activity assays: HDACs 1, 2, 3, and 6,: fluorogenic tetrapeptide from p53 residues 379-382 (RHKK(Ac)AMC); HDACs 4, 5, 7, 9, and 11: fluorogenic HDAC class2a substrate (trifluoroacetyl lysine); HDAC8: twice

acetylated fluorogenic tetrapeptide from p53 residues 379-382 (RHK(Ac)K(Ac)AMC); HDAC10: Ac-spermidine-AMC. Data are given as % residual activity compared with the uninhibited control reaction.

6.2 Biological Characterization

HiBiT assay

HiBiT measurements were performed by Martin Schwalm, as previously described.[314]

The biological evaluation of the synthesized compounds in cancer cell lines was performed by Xin Zhang, Joel R. Schneider and Nick A. Klopp from the group of Prof. Jens T. Siveke.

Cell culture and reagents

Pancreatic ductal adenocarcinoma cell line PaTu 8988T was obtained from ATCC and cultured in Dulbecco's Modified Eagle Medium (DMEM) containing 10% FBS, 25 mM glucose, 4 L-glutamine, 1 mM sodium pyruvate and 1% penicillin-streptomycin. Nut midline carcinoma cell line HCC2429 was kindly provided by Lead Discovery Center GmbH (Dortmund, Germany) and was cultured in RPMI1640 medium containing 10% FBS, 2 mM L-glutamine and 1% penicillin-streptomycin. Cell line PaTu 8988T was authenticated using Multiplex human Cell line Authentication Test (MCA) by Multiplexion GmbH and cell line HCC2429 was authenticated using short tandem repeat (STR) profiling.

Cell viability assays

The assays was performed using Promega's CellTiter-Glo Luminescent Cell Viability Assay kit (Cat. #G7571). First, compounds dissolved in DMSO were printed in 96-well plates (Corning) using Tecan D300e digital dispenser. Then, cells were seeded into the compound-printed plates using Thermo Mulitidrop reagent dispenser. 72 h later, one volume of diluted CellTiter-Glo reagent (1:4 dilution with PBS) was added to individual well using Thermo Multidrop reagent dispenser again. Plates were shaken for 2 min and incubated for 10 min in the dark. Luminescent signals were read by Tecan Spark Multimode Microplate Reader. The values were normalized to the DMSO control wells and presented as percentage of cell viability. Dose-response curves were drawn by GraphPad Prism 8.

Immunoblot analysis

Protein samples were prepared in RIPA buffer (9806S, Cell Signaling Technology) containing protease inhibitor cocktail (Roche). Proteins were separated in SDS-polyacrylamide gels, transferred to nitrocellulose membranes with Trans-Blot Turbo Transfer System (Bio-Rad) and incubated with antibodies dissolved in TBS buffer containing 5% BSA and 0.1% Tween20. The following primary antibodies were used: rabbit anti-β-actin (ab8227, Abcam) and rabbit anti-acetyl-histone H3 (Lys9/Lys14; 9677, Cell Signaling Technology). Primary antibodies were recognized by a peroxidase-coupled secondary antibody (Jackson), and signals were detected by chemiluminescence.

RNA extraction and quantitative RT-PCR analysis

Total RNA was extracted from cell culture using Maxwell RSC simplyRNA Cells Kit (Promega) according to the manufacturer's protocol. cDNA was synthesized using PrimeScript Reverse Transcriptase (TakaRa) and amplified using home-made PCR master mix. The amplicon was detected by EvaGreen Dye using LightCycler 480 instrument (Roche). PCR conditions were 5 min at 95 °C, followed by 45 cycles of 95 °C for 10 sec, 59 °C for 10 sec and 72 °C for 20 sec. The relative gene expression levels were normalized to GUSB and calculated using $2^{-\Delta\Delta Ct}$ method.

6.3 Chemical Synthesis

Chemistry

Compound synthesis is described in detail in the Supporting Information, including analytical data for all final products. All commercial chemicals were purchased from common suppliers in reagent grade and used without further purification. For compound purification by flash chromatography, a puriFlash XS 420 device with a UV-VIS multiwave detector (200–400 nm) from Interchim with pre-packed normal-phase PF-SIHP silica columns with particle sizes of 30 μm (Interchim) was used. Synthesized compounds were characterized by NMR and mass spectrometry (ESI). In addition, final inhibitors were identified by high-resolution mass spectrometry (HRMS), and their purity was evaluated by HPLC. ^{1}H and ^{13}C NMR spectra were measured on an AV300, an AV400, or an AV500 HD AVANCE III spectrometer from Bruker. Chemical shifts (δ) are reported in parts per million (ppm). DMSO-d_6 was used as a solvent, and the spectra were referenced to the residual solvent signal: 2.50 ppm (^{1}H NMR) or 39.52 ppm (^{13}C NMR). Abbreviations: s = singlet, br = broad signal, d = doublet, dd = doublet of doublets, ddd = doublet of doublets of doublets, dt = doublet of triplets, t = triplet, td = triplet of doublets, q = quartet, m = multiplet, {1H} = 1H-decoupled

HRMS was measured on a MALDI LTQ Orbitrap XL from ThermoScientific. Determination of the compound purity by HPLC was carried out on an Agilent 1260 Infinity II device with a 1260 DAD HS detector (G7117C; 254 nm, 280 nm, 310 nm) and an LC/MSD device (G6125B, ESI pos. 100-1000). The compounds were analyzed on a Poroshell 120 EC-C18 (Agilent, 3 x 150 mm, 2.7 μm) reversed phase column using 0.1% formic acid in water (A) and 0.1% formic acid in acetonitrile (B) as a mobile phase. The following gradient was used: 0 min: 5% B - 2 min: 80% B - 5 min: 95% B - 7 min: 95% B (flow rate of 0.6 mL/min.). UV-detection was performed at 320 nm (150 nm bandwidth), and all compounds used for further biological characterization showed > 95% purity. Synthesis of the cubane scaffold was carried out together with Nicolai D. Raig.

General procedure for *N-Boc* deprotection

The *Boc*-protected aniline was dissolved in DCM/TFA (3/1) and stirred for 1 h at ambient temperature. Afterwards, volatiles were removed under reduced pressure, the residue was dissolved in ethyl acetate and washed with sat. aq NaHCO$_3$ and brine. The organic phase was dried over MgSO$_4$, filtered, and volatiles were removed under reduced pressure.

General procedure for Suzuki coupling A

The respective arylboronic acid (1.2 eq), *tert*-Butyl (4-bromo-2-nitrophenyl)carbamate (**33**, 1.0 eq), potassium carbonate (3.0 eq), Pd XPhos G2 (0.05 eq) and XPhos (0.05 eq) were dissolved in DMF/water (2/1, 85 mM) and purged with argon for 10 min. The mixture was heated at 100 °C for 2 h, cooled to ambient temperature and partitioned between water and DCM. The DCM layer was washed with brine, dried over MgSO$_4$, filtered, and volatiles were removed under reduced pressure to provide the crude product. The residue was then triturated with methanol and filtered.

General procedure for Suzuki coupling B

6-Methyl-4-(4,4,5,5-tetramethyl-1,3,2-dioxaborolan-2-yl)-1-tosyl-1,6-dihydro-7*H*-pyrrolo[2,3-*c*]pyridin-7-one (**15**, 1.0 eq), the aryl halide (1.2 eq), K$_3$PO$_4$ (2.5 eq), Pd XPhos G2 (0.05 eq) and XPhos (0.05 eq) were dissolved in dioxane/water (4/1, 50 mM) and purged with argon for 10 minutes. The mixture was heated at 70 °C for 1 h, cooled to ambient temperature and partitioned between water and ethyl acetate. The ethyl acetate layer was washed with brine, dried over MgSO$_4$, filtered, and volatiles were removed under reduced pressure to provide the crude product.

General procedure for reduction of nitro groups

A mixture of the starting material (1.0 eq), ammonium chloride (7.0 eq) and iron powder (7.0 eq) in methanol/water (9/1) was heated at 85 °C for 3 h. After cooling to ambient temperature, the mixture was filtered through a plug of celite, and the filtrate was partitioned between water and DCM. The DCM layer was washed with brine, dried over MgSO$_4$, filtered, and volatiles were removed under reduced pressure.

General procedure for azo coupling

The aniline (1.0 eq) was dissolved in MeOH/ACN (1/1) and cooled to -10 °C. To this solution were added conc. HCl (1.0 eq) and *iso*-amyl nitrite (1.0 eq), and the mixture was stirred for 1 h, during which the mixture turned yellow due to the formation of the diazonium salt. In a separate flask, the phenol (1.0 eq) and K_2CO_3 (5.0 eq) were dissolved in MeOH/H_2O/ACN (3/2/1), the mixture was purged with argon for 10 min and cooled to -10 °C. The dissolved diazonium compound was slowly added to the second mixture, which instantly turned red. The mixture was stirred for 2 h while being slowly warmed to ambient temperature. Then, the mixture was partitioned between water and ethyl acetate, and the organic layer was washed with brine, dried over $MgSO_4$, filtered and concentrated under reduced pressure. The crude product was purified by flash chromatography to provide the title compound.

General procedure for ester and tosylamide hydrolysis

The ester and LiOH · H_2O (7 eq) were dissolved in dioxane/water (4/1, 100 mM) and heated at 80 °C for 2 h. The mixture was cooled to ambient temperature and brought to a pH of 3 by the addition of 5% aq HCl. The resulting precipitate was filtered and dried under reduced pressure to provide the product.

General procedure for amide coupling

Carboxylic acid (1.0 eq), amine (1.2 eq) and (7-Azabenzotriazol-1-yloxy)tripyrrolidinophosphonium hexafluorophosphate (PyAOP, 1.3 eq) were dissolved in anh. DMF (40 mM) and *N,N*-diisopropylethylamine (1.3 eq) was added. The mixture was stirred at ambient temperature for 16 h and partitioned between water and ethyl acetate. The ethyl acetate layer was washed with brine, dried over $MgSO_4$, filtered, and volatiles were removed under reduced pressure.

tert-Butyl (4-bromo-2-nitrophenyl)carbamate (24)
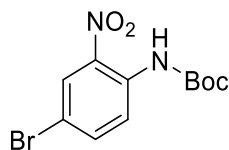
The synthesis was performed as described by Bauer *et al.*[277] 4-Bromo-2-nitroaniline (**23**, 7.00 g, 32.3 mmol, 1.0 eq), was dissolved in anh. THF (100 mL), cooled to -10 °C and sodium hydride (60%, 1.70 g, 71.0 mmol, 2.2 eq) was carefully added. After 10 minutes, a solution of di-*tert*-butyl dicarbonate (7.74 g, 35.5 mmol, 1.1 eq) in THF (60 mL) was added dropwise and the mixture was stirred for 4 h. The reaction was quenched with ice and the mixture was partitioned between water and ethyl acetate. The ethyl acetate layer was washed with brine, dried over $MgSO_4$, filtered, and volatiles were removed under reduced pressure. Purification by chromatography (hexane/ethyl acetate) provided the product as a pale yellow solid (9.45 g, 92%). ^{1}H-NMR (300 MHz, DMSO-d6) δ 9.66

(s, 1H), 8.12 (d, J = 2.3 Hz, 1H), 7.86 (dd, J = 8.8, J = 2.4 Hz, 1H), 7.60 (d, J = 8.8 Hz, 1H), 1.44 (s, 9H). MS (ESI): m/z calc. for $[C_{11}H_{13}BrN_2O_4+Na^+]^+$ = 339.00, found = 338.92

**_tert_-Butyl (2-nitro-4-(thiophen-2-yl)phenyl)carbamate (25a)**
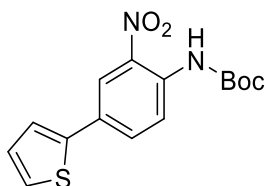
The synthesis was performed as described by Bauer _et al._[277] The synthesis was performed according to "general procedure for Suzuki coupling A". _tert_-Butyl (4-bromo-2-nitrophenyl)carbamate (**24**, 1.90 g, 5.99 mmol, 1.0 eq) and thiophen-2-ylboronic acid (920 mg, 7.19 mmol, 1.2 eq) were used. The product was isolated as an orange solid (1.13 g, 59%). ^{1}H-NMR (300 MHz, DMSO-d_6) δ 9.63 (s, 1H, g), 8.15 (d, J = 2.2 Hz, 1H), 7.94 (dd, J = 8.6, J = 2.3 Hz, 1H), 7.70 (d, J = 8.7 Hz, 1H), 7.64 – 7.60 (m, 2H), 7.17 (dd, J = 5.0, J = 3.7 Hz, 1H), 1.45 (s, 9H). MS (ESI): m/z calc. for $[C_{15}H_{16}N_2O_4S+Na^+]^+$ = 343.07, found = 343.09

tert-Butyl (4-(furan-2-yl)-2-nitrophenyl)carbamate (25b)
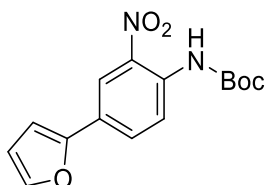
The synthesis was performed as described by Bauer _et al._[277] The synthesis was performed according to "general procedure for Suzuki coupling A". _tert_-Butyl (4-bromo-2-nitrophenyl)carbamate (1.94 g, 6.12 mmol, 1.0 eq) and furan-2-ylboronic acid (821 mg, 7.34 mmol, 1.2 eq) were used. The product was isolated as an orange solid (1.27 g, 68%). ^{1}H-NMR (300 MHz, DMSO-d_6) δ 9.63 (s, 1H), 8.19 (d, J = 2.1 Hz, 1H), 7.97 (dd, J = 8.6, J = 2.1 Hz, 1H), 7.80 (dd, J = 1.8, J = 0.6 Hz, 1H), 7.73 (d, J = 8.6 Hz, 1H), 7.10 (dd, J = 3.4, J = 0.6 Hz, 1H), 6.63 (dd, J = 3.4, J = 1.8 Hz, 1H), 1.45 (s, 9H). MS (ESI): m/z calc. for $[C_{15}H_{16}N_2O_5+Na^+]^+$ = 327.10, found = 327.09

tert-Butyl (3-nitro-[1,1'-biphenyl]-4-yl)carbamate (25d)
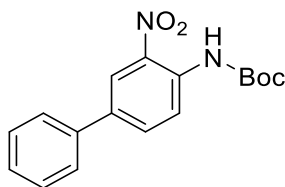
The synthesis was performed as described by Bauer *et al.*[277] The synthesis was performed according to "general procedure for Suzuki coupling A". *tert*-Butyl (4-bromo-2-nitrophenyl)carbamate (**24**, 2.00 g, 6.31 mmol, 1.0 eq) and phenylboronic acid (923 mg, 7.57 mmol, 1.2 eq) were used. The product was isolated as an orange solid (1.65 g, 83%). ^{1}H-NMR (300 MHz, DMSO-d$_6$) δ 9.64 (s, 1H), 8.18 (d, *J* = 2.2 Hz, 1H), 7.99 (dd, *J* = 8.6, *J* = 2.2 Hz, 1H), 7.81 – 7.68 (m, 3H), 7.54 – 7.36 (m, 3H), 1.46 (s, 9H). MS (ESI): m/z calc. for $[C_{17}H_{18}N_2O_4+Na^+]^+$ = 337.12, found = 337.11

tert-Butyl (2-amino-4-(thiophen-2-yl)phenyl)carbamate (26a)
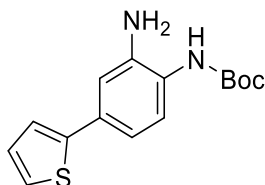
The synthesis was performed as described by Bauer *et al.*[277] The synthesis was performed according to "general procedure for reduction of nitro groups". *tert*-Butyl (2-nitro-4-(thiophen-2-yl)phenyl)carbamate (**25a**, 1.10 g, 3.43 mmol) was used. The product was isolated as a colorless solid (0.928 g, 93%). ^{1}H-NMR (300 MHz, DMSO-d6) δ 8.33 (s, 1H), 7.44 (dd, *J* = 5.1, *J* = 1.1 Hz, 1H), 7.29 (dd, *J* = 3.6, *J* = 1.2 Hz, 1H), 7.27 (d, *J* = 8.4 Hz, 1H), 7.08 (dd, *J* = 5.1, *J* = 3.6 Hz, 1H), 6.98 (d, *J* = 2.1 Hz, 1H), 6.84 (dd, *J* = 8.2, *J* = 2.0 Hz, 1H), 5.00 (s, 2H), 1.47 (s, 9H). MS (ESI): m/z calc. for $[C_{15}H_{18}N_2O_2S+Na^+]^+$ = 313.10, found = 313.06

tert-Butyl (2-amino-4-(furan-2-yl)phenyl)carbamate (26b)
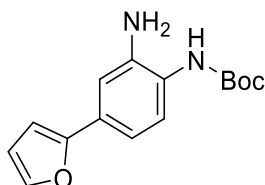
The synthesis was performed as described by Bauer *et al.*[277] The synthesis was performed according to "general procedure for reduction of nitro groups". *tert*-Butyl (4-(furan-2-yl)-2-nitrophenyl)carbamate (**25b**, 1.23 g, 4.04 mmol) was used. The product was isolated as a colorless solid (0.989 g, 89%). ^{1}H-NMR (300 MHz, DMSO-d6) δ 8.32 (s, 1H), 7.66 (dd, *J* = 1.8, *J* = 0.7 Hz, 1H), 7.28 (d, *J* = 8.3 Hz, 1H), 7.04

(d, *J* = 2.0 Hz, 1H), 6.88 (dd, *J* = 8.2, *J* = 2.0 Hz, 1H), 6.68 (dd, *J* = 3.3, *J* = 0.7 Hz, 1H), 6.53 (dd, *J* = 3.4, *J* = 1.8 Hz, 1H), 4.98 (s, 2H), 1.46 (s, 9H). MS (ESI): m/z calc. for $[C_{17}H_{20}N_2O_2+Na^+]^+$ = 297.12, found = 297.11

tert-butyl (2-amino-4-(pyridin-4-yl)phenyl)carbamate (26c)
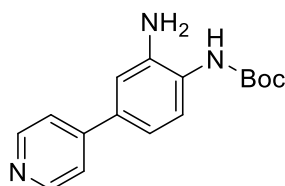
The synthesis was performed as described by Bauer *et al.*[277] The synthesis was performed according to "general procedure for Suzuki coupling A". *tert*-butyl (2-amino-4-bromophenyl)carbamate (1.00 g, 3.48 mmol, 1.0 eq) and phenylboronic acid (471 mg, 3.83 mmol, 1.1 eq) were used. The product was isolated as an orange solid (480 mg, 48%). ^{1}H-NMR (250 MHz, DMSO-d_6) δ 8.62-8.47 (m, 2H), 8.41 (s, 1H), 7.61-7.47 (m, 2H), 7.40 (d, *J* = 8.3 Hz, 1H), 7.10 (d, *J* = 2.1 Hz, 1H), 6.96 (dd, *J* = 8.2, 2.0 Hz, 1H), 5.05 (s, 2H), 1.46 (s, 9H). MS (ESI): m/z calc. for $[M+H^+]^+$ = 286.16, found = 286.19

tert-Butyl (3-amino-[1,1'-biphenyl]-4-yl)carbamate (26d)
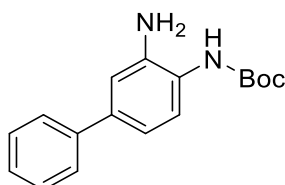
The synthesis was performed as described by Bauer *et al.*[277] The synthesis was performed according to "general procedure for reduction of nitro groups". *tert*-Butyl (3-nitro-[1,1'-biphenyl]-4-yl)carbamate (**25d**, 1.47 g, 4.68 mmol) was used. The product was isolated as a colorless solid (1.288 g, 97%). ^{1}H-NMR (300 MHz, DMSO-d6) δ 8.34 (s, 1H), 7.56 – 7.51 (m, 2H), 7.46 – 7.39 (m, 2H), 7.34 – 7.28 (m, 2H), 6.99 (d, *J* = 2.1 Hz, 1H), 6.83 (dd, *J* = 8.2, *J* = 2.2 Hz, 1H), 4.95 (s, 2H), 1.47 (s, 9H). MS (ESI): m/z calc. for $[C_{17}H_{20}N_2O_2+Na^+]^+$ = 307.14, found = 307.05

tert-Butyl (2-(4-aminobenzamido)-4-(thiophen-2-yl)phenyl)carbamate (29a)
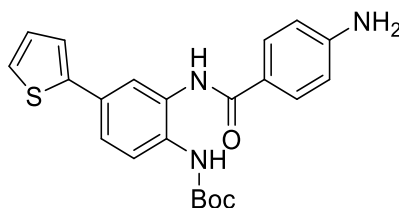
4-((((9H-Fluoren-9-yl)methoxy)carbonyl)amino)benzoic acid (**27**, 217 mg, 603 μmol, 1.0 eq), 1-[bis(dimethylamino)methylene]-1H-1,2,3-triazolo[4,5-b]pyridinium 3-oxide hexafluorophosphate (298 mg, 783 μmol, 1.3 eq) and N,N-diisopropylethylamine (158 μL, 904 μmol, 1.5 eq) were dissolved in DMF (20 mL) and stirred at ambient temperature for 0.5 h. Then, tert-butyl (2-amino-4-(thiophen-2-yl)phenyl)carbamate (**26a**, 176 mg, 603 μmol, 1.0 eq) was added and the mixture was stirred for 16 h. The mixture was partitioned between water and ethyl acetate, the ethyl acetate layer was washed with brine, dried over $MgSO_4$, filtered, and volatiles were removed under reduced pressure. Intermediate **28a** was deprotected without further purification. The residue was then dissolved in DCM/morpholine (1/1, 10 mL) and stirred for 1.5 h at ambient temperature. Volatiles were removed under reduced pressure and the residue was purified by flash chromatography (DCM/methanol) to provide a colorless solid (135 mg, 55%). ^{1}H NMR (400 MHz, DMSO-d_6) δ 9.56 (s, 1H), 8.70 (s, 1H), 7.82 (d, J = 2.2 Hz, 1H), 7.70 (d, J = 8.6 Hz, 2H), 7.55 (d, J = 8.5 Hz, 1H), 7.52 (dd, J = 5.1, 1.1 Hz, 1H), 7.47 (dd, J = 8.5, 2.2 Hz, 1H), 7.44 (dd, J = 3.6, 1.1 Hz, 1H), 7.13 (dd, J = 5.1, 3.6 Hz, 1H), 6.62 (d, J = 8.6 Hz, 2H), 5.83 (s, 2H), 1.47 (s, 9H). MS (ESI): m/z calc. for $[C_{22}H_{23}N_3O_3S+Na^+]^+$ = 432.14, found = 432.07

tert-butyl (2-(4-aminobenzamido)-4-(furan-2-yl)phenyl)carbamate (29b)
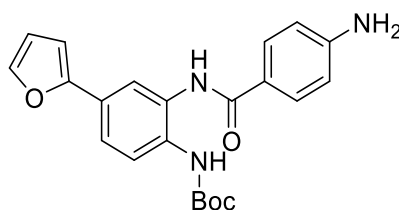
4-((((9H-Fluoren-9-yl)methoxy)carbonyl)amino)benzoic acid (**27**, 317 mg, 882 μmol, 1.1 eq), 1-[bis(dimethylamino)methylene]-1H-1,2,3-triazolo[4,5-b]pyridinium 3-oxide hexafluorophosphate (396 mg, 1.04 mmol, 1.3 eq) and N,N-diisopropylethylamine (182 μL, 1.04 mmol, 1.3 eq) were dissolved in DMF (20 mL) and stirred at ambient temperature for 0.5 h. Then, tert-butyl (2-amino-4-(furan-2-yl)phenyl)carbamate (**26b**, 220 mg, 802 μmol, 1.0 eq) was added and the mixture was stirred for 16 h. The mixture was partitioned between water and ethyl acetate, the ethyl acetate layer was washed with brine, dried over $MgSO_4$, filtered, the volatiles were removed under reduced pressure and the residue was purified by flash chromatography (hexane/ethyl acetate) to provide the Fmoc-protected intermediate (260 mg, 53%). ^{1}H NMR (300 MHz, DMSO-d_6) δ 10.05 (s, 1H), 9.79 (s, 1H), 8.72

(s, 1H), 7.92 (d, *J* = 6.8 Hz, 4H), 7.87 (d, *J* = 2.0 Hz, 1H), 7.77 (d, *J* = 7.3 Hz, 2H), 7.73 (d, *J* = 1.8 Hz, 1H), 7.66 – 7.56 (m, 2H), 7.53 (dd, *J* = 8.5, 2.1 Hz, 1H), 7.48 – 7.32 (m, 5H), 6.88 (d, *J* = 3.4 Hz, 1H), 6.59 (dd, *J* = 3.4, 1.8 Hz, 1H), 4.54 (d, *J* = 6.6 Hz, 2H), 4.34 (t, *J* = 6.5 Hz, 1H), 1.46 (s, 9H). MS (ESI): m/z calc. for $[M+H^+]^+$ = 616.24, found = 615.20

The residue was then dissolved in DCM/morpholine (1/1, 10 mL) and stirred for 1.5 h at ambient temperature. Volatiles were removed under reduced pressure and the residue was purified by flash chromatography (DCM/methanol) to provide a colorless solid (122 mg, 76%). ^{1}H NMR (400 MHz, DMSO-*d*[6]) δ 9.54 (s, 1H), 8.71 (s, 1H), 7.86 (d, *J* = 2.0 Hz, 1H), 7.73 (dd, *J* = 1.8, 0.7 Hz, 1H), 7.70 (d, *J* = 8.7 Hz, 2H), 7.56 (d, *J* = 8.5 Hz, 1H), 7.50 (dd, *J* = 8.5, 2.1 Hz, 1H), 6.86 (dd, *J* = 3.4, 0.8 Hz, 1H), 6.62 (d, *J* = 8.7 Hz, 2H), 6.58 (dd, *J* = 3.4, 1.8 Hz, 1H), 5.83 (s, 2H), 1.47 (s, 9H). MS (ESI): m/z calc. for $[M+H^+]^+$ = 394.17, found = 394.22

tert-butyl (2-(4-aminobenzamido)-4-(pyridin-4-yl)phenyl)carbamate (29c)
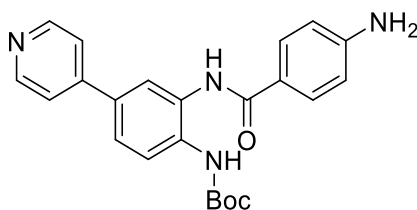
4-((((9*H*-Fluoren-9-yl)methoxy)carbonyl)amino)benzoic acid (**27**, 604 mg, 1.68 mmol, 1.0 eq), 1-[bis(dimethylamino)methylene]-1*H*-1,2,3-triazolo[4,5-*b*]pyridinium 3-oxide hexafluorophosphate (760 mg, 2.00 mmol, 1.2 eq) and *N,N*-diisopropylethylamine (350 μL, 2.01 mmol, 1.2 eq) were dissolved in DMF (20 mL) and stirred at ambient temperature for 0.5 h. Then, *tert*-butyl (2-amino-4-(pyridin-4-yl)phenyl)carbamate (**26c**, 480 mg, 1.68 mmol, 1.0 eq) was added and the mixture was stirred for 16 h. The mixture was partitioned between water and ethyl acetate, the ethyl acetate layer was washed with brine, dried over MgSO₄, filtered, the volatiles were removed under reduced pressure and the residue was purified by flash chromatography (hexane/ethyl acetate) to provide the crude *Fmoc*-protected intermediate. MS (ESI): m/z calc. for $[M+H^+]^+$ = 627.26, found = 627.38

The residue was then dissolved in DCM/morpholine (1/1, 10 mL) and stirred for 1.5 h at ambient temperature. Volatiles were removed under reduced pressure and the residue was purified by flash chromatography (DCM/methanol) to provide a colorless solid (168 mg, 25%). ^{1}H NMR (400 MHz, DMSO-*d*[6]) δ 9.61 (s, 1H), 8.82 (s, 1H), 8.64 – 8.61 (m, 2H), 7.96 (d, *J* = 2.1 Hz, 1H), 7.75 – 7.70 (m, 2H), 7.69 – 7.66 (m, 3H), 7.63 (dd, *J* = 8.5, 2.2 Hz, 1H), 6.62 (d, *J* = 8.6 Hz, 2H), 5.84 (s, 2H), 1.48 (s, 9H). MS (ESI): m/z calc. for $[M+H^+]^+$ = 405.18, found = 405.26

tert-Butyl (3-(4-aminobenzamido)-[1,1'-biphenyl]-4-yl)carbamate (29d)
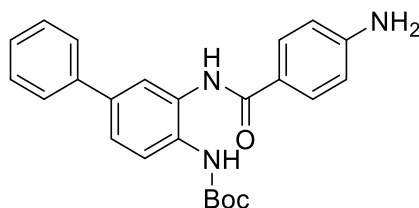
4-(((((9*H*-Fluoren-9-yl)methoxy)carbonyl)amino)benzoic acid (230 mg, 640 µmol, 1.0 eq), 1-[bis(dimethylamino)methylene]-1*H*-1,2,3-triazolo[4,5-*b*]pyridinium 3-oxide hexafluorophosphate (316 mg, 832 µmol, 1.3 eq) and *N*,*N*-diisopropylethylamine (167 µL, 960 µmol, 1.5 eq) were dissolved in DMF (20 mL) and stirred at ambient temperature for 0.5 h. Then, *tert*-butyl (**26a**, 3-amino-[1,1'-biphenyl]-4-yl)carbamate (182 mg, 640 µmol, 1.0 eq) was added and the mixture was stirred for 16 h. The mixture was partitioned between water and ethyl acetate, the ethyl acetate layer was washed with brine, dried over MgSO₄, filtered, and volatiles were removed under reduced pressure. The residue was then dissolved in DCM/morpholine (1/1, 10 mL) and stirred for 1.5 h at ambient temperature. Volatiles were removed under reduced pressure and the residue was purified by flash chromatography (DCM/methanol) to provide a colorless solid (147 mg, 57%). The product was used in the next step without further characterization.

(*S*)-*N*-(2-amino-5-(thiophen-2-yl)phenyl)-4-(2-(4-(4-chlorophenyl)-2,3,9-trimethyl-6*H*-thieno[3,2-*f*][1,2,4]triazolo[4,3-*a*][1,4]diazepin-6-yl)acetamido)benzamide (31a)
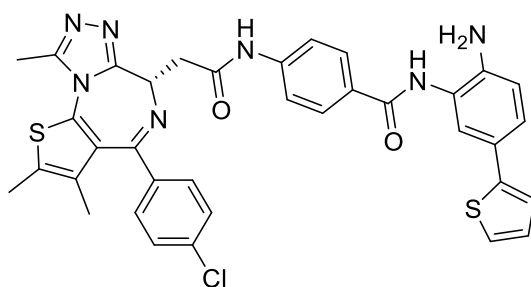
The synthesis was performed according to "general procedure for amide coupling". ¹H NMR (500 MHz, DMSO-*d₆*) δ 10.60 (s, 1H), 9.66 (s, 1H), 8.00 (d, *J* = 8.7 Hz, 2H), 7.77 (d, *J* = 8.8 Hz, 2H), 7.49 (d, *J* = 11.7 Hz, 1H), 7.48 (s, 2H), 7.46 − 7.40 (m, 2H), 7.36 (dd, *J* = 5.1, 1.1 Hz, 1H), 7.30 (dd, *J* = 8.3, 2.2 Hz, 1H), 7.25 (dd, *J* = 3.5, 1.2 Hz, 1H), 7.05 (dd, *J* = 5.1, 3.5 Hz, 1H), 6.82 (d, *J* = 8.4 Hz, 1H), 5.14 (s, 2H), 4.63 (t, *J* = 7.2 Hz, 1H), 3.57 (d, *J* = 7.1 Hz, 2H), 2.61 (s, 3H), 2.43 (s, 3H), 1.64 (s, 3H). ¹³C NMR (126 MHz, DMSO) δ 169.13, 164.88, 163.29, 155.00, 149.96, 144.26, 143.03, 142.03, 136.73, 135.28, 132.32, 130.78, 130.14, 129.89, 129.55, 128.84, 128.81, 128.53, 128.22, 123.91, 123.84, 123.55, 123.21, 122.27, 121.01, 118.17, 116.38, 54.91, 53.68, 14.09, 12.71, 11.32. MS (ESI): m/z calc. for [M+H⁺]⁺ = 692.2, found = 691.5

(*S*)-*N*-(2-amino-5-(furan-2-yl)phenyl)-4-(2-(4-(4-chlorophenyl)-2,3,9-trimethyl-6*H*-thieno[3,2-*f*][1,2,4]-triazolo[4,3-*a*][1,4]diazepin-6-yl)acetamido)benzamide (31b)
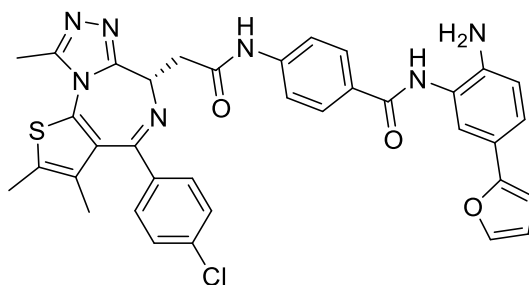
The synthesis was performed according to "general procedure for amide coupling". ^{1}H NMR (500 MHz, DMSO-d_6) δ 10.60 (s, 1H), 9.64 (s, 1H), 8.01 (d, *J* = 8.4 Hz, 2H), 7.78 (d, *J* = 8.4 Hz, 2H), 7.60 (d, *J* = 1.8 Hz, 1H), 7.54 (d, *J* = 2.0 Hz, 1H), 7.49 (d, *J* = 8.5 Hz, 2H), 7.43 (d, *J* = 8.4 Hz, 2H), 7.34 (dd, *J* = 8.4, 2.1 Hz, 1H), 6.83 (d, *J* = 8.4 Hz, 1H), 6.61 (d, *J* = 3.4 Hz, 1H), 6.50 (dd, *J* = 3.3, 1.8 Hz, 1H), 5.15 (s, 2H), 4.64 (t, *J* = 7.1 Hz, 1H), 3.58 (d, *J* = 7.2 Hz, 2H), 2.61 (s, 3H), 2.42 (s, 3H), 1.64 (s, 3H). ^{13}C NMR (126 MHz, DMSO) δ 169.14, 164.91, 163.30, 155.01, 153.82, 149.95, 142.95, 142.02, 141.20, 136.73, 135.29, 132.32, 130.78, 130.14, 129.89, 129.56, 128.87, 128.81, 128.52, 123.43, 122.30, 122.18, 119.24, 118.19, 116.22, 111.79, 102.39, 53.69, 14.07, 12.69, 11.31. MS (ESI): m/z calc. for [M+H^{+}][+] = 676.2, found = 675.8

(*S*)-*N*-(2-amino-5-(pyridin-4-yl)phenyl)-4-(2-(4-(4-chlorophenyl)-2,3,9-trimethyl-6*H*-thieno[3,2-*f*][1,2,4]-triazolo[4,3-*a*][1,4]diazepin-6-yl)acetamido)benzamide (31c)
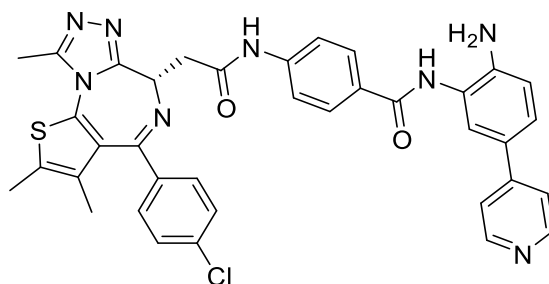
The synthesis was performed according to "general procedure for amide coupling". ^{1}H NMR (400 MHz, DMSO-d_6) δ 10.59 (s, 1H), 9.66 (s, 1H), 8.58 – 8.48 (m, 2H), 8.00 (d, *J* = 8.6 Hz, 2H), 7.77 (d, *J* = 8.7 Hz, 2H), 7.68 (d, *J* = 2.3 Hz, 1H), 7.60 – 7.57 (m, 2H), 7.51 – 7.47 (m, 3H), 7.43 (d, *J* = 8.6 Hz, 2H), 6.89 (d, *J* = 8.4 Hz, 1H), 5.35 (s, 2H), 4.63 (t, *J* = 7.1 Hz, 1H), 3.57 (d, *J* = 7.2 Hz, 2H), 2.61 (s, 3H), 2.45 – 2.39 (m, 3H), 1.73 – 1.51 (m, 3H).

tert-butyl (2-aminophenyl)carbamate (32)
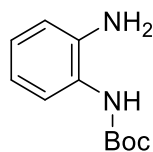
The synthesis was performed as described by Bauer *et al.*[277] Benzene-1,2-diamine (5.00 g, 46.2 mmol, 1.0 eq) was dissolved in DCM (200 mL) and cooled to 0 °C. A solution of di-*tert*-butyl dicarbonate (10.09 g, 46.2 mmol, 1.0 eq) in DCM (100 mL) was added dropwise and the mixture was stirred for 16 h. Afterwards, all volatiles were removed under reduced pressure and the residue was crystallized from hexane/ethyl acetate to provide the title compound as colorless crystals (7.89 g, 82%). ^{1}H NMR (400 MHz, DMSO-d_6) δ 8.26 (s, 1H), 7.19 (d, J = 7.9 Hz, 1H), 6.84 (td, J = 7.6, 1.5 Hz, 1H), 6.69 (dd, J = 8.0, 1.5 Hz, 1H), 6.53 (td, J = 7.5, 1.5 Hz, 1H), 4.80 (s, 2H), 1.47 (d, J = 4.5 Hz, 9H). MS (ESI): m/z calc. for [$C_{11}H_{16}N_2O_2$ +Na$^+$]$^+$ = 231.11, found = 231.05

(9H-Fluoren-9-yl)methyl (4-((2-((tert-butoxycarbonyl)amino)phenyl)carbamoyl)phenyl)-carbamate (33)
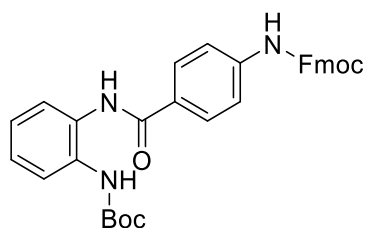
The synthesis was performed as described by Bauer *et al.*[277] The synthesis was performed according to "general procedure for amide coupling". 4-((((9H-fluoren-9-yl)methoxy)carbonyl)amino)benzoic acid (**27**, 5.30 g, 14.8 mmol, 1.0 eq) and compound **32** (3.07 g, 14.8 mmol, 1.0 eq) were used. The crude product (12.74 g (64% purity), quant yield assumed) was used in the next step without further purification. MS (ESI): m/z calc. for [$C_{33}H_{31}N_3O_5$+Na$^+$]$^+$ = 572.22, found = 572.20

tert-Butyl (2-(4-aminobenzamido)phenyl)carbamate (34)
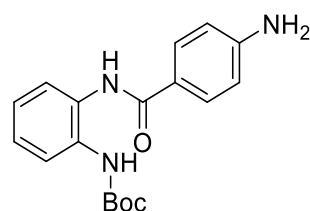
The synthesis was performed as described by Bauer *et al.*[277] **33** (12.74 g, 64% purity, 14.8 mmol) was dissolved in ACN/morpholine (1/1, 200 mL) and stirred at ambient temperature for 16 h. Afterwards, ice water was added and the resulting precipitate was filtered. The filtrate was extracted with DCM, the organic phase was washed with brine, dried over MgSO$_4$ and volatiles were removed under reduced pressure. The crude product was purified by flash chromatography (silica, DCM/MeOH) to provide the title compound as an off-white solid (3.43 g, 71%). ^{1}H NMR (400 MHz, DMSO-d_6) δ 9.48 (s, 1H), 8.65 (s, 1H), 7.73 – 7.65 (m, 2H), 7.55 – 7.52 (m, 1H), 7.50 – 7.46 (m, 1H), 7.14 (ddd, J = 6.6, 3.7, 2.1 Hz, 2H), 6.65 – 6.59 (m, 2H), 5.81 (s, 2H), 1.46 (s, 9H). MS (ESI): m/z calc. for [C$_{18}$H$_{21}$N$_3$O$_3$+H$^+$]$^+$ = 328.16, found = 328.20

Ethyl 1-(*p*-tolyl)-1*H*-1,2,4-triazole-3-carboxylate (37)
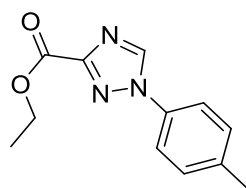
The synthesis was adapted from Zibinsky and Fokin.[271] 4-methyl aniline (**36**, 5.00 g, 46.7 mmol) was dissolved in a mixture of water (25 mL) and HCl (conc., 14 mL) and cooled down to -10 °C in an ice/salt bath. A Solution of NaNO$_2$ (3.22 g, 46.7 mmol) in water (10 mL) was slowly added to the solution of 4-methyl aniline. After the addition was complete, the mixture was stirred for 5 min at 0 °C. The solution of diazonium salt was added dropwise to the mixture of 40.8 g (300 mmol) of NaOAc · 3H$_2$O and ethyl 2-isocyanoacetate (**35**, 5.28 g, 46.7 mmol) in MeOH/H$_2$O (50 mL/5 mL). After addition of a final portion of the diazonium solution, the reaction mixture was stirred at 0 °C for 30 min, warmed up to ambient temperature, and stirred for additional 3 h. After formation of a red precipitate, the mixture was transferred to a round bottom flask and most of methanol was removed *in vacuo*. The remaining suspension of 1,2,4-triazole in water was filtered and the remaining solid precipitate was washed with cold water. Recrystallization of the remaining solid yielded a pinkish solid (4.35 g, 40%). ^{1}H NMR (300 MHz, DMSO-d_6) δ 9.38 (s, 1H), 7.90 – 7.69 (m, 2H), 7.47 – 7.28 (m, 2H), 4.37 (q, J = 7.1 Hz, 2H), 2.37 (s, 3H), 1.33 (t, J = 7.1 Hz, 3H). MS (ESI): m/z calc. for [M+Na$^+$]$^+$ = 254.09, found = 254.08

Ethyl 5-bromo-1-(*p*-tolyl)-1*H*-1,2,4-triazole-3-carboxylate (38)
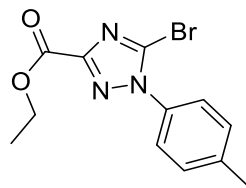
The synthesis was adapted from Zibinsky and Fokin.[271] NaH (60 % in silicon oil, 973 mg, 24.3 mmol) and *N*-bromosuccinimide (6.93 g, 38.9 mmol) were subsequently added to a solution of ethyl 1-p-tolyl-1H-1,2,4-triazole-3-carboxylate (**37**, 2.25 g, 9.73 mmol) in THF (10 mL). The reaction mixture was stirred for 48 h at room temperature. Afterwards, sat. aq NH$_4$Cl was added, and the resulting mixture was extracted with ethyl acetate. Combined organic fractions were dried over sodium sulfate, and then solvents were removed *in vacuo*. The crude product was purified by flash chromatography (silica, hexane/ethyl acetate) to provide the title compound as an off-white solid (2.67 g, 88%). ^{1}H NMR (600 MHz, DMSO-*d*$_6$) δ 7.54 (d, *J* = 8.4 Hz, 2H), 7.44 – 7.39 (m, 2H), 4.37 (q, *J* = 7.1 Hz, 2H), 2.41 (s, 3H), 1.32 (t, *J* = 7.1 Hz, 3H). MS (ESI): m/z calc. for [M+Na$^+$]$^+$ = 332.00, found = 331.87

(5-Bromo-2-nitrophenyl)-*D*-alanine (40)
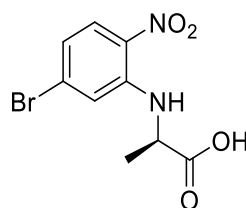
The synthesis was adapted from Hu *et al.*[246] To a solution of 4-bromo-2-fluoro-1-nitrobenzene (**39**, 10.0 g, 45.5 mmol) in EtOH (60 mL) and H$_2$O (20 mL) were added D-alanine (4.45 g, 50.0 mmol) and K$_2$CO$_3$ (6.91 g, 50.0 mmol). The reaction mixture was heated to 80 °C for 3 h. Upon completion, the reaction mixture was acidified with 1 N aq. HCl to pH 2-3. Then, the mixture was filtered, and the solid was dried to give the title compound as a yellow solid (9.12 g, 69%). ^{1}H NMR (400 MHz, DMSO-*d*$_6$) δ 13.30 (s, 1H), 8.38 (d, *J* = 7.1 Hz, 1H), 8.01 (d, *J* = 9.1 Hz, 1H), 7.23 (d, *J* = 2.0 Hz, 1H), 6.90 (dd, *J* = 9.1, 2.0 Hz, 1H), 4.57 (t, *J* = 6.9 Hz, 1H), 1.46 (d, *J* = 6.8 Hz, 3H).

(*R*)-6-bromo-3-methyl-3,4-dihydroquinoxalin-2(1*H*)-one (41)
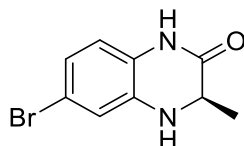
The synthesis was adapted from Hu *et al.*[246] To a solution of compound **40** (8.40 g, 29.1 mmol) and K$_2$CO$_3$ (8.03 g, 58.1 mmol) in H$_2$O (160 mL) was added Na$_2$S$_2$O$_4$ (20.2 g, 116 mmol). The reaction mixture was heated to 60 °C overnight. Upon completion, the reaction mixture was acidified with 1 N aq. HCl to pH 7-8. Then, the mixture was filtered, and the solid was dried to give the title compound as a yellow solid (3.17 g, 45%). ^{1}H NMR (400 MHz, DMSO-d_6) δ 10.29 (s, 1H), 6.81 (d, *J* = 2.2 Hz, 1H), 6.73 (dd, *J* = 8.2, 2.1 Hz, 1H), 6.64 (d, *J* = 8.3 Hz, 1H), 6.26 (d, *J* = 1.7 Hz, 1H), 3.81 (dd, *J* = 6.7, 1.7 Hz, 1H), 1.24 (d, *J* = 6.6 Hz, 3H). MS (ESI): m/z calc. for [M+H$^+$]$^+$ = 240.99, found = 240.96

(*R*)-6-bromo-4-cyclopentyl-3-methyl-3,4-dihydroquinoxalin-2(1*H*)-one (42)
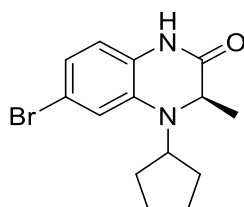
The synthesis was adapted from Hu *et al.*[246] A solution of compound **41** (3.15 g, 13.1 mmol), phenylsilane (4.83 mL, 39.2 mmol), cyclopentanone (3.47 mL, 39.2 mmol), and dibutyltin dichloride (5.95 g, 19.6 mmol) in THF (30 mL) were stirred at ambient temperature for 10 h. Upon completion, the solvent was evaporated, diluted with water, and extracted with dichloromethane. The combined organic layers were washed with brine, dried over sodium sulfate, and concentrated by evaporation under reduced pressure. Purification by flash chromatography (silica, hexane/ethyl acetate) gave the title compound (4.0 g, 99%). MS (ESI): m/z calc. for [M+H$^+$]$^+$ = 309.05, found = 308.99

(*R*)-6-bromo-4-cyclopentyl-1,3-dimethyl-3,4-dihydroquinoxalin-2(1*H*)-one (43)
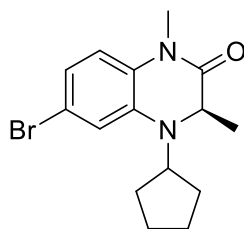
The synthesis was adapted from Hu *et al.*[246] To a solution of compound **42** (4.00 g, 12.9 mmol) in anhydrous DMF (20 mL) was added NaH (60%, 1.03 g, 25.9 mmol) at 0 °C, the mixture was stirred at 0 °C for 30 min, and then iodomethane in THF (2M, 9.1 mL, 18.1 mmol) was added and stirred at room temperature for another 2 h. Upon completion, the reaction mixture was acidified with 1 N aq. HCl to pH 7-8, diluted with water, and extracted with EtOAc. The combined organic fractions were washed with brine, dried over Na$_2$SO$_4$, and concentrated under reduced pressure. Purification by flash chromatography (silica, hexane/ethyl acetate) gave the title compound as a white solid (4.00 g, 96%). ^{1}H NMR (600 MHz, DMSO-d_6) δ 7.49 (dd, *J* = 8.3, 1.8 Hz, 1H), 7.41 (d, *J* = 1.8 Hz, 1H), 7.17 (d, *J* = 8.4 Hz, 1H), 4.14 (q, *J* = 6.7 Hz, 1H), 3.86 (q, *J* = 7.4 Hz, 1H), 3.30 (s, 3H), 1.98 (dtd, *J* = 15.6, 8.2, 7.7, 4.1 Hz, 2H), 1.76 – 1.46 (m, 6H), 0.94 (d, *J* = 6.8 Hz, 3H). MS (ESI): m/z calc. for [M+H$^+$]$^+$ = 323.07, found = 322.97

(*R*)-4-cyclopentyl-1,3-dimethyl-6-(4,4,5,5-tetramethyl-1,3,2-dioxaborolan-2-yl)-3,4-dihydroquinoxalin-2(1*H*)-one (44)
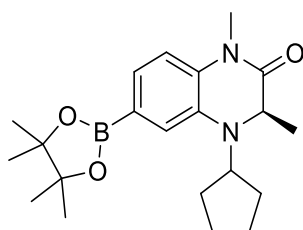
The synthesis was adapted from Hu *et al.*[246] To a solution of compound **43** (4.00 g, 12.4 mmol) and KOAc (2.43 g, 24.8 mmol) in DMSO (10 mL) was added bis(pinacolato)diboron (3.77 g, 14.9 mmol), the mixture was bubbled with Ar for 5 min, then Pd(dppf)$_2$Cl$_2$ · CH$_2$Cl$_2$ (505 mg, 619 μmol) was added, and the mixture was further bubbled with Ar for 5 min. Then, the mixture was heated to 80 °C overnight. Upon completion, the reaction mixture was diluted with water and extracted with EtOAc. The combined organic fractions were washed with brine, dried over Na$_2$SO$_4$, and concentrated under reduced pressure. Purification by flash chromatography (silica, hexane/ethyl acetate) gave the title compound (2.89 g, 63%). MS (ESI): m/z calc. for [M+H$^+$]$^+$ = 371.24, found = 371.18

Ethyl (*R*)-5-(4-cyclopentyl-1,3-dimethyl-2-oxo-1,2,3,4-tetrahydroquinoxalin-6-yl)-1-(*p*-tolyl)-1*H*-1,2,4-triazole-3-carboxylate (45)
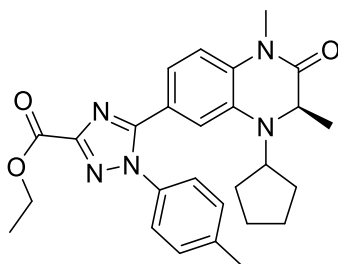
The synthesis was adapted from Hu *et al.*[246] To a solution of compound **44** (1.40 g, 3.78 mmol) and NaHCO$_3$ (635 mg, 7.56 mmol) in THF (14 mL) and H$_2$O (4 mL) was added compound **38** (1.29 g, 4.16 mmol), the mixture was bubbled with Ar for 5 min, then Pd(dppf)$_2$Cl$_2$ · CH$_2$Cl$_2$ (309 mg, 378 µmol) was added, and the mixture was further bubbled with Ar for 5 min. Then, the mixture was heated to 80 °C overnight. Upon completion, the reaction mixture was diluted with water and extracted with EtOAc. The combined organic fractions were washed with brine, dried over Na$_2$SO$_4$, and concentrated under reduced pressure. Purification by flash chromatography (silica, hexane/ethyl acetate) gave the title compound (817 mg, 45%). ^{1}H NMR (400 MHz, DMSO-d_6) δ 7.38 (d, *J* = 1.1 Hz, 4H), 7.21 (dd, *J* = 8.3, 1.8 Hz, 1H), 7.15 (d, *J* = 8.4 Hz, 1H), 6.70 (d, *J* = 1.8 Hz, 1H), 4.38 (q, *J* = 7.1 Hz, 2H), 4.05 (q, *J* = 6.8 Hz, 1H), 3.27 (s, 3H), 2.38 (s, 3H), 1.75 – 1.38 (m, 7H), 1.34 (t, *J* = 7.1 Hz, 3H), 1.19 (dt, *J* = 11.3, 7.5 Hz, 2H), 0.88 (d, *J* = 6.7 Hz, 3H). MS (ESI): m/z calc. for [M+H$^+$]$^+$ = 474.24, found = 474.20

(*R*)-5-(4-cyclopentyl-1,3-dimethyl-2-oxo-1,2,3,4-tetrahydroquinoxalin-6-yl)-1-(*p*-tolyl)-1*H*-1,2,4-triazole-3-carboxylic acid (46)
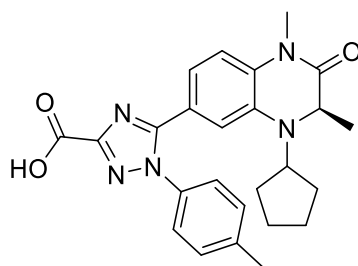
The synthesis was adapted from Hu *et al.*[246] To a solution of compound **45** (560 mg, 1.18 mmol) in THF (6 mL) methanol (4 mL) and H$_2$O (2 mL) was added LiOH · H$_2$O (496 mg, 11.8 mmol), and the mixture was stirred at rt overnight. Upon completion, the reaction mixture was diluted with water, acidified with 1 N aq. HCl to a pH of 3 and extracted with EtOAc. The combined organic fractions were washed with brine, dried over Na$_2$SO$_4$, and concentrated by evaporation under reduced pressure to give a white solid (487 mg, 92%). ^{1}H NMR (250 MHz, DMSO-d_6) δ 12.96 (br s, 1H), 7.37 (s, 4H), 7.20 (dd, *J* = 8.4, 1.6 Hz, 1H), 7.15 (d, *J* = 8.4 Hz, 1H), 6.71 (d, *J* = 1.6 Hz, 1H), 4.26 (t, *J* = 7.0 Hz, 0H), 4.11 – 4.00 (m, 1H), 3.27 (s, 3H), 2.38 (s, 3H), 1.80 – 1.34 (m, 8H), 1.21 – 1.15 (m, 1H), 0.88 (d, *J* = 6.7 Hz, 3H).

(R)-N-(4-((2-aminophenyl)carbamoyl)phenyl)-5-(4-cyclopentyl-1,3-dimethyl-2-oxo-1,2,3,4-tetrahydro-quinoxalin-6-yl)-1-(p-tolyl)-1H-1,2,4-triazole-3-carboxamide (47)
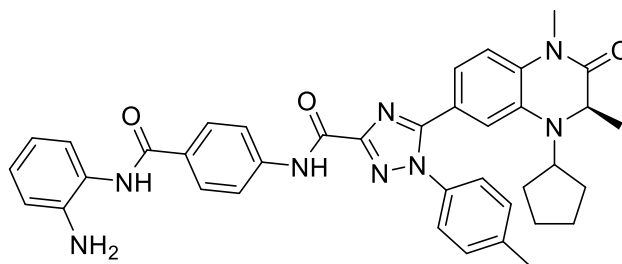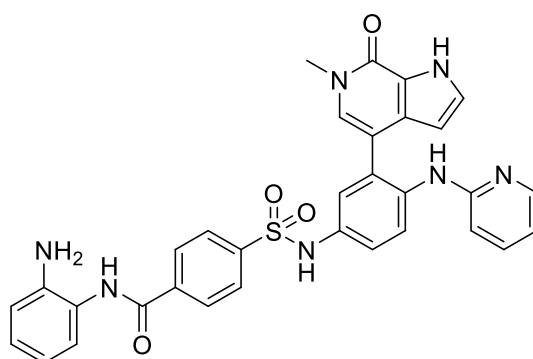

The reaction was performed according to "general procedure for amide coupling". Compound **34** (100 mg, 305 µmol) and compound **46** (163 mg, 367 µmol) were used. MS (ESI): m/z calc. for [M+Na⁺]⁺ = 777.35, found = 777.49

The *Boc*-protected intermediate was reacted according to "General procedure for *N-Boc* deprotection". Purification by flash chromatography (silica, DCM/methanol) gave the title compound as a colorless solid (127 mg, 64%). ^{1}H NMR (250 MHz, DMSO-d_6) δ 10.75 (s, 1H), 9.60 (s, 1H), 8.01 (s, 4H), 7.50 – 7.34 (m, 3H), 7.29 (dd, J = 8.3, 1.7 Hz, 1H), 7.18 (dd, J = 8.1, 1.8 Hz, 2H), 6.97 (td, J = 8.1, 1.5 Hz, 1H), 6.79 (dd, J = 8.3, 1.6 Hz, 2H), 6.61 (td, J = 7.5, 1.5 Hz, 1H), 4.90 (s, 2H), 4.07 (q, J = 6.5 Hz, 1H), 3.29 (s, 3H), 2.40 (s, 3H), 1.82 – 1.37 (m, 8H), 1.23 (d, J = 7.6 Hz, 2H), 0.89 (d, J = 6.7 Hz, 3H). MS (ESI): m/z calc. for [M+H⁺]⁺ = 655.31, found = 655.12

2-Methoxy-4-methyl-3-nitropyridine (49)
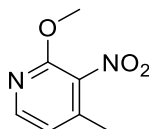
The synthesis was adapted from Crawford *et al* and performed as described by Bauer *et al*.[272,277] Sodium methoxide (100 g, 1.85 mol, 3.8 eq) was dissolved in methanol (300 mL) and cooled to 0 °C. A solution of 2-chloro-4-methyl-3-nitropyridine (**48**, 85.0 g, 0.493 mol, 1.0 eq) in methanol (400 mL) was added dropwise, and the mixture was heated to reflux for 16 h. About half of the solvent was reduced under reduced pressure, and ice water was added. The resulting precipitate was filtered and dried to provide a beige solid (79.5 g, 96%). ^{1}H NMR (400 MHz, DMSO-d_6) δ 8.34 – 8.05 (m, 1H), 7.09 (d, J = 5.7 Hz, 1H), 3.95 (s, 3H), 2.29 (s, 3H). ^{13}C NMR (101 MHz, DMSO) δ 154.19, 148.05, 141.69, 135.62, 119.47, 54.34, 16.06.

5-Bromo-2-methoxy-4-methyl-3-nitropyridine (50)
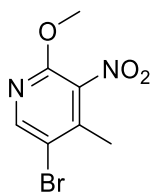
The synthesis was adapted from Crawford *et al* and performed as described by Bauer *et al*.[272,277] Bromine (65.0 mL, 1.27 mol, 2.7 eq) was slowly added to a suspension of 2-Methoxy-4-methyl-3-nitropyridine (**49**, 79.0 g, 0.470 mol, 1.0 eq) and sodium acetate (139 g, 1.69 mol, 3.6 eq) in acetic acid (450 mL) and the mixture was heated at 80 °C for 16 h. Afterwards, ice water and sat. aq Na_2SO_3 were added (1.8 L), and the resulting precipitate was filtered and dried to provide a beige solid (100.5 g, 87%). ^{1}H NMR (400 MHz, DMSO-d_6) δ 8.52 (s, 1H), 3.97 (s, 3H), 2.31 (s, 3H). ^{13}C NMR (101 MHz, DMSO) δ 153.46, 149.19, 140.97, 135.78, 114.36, 54.87, 17.44.

(*E*)-2-(5-Bromo-2-methoxy-3-nitropyridin-4-yl)-*N*,*N*-dimethylethen-1-amine (51)
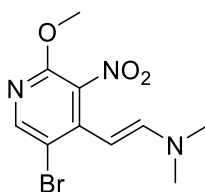
The synthesis was adapted from Crawford *et al* and performed as described by Bauer *et al*.[272,277] 5-Bromo-2-methoxy-4-methyl-3-nitropyridine (**50**, 100 g, 0.405 mol, 1.0 eq) was dissolved in DMF (700 mL) and heated at 80 °C. *N*,*N*-Dimethylformamide dimethyl acetal (500 mL, 3.75 mol, 9.3 eq) was added dropwise, and the mixture was heated at 90 °C for 16 h. After cooling to ambient temperature, water (3 L) was added, and the resulting precipitate was filtered and dried to provide a red solid (120 g, 98%). ^{1}H NMR (300 MHz, DMSO-d_6) δ 8.22 (s, 1H), 7.04 (d, *J* = 13.5 Hz, 1H), 4.80 (d, *J* = 13.5 Hz, 1H), 3.88 (s, 3H), 2.90 (s, 6H). ^{13}C NMR (75 MHz, DMSO) δ 154.49, 148.74, 148.26, 139.83, 111.26, 86.27, 54.84.

4-Bromo-7-methoxy-1*H*-pyrrolo[2,3-*c*]pyridine (52)
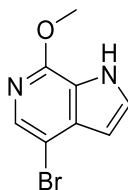
The synthesis was adapted from Crawford *et al* and performed as described by Bauer *et al*.[272,277] A mixture of (*E*)-2-(5-bromo-2-methoxy-3-nitropyridin-4-yl)-*N*,*N*-dimethylethen-1-amine (**51**, 60.0 g, 199 mmol, 1.0 eq) and iron powder (50.0 g, 895 mmol, 4.5 eq) in methanol/acetic acid/water (6/2/1,

450 mL) was heated under reflux for 2 h. The mixture was filtered over a plug of celite, and the solvent was removed under reduced pressure. The residue was partitioned between water and ethyl acetate. The organic layer was washed with brine, dried over MgSO$_4$, filtered, and volatiles were removed under reduced pressure to provide an off-white solid. The procedure was performed twice to provide a combined yield of 85 g (94%). ^{1}H NMR (300 MHz, DMSO-d_6) δ 12.15 (s, 1H), 7.76 (s, 1H), 7.54 (t, J = 2.7 Hz, 1H), 6.54 – 6.34 (m, 1H), 4.02 (s, 3H). ^{13}C NMR (75 MHz, DMSO) δ 150.80, 134.83, 134.10, 129.13, 120.92, 105.17, 101.98, 53.51.

4-Bromo-7-methoxy-1-tosyl-1*H*-pyrrolo[2,3-*c*]pyridine (53)
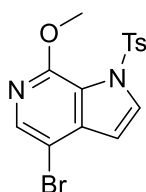
The synthesis was adapted from Crawford *et al* and performed as described by Bauer *et al*.[272,277] Sodium hydride (60%, 28.8 g, 1.20 mol, 3.2 eq) was slowly added to a solution of 4-bromo-7-methoxy-1*H*-pyrrolo[2,3-*c*]pyridine (**52**, 85.0 g, 374 mmol, 1.0 eq) in THF (900 mL) at 0 °C. After stirring for 30 min, tosyl chloride (99.9 g, 524 mmol, 1.4 eq) was slowly added. After 2 h, the reaction was quenched by adding ice water and extracted with ethyl acetate. The organic layer was washed with brine, dried over MgSO$_4$, filtered, and volatiles were removed under reduced pressure. The residue was recrystallized from acetonitrile to provide a beige solid (110 g, 77%). ^{1}H NMR (400 MHz, DMSO-d_6) δ 8.15 (d, J = 3.7 Hz, 1H), 7.94 (s, 1H), 7.84 (d, J = 8.4 Hz, 2H), 7.41 (d, J = 8.3 Hz, 2H), 6.75 (d, J = 3.7 Hz, 1H), 3.81 (s, 3H), 2.33 (s, 3H). ^{13}C NMR (101 MHz, DMSO) δ 149.95, 145.53, 139.14, 138.55, 134.93, 132.20, 129.89, 127.72, 118.37, 105.78, 104.14, 53.18, 21.05.

4-Bromo-1-tosyl-1,6-dihydro-7*H*-pyrrolo[2,3-*c*]pyridin-7-one (54)
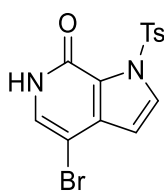
The synthesis was adapted from McDaniel *et al*. and performed as described by Bauer *et al*.[187,277] 4-Bromo-7-methoxy-1-tosyl-1*H*-pyrrolo[2,3-*c*]pyridine (**53**, 80.0 g, 210 mmol) was dissolved in dioxane (300 mL) and HCl in dioxane (4 M, 250 mL) and heated at 50 °C for 2 h. About 300 mL of dioxane were removed under reduced pressure, and the residue was triturated with diethyl ether. The precipitate was filtered and dried to provide an off-white solid (62 g, 81%). ^{1}H NMR (400 MHz, DMSO-d_6) δ 11.63 (s, 1H), 8.02 (d, J = 3.5 Hz, 1H), 7.93 (d, J = 8.4 Hz, 2H), 7.39 (d, J = 8.2 Hz, 2H), 7.34 (s, 1H), 6.58 (d, J =

3.5 Hz, 1H), 2.35 (s, 3H). ^{13}C NMR (101 MHz, DMSO) δ 151.97, 145.36, 136.70, 135.03, 131.11, 129.67, 129.60, 128.39, 121.88, 106.24, 91.19, 21.09.

4-Bromo-6-methyl-1-tosyl-1,6-dihydro-7H-pyrrolo[2,3-c]pyridin-7-one (55)
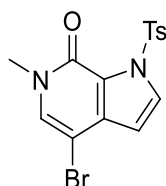
The synthesis was adapted from McDaniel *et al.* and performed as described by Bauer *et al.*[187,277] Sodium hydride (60%, 3.63 g, 151 mmol, 1.5 eq) was slowly added to a solution of 4-bromo-7-methoxy-1H-pyrrolo[2,3-c]pyridine (**54**, 37.0 g, 101 mmol, 1.0 eq) in DMF (400 mL) at 0 °C. After stirring for 20 min, iodomethane (9.41 mL, 151 mmol, 1.5 eq) was slowly added. After 2 h, the reaction was quenched by adding ice water. The resulting precipitate was filtered and dried to provide an off-white solid (36.37 g, 95%). ^{1}H NMR (400 MHz, DMSO-d_6) δ 8.05 (d, J = 3.5 Hz, 1H), 7.95 (d, J = 8.4 Hz, 2H), 7.78 (s, 1H), 7.41 (d, J = 8.2 Hz, 2H), 6.58 (d, J = 3.5 Hz, 1H), 3.39 (s, 3H), 2.36 (s, 3H). ^{13}C NMR (101 MHz, DMSO) δ 151.78, 145.30, 136.10, 135.09, 134.17, 131.38, 129.62, 128.40, 121.42, 105.95, 90.79, 36.31, 21.08.

6-Methyl-4-(4,4,5,5-tetramethyl-1,3,2-dioxaborolan-2-yl)-1-tosyl-1,6-dihydro-7H-pyrrolo-[2,3-c]pyridin-7-one (56)
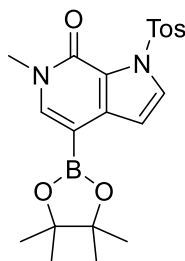
The synthesis was adapted from McDaniel *et al.* and performed as described by Bauer *et al.*[187,277] 4-Bromo-6-methyl-1-tosyl-1,6-dihydro-7H-pyrrolo[2,3-c]pyridin-7-one (**55**, 10.0 g, 26.2 mmol, 1.0 eq), 4,4,4',4',5,5,5',5'-octamethyl-2,2'-bi(1,3,2-dioxaborolane) (13.3 g, 52.4 mmol, 2.0 eq), potassium acetate (5.66 g, 57.7 mmol, 2.2 eq), Pd XPhos G2 (825 mg, 1.05 mmol, 0.04 eq) and XPhos (125 mg, 262 µmol, 0.01 eq) were dissolved in dioxane (150 mL) and purged with argon for 10 min. The mixture was heated at 80 °C for 2 h, cooled to ambient temperature, partitioned between water and ethyl acetate and filtered over a plug of celite. The ethyl acetate layer was washed with brine, dried over MgSO₄, filtered, and volatiles were removed under reduced pressure. The crude residue was triturated with hexane/diethyl ether (2/1), filtered and washed with hexane to provide the title compound as a colorless solid (8.68 g, 77%). ^{1}H NMR (400 MHz, DMSO-d_6) δ 7.97 (d, J = 3.5 Hz, 1H), 7.91 (d, J = 1.8 Hz,

1H), 7.89 (d, J = 1.8 Hz, 1H), 7.72 (s, 1H), 7.42 – 7.40 (m, 1H), 7.42 – 7.36 (m, 1H), 6.81 (d, J = 3.5 Hz, 1H), 3.43 (s, 3H), 2.36 (s, 3H), 1.29 (s, 12H). ^{13}C NMR (101 MHz, DMSO) δ 152.86, 144.91, 143.05, 138.93, 135.53, 131.06, 129.55, 129.52, 128.11, 121.29, 107.80, 82.80, 36.29, 24.60, 21.06. MS (ESI): m/z calc. for $[C_{21}H_{25}BN_2O_5S+H^+]^+$ = 429.16, found = 429.10

6-Methyl-4-(4,4,5,5-tetramethyl-1,3,2-dioxaborolan-2-yl)-1,6-dihydro-7H-pyrrolo[2,3-c]pyridin-7-one (57)
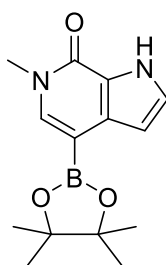
The synthesis was performed as described by Bauer *et al.*[277] Compound **55** (2.00 g, 5.25 mmol) and LiOH · H$_2$O (881 mg, 21.0 mmol) were dissolved in dioxane (30 mL) and H$_2$O (10 mL) and heated at 85 °C for 2.5 h. After cooling to ambient temperature, the pH was brought to 3 through the addition of aq HCl (5%), the dioxane was removed under reduced pressure and the resulting precipitate was filtered and dried to provide a colorless solid (1.074 g, 90%). ^{1}H NMR (400 MHz, DMSO-d_6) δ 12.33 (s, 1H), 7.53 (s, 1H), 7.36 (t, J = 2.8 Hz, 1H), 6.25 (dd, J = 2.8, 2.1 Hz, 1H), 3.50 (s, 3H). MS (ESI): m/z calc. for $[M+H^+]^+$ = 226.97, found = 225.84

The intermediate (730 mg, 3.21 mmol), 4,4,4',4',5,5,5',5'-octamethyl-2,2'-bi(1,3,2-dioxaborolane) (1.63 g, 6.43 mmol), potassium acetate (947 mg, 9.64 mmol), Pd XPhos G2 (136 mg, 161 mmol) and XPhos (77 mg, 0.16 mmol) were dissolved in dioxane (15 mL) and purged with argon for 10 min. The mixture was heated at 80 °C for 5 h, cooled to ambient temperature, partitioned between water and ethyl acetate and filtered over a plug of celite. The ethyl acetate layer was washed with brine, dried over MgSO$_4$, filtered, and volatiles were removed under reduced pressure. Purification by flash chromatography (silica, hexane/ethyl acetate) gave the title compound (593 mg, 73%). ^{1}H NMR (400 MHz, DMSO-d_6) δ 11.88 (s, 1H), 7.51 (s, 1H), 7.25 (t, J = 2.7 Hz, 1H), 6.50 (t, J = 2.4 Hz, 1H), 3.53 (s, 3H), 1.29 (s, 12H). MS (ESI): m/z calc. for $[M+H^+]^+$ = 297.14, found = 297.18

N-(2-bromo-4-nitrophenyl)pyridin-2-amine (60)
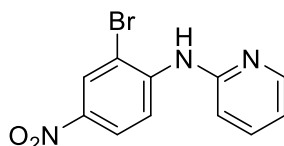
Sodium hydride (60%, 2.18 g, 54.6 mmol) was added to a solution of pyridin-2-amine (**59**, 3.85 g, 40.9 mmol) in DMF (60 mL) at -10 °C. After 30 min, 2-bromo-1-fluoro-4-nitrobenzene (**58**, 6.00 g, 27.3 mmol) dissolved in DMF (40 mL) was added dropwise. After 16 h, the reaction was quenched by adding ice and the mixture was extracted with ethyl acetate. The ethyl acetate layer was washed with brine, dried over MgSO$_4$, filtered, and volatiles were removed under reduced pressure. Purification by chromatography (silica, hexane/ethyl acetate) gave the title compound (4.965 g, 62%). ^{1}H-NMR (250 MHz, DMSO-d_6) δ 8.76 (s, 1H), 8.43 (d, J = 2.7 Hz, 1H), 8.39 (d, J = 9.4 Hz, 1H), 8.29 (dd, J = 6.4, 4.7 Hz, 1H), 8.16 (dd, J = 9.4, 2.8 Hz, 1H), 7.80-7.68 (m, 1H), 7.32 (d, J = 8.3 Hz, 1H), 7.07-6.95 (m, 1H). MS (ESI): m/z calc. for [M+H$^+$]$^+$ = 293.99, found = 294.03

2-Bromo-N^1-(pyridin-2-yl)benzene-1,4-diamine (61)
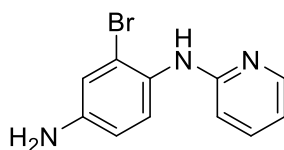
Na$_2$S$_2$O$_4$ (12.4 g, 71.4 mmol) was added to a solution of compound **60** (3.50 g, 11.9 mmol) in EtOH/H$_2$O (5/1, 300 mL) at 100 °C. Then, the pH was brought to 1 through the addition of aq HCl (conc.) and the mixture was heated at 100 °C for 1 h. After cooling to ambient temperature, the mixture was neutralized with sat. aq NaHCO$_3$ and extracted with DCM. The combined organic phases were washed with brine, dried over MgSO$_4$, filtered, and volatiles were removed under reduced pressure to provide the title compound (2.69 g, 86%). ^{1}H-NMR (250 Hz, DMSO-d_6) δ 7.96 (d, J = 4.8 Hz, 1H, I), 7.86 (s, 1H, A), 7.41 (t, J = 7.8 Hz, 1H, G), 7.10 (d, J = 8.5 Hz, 1H, D), 6.86 (s, 1H, E), 6.56 (d, J = 7.1 Hz, 2H, F & H), 6.40 (d, J = 8.3 Hz, 1H, C), 5.25 (s, 2H, B). MS (ESI): m/z calc. for [M+H$^+$]$^+$ = 264.02, found = 264.03

4-(*N*-(3-bromo-4-(pyridin-2-ylamino)phenyl)sulfamoyl)benzoic acid (63)
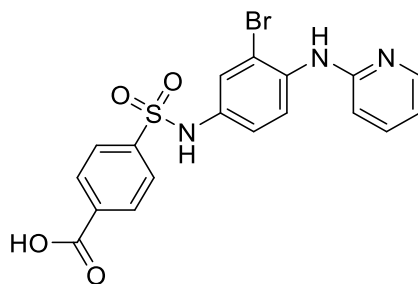
4-(chlorosulfonyl)benzoic acid (**62**, 501 mg, 2.27 mmol) was added to a solution of compound **61** (600 mg, 2.27 mmol) and pyridine (5 mL) in THF (60 mL) and the mixture was stirred at ambient temperature for 16 h. The mixture was partitioned between water and DCM and the aqueous phase was extracted with DCM. The combined organic phases were washed with brine, dried over MgSO$_4$, filtered, and volatiles were removed under reduced pressure. Purification by flash chromatography (silica, DCM/MeOH/AcOH) gave the title compound (256 mg, 25%). ^{1}H NMR (300 MHz, DMSO-d_6) δ 10.45 (s, 1H), 8.12 (d, *J* = 7.3 Hz, 2H), 8.08 (s, 1H), 8.05 − 7.98 (m, 1H), 7.90 − 7.82 (m, 2H), 7.70 (d, *J* = 8.7 Hz, 1H), 7.53 (ddd, *J* = 8.9, 7.1, 2.0 Hz, 1H), 7.29 (d, *J* = 2.5 Hz, 1H), 7.04 (dd, *J* = 8.8, 2.5 Hz, 1H), 6.81 (d, *J* = 8.4 Hz, 1H), 6.72 (ddd, *J* = 7.1, 5.0, 0.7 Hz, 2H). MS (ESI): m/z calc. for [M+H$^+$]$^+$ = 447.99, found = 448.00

***tert*-butyl (2-(4-(*N*-(3-bromo-4-(pyridin-2-ylamino)phenyl)sulfamoyl)benzamido)phenyl)carbamate (64)**
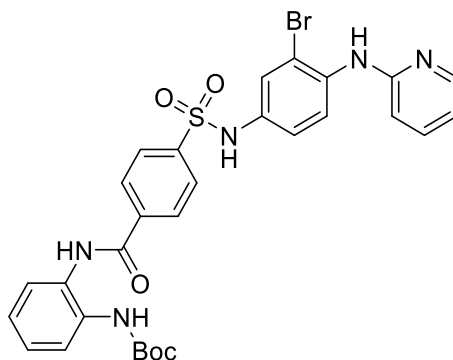
The synthesis was performed according to "general procedure for amide coupling". Compound **64** (150 mg, 335 µmol) and compound **32** (77 mg, 0.37 mmol) were used. Purification by flash chromatography (silica, DCM/MeOH) gave the title compound (211 mg, 99%). ^{1}H NMR (400 MHz, DMSO-d_6) δ 10.48 (s, 1H), 9.92 (s, 1H), 8.68 (s, 1H), 8.14 (s, 1H), 8.10 (d, *J* = 8.1 Hz, 2H), 8.01 (d, *J* = 5.0 Hz, 1H), 7.92 (dd, *J* = 8.4, 1.6 Hz, 2H), 7.71 (dd, *J* = 8.8, 1.5 Hz, 1H), 7.57 (d, *J* = 8.1 Hz, 1H), 7.53 (td, *J* = 7.8, 7.1, 1.8 Hz, 1H), 7.48 (d, *J* = 7.9 Hz, 1H), 7.35 (t, *J* = 2.0 Hz, 1H), 7.20 (t, *J* = 7.7 Hz, 1H), 7.13 (d, *J* = 7.7 Hz, 1H), 7.09 (dd, *J* = 8.9, 2.2 Hz, 1H), 6.83 (d, *J* = 8.4 Hz, 1H), 6.72 (t, *J* = 6.1 Hz, 1H), 1.39 (d, *J* = 1.5 Hz, 9H). MS (ESI): m/z calc. for [M+H$^+$]$^+$ = 638.25, found = 638.10

***tert*-butyl (2-(4-(*N*-(3-(6-methyl-7-oxo-6,7-dihydro-1*H*-pyrrolo[2,3-*c*]pyridin-4-yl)-4-(pyridin-2-ylamino)-phenyl)sulfamoyl)benzamido)phenyl)carbamate (65)**
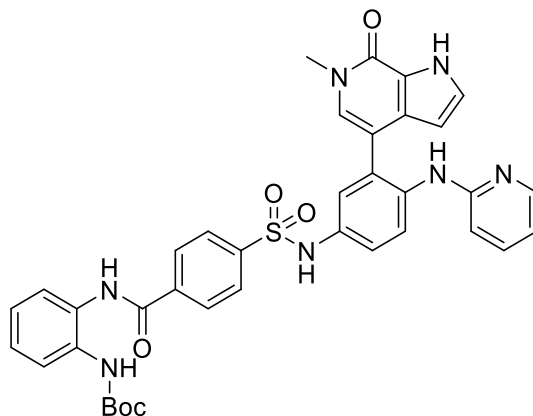
The synthesis was performed according to "general procedure for Suzuki coupling B". Compound **64** (68 mg, 0.25 mmol) and compound **57** (105 mg, 164 µmol) were used. The mixture was partitioned between water and ethyl acetate and the organic phase was filtered to provide the title compound (62 mg, 53%). MS (ESI): m/z calc. for [M+H$^+$]$^+$ = 706.24, found = 706.17

***N*-(2-aminophenyl)-4-(*N*-(3-(6-methyl-7-oxo-6,7-dihydro-1*H*-pyrrolo[2,3-*c*]pyridin-4-yl)-4-(pyridin-2-ylamino)phenyl)sulfamoyl)benzamide (66)**

The synthesis was performed according to "general procedure for *N-Boc* deprotection". Compound **65** (30 mg, 43 µmol) was used. Purification by flash chromatography (silica, DCM/MeOH) gave the title compound (19 mg, 73%). ^{1}H NMR (400 MHz, DMSO-d_6) δ 11.96 (s, 1H), 9.77 (s, 1H), 8.31 (d, *J* = 8.1 Hz, 1H), 8.09 (d, *J* = 8.1 Hz, 2H), 7.99 – 7.95 (m, 2H), 7.90 (d, *J* = 8.3 Hz, 1H), 7.86 (d, *J* = 8.2 Hz, 2H), 7.36 (t, *J* = 7.8 Hz, 2H), 7.18 – 7.13 (m, 2H), 7.02 (d, *J* = 5.0 Hz, 2H), 7.00 – 6.96 (m, 2H), 6.76 (dd, *J* = 8.0, 1.4 Hz, 1H), 6.58 (t, *J* = 7.0 Hz, 2H), 6.52 (d, *J* = 8.3 Hz, 1H), 4.93 (s, 2H), 3.47 (s, 3H). MS (ESI): m/z calc. for [M+H$^+$]$^+$ = 606.2, found = 606.2

N-(2-aminophenyl)-4-(N-(10-methyl-11-oxo-4-(pyridin-2-yl)-3,4,10,11-tetrahydro-1H-1,4,10-triazadibenzo[cd,f]azulen-7-yl)sulfamoyl)benzamide (67)
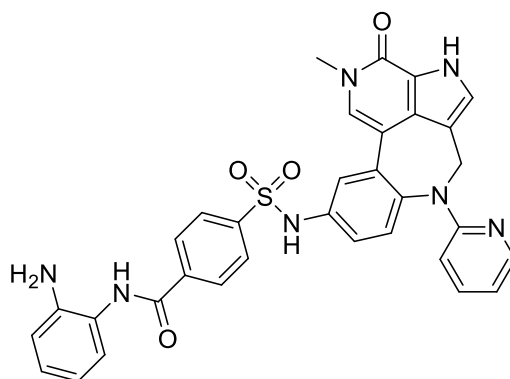
A mixture of compound **65** (28 mg, 40 µmol) and paraformaldehyde (4 mg, 0.1 mmol) in AcOH (2.5 mL) was heated in a sealed vial at 80 °C for 1 h. Afterwards, volatiles were removed under reduced pressure. MS (ESI): m/z calc. for $[M-H^+]^-$ = 716.24, found = 717.68

The residue was reacted according to "general procedure for *N-Boc* deprotection". Purification by flash chromatography (silica, DCM/MeOH) gave the title compound (18 mg, 64%). ^{1}H NMR (400 MHz, DMSO-d_6) δ 11.93 (s, 1H), 11.82 (d, J = 2.8 Hz, 1H), 10.58 (s, 1H), 9.79 (s, 1H), 8.15 (d, J = 8.2 Hz, 2H), 7.98 (d, J = 8.2 Hz, 2H), 7.93 (dd, J = 5.1, 2.0 Hz, 1H), 7.54 (d, J = 2.5 Hz, 1H), 7.38 (s, 1H), 7.26 (p, J = 2.5, 1.9 Hz, 2H), 7.24 – 7.18 (m, 1H), 7.13 (d, J = 7.8 Hz, 1H), 7.09 (dd, J = 8.5, 2.6 Hz, 1H), 6.97 (t, J = 7.9 Hz, 1H), 6.75 (dd, J = 8.0, 1.4 Hz, 1H), 6.57 (t, J = 7.5 Hz, 1H), 6.47 (dd, J = 7.2, 5.0 Hz, 1H), 6.05 (d, J = 8.7 Hz, 1H), 5.71 (d, J = 15.5 Hz, 1H), 4.93 (s, 2H), 3.57 (s, 3H). MS (ESI): m/z calc. for $[M+H^+]^+$ = 618.2, found = 618.2

Methyl **4-((2-((tert-butoxycarbonyl)amino)phenyl)carbamoyl)benzoate (69)**
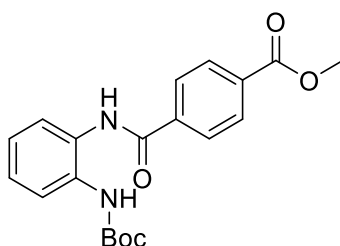
The synthesis was performed according to "general procedure for amide coupling". 4-(methoxycarbonyl)benzoic acid (**70**, 600 mg, 3.33 mmol) and compound **32** (694 mg, 3.33 mmol) were used. The crude product was used in the next step without further purification.

4-((2-((tert-butoxycarbonyl)amino)phenyl)carbamoyl)benzoic acid (70)
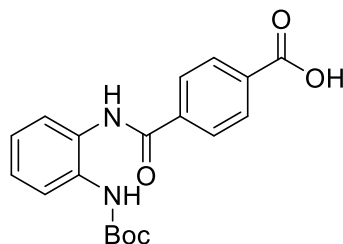
A mixture of compound **69** (1.23 g, 3.33 mmol) and LiOH · H$_2$O (1.00 g mg, 24.0 mmol) in THF (15 mL), MeOH (10 mL) and H$_2$O (5 mL) was stirred at ambient temperature for 16 h. Afterwards, the pH was brought to 1 through the addition of aq HCl (10%) and most of the organic solvents was removed under reduced pressure. The residue was partitioned between water and ethyl acetate and the aqueous phase was extracted with ethyl acetate. The combined organic phases were washed with brine, dried over MgSO$_4$, filtered, and volatiles were removed under reduced pressure to provide the title compound (960 mg, 99%). ^{1}H-NMR (250 MHz, DMSO-d_6) δ 9.93 (s, 1H, E), 8.68 (s, 1H, J), 8.13 – 8.00 (m, 4H), 7.60 – 7.45 (m, 2H), 7.26 – 7.08 (m, 2H), 1.43 (s, 9H). MS (ESI): m/z calc. for [M+H$^+$]$^+$ = 379.14, found = 379.13

tert-butyl (2-(4-((3-bromo-4-(pyridin-2-ylamino)phenyl)carbamoyl)benzamido)phenyl)carbamate (71)
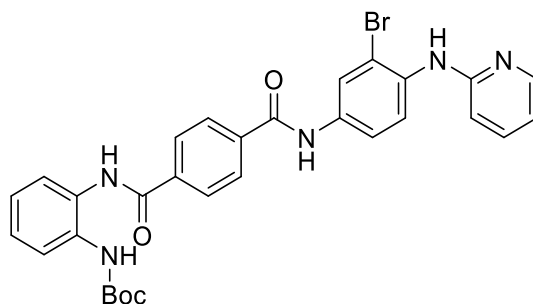
The synthesis was performed according to "general procedure for amide coupling". Compound **70** (500 mg, 1.40 mmol) and compound **61** (371 mg, 1.40 mmol) were used. Purification by flash chromatography (C18 silica, H$_2$O/ACN) gave the title compound (580 mg, 69%). ^{1}H NMR (400 MHz, DMSO-d_6) δ 10.46 (s, 1H), 9.96 (s, 1H), 8.71 (s, 1H), 8.22 (s, 1H), 8.20 (d, J = 2.4 Hz, 1H), 8.11 (d, J = 1.5 Hz, 4H), 8.07 (ddd, J = 5.0, 2.0, 0.8 Hz, 1H), 7.80 (d, J = 8.9 Hz, 1H), 7.73 (dd, J = 8.8, 2.4 Hz, 1H), 7.59 – 7.52 (m, 3H), 7.20 (dtd, J = 22.7, 7.5, 1.7 Hz, 2H), 6.85 (dt, J = 8.4, 1.0 Hz, 1H), 6.74 (ddd, J = 7.1, 5.0, 0.9 Hz, 1H), 1.45 (s, 9H). MS (ESI): m/z calc. for [M+H$^+$]$^+$ = 602.13, found = 602.23

***tert*-butyl (2-(4-((3-(6-methyl-7-oxo-6,7-dihydro-1*H*-pyrrolo[2,3-*c*]pyridin-4-yl)-4-(pyridin-2-ylamino)-phenyl)carbamoyl)benzamido)phenyl)carbamate (72)**
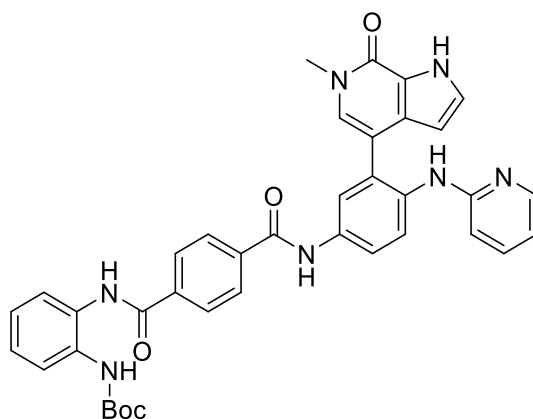
The synthesis was performed according to "general procedure for Suzuki coupling B". Compound **71** (385 mg, 638 µmol) and compound **57** (175 mg, 638 µmol) were used. The mixture was partitioned between water and ethyl acetate and the organic phase was filtered to provide the title compound (220 mg, 51%). MS (ESI): m/z calc. for [M+H$^+$]$^+$ = 670.27, found = 670.16

***N*^{1}-(2-aminophenyl)-*N*^{4}-(3-(6-methyl-7-oxo-6,7-dihydro-1*H*-pyrrolo[2,3-*c*]pyridin-4-yl)-4-(pyridin-2-ylamino)phenyl)terephthalamide (73)**
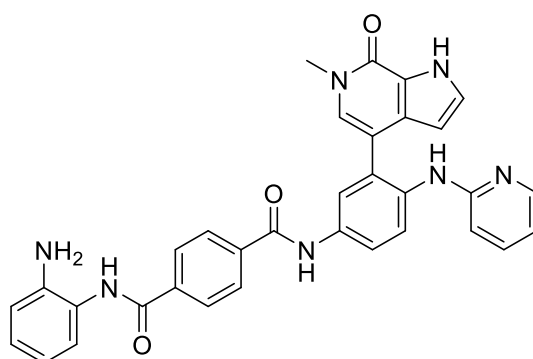
The synthesis was performed according to "general procedure for *N-Boc* deprotection". Compound **72** (90 mg, 134 µmol) was used. Purification by flash chromatography (silica, DCM/MeOH) gave the title compound (35 mg, 46%). ^{1}H NMR (400 MHz, DMSO-*d*$_6$) δ 12.01 (s, 1H), 10.42 (s, 1H), 9.85 (s, 1H), 8.19 − 8.10 (m, 4H), 8.05 (dd, *J* = 5.2, 1.6 Hz, 1H), 7.91 − 7.83 (m, 2H), 7.80 − 7.75 (m, 2H), 7.42 (ddd, *J* = 9.0, 7.1, 2.0 Hz, 1H), 7.26 (s, 1H), 7.23 − 7.17 (m, 2H), 7.00 (td, *J* = 7.7, 7.2, 1.5 Hz, 1H), 6.81 (dd, *J* = 8.0, 1.4 Hz, 1H), 6.69 − 6.58 (m, 3H), 6.05 (d, *J* = 2.2 Hz, 1H), 4.97 (s, 2H), 3.55 (s, 3H). MS (ESI): m/z calc. for [M+H$^+$]$^+$ = 570.2, found = 570.2

N[1]-(2-aminophenyl)-N[4]-(10-methyl-11-oxo-4-(pyridin-2-yl)-3,4,10,11-tetrahydro-1H-1,4,10-triazadibenzo[cd,f]azulen-7-yl)terephthalamide (74)
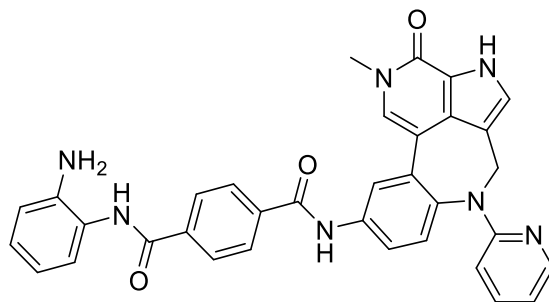

A mixture of compound **72** (125 mg, 187 µmol) and paraformaldehyde (17 mg, 0.56 mmol) in AcOH (4 mL) was heated in a sealed vial at 80 °C for 1 h. Afterwards, volatiles were removed under reduced pressure. MS (ESI): m/z calc. for $[M-H^+]^-$ = 682.27, found = 682.23

The residue was reacted according to "general procedure for *N-Boc* deprotection". Purification by flash chromatography (silica, DCM/MeOH) gave the title compound (67 mg, 63%). ^{1}H NMR (400 MHz, DMSO-d_6) δ 11.84 (s, 1H), 10.56 (s, 1H), 9.84 (s, 1H), 8.22 (d, J = 2.4 Hz, 1H), 8.19 – 8.11 (m, 4H), 7.98 (dd, J = 5.1, 1.9 Hz, 1H), 7.87 (dd, J = 8.6, 2.3 Hz, 1H), 7.59 (s, 1H), 7.35 (d, J = 8.5 Hz, 1H), 7.31 (d, J = 2.1 Hz, 2H), 7.21 (d, J = 7.8 Hz, 1H), 7.05 – 6.97 (m, 1H), 6.82 (dd, J = 8.0, 1.4 Hz, 1H), 6.63 (t, J = 7.6 Hz, 1H), 6.52 (t, J = 6.1 Hz, 1H), 6.21 (s, 1H), 5.80 (d, J = 15.5 Hz, 1H), 4.25 (d, J = 15.4 Hz, 1H), 3.59 (s, 3H). MS (ESI): m/z calc. for $[M+H^+]^+$ = 582.2, found = 582.2

4-((methylsulfonyl)methyl)aniline (76)
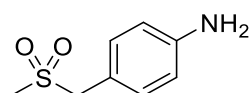
The synthesis was adapted from Fidanze *et al.*[245] 1-((Methylsulfonyl)methyl)-4-nitrobenzene (**75**, 617 mg, 2.8 mmol) was dissolved in THF (7 mL) and combined with Pd/C (10%, 74 mg). The flask was evacuated and filled with H_2 several times and the mixture was afterwards stirred under H_2 for 90 min. The suspension was filtered through celite and the solvent was removed under vacuum to provide the title compound (514 mg, 97%). ^{1}H NMR (250 MHz, DMSO-d6): δ 7.03 (d, J = 8.4 Hz, 2H), 6.54 (d, J = 8.5 Hz, 2H), 5.19 (s, 2H), 4.20 (s, 2H), 2.79 (s, 3H).

2-iodo-4-((methylsulfonyl)methyl)aniline (77)
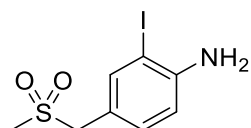
The synthesis was adapted from Fidanze *et al.*[245] *N*-Iodosuccinimide (739 mg, 3.28 mmol, 1.1 eq) was added to a solution of 4-((methylsulfonyl)-methyl)aniline (**76**, 549 mg, 296 mmol, 1 eq) in DMF (18 mL) and the mixture was stirred at ambient temperature. After 1 h, the reaction was quenched by adding sat. aq $Na_2S_2O_3$ and sat. aq $NaHCO_3$. The precipitate was filtered, suspended in water and stirred for 10 min. The solid was filtered again, washed with water and dried to provide the title compound (708 mg, 77%). ^{1}H NMR (400 MHz, DMSO-d6): δ 7.58 (d, J = 1.9 Hz, 1H), 7.10 (dd, J = 8.3, J = 1.9 Hz, 1H), 6.74 (d, J = 8.3 Hz, 1H), 5.36 (s, 2H), 4.24 (s, 2H), 2.83 (s, 3H).

N-cyclohexyl-2-iodo-4-((methylsulfonyl)methyl)aniline (78)
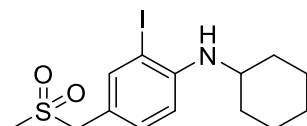
A solution of compound **77** (500 mg, 1.61 mmol) and cyclohexanone (0.50 mL, 4.8 mmol) in DCM (10 mL) and AcOH (1 mL) was stirred at ambient temperature for 2 h. Afterwards, sodium triacetoxyborohydride (1.02 g, 4.82 mmol) was added. After 2 h, the reaction was quenched by adding sat. aq $NaHCO_3$ and extracted with ethyl acetate. The ethyl acetate layer was washed with brine, dried over $MgSO_4$, filtered, and volatiles were removed under reduced pressure. Purification by flash chromatography (silica, hexane/ethyl acetate) gave the title compound (497mg, 79%).

4-(2-(Cyclohexylamino)-5-((methylsulfonyl)methyl)phenyl)-6-methyl-1,6-dihydro-7*H*-pyrrolo[2,3-c]pyridin-7-one (79)
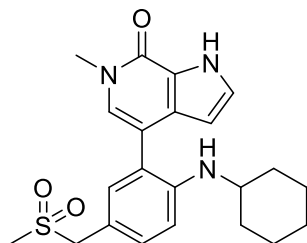
The synthesis was performed according to "general procedure for Suzuki coupling B". Compound **78** (400 mg, 1.02 mmol) and compound **56** (436 mg, 1.02 mmol) were used. Purification by flash chromatography (silica, DCM/MeOH) gave the title compound (0.520 mg, 90%). ^{1}H NMR (250 MHz, DMSO-d_6) δ 8.02 – 7.95 (m, 2H), 7.93 (d, J = 3.5 Hz, 1H), 7.46 – 7.40 (m, 2H), 7.38 (s, 1H), 7.20 (dd, J = 8.5, 2.2 Hz, 1H), 7.02 (d, J = 2.2 Hz, 1H), 6.72 (d, J = 8.6 Hz, 1H), 6.24 (d, J = 3.5 Hz, 1H), 4.27 (s, 2H), 3.43 (s, 3H), 3.27 – 3.15 (m, 1H), 2.84 (s, 3H), 2.50 (p, J = 1.9 Hz, 4H), 2.39 (s, 3H), 1.91 – 1.49 (m, 5H), 1.07 (dd, J = 14.5, 8.4 Hz, 2H). MS (ESI): m/z calc. for [M+H$^+$]$^+$ = 568.19, found = 568.28

The intermediate was reacted according to "general procedure for ester and tosylamide hydrolysis". Purification by flash chromatography (silica, DCM/MeOH) gave the title compound (0.287 mg, 76%). ^{1}H NMR (500 MHz, DMSO-d_6) δ 12.11 (d, J = 2.9 Hz, 1H), 7.29 (t, J = 2.7 Hz, 1H), 7.20 (dd, J = 8.4, 2.2 Hz, 1H), 7.16 (s, 1H), 7.11 (d, J = 2.2 Hz, 1H), 6.73 (d, J = 8.5 Hz, 1H), 6.03 (t, J = 2.3 Hz, 1H), 4.29 (s, 2H), 4.17 (d, J = 8.0 Hz, 1H), 3.55 (s, 3H), 3.32 – 3.26 (m, 1H), 2.86 (s, 3H), 1.87 (dd, J = 12.5, 4.1 Hz, 2H), 1.56 (ddt, J = 29.5, 12.5, 3.8 Hz, 3H), 1.41 – 1.25 (m, 2H), 1.15 – 0.97 (m, 3H). ^{13}C NMR (126 MHz, DMSO) δ 154.20, 145.02, 133.13, 131.25, 129.15, 129.05, 126.82, 123.25, 121.62, 115.29, 111.60, 110.31, 102.56, 59.07, 50.67, 35.55, 32.46, 25.37, 24.49. MS (ESI): m/z calc. for [M+H$^+$]$^+$ = 414.18, found = 414.14

4-Cyclohexyl-10-methyl-7-((methylsulfonyl)methyl)-1,3,4,10-tetrahydro-11*H*-1,4,10-triazadibenzo-[*cd,f*]azulen-11-one (80)
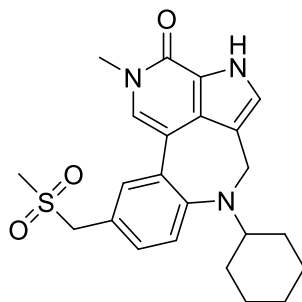
A mixture of compound **79** (50 mg, 0.12 mmol) and paraformaldehyde (11 mg, 0.32 mmol) in AcOH (4 mL) was heated in a sealed vial at 80 °C for 1 h. Afterwards, volatiles were removed under reduced pressure. Purification by flash chromatography (silica, DCM/MeOH) gave the title compound (40 mg, 78%). ^{1}H NMR (500 MHz, DMSO-d_6) δ 11.91 – 11.75 (m, 1H), 7.69 (d, *J* = 2.1 Hz, 1H), 7.54 (s, 1H), 7.22 (dd, *J* = 8.1, 2.0 Hz, 1H), 7.19 – 7.15 (m, 2H), 4.45 (s, 3H), 3.99 (s, 1H), 3.61 (s, 3H), 2.93 (s, 3H), 2.76 – 2.63 (m, 1H), 1.72 (s, 1H), 1.58 (d, *J* = 11.2 Hz, 2H), 1.43 (dd, *J* = 11.7, 4.4 Hz, 2H), 1.15 (d, *J* = 11.3 Hz, 2H), 1.01 (h, *J* = 11.7 Hz, 3H). ^{13}C NMR (126 MHz, DMSO) δ 154.25, 150.10, 134.40, 131.11, 130.68, 129.63, 128.42, 127.80, 126.42, 123.14, 122.72, 117.84, 113.52, 59.55, 57.62, 46.48, 46.44, 36.43, 25.97, 24.96.

Ethyl 4-bromo-7-methoxy-1-tosyl-1*H*-pyrrolo[2,3-*c*]pyridine-2-carboxylate (81)
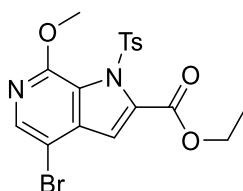
The synthesis was adapted from Sheppard *et al.*[188] 4-Bromo-7-methoxy-1-tosyl-1H-pyrrolo[2,3-c]pyridine (**53**, 16.00 g, 41.97 mmol, 1.0 eq) was dissolved in THF (200 mL) and chilled to -78 °C. A solution of LDA (2.0 M in THF/heptane/ethylbenzene, 33.6 mL, 67.2 mmol, 1.6 eq) was added dropwise and the mixture was stirred at -78 °C for 1 h. Afterwards, ethyl chloroformate (6.0 mL, 63 mmol, 1.5 eq) was added dropwise and the mixture was stirred for 16 h. The reaction was quenched with sat. aq NH₄Cl and extracted with ethyl acetate. The combined organic layers were washed with brine, dried over MgSO₄ and volatiles were removed under reduced pressure. The residue was triturated with DCM/MeOH (1/10) to provide the crude product (18.0 g) which was used in the next step without further purification. ^{1}H-NMR (250 MHz, DMSO) δ 8.21 – 8.09 (m, 3H), 7.56 (d, *J* = 8.7 Hz, 2H), 7.27 (s, 1H), 4.42 (q, *J* = 7.1 Hz, 2H), 3.85 (s, 3H), 2.44 (s, 3H), 1.36 (t, *J* = 7.1 Hz, 3H). MS (ESI): m/z calc. for [M+H$^+$]$^+$ = 455.00, found = 455.00

Ethyl 4-bromo-7-oxo-1-tosyl-6,7-dihydro-1*H*-pyrrolo[2,3-*c*]pyridine-2-carboxylate (82)
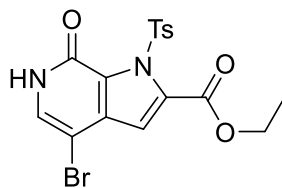
The synthesis was adapted from Sheppard *et al.*[188] Chlorotrimethylsilane (7.1 mL, 56 mmol, 1.4 eq) was added dropwise to a mixture of compound **81** (18.0 g, 39.7 mmol, 1.0 eq) and NaI (8.33 g, 55.6 mmol, 1.4 eq) in ACN (200 mL) and the mixture was stirred at ambient temperature for 1 h. H_2O (0.36 mL 20 mmol, 0.5 eq) was added and the mixture was stirred at 65 °C for 2 h. The reaction mixture was cooled to rt and filtered. The collected solid was dissolved in DCM, filtered, and concentrated to give a brown solid which was washed with hexane and DCM to afford the crude product (16.0 g) which was used in the next step without further purification. ^{1}H-NMR (250 MHz, DMSO) δ 11.78 (s, 1H), 8.26 (d, *J* = 8.4 Hz, 2H), 7.50 (m, 3H), 7.02 (d, *J* = 0.7 Hz, 1H), 4.38 (q, *J* = 7.1 Hz, 2H), 2.42 (s, 3H), 1.34 (t, *J* = 7.1 Hz, 3H). MS (ESI): m/z calc. for [M+H$^+$]$^+$ = 440.99, found = 440.95

Ethyl 4-bromo-6-methyl-7-oxo-1-tosyl-6,7-dihydro-1*H*-pyrrolo[2,3-*c*]pyridine-2-carboxylate (83)
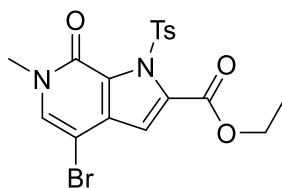
The synthesis was adapted from Sheppard *et al.*[188] Iodomethane (2.7 mL, 44 mmol, 1.2 eq) was added to a mixture of compound **82** (16.0 g, 36.4 mmol, 1.0 eq) and Cs_2CO_3 (14.2 g, 43.7 mol, 1.2 eq) in DMF (150 mL) and stirred at ambient temperature for 16 h. Water was added and the resulting precipitate was filtered and dried to provide the crude product (15.6 g) which was used in the next step without further purification. ^{1}H-NMR (250 MHz, DMSO) δ 8.29 (d, *J* = 8.3 Hz, 2H), 7.94 (d, *J* = 0.7 Hz, 1H), 7.52 (d, *J* = 8.6 Hz, 2H), 7.04 (d, *J* = 0.7 Hz, 1H), 4.39 (q, *J* = 7.1 Hz, 2H), 3.45 (s, 3H), 2.43 (s, 4H), 1.34 (t, *J* = 7.1 Hz, 2H). MS (ESI): m/z calc. for [M+H$^+$]$^+$ = 455.00, found = 455.00

4-Bromo-6-methyl-7-oxo-6,7-dihydro-1*H*-pyrrolo[2,3-*c*]pyridine-2-carboxylic acid (84)
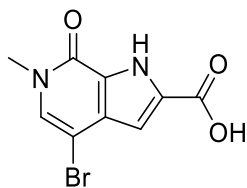
Compound **83** (10.0 g, 22.1 mmol, 1.0 eq) and LiOH·H₂O (7.4 g, 0.18 mol, 8.0 eq) were dissolved in dioxane/water (100 mL, 4/1) and heated at 90 °C for 2 h. Afterwards, volatiles were removed under reduced pressure until about half of the initial volume was reached. The mixture was cooled and brought to a pH of 3 with diluted aq HCl. The resulting precipitate was filtered and dried to provide the title compound as a colorless solid (2.13 g, 36%). ^{1}H NMR (400 MHz, DMSO-d_6) δ 13.18 (br s, 1H), 12.99 (s, 1H), 7.60 (s, 1H), 6.78 (d, J = 2.2 Hz, 1H), 3.50 (s, 3H). ^{13}C NMR (101 MHz, DMSO) δ 161.35, 153.94, 130.63, 130.45, 129.51, 125.29, 107.60, 92.45, 35.73. MS (ESI): m/z calc. for [M+H$^+$]$^+$ = 270.96, found = 270.95

Ethyl 4-bromo-6-methyl-7-oxo-6,7-dihydro-1*H*-pyrrolo[2,3-*c*]pyridine-2-carboxylate (85)
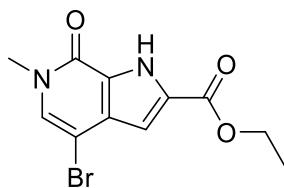
Thionyl chloride (2.0 mL, 28 mmol, 7.5 eq) was added to a solution of compound **84** (1.0 g, 3.7 mmol, 1.0 eq) in ethanol (40 mL) and the mixture was heated at 75 °C for 12 h. Afterwards, the mixture was cooled to rt and ice was added. The resulting precipitate was filtered and dried to provide the title compound as a colorless solid (670 mg, 61%). ^{1}H NMR (400 MHz, DMSO-d_6) δ 13.22 (s, 1H), 7.61 (d, J = 0.7 Hz, 1H), 6.82 (d, J = 2.2 Hz, 1H), 4.30 (q, J = 7.1 Hz, 2H), 3.50 (s, 3H), 1.32 (t, J = 7.1 Hz, 3H). ^{13}C NMR (101 MHz, DMSO) δ 159.87, 153.94, 130.60, 129.47, 125.53, 107.72, 92.36, 60.76, 35.74, 14.06. MS (ESI): m/z calc. for [M+H$^+$]$^+$ = 299.00, found = 299.00

Ethyl 6-methyl-7-oxo-4-(4,4,5,5-tetramethyl-1,3,2-dioxaborolan-2-yl)-6,7-dihydro-1*H*-pyrrolo[2,3-c]pyridine-2-carboxylate (86)
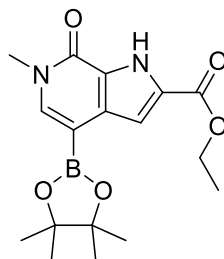
Compound **85** (1.00 g, 3.34 mmol, 1.0 eq), B₂pin₂ (1.70 g, 6.69 mmol, 2.0 eq), potassium ethylhexanoate (1.39 g, 8.36 mmol, 2.5 eq), Pd XPhos G2 (132 mg, 167 μmol, 0.05 eq) and XPhos (80 mg, 0.17 mmol, 0.05 eq) were dissolved in MeTHF/dioxane (50 mL, 4/1) and heated at 50 °C for 16 h. The mixture was partitioned between water and ethyl acetate. The aqueous phase was extracted with ethyl acetate, the combined organic phases were washed with sat. aq NaHCO₃ and brine, dried over MgSO₄ and volatiles were removed under reduced pressure. The residue was purified by flash chromatography (silica, DCM/MeOH) and afterwards triturated with hexane to provide the title compound as a colorless solid (525 mg, 45%). ^{1}H NMR (500 MHz, DMSO-d_6) δ 12.73 (t, 1H), 7.58 (s, 1H), 7.09 (d, *J* = 2.1 Hz, 1H), 4.30 (q, *J* = 7.2 Hz, 2H), 3.55 (s, 3H), 1.32 (t, *J* = 7.1 Hz, 3H), 1.31 (s, 12H). ^{13}C NMR (126 MHz, DMSO) δ 160.35, 155.15, 139.92, 131.33, 129.20, 125.52, 109.68, 83.33, 60.52, 35.79, 24.67, 14.18. MS (ESI): m/z calc. for [M+H$^+$]$^+$ = 347.17, found = 347.15

***tert*-butyl (2-(4-(4-bromo-6-methyl-7-oxo-6,7-dihydro-1*H*-pyrrolo[2,3-c]pyridine-2-carboxamido)-benzamido)phenyl)carbamate (87)**
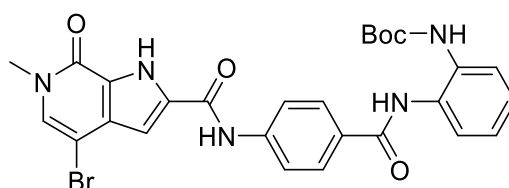
The reaction was performed according to "general procedure for amide coupling". Compound **84** (100 mg, 369 μmol) and compound **34** (146 mg, 443 μmol) were used. The residue was purified by flash chromatography (silica, hexane/ethyl acetate) to provide the title compound as a colorless solid (110 mg, 51%). ^{1}H NMR (250 MHz, DMSO-d_6) δ 12.94 (s, 1H), 10.50 (s, 1H), 9.80 (s, 1H), 8.69 (s, 1H, NH), 8.03 – 7.91 (m, 4H), 7.65 (s, 1H), 7.55 (td, *J* = 7.3, 2.2 Hz, 2H), 7.25 – 7.11 (m, 3H), 3.53 (s, 3H), 1.46 (s, 9H) ppm.

tert-butyl (2-(4-(6-methyl-7-oxo-4-(4,4,5,5-tetramethyl-1,3,2-dioxaborolan-2-yl)-6,7-dihydro-1*H*-pyrrolo[2,3-*c*]pyridine-2-carboxamido)benzamido)phenyl)carbamate (88)
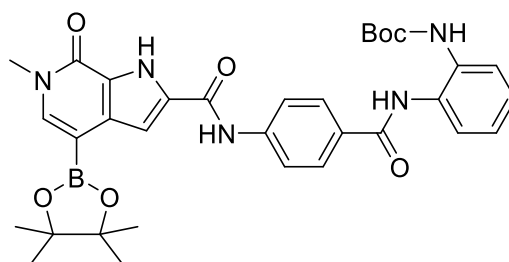
Compound **87** (110 mg, 190 µmol, 1.0 eq), B_2pin_2 (96 mg, 0.38 mmol, 2.0 eq), KOAc (47 mg, 0.47 mmol, 2.5 eq), Pd XPhos G2 (7 mg, 9 µmol, 0.05 eq) and XPhos (5 mg, 9 µmol, 0.05 eq) were dissolved in dioxane (5 mL) and heated at 50 °C for 16 h. The mixture was partitioned between water and ethyl acetate. The aqueous phase was extracted with ethyl acetate, the combined organic phases were washed with sat. aq $NaHCO_3$ and brine, dried over $MgSO_4$ and volatiles were removed under reduced pressure. The residue was purified by flash chromatography (silica, DCM/MeOH) to provide the title compound as a colorless solid (65 mg, 55%).

tert-butyl (2-(4-(4-(2-(cyclohexylamino)-5-((methylsulfonyl)methyl)phenyl)-6-methyl-7-oxo-6,7-dihydro-1*H*-pyrrolo[2,3-*c*]pyridine-2-carboxamido)benzamido)phenyl)carbamate (89)
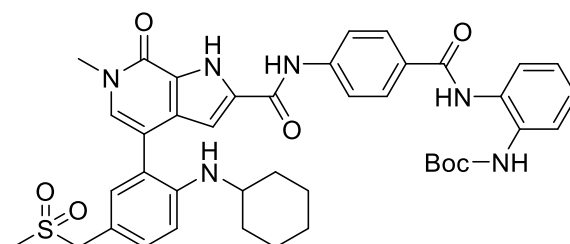
The reaction was performed according to "general procedure for Suzuki coupling B". Compound **88** (65 mg, 0.10 mmol) and compound **78** (61 mg, 155 µmol) were used. The residue was purified by flash chromatography (silica, DCM/MeOH) to provide the title compound (62 mg, 78%).

N-(4-((2-aminophenyl)carbamoyl)phenyl)-4-(2-(cyclohexylamino)-5-((methylsulfonyl)methyl)phenyl)-6-methyl-7-oxo-6,7-dihydro-1H-pyrrolo[2,3-c]pyridine-2-carboxamide (90)
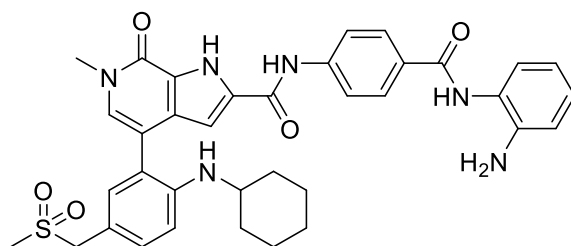
The reaction was performed according to "general procedure for *N-Boc* deprotection". Compound **89** (32 mg, 41 µmol) was used. The residue was purified by flash chromatography (silica, DCM/MeOH) to provide the title compound (18 mg, 65%). ^{1}H NMR (500 MHz, DMSO-d_6) δ 12.54 (s, 1H), 10.34 (s, 1H), 9.72 (s, 1H), 8.04 (d, *J* = 8.5 Hz, 2H), 7.93 – 7.83 (m, 2H), 7.73 (s, 1H), 7.65 (s, 1H), 7.28 (t, *J* = 5.0 Hz, 2H), 7.21 (dd, *J* = 7.9, 1.5 Hz, 1H), 7.01 (td, *J* = 7.6, 1.5 Hz, 1H), 6.85 (dd, *J* = 8.0, 1.5 Hz, 1H), 6.71 – 6.63 (m, 1H), 4.47 (s, 2H), 3.68 (s, 3H), 2.95 (s, 3H), 2.91 – 2.82 (m, 1H), 1.65 – 1.40 (m, 4H), 1.26 – 1.20 (m, 7H), 1.08 – 1.02 (m, 3H).

N-(4-((2-aminophenyl)carbamoyl)phenyl)-4-cyclohexyl-10-methyl-7-((methylsulfonyl)methyl)-11-oxo-3,4,10,11-tetrahydro-1H-1,4,10-triazadibenzo[cd,f]azulene-2-carboxamide (91)
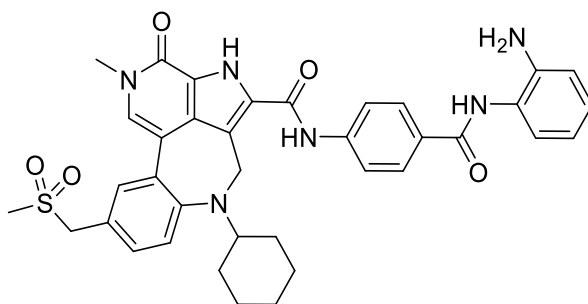
A mixture of compound **89** (30 mg, 39 µmol) and paraformaldehyde (6 mg, 0.2 mmol) in AcOH (1.5 mL) was heated in a sealed vial at 80 °C for 1 h. Afterwards, volatiles were removed under reduced pressure. Purification by flash chromatography (silica, DCM/MeOH) gave the title compound (12 mg, 45%).

(9*H*-fluoren-9-yl)methyl (4-(((tetrahydro-2*H*-pyran-2-yl)oxy)carbamoyl)phenyl)carbamate (97)
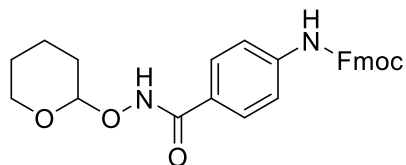
The reaction was performed according to "general procedure for amide coupling". 4-((((9*H*-Fluoren-9-yl)methoxy)carbonyl)amino)benzoic acid (**27**, 4.00 g, 11.1 mmol) and *O*-(tetrahydro-2*H*-pyran-2-yl)hydroxylamine (**96**, 2.61 g, 22.3 mmol) and 60 mL DMF were used. Instead of removing the solvent under reduced pressure, water was added and the resulting precipitate was dried to provide a colorless solid (4.97 g, 97%). ^{1}H NMR (400 MHz, DMSO-d_6) δ 11.48 (s, 1H), 9.97 (s, 1H), 7.91 (dt, J = 7.6, 1.0 Hz, 2H), 7.75 (dd, J = 7.5, 1.1 Hz, 2H), 7.70 (d, J = 8.6 Hz, 2H), 7.52 (d, J = 8.4 Hz, 2H), 7.47 − 7.40 (m, 2H), 7.35 (td, J = 7.4, 1.2 Hz, 2H), 4.97 (d, J = 3.1 Hz, 1H), 4.52 (d, J = 6.6 Hz, 2H), 4.32 (t, J = 6.5 Hz, 1H), 4.05 (ddd, J = 11.9, 8.2, 3.9 Hz, 1H), 3.57 − 3.42 (m, 1H), 1.79 − 1.65 (m, 3H), 1.60 − 1.48 (m, 3H). MS (ESI): m/z calc. for [M-THP+H^{+}][+] = 375.13, found = 375.10

4-Amino-*N*-((tetrahydro-2*H*-pyran-2-yl)oxy)benzamide (98)
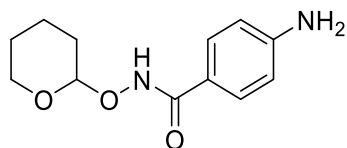
Compound **97** (4.95 g, 10.8 mmol) was dissolved in acetonitrile/morpholine (80 mL, 1/1) and stirred at ambient temperature for 3 h. Water was added, the mixture was filtered, and the filtrate was extracted with DCM. The organic phase was washed with brine, dried over MgSO$_4$, filtered and concentrated under reduced pressure to provide the title compound as an off-white solid (1.97 g, 77%). ^{1}H NMR (400 MHz, DMSO-d_6) δ 11.12 (s, 1H), 7.67 − 7.38 (m, 2H), 6.68 − 6.42 (m, 2H), 5.66 (s, 2H), 5.01 − 4.83 (m, 1H), 4.04 (ddt, *J* = 11.3, 8.7, 4.1 Hz, 1H), 3.52 − 3.46 (m, 1H), 1.75 − 1.65 (m, 3H), 1.58 − 1.48 (m, 3H). MS (ESI): m/z calc. for [M+H^{+}][+] = 237.12, found = 237.20

(*E*)-4-((2-amino-4-hydroxy-5-methylphenyl)diazenyl)-*N*-((tetrahydro-2*H*-pyran-2-yl)oxy)benzamide (99)
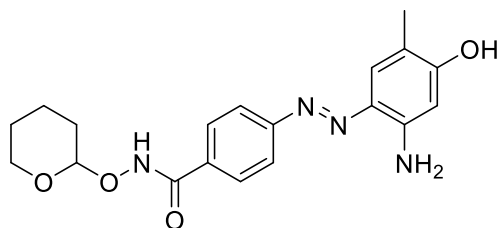
The reaction was performed according to "general procedure for azo coupling". Compound **98** (110 mg, 466 µmol) and 5-amino-2-methylphenol (112 mg, 559 µmol) were used. A red solid (127 mg, 66%) was isolated.

(*E*)-4-((3,5-dibromo-4-hydroxyphenyl)diazenyl)-*N*-((tetrahydro-2*H*-pyran-2-yl)oxy)benzamide (99a)
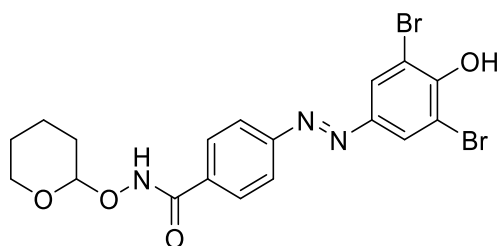
The reaction was performed according to "general procedure for azo coupling". Compound **98** (110 mg, 466 µmol) and 2,6-dibromophenol (129 mg, 512 µmol) were used. A red solid (214 mg, 92%) was isolated. MS (ESI): m/z calc. for [M+H$^+$]$^+$ = 521.95, found = 522.00

(*E*)-4-((4-hydroxy-5-methyl-2-ureidophenyl)diazenyl)-*N*-((tetrahydro-2*H*-pyran-2-yl)oxy)benzamide (99b)
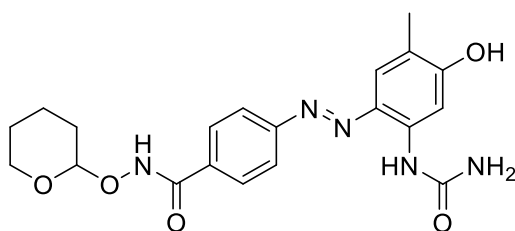
The reaction was performed according to "general procedure for azo coupling". Compound **98** (110 mg, 466 µmol) and 1-(3-hydroxy-4-methylphenyl)urea hydrochloride (113 mg, 559 µmol) were used. A red solid (132 mg, 69%) was isolated. ^{1}H NMR (250 MHz, DMSO-d$_6$) δ 11.75 (s, 1H), 10.46 (s, 1H), 9.04 (s, 1H), 8.06 – 7.98 (m, 3H), 7.93 (d, J = 8.6 Hz, 2H), 7.55 (s, 1H), 6.59 (br s, 2H), 5.03 (s, 1H), 4.17 – 4.05 (m, 1H), 3.61 – 3.49 (m, 1H), 2.09 (s, 3H), 1.80 – 1.70 (m, 3H), 1.62 – 1.43 (m, 3H). MS (ESI): m/z calc. for [M+H$^+$]$^+$ = 521.95, found = 522.00

(*E*)-4-((2-guanidino-4-hydroxy-5-methylphenyl)diazenyl)-*N*-((tetrahydro-2*H*-pyran-2-yl)oxy)benzamide (99c)
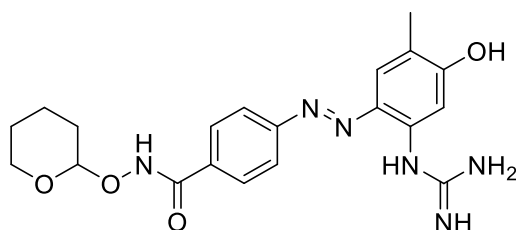
The reaction was performed according to "general procedure for azo coupling". Compound **98** (110 mg, 466 µmol) and 1-(3-hydroxy-4-methylphenyl)guanidinium hydrochloride (112 mg, 559 µmol) were used. A red solid (127 mg, 66%) was isolated. The product was used in the next step without further characterization.

(*E*)-4-((2-amino-5-chloro-4-hydroxyphenyl)diazenyl)-*N*-((tetrahydro-2*H*-pyran-2-yl)oxy)benzamide (99d)
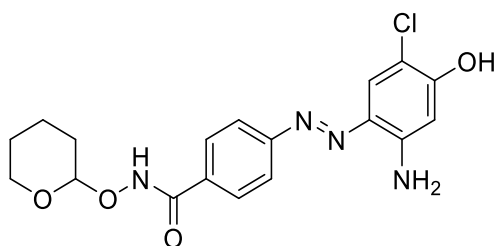
The reaction was performed according to "general procedure for azo coupling". Compound **98** (130 mg, 550 µmol) and 5-amino-2-chlorophenol (87 mg, 0.61 mmol) were used. A red solid (215 mg, quant yield assumed) was isolated. MS (ESI): m/z calc. for [M+H$^+$]$^+$ = 391.11, found = 391.05

(*E*)-4-((2-(benzylamino)-4-hydroxy-5-methylphenyl)diazenyl)-*N*-((tetrahydro-2*H*-pyran-2-yl)oxy)benzamide (99e)
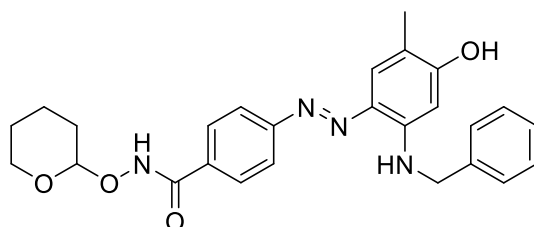
The reaction was performed according to "general procedure for azo coupling". Compound **98** (120 mg, 508 µmol) and 5-(benzylamino)-2-methylphenol 119 mg, 559 µmol) were used. A red solid (134 mg, 57%) was isolated. MS (ESI): m/z calc. for [M+H$^+$]$^+$ = 461.21, found = 461.20

(*E*)-4-((4-hydroxy-5-methyl-2-(2-phenylacetamido)phenyl)diazenyl)-*N*-((tetrahydro-2*H*-pyran-2-yl)oxy)benzamide (99f)
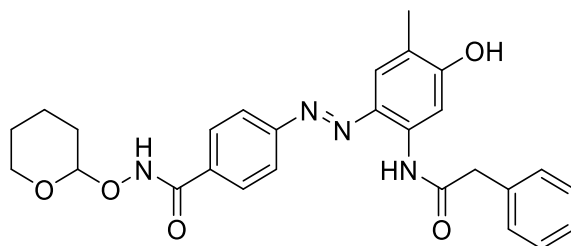
The reaction was performed according to "general procedure for azo coupling". Compound **98** (130 mg, 550 μmol) and *N*-(3-hydroxy-4-methylphenyl)-2-phenylacetamide (146 mg, 605 μmol) were used. A red solid (143 mg, 53%) was isolated. MS (ESI): m/z calc. for [M+H$^+$]$^+$ = 489.21, found = 489.15

***tert*-butyl** **(*E*)-(2-((5-hydroxy-4-methyl-2-((4-(((tetrahydro-2*H*-pyran-2-yl)oxy)carbamoyl)phenyl)diazenyl)phenyl)amino)-2-oxoethyl)carbamate (99g)**
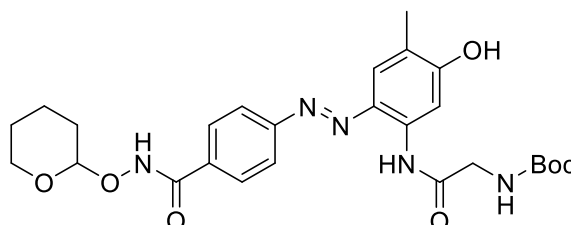
The reaction was performed according to "general procedure for azo coupling". Compound **98** (130 mg, 550 μmol) and *tert*-butyl (2-((3-hydroxy-4-methylphenyl)amino)-2-oxoethyl)carbamatephenylacetamide (170 mg, 605 μmol) were used. A red solid (212 mg, 73%) was isolated. MS (ESI): m/z calc. for [M+H$^+$]$^+$ = 528.24, found = 528.20

(*E*)-4-((2-Amino-4-hydroxy-5-methylphenyl)diazenyl)-*N*-hydroxybenzamide (100)
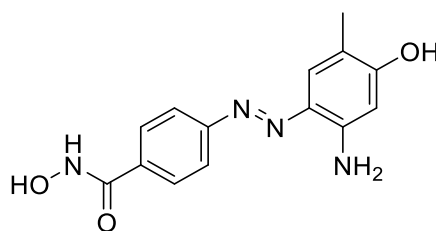
The reaction was performed according to "general procedure for THP deprotection". Compound **99** (127 mg, 293 μmol) was used. A red solid (42 mg, 43%) was isolated. ^{1}H NMR (500 MHz, DMSO-*d*$_6$) δ 11.25 (s, 1H), 10.14 (s, 1H), 9.03 (s, 1H), 7.84 (d, *J* = 8.4 Hz, 2H), 7.80 (d, *J* = 8.4 Hz, 2H), 7.40 (s, 1H), 7.05 (s, 2H), 6.25 (s, 1H), 2.03 (s, 3H). ^{13}C NMR (126 MHz, DMSO) δ 163.82, 161.07, 154.53, 146.20, 131.83, 130.73, 127.86, 121.11, 114.52, 100.10, 15.18. MS (HRMS): m/z calc. for [C$_{14}$H$_{14}$N$_4$O$_3$+H$^+$]$^+$ = 287.1139, found = 287.1140

(*E*)-4-((3,5-dibromo-4-hydroxyphenyl)diazenyl)-*N*-hydroxybenzamide (100a)
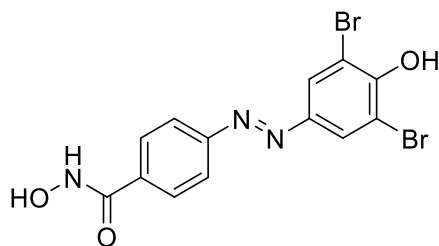
The reaction was performed according to "general procedure for THP deprotection". Compound **99a** (197 mg, 395 μmol) was used. A red solid (121 mg, 74%) was isolated. ^{1}H NMR (500 MHz, DMSO-d$_6$) δ 11.38 (s, 1H), 10.92 (s, 1H), 9.15 (s, 1H), 8.13 (s, 2H), 7.95 (d, J = 8.7 Hz, 2H), 7.91 (d, J = 8.6 Hz, 2H). ^{13}C NMR (126 MHz, DMSO) δ 163.32, 152.90, 145.57, 134.94, 128.18, 126.97, 122.41, 112.44. HRMS (MALDI): m/z calc. for [M+H$^+$]$^+$ = 415.9063, found = 415.9061

(*E*)-*N*-hydroxy-4-((4-hydroxy-5-methyl-2-ureidophenyl)diazenyl)benzamide (100b)
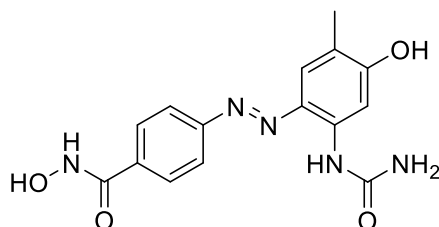
The reaction was performed according to "general procedure for THP deprotection". Compound **99b** (132 mg, 319 μmol) was used. A red solid (83 mg, 79%) was isolated. ^{1}H NMR (500 MHz, DMSO-d$_6$) δ 11.34 (s, 1H), 10.45 (s, 1H), 9.10 (s, 1H), 9.02 (s, 1H), 8.03 (s, 1H), 7.99 (d, J = 8.6 Hz, 2H), 7.91 (d, J = 8.6 Hz, 2H), 7.54 (d, J = 1.1 Hz, 1H), 6.60 (s, 2H), 2.08 (s, 3H). ^{13}C NMR (126 MHz, DMSO) δ 164.02, 161.73, 155.79, 154.32, 140.58, 133.79, 132.88, 128.36, 122.78, 119.30, 118.77, 104.67, 15.81. HRMS (MALDI): m/z calc. for [M+H$^+$]$^+$ = 331.1230, found = 331.1234

(*E*)-4-((2-guanidino-4-hydroxy-5-methylphenyl)diazenyl)-*N*-hydroxybenzamide (100c)
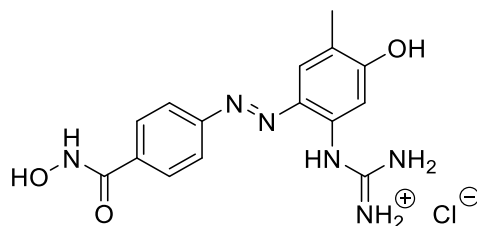
The reaction was performed according to "general procedure for THP deprotection". Compound **99c** (127 mg, 308 µmol) was used. A red solid (79 mg, 70%) was isolated as a HCl salt. ^{1}H NMR (500 MHz, DMSO-d$_6$) δ 11.48 (s, 1H), 11.07 (s, 1H), 10.23 (s, 1H), 9.15 (s, 1H), 7.95 (d, J = 8.7 Hz, 2H), 7.92 (d, J = 8.6 Hz, 2H), 7.82 (s, 4H), 7.61 (s, 1H), 7.07 (s, 1H), 2.15 (s, 3H). ^{13}C NMR (126 MHz, DMSO) δ 163.52, 160.92, 156.91, 153.88, 137.98, 134.74, 134.00, 128.11, 124.16, 122.49, 118.26, 111.40, 15.72. HRMS (MALDI): m/z calc. for [M+H$^+$]$^+$ = 329.1357, found = 329.1365

(*E*)-4-((2-amino-5-chloro-4-hydroxyphenyl)diazenyl)-*N*-hydroxybenzamide (100d)
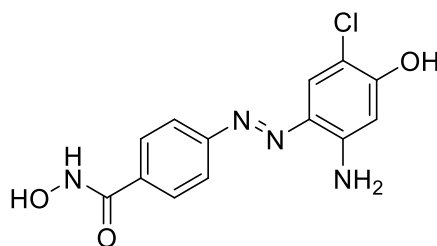
The reaction was performed according to "general procedure for THP deprotection". Compound **99d** (215 mg, 550 µmol) was used. A red solid (79 mg, 47%) was isolated. ^{1}H NMR (500 MHz, DMSO-d$_6$) δ 11.29 (s, 1H), 10.83 (s, 1H), 9.08 (s, 1H), 7.87 (s, 4H), 7.62 (s, 1H), 7.06 (s, 2H), 6.43 (d, J = 7.3 Hz, 1H). HRMS (MALDI): m/z calc. for [M+H$^+$]$^+$ = 307.0592, found = 307.0595

(*E*)-4-((2-(benzylamino)-4-hydroxy-5-methylphenyl)diazenyl)-*N*-hydroxybenzamide (100e)
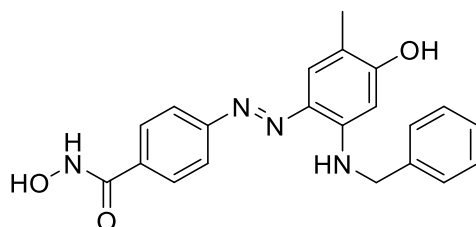
The reaction was performed according to "general procedure for THP deprotection". Compound **99e** (134 mg, 291 µmol) was used. A red solid (20 mg, 18%) was isolated. ^{1}H NMR (500 MHz, DMSO-d$_6$) δ 11.26 (s, 1H), 10.24 (s, 1H), 9.22 (s, 1H), 9.04 (s, 1H), 7.86 (d, J = 8.6 Hz, 2H), 7.81 (d, J = 8.6 Hz, 2H), 7.49 (s, 1H), 7.39 – 7.35 (m, 4H), 7.26 (ddd, J = 8.6, 5.4, 3.3 Hz, 1H), 6.15 (s, 1H), 4.50 (d, J = 6.1 Hz, 2H), 2.04 (s, 3H). ^{13}C NMR (126 MHz, DMSO) δ 163.77, 161.58, 154.30, 145.21, 139.19, 131.93, 130.76,

128.50, 127.89, 126.85, 126.80, 121.09, 114.24, 96.59, 45.71, 15.02. HRMS (MALDI): m/z calc. for [M+H$^+$]$^+$ = 377.1608, found = 377.1611

(*E*)-*N*-hydroxy-4-((4-hydroxy-5-methyl-2-(2-phenylacetamido)phenyl)diazenyl)benzamide (100f)
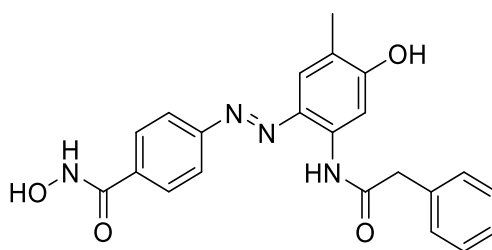
The reaction was performed according to "general procedure for THP deprotection". Compound **99f** (143 mg, 293 µmol) was used. A red solid (78 mg, 66%) was isolated. ^{1}H NMR (500 MHz, DMSO-d$_6$) δ 11.38 (s, 1H), 9.18 (s, 1H), 7.89 – 7.82 (m, 2H), 7.63 – 7.56 (m, 2H), 7.44 (d, J = 1.5 Hz, 1H), 7.19 (dd, J = 5.1, 2.0 Hz, 3H), 6.98 – 6.91 (m, 2H), 6.19 (s, 1H), 3.98 (s, 2H), 3.01 (td, J = 6.7, 3.9 Hz, 1H), 2.11 (s, 3H), 1.78 – 1.63 (m, 1H). ^{13}C NMR (126 MHz, DMSO) δ 184.34, 154.78, 146.87, 141.82, 140.37, 135.18, 129.31, 128.83, 128.48, 127.87, 127.62, 127.33, 110.01, 46.35, 26.41, 17.20. MS (ESI): m/z calc. for [M+H$^+$]$^+$ = 405.15, found = 405.15

(*E*)-4-((2-(2-aminoacetamido)-4-hydroxy-5-methylphenyl)diazenyl)-*N*-hydroxybenzamide (100g)
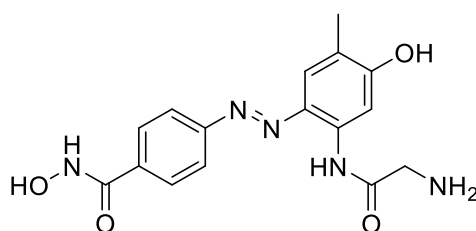
Compound **99g** (212 mg, 402 µmol) was dissolved in DCM (10 mL) and HCl in dioxane (4 M, 1.0 mL, 4.0 mmol) was added. After stirring at ambient temperature for 1 h, all volatiles were removed under reduced pressure and the residue was purified by flash chromatography (C18 silica, H$_2$O/ACN) to provide the title compound as a HCl salt (64 mg, 46%). ^{1}H NMR (500 MHz, DMSO-d$_6$) δ 11.40 (s, 1H), 10.72 (s, 1H), 10.38 (s, 1H), 8.31 (t, J = 5.8 Hz, 3H), 8.04 (d, J = 8.2 Hz, 2H), 7.93 (d, J = 8.3 Hz, 2H), 7.90 (s, 1H), 7.62 (s, 1H), 4.00 (d, J = 5.9 Hz, 2H), 2.15 (s, 3H). ^{13}C NMR (126 MHz, DMSO) δ 165.72, 161.24, 154.15, 137.21, 134.77, 134.32, 128.36, 123.16, 122.05, 118.60, 107.76, 16.05. HRMS (MALDI): m/z calc. for [M+H$^+$]$^+$ = 344.1353, found = 344.1354

***tert*-Butyl (*E*)-(2-(4-((2-amino-4-hydroxy-5-methylphenyl)diazenyl)benzamido)phenyl)carbamate (101a)**
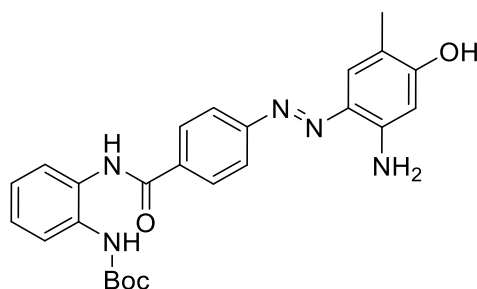
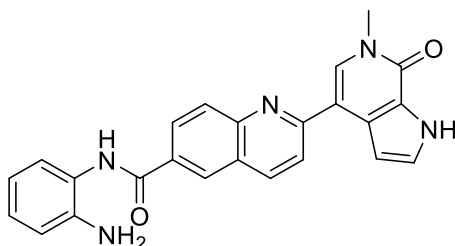The synthesis was performed as described by Bauer *et al.*[277] The synthesis was performed according to "general procedure for azo coupling". *tert*-Butyl (2-(4-aminobenzamido)phenyl)carbamate (**34**, 75 mg, 0.23 mmol, 1.0 eq), conc. HCl (19 μL, 0.23 mmol, 1.0 eq), *iso*-amyl nitrite (31 μL, 0.23 mmol, 1.0 eq), 5-amino-2-methylphenol (27 mg, 0.23 mmol, 1.0 eq) and K_2CO_3 (158 mg, 1.15 mmol, 5.0 eq) were used. The crude product was purified by flash chromatography (hexane/ethyl acetate) to provide the title compound as a red solid (90 mg, 85%). ^{1}H NMR (400 MHz, DMSO-d_6) δ 10.22 (s, 1H), 9.87 (s, 1H), 8.69 (s, 1H), 8.05 (d, *J* = 8.5 Hz, 2H), 7.87 (d, *J* = 8.2 Hz, 2H), 7.55 (ddd, *J* = 7.8, 4.5, 1.7 Hz, 2H), 7.43 (d, *J* = 1.1 Hz, 1H), 7.21 (td, *J* = 7.7, 1.8 Hz, 1H), 7.16 (td, *J* = 7.4, 1.6 Hz, 1H), 7.12 (br s, 2H), 6.24 (s, 1H), 2.04 (s, 3H), 1.46 (s, 9H). MS (ESI): m/z calc. for $[C_{25}H_{27}N_5O_4+H^+]^+$ = 462.21, found = 462.27

***tert*-Butyl (*E*)-(2-(4-((2-amino-4-hydroxy-5-methylphenyl)diazenyl)benzamido)-4-(thiophen-2-yl)phenyl)carbamate (101b)**
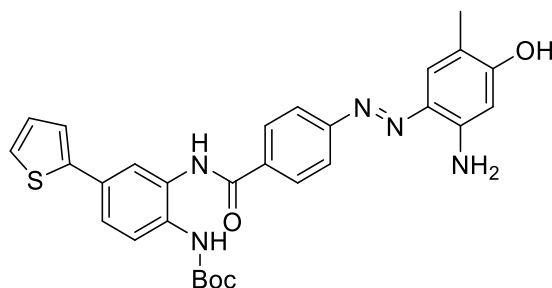
The synthesis was performed according to "general procedure for azo coupling". *tert*-Butyl (2-(4-aminobenzamido)-4-(thiophen-2-yl)phenyl)carbamate (**28a**, 110 mg, 269 μmol, 1.0 eq), conc. HCl (22.4 μL, 269 μmol, 1.0 eq), *iso*-amyl nitrite (35.8 μL, 269 μmol, 1.0 eq), 5-amino-2-methylphenol (33 mg, 0.27 mmol, 1.0 eq) and K_2CO_3 (186 mg, 1.34 mmol, 5.0 eq) were used. The crude product was purified by flash chromatography (DCM/methanol) to provide the title compound as a red solid (79 mg, 54%). MS (ESI): m/z calc. for $[C_{29}H_{29}N_5O_4S+H^+]^+$ = 544.19, found = 544.22

***tert*-Butyl (*E*)-(3-(4-((2-amino-4-hydroxy-5-methylphenyl)diazenyl)benzamido)-[1,1'-biphenyl]-4-yl)carbamate (101c)**
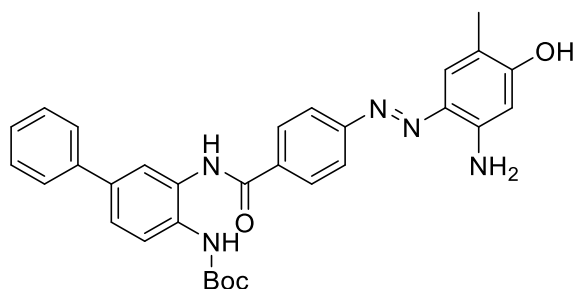
The synthesis was performed according to "general procedure for azo coupling". *tert*-Butyl (3-(4-aminobenzamido)-[1,1'-biphenyl]-4-yl)carbamate (**28d**, 150 mg, 372 μmol, 1.0 eq), conc. HCl (31.0 μL, 372 μmol, 1.0 eq), *iso*-amyl nitrite (49.6 μL, 372 μmol, 1.0 eq), 5-amino-2-methylphenol (46 mg, 0.37 mmol, 1.0 eq) and K_2CO_3 (257 mg, 1.86 mmol, 5.0 eq) were used. The crude product was purified by flash chromatography (DCM/methanol) to provide the title compound as a red solid (100 mg, 50%). ^{1}H NMR (400 MHz, DMSO-d_6) δ 10.17 (s, 1H), 9.97 (s, 1H), 8.79 (s, 1H), 8.08 (d, *J* = 8.4 Hz, 2H), 7.90 (d, *J* = 8.2 Hz, 2H), 7.87 (d, *J* = 2.2 Hz, 1H), 7.70 – 7.67 (m, 2H), 7.66 – 7.64 (m, 2H), 7.53 (dd, *J* = 8.5, 2.2 Hz, 1H), 7.48 (d, *J* = 7.5 Hz, 1H), 7.45 (d, *J* = 6.1 Hz, 1H), 7.39 – 7.33 (m, 1H), 7.14 (s, 2H), 6.27 (s, 1H), 2.05 (s, 3H), 1.48 (s, 9H). MS (ESI): m/z calc. for $[C_{31}H_{31}N_5O_4+H^+]^+$ = 538.24, found = 538.36

(*E*)-4-((2-Amino-4-hydroxy-5-methylphenyl)diazenyl)-*N*-(2-aminophenyl)benzamide (102a)
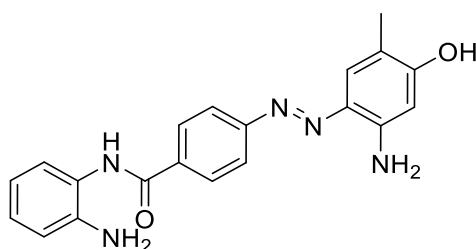
The synthesis was performed as described by Bauer *et al.*[277] The synthesis was performed according to "general procedure for *N-Boc* deprotection". *tert*-Butyl (*E*)-(2-(4-((2-amino-4-hydroxy-5-methylphenyl)diazenyl)benzamido)phenyl)carbamate (**101a**, 85 mg, 0.18 mmol) was used. The crude product was purified by flash chromatography (C18 silica, ACN/H_2O) to provide the title compound as a red solid (42 mg, 63%). ^{1}H NMR (500 MHz, DMSO-d_6) δ 10.20 (s, 1H), 9.71 (s, 1H), 8.08 (d, *J* = 8.2 Hz, 2H), 7.86 (d, *J* = 8.2 Hz, 2H), 7.44 (s, 1H), 7.19 (d, *J* = 7.8 Hz, 1H), 7.09 (s, 2H), 6.98 (td, *J* = 7.6, 1.6 Hz, 1H), 6.80 (dd, *J* = 8.0, 1.5 Hz, 1H), 6.61 (td, *J* = 7.5, 1.4 Hz, 1H), 6.26 (s, 1H), 4.92 (s, 2H), 2.05 (s, 3H). MS (ESI): m/z calc. for $[C_{20}H_{19}N_5O_2+H^+]^+$ = 362.15, found = 362.18. MS (HRMS): m/z calc. for $[C_{20}H_{19}N_5O_2+H^+]^+$ = 362.1612, found = 362.1613

(*E*)-4-((2-Amino-4-hydroxy-5-methylphenyl)diazenyl)-*N*-(2-amino-5-(thiophen-2-yl)phenyl)benzamide (102b)
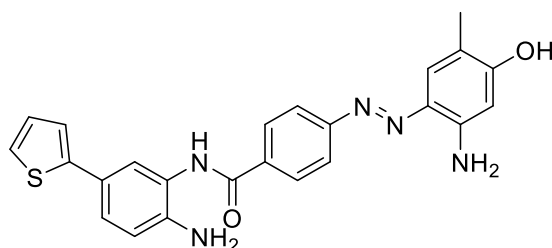
The synthesis was performed according to "general procedure for *N*-Boc deprotection". *tert*-butyl (*E*)-(2-(4-((2-amino-4-hydroxy-5-methylphenyl)diazenyl)benzamido)-4-(thiophen-2-yl)phenyl)carbamate (**101b**, 79 mg, 0.15 mmol) was used. The crude product was purified by flash chromatography (C18 silica, ACN/H$_2$O) to provide the title compound as a red solid (54 mg, 70%). ^{1}H NMR (500 MHz, DMSO-d_6) δ 10.20 (s, 1H), 9.78 (s, 1H), 8.10 (d, *J* = 8.3 Hz, 2H), 7.87 (d, *J* = 8.2 Hz, 2H), 7.50 (d, *J* = 2.3 Hz, 1H), 7.44 (d, *J* = 1.1 Hz, 1H), 7.36 (dd, *J* = 5.1, 1.1 Hz, 1H), 7.31 (dd, *J* = 8.3, 2.2 Hz, 1H), 7.26 (dd, *J* = 3.6, 1.2 Hz, 1H), 7.10 (s, 2H), 7.05 (dd, *J* = 5.1, 3.6 Hz, 1H), 6.83 (d, *J* = 8.3 Hz, 1H), 6.26 (s, 1H), 5.18 (s, 2H), 2.05 (s, 3H). ^{13}C NMR (126 MHz, DMSO) δ 164.99, 161.29, 154.72, 146.26, 144.25, 143.11, 133.39, 130.78, 128.91, 128.21, 123.98, 123.95, 123.42, 123.20, 122.24, 121.01, 116.36, 114.69, 100.08, 15.24. MS (HRMS): m/z calc. for [C$_{24}$H$_{21}$N$_5$O$_2$S+H$^+$]$^+$ = 444.1489, found = 444.1480

(*E*)-4-((2-amino-4-hydroxy-5-methylphenyl)diazenyl)-N-(4-amino-[1,1'-biphenyl]-3-yl)benzamide (102c)
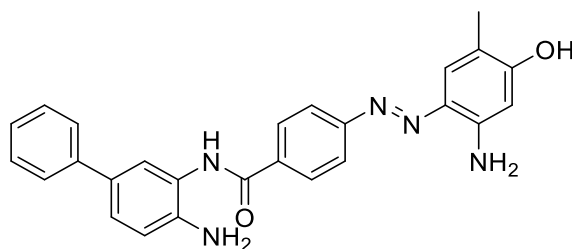
The synthesis was performed according to "general procedure for *N-Boc* deprotection". *tert*-Butyl (*E*)-(3-(4-((2-amino-4-hydroxy-5-methylphenyl)diazenyl)benzamido)-[1,1'-biphenyl]-4-yl)carbamate (**101c**, 95 mg, 0.18 mmol) was used. The crude product was purified by flash chromatography (C18 silica, ACN/H$_2$O) to provide the title compound as a red solid (52 mg, 68%). ^{1}H NMR (500 MHz, DMSO-d_6) δ 10.18 (s, 1H), 9.79 (s, 1H), 8.11 (d, *J* = 8.2 Hz, 2H), 7.87 (d, *J* = 8.1 Hz, 2H), 7.60 – 7.54 (m, 2H), 7.55 (d, *J* = 2.2 Hz, 1H), 7.44 (d, *J* = 1.1 Hz, 1H), 7.40 (t, *J* = 7.8 Hz, 2H), 7.34 (dd, *J* = 8.3, 2.2 Hz, 1H), 7.26 – 7.22 (m, 1H), 7.10 (s, 2H), 6.88 (d, *J* = 8.4 Hz, 1H), 6.26 (s, 1H), 5.12 (s, 2H), 2.04 (s, 3H). ^{13}C NMR (126 MHz, DMSO) δ 165.5, 143.4, 140.7, 131.3, 129.4, 129.3, 128.6, 126.0, 125.3, 125.2, 124.1, 121.5, 121.5, 121.5, 121.4, 117.0, 100.6, 15.7. MS (ESI): m/z calc. for [C$_{26}$H$_{23}$N$_5$O$_2$+H$^+$]$^+$ = 438.19, found = 438.21. MS (HRMS): m/z calc. for [C$_{26}$H$_{23}$N$_5$O$_2$+H$^+$]$^+$ = 438.1925, found = 438.1918

1-(6-chloro-1*H*-indol-1-yl)-2,2-dimethylpropan-1-one (104a)
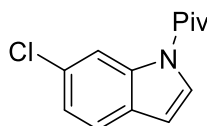
The synthesis was adapted from Lv *et al.*[274] A mixture of 6-chloro-1H-indole (**103a**, 2.00 g, 13.2 mmol), pivaloyl chloride (1.95 mL, 15.8 mmol) and DIPEA (3.22 mL, 18.5 mmol) in DCM (40 mL) was stirred at ambient temperature for 16 h. Afterwards, volatiles were removed under reduced pressure and the residue was purified by flash chromatography (hexane/EE) to provide a colorless solid (1.46 g, 47%). ^{1}H NMR (400 MHz, DMSO-d_6) δ 8.39 (d, J = 2.0 Hz, 1H), 8.12 (d, J = 3.9 Hz, 1H), 7.62 (d, J = 8.3 Hz, 1H), 7.30 (dd, J = 8.3, 2.0 Hz, 1H), 6.76 (dd, J = 3.8, 0.8 Hz, 1H), 1.43 (s, 9H). MS (ESI): m/z calc. for [M+H$^+$]$^+$ = 236.08, found = 236.05

2,2-Dimethyl-1-(6-methyl-1*H*-indol-1-yl)propan-1-one (104b)
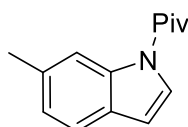
The synthesis was adapted from Lv *et al.*[274] ^{1}H NMR (400 MHz, DMSO-d_6) δ 8.24 – 8.21 (m, 1H), 7.99 (d, *J* = 3.8 Hz, 1H), 7.47 (d, *J* = 7.9 Hz, 1H), 7.09 (ddd, *J* = 7.9, 1.6, 0.7 Hz, 1H), 6.67 (dd, *J* = 3.9, 0.8 Hz, 1H), 2.41 (s, 3H), 1.44 (s, 9H). MS (ESI): m/z calc. for [$C_{14}H_{17}NO+H^+$]$^+$ = 216.13, found = 216.10

6-chloro-1*H*-indol-7-ol (105a)
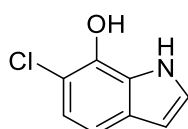
The synthesis was adapted from Lv *et al.*[275] 1-(6-Chloro-1*H*-indol-1-yl)-2,2-dimethylpropan-1-one (**104a**, 800 mg, 3.39 mmol, 1.0 eq) was dissolved in anh. DCM (10 mL) and cooled to 0 °C. Afterwards, a solution of BBr$_3$ in DCM (1 M, 3.7 mL, 3.7 mmol) was added and the mixture was stirred at ambient temperature for 1 h. Volatiles were removed under reduced pressure and the residue was dissolved in anh. THF. Sodium perborate (1.57 g, 10.2 mmol, 3 eq), followed by aq K_2CO_3 (1 M, 10 mL) were added. After stirring at ambient temperature for 1 h, volatiles were removed under reduced pressure and the residue was purified by flash chromatography (hexane/EE) to provide a colorless solid (200 mg, 35%). ^{1}H NMR (400 MHz, DMSO-d_6) δ 10.90 (s, 1H), 9.53 (s, 1H), 7.28 (dd, J = 3.0, 2.5 Hz, 1H), 7.03 (dd, J = 8.4, 0.7 Hz, 1H), 6.90 (d, J = 8.4 Hz, 1H), 6.38 (dd, J = 3.0, 2.0 Hz, 1H). MS (ESI): m/z calc. for [M+H$^+$]$^+$ = 168.01, found = 168.00

6-Methyl-1*H*-indol-7-ol (105b)
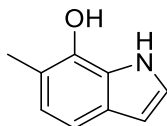
The synthesis was adapted from Lv *et al.*[275] MS (ESI): m/z calc. for $[C_9H_9NO+H^+]^+$ = 148.07, found = 148.10

(*E*)-4-((6-chloro-7-hydroxy-1*H*-indol-4-yl)diazenyl)-*N*-hydroxybenzamide (106)
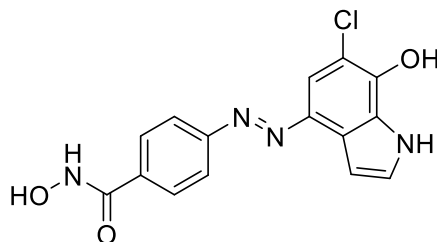
The reaction was performed according to "general procedure for azo coupling". Compound **98** (120 mg, 508 μmol) and 6-chloro-1H-indol-7-ol (**105a**, 101 mg, 605 μmol) were used. A red solid (76 mg, 33%) was isolated. MS (ESI): m/z calc. for $[M+H^+]^+$ = 415.11, found = 415.05

The intermediate was reacted according to "general procedure for THP deprotection". A red solid (23 mg, 38%) was isolated. ^{1}H NMR (500 MHz, DMSO-d$_6$) δ 12.18 (s, 1H), 11.70 (s, 1H), 11.12 (s, 1H), 8.35 (s, 1H), 7.85 – 7.72 (m, 4H), 7.48 (s, 1H), 7.29 (s, 1H), 6.69 (s, 1H). HRMS (MALDI): m/z calc. for $[M+H^+]^+$ = 331.0592, found = 331.0592

(*E*)-*N*-(2-aminophenyl)-4-((6-chloro-7-hydroxy-1*H*-indol-4-yl)diazenyl)benzamide (107a)
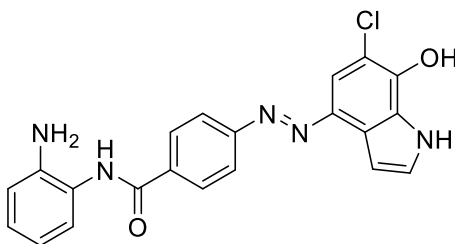
The reaction was performed according to "general procedure for azo coupling". Compound **34** (65 mg, 0.20 mmol) and 6-chloro-1H-indol-7-ol (**105a**, 33 mg, 0.20 mmol) were used. A red solid (25 mg, 25%) was isolated. MS (ESI): m/z calc. for $[M+H^+]^+$ = 528.24, found = 506.10

The intermediate was reacted according to "general procedure for *Boc* deprotection. A red solid (16 mg, 80%) was isolated. HRMS (MALDI): m/z calc. for $[M+Na^+]^+$ = 428.0885, found = 428.0883

(_E_)-_N_-(2-Aminophenyl)-4-((7-hydroxy-6-methyl-1_H_-indol-4-yl)diazenyl)benzamide (107b)
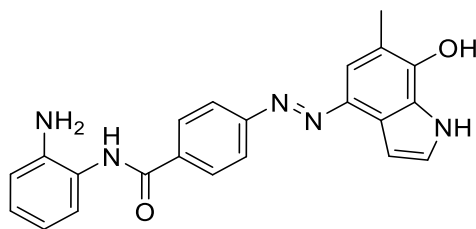
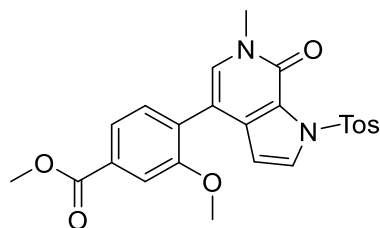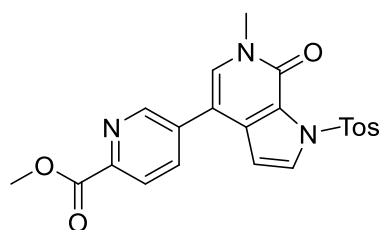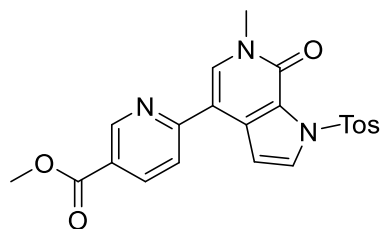The synthesis was performed as described by Bauer _et al._[277] The synthesis was performed according to "general procedure for azo coupling". _tert_-Butyl (2-(4-aminobenzamido)phenyl)carbamate (**34**, 160 mg, 489 µmol, 1.0 eq) and 6-methyl-1_H_-indol-7-ol (**105b**, 86 mg, 0.59 mmol, 1.2 eq) were used. The _Boc_-protected intermediate was used in the next step without further purification. MS (ESI): m/z calc. for $[C_9H_9NO+H^+]^+$ = 486.21, found = 486.20

The intermediate was reacted according to "general procedure for _N-Boc_ deprotection. Crude _tert_-Butyl (_E_)-(2-(4-((7-hydroxy-6-methyl-1_H_-indol-4-yl)diazenyl)benzamido)phenyl)carbamate (max. 237 mg, 488 µmol) was used. The crude product was purified by flash chromatography (C18 silica, ACN/H$_2$O) to provide the title compound as a red solid (19 mg, 8%).^{1}H NMR (500 MHz, DMSO-d_6) δ 11.93 (s, 1H), 11.30 (s, 1H), 9.52 (s, 1H), 7.99 (d, _J_ = 8.6 Hz, 2H), 7.81 (s, 1H), 7.59 (d, _J_ = 8.7 Hz, 1H), 7.46 (d, _J_ = 8.8 Hz, 2H), 7.18 (d, _J_ = 3.0 Hz, 1H), 6.97 (t, _J_ = 7.6 Hz, 1H), 6.79 (dd, _J_ = 7.9, 1.4 Hz, 1H), 6.63 (t, _J_ = 2.5 Hz, 1H), 6.60 (dd, _J_ = 7.5, 1.5 Hz, 1H), 4.90 (br s, 2H), 2.11 (s, 3H). HRMS (MALDI): m/z calc. for $[C_{22}H_{19}N_5O_2+H^+]^+$ = 386.1612, found = 386.1611

6-(Methoxycarbonyl)quinoline 1-oxide (109)
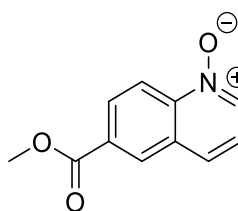
The synthesis was adapted from Ito _et al._ and performed as described by Bauer _et al._[277,315] Methyl quinoline-6-carboxlate (**108**, 8.00 g, 42.7 mmol, 1.0 eq) was dissolved in DCM (200 mL) and cooled to 0 °C. _meta_-chloroperoxybenzoic acid (75 %, wet with water; 19.67 g, 85.47 mmol, 2.0 eq) was added in small portions to the stirring solution. After addition, the cooling bath was removed and the solution was stirred for 3 h at ambient temperature. Afterwards, the reaction mixture was quenched with sat. aq NaHCO$_3$ and the aqueous layer was extracted with DCM. The combined organic layers were washed with brine, dried over MgSO$_4$, filtered and the solvent was removed under reduced pressure to provide a colorless solid (7.97 g, 92%). ^{1}H NMR (400 MHz, DMSO-d_6) δ 8.70 (d, _J_ = 1.6 Hz, 1H), 8.67 (d, _J_ = 5.9 Hz, 1H), 8.58 (d, _J_ = 9.0 Hz, 1H), 8.18 (dd, _J_ = 9.0, 1.6 Hz, 1H), 8.09 (d, _J_ = 8.3 Hz, 1H), 7.54 (dd, _J_ = 8.5,

5.8 Hz, 1H), 3.92 (s, 3H). ^{13}C NMR (101 MHz, DMSO) δ 165.26, 142.43, 136.99, 131.09, 129.85, 129.43, 128.99, 126.06, 122.87, 119.75, 52.58. MS (ESI): m/z calc. for $[C_{11}H_9NO_3+H^+]^+$ = 204.06, found = 204.05

Methyl 2-hydroxyquinoline-6-carboxylate (110)
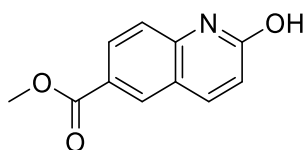
The synthesis was adapted from Xie *et al.* and performed as described by Bauer *et al.*[277,316] Mesyl chloride (6.03 mL, 77.7 mmol, 2.0 eq) was added to a stirred solution of 6-(methoxycarbonyl)quinoline 1-oxide (**109**, 7.90 g, 38.9 mmol, 1.0 eq) in acetonitrile/water (1/1, 140 mL) and the mixture was stirred at ambient temperature for 45 minutes. The resulting precipitate was filtered, washed with hexane and dried to give a colorless solid (5.68 g, 72%). ^{1}H NMR (400 MHz, DMSO-d_6) δ 12.03 (s, 1H), 8.29 (d, *J* = 1.9 Hz, 1H), 8.07 – 7.97 (m, 2H), 7.35 (d, *J* = 8.6 Hz, 1H), 6.56 (d, *J* = 9.6 Hz, 1H), 3.85 (s, 3H). ^{13}C NMR (101 MHz, DMSO) δ 165.66, 162.03, 142.08, 140.37, 130.54, 129.86, 122.82, 122.72, 118.63, 115.37, 52.01. MS (ESI): m/z calc. for $[C_{11}H_9NO_3+H^+]^+$ = 204.06, found = 204.10

Methyl 2-chloroquinoline-6-carboxylate (111)
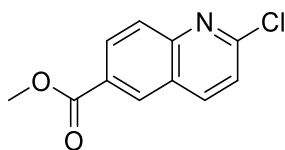
The synthesis was performed as described by Bauer *et al.*[277] Methyl 2-hydroxyquinoline-6-carboxylate (**110**, 5.64 g, 27.8 mmol) was suspended in DCM (80 mL) and cooled to 0 °C. DMF (5.0 mL) and SOCl$_2$ (5.0 mL, 68.9 mmol, 2.5 eq) were subsequently added and the mixture was stirred for 18 h. The reaction was quenched with ice and sat. aq NaHCO$_3$ and extracted with DCM. The organic phase was washed with sat. aq NaHCO$_3$ and brine, dried over MgSO$_4$, filtered and the solvent was removed under reduced pressure. The crude product (8.80 g) was recrystallized from chloroform to provide the title compound as a colorless solid (4.28 g, 70%). ^{1}H NMR (400 MHz, DMSO-d_6) δ 8.73 (d, *J* = 2.0 Hz, 1H), 8.64 (dd, *J* = 8.7, 0.8 Hz, 1H), 8.24 (dd, *J* = 8.8, 2.0 Hz, 1H), 8.02 (d, *J* = 8.8 Hz, 1H), 7.69 (d, *J* = 8.6 Hz, 1H), 3.93 (s, 3H). ^{13}C NMR (101 MHz, DMSO) δ 165.55, 152.28, 148.94, 141.29, 130.79, 129.77, 128.43, 127.90, 126.10, 123.41, 52.49. MS (ESI): m/z calc. for $[C_{11}H_8ClNO_2+H^+]^+$ = 222.02, found = 222.00

Methyl 2-(6-methyl-7-oxo-1-tosyl-6,7-dihydro-1*H*-pyrrolo[2,3-*c*]pyridin-4-yl)quinoline-6-carboxylate (112)
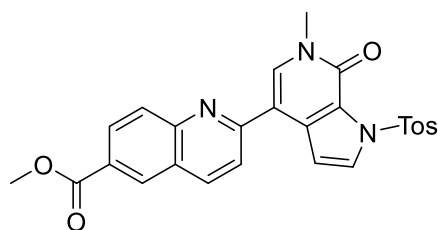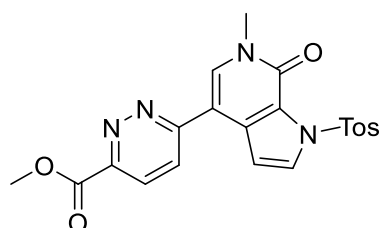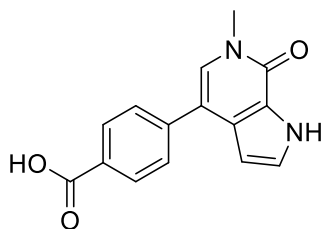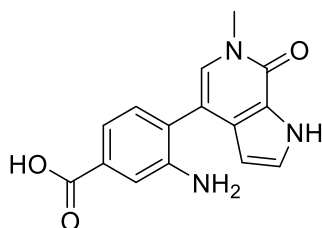

The synthesis was performed as described by Bauer *et al.*[277] The synthesis was performed according to "general procedure for Suzuki coupling B". 6-Methyl-4-(4,4,5,5-tetramethyl-1,3,2-dioxaborolan-2-yl)-1-tosyl-1,6-dihydro-7*H*-pyrrolo[2,3-*c*]pyridin-7-one (1.20 g, 2.80 mmol, 1.0 eq), methyl 2-chloroquinoline-6-carboxylate (869 mg, 3.92 mmol, 1.4 eq) were used. The crude product could be filtered from the reaction mixture to give a colorless solid (1.27 g, 93%). The compound was not soluble enough in DMSO to give an NMR spectrum. MS (ESI): m/z calc. for $[C_{26}H_{21}N_3O_5S+H^+]^+$ = 488.12, found = 488.15

2-(6-Methyl-7-oxo-6,7-dihydro-1*H*-pyrrolo[2,3-*c*]pyridin-4-yl)quinoline-6-carboxylic acid (113)
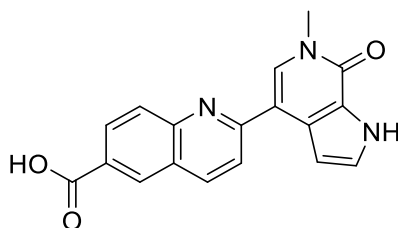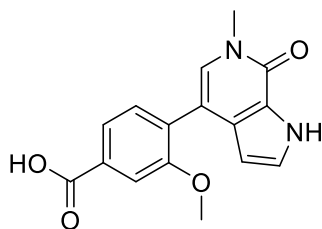

The synthesis was performed as described by Bauer *et al.*[277] The synthesis was performed according to "general procedure for ester and tosylamide hydrolysis". Methyl 2-(6-methyl-7-oxo-1-tosyl-6,7-dihydro-1*H*-pyrrolo[2,3-*c*]pyridin-4-yl)quinoline-6-carboxylate (**112**, 1.20 g, 2.46 mmol) was used. The resulting yellow solid (0.85 g, quant) was not soluble enough in DMSO to give an NMR spectrum. MS (ESI): m/z calc. for $[C_{18}H_{13}N_3O_3+H^+]^+$ = 320.10, found = 320.10

N-(2-Aminophenyl)-2-(6-methyl-7-oxo-6,7-dihydro-1H-pyrrolo[2,3-c]pyridin-4-yl)quinoline-6-carboxamide (114a)
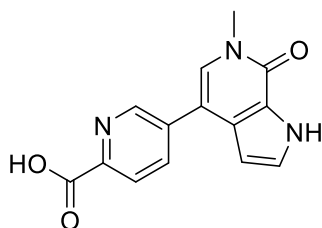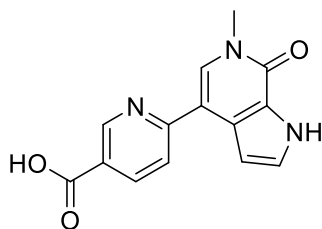

The synthesis was performed as described by Bauer *et al.*[277] The synthesis was performed according to "general procedure for amide coupling". 2-(6-Methyl-7-oxo-6,7-dihydro-1H-pyrrolo[2,3-c]pyridin-4-yl)quinoline-6-carboxylic acid (**113**, 250 mg, 783 μmol, 1.0 eq) and tert-butyl (2-aminophenyl)carbamate (**32**, 179 mg, 861 μmol, 1.1 eq) were used. The resulting colorless solid (399 mg, quant) was not soluble enough in DMSO to give an NMR spectrum. MS (ESI): m/z calc. for $[C_{29}H_{27}N_5O_4+H^+]^+$ = 510.21, found = 510.25

The intermediate was reacted according to "general procedure for *N-Boc* deprotection". The crude product was purified by flash chromatography (DCM/MeOH) to give a beige solid (124 mg, 39%). ^{1}H NMR (500 MHz, DMSO-d_6) δ 12.18 (s, 1H), 9.88 (s, 1H), 8.63 (d, J = 2.1 Hz, 1H), 8.49 (d, J = 8.7 Hz, 1H), 8.30 (dd, J = 8.7, 2.1 Hz, 1H), 8.27 (s, 1H), 8.15 (dd, J = 8.8, 2.2 Hz, 2H), 7.43 (t, J = 2.8 Hz, 1H), 7.38 (t, J = 2.4 Hz, 1H), 7.25 (dd, J = 7.9, 1.5 Hz, 1H), 7.00 (td, J = 7.7, 1.6 Hz, 1H), 6.82 (dd, J = 8.1, 1.5 Hz, 1H), 6.63 (td, J = 7.5, 1.5 Hz, 1H), 4.99 (s, 2H), 3.69 (s, 3H). ^{13}C NMR (126 MHz, DMSO) δ 157.54, 154.91, 149.22, 143.67, 137.71, 132.65, 132.12, 129.12, 129.06, 128.93, 128.66, 128.17, 127.63, 127.19, 127.04, 125.85, 123.99, 123.77, 119.96, 116.73, 116.61, 113.69, 105.65, 36.47. MS (ESI): m/z calc. for $[C_{24}H_{19}N_5O_2+H^+]^+$ = 410.15, found = 410.10 HRMS (MALDI): m/z calc. for $[C_{24}H_{19}N_5O_2+H^+]^+$ = 410.1612, found = 410.1618

N-(2-amino-4-fluorophenyl)-2-(6-methyl-7-oxo-6,7-dihydro-1H-pyrrolo[2,3-c]pyridin-4-yl)quinoline-6-carboxamide (114b)
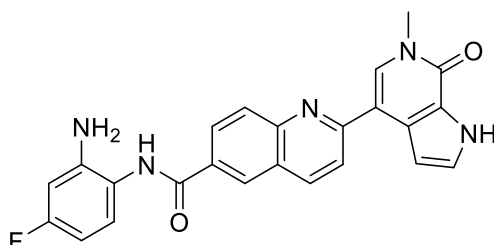
The reaction was performed according to "general procedure for amide coupling". Compound **113** (100 mg, 313 μmol) and 4-fluorobenzene-1,2-diamine (47 mg, 0.38 mmol) were used. After completion, water was added to the reaction mixture and the resulting precipitate was filtered. The crude product was then purified by flash chromatography (silica, DCM/MeOH) to provide the title

compound (74 mg, 55%). ^{1}H NMR (500 MHz, DMSO-d_6) δ 12.18 (s, 1H), 9.81 (s, 1H), 8.63 (d, J = 2.1 Hz, 1H), 8.48 (d, J = 8.8 Hz, 1H), 8.29 (dd, J = 8.8, 2.1 Hz, 1H), 8.27 (s, 1H), 8.14 (dd, J = 8.8, 5.3 Hz, 2H), 7.43 (t, J = 2.8 Hz, 1H), 7.38 (t, J = 2.4 Hz, 1H), 7.19 (dd, J = 8.7, 6.3 Hz, 1H), 6.58 (dd, J = 11.2, 2.9 Hz, 1H), 6.39 (td, J = 8.5, 2.9 Hz, 1H), 5.32 (br s, 2H), 3.69 (s, 3H). ^{13}C NMR (126 MHz, DMSO) δ 165.27, 160.13, 157.06, 154.42, 148.73, 145.56, 145.46, 137.22, 132.18, 131.52, 128.62, 128.52, 128.47, 128.20, 127.67, 127.14, 125.35, 123.50, 119.47, 119.25, 119.23, 113.19, 105.16, 102.13, 101.95, 101.55, 101.35, 35.98. MS (ESI): m/z calc. for [M+H^{+}][+] = 428.14, found = 428.20

6-Methyl-7-oxo-1-tosyl-6,7-dihydro-1*H*-pyrrolo[2,3-*c*]pyridine-4-carboxylic acid (115)
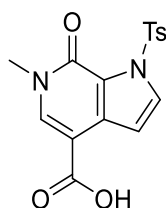
The synthesis was performed as described by Bauer *et al*.[277] 4-Bromo-6-methyl-1-tosyl-1,6-dihydro-7*H*-pyrrolo[2,3-*c*]pyridin-7-one (**55**, 3.00 g, 7.87 mmol, 1.0 eq) was dissolved in anh. THF (50 mL) and cooled to -40 °C. A solution of isopropylmagnesium chloride lithium chloride complex in THF (1.3 M, 12.1 mL, 15.7 mmol, 2.0 eq) was slowly added. The mixture was stirred for 2 h and poured onto powdered dry ice. After stirring for 30 minutes, the reaction was quenched by adding sat. aq NH$_4$Cl and extracted with ethyl acetate. The ethyl acetate layer was washed with brine, dried over MgSO$_4$, filtered, and volatiles were removed under reduced pressure to provide the crude product (2.73 g, quant.). MS (ESI): m/z calc. for [C$_{16}$H$_{14}$N$_2$O$_5$S+H^{+}][+] = 347.06, found = 347.00

6-Methyl-7-oxo-6,7-dihydro-1*H*-pyrrolo[2,3-*c*]pyridine-4-carboxylic acid (116)
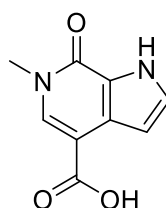
The synthesis was performed as described by Bauer *et al*.[277] 6-Methyl-7-oxo-1-tosyl-6,7-dihydro-1*H*-pyrrolo[2,3-*c*]pyridine-4-carboxylic acid (**115**, 2.73 g, 7.88 mmol, 1 eq) and LiOH · H$_2$O (2.65 g, 63.1 mmol, 8 eq) were dissolved in dioxane/water (60 mL, 3/1) and heated at 90 °C for 1 h. The mixture was cooled to ambient temperature and brought to a pH of 3 by the addition of 5% aq HCl. The resulting precipitate was filtered and dried under reduced pressure to provide the product as a colorless solid (1.27 g, 84%). ^{1}H NMR (400 MHz, DMSO-d_6) δ 12.50 (s, 1H), 12.13 (s, 1H), 8.07 (s, 1H), 7.34 (t, *J* = 2.8 Hz, 1H), 6.73 (dd, *J* = 2.7, 2.1 Hz, 1H), 3.59 (s, 3H). ^{13}C NMR (101 MHz, DMSO) δ 166.58, 154.72, 136.59,

127.70, 127.59, 122.58, 104.78, 104.03, 36.02. MS (ESI): m/z calc. for $[C_9H_8N_2O_3+H^+]^+$ = 193.05, found = 193.00

Methyl 4-(6-methyl-7-oxo-6,7-dihydro-1*H*-pyrrolo[2,3-*c*]pyridine-4-carboxamido)benzoate (117)
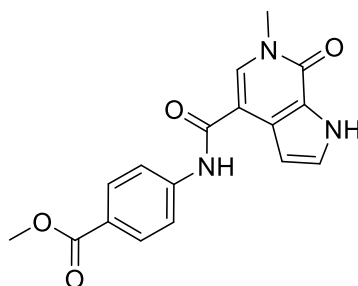
The synthesis was performed as described by Bauer *et al*.[277] 6-Methyl-7-oxo-6,7-dihydro-1*H*-pyrrolo[2,3-*c*]pyridine-4-carboxylic acid (**116**, 350 mg, 1.81 mmol, 1.0 eq) and SOCl$_2$ (211 µL, 2.91 mmol, 1.6 eq) were added to dioxane (15 mL). The mixture was heated at 80 °C for 16 h and cooled to ambient temperature. Afterwards, a solution of methyl 4-aminobenzoate (441 mg, 2.91 mmol, 1.6 eq) and *N,N*-diisopropylethylamine (381 µL, 2.19 mmol, 1.2 eq) in *N,N*-dimethylacetamide (8 mL) was added. The mixture was stirred for 1 h and partitioned between water and ethyl acetate. The ethyl acetate layer was washed with brine, dried over MgSO$_4$, filtered, and volatiles were removed under reduced pressure. The crude product was purified by flash chromatography (DCM -> 10% MeOH in DCM) to provide the title compound as a colorless solid (550 mg, 93 %). ^{1}H NMR (400 MHz, DMSO-*d*$_6$) δ 12.17 (s, 1H), 10.25 (s, 1H), 8.11 (s, 1H), 7.98 – 7.93 (m, 2H), 7.90 – 7.86 (m, 2H), 7.37 (t, *J* = 2.7 Hz, 1H), 6.74 (dd, *J* = 2.7, 2.0 Hz, 1H), 3.84 (s, 3H), 3.61 (s, 3H). ^{13}C NMR (101 MHz, DMSO) δ 165.87, 164.48, 154.49, 143.94, 133.34, 130.14, 127.59, 127.55, 123.77, 122.81, 119.12, 108.77, 103.77, 51.84, 36.05. MS (ESI): m/z calc. for $[C_{17}H_{15}N_3O_4+H^+]^+$ = 326.11, found = 326.05

4-(6-Methyl-7-oxo-6,7-dihydro-1*H***-pyrrolo[2,3-*c*]pyridine-4-carboxamido)benzoic acid (118)**
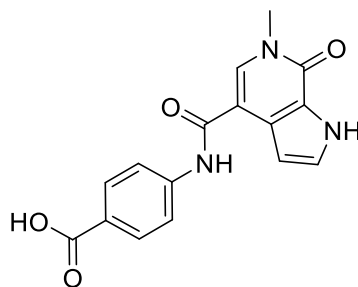
The synthesis was performed as described by Bauer *et al.*[277] Methyl 4-(6-methyl-7-oxo-6,7-dihydro-1*H*-pyrrolo[2,3-*c*]pyridine-4-carboxamido)benzoate (**117**, 425 mg, 1.31 mmol, 1 eq) and LiOH · H$_2$O (329 mg, 7.84 mmol, 6 eq) were dissolved in THF/methanol/water (40 mL, 3/3/2) and heated at 60 °C for 1 h. The mixture was cooled to ambient temperature and brought to a pH of 3 by the addition of 5% aq HCl. The resulting precipitate was filtered and dried under reduced pressure to provide the product as an off-white solid (397 mg, 98%). ^{1}H NMR (400 MHz, DMSO-*d*$_6$) δ 12.70 (s, 1H), 12.18 (s, 1H), 10.27 (s, 1H), 8.16 (s, 1H), 7.97 − 7.93 (m, 2H), 7.91 − 7.86 (m, 2H), 7.38 (t, *J* = 2.8 Hz, 1H), 6.76 (t, *J* = 2.4 Hz, 1H), 3.63 (s, 3H). ^{13}C NMR (101 MHz, DMSO) δ 166.97, 164.45, 154.49, 143.58, 133.32, 130.24, 127.64, 127.54, 124.96, 122.81, 119.04, 108.80, 103.79, 36.03. MS (ESI): m/z calc. for [C$_{16}$H$_{13}$N$_3$O$_4$+H$^+$]$^+$ = 312.09, found = 312.05

***N*-(4-((2-Aminophenyl)carbamoyl)phenyl)-6-methyl-7-oxo-6,7-dihydro-1*H*-pyrrolo[2,3-*c*]pyridine-4-carboxamide (119)**
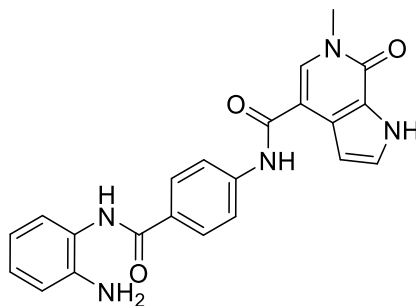
The synthesis was performed as described by Bauer *et al.*[277] The synthesis was performed according to "general procedure for amide coupling". 4-(6-Methyl-7-oxo-6,7-dihydro-1*H*-pyrrolo[2,3-*c*]pyridine-4-carboxamido)benzoic acid (**118**, 190 mg, 793 μmol, 1.0 eq) and benzene-1,2-diamine (86 mg, 0.79 mmol, 1.3 eq) were used. The crude product was triturated with methanol and filtered to provide the title compound as a colorless solid (161 mg, 66%). ^{1}H NMR (500 MHz, DMSO-*d*$_6$) δ 12.18 (s, 1H), 10.18 (s, 1H), 9.60 (s, 1H), 8.12 (s, 1H), 8.01 (d, *J* = 8.4 Hz, 2H), 7.86 (d, *J* = 8.5 Hz, 2H), 7.38 (t, *J* = 2.8 Hz, 1H), 7.19 (d, *J* = 7.2 Hz, 1H), 6.98 (td, *J* = 7.7, 1.6 Hz, 1H), 6.80 (dd, *J* = 8.0, 1.5 Hz, 1H), 6.76 (t, *J* = 2.4 Hz, 1H), 6.61 (td, *J* = 7.5, 1.4 Hz, 1H), 4.89 (s, 2H), 3.63 (s, 3H). ^{13}C NMR (126 MHz, DMSO) δ 164.78, 164.40, 154.52, 143.13, 142.29, 133.17, 128.89, 128.58, 127.66, 127.55, 126.66, 126.37, 123.54,

122.86, 118.94, 116.31, 116.17, 108.94, 103.82, 36.06. MS (ESI): m/z calc. for $[C_{22}H_{19}N_5O_3+H^+]^+$ = 402.15, found = 402.10. HRMS (MALDI): m/z calc. for $[C_{22}H_{19}N_5O_3+Na^+]^+$ = 424.1380, found = 424.1390
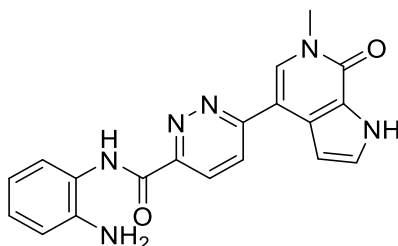
Methyl 4-(6-methyl-7-oxo-1-tosyl-6,7-dihydro-1*H*-pyrrolo[2,3-*c*]pyridin-4-yl)benzoate (121a)
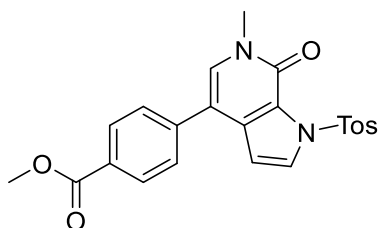
The synthesis was performed as described by Bauer *et al.*[277] The synthesis was performed according to "general procedure for Suzuki coupling B". 6-Methyl-4-(4,4,5,5-tetramethyl-1,3,2-dioxaborolan-2-yl)-1-tosyl-1,6-dihydro-7*H*-pyrrolo[2,3-*c*]pyridin-7-one (**56**, 1.00 g, 2.33 mmol, 1.0 eq), methyl 4-bromobenzoate (**120a**, 603 mg, 2.80 mmol, 1.2 eq), K$_3$PO$_4$ (1.24 g, 5.84 mmol, 2.5 eq), Pd XPhos G2 (92 mg, 0.12 mmol, 0.05 eq) and XPhos (56 mg, 0.12 mmol, 0.05 eq) were used. The crude product (1.00 g, 98%) was used in the next step without further characterization. MS (ESI): m/z calc. for $[C_{23}H_{20}N_2O_5S+H^+]^+$ = 437.11, found = 437.05

Methyl 3-amino-4-(6-methyl-7-oxo-1-tosyl-6,7-dihydro-1*H*-pyrrolo[2,3-*c*]pyridin-4-yl)benzoate (121b)
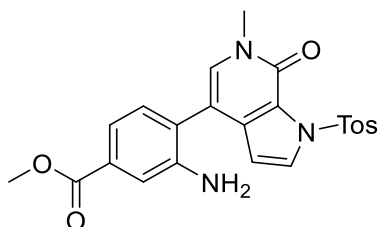

The synthesis was performed as described by Bauer *et al.*[277] The synthesis was performed according to "general procedure for Suzuki coupling B". 6-Methyl-4-(4,4,5,5-tetramethyl-1,3,2-dioxaborolan-2-yl)-1-tosyl-1,6-dihydro-7*H*-pyrrolo[2,3-*c*]pyridin-7-one (**56**, 1.60 g, 3.74 mmol, 1.0 eq), methyl 3-amino-4-bromobenzoate (1.12 g, 4.86 mmol, 1.3 eq), K$_3$PO$_4$ (**102b**, 1.98 g, 9.34 mmol, 2.5 eq), Pd XPhos G2 (147 mg, 187 µmol, 0.05 eq) and XPhos (89 mg, 0.19 mmol, 0.05 eq) were used. The crude product (1.60 g, 95%) was used in the next step without further characterization. MS (ESI): m/z calc. for $[C_{23}H_{21}N_3O_5S+H^+]^+$ = 452.12, found = 452.10

Methyl 3-methoxy-4-(6-methyl-7-oxo-1-tosyl-6,7-dihydro-1*H*-pyrrolo[2,3-*c*]pyridin-4-yl)benzoate (121c)

The synthesis was performed as described by Bauer *et al.*[277] The synthesis was performed according to "general procedure for Suzuki coupling B". 6-Methyl-4-(4,4,5,5-tetramethyl-1,3,2-dioxaborolan-2-yl)-1-tosyl-1,6-dihydro-7*H*-pyrrolo[2,3-*c*]pyridin-7-one (**56**, 1.00 g, 2.33 mmol, 1.0 eq), methyl 4-bromo-3-methoxybenzoate (**120c**, 629 mg, 2.57 mmol, 1.1 eq), K_3PO_4 (1.24 g, 5.84 mmol, 2.5 eq), Pd XPhos G2 (110 mg, 140 µmol, 0.05 eq) and XPhos (67 mg, 0.14 mmol, 0.05 eq) were used. The crude product (1.00 g, 92%) was used in the next step without further characterization. MS (ESI): m/z calc. for $[C_{24}H_{22}N_2O_6S+H^+]^+ = 467.00$, found = 467.12

**Methyl 5-(6-methyl-7-oxo-1-tosyl-6,7-dihydro-1*H*-pyrrolo[2,3-*c*]pyridin-4-yl)picolinate (121d)**

The synthesis was performed as described by Bauer *et al.*[277] The synthesis was performed according to "general procedure for Suzuki coupling B". 6-Methyl-4-(4,4,5,5-tetramethyl-1,3,2-dioxaborolan-2-yl)-1-tosyl-1,6-dihydro-7*H*-pyrrolo[2,3-*c*]pyridin-7-one (**56**, 3.50 g, 8.17 mmol, 1.0 eq), methyl 5-chloropicolinate (**120d**, 1.68 g, 9.81 mmol, 1.2 eq), K_3PO_4 (4.34 g, 20.43 mmol, 2.5 eq), Pd XPhos G2 (193 mg, 245 µmol, 0.03 eq) and XPhos (117 mg, 245 µmol, 0.03 eq) were dissolved in dioxane/water (160 mL, 3/1) and purged with argon for 10 minutes. The mixture was heated at 70 °C for 1 h, cooled to ambient temperature, diluted with water and the resulting solid was filtered. Dioxane was removed from the solution under reduced pressure, the solution was cooled to 4 °C overnight and the resulting precipitate was filtered. The combined solids were dried under reduced pressure to provide the crude product (1.90 g, 53%).^{1}H NMR (400 MHz, DMSO-*d*$_6$) δ 8.86 (s, 1H), 8.13 (s, 2H), 8.08 (d, *J* = 3.6 Hz, 1H), 7.97 (d, *J* = 8.0 Hz, 2H), 7.85 (s, 1H), 7.43 (d, *J* = 8.2 Hz, 2H), 6.79 (d, *J* = 3.6 Hz, 1H), 3.91 (s, 3H), 3.49 (s, 3H), 2.38 (s, 3H). MS (ESI): m/z calc. for $[C_{22}H_{19}N_3O_5S+H^+]^+ = 438.10$, found = 438.00

Methyl 6-(6-methyl-7-oxo-1-tosyl-6,7-dihydro-1*H*-pyrrolo[2,3-*c*]pyridin-4-yl)nicotinate (121e)

The synthesis was performed as described by Bauer *et al.*[277] The synthesis was performed according to "general procedure for Suzuki coupling B". 6-Methyl-4-(4,4,5,5-tetramethyl-1,3,2-dioxaborolan-2-yl)-1-tosyl-1,6-dihydro-7*H*-pyrrolo[2,3-*c*]pyridin-7-one (**56**, 400 mg, 934 μmol, 1.0 eq), methyl 6-chloronicotinate (**102e**, 208 mg, 1.21 mmol, 1.2 eq), K$_3$PO$_4$ (496 mg, 2.33 mmol, 2.5 eq), Pd XPhos G2 (37 mg, 47 μmol, 0.05 eq) and XPhos (22 mg, 47 μmol, 0.05 eq) were used. The product was used in the next step without being isolated. MS (ESI): m/z calc. for [C$_{22}$H$_{19}$N$_3$O$_5$S+H$^+$]$^+$ = 438.10, found = 438.05

Methyl 6-(6-methyl-7-oxo-1-tosyl-6,7-dihydro-1*H*-pyrrolo[2,3-*c*]pyridin-4-yl)pyridazine-3-carboxylate (121f)

The synthesis was performed as described by Bauer *et al.*[277] The synthesis was performed according to "general procedure for Suzuki coupling B". 6-Methyl-4-(4,4,5,5-tetramethyl-1,3,2-dioxaborolan-2-yl)-1-tosyl-1,6-dihydro-7*H*-pyrrolo[2,3-*c*]pyridin-7-one (**56**, 400 mg, 934 μmol, 1.0 eq), methyl 6-chloropyridazine-3-carboxylate (**102f**, 209 mg, 1.21 mmol, 1.2 eq), K$_3$PO$_4$ (496 mg, 2.33 mmol, 2.5 eq), Pd XPhos G2 (37 mg, 47 μmol, 0.05 eq) and XPhos (22 mg, 47 μmol, 0.05 eq) were used. The product was used in the next step without being isolated. MS (ESI): m/z calc. for [C$_{21}$H$_{18}$N$_4$O$_5$S+H$^+$]$^+$ = 439.10, found = 439.05

4-(6-Methyl-7-oxo-6,7-dihydro-1H-pyrrolo[2,3-c]pyridin-4-yl)benzoic acid (122a)

The synthesis was performed as described by Bauer *et al.*[277] The synthesis was performed according to "general procedure for ester and tosylamide hydrolysis". Methyl 4-(6-methyl-7-oxo-1-tosyl-6,7-dihydro-1H-pyrrolo[2,3-c]pyridin-4-yl)benzoate (**121a**, 1.00 g, 2.29 mmol) was used. The product was obtained as a colorless solid (602 mg, 98%). ^{1}H NMR (500 MHz, DMSO-d_6) δ 12.97 (s, 1H), 12.19 (s, 1H), 8.02 (d, *J* = 8.0 Hz, 2H), 7.73 (d, *J* = 8.0 Hz, 2H), 7.51 (s, 1H), 7.37 (d, *J* = 3.1 Hz, 1H), 6.50 (d, *J* = 2.4 Hz, 1H), 3.60 (s, 3H). ^{13}C NMR (126 MHz, DMSO) δ 167.19, 154.15, 141.70, 131.70, 131.30, 129.88, 128.94, 128.81, 127.97, 127.31, 127.14, 123.40, 113.71, 102.17, 35.64. MS (ESI): m/z calc. for $[C_{15}H_{12}N_2O_3+H^+]^+$ = 269.08, found = 269.05

3-Amino-4-(6-methyl-7-oxo-6,7-dihydro-1H-pyrrolo[2,3-c]pyridin-4-yl)benzoic acid (122b)

The synthesis was performed as described by Bauer *et al.*[277] The synthesis was performed according to "general procedure for ester and tosylamide hydrolysis". Methyl 3-amino-4-(6-methyl-7-oxo-1-tosyl-6,7-dihydro-1H-pyrrolo[2,3-c]pyridin-4-yl)benzoate (**121b**, 1.60 g, 3.54 mmol) was used. The product (970 mg, 97%) was used in the next step without further characterization. MS (ESI): m/z calc. for $[C_{15}H_{13}N_3O_3+H^+]^+$ = 284.10, found = 284.05

3-Methoxy-4-(6-methyl-7-oxo-6,7-dihydro-1*H*-pyrrolo[2,3-*c*]pyridin-4-yl)benzoic acid (122c)

The synthesis was performed as described by Bauer *et al.*[277] The synthesis was performed according to "general procedure for ester and tosylamide hydrolysis". Methyl 3-methoxy-4-(6-methyl-7-oxo-1-tosyl-6,7-dihydro-1*H*-pyrrolo[2,3-*c*]pyridin-4-yl)benzoate (**121c**, 1.00 g, 2.14 mmol) was used. The product was obtained as a colorless solid (621 mg, 97%). ^{1}H NMR (400 MHz, DMSO-d_6) δ 12.99 (s, 1H), 12.00 (s, 1H), 7.66 – 7.57 (m, 2H), 7.45 (d, J = 7.8 Hz, 1H), 7.30 – 7.24 (m, 2H), 6.07 (t, J = 2.5 Hz, 1H), 3.80 (s, 3H), 3.56 (s, 3H). ^{13}C NMR (101 MHz, DMSO) δ 167.11, 156.58, 154.11, 130.89, 130.63, 130.31, 129.57, 129.28, 126.62, 122.87, 121.69, 111.66, 111.07, 102.88, 55.35, 35.54. MS (ESI): m/z calc. for $[C_{16}H_{14}N_2O_4+H^+]^+$ = 299.10, found = 299.05

5-(6-Methyl-7-oxo-6,7-dihydro-1*H*-pyrrolo[2,3-*c*]pyridin-4-yl)picolinic acid (122d)

The synthesis was performed as described by Bauer *et al.*[277] The synthesis was performed according to "general procedure for ester and tosylamide hydrolysis". Methyl 5-(6-methyl-7-oxo-1-tosyl-6,7-dihydro-1*H*-pyrrolo[2,3-*c*]pyridin-4-yl)picolinate (**121d**, 1.85 g, 4.23 mmol) was used. The product was obtained as a yellow solid (1.09 g, 96%). ^{1}H NMR (500 MHz, DMSO-d_6) δ 12.26 (s, 1H), 8.96 – 8.92 (m, 2H), 8.18 (dd, J = 8.1, 2.3 Hz, 1H), 8.12 (d, J = 7.9 Hz, 1H), 7.65 (s, 1H), 7.40 (t, J = 2.8 Hz, 1H), 6.52 (dd, J = 2.8, 2.0 Hz, 1H), 3.61 (s, 3H). ^{13}C NMR (126 MHz, DMSO) δ 166.05, 154.18, 147.54, 146.18, 136.09, 135.27, 129.75, 127.65, 127.61, 124.89, 123.41, 110.43, 101.92, 35.74. MS (ESI): m/z calc. for $[C_{14}H_{11}N_3O_3+H^+]^+$ = 270.08, found = 270.00

6-(6-methyl-7-oxo-6,7-dihydro-1*H*-pyrrolo[2,3-*c*]pyridin-4-yl)nicotinic acid (122e)

The synthesis was performed as described by Bauer *et al.*[277] The synthesis was performed according to "general procedure for ester and tosylamide hydrolysis". Hydrolysis was performed directly after Suzuki coupling. LiOH · H$_2$O (274 mg, 6.53 mmol, 7 eq) was added to the solution of methyl 6-(6-methyl-7-oxo-1-tosyl-6,7-dihydro-1*H*-pyrrolo[2,3-*c*]pyridin-4-yl)nicotinate (**121e**, 409 mg, 933 µmol, 1 eq). The product was obtained as a yellow solid (170 mg, 68%). MS (ESI): m/z calc. for [C$_{14}$H$_{11}$N$_3$O$_3$+H$^+$]$^+$ = 270.08, found = 270.00

6-(6-methyl-7-oxo-6,7-dihydro-1*H*-pyrrolo[2,3-*c*]pyridin-4-yl)pyridazine-3-carboxylic acid (122f)
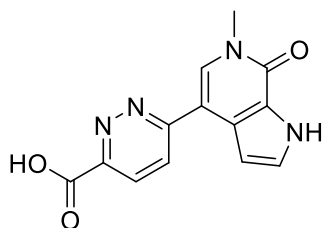
The synthesis was performed as described by Bauer *et al.*[277] The synthesis was performed according to "general procedure for ester and tosylamide hydrolysis". Hydrolysis was performed directly after Suzuki coupling. LiOH · H$_2$O (274 mg, 6.53 mmol, 7 eq) was added to the solution of methyl 6-(6-methyl-7-oxo-1-tosyl-6,7-dihydro-1*H*-pyrrolo[2,3-*c*]pyridin-4-yl)pyridazine-3-carboxylate (**121f**, 409 mg, 933 µmol, 1 eq). The product was obtained as a yellow solid (130 mg, 52%). MS (ESI): m/z calc. for [C$_{13}$H$_{10}$N$_4$O$_3$+H$^+$]$^+$ = 271.08, found = 271.05

N-(2-Aminophenyl)-4-(6-methyl-7-oxo-6,7-dihydro-1H-pyrrolo[2,3-c]pyridin-4-yl)benzamide (123a)
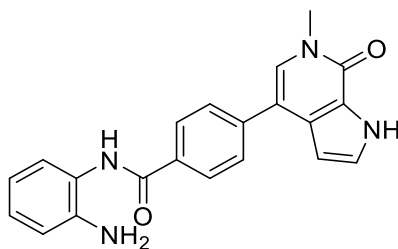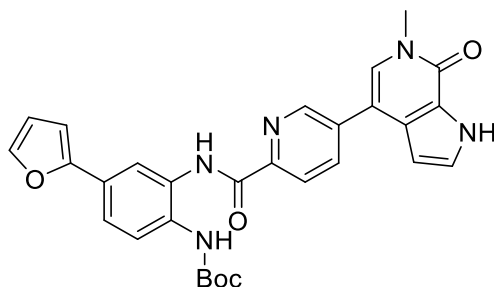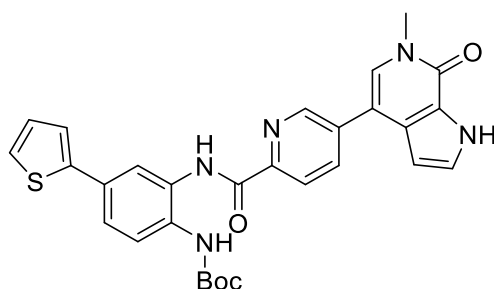

The synthesis was performed as described by Bauer *et al.*[277] The synthesis was performed according to "general procedure for amide coupling". 4-(6-Methyl-7-oxo-6,7-dihydro-1H-pyrrolo[2,3-c]pyridin-4-yl)benzoic acid (**122a**, 350 mg, 1.30 mmol, 1.0 eq) and benzene-1,2-diamine (169 mg, 1.57 mmol, 1.2 eq) were used. The crude product was triturated with methanol and filtered to provide the title compound as a colorless solid (198 mg, 42%). ^{1}H NMR (500 MHz, DMSO-d_6) δ 12.20 (s, 1H), 9.72 (s, 1H), 8.10 (d, *J* = 7.9 Hz, 2H), 7.74 (d, *J* = 8.0 Hz, 2H), 7.52 (s, 1H), 7.39 (d, *J* = 3.7 Hz, 1H), 7.21 (d, *J* = 7.8 Hz, 1H), 6.99 (t, *J* = 7.7 Hz, 1H), 6.82 (d, *J* = 8.0 Hz, 1H), 6.63 (t, *J* = 7.5 Hz, 1H), 6.51 (s, 1H), 4.94 (s, 2H), 3.62 (s, 3H). ^{13}C NMR (126 MHz, DMSO) δ 165.03, 154.16, 143.18, 140.26, 132.67, 128.65, 128.36, 128.12, 127.30, 126.90, 126.74, 126.51, 123.44, 123.42, 116.34, 116.20, 113.87, 102.14, 54.91, 35.64. MS (ESI): m/z calc. for $[C_{21}H_{18}N_4O_2+H^+]^+$ = 359.14, found = 359.10. HRMS (MALDI): m/z calc. for $[C_{21}H_{18}N_4O_2+Na^+]^+$ = 381.1322, found = 381.1332

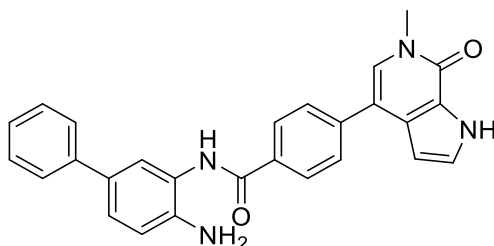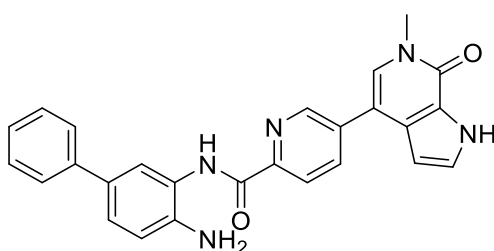**3-Amino-N-(2-aminophenyl)-4-(6-methyl-7-oxo-6,7-dihydro-1H-pyrrolo[2,3-c]pyridin-4-yl)benzamide (123b)**
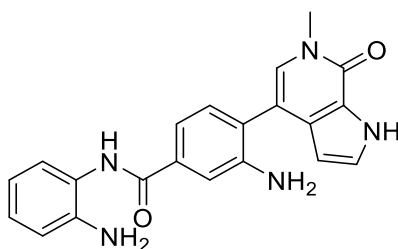
The synthesis was performed as described by Bauer *et al.*[277] The synthesis was performed according to "general procedure for amide coupling". 3-Amino-4-(6-methyl-7-oxo-6,7-dihydro-1H-pyrrolo[2,3-c]pyridin-4-yl)benzoic acid (**122b**, 970 mg, 3.42 mmol, 1.0 eq) and benzene-1,2-diamine (555 mg, 5.14 mmol, 1.5 eq) were used. The crude product was triturated with methanol and filtered to provide the title compound as a beige solid (417 mg, 33%). ^{1}H NMR (500 MHz, DMSO-d_6) δ 12.08 (s, 1H), 9.54 (s, 1H), 7.35 (d, *J* = 1.8 Hz, 1H), 7.30 (t, *J* = 2.8 Hz, 1H), 7.22 (ddd, *J* = 17.0, 7.7, 1.6 Hz, 2H), 7.20 (s, 1H), 7.17 (d, *J* = 7.8 Hz, 1H), 6.97 (ddd, *J* = 8.1, 7.3, 1.5 Hz, 1H), 6.79 (dd, *J* = 8.0, 1.5 Hz, 1H), 6.61 (td, *J* = 7.5, 1.4 Hz, 1H), 6.07 (dd, *J* = 2.7, 2.0 Hz, 1H), 4.99 (s, 2H), 4.88 (s, 2H), 3.57 (s, 3H). ^{13}C NMR (126 MHz, DMSO) δ 165.78, 154.22, 146.03, 142.85, 134.57, 130.20, 129.32, 128.85, 126.78, 126.35, 126.21, 123.87, 123.78, 123.31, 116.38, 116.26, 115.18, 114.41, 111.71, 102.50, 35.55. MS (ESI): m/z calc. for

$[C_{21}H_{19}N_5O_2+H^+]^+ = 374.15$, found = 374.10. HRMS (MALDI): m/z calc. for $[C_{21}H_{19}N_5O_2+Na^+]^+ = 396.1431$, found = 396.1441

N-(2-Aminophenyl)-3-methoxy-4-(6-methyl-7-oxo-6,7-dihydro-1H-pyrrolo[2,3-c]pyridin-4-yl)benzamide (123c)
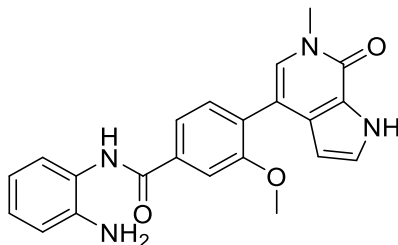
The synthesis was performed as described by Bauer *et al.*[277] The synthesis was performed according to "general procedure for amide coupling". 3-Methoxy-4-(6-methyl-7-oxo-6,7-dihydro-1H-pyrrolo[2,3-c]pyridin-4-yl)benzoic acid (**122c**, 400 mg, 1.34 mmol, 1.0 eq) and benzene-1,2-diamine (189 mg, 1.74 mmol, 1.3 eq) were used. The crude product was triturated with methanol and filtered to provide the title compound as a colorless solid (388 mg, 74%). ^{1}H NMR (500 MHz, DMSO-d_6) δ 12.01 (s, 1H), 9.76 (s, 1H), 7.71 (d, J = 1.7 Hz, 1H), 7.67 (dd, J = 7.8, 1.7 Hz, 1H), 7.45 (d, J = 7.8 Hz, 1H), 7.28 (t, J = 2.8 Hz, 1H), 7.26 (s, 1H), 7.19 (dd, J = 7.9, 1.6 Hz, 1H), 7.00 (td, J = 7.6, 1.5 Hz, 1H), 6.81 (dd, J = 8.0, 1.5 Hz, 1H), 6.63 (td, J = 7.5, 1.4 Hz, 1H), 6.07 (t, J = 2.4 Hz, 1H), 4.93 (s, 2H), 3.83 (s, 3H), 3.57 (s, 3H). ^{13}C NMR (126 MHz, DMSO) δ 164.91, 156.54, 154.14, 143.29, 134.76, 130.36, 129.75, 129.10, 128.77, 126.84, 126.63, 126.58, 123.30, 122.89, 120.06, 116.29, 116.16, 111.30, 110.77, 102.87, 55.51, 35.57. MS (ESI): m/z calc. for $[C_{22}H_{20}N_4O_3+H^+]^+ = 389.15$, found = 389.10. HRMS (MALDI): m/z calc. for $[C_{22}H_{20}N_4O_3+Na^+]^+ = 411.1428$, found = 411.1434
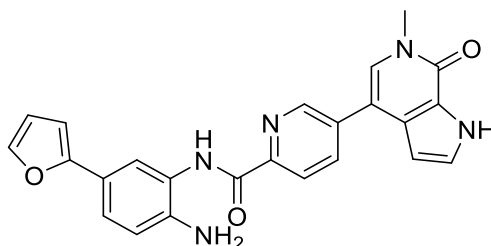
N-(2-Aminophenyl)-5-(6-methyl-7-oxo-6,7-dihydro-1H-pyrrolo[2,3-c]pyridin-4-yl)picolinamide (123d)
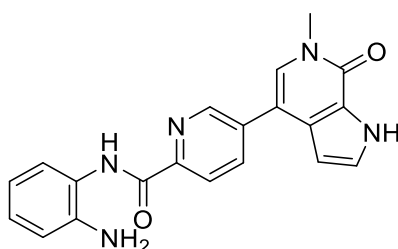
The synthesis was performed as described by Bauer *et al.*[277] The synthesis was performed according to "general procedure for amide coupling". 5-(6-Methyl-7-oxo-6,7-dihydro-1H-pyrrolo[2,3-c]pyridin-4-yl)picolinic acid (**122d**, 170 mg, 631 μmol, 1.0 eq) and benzene-1,2-diamine (82 mg, 0.76 mmol, 1.2 eq) were used. The crude product was triturated with methanol and filtered to provide the title compound as a pale yellow solid (80 mg, 35%). ^{1}H NMR (500 MHz, DMSO-d_6) δ 12.28 (s, 1H), 10.08 (s, 1H), 8.95 (dd, J = 2.2, 0.9 Hz, 1H), 8.26 (dd, J = 8.1, 2.2 Hz, 1H), 8.22 (dd, J = 8.1, 0.9 Hz, 1H), 7.67 (s, 1H), 7.54

(dd, *J* = 8.0, 1.5 Hz, 1H), 7.42 (t, *J* = 2.8 Hz, 1H), 6.97 (td, *J* = 7.6, 1.5 Hz, 1H), 6.85 (dd, *J* = 8.0, 1.5 Hz, 1H), 6.67 (td, *J* = 7.6, 1.5 Hz, 1H), 6.53 (dd, *J* = 2.8, 2.0 Hz, 1H), 4.92 (s, 2H), 3.63 (s, 3H). ^{13}C NMR (126 MHz, DMSO) δ 162.07, 148.02, 146.48, 141.67, 135.86, 135.76, 129.57, 127.69, 127.56, 125.82, 124.39, 124.13, 123.39, 122.33, 117.06, 116.80, 110.49, 101.84, 35.72. MS (ESI): m/z calc. for $[C_{20}H_{17}N_5O_2+H^+]^+$ = 360.14, found = 360.05. HRMS (MALDI): m/z calc. for $[C_{20}H_{17}N_5O_2+Na^+]^+$ = 382.1275, found = 382.1286

N-(2-Aminophenyl)-6-(6-methyl-7-oxo-6,7-dihydro-1H-pyrrolo[2,3-c]pyridin-4-yl)pyridazine-3-carboxamide (123e)
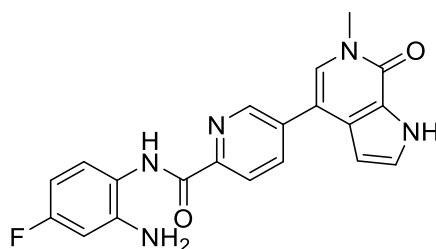

The synthesis was performed as described by Bauer *et al.*[277] The synthesis was performed according to "general procedure for amide coupling". 6-(6-Methyl-7-oxo-6,7-dihydro-1H-pyrrolo[2,3-c]pyridin-4-yl)pyridazine-3-carboxylic acid (**122e**, 130 mg, 481 µmol, 1.0 eq) and benzene-1,2-diamine (62 mg, 0.58 mmol, 1.2 eq) were used. The crude product was triturated with methanol and filtered to provide the title compound as a pale yellow solid (100 mg, 58%). ^{1}H NMR (500 MHz, DMSO-d_6) δ 12.26 (s, 1H), 10.38 (s, 1H), 8.36 (d, *J* = 9.0 Hz, 1H), 8.28 (d, *J* = 8.9 Hz, 1H), 8.24 (s, 1H), 7.45 (dd, *J* = 7.9, 1.5 Hz, 1H), 7.43 (t, *J* = 2.8 Hz, 1H), 7.09 (t, *J* = 2.4 Hz, 1H), 7.00 (td, *J* = 7.6, 1.5 Hz, 1H), 6.84 (dd, *J* = 8.1, 1.5 Hz, 1H), 6.66 (td, *J* = 7.5, 1.5 Hz, 1H), 5.01 (s, 2H), 3.67 (s, 3H). ^{13}C NMR (126 MHz, DMSO) δ 161.32, 159.32, 154.39, 150.75, 142.43, 132.49, 127.45, 126.99, 126.35, 125.87, 125.47, 124.69, 123.41, 123.37, 116.72, 116.56, 109.96, 104.53, 36.04. MS (ESI): m/z calc. for $[C_{19}H_{16}N_6O_2+H^+]^+$ = 361.13, found = 361.05. HRMS (MALDI): m/z calc. for $[C_{19}H_{16}N_6O_2+Na^+]^+$ = 383.1227, found = 383.1240

N-(2-Aminophenyl)-6-(6-methyl-7-oxo-6,7-dihydro-1H-pyrrolo[2,3-c]pyridin-4-yl)nicotinamide (123f)
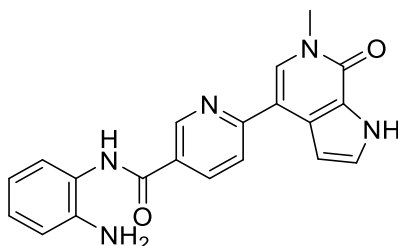
The synthesis was performed as described by Bauer *et al.*[277] The synthesis was performed according to "general procedure for amide coupling". 6-(6-Methyl-7-oxo-6,7-dihydro-1H-pyrrolo[2,3-c]pyridin-4-yl)nicotinic acid (**122f**, 170 mg, 631 µmol, 1.0 eq) and benzene-1,2-diamine (82 mg, 0.76 mmol, 1.2 eq) were used. The crude product was triturated with methanol and filtered to provide the title compound as a beige solid (126 mg, 56%). ^{1}H NMR (500 MHz, DMSO-d_6) δ 12.18 (s, 1H), 9.81 (s, 1H), 9.21 (d, J = 2.3 Hz, 1H), 8.38 (dd, J = 8.3, 2.4 Hz, 1H), 8.10 (s, 1H), 7.98 (d, J = 8.3 Hz, 1H), 7.40 (t, J = 2.8 Hz, 1H), 7.20 (dd, J = 7.9, 1.4 Hz, 1H), 7.03 – 6.94 (m, 2H), 6.80 (dd, J = 8.1, 1.4 Hz, 1H), 6.61 (td, J = 7.5, 1.4 Hz, 1H), 4.99 (s, 2H), 3.66 (s, 3H). ^{13}C NMR (126 MHz, DMSO) δ 163.83, 157.53, 154.35, 148.74, 143.38, 136.14, 131.19, 127.41, 127.22, 126.92, 126.73, 123.45, 122.81, 119.47, 116.12, 115.97, 112.76, 104.00, 35.90. MS (ESI): m/z calc. for $[C_{20}H_{17}N_5O_2+H^+]^+$ = 360.14, found = 360.10. HRMS (MALDI): m/z calc. for $[C_{20}H_{17}N_5O_2+Na^+]^+$ = 382.1275, found = 382.1285

4-Bromo-N-ethyl-6-methyl-7-oxo-6,7-dihydro-1H-pyrrolo[2,3-c]pyridine-2-carboxamide (124)
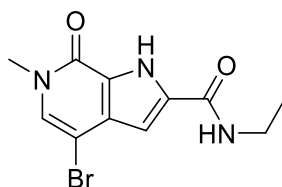
The synthesis was adapted from Sheppard *et al.*[188] Compound **83** (0.500 g, 1.10 mmol, 1.0 eq) was dissolved in ethylamine (2 M in THF, 4.41 mL, 8.0 eq) and to this was added magnesium methoxide (8-10% in MeOH, 4.38 mL, 3.0 eq). The mixture was heated to 55 °C for 20 h and then cooled to RT. After adding 20 mL of 5% HCl, the mixture was stirred for 30 min and the product precipitated as a colorless solid. The precipitate was dried under reduced pressure and the product was obtained as colorless solid (0.279 g, 85%). ^{1}H-NMR (250 MHz, DMSO-d6): δ = 12.57 (s, 1H), 8.44 (t, J = 5.4 Hz, 1H), 7.59 (s, 1H), 6.86 (s, 1H), 3.50 (s, 3H), 3.27 (m, 2H), 1.13 (t, J = 7.2 Hz, 3H) ppm. MS (ESI): m/z calc. for $[M-H^+]^-$ = 296.00, found = 295.96

N-ethyl-6-methyl-7-oxo-4-(4,4,5,5-tetramethyl-1,3,2-dioxaborolan-2-yl)-6,7-dihydro-1H-pyrrolo[2,3-c]pyridine-2-carboxamide (125)
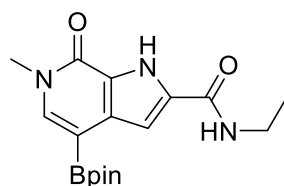
Compound **124** (120 mg, 403 µmol, 1.0 eq), B$_2$pin$_2$ (204 mg, 805 µmol, 2.0 eq), potassium ethylhexanoate (183 mg, 1.01 mmol, 2.5 eq), Pd XPhos G2 (32 mg, 40 µmol, 0.05 eq) and XPhos (19 mg, 40 µmol, 0.05 eq) were dissolved in MeTHF (5 mL) and heated at 55 °C for 16 h. The mixture was partitioned between water and ethyl acetate. The aqueous phase was extracted with ethyl acetate, the combined organic phases were washed with brine, dried over MgSO$_4$ and volatiles were removed under reduced pressure. The residue was purified by flash chromatography (silica, DCM/MeOH) and afterwards triturated with hexane to provide the title compound as a colorless solid (94 mg, 68%). ^{1}H-NMR (250 MHz, DMSO-d6): δ = 12.10 (s, 1H), 8.39 (t, J = 5.4 Hz, 1H), 7.56 (s, 1H), 7.06 (s, 1H), 3.55 (s, 3H), 3.27 (m, 2H), 1.32 (s, 12H), 1.14 (t, 3H). MS (ESI): m/z calc. for [M+H$^+$]$^+$ = 346.19, found = 346.15

Methyl 2-(2-(ethylcarbamoyl)-6-methyl-7-oxo-6,7-dihydro-1H-pyrrolo[2,3-c]pyridin-4-yl)quinoline-6-carboxylate (126)
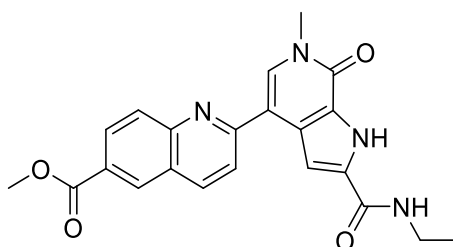
The reaction was performed according to "general procedure for Suzuki coupling B". **111** (87 mg, 0.39 mmol) and **125** (75 mg, 0.22 mmol) were used. The crude product was purified by flash chromatography to provide the title compound (50 mg, 57%). ^{1}H NMR (400 MHz, DMSO-d$_6$) δ 12.36 (s, 1H), 8.68 (d, J = 1.8 Hz, 1H), 8.59 (d, J = 8.8 Hz, 1H), 8.51 (t, J = 5.4 Hz, 1H), 8.34 (s, 1H), 8.25 (dd, J = 8.8, 1.8 Hz, 1H), 8.21 (d, J = 8.8 Hz, 1H), 8.17 (d, J = 8.8 Hz, 1H), 7.95 (s, 1H), 3.95 (s, 3H), 3.69 (s, 3H), 3.37 – 3.31 (m, 2H), 1.18 (t, J = 7.2 Hz, 3H). MS (ESI): m/z calc. for [M+H$^+$]$^+$ = 405.15, found = 405.15

2-(2-(ethylcarbamoyl)-6-methyl-7-oxo-6,7-dihydro-1*H*-pyrrolo[2,3-*c*]pyridin-4-yl)quinoline-6-carboxylic acid (127)
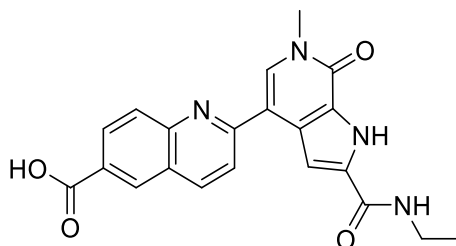
Compound **126** (50 mg, 124 µmol) and LiOH (26 mg, 0.62 mmol) were dissolved in dioxane/methanol/water (3/2/1, 12 mL) and stirred at ambient temperature for 19 h. Afterwards, water was added and the pH of the solution was brought to 4 through the addition of diluted aq HCl. The resulting precipitate was filtered and dried to provide the title compound (30 mg, 62%). MS (ESI): m/z calc. for $[M+H^+]^+$ = 391.13, found = 391.10

***N*-(2-aminophenyl)-2-(2-(ethylcarbamoyl)-6-methyl-7-oxo-6,7-dihydro-1*H*-pyrrolo[2,3-*c*]pyridin-4-yl)quinoline-6-carboxamide (128)**
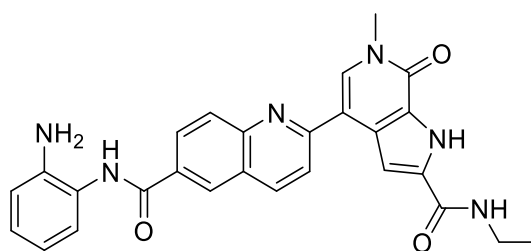
The reaction was performed according to "general procedure for amide coupling". Compound **127** (30 mg, 77 µmol) and benzene-1,2-diamine (17 mg, 0.15 mmol) were used. After completion, water was added to the reaction mixture and the resulting precipitate was filtered and dried to provide the title compound (33 mg, 89%). ^{1}H NMR (400 MHz, DMSO-d$_6$) δ 12.34 (s, 1H), 9.91 (s, 1H), 8.72 − 8.43 (m, 3H), 8.32 (s, 2H), 8.26 − 8.12 (m, 2H), 7.97 (s, 1H), 7.48 − 6.48 (m, 4H), 5.20 (br s, 2H), 3.69 (s, 3H), 2.95 − 2.61 (m, 2H), 1.19 (s, 3H). MS (ESI): m/z calc. for $[M+H^+]^+$ = 481.19, found = 481.15

5-(2-(ethylcarbamoyl)-6-methyl-7-oxo-6,7-dihydro-1*H*-pyrrolo[2,3-*c*]pyridin-4-yl)picolinic acid (129)
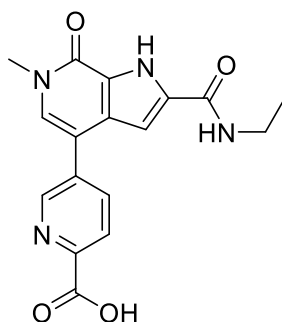
The reaction was performed according to "general procedure for Suzuki coupling B". Compound **120d** (58 mg, 0.34 mmol) and compound **125** (90 mg, 0.26 mmol) were used. After the reaction was complete, LiOH · H₂O (30 mg) was added and the mixture was stirred at ambient temperature for 1 h. Then, the pH was brought to 3 through the addition of aq HCl (5%) and the resulting precipitate was filtered and dried to provide the title compound (50 mg, 56%). MS (ESI): m/z calc. for [M+H$^+$]$^+$ = 341.12, found = 341.10

4-(6-((2-aminophenyl)carbamoyl)pyridin-3-yl)-*N*-ethyl-6-methyl-7-oxo-6,7-dihydro-1*H*-pyrrolo[2,3-*c*]pyridine-2-carboxamide (130)
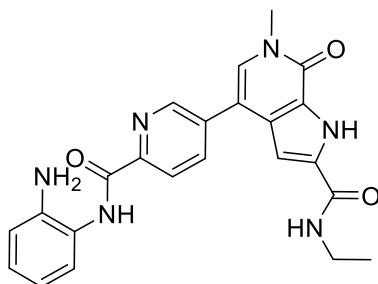
The synthesis was performed according to "general procedure for amide coupling". Compound **129** (50 mg, 0.15 mmol) and benzene-1,2-diamine (19 mg, 0.18 mmol) were used. The crude product was suspended in a small amount of MeOH and filtered to provide the title compound (25 mg, 40%). MS (ESI): m/z calc. for [M+H$^+$]$^+$ = 431.18, found = 431.15

***tert*-Butyl (3-(4-(6-methyl-7-oxo-6,7-dihydro-1*H*-pyrrolo[2,3-*c*]pyridin-4-yl)benzamido)-[1,1'-biphenyl]-4-yl)carbamate (131a)**
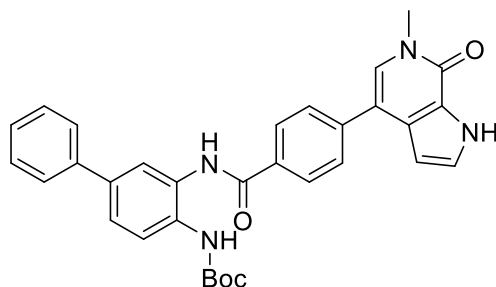
The synthesis was performed as described by Bauer *et al.*[277] The synthesis was performed according to "general procedure for amide coupling". 4-(6-Methyl-7-oxo-6,7-dihydro-1*H*-pyrrolo[2,3-*c*]pyridin-4-yl)benzoic acid (**122a**, 160 mg, 596 µmol, 1.0 eq) and *tert*-butyl (3-amino-[1,1'-biphenyl]-4-yl)carbamate (**26d**, 170 mg, 596 µmol, 1.0 eq) were used. The obtained beige solid (210 mg, 66%) was used in the next step without further characterization. MS (ESI): m/z calc. for $[C_{32}H_{30}N_4O_4+H^+]^+$ = 535.23, found = 535.20

***tert*-Butyl (3-(5-(6-methyl-7-oxo-6,7-dihydro-1*H*-pyrrolo[2,3-*c*]pyridin-4-yl)picolinamido)-[1,1'-biphenyl]-4-yl)carbamate (131b)**
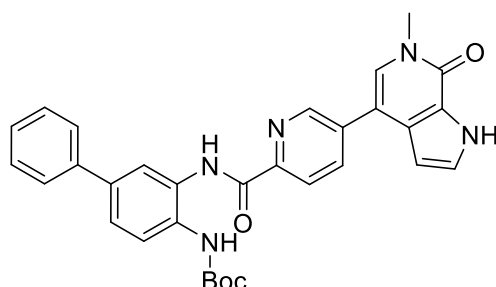
The synthesis was performed as described by Bauer *et al.*[277] The synthesis was performed according to "general procedure for amide coupling". 5-(6-Methyl-7-oxo-6,7-dihydro-1*H*-pyrrolo[2,3-*c*]pyridin-4-yl)picolinic acid (**122d**, 100 mg, 371 µmol, 1.0 eq) and *tert*-butyl (3-amino-[1,1'-biphenyl]-4-yl)carbamate (**26d**, 116 mg, 409 µmol, 1.1 eq) were used. The product was obtained as a beige solid (198 mg, quant.). ^{1}H NMR (500 MHz, DMSO-d_6) δ 12.29 (s, 1H), 10.58 (s, 1H), 9.24 (s, 1H), 8.88 (dd, *J* = 2.2, 0.9 Hz, 1H), 8.33 (d, *J* = 2.1 Hz, 1H), 8.29 (dd, *J* = 8.2, 2.2 Hz, 1H), 8.26 (dd, *J* = 8.1, 0.9 Hz, 1H), 7.71 − 7.63 (m, 3H), 7.51 − 7.46 (m, 3H), 7.43 (t, *J* = 2.8 Hz, 1H), 7.41 − 7.36 (m, 2H), 6.50 (dd, *J* = 2.9, 2.0 Hz, 1H), 3.63 (s, 3H), 1.52 (s, 9H). ^{13}C NMR (126 MHz, DMSO) δ 161.98, 154.14, 153.93, 147.41, 146.41, 139.54, 137.37, 136.23, 136.11, 132.13, 129.78, 129.17, 129.00, 127.63, 127.48, 126.54, 123.37, 123.10, 122.49, 110.34, 101.69, 79.85, 35.73, 28.06. MS (ESI): m/z calc. for $[C_{31}H_{29}N_5O_4+H^+]^+$ = 536.22, found = 536.20

tert-Butyl (4-(furan-2-yl)-2-(5-(6-methyl-7-oxo-6,7-dihydro-1H-pyrrolo[2,3-c]pyridin-4-yl)picolinamido)-phenyl)carbamate (131c)

The synthesis was performed as described by Bauer *et al.*[277] The synthesis was performed according to "general procedure for amide coupling". 5-(6-Methyl-7-oxo-6,7-dihydro-1H-pyrrolo[2,3-c]pyridin-4-yl)picolinic acid (**122d**, 100 mg, 371 µmol, 1.0 eq) and *tert*-butyl (2-amino-4-(furan-2-yl)phenyl)carbamate (**26b**, 112 mg, 409 µmol, 1.1 eq) were used. The crude product (195 mg, quant.) was used in the next step without further characterization. MS (ESI): m/z calc. for $[C_{29}H_{27}N_5O_5+H^+]^+$ = 526.20, found = 526.15

tert-Butyl (2-(5-(6-methyl-7-oxo-6,7-dihydro-1H-pyrrolo[2,3-c]pyridin-4-yl)picolinamido)-4-(thiophen-2-yl)phenyl)carbamate (131d)

The synthesis was performed as described by Bauer *et al.*[277] The synthesis was performed according to "general procedure for amide coupling". 5-(6-Methyl-7-oxo-6,7-dihydro-1H-pyrrolo[2,3-c]pyridin-4-yl)picolinic acid (**122d**, 50 mg, 186 µmol, 1.0 eq) and *tert*-butyl (2-amino-4-(thiophen-2-yl)phenyl)carbamate (**26a**, 54 mg, 0.19 mmol, 1.0 eq) were used. The crude product (100 mg, quant.) was used in the next step without further characterization. MS (ESI): m/z calc. for $[C_{29}H_{27}N_5O_4S+H^+]^+$ = 542.18, found = 542.15

_N_-(4-Amino-[1,1'-biphenyl]-3-yl)-4-(6-methyl-7-oxo-6,7-dihydro-1_H_-pyrrolo[2,3-_c_]pyridin-4-yl)benz-amide (132a)

The synthesis was performed as described by Bauer _et al._[277] The synthesis was performed according to "general procedure for _N-Boc_ deprotection". _tert_-Butyl (3-(4-(6-methyl-7-oxo-6,7-dihydro-1_H_-pyrrolo[2,3-_c_]pyridin-4-yl)benzamido)-[1,1'-biphenyl]-4-yl)carbamate (**131a**, 210 mg, 393 μmol) was dissolved in DCM/TFA (10 mL, 3/1). The crude product was triturated with methanol and filtered to provide the title compound as a beige solid (128 mg, 75%). ^{1}H NMR (500 MHz, DMSO-d_6) δ 12.22 (s, 1H), 10.29 (s, 1H), 8.18 (d, J = 8.3 Hz, 2H), 7.79 (d, J = 8.3 Hz, 2H), 7.74 (d, J = 2.2 Hz, 1H), 7.64 (d, J = 7.1 Hz, 2H), 7.56 (s, 1H), 7.54 (dd, J = 8.4, 2.3 Hz, 1H), 7.45 (t, J = 7.7 Hz, 2H), 7.41 (t, J = 2.8 Hz, 1H), 7.34 (t, J = 7.4 Hz, 1H), 7.27 (d, J = 8.3 Hz, 1H), 6.70 (br s, 2H), 6.52 (t, J = 2.4 Hz, 1H), 3.63 (s, 3H). ^{13}C NMR (126 MHz, DMSO) δ 165.54, 154.17, 140.75, 139.31, 131.97, 129.00, 128.82, 128.60, 128.08, 127.36, 127.17, 126.96, 126.17, 124.97, 124.85, 123.44, 113.77, 102.14, 35.67. MS (ESI): m/z calc. for [$C_{27}H_{22}N_4O_2$+H$^+$]$^+$ = 435.17, found = 435.10. HRMS (MALDI): m/z calc. for [$C_{27}H_{22}N_4O_2$+H$^+$]$^+$ = 457.1635, found = 457.1639

_N_-(4-Amino-[1,1'-biphenyl]-3-yl)-5-(6-methyl-7-oxo-6,7-dihydro-1_H_-pyrrolo[2,3-_c_]pyridin-4-yl)picolin-amide (132b)

The synthesis was performed as described by Bauer _et al._[277] The synthesis was performed according to "general procedure for _N-Boc_ deprotection". _tert_-Butyl (3-(5-(6-methyl-7-oxo-6,7-dihydro-1_H_-pyrrolo[2,3-_c_]pyridin-4-yl)picolinamido)-[1,1'-biphenyl]-4-yl)carbamate (**131b**, 198 mg, 370 μmol) was dissolved in DCM/TFA (10 mL, 3/1). The crude product was triturated with methanol and filtered to provide the title compound as a pale yellow solid (100 mg, 62%). ^{1}H NMR (500 MHz, DMSO-d_6) δ 12.28 (s, 1H), 10.17 (s, 1H), 8.97 (dd, J = 2.2, 0.9 Hz, 1H), 8.28 (dd, J = 8.1, 2.2 Hz, 1H), 8.24 (dd, J = 8.2, 0.8 Hz, 1H), 7.88 (d, J = 2.1 Hz, 1H), 7.68 (s, 1H), 7.60 – 7.55 (m, 2H), 7.44 – 7.38 (m, 3H), 7.32 (dd, J = 8.3, 2.2 Hz, 1H), 7.28 – 7.24 (m, 1H), 6.93 (d, J = 8.3 Hz, 1H), 6.54 (dd, J = 2.8, 2.0 Hz, 1H), 5.11 (s, 2H), 3.63 (s,

3H). ^{13}C NMR (126 MHz, DMSO) δ 162.29, 154.15, 147.99, 146.50, 141.51, 140.31, 135.89, 135.82, 129.60, 128.90, 128.80, 127.70, 127.58, 126.12, 125.65, 124.27, 124.16, 123.39, 122.80, 122.40, 117.11, 110.50, 101.84, 35.73. MS (ESI): m/z calc. for $[C_{26}H_{21}N_5O_2+H^+]^+$ = 436.17, found = 436.15. HRMS (MALDI): m/z calc. for $[C_{26}H_{21}N_5O_2+Na^+]^+$ = 458.1588, found = 458.1582

N-(2-Amino-5-(furan-2-yl)phenyl)-5-(6-methyl-7-oxo-6,7-dihydro-1H-pyrrolo[2,3-c]pyridin-4-yl)picolin-amide (132c)

The synthesis was performed as described by Bauer *et al.*[277] The synthesis was performed according to "general procedure for *N-Boc* deprotection". *tert*-Butyl (4-(furan-2-yl)-2-(5-(6-methyl-7-oxo-6,7-dihydro-1H-pyrrolo[2,3-c]pyridin-4-yl)picolinamido)phenyl)-carbamate (**131c**, 195 mg, 371 μmol) was dissolved in DCM/TFA (10 mL, 3/1). The crude product was triturated with methanol and filtered to provide the title compound as a beige solid (87 mg, 55%). ^{1}H NMR (500 MHz, DMSO-d_6) δ 12.28 (s, 1H), 10.12 (s, 1H), 8.96 (d, J = 2.2 Hz, 1H), 8.30 – 8.20 (m, 2H), 7.89 (d, J = 2.1 Hz, 1H), 7.72 – 7.59 (m, 2H), 7.42 (t, J = 2.8 Hz, 1H), 7.33 (dd, J = 8.3, 2.1 Hz, 1H), 6.88 (d, J = 8.4 Hz, 1H), 6.63 (d, J = 3.3 Hz, 1H), 6.54 (t, J = 2.4 Hz, 1H), 6.52 (dd, J = 3.3, 1.8 Hz, 1H), 5.26 – 5.01 (m, 2H), 3.63 (s, 3H). ^{13}C NMR (126 MHz, DMSO) δ 162.35, 154.15, 153.80, 147.94, 146.49, 141.62, 141.34, 135.88, 135.83, 129.61, 127.69, 127.58, 123.98, 123.39, 122.40, 121.70, 120.17, 119.87, 116.80, 111.80, 110.49, 102.66, 101.84, 35.73. MS (ESI): m/z calc. for $[C_{24}H_{19}N_5O_3+H^+]^+$ = 426.15, found = 426.10. HRMS (MALDI): m/z calc. for $[C_{24}H_{19}N_5O_3+Na^+]^+$ = 448.1380, found = 448.1385

N-(2-Amino-5-(thiophen-2-yl)phenyl)-5-(6-methyl-7-oxo-6,7-dihydro-1H-pyrrolo[2,3-c]pyridin-4-yl)-picolinamide (132d)
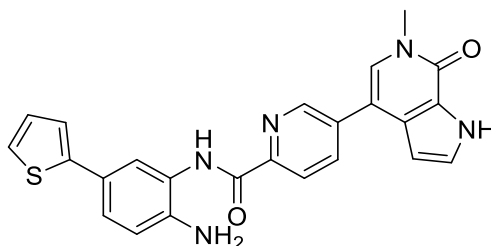
The synthesis was performed as described by Bauer *et al.*[277] The synthesis was performed according to "general procedure for *N-Boc* deprotection". *tert*-Butyl (2-(5-(6-methyl-7-oxo-6,7-dihydro-1H-pyrrolo[2,3-c]pyridin-4-yl)picolinamido)-4-(thiophen-2-yl)phenyl)-carbamate (**131d**, 100 mg, 185 μmol) was dissolved in DCM/TFA (8 mL, 3/1). The crude product was triturated with methanol and filtered to provide the title compound as a beige solid (34 mg, 41%). ^{1}H NMR (500 MHz, DMSO-d_6) δ 12.29 (s, 1H), 10.19 (s, 1H), 8.98 – 8.96 (m, 1H), 8.29 (dd, *J* = 8.2, 2.2 Hz, 1H), 8.27 – 8.22 (m, 1H), 7.85 (d, *J* = 2.2 Hz, 1H), 7.69 (s, 1H), 7.43 (t, *J* = 2.8 Hz, 1H), 7.39 (dd, *J* = 5.1, 1.2 Hz, 1H), 7.32 (dd, *J* = 8.3, 2.2 Hz, 1H), 7.28 (dd, *J* = 3.6, 1.2 Hz, 1H), 7.08 (dd, *J* = 5.1, 3.6 Hz, 1H), 6.90 (d, *J* = 8.3 Hz, 1H), 6.56 – 6.53 (m, 1H), 5.08 (br s, 2H), 3.64 (s, 3H). ^{13}C NMR (126 MHz, DMSO) δ 162.40, 154.15, 147.88, 146.50, 144.18, 135.88, 135.87, 129.62, 128.24, 127.69, 127.59, 124.39, 123.54, 123.39, 123.37, 123.33, 123.31, 122.45, 121.98, 121.35, 117.24, 110.48, 101.84, 35.73. MS (ESI): m/z calc. for $[C_{24}H_{19}N_5O_2S+H^+]^+$ = 442.13, found = 442.10. HRMS (MALDI): m/z calc. for $[C_{24}H_{19}N_5O_2S +Na^+]^+$ = 464.1152, found = 464.1151

N-(2-Amino-4-fluorophenyl)-5-(6-methyl-7-oxo-6,7-dihydro-1H-pyrrolo[2,3-c]pyridin-4-yl)picolinamide (133)

The synthesis was performed as described by Bauer *et al.*[277] The synthesis was performed according to "general procedure for amide coupling". 5-(6-Methyl-7-oxo-6,7-dihydro-1H-pyrrolo[2,3-c]pyridin-4-yl)picolinic acid (**122d**, 90 mg, 0.33 mmol, 1.0 eq) and 4-fluorobenzene-1,2-diamine (51 mg, 0.40 mmol, 1.2 eq) were used. The crude product was triturated with methanol and filtered to provide the title compound as a beige solid (48 mg, 38%). ^{1}H NMR (500 MHz, DMSO-d_6) δ 12.27 (s, 1H), 9.99 (s, 1H), 8.94 (dd, *J* = 2.2, 0.8 Hz, 1H), 8.25 (dd, *J* = 8.2, 2.3 Hz, 1H), 8.20 (dd, *J* = 8.2, 0.8 Hz, 1H), 7.66 (s, 1H), 7.42 (t, *J* = 2.8 Hz, 1H), 7.37 (dd, *J* = 8.7, 6.3 Hz, 1H), 6.60 (dd, *J* = 11.1, 2.9 Hz, 1H), 6.52 (dd, *J* = 2.8,

2.0 Hz, 1H), 6.42 (td, J = 8.6, 2.9 Hz, 1H), 5.25 (s, 2H), 3.62 (s, 3H). ^{19}F NMR (471 MHz, DMSO-d_6) δ -116.72 (ddd, J = 11.7, 8.9, 6.6 Hz). ^{13}C NMR (126 MHz, DMSO) δ 162.51, 154.14, 148.00, 146.45, 144.60, 144.50, 135.81, 135.75, 129.55, 127.70, 127.57, 126.95, 126.87, 123.38, 122.40, 119.70, 119.68, 110.50, 102.63, 102.45, 102.17, 101.97, 101.82, 35.72. MS (ESI): m/z calc. for $[C_{20}H_{16}FN_5O_2+H^+]^+$ = 378.13, found = 360.10. HRMS (MALDI): m/z calc. for $[C_{20}H_{16}FN_5O_2+Na^+]^+$ = 400.1180, found = 400.1183

1,4-dioxaspiro[4.4]nonane (135)
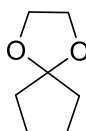
A mixture of cyclopentanone (**134**, 250 mL, 2.82 mol), ethylene glycol (189 mL, 3.38 mol) and DOWEX 50W X8 acidic ion exchange resin (4 g) in benzene (500 mL) was heated unter reflux for 3 d, while water was removed *via* a Dean-Stark apparatus. Distillation under reduced pressure provided the title compound as a colorless liquid (310 g, 86%). ^{1}H NMR (400 MHz, DMSO-d_6) δ 3.80 (s, 4H), 1.71 – 1.64 (m, 4H), 1.63 – 1.56 (m, 4H). ^{13}C NMR (101 MHz, DMSO) δ 117.52, 63.57, 35.35, 23.01.

(3a'S,4'S,7'S,7a'R)-2',4'-dibromo-3a',4',7',7a'-tetrahydrodispiro[[1,3]dioxolane-2,1'-[4,7]methano-indene-8',2''-[1,3]dioxolane] (138)
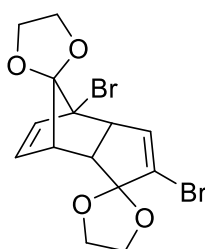
The synthesis was adapted from Falkiner *et al*.[295] To a solution of compound **135** (144 g, 1.13 mol) in dioxane (800 mL), Br_2 (185 mL, 3.61 mol) was added dropwise at 0 °C. Afterwards, the mixture was stirred at ambient temperature for 16 h under a stream of Ar to facilitate removal of HBr. Then, the mixture was cooled to 0 °C and a solution of NaOH (234 g, 5.86 mol) in MeOH (600 mL) was added dropwise. Afterwards, the reaction was heated under reflux for 16 h. After cooling to ambient temperature, the mixture was poured onto ice and the resulting precipitate was filtered, subsequently washed with water and methanol, and dried to provide a beige solid (162.8 g, 71%). ^{1}H NMR (400 MHz, Chloroform-d) δ 6.17 (dd, J = 6.4, 3.6 Hz, 1H), 6.05 (dd, J = 2.5, 0.6 Hz, 1H), 5.82 (dd, J = 6.5, 1.3 Hz, 1H), 4.26 – 4.09 (m, 4H), 4.03 – 3.85 (m, 4H), 3.49 (dd, J = 7.4, 2.4 Hz, 1H), 3.06 (dd, J = 7.4, 4.7 Hz, 1H), 2.71 (ddt, J = 4.8, 3.8, 0.8 Hz, 1H).

(3aS,4S,7S,7aR)-2,4-dibromo-3a,4,7,7a-tetrahydro-1H-4,7-methanoindene-1,8-dione (139)
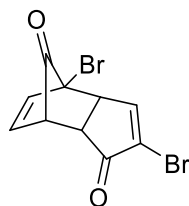
The synthesis was adapted from Falkiner *et al.*[295] Compound **138** (162.8 g, 400.1 mmol) was slowly added to concentrated H_2SO_4 (500 mL) at ambient temperature and the reaction was stirred for 30 h. Afterwards, the mixture was poured onto ice and the resulting precipitate was filtered, washed with water and dried to provide a brown solid. Recrystallization from methanol then afforded a pale beige solid (98 g, 77%). ^{1}H NMR (400 MHz, Chloroform-*d*) δ 7.67 (d, *J* = 2.9 Hz, 1H), 6.36 (dd, *J* = 6.9, 3.9 Hz, 1H), 6.25 (dd, *J* = 7.0, 1.4 Hz, 1H), 3.59 (td, *J* = 4.5, 3.7, 1.4 Hz, 1H), 3.52 (dd, *J* = 6.4, 2.9 Hz, 1H), 3.21 (dd, *J* = 6.4, 5.0 Hz, 1H).

Intermediate 140
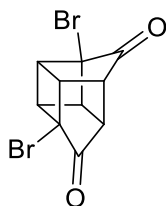
Conc. H_2SO_4 (2 mL) was added to a solution of compound **139** (20.0 g, 62.9 mmol) in H_2O (1.6 L) and MeOH (200 mL) and the mixture was left outside and exposed to sunlight for 21 d. After monitoring by ^{1}H NMR indicated full conversion, all volatiles were removed under reduced pressure. The crude product was used in the next step without further purification.

Cubane-1,4-dicarboxylic acid (141)
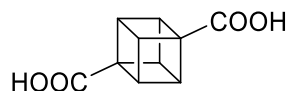
Crude compound **140** (20.0 g, 62.9 mmol, quant. yield assumed) was dissolved in aq NaOH (20%, 300 mL) and heated under reflux for 3 h. Afterwards, the mixture was cooled to 0 °C and aq HCl (conc.) was added until a pH of 1-2 was reached. The mixture was left at 4 °C for 16 h and the resulting precipitate was filtered, washed with water and dried to provide a light brown solid (9.16 g, 76%). ^{1}H NMR (400 MHz, DMSO-d_6) δ 12.44 (br s, 2H), 4.10 (s, 6H). HRMS (MALDI): m/z calc. for $[C_{20}H_{16}FN_5O_2+H^+]^+$ = 193.0495, found = 193.0495

Dimethyl cubane-1,4-dicarboxylate (142)
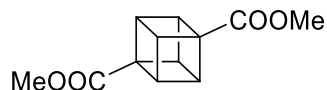
A mixture of compound **141** (8.4 g, 44 mmol) and DOWEX 50W X8 acidic ion exchange resin (700 mg) in MeOH (100 mL) was heated under reflux for 18 h. Afterwards, the mixture was filtered and volatiles were removed under reduced pressure to provide a brown solid (6.62 g, 69%). ^{1}H NMR (250 MHz, Chloroform-*d*) δ 4.22 (s, 6H), 3.69 (s, 6H).

4-(methoxycarbonyl)cubane-1-carboxylic acid (143)
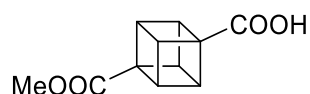
A solution of NaOH (1.20 g, 30.1 mmol) in MeOH (15 mL) was added to a solution of compound **142** (6.62 g, 30.1 mmol) in THF (90 mL) and the mixture was stirred at ambient temperature for 16 h. Afterwards, most of the solvent was removed under reduced pressure, the residue was acidified with aq HCL (5%) and extracted with DCM and ethyl acetate. The combined organic layers were washed with brine, dried over MgSO$_4$, filtered and the solvent was removed *in vacuo* to give a brown residue which was recrystallized from MeOH to provide the title compound as a beige solid (3.94 g, 64%).^{1}H NMR (250 MHz, DMSO-*d*$_6$) δ 12.41 (s, 1H), 4.14 (d, *J* = 0.7 Hz, 6H), 3.62 (s, 3H).

4,5,6,7-tetrachloro-1,3-dioxoisoindolin-2-yl 4-acetoxycubane-1-carboxylate (144)
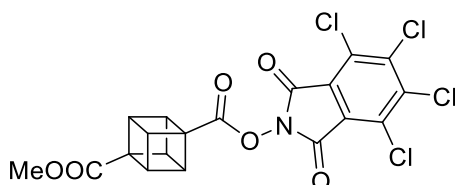
The synthesis was adapted from Wiesenfeldt *et al.*[293] EDC (846 mg, 4.41 mmol, 1.0 eq) was dissolved in DCM (5 ml). DIPEA (767 µl, 4.41 mmol, 1.0 eq) was added and the solution was stirred at room temperature for 15 minutes. Compound **143** (910 mg, 4.41 mmol, 1.0 eq), 4,5,6,7-Tetrachloro-2-hydroxyisoindoline-1,3-dione (1.39 g, 4.63 mmol, 1.05 eq) and DMAP (54 mg, 0.44 mmol, 0.1 eq), dissolved in DCM (12 ml), were added to the reaction mixture and stirred at room temperature for 18 h. The solvent was removed *in vacuo* and the crude product was rapidly purified *via* flash chromatography (silica, DCM) to give a colourless solid (530 mg, 25%). ^{1}H NMR (400 MHz, Chloroform-*d*) δ 4.52 − 4.45 (m, 3H), 4.41 − 4.34 (m, 3H), 3.73 (s, 3H). ^{13}C NMR (101 MHz, CDCl$_3$) δ 171.52, 166.58, 157.80, 141.21, 130.65, 124.89, 55.92, 52.91, 51.92, 47.86, 47.76.

N-(*tert*-butyl)-*N*,1,1,1,3,3,3-heptamethyl-2-(trimethylsilyl)trisilan-2-amine (146)
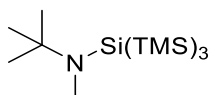
The synthesis was adapted from Wiesenfeldt *et al.*[293] Trifluoromethanesulfonic acid (0.94 mL, 11 mmol) was dissolved in anh. DCM (30 mL) and cooled to 0 °C. Then, supersilane (3.0 mL, 11 mmol) was added dropwise and the mixture was stirred for 1 h at ambient temperature. The mixture was allowed to warm up to room temperature over the course of 1 h. Then, a solution of *N*,*N*-diisopropylethylamine (2.5 mL, 14 mmol) and *tert*butyl-methyl amine (1.3 mL, 11 mmol) was added slowly at 0 °C. The ice bath was removed, and the resulting solution was stirred for 16 h at ambient temperature. Afterwards, the solvent was removed under reduced pressure and the residue was triturated with methanol and filtered to provide a colorless solid (1.13 g, 33%). ^{1}H NMR (400 MHz, Chloroform-*d*) δ 2.59 (s, 3H), 1.14 (s, 9H), 0.20 (s, 27H).

Methyl 4-(6-methyl-7-oxo-1-tosyl-6,7-dihydro-1*H*-pyrrolo[2,3-*c*]pyridin-4-yl)cubane-1-carboxylate (147)
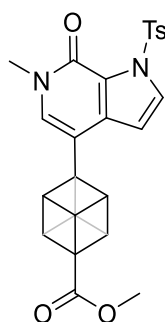
Compound **55** (270 mg, 0.708 mmol, 3 eq) was dissolved in THF (5 mL) and cooled to -10 °C. Isopropylmagnesium chloride (980 µl, 1.27 mmol, 5.4 eq) in THF (2 M) was added dropwise and the reaction mixture was stirred at -10 °C for 30 min. After full conversion of the starting material (monitored *via* HPLC-MS), ZnCl$_2$ (96 mg, 0.71 mmol, 1.0 eq) was added to the reaction mixture and stirred at ambient temperature for 10 min. **144** (100 mg, 0.204 mmol, 1.0 eq) and [4,4'-Bis(1,1-dimethylethyl)-2,2'-bipyridine] nickel (II) dichloride (81 mg, 0.20 mmol, 1.0 eq) were dissolved in DMF (2 mL), slowly added to the reaction mixture and stirred at room temperature for 2 h. The reaction mixture was quenched with sat. aq NH$_4$Cl (10 ml) and the aqueous phase was extracted with DCM (3x 10 ml). The combined organic layers were washed with brine (3x 10 ml), dried over MgSO$_4$, filtered and the solvent was removed *in vacuo* to give a yellow resin. The crude product was used without further purification. MS (ESI): m/z calc. for [M+H$^+$]$^+$ = 463.12, found = 463.10

4-(6-methyl-7-oxo-1-tosyl-6,7-dihydro-1*H*-pyrrolo[2,3-*c*]pyridin-4-yl)cubane-1-carboxylic acid (149)
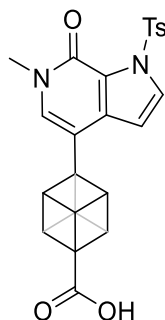
Compound **147** (30 mg, 65 µmol, 1 eq) and LiOH · H$_2$O (21 mg, 0.51 mmol, 8 eq) were dissolved in methanol/water (4 ml, 3/1) and heated at ambient temperature for 16 h. The mixture was cooled to ambient temperature and quenched by the addition of sat. aq NH$_4$CL (10 ml) and the aqueous phase extracted with DCM (3x 10 ml). The combined organic layers were washed with brine (3x 10 ml) and dried *in vacuo*. The crude product was purified *via* flash chromatography (C18 silica, H$_2$O/ACN with 0.2% TFA) to give the title compound as a yellow resin (3.1 mg, 16%). MS (ESI): m/z calc. for [M+H$^+$]$^+$ = 449.11, found = 449.05

***N*-(2-aminophenyl)-4-(6-methyl-7-oxo-1-tosyl-6,7-dihydro-1*H*-pyrrolo[2,3-*c*]pyridin-4-yl)cubane-1-carboxamide (150)**
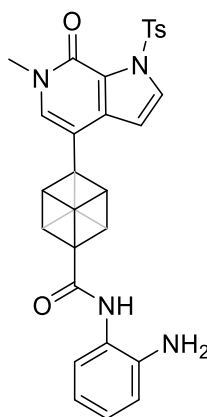
Compound **149** (3.1 mg, 6.7 µmol, 1.0 eq) and PyAOP (4.1 mg, 8.1 µmol, 1.2 eq) were dissolved in DMF (0.5 mL). DIPEA (2.6 µl, 20 µmol, 3.0 eq) was added and the reaction mixture was stirred at ambient temperature for 15 minutes. 1,2-Phenylenediamine (0.7 mg, 6.7 µmol, 1.0 eq) was added to the solution and the reaction mixture was stirred for 1 h. The reaction mixture was quenched with sat. aq NH$_4$Cl (3 ml) and the aqueous phase was extracted with DCM (3x 5 ml). The combined organic layers were washed with brine (3x 5 ml) and dried *in vacuo*. The reaction mixture was purified via preparative HPLC (C18 silica, H$_2$O/ACN with 0.1% TFA) and the title compound was obtained as a yellow resin (0.3 mg, 8%). MS (ESI): m/z calc. for [M+H$^+$]$^+$ = 539.17, found = 539.15

(2*r*,3*r*,5*r*,6*r*,7*r*,8*r*)-*N*-(2-aminophenyl)-4-(6-methyl-7-oxo-6,7-dihydro-1*H*-pyrrolo[2,3-*c*]pyridin-4-yl)cubane-1-carboxamide (151)
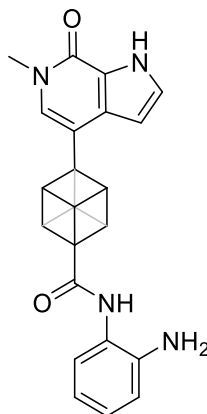
Compound **150** (0.3 mg, 0.6 µmol, 1 eq) and LiOH · H$_2$O (0.2 mg, 4.5 µmol, 8 eq) were dissolved in dioxane/water (1 ml, 3/1) and heated at 70 °C for 16 h. The mixture was cooled to ambient temperature and quenched by the addition of sat. aq NH$_4$CL (1 ml) and the aqueous phase was extracted with DCM (3x 2 ml). The combined organic layers were washed with brine (3x 2 ml) and dried *in vacuo* to give the title compound as a yellow resin (0.2 mg, 80%). MS (ESI): m/z calc. for [M+H$^+$]$^+$ = 385.16, found = 385.10

4-(2-(2-aminoethoxy)ethoxy)-2-(2,6-dioxopiperidin-3-yl)isoindoline-1,3-dione (154a)
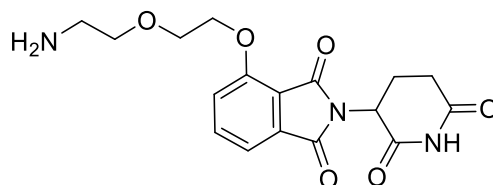
A mixture of 4-hydroxy-thalidomide (**153**, 500 mg, 1.82 mmol, 1.0 eq), *tert*-butyl (2-(2-hydroxyethyl)ethyl)carbamate (**152**, 393 mg, 1.91 mmol, 1.05 eq), PPh$_3$ (956 mg, 3.65 mmol, 2.0 eq) and MgSO$_4$ (263 mg, 2.19 mmol, 1.2 eq) in THF/DMF (10/1, 15 mL) was cooled to 0 °C and a solution of DIAD (716 µL, 3.65 mmol, 2.0 eq) in THF (5 mL) was added dropwise. After 16 h, all volatiles were removed under reduced pressure and the residue was purified by flash chromatography (C18 silica, water/ACN) to provide the *Boc*-protected intermediate. MS (ESI): m/z calc. for [M+Na$^+$]$^+$ = 484.17, found = 484.15

The residue was dissolved in DCM/TFA (3/1, 20 mL) and stirred at ambient temperature for 2 h. Afterwards, all volatiles were removed under reduced pressure and the residue was purified by flash chromatography (C18 silica, water/ACN) to provide the title compound as a TFA salt (400 mg, 46%). ^{1}H NMR (400 MHz, DMSO-*d$_6$*) δ 11.04 (br s, 1H), 7.90 (br s, 3H), 7.83 (dd, *J* = 8.5, 7.3 Hz, 1H), 7.54 (d, *J* = 8.5 Hz, 1H), 7.48 (d, *J* = 7.2 Hz, 1H), 5.08 (dd, *J* = 12.8, 5.4 Hz, 1H), 4.38 (t, *J* = 4.4 Hz, 2H), 3.89 – 3.83

(m, 1H), 3.74 (t, J = 5.2 Hz, 2H), 3.01 (t, J = 5.2 Hz, 2H), 2.89 (ddd, J = 16.6, 13.7, 5.2 Hz, 1H), 2.65 – 2.53 (m, 2H), 2.13 – 1.96 (m, 1H). MS (ESI): m/z calc. for $[M+H^+]^+$ = 362.13, found = 362.10

4-(2-(2-(2-aminoethoxy)ethoxy)ethoxy)-2-(2,6-dioxopiperidin-3-yl)isoindoline-1,3-dione (154b)
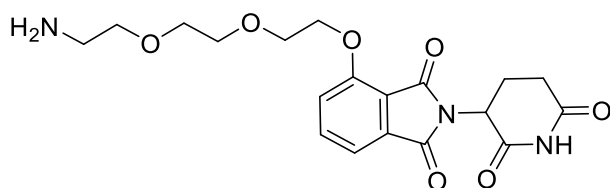
A mixture of 4-hydroxy-thalidomide (**153**, 150 mg, 547 µmol, 1.0 eq), *tert*-butyl (2-(2-(2-bromoethoxy)ethoxy)ethyl)carbamate (**155a**, 188 mg, 602 µmol, 1.1 eq), NaI (82 mg, 0.55 mmol, 1.0 eq) and NaHCO$_3$ (129 mg, 1.53 mmol, 2.8 eq) in DMF (1.5 mL) was heated at 80 °C for 3 d. Afterwards, all volatiles were removed under reduced pressure and the residue was purified by flash chromatography (C18 silica, water/ACN) to provide the *Boc*-protected intermediate. MS (ESI): m/z calc. for $[M+Na^+]^+$ = 528.20, found = 528.15

The residue was dissolved in DCM/TFA (3/1, 10 mL) and stirred at ambient temperature for 2 h. Afterwards, all volatiles were removed under reduced pressure and the residue was purified by flash chromatography (C18 silica, water/ACN) to provide the title compound as a TFA salt (107 mg, 38%).^{1}H NMR (400 MHz, DMSO-d_6) δ 11.09 (s, 1H), 7.82 (dd, J = 8.5, 7.3 Hz, 1H), 7.78 (br s, 3H), 7.54 (d, J = 8.5 Hz, 1H), 7.47 (d, J = 7.2 Hz, 1H), 5.08 (dd, J = 12.7, 5.4 Hz, 1H), 4.39 – 4.30 (m, 2H), 3.84 – 3.79 (m, 2H), 3.69 (dd, J = 5.9, 3.4 Hz, 2H), 3.60 (t, J = 5.0 Hz, 4H), 2.96 (q, J = 5.4 Hz, 2H), 2.89 (ddd, J = 16.8, 13.7, 5.4 Hz, 1H), 2.68 – 2.50 (m, 2H), 2.07 – 1.98 (m, 1H). MS (ESI): m/z calc. for $[M+H^+]^+$ = 406.15, found = 406.10

4-(2-(2-(2-(2-aminoethoxy)ethoxy)ethoxy)ethoxy)-2-(2,6-dioxopiperidin-3-yl)isoindoline-1,3-dione (154c)
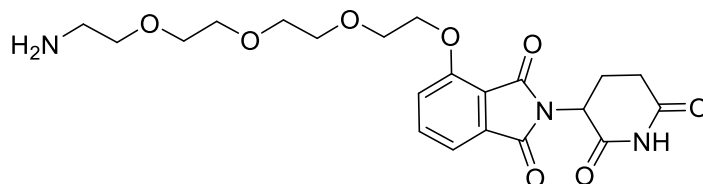
A mixture of 4-hydroxy-thalidomide (**153**, 150 mg, 547 µmol, 1.0 eq), *tert*-butyl (2-(2-(2-(2-bromoethoxy)ethoxy)ethoxy)ethyl)carbamate (**155b**, 214 mg, 602 µmol, 1.1 eq), NaI (82 mg, 0.55 mmol, 1.0 eq) and NaHCO$_3$ (129 mg, 1.53 mmol, 2.8 eq) in DMF (1.5 mL) was heated at 80 °C for 3 d. Afterwards, all volatiles were removed under reduced pressure and the residue was purified by flash chromatography (C18 silica, water/ACN) to provide the *Boc*-protected intermediate.

The residue was dissolved in DCM/TFA (3/1, 10 mL) and stirred at ambient temperature for 2 h. Afterwards, all volatiles were removed under reduced pressure and the residue was purified by flash chromatography (C18 silica, water/ACN) to provide the title compound as a TFA salt (173 mg, 56%).^{1}H NMR (400 MHz, DMSO-d_6) δ 11.09 (s, 1H), 7.82 (dd, J = 8.5, 7.3 Hz, 1H), 7.76 (br s, 3H), 7.53 (d, J = 8.6 Hz, 1H), 7.47 (d, J = 7.2 Hz, 1H), 5.08 (dd, J = 12.7, 5.4 Hz, 1H), 4.35 (dd, J = 5.7, 3.4 Hz, 2H), 3.89 – 3.78 (m, 2H), 3.60 – 3.54 (m, 10H), 2.97 (q, J = 5.6 Hz, 2H), 2.89 (ddd, J = 16.8, 13.7, 5.4 Hz, 1H), 2.65 – 2.53 (m, 2H), 2.06 – 1.99 (m, 1H). MS (ESI): m/z calc. for [M+H$^+$]$^+$ = 450.18, found = 450.15

4-((3-aminopropyl)amino)-2-(2,6-dioxopiperidin-3-yl)isoindoline-1,3-dione (154d)
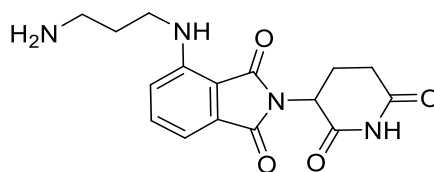
A mixture of 4-fluoro-thalidomide (**157**, 300 mg, 1.09 mmol, 1.0 eq), *tert*-butyl (3-aminopropyl)carbamate (**156a**, 208 mg, 1.19 mmol, 1.1 eq) and DIPEA (568 mL, 3.26 mmol, 3.0 eq) in DMSO (2 mL) was heated at 130 °C for 16 h. Afterwards, the mixture was partitioned between brine and ethyl acetate, the organic phase was washed with brine, dried over MgSO$_4$ and volatiles were removed under reduced pressure and the residue was purified by flash chromatography (silica, DCM/MeOH) to provide the *Boc*-protected intermediate. ^{1}H NMR (400 MHz, DMSO-d_6) δ 11.08 (s, 1H), 7.57 (dd, J = 8.6, 7.1 Hz, 1H), 7.08 (d, J = 8.6 Hz, 1H), 7.02 (d, J = 7.0 Hz, 1H), 6.90 (t, J = 5.7 Hz, 1H), 6.65 (t, J = 6.2 Hz, 1H), 5.05 (dd, J = 12.9, 5.4 Hz, 1H), 3.36 – 3.26 (m, 2H), 3.00 (q, J = 6.4 Hz, 2H), 2.88 (ddd, J = 17.4, 14.0, 5.5 Hz, 1H), 2.65 – 2.53 (m, 2H), 2.09 – 1.95 (m, 1H), 1.67 (q, J = 6.6 Hz, 2H), 1.38 (s, 9H).

The residue was dissolved in DCM/TFA (3/1, 10 mL) and stirred at ambient temperature for 2 h. Afterwards, all volatiles were removed under reduced pressure and the residue was purified by flash chromatography (C18 silica, water/ACN) to provide the title compound as a TFA salt (239 mg, 49%). MS (ESI): m/z calc. for [M+H$^+$]$^+$ = 331.13, found = 331.05

4-((8-aminooctyl)amino)-2-(2,6-dioxopiperidin-3-yl)isoindoline-1,3-dione (154e)
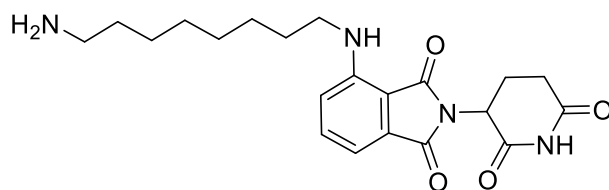
A mixture of 4-fluoro-thalidomide (**157**, 300 mg, 1.09 mmol, 1.0 eq), *tert*-butyl (**156b**, 8-aminooctyl)carbamate (292 mg, 1.19 mmol, 1.1 eq) and DIPEA (568 mL, 3.26 mmol, 3.0 eq) in DMSO (2 mL) was heated at 130 °C for 16 h. Afterwards, the mixture was partitioned between brine and ethyl acetate, the organic phase was washed with brine, dried over MgSO₄ and volatiles were removed under reduced pressure and the residue was purified by flash chromatography (C18 silica, water/ACN) to provide the *Boc*-protected intermediate. MS (ESI): m/z calc. for [M+Na⁺]⁺ = 523.25, found = 523.25

The residue was dissolved in DCM/TFA (3/1, 12 mL) and stirred at ambient temperature for 2 h. Afterwards, all volatiles were removed under reduced pressure and the residue was purified by flash chromatography (C18 silica, water/ACN) to provide the title compound as a TFA salt (248 mg, 44%).¹H NMR (400 MHz, DMSO-d_6) δ 8.40 (br s, 3H), 7.58 (dd, *J* = 8.5, 7.1 Hz, 1H), 7.08 (d, *J* = 8.6 Hz, 1H), 7.02 (d, *J* = 7.0 Hz, 1H), 6.52 (t, *J* = 5.9 Hz, 1H), 5.05 (dd, *J* = 12.8, 5.4 Hz, 1H), 3.29 (q, *J* = 6.7 Hz, 2H), 2.88 (ddd, *J* = 16.8, 13.7, 5.2 Hz, 1H), 2.79 – 2.72 (m, 2H), 2.65 – 2.44 (m, 2H), 2.09 – 1.97 (m, 1H), 1.54 (dp, *J* = 22.5, 7.1 Hz, 4H), 1.40 – 1.23 (m, 9H). MS (ESI): m/z calc. for [M+H⁺]⁺ = 401.21, found = 401.20

tert-butyl (3-(4-bromobenzamido)-[1,1'-biphenyl]-4-yl)carbamate (158)
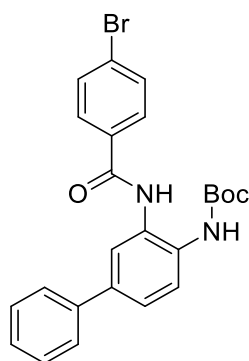
4-bromobenzoyl chloride (365 mg, 1.66 mmol, 1.1 eq) was added to a solution of **26d** (430 mg, 1.51 mmol, 1.0 eq) and DIPEA (316 µL, 1.81 mmol, 1.2 eq) in DCM (30 mL) at 0 °C and the mixture was stirred for 2 h while warming up to ambient temperature. Afterwards, the mixture was partitioned between water and DCM, the aqueous phase was extracted with DCM, the combined organic phases were washed with brine, dried over MgSO₄ and volatiles were removed under reduced pressure to provide the title compound. ¹H NMR (500 MHz, DMSO-d_6) δ 9.97 (s, 1H), 8.76 (s, 1H), 7.98 – 7.92 (m, 2H), 7.83 (d, *J* = 2.2 Hz, 1H), 7.80 – 7.76 (m, 2H), 7.69 (d, *J* = 8.4 Hz, 1H), 7.66 – 7.62 (m, 2H), 7.53 (dd, *J* = 8.5, 2.2 Hz, 1H), 7.46 (t, *J* = 7.7 Hz, 2H), 7.38 – 7.32 (m, 1H), 1.46 (s, 9H). ¹³C NMR (126 MHz, DMSO)

δ 153.31, 139.26, 135.67, 133.47, 131.69, 131.51, 131.47, 131.27, 129.79, 129.54, 128.96, 127.32, 126.33, 125.57, 124.35, 123.97, 79.71, 28.04. MS (ESI): m/z calc. for [M+Na$^+$]$^+$ = 489.08, found = 489.05

Ethyl 4-(4-((4-((tert-butoxycarbonyl)amino)-[1,1'-biphenyl]-3-yl)carbamoyl)phenyl)-6-methyl-7-oxo-6,7-dihydro-1*H*-pyrrolo[2,3-*c*]pyridine-2-carboxylate (159)
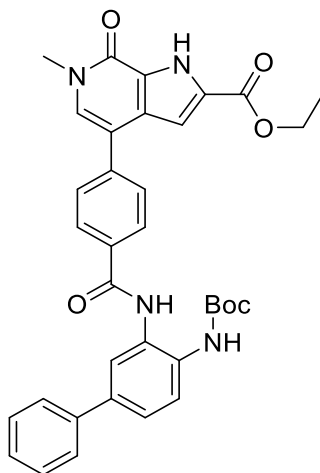
A mixture of compound **158** (675 mg, 1.44 mmol, 1.0 eq), compound **86** (500 mg, 1.44 mmol, 1.0 eq), K$_3$PO$_4$ (766 mg, 3.61 mmol, 2.5 eq), Pd XPhos G2 (57 mg, 72 μmol, 0.05 eq) and XPhos (34 mg, 72 μmol, 0.05 eq) in dioxane/water (37.5 mL, 4/1) was heated at 70 °C for 2 h. Afterwards, the mixture was partitioned between water and DCM, the aqueous phase was extracted with DCM, the combined organic phases were washed with brine, dried over MgSO$_4$ and volatiles were removed under reduced pressure. The crude product was purified by flash chromatography (silica, DCM/MeOH) to provide the title compound (669 mg, 76%). MS (ESI): m/z calc. for [M+H$^+$]$^+$ = 607.25, found = 607.25

4-(4-((4-((tert-butoxycarbonyl)amino)-[1,1'-biphenyl]-3-yl)carbamoyl)phenyl)-6-methyl-7-oxo-6,7-dihydro-1*H*-pyrrolo[2,3-*c*]pyridine-2-carboxylic acid (160)
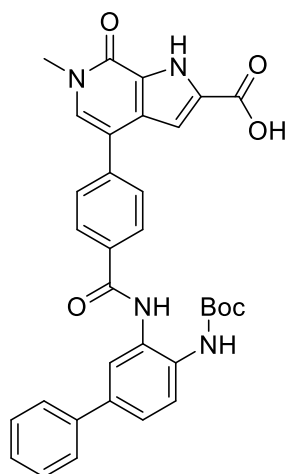
Compound **159** (669 mg, 1.10 mmol, 1.0 eq) and LiOH·H_2O (185 mg, 4.41 mmol, 4.0 eq) were dissolved in MeOH/THF/water (70 mL, 3/2/2) and heated at 40 °C for 4 h. Afterwards, volatiles were removed under reduced pressure until about half of the initial volume was reached. The mixture was cooled, brought to a pH of 7 with diluted aq HCl and extracted with ethyl acetate. The combined organic phases were washed with brine, dried over $MgSO_4$ and volatiles were removed under reduced pressure to provide the title compound (465 mg, 73%). MS (ESI): m/z calc. for [M+H$^+$]$^+$ = 579.22, found = 579.20

4-(4-((4-amino-[1,1'-biphenyl]-3-yl)carbamoyl)phenyl)-*N*-(6-((2-(2,6-dioxopiperidin-3-yl)-1,3-dioxoisoindolin-4-yl)oxy)hexyl)-6-methyl-7-oxo-6,7-dihydro-1*H*-pyrrolo[2,3-*c*]pyridine-2-carboxamide (161a)
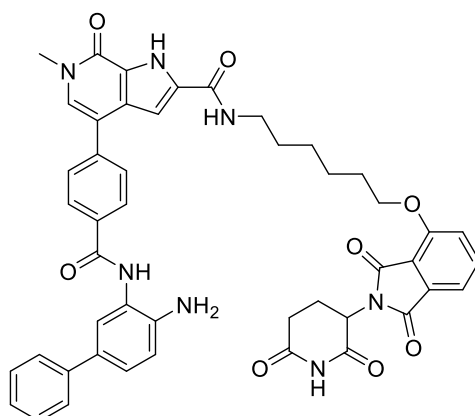
4-((6-aminohexyl)oxy)-2-(2,6-dioxopiperidin-3-yl)isoindoline-1,3-dione (32 mg, 86 µmol) and compound **160** (50 mg, 86 µmol) were reacted according to "general procedure for amide coupling". The mixture was partitioned between water and DCM and the organic phase was washed with brine, dried over MgSO$_4$ and volatiles were removed under reduced pressure. The residue was then purified by flash chromatography (C18 silica, H$_2$O/ACN) to provide the *Boc*-protected intermediate (20 mg, 25%).

The residue was then dissolved in DCM/TFA (2 mL, 3/1) and stirred at ambient temperature for 1 h. Afterwards, all volatiles were removed under reduced pressure and the residue was purified by prep HPLC (C18 silica, H$_2$O/ACN with 0.1% TFA) to provide the title compound as an off-white solid (13 mg, 73%). ^{1}H NMR (500 MHz, DMSO-*d$_6$*) δ 12.41 (d, *J* = 2.3 Hz, 1H), 11.08 (s, 1H), 9.89 (s, 1H), 8.41 (t, *J* = 5.5 Hz, 1H), 8.14 (d, *J* = 8.0 Hz, 2H), 7.81 – 7.76 (m, 3H), 7.61 – 7.57 (m, 4H), 7.50 (d, *J* = 8.5 Hz, 1H), 7.45 – 7.36 (m, 4H), 7.30 – 7.25 (m, 1H), 7.12 (d, *J* = 2.2 Hz, 1H), 6.97 (d, *J* = 8.3 Hz, 1H), 5.07 (dd, *J* = 12.8, 5.5 Hz, 1H), 4.21 (t, *J* = 6.4 Hz, 2H), 3.63 (s, 3H), 3.29 (q, *J* = 6.6 Hz, 2H), 2.92 – 2.81 (m, 1H), 2.62 – 2.52 (m, 2H), 2.01 (dtd, *J* = 13.0, 5.6, 5.2, 2.1 Hz, 1H), 1.78 (p, *J* = 6.6 Hz, 2H), 1.60 – 1.47 (m, 4H), 1.46 – 1.38 (m, 2H). ^{13}C NMR (126 MHz, DMSO) δ 172.76, 169.94, 166.83, 165.30, 159.44, 155.99, 154.21, 139.99, 139.82, 136.99, 133.97, 133.22, 132.67, 129.44, 128.83, 128.44, 127.60, 126.98, 126.25, 125.63, 124.82, 124.68, 119.75, 116.20, 115.10, 113.69, 104.70, 68.74, 48.72, 38.84, 35.81, 35.76, 30.94, 30.76, 28.86, 28.33, 26.10, 25.03, 21.98. MS (ESI): m/z calc. for [M+H$^+$]$^+$ = 834.32, found = 834.35

4-(4-((4-amino-[1,1'-biphenyl]-3-yl)carbamoyl)phenyl)-*N*-(2-(2-(2-((2-(2,6-dioxopiperidin-3-yl)-1,3-dioxoisoindolin-4-yl)oxy)ethoxy)ethoxy)ethyl)-6-methyl-7-oxo-6,7-dihydro-1*H*-pyrrolo[2,3-c]pyridine-2-carboxamide (161b)
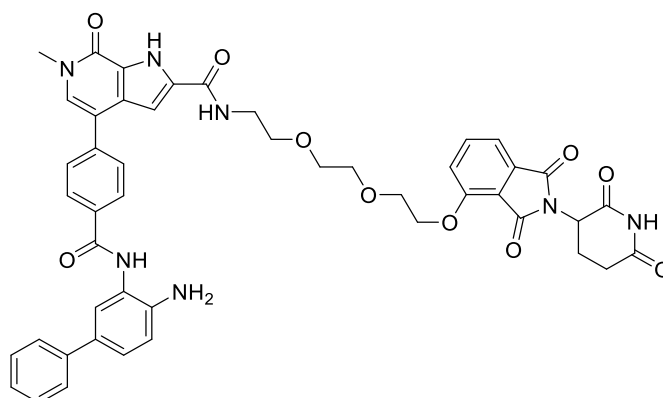
4-(2-(2-(2-aminoethoxy)ethoxy)ethoxy)-2-(2,6-dioxopiperidin-3-yl)isoindoline-1,3-dione (**154b**, 35 mg, 86 μmol) and compound **160** (50 mg, 86 μmol) were reacted according to "general procedure for amide coupling". The residue was then dissolved in DCM/TFA (2 mL, 3/1) and stirred at ambient temperature for 1 h. Afterwards, all volatiles were removed under reduced pressure and the residue was purified by prep HPLC (C18 silica, H$_2$O/ACN with 0.1% TFA) to provide the title compound as an off-white solid (52 mg, 70%). 1H NMR (500 MHz, DMSO-d6) δ 12.62 – 12.41 (m, 1H), 11.08 (s, 1H), 10.14 (s, 1H), 8.54 (t, J = 5.6 Hz, 1H), 8.15 (d, J = 8.1 Hz, 2H), 7.81 – 7.75 (m, 3H), 7.69 – 7.57 (m, 4H), 7.49 (dd, J = 8.3, 2.1 Hz, 1H), 7.48 – 7.40 (m, 4H), 7.32 (t, J = 7.4 Hz, 1H), 7.18 – 7.11 (m, 2H), 5.06 (dd, J = 12.8, 5.5 Hz, 1H), 4.29 (t, J = 4.5 Hz, 2H), 3.80 (t, J = 4.5 Hz, 2H), 3.67 (dd, J = 5.9, 3.5 Hz, 2H), 3.62 (s, 3H), 3.57 (dt, J = 13.7, 5.4 Hz, 4H), 3.43 (q, J = 5.6 Hz, 2H), 2.66 – 2.51 (m, 2H), 2.00 (ddt, J = 13.0, 5.8, 3.4 Hz, 1H), 1.86 – 1.81 (m, 1H). ^{13}C NMR (126 MHz, DMSO) δ 172.74, 169.90, 166.77, 165.34, 165.23, 159.59, 155.77, 154.21, 140.01, 139.50, 136.88, 133.76, 133.19, 132.31, 129.50, 128.92, 128.50, 127.50, 126.98, 126.83, 125.95, 124.83, 124.77, 119.90, 116.71, 116.27, 115.33, 114.40, 113.60, 104.98, 70.07, 69.71, 68.91, 68.82, 68.68, 48.74, 44.88, 35.80, 30.93, 23.61, 21.96. MS (ESI): m/z calc. for [M+H$^+$]$^+$ = 866.31, found = 866.35

4-(4-((4-amino-[1,1'-biphenyl]-3-yl)carbamoyl)phenyl)-*N*-(2-(2-(2-((2-(2,6-dioxopiperidin-3-yl)-1,3-dioxoisoindolin-4-yl)oxy)acetamido)ethoxy)ethoxy)ethyl)-6-methyl-7-oxo-6,7-dihydro-1*H*-pyrrolo[2,3-*c*]pyridine-2-carboxamide (161c)
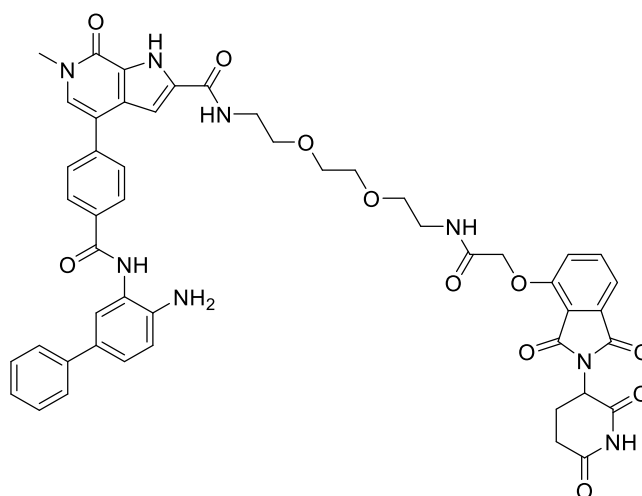
N-(2-(2-(2-aminoethoxy)ethoxy)ethyl)-2-((2-(2,6-dioxopiperidin-3-yl)-1,3-dioxoisoindolin-4-yl)oxy)acet-amide (32 mg 69 μmol) and compound **160** (40 mg, 69 μmol) were reacted according to "general procedure for amide coupling". The residue was then dissolved in DCM/TFA (2 mL, 3/1) and stirred at ambient temperature for 1 h. Afterwards, all volatiles were removed under reduced pressure and the residue was purified by prep HPLC (C18 silica, H_2O/ACN with 0.1% TFA) to provide the title compound as an off-white solid (43 mg, 67%). ^{1}H NMR (500 MHz, DMSO-d_6) δ 12.46 (d, *J* = 2.3 Hz, 1H), 11.10 (s, 1H), 9.98 (s, 1H), 8.53 (t, *J* = 5.5 Hz, 1H), 8.14 (d, *J* = 8.0 Hz, 2H), 7.98 (t, *J* = 5.7 Hz, 1H), 7.77 (dt, *J* = 8.6, 3.7 Hz, 3H), 7.63 – 7.58 (m, 4H), 7.46 (d, *J* = 7.3 Hz, 1H), 7.45 – 7.40 (m, 3H), 7.37 (d, *J* = 8.5 Hz, 1H), 7.32 – 7.27 (m, 1H), 7.13 (d, *J* = 2.3 Hz, 1H), 7.04 (d, *J* = 8.3 Hz, 1H), 5.10 (dd, *J* = 12.8, 5.5 Hz, 1H), 4.77 (s, 2H), 3.62 (s, 3H), 3.55 (dt, *J* = 8.6, 4.0 Hz, 6H), 3.45 (dt, *J* = 14.9, 5.7 Hz, 4H), 3.31 (q, *J* = 5.7 Hz, 2H), 2.89 (ddd, *J* = 16.9, 13.8, 5.4 Hz, 1H), 2.65 – 2.50 (m, 2H), 2.03 (dtd, *J* = 13.0, 5.2, 2.1 Hz, 1H). ^{13}C NMR (126 MHz, DMSO) δ 172.73, 169.84, 166.88, 166.69, 165.41, 165.23, 159.63, 154.92, 154.21, 139.88, 139.79, 136.85, 133.72, 132.98, 132.52, 129.47, 128.86, 128.45, 127.54, 126.98, 126.47, 125.75, 124.81, 124.78, 120.29, 116.72, 115.99, 113.64, 104.93, 69.60, 69.58, 68.95, 68.81, 67.49, 48.79, 38.38, 35.80, 30.92, 21.97, 1.12. MS (ESI): m/z calc. for [M+H^{+}][+] = 923.33, found = 923.35

3-(2-(2-(4-(4-((4-((tert-butoxycarbonyl)amino)-[1,1'-biphenyl]-3-yl)carbamoyl)phenyl)-6-methyl-7-oxo-6,7-dihydro-1*H*-pyrrolo[2,3-*c*]pyridine-2-carboxamido)ethoxy)ethoxy)propanoic acid (163a)
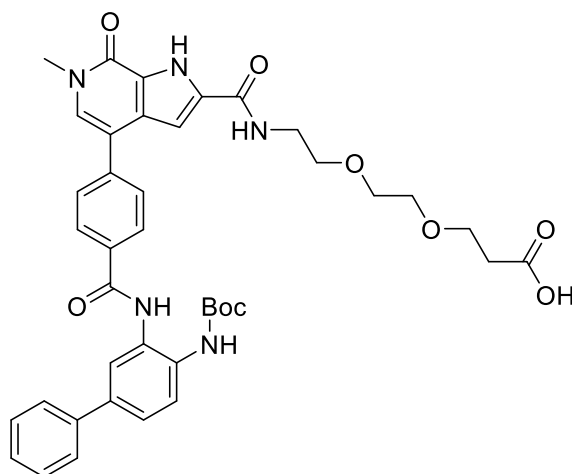
The reaction was performed according to "general procedure for amide coupling". Compound **160** (60 mg, 0.10 mmol) and *tert*-butyl 3-(2-(2-aminoethoxy)ethoxy)propanoate (**162a**, 29 mg, 0.12 mmol) were used. The mixture was partitioned between water and ethyl acetate and the organic phase was washed with brine, dried over MgSO₄ and volatiles were removed under reduced pressure to provide the intermediate *t*-Bu ester. The residue was dissolved in MeOH/H₂O/THF (8/3/3) and LiOH·H₂O (87 mg, 2.1 mmol) was added. After stirring at ambient temperature for 30 h, the mixture was chilled and the pH was brought to 4 through the addition of aq HCl (5%). The resulting precipitate was filtered and dried to provide an off-white solid (70 mg, 92%). ^{1}H NMR (500 MHz, DMSO-d_6) δ 12.48 (s, 1H), 12.14 (br s, 1H), 10.01 (s, 1H), 8.80 (s, 1H), 8.55 (t, *J* = 5.6 Hz, 1H), 8.11 (d, *J* = 8.1 Hz, 2H), 7.89 (d, *J* = 2.2 Hz, 1H), 7.80 (d, *J* = 8.1 Hz, 2H), 7.67 (t, *J* = 7.6 Hz, 3H), 7.61 (s, 1H), 7.54 (dd, *J* = 8.5, 2.2 Hz, 1H), 7.48 (t, *J* = 7.7 Hz, 2H), 7.37 (t, *J* = 7.3 Hz, 1H), 7.16 (d, *J* = 2.2 Hz, 1H), 3.63 (s, 3H), 3.60 (t, *J* = 6.4 Hz, 2H), 3.57 – 3.50 (m, 6H), 3.43 (q, *J* = 5.8 Hz, 2H), 2.42 (t, *J* = 6.3 Hz, 2H), 1.48 (s, 9H). ^{13}C NMR (126 MHz, DMSO) δ 172.60, 165.15, 159.64, 154.24, 153.42, 140.19, 139.33, 135.83, 133.78, 132.42, 131.24, 129.93, 128.98, 128.26, 127.55, 127.36, 127.16, 126.37, 126.33, 124.78, 124.17, 123.81, 113.57, 104.90, 79.80, 69.57, 69.53, 68.94, 66.23, 35.82, 34.70, 28.06. MS (ESI): m/z calc. for [M+Na^{+}]$^{+}$ = 760.30, found = 760.25

1-(4-(4-((4-((tert-butoxycarbonyl)amino)-[1,1'-biphenyl]-3-yl)carbamoyl)phenyl)-6-methyl-7-oxo-6,7-dihydro-1*H*-pyrrolo[2,3-*c*]pyridin-2-yl)-1-oxo-5,8,11-trioxa-2-azatetradecan-14-oic acid (163b)
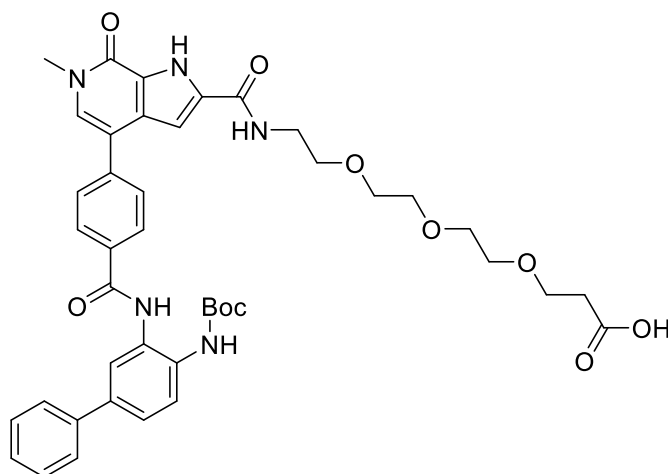
The reaction was performed according to "general procedure for amide coupling". Compound **160** (60 mg, 0.10 mmol) and tert-butyl 3-(2-(2-(2-aminoethoxy)ethoxy)ethoxy)propanoate (**162b**, 35 mg, 0.12 mmol) were used. The mixture was partitioned between water and ethyl acetate and the organic phase was washed with brine, dried over $MgSO_4$ and volatiles were removed under reduced pressure to provide the intermediate *t*-Bu ester. The residue was dissolved in MeOH/H_2O/THF (8/3/3) and LiOH·H_2O (87 mg, 2.1 mmol) was added. After stirring at ambient temperature for 20 h, the mixture was chilled and the pH was brought to 4 through the addition of aq HCl (5%). The resulting precipitate was filtered and dried to provide an off-white solid (44 mg, 54%). ^{1}H NMR (500 MHz, DMSO-d_6) δ 12.48 (s, 1H), 12.13 (s, 1H), 9.99 (s, 1H), 8.79 (s, 1H), 8.54 (t, *J* = 5.5 Hz, 1H), 8.11 (d, *J* = 8.0 Hz, 2H), 7.89 (d, *J* = 2.2 Hz, 1H), 7.80 (d, *J* = 8.0 Hz, 2H), 7.67 (t, *J* = 7.4 Hz, 3H), 7.60 (s, 1H), 7.54 (dd, *J* = 8.5, 2.2 Hz, 1H), 7.48 (t, *J* = 7.6 Hz, 2H), 7.37 (t, *J* = 7.4 Hz, 1H), 7.15 (d, *J* = 2.2 Hz, 1H), 3.63 (s, 3H), 3.59 − 3.52 (m, 8H), 3.52 − 3.40 (m, 6H), 2.41 (t, *J* = 6.3 Hz, 2H), 1.48 (s, 9H). ^{13}C NMR (126 MHz, DMSO) δ 172.59, 165.15, 159.63, 154.23, 153.42, 145.25, 140.19, 139.32, 135.83, 133.78, 132.42, 131.23, 129.91, 129.58, 128.98, 128.25, 127.54, 127.35, 127.16, 126.37, 124.77, 124.16, 123.82, 119.44, 113.56, 104.90, 79.80, 69.70, 69.62, 69.59, 68.92, 66.19, 35.83, 34.70, 30.29, 28.06, 25.50, 24.03, 22.63. MS (ESI): m/z calc. for $[M+H^+]^+$ = 782.33, found = 782.30

9-(4-(4-((4-((tert-butoxycarbonyl)amino)-[1,1'-biphenyl]-3-yl)carbamoyl)phenyl)-6-methyl-7-oxo-6,7-dihydro-1*H*-pyrrolo[2,3-*c*]pyridine-2-carboxamido)nonanoic acid (163c)
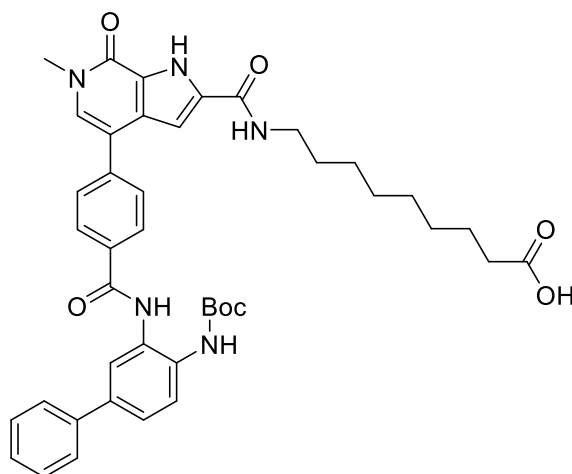
The reaction was performed according to "general procedure for amide coupling". Compound **160** (60 mg, 0.10 mmol) and tert-butyl 9-aminononanoate (**162c**, 29 mg, 0.12 mmol) were used. The mixture was partitioned between water and ethyl acetate and the organic phase was washed with brine, dried over MgSO$_4$ and volatiles were removed under reduced pressure to provide the intermediate *t*-Bu ester. The residue was dissolved in MeOH/H$_2$O/THF (8/3/3) and LiOH·H$_2$O (87 mg, 2.1 mmol) was added. After stirring at ambient temperature for 5 d, the mixture was chilled and the pH was brought to 4 through the addition of aq HCl (5%). The resulting precipitate was filtered and dried to provide an off-white solid (44 mg, 58%). ^{1}H NMR (500 MHz, DMSO-d_6) δ 12.42 (s, 1H), 9.99 (s, 1H), 8.80 (s, 1H), 8.38 (t, *J* = 5.5 Hz, 1H), 8.11 (d, *J* = 8.2 Hz, 2H), 7.89 (d, *J* = 2.2 Hz, 1H), 7.83 – 7.77 (m, 2H), 7.70 – 7.65 (m, 3H), 7.60 (s, 1H), 7.54 (dd, *J* = 8.5, 2.2 Hz, 1H), 7.48 (t, *J* = 7.7 Hz, 2H), 7.39 – 7.34 (m, 1H), 7.12 (d, *J* = 2.3 Hz, 1H), 3.63 (s, 3H), 3.26 (q, *J* = 6.7 Hz, 2H), 2.18 (t, *J* = 7.3 Hz, 2H), 1.48 (s, 9H), 1.34 – 1.21 (m, 12H). ^{13}C NMR (126 MHz, DMSO) δ 174.47, 165.14, 159.40, 154.23, 153.42, 145.25, 140.21, 139.32, 135.84, 134.01, 132.42, 131.22, 129.92, 129.54, 128.98, 128.25, 127.57, 127.35, 127.17, 126.37, 124.67, 124.15, 119.44, 113.58, 104.66, 79.80, 35.81, 33.63, 28.93, 28.69, 28.63, 28.52, 28.05, 26.43, 24.47, 24.03. MS (ESI): m/z calc. for [M+Na$^+$]$^+$ = 756.34, found = 756.30

4-(4-((4-amino-[1,1'-biphenyl]-3-yl)carbamoyl)phenyl)-N-(2-(2-(3-(((S)-1-((2S,4R)-4-hydroxy-2-((4-(4-methylthiazol-5-yl)benzyl)carbamoyl)pyrrolidin-1-yl)-3,3-dimethyl-1-oxobutan-2-yl)amino)-3-oxopropoxy)ethoxy)ethyl)-6-methyl-7-oxo-6,7-dihydro-1H-pyrrolo[2,3-c]pyridine-2-carboxamide (164a)
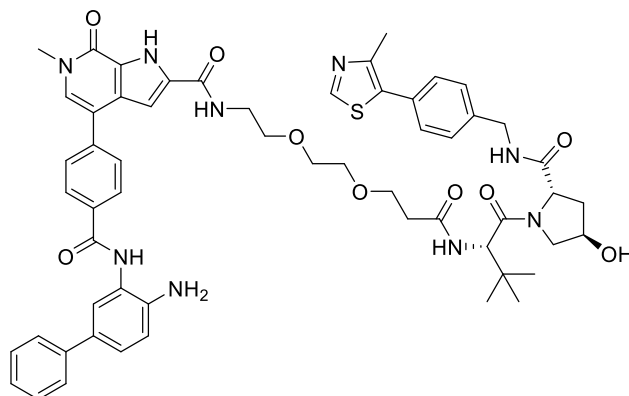
The reaction was performed according to "general procedure for amide coupling". Compound **163a** (60 mg, 81 µmol) and VHL ligand 1 (hydrochloride) (38 mg, 81 µmol) were used. MS (ESI): m/z calc. for [(M+2H$^+$)/2]$^+$ = 575.75, found = 575.90

The residue was then dissolved in DCM/TFA (2 mL, 3/1) and stirred at ambient temperature for 1 h. Afterwards, all volatiles were removed under reduced pressure and the residue was purified by prep HPLC (C18 silica, H$_2$O/ACN with 0.1% TFA) to provide the title compound as an off-white solid (46 mg, 54%). ^{1}H NMR (500 MHz, DMSO-d_6) δ 12.48 (d, J = 2.3 Hz, 1H), 10.14 (s, 1H), 8.98 (s, 1H), 8.56 (td, J = 5.8, 3.0 Hz, 2H), 8.21 − 8.08 (m, 2H), 8.02 − 7.88 (m, 2H), 7.79 (d, J = 8.3 Hz, 2H), 7.70 − 7.58 (m, 4H), 7.50 (dd, J = 8.4, 2.2 Hz, 1H), 7.47 − 7.42 (m, 2H), 7.42 − 7.35 (m, 4H), 7.32 (td, J = 7.2, 1.2 Hz, 1H), 7.17 − 7.13 (m, 2H), 4.55 (d, J = 9.4 Hz, 1H), 4.46 − 4.40 (m, 2H), 4.35 (dp, J = 4.5, 2.5 Hz, 1H), 4.21 (dd, J = 15.8, 5.4 Hz, 1H), 3.71 − 3.55 (m, 7H), 3.57 − 3.49 (m, 6H), 3.43 (q, J = 5.6 Hz, 2H), 2.57 − 2.52 (m, 1H), 2.43 (s, 3H), 2.35 (dt, J = 14.5, 6.1 Hz, 1H), 2.06 − 2.00 (m, 1H), 1.90 (ddd, J = 12.9, 8.6, 4.7 Hz, 1H), 0.92 (s, 9H). ^{13}C NMR (126 MHz, DMSO) δ 171.91, 169.94, 169.54, 165.38, 159.65, 154.24, 151.46, 147.64, 140.04, 139.48, 133.77, 132.31, 131.18, 129.60, 129.53, 129.13, 128.94, 128.61, 128.52, 127.56, 127.41, 127.19, 127.01, 126.87, 125.98, 124.87, 124.84, 124.80, 116.72, 114.41, 113.65, 104.98, 69.59, 69.49, 68.98, 68.87, 66.96, 58.71, 56.37, 56.30, 41.66, 37.93, 35.83, 35.65, 35.36, 26.30, 15.90. MS (ESI): m/z calc. for [M+H$^+$]$^+$ = 1050.45, found = 1050.45

4-(4-((4-amino-[1,1'-biphenyl]-3-yl)carbamoyl)phenyl)-N-((S)-14-((2S,4R)-4-hydroxy-2-((4-(4-methylthiazol-5-yl)benzyl)carbamoyl)pyrrolidine-1-carbonyl)-15,15-dimethyl-12-oxo-3,6,9-trioxa-13-azahexadecyl)-6-methyl-7-oxo-6,7-dihydro-1H-pyrrolo[2,3-c]pyridine-2-carboxamide (164b)
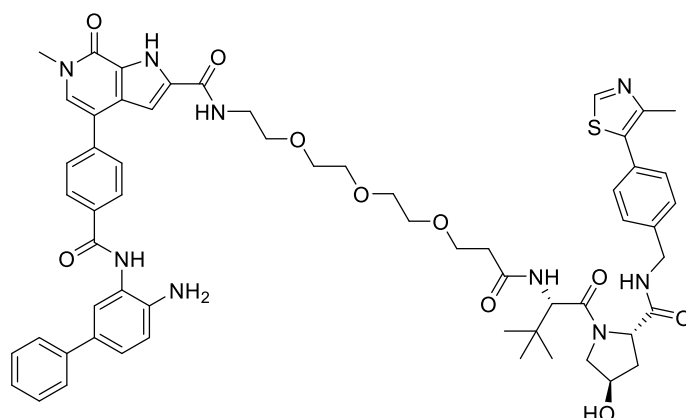
The reaction was performed according to "general procedure for amide coupling". Compound **163b** (40 mg, 51 μmol) and VHL ligand 1 (hydrochloride) (24 mg, 51 μmol) were used. MS (ESI): m/z calc. for $[(M+2H^+)/2]^+ = 597.77$, found = 597.95

The residue was then dissolved in DCM/TFA (2 mL, 3/1) and stirred at ambient temperature for 1 h. Afterwards, all volatiles were removed under reduced pressure and the residue was purified by prep HPLC (C18 silica, H_2O/ACN with 0.1% TFA) to provide the title compound as an off-white solid (38 mg, 68%). ^{1}H NMR (500 MHz, DMSO-d_6) δ 12.64 – 12.34 (m, 1H), 10.19 (s, 1H), 8.98 (s, 1H), 8.60 – 8.50 (m, 2H), 8.16 (d, J = 8.2 Hz, 2H), 7.90 (d, J = 9.3 Hz, 1H), 7.79 (d, J = 8.5 Hz, 2H), 7.69 (d, J = 2.1 Hz, 1H), 7.66 – 7.62 (m, 2H), 7.60 (s, 1H), 7.52 (dd, J = 8.3, 2.2 Hz, 1H), 7.45 (t, J = 7.8 Hz, 2H), 7.41 (d, J = 8.2 Hz, 2H), 7.37 (d, J = 8.3 Hz, 2H), 7.35 – 7.31 (m, 1H), 7.20 (d, J = 8.4 Hz, 1H), 7.15 (d, J = 2.2 Hz, 1H), 4.55 (d, J = 9.4 Hz, 1H), 4.46 – 4.39 (m, 2H), 4.35 (dt, J = 4.5, 2.1 Hz, 1H), 4.21 (dd, J = 15.8, 5.5 Hz, 1H), 3.69 – 3.64 (m, 1H), 3.63 (s, 3H), 3.54 (td, J = 5.8, 2.4 Hz, 6H), 3.50 – 3.48 (m, 2H), 3.47 – 3.43 (m, 3H), 3.02 (td, J = 6.6, 3.8 Hz, 3H), 2.55 (t, J = 5.5 Hz, 1H), 2.43 (s, 3H), 2.34 (dt, J = 14.7, 5.8 Hz, 1H), 2.08 – 2.00 (m, 1H), 1.90 (ddd, J = 12.9, 8.5, 4.6 Hz, 1H), 1.76 – 1.71 (m, 2H), 0.92 (s, 9H). ^{13}C NMR (126 MHz, DMSO) δ 172.38, 170.40, 170.02, 165.90, 160.12, 154.73, 151.94, 148.11, 140.57, 139.97, 139.85, 134.26, 132.72, 131.67, 130.08, 130.03, 129.44, 129.09, 129.02, 128.03, 127.90, 127.50, 127.48, 126.52, 125.36, 125.32, 125.28, 117.11, 114.80, 114.11, 105.47, 70.22, 70.19, 70.11, 69.94, 69.40, 69.35, 67.40, 59.19, 56.84, 56.77, 42.14, 38.41, 36.31, 36.13, 35.83, 34.83, 26.78, 16.36. MS (ESI): m/z calc. for $[M+H^+]^+ = 1094.47$, found = 1094.50

4-(4-((4-amino-[1,1'-biphenyl]-3-yl)carbamoyl)phenyl)-N-(9-(((S)-1-((2S,4R)-4-hydroxy-2-((4-(4-methylthiazol-5-yl)benzyl)carbamoyl)pyrrolidin-1-yl)-3,3-dimethyl-1-oxobutan-2-yl)amino)-9-oxononyl)-6-methyl-7-oxo-6,7-dihydro-1H-pyrrolo[2,3-c]pyridine-2-carboxamide (164c)
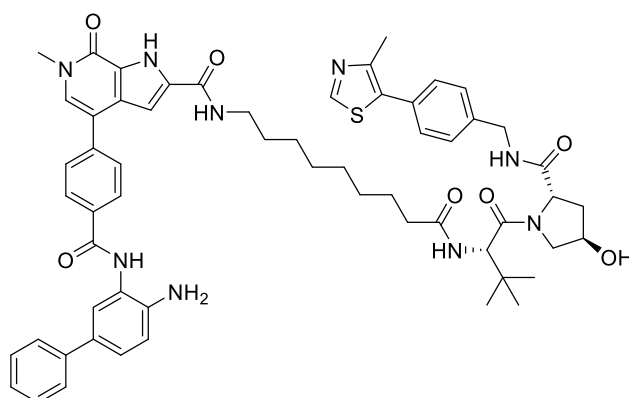
The reaction was performed according to "general procedure for amide coupling". Compound **163c** (40 mg, 55 µmol) and VHL ligand 1 (hydrochloride) (25 mg, 55 µmol) were used. MS (ESI): m/z calc. for [(M+2H$^+$)/2]$^+$ = 597.77, found = 597.95

The residue was then dissolved in DCM/TFA (2 mL, 3/1) and stirred at ambient temperature for 1 h. Afterwards, all volatiles were removed under reduced pressure and the residue was purified by prep HPLC (C18 silica, H$_2$O/ACN with 0.1% TFA) to provide the title compound as an off-white solid (40 mg, 71%). ^{1}H NMR (500 MHz, DMSO-d_6) δ 12.41 (d, J = 2.1 Hz, 1H), 10.14 (s, 1H), 8.98 (s, 1H), 8.54 (t, J = 6.1 Hz, 1H), 8.40 (t, J = 5.5 Hz, 1H), 8.18 – 8.14 (m, 2H), 7.83 (d, J = 9.5 Hz, 1H), 7.80 – 7.77 (m, 2H), 7.67 (d, J = 2.2 Hz, 1H), 7.65 – 7.61 (m, 2H), 7.60 (s, 1H), 7.50 (dd, J = 8.3, 2.2 Hz, 1H), 7.45 (t, J = 7.8 Hz, 2H), 7.42 – 7.39 (m, 2H), 7.37 (d, J = 8.3 Hz, 2H), 7.32 (td, J = 7.1, 1.2 Hz, 1H), 7.22 (s, 1H), 7.16 (d, J = 8.3 Hz, 1H), 7.12 (d, J = 2.6 Hz, 2H), 7.01 (s, 1H), 4.54 (d, J = 9.4 Hz, 1H), 4.47 – 4.39 (m, 2H), 4.38 – 4.32 (m, 1H), 4.21 (dd, J = 15.9, 5.4 Hz, 1H), 3.67 – 3.63 (m, 3H), 3.62 (s, 3H), 3.26 (q, J = 6.5 Hz, 2H), 3.02 (td, J = 6.6, 3.9 Hz, 1H), 2.56 – 2.51 (m, 1H), 2.43 (s, 3H), 2.26 (dt, J = 14.8, 7.6 Hz, 1H), 2.15 – 2.09 (m, 1H), 2.06 – 2.00 (m, 1H), 1.90 (ddd, J = 12.9, 8.5, 4.6 Hz, 1H), 1.75 – 1.71 (m, 1H), 1.56 – 1.39 (m, 6H), 0.92 (s, 9H). ^{13}C NMR (126 MHz, DMSO) δ 172.06, 171.92, 169.72, 165.37, 159.41, 154.24, 151.45, 147.64, 140.05, 139.48, 133.99, 132.31, 131.18, 129.60, 128.93, 128.62, 128.60, 128.52, 127.58, 127.41, 127.02, 126.87, 125.97, 124.84, 124.69, 116.71, 114.40, 113.66, 104.73, 68.85, 58.68, 56.33, 56.26, 41.65, 38.86, 37.93, 35.82, 35.19, 34.82, 28.91, 28.64, 28.61, 28.59, 26.41, 26.34, 25.37, 15.89. MS (ESI): m/z calc. for [(M+2H$^+$)/2]$^+$ = 523.75, found = 523.85

Methyl (*S*)-2-(4-(4-chlorophenyl)-2,3,9-trimethyl-6*H*-thieno[3,2-*f*][1,2,4]triazolo[4,3-*a*][1,4]diazepin-6-yl)acetate (165)
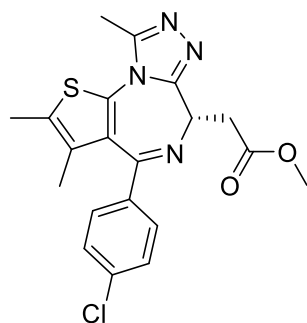
The synthesis was adapted from Nowak *et al.*[270] (+)-JQ1 (**7**, 9.90 g, 21.7 mmol, 1.0 eq) was dissolved in MeOH (100 mL) and conc. H_2SO_4 (3.1 mL, 58 mmol, 2.7 eq) and heated under reflux for 20 h. After cooling to ambient temperature, the mixture was neutralized with diluted aq NaOH and sat. aq $NaHCO_3$ and afterwards extracted with ethyl acetate. The combined organic layers were washed with brine, dried over $MgSO_4$ and volatiles were removed under reduced pressure to provide the title compound as a brown foam (7.88 g, 88%). ^1H NMR (400 MHz, DMSO-d_6) δ 7.49 (d, *J* = 8.4 Hz, 2H), 7.43 (d, *J* = 8.6 Hz, 2H), 4.50 (t, *J* = 7.2 Hz, 1H), 3.67 (s, 3H), 3.45 (dd, *J* = 12.9, 7.2 Hz, 2H), 2.60 (s, 3H), 2.42 (s, 3H), 1.63 (s, 3H). MS (ESI): m/z calc. for [M+H$^+$]$^+$ = 415.09, found = 415.10

methyl (*S*)-2-(2-(acetoxymethyl)-4-(4-chlorophenyl)-3,9-dimethyl-6*H*-thieno[3,2-*f*][1,2,4]triazolo[4,3-*a*][1,4]diazepin-6-yl)acetate (166)
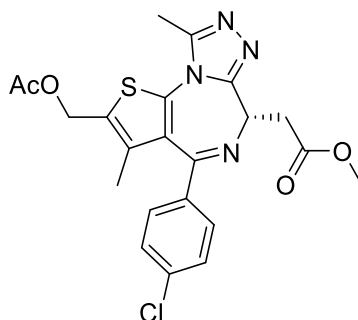
The synthesis was adapted from Nowak *et al.*[270] Compound **165** (7.70 g, 18.6 mmol, 1.0 eq) and Mn(OAc)$_3$·2H$_2$O (9.95 g, 371.1 mmol, 2.0 eq) were dissolved in a mixture of acetic acid (66 mL), acetic anhydride (38 mL) and conc. H_2SO_4 (10 mL) and the mixture was stirred at ambient temperature for 3 d. Additional Mn(OAc)$_3$·2H$_2$O (4.98 g, 18.6 mmol, 1.0 eq) and H_2SO_4 (5 mL) were added and the mixture was stirred at 50 °C for 3 d. Afterwards, the mixture was poured onto ice and brought to a pH of 5 with diluted aq NaOH. The mixture was extracted with ethyl acetate, the combined organic layers were washed with sat. aq $NaHCO_3$ and brine, dried over $MgSO_4$ and volatiles were removed under reduced pressure to provide the title compound as a brown foam (8.56 g, 98%). ^1H NMR (400 MHz, DMSO-d$_6$) δ 7.53 – 7.47 (m, 2H), 7.45 – 7.40 (m, 2H), 4.53 (dd, *J* = 7.8, 6.6 Hz, 1H), 3.67 (s, 3H), 3.45 (dd,

J = 11.9, 7.2 Hz, 2H), 2.65 – 2.59 (m, 3H), 2.21 – 2.04 (m, 3H), 1.91 (s, 2H), 1.76 (d, J = 18.9 Hz, 3H). MS (ESI): m/z calc. for [M+H$^+$]$^+$ = 473.10, found = 473.05

methyl (S)-2-(4-(4-chlorophenyl)-2-(hydroxymethyl)-3,9-dimethyl-6H-thieno[3,2-f][1,2,4]triazolo[4,3-a][1,4]diazepin-6-yl)acetate (167)
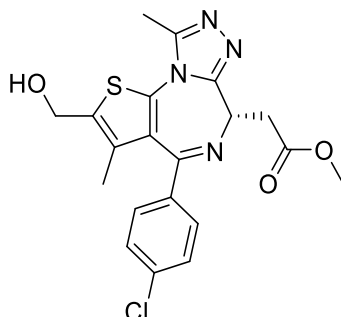
The synthesis was adapted from Nowak *et al.*[270] Compound **166** (8.45 g, 17.9 mmol, 1.0 eq) was dissolved in MeOH (160 mL) and K$_2$CO$_3$ was added. After stirring at ambient temperature for 2 h, the mixture was neutralized with 1N aq HCl and extracted with DCM and ethyl acetate. The combined organic layers were washed with brine, dried over MgSO$_4$ and volatiles were removed under reduced pressure to provide the title compound as a brown foam (7.77 g, quant.). MS (ESI): m/z calc. for [M+H$^+$]$^+$ = 431.09, found = 431.05

methyl (S)-2-(4-(4-chlorophenyl)-2-formyl-3,9-dimethyl-6H-thieno[3,2-f][1,2,4]triazolo[4,3-a][1,4]-diazepin-6-yl)acetate (168)
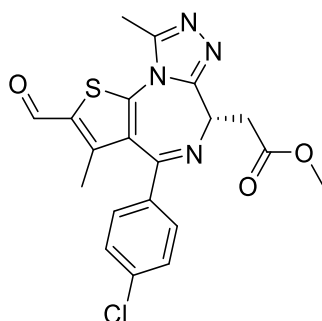
The synthesis was adapted from Nowak *et al.*[270] Compound **167** (7.70 g, 17.9 mmol, 1.0 eq) was dissolved in DCM (180 mL) and cooled to 0 °C. Dess–Martin periodinane (8.34 g, 19.7 mmol, 1.1 eq) was added and the mixture was stirred at ambient temperature for 2 h. The mixture was diluted with additional DCM was washed with sat. aq NaHCO$_3$ and brine, dried over MgSO$_4$ and volatiles were removed under reduced pressure to provide the crude compound as a brown foam (10.24 g (75% purity), quant yield assumed). ^{1}H NMR (400 MHz, DMSO-d_6) δ 10.14 (s, 1H), 7.57 – 7.45 (m, 4H), 4.64 (dd, J = 7.7, 6.7 Hz, 1H), 3.67 (s, 3H), 3.46 (dd, J = 12.2, 7.2 Hz, 2H), 2.67 (s, 3H), 2.10 (s, 3H). MS (ESI): m/z calc. for [M+H$^+$]$^+$ = 429.07, found = 429.05

(S)-4-(4-chlorophenyl)-6-(2-methoxy-2-oxoethyl)-3,9-dimethyl-6H-thieno[3,2-f][1,2,4]triazolo[4,3-a][1,4]diazepine-2-carboxylic acid (169)
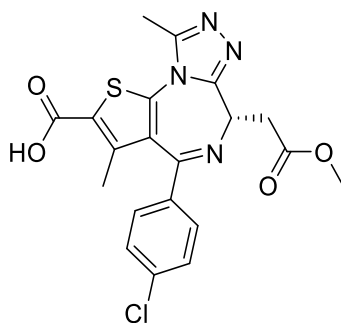
The synthesis was adapted from Nowak *et al.*[270] Compound **168** (10.24 g, 75% purity, 17.9 mmol, 1.0 eq) was dissolved in ACN (70 mL), cooled to 0 °C and a solution of $NaHPO_4$ (2.14 g, 17.9 mmol, 1.0 eq) in water (30 mL) and H_2O_2 (30% in water, 9.12 mL, 89.3 mmol, 5.0 eq) were added. Afterwards, a solution of $NaClO_2$ (2.26 g, 25.0 mmol, 1.4 eq) was added dropwise and the mixture was stirred at ambient temperature for 30 min. To the mixture was added ice and sat. aq Na_2SO_3 and the pH was brought to 4 through the addition of diluted aq HCl. The precipitate was filtrated, and the crude product was afterwards purified by flash chromatography (silica, DCM/MeOH) to provide the title compound as a yellowish solid (6.03 g, 76%). MS (ESI): m/z calc. for $[M+H^+]^+$ = 445.07, found = 445.05

isopropyl (S)-4-(4-chlorophenyl)-6-(2-methoxy-2-oxoethyl)-3,9-dimethyl-6H-thieno[3,2-f][1,2,4]-triazolo[4,3-a][1,4]diazepine-2-carboxylate (171)
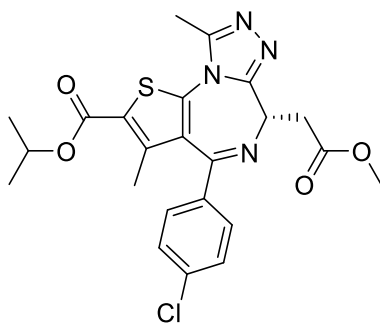
Compound **169** (3.30 g, 7.42 mmol, 1.0 eq) and DMAP (227 mg, 1.85 mmol, 0.25 eq) were dissolved in DMF/*i*PrOH (1/1, 40 mL). PyAOP (4.64 g, 8.90 mmol, 1.2 eq) and DIPEA (1.55 mL, 8.90 mmol, 1.2 eq) were added and the solution was stirred at ambient temperature for 16 h. Afterwards, the mixture was partitioned between water and ethyl acetate, the organic phase was washed with brine, dried over $MgSO_4$ and volatiles were removed under reduced pressure to provide the crude product which was used without further purification. MS (ESI): m/z calc. for $[M+H^+]^+$ = 487.11, found = 487.10

(*S*)-2-(4-(4-chlorophenyl)-2-(isopropoxycarbonyl)-3,9-dimethyl-6*H*-thieno[3,2-*f*][1,2,4]triazolo[4,3-*a*][1,4]diazepin-6-yl)acetic acid (172)
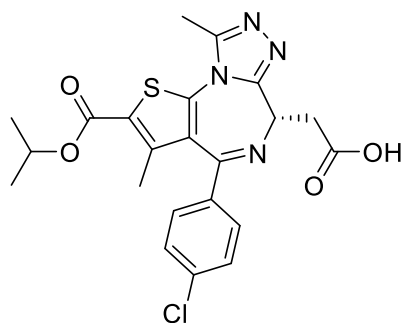
The procedure was adapted from Nicolaou *et al.*[311] Compound **171** (3.61 g, 7.41 mmol, 1.0 eq) and trimethyltin hydroxide (9.83 g, 51.9 mmol, 7.0 eq) were dissolved in DCE (60 mL) and heated at 80 °C for 5 d. Afterwards, water was added and the aqueous phase was brought to a pH of 5 through addition of diluted aq HCl and extracted with DCM. The combined organic phases were washed with brine, dried over $MgSO_4$ and volatiles were removed under reduced pressure. The crude product was afterwards purified by flash chromatography (silica, DCM/MeOH) to provide the title compound as an off-white solid (1.68 g, 48%). ^{1}H NMR (400 MHz, DMSO-d_6) δ 12.49 (s, 1H), 7.54 – 7.44 (m, 4H), 5.15 (hept, *J* = 6.2 Hz, 1H), 4.57 (t, *J* = 7.1 Hz, 1H), 3.44 (ddd, *J* = 16.7, 6.8, 4.7 Hz, 1H), 3.32 (ddd, *J* = 16.7, 7.4, 6.2 Hz, 1H), 2.67 (s, 3H), 2.02 (s, 3H), 1.32 (t, *J* = 5.9 Hz, 6H). MS (ESI): m/z calc. for [M+H$^+$]$^+$ = 473.10, found = 473.05

isopropyl (*S*)-6-(2-((4-((2-((tert-butoxycarbonyl)amino)phenyl)carbamoyl)phenyl)amino)-2-oxoethyl)-4-(4-chlorophenyl)-3,9-dimethyl-6*H*-thieno[3,2-*f*][1,2,4]triazolo[4,3-*a*][1,4]diazepine-2-carboxylate (173)
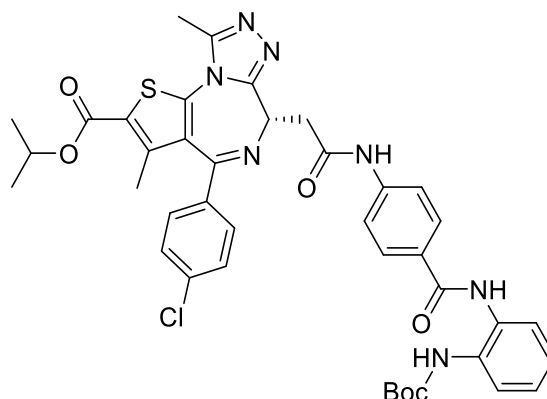
Compound **172** (497 mg, 1.05 mmol, 1.0 eq) and Compound **34** (344 mg, 1.05 mmol, 1.0 eq) were dissolved in ACN (15 mL) and pyridine (1.5 mL). T3P (50% in ethyl acetate, 1.25 mL, 2.10 mmol, 2.0 eq) was added and the mixture was stirred at ambient temperature for 2 h. Afterwards, the mixture was partitioned between water and DCM, the organic phase was washed with aq HCl (1%) and brine, dried over MgSO$_4$ and volatiles were removed under reduced pressure to provide the product which was used without further purification (744 mg, 91%). ^{1}H NMR (400 MHz, DMSO-d_6) δ 10.63 (s, 1H), 9.77 (s, 1H), 8.67 (s, 1H), 7.95 (d, *J* = 8.8 Hz, 2H), 7.79 (d, *J* = 8.8 Hz, 2H), 7.54 (ddd, *J* = 11.1, 7.9, 2.0 Hz, 2H), 7.51 − 7.43 (m, 4H), 7.17 (dtd, *J* = 17.0, 7.4, 1.7 Hz, 2H), 5.16 (hept, *J* = 6.2 Hz, 1H), 4.74 (t, *J* = 7.1 Hz, 1H), 3.59 (d, *J* = 6.9 Hz, 2H), 2.68 (s, 3H), 2.04 (s, 3H), 1.45 (s, 9H), 1.33 (dd, *J* = 6.3, 4.6 Hz, 6H). MS (ESI): m/z calc. for [M+H$^+$]$^+$ = 782.24, found = 782.25

(S)-6-(2-((4-((2-((tert-butoxycarbonyl)amino)phenyl)carbamoyl)phenyl)amino)-2-oxoethyl)-4-(4-chlorophenyl)-3,9-dimethyl-6H-thieno[3,2-f][1,2,4]triazolo[4,3-a][1,4]diazepine-2-carboxylic acid (174)
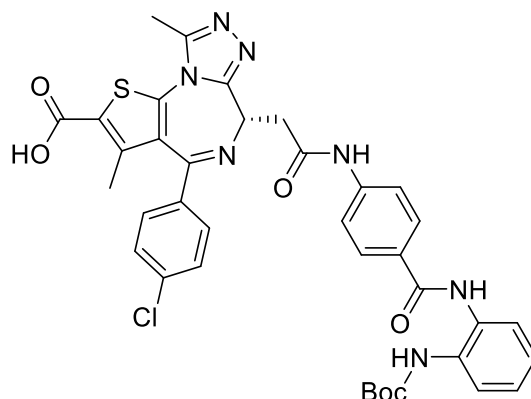
Compound **173** (1.74 g, 2.23 mmol, 1.0 eq) and LiOH·H$_2$O (468 mg, 11.2 mmol, 5.0 eq) were dissolved in MeOH/water (2/1, 30 mL) and stirred at ambient temperature for 3 h. The residue was diluted with water and brought to a pH of 6 with diluted aq HCl. The resulting precipitate was filtered, dissolved in MeOH and dried under reduced pressure. The residue was purified by flash chromatography (silica, DCM/MeOH) to provide the title compound as a brownish solid (1.00 g, 61%). ^{1}H NMR (400 MHz, DMSO-d_6) δ 10.66 (s, 1H), 9.82 (s, 1H), 8.69 (s, 1H), 7.95 (d, J = 8.9 Hz, 2H), 7.80 (d, J = 8.9 Hz, 2H), 7.54 (ddd, J = 9.2, 7.8, 1.8 Hz, 2H), 7.46 (q, J = 8.8 Hz, 4H), 7.24 − 7.11 (m, 2H), 4.69 (t, J = 7.1 Hz, 1H), 3.57 (d, J = 7.2 Hz, 2H), 2.65 (s, 3H), 2.02 (s, 3H), 1.45 (s, 9H). MS (ESI): m/z calc. for [M+H$^+$]$^+$ = 740.20, found = 740.25

(6*S*)-6-(2-((4-((2-aminophenyl)carbamoyl)phenyl)amino)-2-oxoethyl)-4-(4-chlorophenyl)-*N*-(2-(2-((2-(2,6-dioxopiperidin-3-yl)-1,3-dioxoisoindolin-4-yl)oxy)-ethoxy)ethyl)-3,9-dimethyl-6*H*-thieno[3,2-*f*][1,2,4]triazolo[4,3-*a*][1,4]diazepine-2-carboxamide (175a)
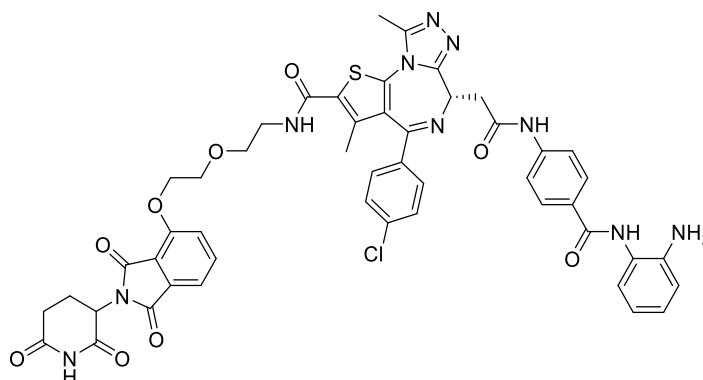
Compound **174** (50 mg, 68 µmol) and compound **154a** (26 mg, 71 µmol) were reacted according to "general procedure for amide coupling". The crude product was purified by flash chromatography (silica, DCM/MeOH) to provide the *Boc*-protected intermediate (66 mg, 93%). MS (ESI): m/z calc. for $[M+H^+]^+$ = 1082.3, found = 1083.3

The intermediate was then dissolved in DCM/TFA (4 mL, 3/1) and stirred at ambient temperature for 1 h. Afterwards, all volatiles were removed under reduced pressure and the residue was purified by flash chromatography (C18 silica, H_2O/ACN) to provide the title compound as an off-white solid (5 mg, 9%). ^{1}H NMR (500 MHz, DMSO-d_6) δ 11.08 (s, 1H), 10.59 (s, 1H), 9.57 (s, 1H), 8.32 (td, *J* = 5.6, 2.7 Hz, 1H), 7.97 (d, *J* = 8.7 Hz, 2H), 7.77 (dd, *J* = 16.4, 8.3 Hz, 3H), 7.52 (d, *J* = 8.6 Hz, 1H), 7.48 (d, *J* = 8.8 Hz, 2H), 7.45 (s, 2H), 7.44 − 7.41 (m, 1H), 7.16 (d, *J* = 7.0 Hz, 1H), 6.99 − 6.94 (m, 1H), 6.78 (dd, *J* = 8.0, 1.3 Hz, 1H), 6.60 (td, *J* = 7.6, 1.3 Hz, 1H), 5.07 (ddd, *J* = 12.8, 5.5, 1.9 Hz, 1H), 4.87 (s, 2H), 4.69 (t, *J* = 6.9 Hz, 1H), 4.37 − 4.32 (m, 2H), 3.85 − 3.81 (m, 2H), 3.67 (t, *J* = 5.8 Hz, 2H), 3.58 (d, *J* = 7.1 Hz, 2H), 3.45 (tdd, *J* = 13.7, 7.9, 5.8 Hz, 2H), 2.92 − 2.83 (m, 1H), 2.63 (d, *J* = 0.4 Hz, 3H), 2.61 − 2.55 (m, 1H), 2.01 (dd, *J* = 7.3, 5.5 Hz, 1H), 1.89 (d, *J* = 1.6 Hz, 3H). ^{13}C NMR {^{1}H} (126 MHz, DMSO-d_6) δ 172.75, 169.90, 169.03, 166.78, 165.28, 164.70, 162.90, 161.18, 155.81, 155.02, 150.28, 143.13, 141.91, 136.95, 136.64, 136.60, 135.53, 135.39, 133.19, 130.16, 130.10, 130.04, 128.98, 128.75, 128.52, 126.65, 126.37, 123.48, 120.03, 118.19, 116.31, 116.28, 116.14, 115.39, 68.99, 68.85, 68.45, 48.74, 30.94, 21.99, 16.09, 11.35. HRMS (MALDI): m/z calc. for $[M+Na^+]^+$ = 1005.2516, found = 1005.2515

(6S)-6-(2-((4-((2-aminophenyl)carbamoyl)phenyl)amino)-2-oxoethyl)-4-(4-chlorophenyl)-*N*-(2-(2-(2-((2-(2,6-dioxopiperidin-3-yl)-1,3-dioxoisoindolin-4-yl)oxy)-ethoxy)ethoxy)ethyl)-3,9-dimethyl-6*H*-thieno[3,2-*f*][1,2,4]triazolo[4,3-*a*][1,4]diazepine-2-carboxamide (175b)
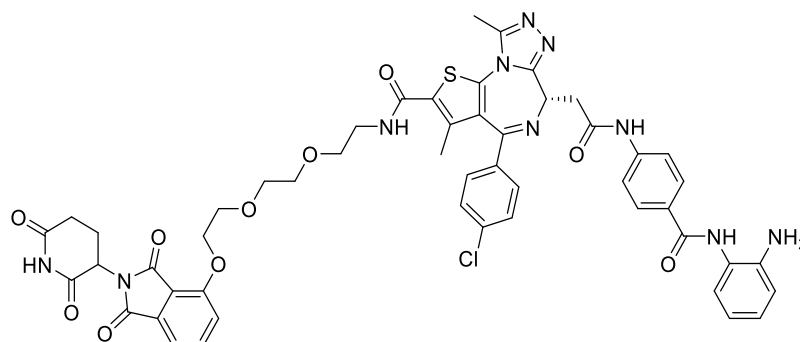
Compound **174** (50 mg, 68 μmol) and compound **154b** (29 mg, 71 μmol) were reacted according to "general procedure for amide coupling". The crude product was purified by flash chromatography (silica, DCM/MeOH) to provide the *Boc*-protected intermediate (42 mg, 55%). MS (ESI): m/z calc. for $[M+H^+(-Boc)]^+$ = 1027.51, found = 1028.10

The intermediate was then dissolved in DCM/TFA (4 mL, 3/1) and stirred at ambient temperature for 1 h. Afterwards, all volatiles were removed under reduced pressure and the residue was purified by flash chromatography (C18 silica, H_2O/ACN) to provide the title compound as an off-white solid (19 mg, 50%). ^{1}H NMR (500 MHz, DMSO-d_6) δ 11.09 (s, 1H), 10.59 (s, 1H), 9.57 (s, 1H), 8.31 (t, *J* = 5.6 Hz, 1H), 7.97 (d, *J* = 8.6 Hz, 2H), 7.79 (dd, *J* = 8.3, 7.5 Hz, 1H), 7.76 (d, *J* = 8.7 Hz, 2H), 7.53 − 7.48 (m, 2H), 7.48 − 7.43 (m, 6H), 7.17 (d, *J* = 7.5 Hz, 1H), 7.00 − 6.94 (m, 1H), 6.78 (dd, *J* = 8.0, 1.2 Hz, 1H), 6.60 (td, *J* = 7.6, 1.3 Hz, 1H), 5.07 (dd, *J* = 12.8, 5.5 Hz, 1H), 4.88 (s, 2H), 4.69 (t, *J* = 7.1 Hz, 1H), 4.34 − 4.30 (m, 2H), 3.82 − 3.77 (m, 2H), 3.68 − 3.65 (m, 2H), 3.58 − 3.52 (m, 6H), 3.48 − 3.35 (m, 2H), 2.88 (ddd, *J* = 17.0, 13.9, 5.4 Hz, 1H), 2.64 (s, 3H), 2.61 − 2.54 (m, 1H), 2.54 − 2.51 (m, 1H), 2.02 (ddd, *J* = 10.3, 5.3, 3.0 Hz, 2H), 1.92 (s, 3H). ^{13}C NMR {^{1}H} (126 MHz, DMSO-d_6) δ 172.76, 169.91, 169.02, 166.79, 165.27, 164.70, 162.90, 161.17, 155.80, 155.01, 150.29, 143.12, 141.91, 136.95, 136.66, 136.61, 135.50, 135.40, 133.24, 130.17, 130.12, 130.03, 128.97, 128.74, 128.52, 126.65, 126.36, 123.48, 119.98, 118.18, 116.32, 116.28, 116.14, 115.40, 70.13, 69.60, 68.86, 68.66, 54.89, 53.68, 48.75, 30.94, 21.98, 16.11, 11.37. HRMS (MALDI): m/z calc. for $[M+Na^+]^+$ = 1049.2778, found = 1049.2770

(6S)-6-(2-((4-((2-aminophenyl)carbamoyl)phenyl)amino)-2-oxoethyl)-4-(4-chlorophenyl)-N-(2-(2-(2-(2-((2-(2,6-dioxopiperidin-3-yl)-1,3-dioxoisoindolin-4-yl)oxy)-ethoxy)ethoxy)ethoxy)ethyl)-3,9-dimethyl-6H-thieno[3,2-f][1,2,4]triazolo[4,3-a][1,4]-diazepine-2-carboxamide (175c)
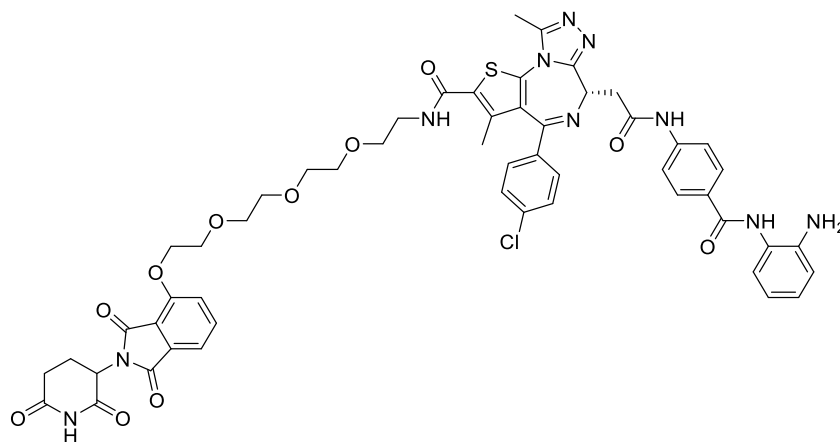
Compound **174** (50 mg, 68 µmol) and compound **154c** (32 mg, 71 µmol) were reacted according to "general procedure for amide coupling". The crude product was purified by flash chromatography (silica, DCM/MeOH) to provide the *Boc*-protected intermediate (44 mg, 56%). MS (ESI): m/z calc. for [M+H⁺]⁺ = 1171.40 , found = 1171.37

The intermediate was then dissolved in DCM/TFA (4 mL, 3/1) and stirred at ambient temperature for 1 h. Afterwards, all volatiles were removed under reduced pressure and the residue was purified by flash chromatography (C18 silica, H₂O/ACN) to provide the title compound as an off-white solid (28 mg, 70%). ¹H NMR (500 MHz, DMSO-d_6) δ 11.09 (s, 1H), 10.58 (s, 1H), 9.57 (s, 1H), 8.32 (t, *J* = 5.6 Hz, 1H), 7.97 (d, *J* = 8.7 Hz, 2H), 7.82 − 7.77 (m, 1H), 7.75 (d, *J* = 8.7 Hz, 2H), 7.54 − 7.49 (m, 2H), 7.46 (dd, *J* = 10.4, 7.6 Hz, 4H), 7.16 (d, *J* = 7.1 Hz, 1H), 6.97 (td, *J* = 8.0, 1.5 Hz, 1H), 6.78 (dd, *J* = 8.0, 1.3 Hz, 1H), 6.63 − 6.57 (m, 1H), 5.07 (dd, *J* = 12.8, 5.4 Hz, 1H), 4.89 (s, 0H), 4.69 (t, *J* = 7.1 Hz, 1H), 4.35 − 4.30 (m, 2H), 3.79 − 3.75 (m, 2H), 3.62 (dd, *J* = 5.9, 3.6 Hz, 2H), 3.57 (d, *J* = 7.0 Hz, 2H), 3.41 (dd, *J* = 12.5, 6.0 Hz, 2H), 3.17 (d, *J* = 5.2 Hz, 1H), 2.65 (s, 3H), 2.62 − 2.59 (m, 1H), 2.57 (t, *J* = 3.3 Hz, 1H), 2.54 − 2.52 (m, 1H), 2.06 − 1.99 (m, 1H), 1.93 (s, 3H). ¹³C NMR {¹H} (126 MHz, DMSO-d_6) δ 172.76, 169.90, 169.01, 166.79, 165.25, 164.70, 162.91, 161.18, 155.82, 155.02, 150.30, 143.12, 141.91, 136.95, 136.67, 136.62, 135.50, 135.40, 133.24, 130.16, 130.04, 128.97, 128.74, 128.53, 126.65, 126.37, 123.49, 120.01, 118.18, 116.32, 116.28, 116.14, 115.38, 70.16, 69.81, 69.73, 69.55, 68.84, 68.68, 68.60, 48.74, 48.59, 30.94, 21.99, 16.12, 11.37. HRMS (MALDI): m/z calc. for [M+Na⁺]⁺ = 1093.3040, found = 1093.3033

(6S)-6-(2-((4-((2-aminophenyl)carbamoyl)phenyl)amino)-2-oxoethyl)-4-(4-chlorophenyl)-N-(3-((2-(2,6-dioxopiperidin-3-yl)-1,3-dioxoisoindolin-4-yl)amino)-propyl)-3,9-dimethyl-6H-thieno[3,2-f][1,2,4]-triazole[4,3-a][1,4]diazepine-2-carboxamide (175d)
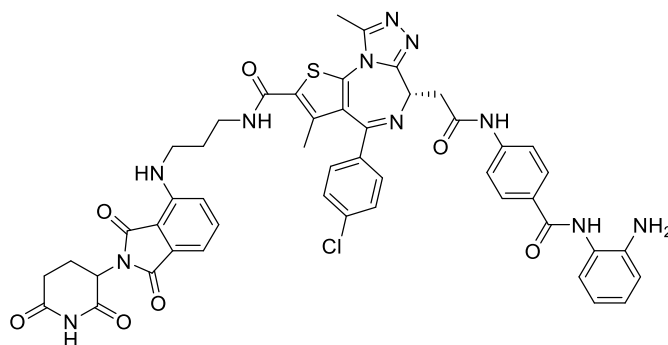
Compound **174** (40 mg, 54 µmol) and compound **154d** (19 mg, 57 µmol) were reacted according to "general procedure for amide coupling". The crude product was purified by flash chromatography (silica, DCM/MeOH) to provide the *Boc*-protected intermediate (44 mg, 56%). MS (ESI): m/z calc. for [M+H$^+$]$^+$ = 1052.6, found = 1052.3

The intermediate was then dissolved in DCM/TFA (4 mL, 3/1) and stirred at ambient temperature for 1 h. Afterwards, all volatiles were removed under reduced pressure and the residue was purified by flash chromatography (C18 silica, H$_2$O/ACN) to provide the title compound as a yellow solid (16 mg, 51%). ^{1}H NMR (500 MHz, DMSO-d_6) δ 11.08 (s, 1H), 10.59 (s, 1H), 9.57 (s, 1H), 8.40 (t, J = 5.6 Hz, 1H), 7.96 (t, J = 6.7 Hz, 2H), 7.75 (d, J = 8.7 Hz, 2H), 7.59 (dd, J = 8.4, 7.3 Hz, 1H), 7.50 (d, J = 8.9 Hz, 2H), 7.46 (d, J = 8.6 Hz, 2H), 7.16 (d, J = 7.1 Hz, 1H), 7.12 (d, J = 8.6 Hz, 1H), 7.03 (d, J = 7.0 Hz, 1H), 6.99 − 6.94 (m, 1H), 6.78 (dd, J = 8.0, 1.3 Hz, 1H), 6.74 (t, J = 6.2 Hz, 1H), 6.60 (td, J = 7.6, 1.3 Hz, 1H), 5.05 (dd, J = 12.7, 5.4 Hz, 1H), 4.88 (s, 2H), 4.69 (t, J = 7.1 Hz, 1H), 3.57 (d, J = 7.1 Hz, 2H), 3.43 − 3.35 (m, 3H), 2.89 (s, 2H), 2.73 (d, J = 0.5 Hz, 1H), 2.66 (s, 3H), 2.58 (d, J = 20.2 Hz, 1H), 2.06 − 1.99 (m, 1H), 1.94 (s, 3H), 1.86 − 1.79 (m, 2H), 1.23 (s, 6H), 0.89 − 0.79 (m, 2H). ^{13}C NMR {^{1}H} (126 MHz, DMSO-d_6) δ 172.80, 170.08, 169.03, 168.81, 167.30, 164.71, 162.93, 162.30, 161.28, 157.90, 157.65, 155.04, 150.30, 146.25, 143.13, 141.92, 136.65, 136.62, 136.27, 135.46, 135.42, 132.29, 130.16, 130.11, 128.98, 128.75, 128.56, 126.65, 126.36, 123.49, 118.46, 118.19, 117.16, 116.28, 116.14, 116.06, 110.43, 109.22, 54.05, 48.54, 37.01, 35.62, 31.28, 30.97, 30.77, 29.00, 28.88, 28.68, 28.63, 22.17, 22.08, 16.17, 11.38. HRMS (MALDI): m/z calc. for [M+Na$^+$]$^+$ = 974.2570, found = 974.2587

(6*S*)-6-(2-((4-((2-aminophenyl)carbamoyl)phenyl)amino)-2-oxoethyl)-4-(4-chlorophenyl)-*N*-(8-((2-(2,6-dioxopiperidin-3-yl)-1,3-dioxoisoindolin-4-yl)amino)octyl)-3,9-dimethyl-6*H*-thieno[3,2-*f*][1,2,4]triazole-[4,3-*a*][1,4]diazepine-2-carboxamide (175e)
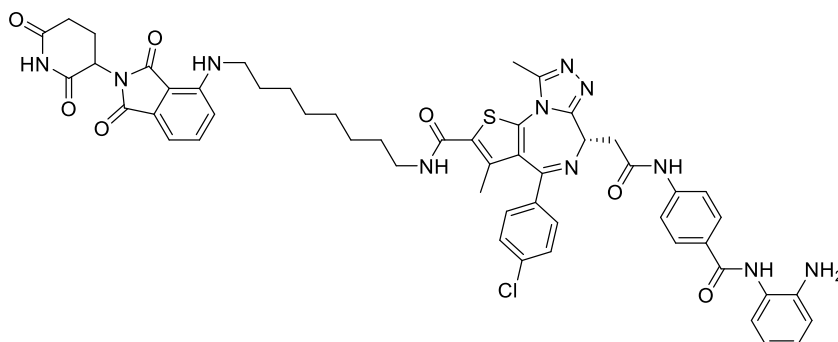
Compound **174** (50 mg, 68 µmol) and compound **154e** (29 mg, 71 µmol) were reacted according to "general procedure for amide coupling". The crude product was purified by flash chromatography (silica, DCM/MeOH) to provide the *Boc*-protected intermediate (109 mg (63% purity), quant yield assumed). MS (ESI): m/z calc. for [M+H$^+$]$^+$ = 1022.6, found = 1022.2

The intermediate was then dissolved in DCM/TFA (4 mL, 3/1) and stirred at ambient temperature for 1 h. Afterwards, all volatiles were removed under reduced pressure and the residue was purified by flash chromatography (C18 silica, H$_2$O/ACN) to provide the title compound as a yellow solid (9 mg, 13%). ^{1}H NMR (500 MHz, DMSO-*d$_6$*) δ 11.08 (s, 1H), 10.59 (s, 1H), 9.57 (s, 1H), 8.30 (t, *J* = 5.6 Hz, 1H), 7.97 (d, *J* = 8.6 Hz, 2H), 7.76 (d, *J* = 8.7 Hz, 2H), 7.57 (dd, *J* = 8.3, 7.3 Hz, 1H), 7.47 (dd, *J* = 19.1, 8.7 Hz, 4H), 7.17 (d, *J* = 7.5 Hz, 1H), 7.08 (d, *J* = 8.6 Hz, 1H), 7.01 (d, *J* = 7.0 Hz, 1H), 6.99 − 6.94 (m, 1H), 6.78 (dd, *J* = 8.0, 1.1 Hz, 1H), 6.63 − 6.58 (m, 1H), 6.51 (t, *J* = 5.8 Hz, 1H), 5.04 (dd, *J* = 12.7, 5.4 Hz, 1H), 4.88 (s, 1H), 4.69 (t, *J* = 7.1 Hz, 1H), 3.57 (d, *J* = 7.0 Hz, 2H), 3.31 − 3.23 (m, 4H), 3.18 (dd, *J* = 12.3, 5.2 Hz, 1H), 2.88 (ddd, *J* = 16.9, 13.8, 5.3 Hz, 1H), 2.65 (s, 3H), 2.62 − 2.53 (m, 2H), 2.08 − 1.97 (m, 1H), 1.92 (s, 3H), 1.62 − 1.48 (m, 4H), 1.31 (s, 8H). ^{13}C NMR {^{1}H} (126 MHz, DMSO-*d$_6$*) δ 172.79, 170.08, 169.02, 168.95, 167.29, 164.70, 162.93, 160.98, 155.04, 150.28, 146.43, 143.12, 141.91, 136.63, 136.50, 136.26, 135.41, 135.14, 132.18, 130.40, 130.16, 130.05, 128.97, 128.74, 128.54, 126.65, 126.36, 123.49, 118.18, 117.16, 116.28, 116.14, 110.37, 109.01, 54.90, 53.69, 48.59, 48.53, 42.06, 30.97, 28.92, 28.67, 28.64, 26.37, 26.26, 22.15, 16.10, 11.37. HRMS (MALDI): m/z calc. for [M+Na$^+$]$^+$ = 1044.3353, found = 1044.3360

(6S)-6-(2-((4-((2-aminophenyl)carbamoyl)phenyl)amino)-2-oxoethyl)-4-(4-chlorophenyl)-*N*-(6-((2-(2,6-dioxopiperidin-3-yl)-1,3-dioxoisoindolin-4-yl)oxy)hexyl)-3,9-dimethyl-6*H*-thieno[3,2-*f*][1,2,4]triazole-[4,3-*a*][1,4]diazepine-2-carboxamide (175f)
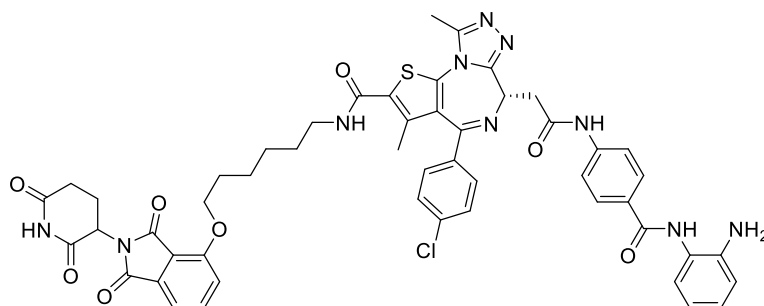
Compound **174** (50 mg, 68 µmol) and compound **154f** (27 mg, 71 µmol) were reacted according to "general procedure for amide coupling". The crude product was purified by flash chromatography (silica, DCM/MeOH) to provide the *Boc*-protected intermediate (43 mg, 58%). MS (ESI): m/z calc. for $[M+H^+]^+$ = 996.30 , found = 996.20

The intermediate was then dissolved in DCM/TFA (4 mL, 3/1) and stirred at ambient temperature for 1 h. Afterwards, all volatiles were removed under reduced pressure and the residue was purified by flash chromatography (C18 silica, H_2O/ACN) to provide the title compound as an off-white solid (20 mg, 30%). ^{1}H NMR (500 MHz, DMSO-d_6) δ 11.09 (s, 1H), 10.63 (s, 1H), 10.02 (s, 1H), 8.31 (t, *J* = 5.6 Hz, 1H), 8.00 (d, *J* = 8.7 Hz, 2H), 7.83 – 7.75 (m, 4H), 7.47 (ddd, *J* = 19.7, 9.7, 6.9 Hz, 8H), 7.33 (d, *J* = 7.4 Hz, 1H), 7.19 (t, *J* = 7.7 Hz, 1H), 7.13 (d, *J* = 7.9 Hz, 1H), 7.05 (t, *J* = 7.0 Hz, 1H), 5.07 (dd, *J* = 12.8, 5.4 Hz, 2H), 4.69 (t, *J* = 6.9 Hz, 2H), 4.21 (t, *J* = 6.3 Hz, 3H), 3.59 (d, *J* = 7.4 Hz, 2H), 3.26 (dt, *J* = 14.2, 7.2 Hz, 2H), 2.88 (ddd, *J* = 17.0, 13.9, 5.4 Hz, 1H), 2.65 (s, 4H), 2.63 – 2.55 (m, 1H), 2.06 – 1.98 (m, 1H), 1.92 (s, 4H), 1.82 – 1.73 (m, 3H), 1.60 – 1.45 (m, 6H), 1.40 (dd, *J* = 14.7, 7.7 Hz, 3H). ^{13}C NMR {^{1}H} (126 MHz, DMSO-d_6) δ 172.77, 169.94, 169.49, 169.11, 166.84, 165.32, 165.11, 163.00, 162.96, 160.99, 158.32, 158.03, 157.74, 156.00, 155.03, 154.98, 150.31, 149.12, 142.30, 137.00, 136.62, 136.50, 135.42, 135.20, 133.24, 130.40, 130.17, 130.07, 128.96, 128.55, 128.25, 126.76, 126.65, 125.51, 119.78, 119.31, 118.22, 116.23, 115.14, 113.95, 68.70, 54.18, 48.73, 30.95, 28.90, 28.30, 26.04, 24.98, 22.00, 16.12, 11.36. HRMS (MALDI): m/z calc. for $[M+Na^+]^+$ = 1017.2880, found = 1017.2893

(*S*)-6-(2-((4-((2-aminophenyl)carbamoyl)phenyl)amino)-2-oxoethyl)-4-(4-chlorophenyl)-*N*-(2-(2-(((*S*)-1-((2*S*,4*R*)-4-hydroxy-2-((4-(4-methylthiazol-5-yl)benzyl)-carbamoyl)pyrrolidin-1-yl)-3,3-dimethyl-1-oxobutan-2-yl)amino)-2-oxoethoxy)ethyl)-3,9-dimethyl-6*H*-thieno[3,2-*f*][1,2,4]triazolo[4,3-*a*][1,4]diazepine-2-carboxamide (177a)
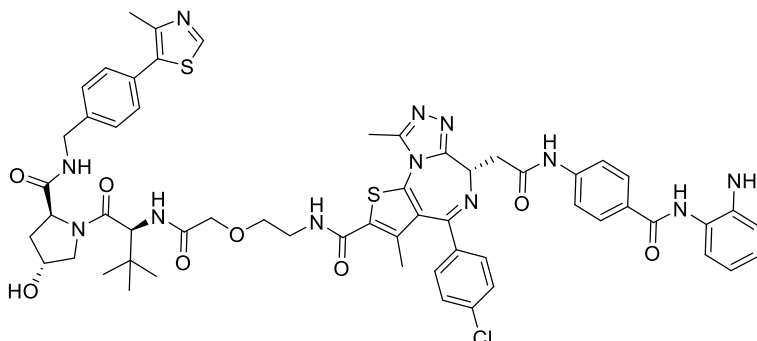
Compound **176a** (47 mg, 74 µmol) was dissolved in DCM/TFA (4 mL, 3/1) and stirred at ambient temperature. After 1 h, all volatiles were removed under reduced pressure. The deprotected amine and compound **174** (50 mg, 68 µmol) were afterwards reacted according to "general procedure for amide coupling". The crude product was purified by flash chromatography (silica, DCM/MeOH) to provide the *Boc*-protected intermediate (45 mg, 53%). MS (ESI): m/z calc. for [(M+2H$^+$-*Boc*)/2]$^+$ = 577.19, found = 577.40

The intermediate was then dissolved in DCM/TFA (4 mL, 3/1) and stirred at ambient temperature for 1 h. Afterwards, all volatiles were removed under reduced pressure and the residue was purified by flash chromatography (C18 silica, H$_2$O/ACN) to provide the title compound as an off-white solid (28 mg, 68%). ^{1}H NMR (500 MHz, DMSO-*d*$_6$) δ 10.63 (s, 1H), 10.05 (s, 1H), 8.96 (s, 1H), 8.56 (t, *J* = 6.0 Hz, 1H), 8.43 (t, *J* = 5.5 Hz, 1H), 8.00 (d, *J* = 8.7 Hz, 2H), 7.79 (d, *J* = 8.8 Hz, 2H), 7.50 – 7.43 (m, 6H), 7.38 (d, *J* = 1.9 Hz, 6H), 7.34 (d, *J* = 7.8 Hz, 1H), 7.25 – 7.19 (m, 1H), 7.15 (d, *J* = 7.7 Hz, 1H), 7.08 (t, *J* = 7.3 Hz, 1H), 4.70 (t, *J* = 7.1 Hz, 2H), 4.56 (d, *J* = 9.6 Hz, 1H), 4.43 (t, *J* = 8.2 Hz, 2H), 4.38 (dd, *J* = 15.9, 6.4 Hz, 2H), 4.25 (dd, *J* = 15.8, 5.7 Hz, 2H), 4.00 (d, *J* = 2.9 Hz, 2H), 3.70 – 3.55 (m, 8H), 3.52 – 3.45 (m, 2H), 2.65 (d, *J* = 3.1 Hz, 3H), 2.43 (s, 3H), 2.04 (d, *J* = 8.0 Hz, 1H), 1.94 (s, 3H), 0.91 (s, 9H). ^{13}C NMR {^{1}H} (126 MHz, DMSO-*d*$_6$) δ 171.73, 169.47, 169.13, 169.09, 168.53, 165.14, 162.95, 161.23, 158.61, 158.33, 158.04, 157.75, 155.03, 151.42, 150.30, 149.08, 147.70, 142.33, 139.42, 138.93, 136.71, 136.63, 135.65, 135.42, 131.15, 130.16, 130.10, 129.68, 128.97, 128.87, 128.69, 128.54, 128.19, 128.10, 127.45, 126.76, 126.67, 125.58, 119.31, 118.22, 113.93, 69.28, 69.22, 68.86, 58.74, 56.52, 55.77, 26.26, 26.17, 16.20, 15.89, 11.37. HRMS (MALDI): m/z calc. for [M+Na$^+$]$^+$ = 1175.3758, found = 1175.3747

(S)-6-(2-((4-((2-aminophenyl)carbamoyl)phenyl)amino)-2-oxoethyl)-4-(4-chloro-phenyl)-N-(2-(2-(2-(((S)-1-((2S,4R)-4-hydroxy-2-((4-(4-methylthiazol-5-yl)benzyl)-carbamoyl)pyrrolidin-1-yl)-3,3-dimethyl-1-oxobutan-2-yl)amino)-2-oxoethoxy)-ethoxy)ethyl)-3,9-dimethyl-6H-thieno[3,2-f][1,2,4]triazolo[4,3-a][1,4]diazepine-2-carboxamide (177b)
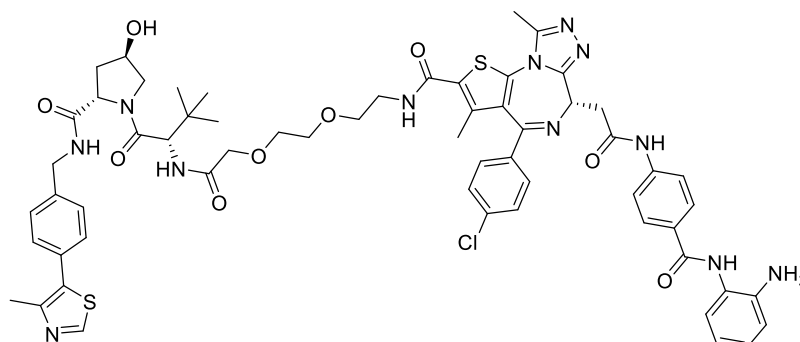
Compound **176b** (59 mg, 88 µmol) was dissolved in DCM/TFA (4 mL, 3/1) and stirred at ambient temperature. After 1 h, all volatiles were removed under reduced pressure. The deprotected amine and compound **174** (50 mg, 68 µmol) were afterwards reacted according to "general procedure for amide coupling". The crude product was purified by flash chromatography (silica, DCM/MeOH) to provide the *Boc*-protected intermediate (59 mg, 68%). MS (ESI): m/z calc. for [(M+2H$^+$-*Boc*)/2]$^+$ = 599.21, found = 599.35

The intermediate was then dissolved in DCM/TFA (4 mL, 3/1) and stirred at ambient temperature for 1 h. Afterwards, all volatiles were removed under reduced pressure and the residue was purified by flash chromatography (C18 silica, H$_2$O/ACN) to provide the title compound as an off-white solid (41 mg, 75%). ^{1}H NMR (500 MHz, DMSO-d_6) δ 10.58 (s, 1H), 9.57 (s, 1H), 8.95 (s, 1H), 8.56 (t, J = 6.0 Hz, 1H), 8.33 (t, J = 5.6 Hz, 1H), 7.97 (d, J = 8.5 Hz, 2H), 7.76 (d, J = 8.5 Hz, 2H), 7.48 (d, J = 8.9 Hz, 2H), 7.47 – 7.42 (m, 4H), 7.39 (s, 4H), 7.16 (d, J = 7.6 Hz, 1H), 7.01 – 6.94 (m, 1H), 6.78 (d, J = 7.7 Hz, 1H), 6.64 – 6.57 (m, 1H), 5.14 (d, J = 3.5 Hz, 1H), 4.88 (s, 2H), 4.70 (t, J = 7.1 Hz, 1H), 4.57 (d, J = 9.6 Hz, 1H), 4.44 (t, J = 8.2 Hz, 1H), 4.38 (dd, J = 15.9, 6.4 Hz, 2H), 4.26 (dd, J = 15.8, 5.7 Hz, 1H), 3.96 (d, J = 2.0 Hz, 2H), 3.67 (dd, J = 10.7, 3.8 Hz, 1H), 3.60 (ddd, J = 16.3, 7.0, 3.5 Hz, 10H), 3.45 (ddd, J = 27.2, 13.4, 7.5 Hz, 2H), 2.64 (s, 3H), 2.43 (s, 3H), 2.09 – 2.03 (m, 1H), 1.92 (s, 3H), 0.94 (s, 9H). ^{13}C NMR {^{1}H} (126 MHz, DMSO-d_6) δ 171.70, 171.23, 169.57, 169.17, 169.01, 168.56, 164.70, 162.91, 161.19, 155.03, 151.49, 151.39, 150.29, 147.81, 147.74, 143.13, 141.92, 139.38, 136.67, 136.61, 135.60, 135.42, 131.12, 130.17, 130.04, 129.72, 128.97, 128.87, 128.75, 128.69, 128.53, 128.17, 127.45, 126.65, 126.37, 123.49, 118.18, 116.28, 116.14, 70.38, 69.57, 69.36, 68.85, 68.78, 58.74, 56.59, 55.70, 54.89, 53.68, 35.74, 35.53, 26.28, 26.18, 16.14, 15.95, 15.91, 11.37. HRMS (MALDI): m/z calc. for [M+Na$^+$]$^+$ = 1219.4019, found = 1219.4029

(S)-6-(2-((4-((2-aminophenyl)carbamoyl)phenyl)amino)-2-oxoethyl)-4-(4-chloro-phenyl)-*N*-((*S*)-3-((2*S*,4*R*)-4-hydroxy-2-((4-(4-methylthiazol-5-yl)benzyl)carbamoyl)-pyrrolidine-1-carbonyl)-2,2-dimethyl-5-oxo-7,10,13-trioxa-4-azahexadecan-16-yl)-3,9-dimethyl-6*H*-thieno[3,2-*f*][1,2,4]triazolo[4,3-*a*][1,4]diazepine-2-carboxamide (177c)
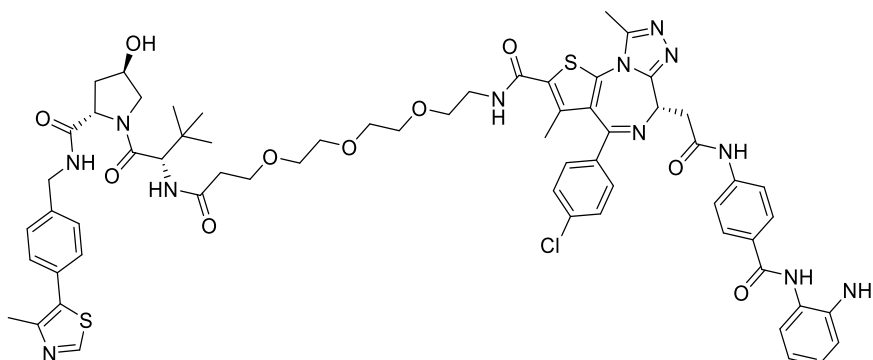
Compound **176c** (52 mg, 71 µmol) was dissolved in DCM/TFA (4 mL, 3/1) and stirred at ambient temperature. After 1 h, all volatiles were removed under reduced pressure. The deprotected amine and compound **174** (50 mg, 68 µmol) were afterwards reacted according to "general procedure for amide coupling". The crude product was purified by flash chromatography (silica, DCM/MeOH) to provide the *Boc*-protected intermediate (74 mg, 81%). MS (ESI): m/z calc. for $[(M+2H^+-Boc)/2]^+$ = 628.23, found = 628.45. The intermediate was then dissolved in DCM/TFA (4 mL, 3/1) and stirred at ambient temperature for 1 h. Afterwards, all volatiles were removed under reduced pressure and the residue was purified by flash chromatography (C18 silica, H_2O/ACN) to provide the title compound as an off-white solid (34 mg, 50%). ^{1}H NMR (500 MHz, DMSO-d_6) δ 10.58 (s, 1H), 9.57 (s, 1H), 8.97 (s, 1H), 8.55 (t, *J* = 6.0 Hz, 1H), 8.34 (t, *J* = 5.6 Hz, 1H), 7.97 (d, *J* = 8.6 Hz, 2H), 7.90 (d, *J* = 9.4 Hz, 1H), 7.76 (d, *J* = 8.7 Hz, 2H), 7.47 (q, *J* = 8.8 Hz, 4H), 7.43 – 7.36 (m, 4H), 7.16 (d, *J* = 7.2 Hz, 1H), 6.99 – 6.94 (m, 1H), 6.78 (dd, *J* = 8.0, 1.2 Hz, 1H), 6.62 – 6.55 (m, 1H), 5.12 (d, *J* = 3.5 Hz, 1H), 4.88 (s, 2H), 4.70 (t, *J* = 7.1 Hz, 1H), 4.55 (d, *J* = 9.4 Hz, 1H), 4.46 – 4.40 (m, 2H), 4.35 (s, 1H), 4.22 (dd, *J* = 15.9, 5.5 Hz, 1H), 3.67 (dd, *J* = 10.5, 4.0 Hz, 1H), 3.63 (s, 1H), 3.60 (d, *J* = 3.2 Hz, 1H), 3.58 (d, *J* = 6.9 Hz, 4H), 3.52 (dd, *J* = 7.7, 3.7 Hz, 6H), 3.48 (s, 2H), 3.48 – 3.46 (m, 2H), 3.42 (dt, *J* = 19.6, 7.0 Hz, 4H), 2.65 (s, 3H), 2.44 (s, 3H), 2.35 (dt, *J* = 14.6, 6.1 Hz, 1H), 2.07 – 2.01 (m, 1H), 1.93 (s, 3H), 0.93 (s, 9H). ^{13}C NMR {^{1}H} (126 MHz, DMSO-d_6) δ 171.91, 169.92, 169.52, 169.00, 164.70, 162.92, 162.30, 161.19, 155.03, 151.42, 150.30, 147.71, 143.12, 141.92, 139.49, 136.66, 136.63, 135.50, 135.41, 131.15, 130.18, 130.14, 130.04, 129.63, 128.97, 128.84, 128.74, 128.63, 128.53, 128.04, 127.42, 126.65, 126.36, 123.49, 118.18, 116.28, 116.14, 69.73, 69.69, 69.54, 69.46, 68.86, 68.63, 66.94, 58.70, 56.35, 56.28, 53.68, 35.90, 35.66, 35.35, 35.11, 26.31, 16.11, 15.92, 11.37. HRMS (MALDI): m/z calc. for $[M+Na^+]^+$ = 1277.4438, found = 1277.4428

(*S*)-6-(2-((4-((2-aminophenyl)carbamoyl)phenyl)amino)-2-oxoethyl)-4-(4-chlorophenyl)-*N*-(7-(((*S*)-1-((2*S*,4*R*)-4-hydroxy-2-((4-(4-methylthiazol-5-yl)benzyl)-carbamoyl)pyrrolidin-1-yl)-3,3-dimethyl-1-oxobutan-2-yl)amino)-7-oxoheptyl)-3,9-dimethyl-6*H*-thieno[3,2-*f*][1,2,4]triazolo[4,3-*a*][1,4]diazepine-2-carboxamide (177d)
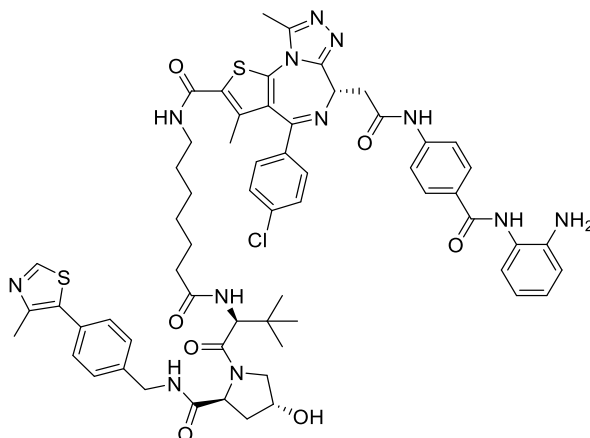
Compound **176d** (49 mg, 74 µmol) was dissolved in DCM/TFA (4 mL, 3/1) and stirred at ambient temperature. After 1 h, all volatiles were removed under reduced pressure. The deprotected amine and compound **174** (50 mg, 68 µmol) were afterwards reacted according to "general procedure for amide coupling". The crude product was purified by flash chromatography (silica, DCM/MeOH) to provide the *Boc*-protected intermediate (70 mg, 80%). MS (ESI): m/z calc. for [(M+2H$^+$-*Boc*)/2]$^+$ = 590.22, found = 590.45. The intermediate was then dissolved in DCM/TFA (4 mL, 3/1) and stirred at ambient temperature for 1 h. Afterwards, all volatiles were removed under reduced pressure and the residue was purified by flash chromatography (C18 silica, H$_2$O/ACN) to provide the title compound as an off-white solid (22 mg, 37%). ^{1}H NMR (500 MHz, DMSO-*d$_6$*) δ 10.59 (s, 1H), 9.57 (s, 1H), 8.97 (s, 1H), 8.55 (t, *J* = 6.0 Hz, 1H), 8.30 (t, *J* = 5.6 Hz, 1H), 7.97 (d, *J* = 8.4 Hz, 2H), 7.84 (d, *J* = 9.3 Hz, 1H), 7.76 (d, *J* = 8.5 Hz, 2H), 7.47 (q, *J* = 8.7 Hz, 4H), 7.43 – 7.37 (m, 4H), 7.17 (d, *J* = 7.6 Hz, 1H), 7.00 – 6.94 (m, 1H), 6.78 (d, *J* = 7.9 Hz, 1H), 6.63 – 6.57 (m, 1H), 5.11 (d, *J* = 3.4 Hz, 1H), 4.88 (s, 2H), 4.70 (t, *J* = 7.1 Hz, 1H), 4.55 (d, *J* = 9.4 Hz, 1H), 4.43 (dd, *J* = 13.9, 7.6 Hz, 2H), 4.35 (s, 1H), 4.22 (dd, *J* = 15.9, 5.4 Hz, 1H), 3.66 (q, *J* = 10.9, 8.9 Hz, 2H), 3.58 (d, *J* = 6.9 Hz, 2H), 3.24 (dt, *J* = 13.1, 6.8 Hz, 2H), 2.65 (s, 3H), 2.44 (s, 3H), 2.26 (dd, *J* = 14.4, 7.2 Hz, 1H), 2.17 – 2.09 (m, 1H), 2.02 (d, *J* = 9.4 Hz, 1H), 1.92 (s, 3H), 1.49 (dt, *J* = 14.4, 7.0 Hz, 6H), 1.29 (s, 6H), 0.93 (s, 9H). ^{13}C NMR {^{1}H} (126 MHz, DMSO-*d$_6$*) δ 172.07, 171.94, 171.35, 169.71, 169.01, 164.71, 162.94, 160.99, 155.04, 151.42, 150.29, 147.71, 143.12, 141.92, 139.49, 136.63, 136.51, 135.41, 135.17, 131.16, 130.39, 130.16, 130.05, 129.63, 128.97, 128.83, 128.75, 128.63, 128.55, 128.03, 127.41, 126.65, 126.36, 123.49, 118.19, 116.28, 116.15, 68.86, 58.68, 56.34, 56.27, 53.69, 28.88, 28.37, 26.45, 26.38, 26.20, 25.37, 16.11, 15.93, 11.37. HRMS (MALDI): m/z calc. for [M+Na$^+$]$^+$ = 1201.4278, found = 1201.4267

(S)-6-(2-((4-((2-aminophenyl)carbamoyl)phenyl)amino)-2-oxoethyl)-4-(4-chlorophenyl)-N-(8-(((S)-1-((2S,4R)-4-hydroxy-2-((4-(4-methylthiazol-5-yl)benzyl)-carbamoyl)pyrrolidin-1-yl)-3,3-dimethyl-1-oxobutan-2-yl)amino)-8-oxooctyl)-3,9-dimethyl-6H-thieno[3,2-f][1,2,4]triazolo[4,3-a][1,4]diazepine-2-carboxamide (177e)
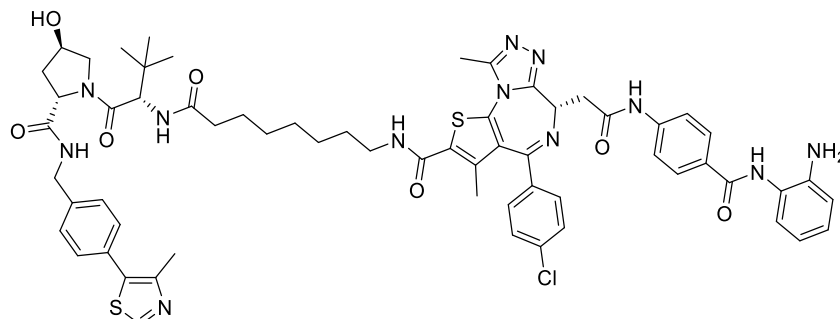
Compound **176e** (50 mg, 74 µmol) was dissolved in DCM/TFA (4 mL, 3/1) and stirred at ambient temperature. After 1 h, all volatiles were removed under reduced pressure. The deprotected amine and compound **174** (50 mg, 68 µmol) were afterwards reacted according to "general procedure for amide coupling". The crude product was purified by flash chromatography (silica, DCM/MeOH) to provide the *Boc*-protected intermediate (70 mg, 80%). MS (ESI): m/z calc. for $[(M+2H^+-Boc)/2]^+$ = 597.23, found = 597.40

The intermediate was then dissolved in DCM/TFA (4 mL, 3/1) and stirred at ambient temperature for 1 h. Afterwards, all volatiles were removed under reduced pressure and the residue was purified by flash chromatography (C18 silica, H_2O/ACN) to provide the title compound as an off-white solid (28 mg, 44%). [^1]H NMR (500 MHz, DMSO-d_6) δ 10.63 (s, 1H), 10.03 (s, 1H), 8.98 (s, 1H), 8.55 (t, J = 6.1 Hz, 1H), 8.31 (t, J = 5.6 Hz, 1H), 8.00 (d, J = 8.7 Hz, 2H), 7.83 (d, J = 9.3 Hz, 1H), 7.79 (d, J = 8.8 Hz, 2H), 7.48 (q, J = 8.8 Hz, 6H), 7.43 – 7.36 (m, 6H), 7.33 (d, J = 7.8 Hz, 1H), 7.20 (t, J = 7.6 Hz, 1H), 7.14 (d, J = 7.7 Hz, 1H), 7.06 (t, J = 7.2 Hz, 1H), 4.70 (t, J = 7.0 Hz, 2H), 4.54 (d, J = 9.4 Hz, 1H), 4.44 (d, J = 6.4 Hz, 1H), 4.41 (d, J = 7.7 Hz, 2H), 4.35 (s, 1H), 4.21 (dd, J = 15.9, 5.5 Hz, 2H), 3.71 – 3.61 (m, 2H), 3.58 (d, J = 7.4 Hz, 2H), 3.31 – 3.19 (m, 2H), 2.65 (s, 3H), 2.44 (s, 3H), 2.26 (dd, J = 14.4, 7.1 Hz, 1H), 2.11 (dt, J = 14.2, 7.2 Hz, 1H), 2.02 (d, J = 9.3 Hz, 3H), 1.54 – 1.40 (m, 6H), 1.28 (s, 6H), 0.93 (s, 9H). [^13]C NMR {[^1]H} (126 MHz, DMSO-d_6) δ 172.07, 171.94, 171.35, 169.71, 169.47, 169.09, 165.12, 162.96, 160.97, 158.60, 158.32, 158.03, 155.03, 151.45, 150.31, 149.11, 147.68, 142.31, 139.51, 136.62, 136.48, 135.43, 135.14, 131.18, 130.43, 130.17, 130.06, 129.62, 128.96, 128.84, 128.63, 128.55, 128.24, 127.42, 126.75, 126.65, 125.51, 119.32, 118.22, 113.94, 68.86, 58.68, 56.33, 56.25, 41.68, 37.92, 35.20, 34.86, 34.50, 28.96, 28.61, 28.46, 26.37, 25.38, 16.10, 15.92, 11.36. HRMS (MALDI): m/z calc. for $[M+Na^+]^+$ = 1215.4434, found = 1215.4470

7 Literature

(1)   Crick, F. H. On Protein Synthesis. *Symp. Soc. Exp. Biol.* **1958**, *12*, 138–163.

(2)   Cobb, M. 60 Years Ago, Francis Crick Changed the Logic of Biology. *PLOS Biol.* **2017**, *15* (9), e2003243. https://doi.org/10.1371/journal.pbio.2003243.

(3)   Crick, F. Central Dogma of Molecular Biology. *Nature* **1970**, *227* (5258), 561–563. https://doi.org/10.1038/227561a0.

(4)   Altshuler, D.; Daly, M. J.; Lander, E. S. Genetic Mapping in Human Disease. *Science* **2008**, *322* (5903), 881–888. https://doi.org/10.1126/science.1156409.

(5)   *DNA transcription*. National Human Genome Research Institute. https://www.genome.gov/Images/EdKit/bio2c_large.gif (accessed 2023-07-25).

(6)   Russo, V. E. A.; Martienssen, R. A.; Riggs, A. D. *Epigenetic Mechanisms of Gene Regulation*; Cold Spring Harbor monograph series; Cold Spring Harbor Laboratory Press: Plainview, N.Y, 1996.

(7)   Chahwan, R.; Wontakal, S. N.; Roa, S. The Multidimensional Nature of Epigenetic Information and Its Role in Disease. *Discov. Med.* **2011**, *11* (58), 233–243.

(8)   Skinner, M. K. Role of Epigenetics in Developmental Biology and Transgenerational Inheritance. *Birth Defects Res. Part C Embryo Today Rev.* **2011**, *93* (1), 51–55. https://doi.org/10.1002/bdrc.20199.

(9)   Jabbari, K.; Bernardi, G. Cytosine Methylation and CpG, TpG (CpA) and TpA Frequencies. *Gene* **2004**, *333*, 143–149. https://doi.org/10.1016/j.gene.2004.02.043.

(10)   Lander, E. S.; Linton, L. M.; Birren, B.; Nusbaum, C.; Zody, M. C.; Baldwin, J.; Devon, K.; Dewar, K.; Doyle, M.; FitzHugh, W.; Funke, R.; Gage, D.; Harris, K.; Heaford, A.; Howland, J.; Kann, L.; Lehoczky, J.; LeVine, R.; McEwan, P.; McKernan, K.; Meldrim, J.; Mesirov, J. P.; Miranda, C.; Morris, W.; Naylor, J.; Raymond, C.; Rosetti, M.; Santos, R.; Sheridan, A.; Sougnez, C.; Stange-Thomann, N.; Stojanovic, N.; Subramanian, A.; Wyman, D.; Rogers, J.; Sulston, J.; Ainscough, R.; Beck, S.; Bentley, D.; Burton, J.; Clee, C.; Carter, N.; Coulson, A.; Deadman, R.; Deloukas, P.; Dunham, A.; Dunham, I.; Durbin, R.; French, L.; Grafham, D.; Gregory, S.; Hubbard, T.; Humphray, S.; Hunt, A.; Jones, M.; Lloyd, C.; McMurray, A.; Matthews, L.; Mercer, S.; Milne, S.; Mullikin, J. C.; Mungall, A.; Plumb, R.; Ross, M.; Shownkeen, R.; Sims, S.; Waterston, R. H.; Wilson, R. K.; Hillier, L. W.; McPherson, J. D.; Marra, M. A.; Mardis, E. R.; Fulton, L. A.; Chinwalla, A. T.; Pepin, K. H.; Gish, W. R.; Chissoe, S. L.; Wendl, M. C.; Delehaunty, K. D.; Miner, T. L.; Delehaunty, A.; Kramer, J. B.; Cook, L. L.; Fulton, R. S.; Johnson, D. L.; Minx, P. J.; Clifton, S. W.; Hawkins, T.; Branscomb, E.; Predki, P.; Richardson, P.; Wenning, S.; Slezak, T.; Doggett, N.; Cheng, J.-F.; Olsen, A.; Lucas, S.; Elkin, C.; Uberbacher, E.; Frazier, M.; Gibbs, R. A.; Muzny, D. M.; Scherer, S. E.; Bouck, J. B.; Sodergren, E. J.; Worley, K. C.; Rives, C. M.; Gorrell, J. H.; Metzker, M. L.; Naylor, S. L.; Kucherlapati, R. S.; Nelson, D. L.; Weinstock, G. M.; Sakaki, Y.; Fujiyama, A.; Hattori, M.; Yada, T.; Toyoda, A.; Itoh, T.; Kawagoe, C.; Watanabe, H.; Totoki, Y.; Taylor, T.; Weissenbach, J.; Heilig, R.; Saurin, W.; Artiguenave, F.; Brottier, P.; Bruls, T.; Pelletier, E.; Robert, C.; Wincker, P.; Rosenthal, A.; Platzer, M.; Nyakatura, G.; Taudien, S.; Rump, A.; Smith, D. R.; Doucette-Stamm, L.; Rubenfield, M.; Weinstock, K.; Lee, H. M.; Dubois, J.; Yang, H.; Yu, J.; Wang, J.; Huang, G.; Gu, J.; Hood, L.; Rowen, L.; Madan, A.; Qin, S.; Davis, R. W.; Federspiel, N. A.; Abola, A. P.; Proctor, M. J.; Roe, B. A.; Chen, F.; Pan, H.; Ramser, J.; Lehrach, H.; Reinhardt, R.; McCombie, W. R.; de la Bastide, M.; Dedhia, N.; Blöcker, H.; Hornischer, K.; Nordsiek, G.; Agarwala, R.; Aravind, L.; Bailey, J. A.; Bateman, A.; Batzoglou, S.; Birney, E.; Bork, P.; Brown, D. G.; Burge, C. B.; Cerutti, L.; Chen, H.-C.; Church, D.; Clamp, M.; Copley, R. R.; Doerks, T.; Eddy, S. R.; Eichler, E. E.; Furey, T. S.; Galagan, J.; Gilbert, J. G. R.; Harmon, C.; Hayashizaki, Y.; Haussler, D.; Hermjakob, H.; Hokamp, K.; Jang, W.; Johnson, L. S.; Jones, T. A.; Kasif, S.; Kaspryzk, A.; Kennedy, S.; Kent, W. J.; Kitts, P.; Koonin, E. V.; Korf, I.; Kulp, D.; Lancet, D.; Lowe, T. M.; McLysaght, A.; Mikkelsen, T.; Moran, J. V.; Mulder, N.; Pollara, V. J.; Ponting, C. P.; Schuler, G.; Schultz, J.; Slater, G.; Smit, A. F. A.; Stupka, E.; Szustakowski, J.; Thierry-Mieg, D.; Thierry-Mieg, J.; Wagner, L.; Wallis, J.; Wheeler, R.; Williams, A.; Wolf, Y. I.; Wolfe, K. H.; Yang, S.-P.; Yeh, R.-F.; Collins, F.; Guyer, M. S.; Peterson, J.; Felsenfeld, A.; Wetterstrand, K. A.; Myers, R. M.; Schmutz, J.; Dickson, M.; Grimwood, J.; Cox, D. R.; Olson, M. V.; Kaul, R.; Raymond, C.; Shimizu, N.; Kawasaki, K.; Minoshima, S.; Evans, G. A.; Athanasiou, M.; Schultz, R.; Patrinos, A.; Morgan,

M. J.; International Human Genome Sequencing Consortium; Whitehead Institute for Biomedical Research, C. for G. R.; The Sanger Centre:; Washington University Genome Sequencing Center; US DOE Joint Genome Institute:; Baylor College of Medicine Human Genome Sequencing Center:; RIKEN Genomic Sciences Center:; Genoscope and CNRS UMR-8030:; Department of Genome Analysis, I. of M. B.; GTC Sequencing Center:; Beijing Genomics Institute/Human Genome Center:; Multimegabase Sequencing Center, T. I. for S. B.; Stanford Genome Technology Center:; University of Oklahoma's Advanced Center for Genome Technology:; Max Planck Institute for Molecular Genetics:; Cold Spring Harbor Laboratory, L. A. H. G. C.; GBF—German Research Centre for Biotechnology:; *Genome Analysis Group (listed in alphabetical order, also includes individuals listed under other headings):; Scientific management: National Human Genome Research Institute, U. N. I. of H.; Stanford Human Genome Center:; University of Washington Genome Center:; Department of Molecular Biology, K. U. S. of M.; University of Texas Southwestern Medical Center at Dallas:; Office of Science, U. D. of E.; The Wellcome Trust: Initial Sequencing and Analysis of the Human Genome. *Nature* **2001**, *409* (6822), 860–921. https://doi.org/10.1038/35057062.

(11)   Walsh, C. P.; Xu, G. L. Cytosine Methylation and DNA Repair. In *DNA Methylation: Basic Mechanisms*; Doerfler, W., Böhm, P., Eds.; Current Topics in Microbiology and Immunology; Springer: Berlin, Heidelberg, 2006; pp 283–315. https://doi.org/10.1007/3-540-31390-7_11.

(12)   Seisenberger, S.; Peat, J. R.; Hore, T. A.; Santos, F.; Dean, W.; Reik, W. Reprogramming DNA Methylation in the Mammalian Life Cycle: Building and Breaking Epigenetic Barriers. *Philos. Trans. R. Soc. B Biol. Sci.* **2013**, *368* (1609), 20110330. https://doi.org/10.1098/rstb.2011.0330.

(13)   Chatterjee, R.; Vinson, C. CpG Methylation Recruits Sequence Specific Transcription Factors Essential for Tissue Specific Gene Expression. *Biochim. Biophys. Acta BBA - Gene Regul. Mech.* **2012**, *1819* (7), 763–770. https://doi.org/10.1016/j.bbagrm.2012.02.014.

(14)   Alberts, B. *Molecular Biology of the Cell*; New York, NY : Garland Science, Taylor and Francis Group, 2015.

(15)   Saxonov, S.; Berg, P.; Brutlag, D. L. A Genome-Wide Analysis of CpG Dinucleotides in the Human Genome Distinguishes Two Distinct Classes of Promoters. *Proc. Natl. Acad. Sci. U. S. A.* **2006**, *103* (5), 1412–1417. https://doi.org/10.1073/pnas.0510310103.

(16)   Deaton, A. M.; Bird, A. CpG Islands and the Regulation of Transcription. *Genes Dev.* **2011**, *25* (10), 1010–1022. https://doi.org/10.1101/gad.2037511.

(17)   Beggs, A. D.; Jones, A.; El-Bahwary, M.; Abulafi, M.; Hodgson, S. V.; Tomlinson, I. P. Whole-Genome Methylation Analysis of Benign and Malignant Colorectal Tumours. *J. Pathol.* **2013**, *229* (5), 697–704. https://doi.org/10.1002/path.4132.

(18)   Rieke, D. T.; Ochsenreither, S.; Klinghammer, K.; Seiwert, T. Y.; Klauschen, F.; Tinhofer, I.; Keilholz, U. Methylation of RAD51B, XRCC3 and Other Homologous Recombination Genes Is Associated with Expression of Immune Checkpoints and an Inflammatory Signature in Squamous Cell Carcinoma of the Head and Neck, Lung and Cervix. *Oncotarget* **2016**, *7* (46), 75379–75393. https://doi.org/10.18632/oncotarget.12211.

(19)   Wei, J.; Li, G.; Dang, S.; Zhou, Y.; Zeng, K.; Liu, M. Discovery and Validation of Hypermethylated Markers for Colorectal Cancer. *Dis. Markers* **2016**, *2016*, 2192853. https://doi.org/10.1155/2016/2192853.

(20)   Jin, B.; Robertson, K. D. DNA Methyltransferases (DNMTs), DNA Damage Repair, and Cancer. *Adv. Exp. Med. Biol.* **2013**, *754*, 3–29. https://doi.org/10.1007/978-1-4419-9967-2_1.

(21)   Kisseljova, N. P.; Kisseljov, F. L. DNA Demethylation and Carcinogenesis. *Biochem. Mosc.* **2005**, *70* (7), 743–752. https://doi.org/10.1007/s10541-005-0179-z.

(22)   Kouzarides, T. Chromatin Modifications and Their Function. *Cell* **2007**, *128* (4), 693–705. https://doi.org/10.1016/j.cell.2007.02.005.

(23)   Ruthenburg, A. J.; Li, H.; Patel, D. J.; Allis, C. D. Multivalent Engagement of Chromatin Modifications by Linked Binding Modules. *Nat. Rev. Mol. Cell Biol.* **2007**, *8* (12), 983–994. https://doi.org/10.1038/nrm2298.

(24)   *Histone*. National Human Genome Research Institute. https://www.genome.gov/sites/default/files/media/images/2022-05/Histone.jpg (accessed 2023-07-25).

(25) Turner, B. M. Histone Acetylation and an Epigenetic Code. *BioEssays* **2000**, *22* (9), 836–845. https://doi.org/10.1002/1521-1878(200009)22:9<836::AID-BIES9>3.0.CO;2-X.

(26) Bannister, A. J.; Kouzarides, T. Regulation of Chromatin by Histone Modifications. *Cell Res.* **2011**, *21* (3), 381–395. https://doi.org/10.1038/cr.2011.22.

(27) Oki, M.; Aihara, H.; Ito, T. Role of Histone Phosphorylation in Chromatin Dynamics and Its Implications in Diseases. *Subcell. Biochem.* **2007**, *41*, 319–336.

(28) Ng, S. S.; Yue, W. W.; Oppermann, U.; Klose, R. J. Dynamic Protein Methylation in Chromatin Biology. *Cell. Mol. Life Sci.* **2008**, *66* (3), 407. https://doi.org/10.1007/s00018-008-8303-z.

(29) Rea, S.; Eisenhaber, F.; O'Carroll, D.; Strahl, B. D.; Sun, Z.-W.; Schmid, M.; Opravil, S.; Mechtler, K.; Ponting, C. P.; Allis, C. D.; Jenuwein, T. Regulation of Chromatin Structure by Site-Specific Histone H3 Methyltransferases. *Nature* **2000**, *406* (6796), 593–599. https://doi.org/10.1038/35020506.

(30) Tamaru, H.; Zhang, X.; McMillen, D.; Singh, P. B.; Nakayama, J.; Grewal, S. I.; Allis, C. D.; Cheng, X.; Selker, E. U. Trimethylated Lysine 9 of Histone H3 Is a Mark for DNA Methylation in Neurospora Crassa. *Nat. Genet.* **2003**, *34* (1), 75–79. https://doi.org/10.1038/ng1143.

(31) Xiao, B.; Jing, C.; Wilson, J. R.; Walker, P. A.; Vasisht, N.; Kelly, G.; Howell, S.; Taylor, I. A.; Blackburn, G. M.; Gamblin, S. J. Structure and Catalytic Mechanism of the Human Histone Methyltransferase SET7/9. *Nature* **2003**, *421* (6923), 652–656. https://doi.org/10.1038/nature01378.

(32) Barski, A.; Cuddapah, S.; Cui, K.; Roh, T.-Y.; Schones, D. E.; Wang, Z.; Wei, G.; Chepelev, I.; Zhao, K. High-Resolution Profiling of Histone Methylations in the Human Genome. *Cell* **2007**, *129* (4), 823–837. https://doi.org/10.1016/j.cell.2007.05.009.

(33) Rosenfeld, J. A.; Wang, Z.; Schones, D. E.; Zhao, K.; DeSalle, R.; Zhang, M. Q. Determination of Enriched Histone Modifications in Non-Genic Portions of the Human Genome. *BMC Genomics* **2009**, *10* (1), 143. https://doi.org/10.1186/1471-2164-10-143.

(34) Goldknopf, I. L.; Taylor, C. W.; Baum, R. M.; Yeoman, L. C.; Olson, M. O.; Prestayko, A. W.; Busch, H. Isolation and Characterization of Protein A24, a "Histone-like" Non-Histone Chromosomal Protein. *J. Biol. Chem.* **1975**, *250* (18), 7182–7187. https://doi.org/10.1016/S0021-9258(19)40926-5.

(35) Matsui, S. I.; Seon, B. K.; Sandberg, A. A. Disappearance of a Structural Chromatin Protein A24 in Mitosis: Implications for Molecular Basis of Chromatin Condensation. *Proc. Natl. Acad. Sci. U. S. A.* **1979**, *76* (12), 6386–6390.

(36) West, M. H.; Bonner, W. M. Histone 2B Can Be Modified by the Attachment of Ubiquitin. *Nucleic Acids Res.* **1980**, *8* (20), 4671–4680. https://doi.org/10.1093/nar/8.20.4671.

(37) Wang, H.; Zhai, L.; Xu, J.; Joo, H.-Y.; Jackson, S.; Erdjument-Bromage, H.; Tempst, P.; Xiong, Y.; Zhang, Y. Histone H3 and H4 Ubiquitylation by the CUL4-DDB-ROC1 Ubiquitin Ligase Facilitates Cellular Response to DNA Damage. *Mol. Cell* **2006**, *22* (3), 383–394. https://doi.org/10.1016/j.molcel.2006.03.035.

(38) Mailand, N.; Bekker-Jensen, S.; Faustrup, H.; Melander, F.; Bartek, J.; Lukas, C.; Lukas, J. RNF8 Ubiquitylates Histones at DNA Double-Strand Breaks and Promotes Assembly of Repair Proteins. *Cell* **2007**, *131* (5), 887–900. https://doi.org/10.1016/j.cell.2007.09.040.

(39) Zhang, Y. Transcriptional Regulation by Histone Ubiquitination and Deubiquitination. *Genes Dev.* **2003**, *17* (22), 2733–2740. https://doi.org/10.1101/gad.1156403.

(40) Cao, J.; Yan, Q. Histone Ubiquitination and Deubiquitination in Transcription, DNA Damage Response, and Cancer. *Front. Oncol.* **2012**, *2*, 26. https://doi.org/10.3389/fonc.2012.00026.

(41) Dover, J.; Schneider, J.; Tawiah-Boateng, M. A.; Wood, A.; Dean, K.; Johnston, M.; Shilatifard, A. Methylation of Histone H3 by COMPASS Requires Ubiquitination of Histone H2B by Rad6*. *J. Biol. Chem.* **2002**, *277* (32), 28368–28371. https://doi.org/10.1074/jbc.C200348200.

(42) Sun, Z.-W.; Allis, C. D. Ubiquitination of Histone H2B Regulates H3 Methylation and Gene Silencing in Yeast. *Nature* **2002**, *418* (6893), 104–108. https://doi.org/10.1038/nature00883.

(43) Djebali, S.; Davis, C. A.; Merkel, A.; Dobin, A.; Lassmann, T.; Mortazavi, A. M.; Tanzer, A.; Lagarde, J.; Lin, W.; Schlesinger, F.; Xue, C.; Marinov, G. K.; Khatun, J.; Williams, B. A.; Zaleski, C.; Rozowsky, J.; Röder, M.; Kokocinski, F.; Abdelhamid, R. F.; Alioto, T.; Antoshechkin, I.; Baer, M. T.; Bar, N. S.; Batut, P.; Bell, K.; Bell, I.; Chakrabortty, S.; Chen, X.; Chrast, J.; Curado, J.;

Derrien, T.; Drenkow, J.; Dumais, E.; Dumais, J.; Duttagupta, R.; Falconnet, E.; Fastuca, M.; Fejes-Toth, K.; Ferreira, P.; Foissac, S.; Fullwood, M. J.; Gao, H.; Gonzalez, D.; Gordon, A.; Gunawardena, H.; Howald, C.; Jha, S.; Johnson, R.; Kapranov, P.; King, B.; Kingswood, C.; Luo, O. J.; Park, E.; Persaud, K.; Preall, J. B.; Ribeca, P.; Risk, B.; Robyr, D.; Sammeth, M.; Schaffer, L.; See, L.-H.; Shahab, A.; Skancke, J.; Suzuki, A. M.; Takahashi, H.; Tilgner, H.; Trout, D.; Walters, N.; Wang, H.; Wrobel, J.; Yu, Y.; Ruan, X.; Hayashizaki, Y.; Harrow, J.; Gerstein, M.; Hubbard, T.; Reymond, A.; Antonarakis, S. E.; Hannon, G.; Giddings, M. C.; Ruan, Y.; Wold, B.; Carninci, P.; Guigó, R.; Gingeras, T. R. Landscape of Transcription in Human Cells. *Nature* **2012**, *489* (7414), 101–108. https://doi.org/10.1038/nature11233.

(44) Bartel, D. P. MicroRNAs: Target Recognition and Regulatory Functions. *Cell* **2009**, *136* (2), 215–233. https://doi.org/10.1016/j.cell.2009.01.002.

(45) Thakur, J.; Henikoff, S. Architectural RNA in Chromatin Organization. *Biochem. Soc. Trans.* **2020**, *48* (5), 1967–1978. https://doi.org/10.1042/BST20191226.

(46) Liu, N.; Pan, T. RNA Epigenetics. *Transl. Res. J. Lab. Clin. Med.* **2015**, *165* (1), 28–35. https://doi.org/10.1016/j.trsl.2014.04.003.

(47) Willbanks, A.; Wood, S.; Cheng, J. X. RNA Epigenetics: Fine-Tuning Chromatin Plasticity and Transcriptional Regulation, and the Implications in Human Diseases. *Genes* **2021**, *12* (5). https://doi.org/10.3390/genes12050627.

(48) Piekna-Przybylska, D.; Decatur, W. A.; Fournier, M. J. The 3D rRNA Modification Maps Database: With Interactive Tools for Ribosome Analysis. *Nucleic Acids Res.* **2008**, *36* (Database issue), D178–D183. https://doi.org/10.1093/nar/gkm855.

(49) Fu, Y.; Jia, G.; Pang, X.; Wang, R. N.; Wang, X.; Li, C. J.; Smemo, S.; Dai, Q.; Bailey, K. A.; Nobrega, M. A.; Han, K.; Cui, Q.; He, C. FTO-Mediated Formation of N6-Hydroxymethyladenosine and N6-Formyladenosine in Mammalian RNA. *Nat. Commun.* **2013**, *4*, 1798. https://doi.org/10.1038/ncomms2822.

(50) Jia, G.; Fu, Y.; Zhao, X.; Dai, Q.; Zheng, G.; Yang, Y.; Yi, C.; Lindahl, T.; Pan, T.; Yang, Y.-G.; He, C. N6-Methyladenosine in Nuclear RNA Is a Major Substrate of the Obesity-Associated FTO. *Nat. Chem. Biol.* **2011**, *7* (12), 885–887. https://doi.org/10.1038/nchembio.687.

(51) Zheng, G.; Dahl, J. A.; Niu, Y.; Fedorcsak, P.; Huang, C.-M.; Li, C. J.; Vågbø, C. B.; Shi, Y.; Wang, W.-L.; Song, S.-H.; Lu, Z.; Bosmans, R. P. G.; Dai, Q.; Hao, Y.-J.; Yang, X.; Zhao, W.-M.; Tong, W.-M.; Wang, X.-J.; Bogdan, F.; Furu, K.; Fu, Y.; Jia, G.; Zhao, X.; Liu, J.; Krokan, H. E.; Klungland, A.; Yang, Y.-G.; He, C. ALKBH5 Is a Mammalian RNA Demethylase That Impacts RNA Metabolism and Mouse Fertility. *Mol. Cell* **2013**, *49* (1), 18–29. https://doi.org/10.1016/j.molcel.2012.10.015.

(52) Heiliger, K.-J.; Hess, J.; Vitagliano, D.; Salerno, P.; Braselmann, H.; Salvatore, G.; Ugolini, C.; Summerer, I.; Bogdanova, T.; Unger, K.; Thomas, G.; Santoro, M.; Zitzelsberger, H. Novel Candidate Genes of Thyroid Tumourigenesis Identified in Trk-T1 Transgenic Mice. *Endocr. Relat. Cancer* **2012**, *19* (3), 409–421. https://doi.org/10.1530/ERC-11-0387.

(53) Chen, Y.; Sprung, R.; Tang, Y.; Ball, H.; Sangras, B.; Kim, S. C.; Falck, J. R.; Peng, J.; Gu, W.; Zhao, Y. Lysine Propionylation and Butyrylation Are Novel Post-Translational Modifications in Histones. *Mol. Cell. Proteomics MCP* **2007**, *6* (5), 812–819. https://doi.org/10.1074/mcp.M700021-MCP200.

(54) Tan, M.; Luo, H.; Lee, S.; Jin, F.; Yang, J. S.; Montellier, E.; Buchou, T.; Cheng, Z.; Rousseaux, S.; Rajagopal, N.; Lu, Z.; Ye, Z.; Zhu, Q.; Wysocka, J.; Ye, Y.; Khochbin, S.; Ren, B.; Zhao, Y. Identification of 67 Histone Marks and Histone Lysine Crotonylation as a New Type of Histone Modification. *Cell* **2011**, *146* (6), 1016–1028. https://doi.org/10.1016/j.cell.2011.08.008.

(55) Ntorla, A.; Burgoyne, J. R. The Regulation and Function of Histone Crotonylation. *Front. Cell Dev. Biol.* **2021**, *9*, 624914. https://doi.org/10.3389/fcell.2021.624914.

(56) Yuan, H.; Marmorstein, R. Histone Acetyltransferases: Rising Ancient Counterparts to Protein Kinases. *Biopolymers* **2013**, *99* (2), 98–111. https://doi.org/10.1002/bip.22128.

(57) Grunstein, M. Histone Acetylation in Chromatin Structure and Transcription. *Nature* **1997**, *389* (6649), 349–352. https://doi.org/10.1038/38664.

(58) New, M.; Olzscha, H.; La Thangue, N. B. HDAC Inhibitor-Based Therapies: Can We Interpret the Code? *Mol. Oncol.* **2012**, *6* (6), 637–656. https://doi.org/10.1016/j.molonc.2012.09.003.

(59)   Gregoretti, I.; Lee, Y.-M.; Goodson, H. V. Molecular Evolution of the Histone Deacetylase Family: Functional Implications of Phylogenetic Analysis. *J. Mol. Biol.* **2004**, *338* (1), 17–31. https://doi.org/10.1016/j.jmb.2004.02.006.

(60)   Haberland, M.; Montgomery, R. L.; Olson, E. N. The Many Roles of Histone Deacetylases in Development and Physiology: Implications for Disease and Therapy. *Nat. Rev. Genet.* **2009**, *10* (1), 32–42. https://doi.org/10.1038/nrg2485.

(61)   Parbin, S.; Kar, S.; Shilpi, A.; Sengupta, D.; Deb, M.; Rath, S. K.; Patra, S. K. Histone Deacetylases: A Saga of Perturbed Acetylation Homeostasis in Cancer. *J. Histochem. Cytochem.* **2014**, *62* (1), 11–33. https://doi.org/10.1369/0022155413506582.

(62)   Hu, J.; Jing, H.; Lin, H. Sirtuin Inhibitors as Anticancer Agents. *Future Med. Chem.* **2014**, *6* (8), 945–966. https://doi.org/10.4155/fmc.14.44.

(63)   Yang, X.-J.; Seto, E. Collaborative Spirit of Histone Deacetylases in Regulating Chromatin Structure and Gene Expression. *Curr. Opin. Genet. Dev.* **2003**, *13* (2), 143–153. https://doi.org/10.1016/S0959-437X(03)00015-7.

(64)   Basta, J.; Rauchman, M. The Nucleosome Remodeling and Deacetylase (NuRD) Complex in Development and Disease. *Transl. Res. J. Lab. Clin. Med.* **2015**, *165* (1), 36–47. https://doi.org/10.1016/j.trsl.2014.05.003.

(65)   Turnbull, R. E.; Fairall, L.; Saleh, A.; Kelsall, E.; Morris, K. L.; Ragan, T. J.; Savva, C. G.; Chandru, A.; Millard, C. J.; Makarova, O. V.; Smith, C. J.; Roseman, A. M.; Fry, A. M.; Cowley, S. M.; Schwabe, J. W. R. The MiDAC Histone Deacetylase Complex Is Essential for Embryonic Development and Has a Unique Multivalent Structure. *Nat. Commun.* **2020**, *11* (1), 3252. https://doi.org/10.1038/s41467-020-17078-8.

(66)   Marchion, D. C.; Bicaku, E.; Turner, J. G.; Schmitt, M. L.; Morelli, D. R.; Munster, P. N. HDAC2 Regulates Chromatin Plasticity and Enhances DNA Vulnerability. *Mol. Cancer Ther.* **2009**, *8* (4), 794–801. https://doi.org/10.1158/1535-7163.MCT-08-0985.

(67)   Luo, J.; Su, F.; Chen, D.; Shiloh, A.; Gu, W. Deacetylation of P53 Modulates Its Effect on Cell Growth and Apoptosis. *Nature* **2000**, *408* (6810), 377–381. https://doi.org/10.1038/35042612.

(68)   Gu, W.; Roeder, R. G. Activation of P53 Sequence-Specific DNA Binding by Acetylation of the P53 C-Terminal Domain. *Cell* **1997**, *90* (4), 595–606. https://doi.org/10.1016/s0092-8674(00)80521-8.

(69)   Harms, K. L.; Chen, X. Histone Deacetylase 2 Modulates P53 Transcriptional Activities through Regulation of P53-DNA Binding Activity. *Cancer Res.* **2007**, *67* (7), 3145–3152. https://doi.org/10.1158/0008-5472.CAN-06-4397.

(70)   Guenther, M. G.; Lane, W. S.; Fischle, W.; Verdin, E.; Lazar, M. A.; Shiekhattar, R. A Core SMRT Corepressor Complex Containing HDAC3 and TBL1, a WD40-Repeat Protein Linked to Deafness. *Genes Dev.* **2000**, *14* (9), 1048–1057.

(71)   Oberoi, J.; Fairall, L.; Watson, P. J.; Yang, J.-C.; Czimmerer, Z.; Kampmann, T.; Goult, B. T.; Greenwood, J. A.; Gooch, J. T.; Kallenberger, B. C.; Nagy, L.; Neuhaus, D.; Schwabe, J. W. R. Structural Basis for the Assembly of the SMRT/NCoR Core Transcriptional Repression Machinery. *Nat. Struct. Mol. Biol.* **2011**, *18* (2), 177–184. https://doi.org/10.1038/nsmb.1983.

(72)   Wong, M. M.; Guo, C.; Zhang, J. Nuclear Receptor Corepressor Complexes in Cancer: Mechanism, Function and Regulation. *Am. J. Clin. Exp. Urol.* **2014**, *2* (3), 169–187.

(73)   Yang, X.-J.; Seto, E. The Rpd3/Hda1 Family of Lysine Deacetylases: From Bacteria and Yeast to Mice and Men. *Nat. Rev. Mol. Cell Biol.* **2008**, *9* (3), 206–218. https://doi.org/10.1038/nrm2346.

(74)   Dokmanovic, M.; Clarke, C.; Marks, P. A. Histone Deacetylase Inhibitors: Overview and Perspectives. *Mol. Cancer Res.* **2007**, *5* (10), 981–989. https://doi.org/10.1158/1541-7786.MCR-07-0324.

(75)   Witt, O.; Deubzer, H. E.; Milde, T.; Oehme, I. HDAC Family: What Are the Cancer Relevant Targets? *Cancer Lett.* **2009**, *277* (1), 8–21. https://doi.org/10.1016/j.canlet.2008.08.016.

(76)   Hudson, G. M.; Watson, P. J.; Fairall, L.; Jamieson, A. G.; Schwabe, J. W. R. Insights into the Recruitment of Class IIa Histone Deacetylases (HDACs) to the SMRT/NCoR Transcriptional Repression Complex*. *J. Biol. Chem.* **2015**, *290* (29), 18237–18244. https://doi.org/10.1074/jbc.M115.661058.

(77)   Park, S.-Y.; Kim, J.-S. A Short Guide to Histone Deacetylases Including Recent Progress on Class II Enzymes. *Exp. Mol. Med.* **2020**, *52* (2), 204–212. https://doi.org/10.1038/s12276-020-0382-4.

(78)   Mihaylova, M. M.; Shaw, R. J. Metabolic Reprogramming by Class I and II Histone Deacetylases. *Trends Endocrinol. Metab.* **2013**, *24* (1), 48–57. https://doi.org/10.1016/j.tem.2012.09.003.

(79)   Hubbert, C.; Guardiola, A.; Shao, R.; Kawaguchi, Y.; Ito, A.; Nixon, A.; Yoshida, M.; Wang, X.-F.; Yao, T.-P. HDAC6 Is a Microtubule-Associated Deacetylase. *Nature* **2002**, *417* (6887), 455–458. https://doi.org/10.1038/417455a.

(80)   Matsuyama, A.; Shimazu, T.; Sumida, Y.; Saito, A.; Yoshimatsu, Y.; Seigneurin-Berny, D.; Osada, H.; Komatsu, Y.; Nishino, N.; Khochbin, S.; Horinouchi, S.; Yoshida, M. In Vivo Destabilization of Dynamic Microtubules by HDAC6-Mediated Deacetylation. *EMBO J.* **2002**, *21* (24), 6820–6831. https://doi.org/10.1093/emboj/cdf682.

(81)   Fischer, D. D.; Cai, R.; Bhatia, U.; Asselbergs, F. A. M.; Song, C.; Terry, R.; Trogani, N.; Widmer, R.; Atadja, P.; Cohen, D. Isolation and Characterization of a Novel Class II Histone Deacetylase, HDAC10*. *J. Biol. Chem.* **2002**, *277* (8), 6656–6666. https://doi.org/10.1074/jbc.M108055200.

(82)   Guardiola, A. R.; Yao, T.-P. Molecular Cloning and Characterization of a Novel Histone Deacetylase HDAC10*. *J. Biol. Chem.* **2002**, *277* (5), 3350–3356. https://doi.org/10.1074/jbc.M109861200.

(83)   Kao, H.-Y.; Lee, C.-H.; Komarov, A.; Han, C. C.; Evans, R. M. Isolation and Characterization of Mammalian HDAC10, a Novel Histone Deacetylase*. *J. Biol. Chem.* **2002**, *277* (1), 187–193. https://doi.org/10.1074/jbc.M108931200.

(84)   Tong, J. J.; Liu, J.; Bertos, N. R.; Yang, X.-J. Identification of HDAC10, a Novel Class II Human Histone Deacetylase Containing a Leucine-Rich Domain. *Nucleic Acids Res.* **2002**, *30* (5), 1114–1123.

(85)   Hai, Y.; Shinsky, S. A.; Porter, N. J.; Christianson, D. W. Histone Deacetylase 10 Structure and Molecular Function as a Polyamine Deacetylase. *Nat. Commun.* **2017**, *8* (1), 15368. https://doi.org/10.1038/ncomms15368.

(86)   Núñez-Álvarez, Y.; Suelves, M. HDAC11: A Multifaceted Histone Deacetylase with Proficient Fatty Deacylase Activity and Its Roles in Physiological Processes. *FEBS J.* **2022**, *289* (10), 2771–2792. https://doi.org/10.1111/febs.15895.

(87)   Gao, L.; Cueto, M. A.; Asselbergs, F.; Atadja, P. Cloning and Functional Characterization of HDAC11, a Novel Member of the Human Histone Deacetylase Family*. *J. Biol. Chem.* **2002**, *277* (28), 25748–25755. https://doi.org/10.1074/jbc.M111871200.

(88)   Villar-Garea, A.; Esteller, M. Histone Deacetylase Inhibitors: Understanding a New Wave of Anticancer Agents. *Int. J. Cancer* **2004**, *112* (2), 171–178. https://doi.org/10.1002/ijc.20372.

(89)   Finnin, M. S.; Donigian, J. R.; Cohen, A.; Richon, V. M.; Rifkind, R. A.; Marks, P. A.; Breslow, R.; Pavletich, N. P. Structures of a Histone Deacetylase Homologue Bound to the TSA and SAHA Inhibitors. *Nature* **1999**, *401* (6749), 188–193. https://doi.org/10.1038/43710.

(90)   Watson, P. J.; Millard, C. J.; Riley, A. M.; Robertson, N. S.; Wright, L. C.; Godage, H. Y.; Cowley, S. M.; Jamieson, A. G.; Potter, B. V. L.; Schwabe, J. W. R. Insights into the Activation Mechanism of Class I HDAC Complexes by Inositol Phosphates. *Nat. Commun.* **2016**, *7*, 11262. https://doi.org/10.1038/ncomms11262.

(91)   Phiel, C. J.; Zhang, F.; Huang, E. Y.; Guenther, M. G.; Lazar, M. A.; Klein, P. S. Histone Deacetylase Is a Direct Target of Valproic Acid, a Potent Anticonvulsant, Mood Stabilizer, and Teratogen*. *J. Biol. Chem.* **2001**, *276* (39), 36734–36741. https://doi.org/10.1074/jbc.M101287200.

(92)   Boivin, A.-J.; Momparler, L. F.; Hurtubise, A.; Momparler, R. L. Antineoplastic Action of 5-Aza-2'-Deoxycytidine and Phenylbutyrate on Human Lung Carcinoma Cells. *Anticancer. Drugs* **2002**, *13* (8), 869–874. https://doi.org/10.1097/00001813-200209000-00013.

(93)   Yoshida, M.; Kijima, M.; Akita, M.; Beppu, T. Potent and Specific Inhibition of Mammalian Histone Deacetylase Both in Vivo and in Vitro by Trichostatin A. *J. Biol. Chem.* **1990**, *265* (28), 17174–17179. https://doi.org/10.1016/S0021-9258(17)44885-X.

(94)   Eckschlager, T.; Plch, J.; Stiborova, M.; Hrabeta, J. Histone Deacetylase Inhibitors as Anticancer Drugs. *Int. J. Mol. Sci.* **2017**, *18* (7), 1414. https://doi.org/10.3390/ijms18071414.

(95) Ho, T. C. S.; Chan, A. H. Y.; Ganesan, A. Thirty Years of HDAC Inhibitors: 2020 Insight and Hindsight. *J. Med. Chem.* **2020**, *63* (21), 12460–12484. https://doi.org/10.1021/acs.jmedchem.0c00830.

(96) Nakajima, H.; Kim, Y. B.; Terano, H.; Yoshida, M.; Horinouchi, S. FR901228, a Potent Antitumor Antibiotic, Is a Novel Histone Deacetylase Inhibitor. *Exp. Cell Res.* **1998**, *241* (1), 126–133. https://doi.org/10.1006/excr.1998.4027.

(97) Shah, R. R. Safety and Tolerability of Histone Deacetylase (HDAC) Inhibitors in Oncology. *Drug Saf.* **2019**, *42* (2), 235–245. https://doi.org/10.1007/s40264-018-0773-9.

(98) Gryder, B. E.; Sodji, Q. H.; Oyelere, A. K. Targeted Cancer Therapy: Giving Histone Deacetylase Inhibitors All They Need to Succeed. *Future Med. Chem.* **2012**, *4* (4), 505–524. https://doi.org/10.4155/fmc.12.3.

(99) *Withdrawal assessment report for Vorinostat*. https://www.ema.europa.eu/en/documents/withdrawal-report/withdrawal-assessment-report-vorinostat-msd_en.pdf.

(100) *Refusal of the marketing authorisation for Istodax (romidepsin)*. https://www.ema.europa.eu/en/documents/smop-initial/questions-answers-refusal-marketing-authorisation-istodax-romidepsin-outcome-re-examination_en.pdf.

(101) Berger, M. R.; Richter, H.; Seelig, M. H.; Eibl, H.; Schmähl, D. New Cytostatics—More Activity and Less Toxicity. *Cancer Treat. Rev.* **1990**, *17* (2), 143–154. https://doi.org/10.1016/0305-7372(90)90039-I.

(102) LoRusso, P. M.; Demchik, L.; Foster, B.; Knight, J.; Bissery, M.-C.; Polin, L. M.; Leopold, W. R.; Corbett, T. H. Preclinical Antitumor Activity of CI-994. *Invest. New Drugs* **1996**, *14* (4), 349–356. https://doi.org/10.1007/BF00180810.

(103) Loprevite, M.; Tiseo, M.; Grossi, F.; Scolaro, T.; Semino, C.; Pandolfi, A.; Favoni, R.; Ardizzoni, A. In Vitro Study of CI-994, a Histone Deacetylase Inhibitor, in Non-Small Cell Lung Cancer Cell Lines. *Oncol. Res.* **2005**, *15* (1), 39–48. https://doi.org/10.3727/096504005775082066.

(104) Khan, N.; Jeffers, M.; Kumar, S.; Hackett, C.; Boldog, F.; Khramtsov, N.; Qian, X.; Mills, E.; Berghs, S. C.; Carey, N.; Finn, P. W.; Collins, L. S.; Tumber, A.; Ritchie, J. W.; Jensen, P. B.; Lichenstein, H. S.; Sehested, M. Determination of the Class and Isoform Selectivity of Small-Molecule Histone Deacetylase Inhibitors. *Biochem. J.* **2008**, *409* (2), 581–589. https://doi.org/10.1042/BJ20070779.

(105) Fournel, M.; Bonfils, C.; Hou, Y.; Yan, P. T.; Trachy-Bourget, M.-C.; Kalita, A.; Liu, J.; Lu, A.-H.; Zhou, N. Z.; Robert, M.-F.; Gillespie, J.; Wang, J. J.; Ste-Croix, H.; Rahil, J.; Lefebvre, S.; Moradei, O.; Delorme, D.; Macleod, A. R.; Besterman, J. M.; Li, Z. MGCD0103, a Novel Isotype-Selective Histone Deacetylase Inhibitor, Has Broad Spectrum Antitumor Activity in Vitro and in Vivo. *Mol. Cancer Ther.* **2008**, *7* (4), 759–768. https://doi.org/10.1158/1535-7163.MCT-07-2026.

(106) Bretz, A. C.; Parnitzke, U.; Kronthaler, K.; Dreker, T.; Bartz, R.; Hermann, F.; Ammendola, A.; Wulff, T.; Hamm, S. Domatinostat Favors the Immunotherapy Response by Modulating the Tumor Immune Microenvironment (TIME). *J. Immunother. Cancer* **2019**, *7* (1), 294. https://doi.org/10.1186/s40425-019-0745-3.

(107) Eyre, T. A.; Collins, G. P.; Gupta, A.; Coupe, N.; Sheikh, S.; Whittaker, J.; Wang, L. M.; Campo, L.; Soilleux, E.; Tysoe, F.; Cousins, R.; La Thangue, N.; Folkes, L. K.; Stratford, M. R. L.; Kerr, D.; Middleton, M. R. A Phase 1 Study to Assess the Safety, Tolerability, and Pharmacokinetics of CXD101 in Patients with Advanced Cancer. *Cancer* **2019**, *125* (1), 99–108. https://doi.org/10.1002/cncr.31791.

(108) Moradei, O.; Leit, S.; Zhou, N.; Fréchette, S.; Paquin, I.; Raeppel, S.; Gaudette, F.; Bouchain, G.; Woo, S. H.; Vaisburg, A.; Fournel, M.; Kalita, A.; Lu, A.; Trachy-Bourget, M.-C.; Yan, P. T.; Liu, J.; Li, Z.; Rahil, J.; MacLeod, A. R.; Besterman, J. M.; Delorme, D. Substituted N-(2-Aminophenyl)-Benzamides, (E)-N-(2-Aminophenyl)-Acrylamides and Their Analogues: Novel Classes of Histone Deacetylase Inhibitors. *Bioorg. Med. Chem. Lett.* **2006**, *16* (15), 4048–4052. https://doi.org/10.1016/j.bmcl.2006.05.005.

(109) Lu, X.; Ning, Z.; Li, Z.; Cao, H.; Wang, X. Development of Chidamide for Peripheral T-Cell Lymphoma, the First Orphan Drug Approved in China. *Intractable Rare Dis. Res.* **2016**, *5* (3), 185–191. https://doi.org/10.5582/irdr.2016.01024.

(110) Rai, S.; Kim, W. S.; Ando, K.; Choi, I.; Izutsu, K.; Tsukamoto, N.; Yokoyama, M.; Tsukasaki, K.; Kuroda, J.; Ando, J.; Hidaka, M.; Koh, Y.; Shibayama, H.; Uchida, T.; Yang, D. H.; Ishitsuka, K.; Ishizawa, K.; Kim, J. S.; Lee, H. G.; Minami, H.; Eom, H. S.; Kurosawa, M.; Lee, J. H.; Lee, J. S.; Lee, W. S.; Nagai, H.; Shindo, T.; Yoon, D. H.; Yoshida, S.; Gillings, M.; Onogi, H.; Tobinai, K. Oral HDAC Inhibitor Tucidinostat in Patients with Relapsed or Refractory Peripheral T-Cell Lymphoma: Phase IIb Results. *Haematologica* **2023**, *108* (3), 811–821. https://doi.org/10.3324/haematol.2022.280996.

(111) *Marketing Approval of HBI-8000 (Tucidinostat) for Relapsed or Refractory ATLL Treatment in Japan*. https://www.meiji.com/global/news/2021/pdf/210624_01.pdf.

(112) Bressi, J. C.; Jennings, A. J.; Skene, R.; Wu, Y.; Melkus, R.; Jong, R. D.; O'Connell, S.; Grimshaw, C. E.; Navre, M.; Gangloff, A. R. Exploration of the HDAC2 Foot Pocket: Synthesis and SAR of Substituted N-(2-Aminophenyl)Benzamides. *Bioorg. Med. Chem. Lett.* **2010**, *20* (10), 3142–3145. https://doi.org/10.1016/j.bmcl.2010.03.091.

(113) Lauffer, B. E. L.; Mintzer, R.; Fong, R.; Mukund, S.; Tam, C.; Zilberleyb, I.; Flicke, B.; Ritscher, A.; Fedorowicz, G.; Vallero, R.; Ortwine, D. F.; Gunzner, J.; Modrusan, Z.; Neumann, L.; Koth, C. M.; Lupardus, P. J.; Kaminker, J. S.; Heise, C. E.; Steiner, P. Histone Deacetylase (HDAC) Inhibitor Kinetic Rate Constants Correlate with Cellular Histone Acetylation but Not Transcription and Cell Viability. *J. Biol. Chem.* **2013**, *288* (37), 26926–26943. https://doi.org/10.1074/jbc.M113.490706.

(114) Moradei, O. M.; Mallais, T. C.; Frechette, S.; Paquin, I.; Tessier, P. E.; Leit, S. M.; Fournel, M.; Bonfils, C.; Trachy-Bourget, M.-C.; Liu, J.; Yan, T. P.; Lu, A.-H.; Rahil, J.; Wang, J.; Lefebvre, S.; Li, Z.; Vaisburg, A. F.; Besterman, J. M. Novel Aminophenyl Benzamide-Type Histone Deacetylase Inhibitors with Enhanced Potency and Selectivity. *J. Med. Chem.* **2007**, *50* (23), 5543–5546. https://doi.org/10.1021/jm701079h.

(115) Kattar, S. D.; Surdi, L. M.; Zabierek, A.; Methot, J. L.; Middleton, R. E.; Hughes, B.; Szewczak, A. A.; Dahlberg, W. K.; Kral, A. M.; Ozerova, N.; Fleming, J. C.; Wang, H.; Secrist, P.; Harsch, A.; Hamill, J. E.; Cruz, J. C.; Kenific, C. M.; Chenard, M.; Miller, T. A.; Berk, S. C.; Tempest, P. Parallel Medicinal Chemistry Approaches to Selective HDAC1/HDAC2 Inhibitor (SHI-1:2) Optimization. *Bioorg. Med. Chem. Lett.* **2009**, *19* (4), 1168–1172. https://doi.org/10.1016/j.bmcl.2008.12.083.

(116) Methot, J. L.; Chakravarty, P. K.; Chenard, M.; Close, J.; Cruz, J. C.; Dahlberg, W. K.; Fleming, J.; Hamblett, C. L.; Hamill, J. E.; Harrington, P.; Harsch, A.; Heidebrecht, R.; Hughes, B.; Jung, J.; Kenific, C. M.; Kral, A. M.; Meinke, P. T.; Middleton, R. E.; Ozerova, N.; Sloman, D. L.; Stanton, M. G.; Szewczak, A. A.; Tyagarajan, S.; Witter, D. J.; Paul Secrist, J.; Miller, T. A. Exploration of the Internal Cavity of Histone Deacetylase (HDAC) with Selective HDAC1/HDAC2 Inhibitors (SHI-1:2). *Bioorg. Med. Chem. Lett.* **2008**, *18* (3), 973–978. https://doi.org/10.1016/j.bmcl.2007.12.031.

(117) Wagner, F. F.; Zhang, Y.-L.; Fass, D. M.; Joseph, N.; Gale, J. P.; Weïwer, M.; McCarren, P.; Fisher, S. L.; Kaya, T.; Zhao, W.-N.; Reis, S. A.; Hennig, K. M.; Thomas, M.; Lemercier, B. C.; Lewis, M. C.; Guan, J. S.; Moyer, M. P.; Scolnick, E.; Haggarty, S. J.; Tsai, L.-H.; Holson, E. B. Kinetically Selective Inhibitors of Histone Deacetylase 2 (HDAC2) as Cognition Enhancers †Electronic Supplementary Information (ESI) Available: Compound Synthesis and Characterization; 1HNMR Spectra, HPLC or UPLC Spectral Traces; HDAC Enzymatic Assay Protocol; IC50s for Representative Compounds for HDACs 1–9; Full Kinetic Parameters for BRD4884 and BRD6688; Progression and Dissociation Curves for BRD6688; Pharmacokinetic Graphs and Parameters for Representative Compounds; Kinetic Selectivity Profiles for BRD4884 and BRD6688; in Vitro Pharmacology, Pharmacokinetic Protocols; Target Engagement Simulation Protocol; Molecular Modelling and Docking Protocols; Neuronal Cell Based Assay Protocol, Behavioural Studies Protocols. See DOI: 10.1039/C4sc02130d Click Here for Additional Data File. *Chem. Sci.* **2015**, *6* (1), 804–815. https://doi.org/10.1039/c4sc02130d.

(118) Bresciani, A.; Ontoria, J. M.; Biancofiore, I.; Cellucci, A.; Ciammaichella, A.; Di Marco, A.; Ferrigno, F.; Francone, A.; Malancona, S.; Monteagudo, E.; Nizi, E.; Pace, P.; Ponzi, S.; Rossetti, I.; Veneziano, M.; Summa, V.; Harper, S. Improved Selective Class I HDAC and Novel Selective HDAC3 Inhibitors: Beyond Hydroxamic Acids and Benzamides. *ACS Med. Chem. Lett.* **2019**, *10* (4), 481–486. https://doi.org/10.1021/acsmedchemlett.8b00517.

(119) Liu, J.; Kelly, J.; Yu, W.; Clausen, D.; Yu, Y.; Kim, H.; Duffy, J. L.; Chung, C. C.; Myers, R. W.; Carroll, S.; Klein, D. J.; Fells, J.; Holloway, M. K.; Wu, J.; Wu, G.; Howell, B. J.; Barnard, R. J. O.; Kozlowski, J. A. Selective Class I HDAC Inhibitors Based on Aryl Ketone Zinc Binding Induce HIV-1 Protein for Clearance. *ACS Med. Chem. Lett.* **2020**, *11* (7), 1476–1483. https://doi.org/10.1021/acsmedchemlett.0c00302.

(120) Liu, J.; Yu, Y.; Kelly, J.; Sha, D.; Alhassan, A.-B.; Yu, W.; Maletic, M. M.; Duffy, J. L.; Klein, D. J.; Holloway, M. K.; Carroll, S.; Howell, B. J.; Barnard, R. J. O.; Wolkenberg, S.; Kozlowski, J. A. Discovery of Highly Selective and Potent HDAC3 Inhibitors Based on a 2-Substituted Benzamide Zinc Binding Group. *ACS Med. Chem. Lett.* **2020**, *11* (12), 2476–2483. https://doi.org/10.1021/acsmedchemlett.0c00462.

(121) Millard, C. J.; Watson, P. J.; Fairall, L.; Schwabe, J. W. R. Targeting Class I Histone Deacetylases in a "Complex" Environment. *Trends Pharmacol. Sci.* **2017**, *38* (4), 363–377. https://doi.org/10.1016/j.tips.2016.12.006.

(122) Archibald, L. J.; Brown, E. A.; Millard, C. J.; Watson, P. J.; Robertson, N. S.; Wang, S.; Schwabe, J. W. R.; Jamieson, A. G. Hydroxamic Acid-Modified Peptide Library Provides Insights into the Molecular Basis for the Substrate Selectivity of HDAC Corepressor Complexes. *ACS Chem. Biol.* **2022**, *17* (9), 2572–2582. https://doi.org/10.1021/acschembio.2c00510.

(123) Bantscheff, M.; Hopf, C.; Savitski, M. M.; Dittmann, A.; Grandi, P.; Michon, A.-M.; Schlegl, J.; Abraham, Y.; Becher, I.; Bergamini, G.; Boesche, M.; Delling, M.; Dümpelfeld, B.; Eberhard, D.; Huthmacher, C.; Mathieson, T.; Poeckel, D.; Reader, V.; Strunk, K.; Sweetman, G.; Kruse, U.; Neubauer, G.; Ramsden, N. G.; Drewes, G. Chemoproteomics Profiling of HDAC Inhibitors Reveals Selective Targeting of HDAC Complexes. *Nat. Biotechnol.* **2011**, *29* (3), 255–265. https://doi.org/10.1038/nbt.1759.

(124) Pan, Z.; Zhao, Y.; Wang, X.; Xie, X.; Liu, M.; Zhang, K.; Wang, L.; Bai, D.; Foster, L. J.; Shu, R.; He, G. Targeting Bromodomain-Containing Proteins: Research Advances of Drug Discovery. *Mol. Biomed.* **2023**, *4* (1), 13. https://doi.org/10.1186/s43556-023-00127-1.

(125) Yang, X.-J.; Ogryzko, V. V.; Nishikawa, J.; Howard, B. H.; Nakatani, Y. A P300/CBP-Associated Factor That Competes with the Adenoviral Oncoprotein E1A. *Nature* **1996**, *382* (6589), 319–324. https://doi.org/10.1038/382319a0.

(126) Dhalluin, C.; Carlson, J. E.; Zeng, L.; He, C.; Aggarwal, A. K.; Zhou, M.-M. Structure and Ligand of a Histone Acetyltransferase Bromodomain. *Nature* **1999**, *399* (6735), 491–496. https://doi.org/10.1038/20974.

(127) Kuo, M.-H.; Brownell, J. E.; Sobel, R. E.; Ranalli, T. A.; Cook, R. G.; Edmondson, D. G.; Roth, S. Y.; Allis, C. D. Transcription-Linked Acetylation by Gcn5p of Histones H3 and H4 at Specific Lysines. *Nature* **1996**, *383* (6597), 269–272. https://doi.org/10.1038/383269a0.

(128) Brownell, J. E.; Zhou, J.; Ranalli, T.; Kobayashi, R.; Edmondson, D. G.; Roth, S. Y.; Allis, C. D. Tetrahymena Histone Acetyltransferase A: A Homolog to Yeast Gcn5p Linking Histone Acetylation to Gene Activation. *Cell* **1996**, *84* (6), 843–851. https://doi.org/10.1016/S0092-8674(00)81063-6.

(129) Gregory, G. D.; Vakoc, C. R.; Rozovskaia, T.; Zheng, X.; Patel, S.; Nakamura, T.; Canaani, E.; Blobel, G. A. Mammalian ASH1L Is a Histone Methyltransferase That Occupies the Transcribed Region of Active Genes. *Mol. Cell. Biol.* **2007**, *27* (24), 8466–8479. https://doi.org/10.1128/MCB.00993-07.

(130) Malik, S.; Bhaumik, S. R. Mixed Lineage Leukemia: Histone H3 Lysine 4 Methyltransferases from Yeast to Human. *FEBS J.* **2010**, *277* (8), 1805–1821. https://doi.org/10.1111/j.1742-4658.2010.07607.x.

(131) Cavellán, E.; Asp, P.; Percipalle, P.; Farrants, A.-K. Ö. The WSTF-SNF2h Chromatin Remodeling Complex Interacts with Several Nuclear Proteins in Transcription*. *J. Biol. Chem.* **2006**, *281* (24), 16264–16271. https://doi.org/10.1074/jbc.M600233200.

(132) Mashtalir, N.; D'Avino, A. R.; Michel, B. C.; Luo, J.; Pan, J.; Otto, J. E.; Zullow, H. J.; McKenzie, Z. M.; Kubiak, R. L.; St. Pierre, R.; Valencia, A. M.; Poynter, S. J.; Cassel, S. H.; Ranish, J. A.; Kadoch, C. Modular Organization and Assembly of SWI/SNF Family Chromatin Remodeling Complexes. *Cell* **2018**, *175* (5), 1272-1288.e20. https://doi.org/10.1016/j.cell.2018.09.032.

(133) Jain, A. K.; Barton, M. C. Regulation of P53: TRIM24 Enters the RING. *Cell Cycle* **2009**, *8* (22), 3668–3674. https://doi.org/10.4161/cc.8.22.9979.

(134) Wanior, M.; Preuss, F.; Ni, X.; Krämer, A.; Mathea, S.; Göbel, T.; Heidenreich, D.; Simonyi, S.; Kahnt, A. S.; Joerger, A. C.; Knapp, S. Pan-SMARCA/PB1 Bromodomain Inhibitors and Their Role in Regulating Adipogenesis. *J. Med. Chem.* **2020**, *63* (23), 14680–14699. https://doi.org/10.1021/acs.jmedchem.0c01242.

(135) Meslamani, J.; Smith, S. G.; Sanchez, R.; Zhou, M.-M. Structural Features and Inhibitors of Bromodomains. *Drug Discov. Today Technol.* **2016**, *19*, 3–15. https://doi.org/10.1016/j.ddtec.2016.09.001.

(136) Filippakopoulos, P.; Picaud, S.; Mangos, M.; Keates, T.; Lambert, J.-P.; Barsyte-Lovejoy, D.; Felletar, I.; Volkmer, R.; Müller, S.; Pawson, T.; Gingras, A.-C.; Arrowsmith, C. H.; Knapp, S. Histone Recognition and Large-Scale Structural Analysis of the Human Bromodomain Family. *Cell* **2012**, *149* (1), 214–231. https://doi.org/10.1016/j.cell.2012.02.013.

(137) Vollmuth, F.; Blankenfeldt, W.; Geyer, M. Structures of the Dual Bromodomains of the P-TEFb-Activating Protein Brd4 at Atomic Resolution*. *J. Biol. Chem.* **2009**, *284* (52), 36547–36556. https://doi.org/10.1074/jbc.M109.033712.

(138) Florence, B.; Faller, D. V. You BET-Cha: A Novel Family of Transcriptional Regulators. *Front. Biosci.-Landmark* **2001**, *6* (3), 1008–1018. https://doi.org/10.2741/florence.

(139) Wu, S.-Y.; Chiang, C.-M. The Double Bromodomain-Containing Chromatin Adaptor Brd4 and Transcriptional Regulation*. *J. Biol. Chem.* **2007**, *282* (18), 13141–13145. https://doi.org/10.1074/jbc.R700001200.

(140) Schwalm, M. P.; Knapp, S. BET Bromodomain Inhibitors. *Curr. Opin. Chem. Biol.* **2022**, *68*, 102148. https://doi.org/10.1016/j.cbpa.2022.102148.

(141) Muller, S.; Filippakopoulos, P.; Knapp, S. Bromodomains as Therapeutic Targets. *Expert Rev. Mol. Med.* **2011**, *13*, e29. https://doi.org/10.1017/S1462399411001992.

(142) Dey, A.; Yang, W.; Gegonne, A.; Nishiyama, A.; Pan, R.; Yagi, R.; Grinberg, A.; Finkelman, F. D.; Pfeifer, K.; Zhu, J.; Singer, D.; Zhu, J.; Ozato, K. BRD4 Directs Hematopoietic Stem Cell Development and Modulates Macrophage Inflammatory Responses. *EMBO J.* **2019**, *38* (7), e100293. https://doi.org/10.15252/embj.2018100293.

(143) Denis, G. V. Bromodomain Coactivators in Cancer, Obesity, Type 2 Diabetes, and Inflammation. *Discov. Med.* **2010**, *10* (55), 489–499.

(144) Shang, E.; Nickerson, H. D.; Wen, D.; Wang, X.; Wolgemuth, D. J. The First Bromodomain of Brdt, a Testis-Specific Member of the BET Sub-Family of Double-Bromodomain-Containing Proteins, Is Essential for Male Germ Cell Differentiation. *Development* **2007**, *134* (19), 3507–3515. https://doi.org/10.1242/dev.004481.

(145) Yang, Z.; Yik, J. H. N.; Chen, R.; He, N.; Jang, M. K.; Ozato, K.; Zhou, Q. Recruitment of P-TEFb for Stimulation of Transcriptional Elongation by the Bromodomain Protein Brd4. *Mol. Cell* **2005**, *19* (4), 535–545. https://doi.org/10.1016/j.molcel.2005.06.029.

(146) Schröder, S.; Cho, S.; Zeng, L.; Zhang, Q.; Kaehlcke, K.; Mak, L.; Lau, J.; Bisgrove, D.; Schnölzer, M.; Verdin, E.; Zhou, M.-M.; Ott, M. Two-Pronged Binding with Bromodomain-Containing Protein 4 Liberates Positive Transcription Elongation Factor b from Inactive Ribonucleoprotein Complexes*. *J. Biol. Chem.* **2012**, *287* (2), 1090–1099. https://doi.org/10.1074/jbc.M111.282855.

(147) Itzen, F.; Greifenberg, A. K.; Bösken, C. A.; Geyer, M. Brd4 Activates P-TEFb for RNA Polymerase II CTD Phosphorylation. *Nucleic Acids Res.* **2014**, *42* (12), 7577–7590. https://doi.org/10.1093/nar/gku449.

(148) Sahai, V.; Redig, A. J.; Collier, K. A.; Eckerdt, F. D.; Munshi, H. G. Targeting BET Bromodomain Proteins in Solid Tumors. *Oncotarget* **2016**, *7* (33), 53997–54009. https://doi.org/10.18632/oncotarget.9804.

(149) Hsu, S. C.; Gilgenast, T. G.; Bartman, C. R.; Edwards, C. R.; Stonestrom, A. J.; Huang, P.; Emerson, D. J.; Evans, P.; Werner, M. T.; Keller, C. A.; Giardine, B.; Hardison, R. C.; Raj, A.; Phillips-Cremins, J. E.; Blobel, G. A. The BET Protein BRD2 Cooperates with CTCF to Enforce Transcriptional and Architectural Boundaries. *Mol. Cell* **2017**, *66* (1), 102-116.e7. https://doi.org/10.1016/j.molcel.2017.02.027.

(150) Cheung, K. L.; Zhang, F.; Jaganathan, A.; Sharma, R.; Zhang, Q.; Konuma, T.; Shen, T.; Lee, J.-Y.; Ren, C.; Chen, C.-H.; Lu, G.; Olson, M. R.; Zhang, W.; Kaplan, M. H.; Littman, D. R.; Walsh, M. J.; Xiong, H.; Zeng, L.; Zhou, M.-M. Distinct Roles of Brd2 and Brd4 in Potentiating the Transcriptional Program for Th17 Cell Differentiation. *Mol. Cell* **2017**, *65* (6), 1068-1080.e5. https://doi.org/10.1016/j.molcel.2016.12.022.

(151) Pott, S.; Lieb, J. D. What Are Super-Enhancers? *Nat. Genet.* **2015**, *47* (1), 8–12. https://doi.org/10.1038/ng.3167.

(152) Blackwood, E. M.; Kadonaga, J. T. Going the Distance: A Current View of Enhancer Action. *Science* **1998**, *281* (5373), 60–63. https://doi.org/10.1126/science.281.5373.60.

(153) Lovén, J.; Hoke, H. A.; Lin, C. Y.; Lau, A.; Orlando, D. A.; Vakoc, C. R.; Bradner, J. E.; Lee, T. I.; Young, R. A. Selective Inhibition of Tumor Oncogenes by Disruption of Super-Enhancers. *Cell* **2013**, *153* (2), 320–334. https://doi.org/10.1016/j.cell.2013.03.036.

(154) Jahangiri, L.; Tsaprouni, L.; Trigg, R. M.; Williams, J. A.; Gkoutos, G. V.; Turner, S. D.; Pereira, J. Core Regulatory Circuitries in Defining Cancer Cell Identity across the Malignant Spectrum. *Open Biol.* **2020**, *10* (7), 200121. https://doi.org/10.1098/rsob.200121.

(155) Mertz, J. A.; Conery, A. R.; Bryant, B. M.; Sandy, P.; Balasubramanian, S.; Mele, D. A.; Bergeron, L.; Sims, R. J. Targeting MYC Dependence in Cancer by Inhibiting BET Bromodomains. *Proc. Natl. Acad. Sci.* **2011**, *108* (40), 16669–16674. https://doi.org/10.1073/pnas.1108190108.

(156) Wyce, A.; Ganji, G.; Smitheman, K. N.; Chung, C.; Korenchuk, S.; Bai, Y.; Barbash, O.; Le, B.; Craggs, P. D.; McCabe, M. T.; Kennedy-Wilson, K. M.; Sanchez, L. V.; Gosmini, R. L.; Parr, N.; McHugh, C. F.; Dhanak, D.; Prinjha, R. K.; Auger, K. R.; Tummino, P. J. BET Inhibition Silences Expression of MYCN and BCL2 and Induces Cytotoxicity in Neuroblastoma Tumor Models. *PLoS ONE* **2013**, *8* (8), e72967. https://doi.org/10.1371/journal.pone.0072967.

(157) Hu, J.; Pan, D.; Li, G.; Chen, K.; Hu, X. Regulation of Programmed Cell Death by Brd4. *Cell Death Dis.* **2022**, *13* (12), 1–15. https://doi.org/10.1038/s41419-022-05505-1.

(158) Sahai, V.; Kumar, K.; Knab, L. M.; Chow, C. R.; Raza, S. S.; Bentrem, D. J.; Ebine, K.; Munshi, H. G. BET Bromodomain Inhibitors Block Growth of Pancreatic Cancer Cells in Three-Dimensional Collagen. *Mol. Cancer Ther.* **2014**, *13* (7), 1907–1917. https://doi.org/10.1158/1535-7163.MCT-13-0925.

(159) Leal, A. S.; Williams, C. R.; Royce, D. B.; Pioli, P. A.; Sporn, M. B.; Liby, K. T. Bromodomain Inhibitors, JQ1 and I-BET 762, as Potential Therapies for Pancreatic Cancer. *Cancer Lett.* **2017**, *394*, 76–87. https://doi.org/10.1016/j.canlet.2017.02.021.

(160) Huang, Y.; Nahar, S.; Nakagawa, A.; Fernandez de Barrena, M. G.; Mertz, J. A.; Bryant, B. M.; Adams, C. E.; Mino-Kenudson, M.; Von Alt, K. N.; Chang, K.; Conery, A. R.; Hatton, C.; Sims, R. J.; Fernandez-Zapico, M. E.; Wang, X.; Lillemoe, K. D.; Castillo, C. F.; Warshaw, A. L.; Thayer, S. P.; Liss, A. S. Regulation of GLI Underlies a Role for BET Bromodomains in Pancreatic Cancer Growth and the Tumor Microenvironment. *Clin. Cancer Res. Off. J. Am. Assoc. Cancer Res.* **2016**, *22* (16), 4259–4270. https://doi.org/10.1158/1078-0432.CCR-15-2068.

(161) French, C. A.; Miyoshi, I.; Aster, J. C.; Kubonishi, I.; Kroll, T. G.; Dal Cin, P.; Vargas, S. O.; Perez-Atayde, A. R.; Fletcher, J. A. BRD4 Bromodomain Gene Rearrangement in Aggressive Carcinoma with Translocation t(15;19). *Am. J. Pathol.* **2001**, *159* (6), 1987–1992.

(162) Reynoird, N.; Schwartz, B. E.; Delvecchio, M.; Sadoul, K.; Meyers, D.; Mukherjee, C.; Caron, C.; Kimura, H.; Rousseaux, S.; Cole, P. A.; Panne, D.; French, C. A.; Khochbin, S. Oncogenesis by Sequestration of CBP/P300 in Transcriptionally Inactive Hyperacetylated Chromatin Domains. *EMBO J.* **2010**, *29* (17), 2943–2952. https://doi.org/10.1038/emboj.2010.176.

(163) Grunwald, C.; Koslowski, M.; Arsiray, T.; Dhaene, K.; Praet, M.; Victor, A.; Morresi-Hauf, A.; Lindner, M.; Passlick, B.; Lehr, H.-A.; Schäfer, S. C.; Seitz, G.; Huber, C.; Sahin, U.; Türeci, O. Expression of Multiple Epigenetically Regulated Cancer/Germline Genes in Nonsmall Cell Lung Cancer. *Int. J. Cancer* **2006**, *118* (10), 2522–2528. https://doi.org/10.1002/ijc.21669.

(164) Scanlan, M. J.; Altorki, N. K.; Gure, A. O.; Williamson, B.; Jungbluth, A.; Chen, Y. T.; Old, L. J. Expression of Cancer-Testis Antigens in Lung Cancer: Definition of Bromodomain Testis-Specific Gene (BRDT) as a New CT Gene, CT9. *Cancer Lett.* **2000**, *150* (2), 155–164. https://doi.org/10.1016/s0304-3835(99)00385-7.

(165) Xiang, T.; Bai, J.; She, C.; Yu, D.; Zhou, X.; Zhao, T. Bromodomain Protein BRD4 Promotes Cell Proliferation in Skin Squamous Cell Carcinoma. *Cell. Signal.* **2018**, *42*, 106–113. https://doi.org/10.1016/j.cellsig.2017.10.010.

(166) Chaidos, A.; Caputo, V.; Gouvedenou, K.; Liu, B.; Marigo, I.; Chaudhry, M. S.; Rotolo, A.; Tough, D. F.; Smithers, N. N.; Bassil, A. K.; Chapman, T. D.; Harker, N. R.; Barbash, O.; Tummino, P.; Al-Mahdi, N.; Haynes, A. C.; Cutler, L.; Le, B.; Rahemtulla, A.; Roberts, I.; Kleijnen, M.; Witherington, J. J.; Parr, N. J.; Prinjha, R. K.; Karadimitris, A. Potent Antimyeloma Activity of the Novel Bromodomain Inhibitors I-BET151 and I-BET762. *Blood* **2014**, *123* (5), 697–705. https://doi.org/10.1182/blood-2013-01-478420.

(167) Dawson, M. A.; Prinjha, R. K.; Dittmann, A.; Giotopoulos, G.; Bantscheff, M.; Chan, W.-I.; Robson, S. C.; Chung, C.; Hopf, C.; Savitski, M. M.; Huthmacher, C.; Gudgin, E.; Lugo, D.; Beinke, S.; Chapman, T. D.; Roberts, E. J.; Soden, P. E.; Auger, K. R.; Mirguet, O.; Doehner, K.; Delwel, R.; Burnett, A. K.; Jeffrey, P.; Drewes, G.; Lee, K.; Huntly, B. J. P.; Kouzarides, T. Inhibition of BET Recruitment to Chromatin as an Effective Treatment for MLL-Fusion Leukaemia. *Nature* **2011**, *478* (7370), 529–533. https://doi.org/10.1038/nature10509.

(168) Rajagopalan, V.; Vaidyanathan, M.; Janardhanam, V. A.; Bradner, J. E. Pre-Clinical Analysis of Changes in Intra-Cellular Biochemistry of Glioblastoma Multiforme (GBM) Cells Due to c-Myc Silencing. *Cell. Mol. Neurobiol.* **2014**, *34* (7), 1059–1069. https://doi.org/10.1007/s10571-014-0083-4.

(169) Ott, C. J.; Kopp, N.; Bird, L.; Paranal, R. M.; Qi, J.; Bowman, T.; Rodig, S. J.; Kung, A. L.; Bradner, J. E.; Weinstock, D. M. BET Bromodomain Inhibition Targets Both C-Myc and IL7R in High-Risk Acute Lymphoblastic Leukemia. *Blood* **2012**, *120* (14), 2843–2852. https://doi.org/10.1182/blood-2012-02-413021.

(170) Asangani, I. A.; Dommeti, V. L.; Wang, X.; Malik, R.; Cieslik, M.; Yang, R.; Escara-Wilke, J.; Wilder-Romans, K.; Dhanireddy, S.; Engelke, C.; Iyer, M. K.; Jing, X.; Wu, Y.-M.; Cao, X.; Qin, Z. S.; Wang, S.; Feng, F. Y.; Chinnaiyan, A. M. Therapeutic Targeting of BET Bromodomain Proteins in Castration-Resistant Prostate Cancer. *Nature* **2014**, *510* (7504), 278–282. https://doi.org/10.1038/nature13229.

(171) Henssen, A. G.; Thor, T.; Odersky, A.; Heukamp, L.; El-Hindy, N.; Beckers, A.; Slpeleman, F.; Althoff, K.; Schäfers, S.; Schramm, A.; Sure, U.; Fleischhack, G.; Eggert, A.; Schulte, J. H. BET Bromodomain Protein Inhibition Is a Therapeutic Option for Medulloblastoma. *Oncotarget* **2013**, *4* (11), 2080–2095. https://doi.org/10.18632/oncotarget.1534.

(172) Nicodeme, E.; Jeffrey, K. L.; Schaefer, U.; Beinke, S.; Dewell, S.; Chung, C.; Chandwani, R.; Marazzi, I.; Wilson, P.; Coste, H.; White, J.; Kirilovsky, J.; Lora, J. M.; Prinjha, R. K.; Lee, K.; Tarakhovsky, A. Suppression of Inflammation by a Synthetic Histone Mimic. *Nature* **2010**, *468* (7327), 1119–1123. https://doi.org/10.1038/nature09589.

(173) Mahdi, H.; Fisher, B. A.; Källberg, H.; Plant, D.; Malmström, V.; Rönnelid, J.; Charles, P.; Ding, B.; Alfredsson, L.; Padyukov, L.; Symmons, D. P. M.; Venables, P. J.; Klareskog, L.; Lundberg, K. Specific Interaction between Genotype, Smoking and Autoimmunity to Citrullinated Alpha-Enolase in the Etiology of Rheumatoid Arthritis. *Nat. Genet.* **2009**, *41* (12), 1319–1324. https://doi.org/10.1038/ng.480.

(174) WANG, F.; LIU, H.; BLANTON, W. P.; BELKINA, A.; LEBRASSEUR, N. K.; DENIS, G. V. Brd2 Disruption in Mice Causes Severe Obesity without Type 2 Diabetes. *Biochem. J.* **2009**, *425* (1), 71–83. https://doi.org/10.1042/BJ20090928.

(175) Shorstova, T.; Foulkes, W. D.; Witcher, M. Achieving Clinical Success with BET Inhibitors as Anti-Cancer Agents. *Br. J. Cancer* **2021**, *124* (9), 1478–1490. https://doi.org/10.1038/s41416-021-01321-0.

(176) Andrieu, G.; Belkina, A. C.; Denis, G. V. Clinical Trials for BET Inhibitors Run Ahead of the Science. *Drug Discov. Today Technol.* **2016**, *19*, 45–50. https://doi.org/10.1016/j.ddtec.2016.06.004.

(177) Filippakopoulos, P.; Qi, J.; Picaud, S.; Shen, Y.; Smith, W. B.; Fedorov, O.; Morse, E. M.; Keates, T.; Hickman, T. T.; Felletar, I.; Philpott, M.; Munro, S.; McKeown, M. R.; Wang, Y.; Christie, A. L.; West, N.; Cameron, M. J.; Schwartz, B.; Heightman, T. D.; La Thangue, N.; French, C. A.; Wiest, O.; Kung, A. L.; Knapp, S.; Bradner, J. E. Selective Inhibition of BET Bromodomains. *Nature* **2010**, *468* (7327), 1067–1073. https://doi.org/10.1038/nature09504.

(178) Hong, S. H.; Eun, J. W.; Choi, S. K.; Shen, Q.; Choi, W. S.; Han, J.-W.; Nam, S. W.; You, J. S. Epigenetic Reader BRD4 Inhibition as a Therapeutic Strategy to Suppress E2F2-Cell Cycle Regulation Circuit in Liver Cancer. *Oncotarget* **2016**, *7* (22), 32628–32640. https://doi.org/10.18632/oncotarget.8701.

(179) Sengupta, S.; Biarnes, M. C.; Clarke, R.; Jordan, V. C. Inhibition of BET Proteins Impair Estrogen Mediated Growth and Transcription in Breast Cancers by Pausing RNA Polymerase Advancement. *Breast Cancer Res. Treat.* **2015**, *150* (2), 265–278. https://doi.org/10.1007/s10549-015-3319-1.

(180) Feng, Q.; Zhang, Z.; Shea, M. J.; Creighton, C. J.; Coarfa, C.; Hilsenbeck, S. G.; Lanz, R.; He, B.; Wang, L.; Fu, X.; Nardone, A.; Song, Y.; Bradner, J.; Mitsiades, N.; Mitsiades, C. S.; Osborne, C. K.; Schiff, R.; O'Malley, B. W. An Epigenomic Approach to Therapy for Tamoxifen-Resistant Breast Cancer. *Cell Res.* **2014**, *24* (7), 809–819. https://doi.org/10.1038/cr.2014.71.

(181) Lockwood, W. W.; Zejnullahu, K.; Bradner, J. E.; Varmus, H. Sensitivity of Human Lung Adenocarcinoma Cell Lines to Targeted Inhibition of BET Epigenetic Signaling Proteins. *Proc. Natl. Acad. Sci.* **2012**, *109* (47), 19408–19413. https://doi.org/10.1073/pnas.1216363109.

(182) Shimamura, T.; Chen, Z.; Soucheray, M.; Carretero, J.; Kikuchi, E.; Tchaicha, J. H.; Gao, Y.; Cheng, K. A.; Cohoon, T. J.; Qi, J.; Akbay, E.; Kimmelman, A. C.; Kung, A. L.; Bradner, J. E.; Wong, K.-K. Efficacy of BET Bromodomain Inhibition in Kras-Mutant Non-Small Cell Lung Cancer. *Clin. Cancer Res. Off. J. Am. Assoc. Cancer Res.* **2013**, *19* (22), 10.1158/1078-0432.CCR-12–3904. https://doi.org/10.1158/1078-0432.CCR-12-3904.

(183) Garcia, P. L.; Miller, A. L.; Kreitzburg, K. M.; Council, L. N.; Gamblin, T. L.; Christein, J. D.; Heslin, M. J.; Arnoletti, J. P.; Richardson, J. H.; Chen, D.; Hanna, C. A.; Cramer, S. L.; Yang, E. S.; Qi, J.; Bradner, J. E.; Yoon, K. J. The BET Bromodomain Inhibitor JQ1 Suppresses Growth of Pancreatic Ductal Adenocarcinoma in Patient-Derived Xenograft Models. *Oncogene* **2016**, *35* (7), 833–845. https://doi.org/10.1038/onc.2015.126.

(184) Kumar, K.; Raza, S. S.; Knab, L. M.; Chow, C. R.; Kwok, B.; Bentrem, D. J.; Popovic, R.; Ebine, K.; Licht, J. D.; Munshi, H. G. GLI2-Dependent c-MYC Upregulation Mediates Resistance of Pancreatic Cancer Cells to the BET Bromodomain Inhibitor JQ1. *Sci. Rep.* **2015**, *5* (1), 9489. https://doi.org/10.1038/srep09489.

(185) Zuber, J.; Shi, J.; Wang, E.; Rappaport, A. R.; Herrmann, H.; Sison, E. A.; Magoon, D.; Qi, J.; Blatt, K.; Wunderlich, M.; Taylor, M. J.; Johns, C.; Chicas, A.; Mulloy, J. C.; Kogan, S. C.; Brown, P.; Valent, P.; Bradner, J. E.; Lowe, S. W.; Vakoc, C. R. RNAi Screen Identifies Brd4 as a Therapeutic Target in Acute Myeloid Leukaemia. *Nature* **2011**, *478* (7370), 524–528. https://doi.org/10.1038/nature10334.

(186) Moyer, M. W. First Drugs Found to Inhibit Elusive Cancer Target. *Nat. Med.* **2011**, *17* (11), 1325–1325. https://doi.org/10.1038/nm1111-1325.

(187) McDaniel, K. F.; Wang, L.; Soltwedel, T.; Fidanze, S. D.; Hasvold, L. A.; Liu, D.; Mantei, R. A.; Pratt, J. K.; Sheppard, G. S.; Bui, M. H.; Faivre, E. J.; Huang, X.; Li, L.; Lin, X.; Wang, R.; Warder, S. E.; Wilcox, D.; Albert, D. H.; Magoc, T. J.; Rajaraman, G.; Park, C. H.; Hutchins, C. W.; Shen, J. J.; Edalji, R. P.; Sun, C. C.; Martin, R.; Gao, W.; Wong, S.; Fang, G.; Elmore, S. W.; Shen, Y.; Kati, W. M. Discovery of N-(4-(2,4-Difluorophenoxy)-3-(6-Methyl-7-Oxo-6,7-Dihydro-1H-Pyrrolo[2,3-c]Pyridin-4-Yl)Phenyl)Ethanesulfonamide (ABBV-075/Mivebresib), a Potent and Orally Available Bromodomain and Extraterminal Domain (BET) Family Bromodomain Inhibitor. *J. Med. Chem.* **2017**, *60* (20), 8369–8384. https://doi.org/10.1021/acs.jmedchem.7b00746.

(188) Sheppard, G. S.; Wang, L.; Fidanze, S. D.; Hasvold, L. A.; Liu, D.; Pratt, J. K.; Park, C. H.; Longenecker, K.; Qiu, W.; Torrent, M.; Kovar, P. J.; Bui, M.; Faivre, E.; Huang, X.; Lin, X.; Wilcox, D.; Zhang, L.; Shen, Y.; Albert, D. H.; Magoc, T. J.; Rajaraman, G.; Kati, W. M.; McDaniel, K. F. Discovery of N-Ethyl-4-[2-(4-Fluoro-2,6-Dimethyl-Phenoxy)-5-(1-Hydroxy-1-Methyl-Ethyl)Phenyl]-6-Methyl-7-Oxo-1H-Pyrrolo[2,3-c]Pyridine-2-Carboxamide (ABBV-744), a BET Bromodomain Inhibitor with Selectivity for the Second Bromodomain. *J. Med. Chem.* **2020**, *63* (10), 5585–5623. https://doi.org/10.1021/acs.jmedchem.0c00628.

(189) Faivre, E. J.; McDaniel, K. F.; Albert, D. H.; Mantena, S. R.; Plotnik, J. P.; Wilcox, D.; Zhang, L.; Bui, M. H.; Sheppard, G. S.; Wang, L.; Sehgal, V.; Lin, X.; Huang, X.; Lu, X.; Uziel, T.; Hessler, P.; Lam, L. T.; Bellin, R. J.; Mehta, G.; Fidanze, S.; Pratt, J. K.; Liu, D.; Hasvold, L. A.; Sun, C.; Panchal, S. C.;

Nicolette, J. J.; Fossey, S. L.; Park, C. H.; Longenecker, K.; Bigelow, L.; Torrent, M.; Rosenberg, S. H.; Kati, W. M.; Shen, Y. Selective Inhibition of the BD2 Bromodomain of BET Proteins in Prostate Cancer. *Nature* **2020**, *578* (7794), 306–310. https://doi.org/10.1038/s41586-020-1930-8.

(190) Watson, R. J.; Bamborough, P.; Barnett, H.; Chung, C.; Davis, R.; Gordon, L.; Grandi, P.; Petretich, M.; Phillipou, A.; Prinjha, R. K.; Rioja, I.; Soden, P.; Werner, T.; Demont, E. H. GSK789: A Selective Inhibitor of the First Bromodomains (BD1) of the Bromo and Extra Terminal Domain (BET) Proteins. *J. Med. Chem.* **2020**, *63* (17), 9045–9069. https://doi.org/10.1021/acs.jmedchem.0c00614.

(191) Modukuri, R. K.; Yu, Z.; Tan, Z.; Ta, H. M.; Ucisik, M. N.; Jin, Z.; Anglin, J. L.; Sharma, K. L.; Nyshadham, P.; Li, F.; Riehle, K.; Faver, J. C.; Duong, K.; Nagarajan, S.; Simmons, N.; Palmer, S. S.; Teng, M.; Young, D. W.; Yi, J. S.; Kim, C.; Matzuk, M. M. Discovery of Potent BET Bromodomain 1 Stereoselective Inhibitors Using DNA-Encoded Chemical Library Selections. *Proc. Natl. Acad. Sci.* **2022**, *119* (22), e2122506119. https://doi.org/10.1073/pnas.2122506119.

(192) Gilan, O.; Rioja, I.; Knezevic, K.; Bell, M. J.; Yeung, M. M.; Harker, N. R.; Lam, E. Y. N.; Chung, C.; Bamborough, P.; Petretich, M.; Urh, M.; Atkinson, S. J.; Bassil, A. K.; Roberts, E. J.; Vassiliadis, D.; Burr, M. L.; Preston, A. G. S.; Wellaway, C.; Werner, T.; Gray, J. R.; Michon, A.-M.; Gobbetti, T.; Kumar, V.; Soden, P. E.; Haynes, A.; Vappiani, J.; Tough, D. F.; Taylor, S.; Dawson, S.-J.; Bantscheff, M.; Lindon, M.; Drewes, G.; Demont, E. H.; Daniels, D. L.; Grandi, P.; Prinjha, R. K.; Dawson, M. A. Selective Targeting of BD1 and BD2 of the BET Proteins in Cancer and Immunoinflammation. *Science* **2020**, *368* (6489), 387–394. https://doi.org/10.1126/science.aaz8455.

(193) Liu, C.-S.; Rioja, I.; Bakr, A.; Veldwijk, M. R.; Sperk, E.; Herskind, C.; Weichenhan, D.; Prinjha, R. K.; Plass, C.; Schmezer, P.; Popanda, O. Selective Inhibitors of Bromodomain BD1 and BD2 of BET Proteins Modulate Radiation-Induced Profibrotic Fibroblast Responses. *Int. J. Cancer* **2022**, *151* (2), 275–286. https://doi.org/10.1002/ijc.33989.

(194) Tanaka, M.; Roberts, J. M.; Seo, H.-S.; Souza, A.; Paulk, J.; Scott, T. G.; DeAngelo, S. L.; Dhe-Paganon, S.; Bradner, J. E. Design and Characterization of Bivalent BET Inhibitors. *Nat. Chem. Biol.* **2016**, *12* (12), 1089–1096. https://doi.org/10.1038/nchembio.2209.

(195) Ren, C.; Zhang, G.; Han, F.; Fu, S.; Cao, Y.; Zhang, F.; Zhang, Q.; Meslamani, J.; Xu, Y.; Ji, D.; Cao, L.; Zhou, Q.; Cheung, K.; Sharma, R.; Babault, N.; Yi, Z.; Zhang, W.; Walsh, M. J.; Zeng, L.; Zhou, M.-M. Spatially Constrained Tandem Bromodomain Inhibition Bolsters Sustained Repression of BRD4 Transcriptional Activity for TNBC Cell Growth. *Proc. Natl. Acad. Sci. U. S. A.* **2018**, *115* (31), 7949–7954. https://doi.org/10.1073/pnas.1720000115.

(196) Bradbury, R. H.; Callis, R.; Carr, G. R.; Chen, H.; Clark, E.; Feron, L.; Glossop, S.; Graham, M. A.; Hattersley, M.; Jones, C.; Lamont, S. G.; Ouvry, G.; Patel, A.; Patel, J.; Rabow, A. A.; Roberts, C. A.; Stokes, S.; Stratton, N.; Walker, G. E.; Ward, L.; Whalley, D.; Whittaker, D.; Wrigley, G.; Waring, M. J. Optimization of a Series of Bivalent Triazolopyridazine Based Bromodomain and Extraterminal Inhibitors: The Discovery of (3R)-4-[2-[4-[1-(3-Methoxy-[1,2,4]Triazolo[4,3-b]Pyridazin-6-Yl)-4-Piperidyl]Phenoxy]Ethyl]-1,3-Dimethyl-Piperazin-2-One (AZD5153). *J. Med. Chem.* **2016**, *59* (17), 7801–7817. https://doi.org/10.1021/acs.jmedchem.6b00070.

(197) Waring, M. J.; Chen, H.; Rabow, A. A.; Walker, G.; Bobby, R.; Boiko, S.; Bradbury, R. H.; Callis, R.; Clark, E.; Dale, I.; Daniels, D. L.; Dulak, A.; Flavell, L.; Holdgate, G.; Jowitt, T. A.; Kikhney, A.; McAlister, M.; Méndez, J.; Ogg, D.; Patel, J.; Petteruti, P.; Robb, G. R.; Robers, M. B.; Saif, S.; Stratton, N.; Svergun, D. I.; Wang, W.; Whittaker, D.; Wilson, D. M.; Yao, Y. Potent and Selective Bivalent Inhibitors of BET Bromodomains. *Nat. Chem. Biol.* **2016**, *12* (12), 1097–1104. https://doi.org/10.1038/nchembio.2210.

(198) Owen, D. Doubling down on BET Inhibition. *Nat. Chem. Biol.* **2016**, *12* (12), 991–992. https://doi.org/10.1038/nchembio.2242.

(199) Guan, X.; Cheryala, N.; Karim, R. Md.; Chan, A.; Berndt, N.; Qi, J.; Georg, G. I.; Schönbrunn, E. Bivalent BET Bromodomain Inhibitors Confer Increased Potency and Selectivity for BRDT via Protein Conformational Plasticity. *J. Med. Chem.* **2022**, *65* (15), 10441–10458. https://doi.org/10.1021/acs.jmedchem.2c00453.

(200) Wu, Q.; Chen, D.-Q.; Sun, L.; Huan, X.-J.; Bao, X.-B.; Tian, C.-Q.; Hu, J.; Lv, K.-K.; Wang, Y.-Q.; Xiong, B.; Miao, Z.-H. Novel Bivalent BET Inhibitor N2817 Exhibits Potent Anticancer Activity and

Inhibits TAF1. *Biochem. Pharmacol.* **2021**, *185*, 114435. https://doi.org/10.1016/j.bcp.2021.114435.

(201) Quintela, M.; James, D. W.; Pociute, A.; Powell, L.; Edwards, K.; Coombes, Z.; Garcia, J.; Garton, N.; Das, N.; Lutchman-Singh, K.; Margarit, L.; Beynon, A. L.; Rioja, I.; Prinjha, R. K.; Harker, N. R.; Gonzalez, D.; Conlan, R. S.; Francis, L. W. Bromodomain Inhibitor I-BET858 Triggers a Unique Transcriptional Response Coupled to Enhanced DNA Damage, Cell Cycle Arrest and Apoptosis in High-Grade Ovarian Carcinoma Cells. *Clin. Epigenetics* **2023**, *15* (1), 63. https://doi.org/10.1186/s13148-023-01477-x.

(202) Luo, M.; Wu, Q.; Yang, Y.; Sun, L.; Huan, X.; Tian, C.; Xiong, B.; Miao, Z.; Wang, Y.; Chen, D. Design and Development of a Novel Series of Oral Bivalent BET Inhibitors with Potent Anticancer Activities. *Eur. J. Med. Chem.* **2022**, *239*, 114519. https://doi.org/10.1016/j.ejmech.2022.114519.

(203) Yang, Y.; Fang, L.; Chen, P.; Zhang, H.; Zhou, J. Identification of 3,5-Dimethylisoxazole Derivatives as BRD4 Inhibitors for the Treatment of Colorectal Cancer. *ACS Med. Chem. Lett.* **2020**, *11* (11), 2174–2181. https://doi.org/10.1021/acsmedchemlett.0c00294.

(204) Gina Battaglia, P. BET Inhibitors in Cancer Therapy: Finding the Right Combination. **2023**, *24*.

(205) Stathis, A.; Bertoni, F. BET Proteins as Targets for Anticancer Treatment. *Cancer Discov.* **2018**, *8* (1), 24–36. https://doi.org/10.1158/2159-8290.CD-17-0605.

(206) Anighoro, A.; Bajorath, J.; Rastelli, G. Polypharmacology: Challenges and Opportunities in Drug Discovery. *J. Med. Chem.* **2014**, *57* (19), 7874–7887. https://doi.org/10.1021/jm5006463.

(207) Chatterjee, N.; Bivona, T. G. Polytherapy and Targeted Cancer Drug Resistance. *Trends Cancer* **2019**, *5* (3), 170–182. https://doi.org/10.1016/j.trecan.2019.02.003.

(208) Zhao, B.; Cheng, X.; Zhou, X. The BET-Bromodomain Inhibitor JQ1 Mitigates Vemurafenib Drug Resistance in Melanoma. *Melanoma Res.* **2018**, *28* (6), 521–526. https://doi.org/10.1097/CMR.0000000000000497.

(209) Jing, Y.; Zhang, Z.; Ma, P.; An, S.; Shen, Y.; Zhu, L.; Zhuang, G. Concomitant BET and MAPK Blockade for Effective Treatment of Ovarian Cancer. *Oncotarget* **2015**, *7* (3), 2545–2554. https://doi.org/10.18632/oncotarget.6309.

(210) Fiskus, W.; Sharma, S.; Qi, J.; Shah, B.; Devaraj, S. G. T.; Leveque, C.; Portier, B. P.; Iyer, S.; Bradner, J. E.; Bhalla, K. N. BET Protein Antagonist JQ1 Is Synergistically Lethal with FLT3 Tyrosine Kinase Inhibitor (TKI) and Overcomes Resistance to FLT3-TKI in AML Cells Expressing FLT-ITD. *Mol. Cancer Ther.* **2014**, *13* (10), 2315–2327. https://doi.org/10.1158/1535-7163.MCT-14-0258.

(211) Schafer, J. M.; Lehmann, B. D.; Gonzalez-Ericsson, P. I.; Marshall, C. B.; Beeler, J. S.; Redman, L. N.; Jin, H.; Sanchez, V.; Stubbs, M. C.; Scherle, P.; Johnson, K. N.; Sheng, Q.; Roland, J. T.; Bauer, J. A.; Shyr, Y.; Chakravarthy, B.; Mobley, B. C.; Hiebert, S. W.; Balko, J. M.; Sanders, M. E.; Liu, P. C. C.; Pietenpol, J. A. Targeting MYCN-Expressing Triple-Negative Breast Cancer with BET and MEK Inhibitors. *Sci. Transl. Med.* **2020**, *12* (534), eaaw8275. https://doi.org/10.1126/scitranslmed.aaw8275.

(212) Fiskus, W.; Sharma, S.; Qi, J.; Valenta, J. A.; Schaub, L. J.; Shah, B.; Peth, K.; Portier, B. P.; Rodriguez, M.; Devaraj, S. G. T.; Zhan, M.; Sheng, J.; Iyer, S. P.; Bradner, J. E.; Bhalla, K. N. Highly Active Combination of BRD4 Antagonist and Histone Deacetylase Inhibitor against Human Acute Myelogenous Leukemia Cells. *Mol. Cancer Ther.* **2014**, *13* (5), 1142–1154. https://doi.org/10.1158/1535-7163.MCT-13-0770.

(213) Bhadury, J.; Nilsson, L. M.; Veppil Muralidharan, S.; Green, L. C.; Li, Z.; Gesner, E. M.; Hansen, H. C.; Keller, U. B.; McLure, K. G.; Nilsson, J. A. BET and HDAC Inhibitors Induce Similar Genes and Biological Effects and Synergize to Kill in Myc-Induced Murine Lymphoma. *Proc. Natl. Acad. Sci.* **2014**, *111* (26), E2721–E2730. https://doi.org/10.1073/pnas.1406722111.

(214) Shahbazi, J.; Liu, P. Y.; Atmadibrata, B.; Bradner, J. E.; Marshall, G. M.; Lock, R. B.; Liu, T. The Bromodomain Inhibitor JQ1 and the Histone Deacetylase Inhibitor Panobinostat Synergistically Reduce N-Myc Expression and Induce Anticancer Effects. *Clin. Cancer Res. Off. J. Am. Assoc. Cancer Res.* **2016**, *22* (10), 2534–2544. https://doi.org/10.1158/1078-0432.CCR-15-1666.

(215) Jostes, S.; Nettersheim, D.; Fellermeyer, M.; Schneider, S.; Hafezi, F.; Honecker, F.; Schumacher, V.; Geyer, M.; Kristiansen, G.; Schorle, H. The Bromodomain Inhibitor JQ1 Triggers Growth

Arrest and Apoptosis in Testicular Germ Cell Tumours in Vitro and in Vivo. *J. Cell. Mol. Med.* **2017**, *21* (7), 1300–1314. https://doi.org/10.1111/jcmm.13059.

(216) Heinemann, A.; Cullinane, C.; De Paoli-Iseppi, R.; Wilmott, J. S.; Gunatilake, D.; Madore, J.; Strbenac, D.; Yang, J. Y.; Gowrishankar, K.; Tiffen, J. C.; Prinjha, R. K.; Smithers, N.; McArthur, G. A.; Hersey, P.; Gallagher, S. J. Combining BET and HDAC Inhibitors Synergistically Induces Apoptosis of Melanoma and Suppresses AKT and YAP Signaling. *Oncotarget* **2015**, *6* (25), 21507–21521.

(217) Hölscher, A. S.; Schulz, W. A.; Pinkerneil, M.; Niegisch, G.; Hoffmann, M. J. Combined Inhibition of BET Proteins and Class I HDACs Synergistically Induces Apoptosis in Urothelial Carcinoma Cell Lines. *Clin. Epigenetics* **2018**, *10* (1), 1. https://doi.org/10.1186/s13148-017-0434-3.

(218) Enßle, J. C.; Boedicker, C.; Wanior, M.; Vogler, M.; Knapp, S.; Fulda, S. Co-Targeting of BET Proteins and HDACs as a Novel Approach to Trigger Apoptosis in Rhabdomyosarcoma Cells. *Cancer Lett.* **2018**, *428*, 160–172. https://doi.org/10.1016/j.canlet.2018.04.032.

(219) Liu, T.; Wan, Y.; Xiao, Y.; Xia, C.; Duan, G. Dual-Target Inhibitors Based on HDACs: Novel Antitumor Agents for Cancer Therapy. *J. Med. Chem.* **2020**, *63* (17), 8977–9002. https://doi.org/10.1021/acs.jmedchem.0c00491.

(220) Peng, X.; Sun, Z.; Kuang, P.; Chen, J. Recent Progress on HDAC Inhibitors with Dual Targeting Capabilities for Cancer Treatment. *Eur. J. Med. Chem.* **2020**, *208*, 112831. https://doi.org/10.1016/j.ejmech.2020.112831.

(221) Roy, R.; Ria, T.; RoyMahaPatra, D.; Sk, U. H. Single Inhibitors versus Dual Inhibitors: Role of HDAC in Cancer. *ACS Omega* **2023**, *8* (19), 16532–16544. https://doi.org/10.1021/acsomega.3c00222.

(222) Orth, M.; Metzger, P.; Gerum, S.; Mayerle, J.; Schneider, G.; Belka, C.; Schnurr, M.; Lauber, K. Pancreatic Ductal Adenocarcinoma: Biological Hallmarks, Current Status, and Future Perspectives of Combined Modality Treatment Approaches. *Radiat. Oncol. Lond. Engl.* **2019**, *14*, 141. https://doi.org/10.1186/s13014-019-1345-6.

(223) Mazur, P. K.; Herner, A.; Mello, S. S.; Wirth, M.; Hausmann, S.; Sánchez-Rivera, F. J.; Lofgren, S. M.; Kuschma, T.; Hahn, S. A.; Vangala, D.; Trajkovic-Arsic, M.; Gupta, A.; Heid, I.; Noël, P. B.; Braren, R.; Erkan, M.; Kleeff, J.; Sipos, B.; Sayles, L. C.; Heikenwalder, M.; Heßmann, E.; Ellenrieder, V.; Esposito, I.; Jacks, T.; Bradner, J. E.; Khatri, P.; Sweet-Cordero, E. A.; Attardi, L. D.; Schmid, R. M.; Schneider, G.; Sage, J.; Siveke, J. T. Combined Inhibition of BET Family Proteins and Histone Deacetylases as a Potential Epigenetics-Based Therapy for Pancreatic Ductal Adenocarcinoma. *Nat. Med.* **2015**, *21* (10), 1163–1171. https://doi.org/10.1038/nm.3952.

(224) Manzotti, G.; Ciarrocchi, A.; Sancisi, V. Inhibition of BET Proteins and Histone Deacetylase (HDACs): Crossing Roads in Cancer Therapy. *Cancers* **2019**, *11* (3), 304. https://doi.org/10.3390/cancers11030304.

(225) Scripture, C. D.; Figg, W. D. Drug Interactions in Cancer Therapy. *Nat. Rev. Cancer* **2006**, *6* (7), 546–558. https://doi.org/10.1038/nrc1887.

(226) Amin, A. R.; Attur, M. G.; Pillinger, M.; Abramson, S. B. The Pleiotropic Functions of Aspirin: Mechanisms of Action. *Cell. Mol. Life Sci. CMLS* **1999**, *56* (3), 305–312. https://doi.org/10.1007/s000180050432.

(227) Proschak, E.; Stark, H.; Merk, D. Polypharmacology by Design: A Medicinal Chemist's Perspective on Multitargeting Compounds. *J. Med. Chem.* **2019**, *62* (2), 420–444. https://doi.org/10.1021/acs.jmedchem.8b00760.

(228) Maach, S.; Chiaramonte, N.; Borgonetti, V.; Sarno, F.; Pierucci, F.; Dei, S.; Teodori, E.; Altucci, L.; Meacci, E.; Galeotti, N.; Romanelli, M. N. Dual HDAC–BRD4 Inhibitors Endowed with Antitumor and Antihyperalgesic Activity. *Med. Chem. Res.* **2022**, *31* (6), 960–974. https://doi.org/10.1007/s00044-022-02896-w.

(229) He, S.; Dong, G.; Li, Y.; Wu, S.; Wang, W.; Sheng, C. Potent Dual BET/HDAC Inhibitors for Efficient Treatment of Pancreatic Cancer. *Angew. Chem. Int. Ed Engl.* **2020**, *59* (8), 3028–3032. https://doi.org/10.1002/anie.201915896.

(230) Zhang, X.; Zegar, T.; Weiser, T.; Hamdan, F. H.; Berger, B.-T.; Lucas, R.; Balourdas, D.-Ii; Ladigan, S.; Cheung, P. F.; Liffers, S.-T.; Trajkovic-Arsic, M.; Scheffler, B.; Joerger, A. C.; Hahn, S. A.; Johnsen, S. A.; Knapp, S.; Siveke, J. T. Characterization of a Dual BET/HDAC Inhibitor for

Treatment of Pancreatic Ductal Adenocarcinoma. *Int. J. Cancer* **2020**, *147* (10), 2847–2861. https://doi.org/10.1002/ijc.33137.

(231) Li, Z.; Huang, Y.; Tu, J.; Yang, W.; Liu, N.; Wang, W.; Sheng, C. Discovery of BRD4–HDAC Dual Inhibitors with Improved Fungal Selectivity and Potent Synergistic Antifungal Activity against Fluconazole-Resistant Candida Albicans. *J. Med. Chem.* **2023**, *66* (8), 5950–5964. https://doi.org/10.1021/acs.jmedchem.3c00165.

(232) Chen, J.; Li, Y.; Zhang, J.; Zhang, M.; Wei, A.; Liu, H.; Xie, Z.; Ren, W.; Duan, W.; Zhang, Z.; Shen, A.; Hu, Y. Discovery of Selective HDAC/BRD4 Dual Inhibitors as Epigenetic Probes. *Eur. J. Med. Chem.* **2021**, *209*, 112868. https://doi.org/10.1016/j.ejmech.2020.112868.

(233) Shao, M.; He, L.; Zheng, L.; Huang, L.; Zhou, Y.; Wang, T.; Chen, Y.; Shen, M.; Wang, F.; Yang, Z.; Chen, L. Structure-Based Design, Synthesis and in Vitro Antiproliferative Effects Studies of Novel Dual BRD4/HDAC Inhibitors. *Bioorg. Med. Chem. Lett.* **2017**, *27* (17), 4051–4055. https://doi.org/10.1016/j.bmcl.2017.07.054.

(234) Atkinson, S. J.; Soden, P. E.; Angell, D. C.; Bantscheff, M.; Chung, C.; Giblin, K. A.; Smithers, N.; Furze, R. C.; Gordon, L.; Drewes, G.; Rioja, I.; Witherington, J.; Parr, N. J.; Prinjha, R. K. The Structure Based Design of Dual HDAC/BET Inhibitors as Novel Epigenetic Probes. *MedChemComm* **2014**, *5* (3), 342–351. https://doi.org/10.1039/C3MD00285C.

(235) Cheng, G.; Wang, Z.; Yang, J.; Bao, Y.; Xu, Q.; Zhao, L.; Liu, D. Design, Synthesis and Biological Evaluation of Novel Indole Derivatives as Potential HDAC/BRD4 Dual Inhibitors and Anti-Leukemia Agents. *Bioorganic Chem.* **2019**, *84*, 410–417. https://doi.org/10.1016/j.bioorg.2018.12.011.

(236) Amemiya, S.; Yamaguchi, T.; Hashimoto, Y.; Noguchi-Yachide, T. Synthesis and Evaluation of Novel Dual BRD4/HDAC Inhibitors. *Bioorg. Med. Chem.* **2017**, *25* (14), 3677–3684. https://doi.org/10.1016/j.bmc.2017.04.043.

(237) Schäker-Hübner, L.; Warstat, R.; Ahlert, H.; Mishra, P.; Kraft, F. B.; Schliehe-Diecks, J.; Schöler, A.; Borkhardt, A.; Breit, B.; Bhatia, S.; Hügle, M.; Günther, S.; Hansen, F. K. 4-Acyl Pyrrole Capped HDAC Inhibitors: A New Scaffold for Hybrid Inhibitors of BET Proteins and Histone Deacetylases as Antileukemia Drug Leads. *J. Med. Chem.* **2021**, *64* (19), 14620–14646. https://doi.org/10.1021/acs.jmedchem.1c01119.

(238) Pan, Z.; Li, X.; Wang, Y.; Jiang, Q.; Jiang, L.; Zhang, M.; Zhang, N.; Wu, F.; Liu, B.; He, G. Discovery of Thieno[2,3-d]Pyrimidine-Based Hydroxamic Acid Derivatives as Bromodomain-Containing Protein 4/Histone Deacetylase Dual Inhibitors Induce Autophagic Cell Death in Colorectal Carcinoma Cells. *J. Med. Chem.* **2020**, *63* (7), 3678–3700. https://doi.org/10.1021/acs.jmedchem.9b02178.

(239) Borgonetti, V.; Meacci, E.; Pierucci, F.; Romanelli, M. N.; Galeotti, N. Dual HDAC/BRD4 Inhibitors Relieves Neuropathic Pain by Attenuating Inflammatory Response in Microglia After Spared Nerve Injury. *Neurother. J. Am. Soc. Exp. Neurother.* **2022**, *19* (5), 1634–1648. https://doi.org/10.1007/s13311-022-01243-6.

(240) Zhang, Z.; Hou, S.; Chen, H.; Ran, T.; Jiang, F.; Bian, Y.; Zhang, D.; Zhi, Y.; Wang, L.; Zhang, L.; Li, H.; Zhang, Y.; Tang, W.; Lu, T.; Chen, Y. Targeting Epigenetic Reader and Eraser: Rational Design, Synthesis and in Vitro Evaluation of Dimethylisoxazoles Derivatives as BRD4/HDAC Dual Inhibitors. *Bioorg. Med. Chem. Lett.* **2016**, *26* (12), 2931–2935. https://doi.org/10.1016/j.bmcl.2016.04.034.

(241) Lipinski, C. A.; Lombardo, F.; Dominy, B. W.; Feeney, P. J. Experimental and Computational Approaches to Estimate Solubility and Permeability in Drug Discovery and Development Settings. *Adv. Drug Deliv. Rev.* **1997**, *23* (1), 3–25. https://doi.org/10.1016/S0169-409X(96)00423-1.

(242) Veber, D. F.; Johnson, S. R.; Cheng, H.-Y.; Smith, B. R.; Ward, K. W.; Kopple, K. D. Molecular Properties That Influence the Oral Bioavailability of Drug Candidates. *J. Med. Chem.* **2002**, *45* (12), 2615–2623. https://doi.org/10.1021/jm020017n.

(243) Ren, Q.; Gao, W. Current Status in the Discovery of Dual BET/HDAC Inhibitors. *Bioorg. Med. Chem. Lett.* **2021**, *38*, 127829. https://doi.org/10.1016/j.bmcl.2021.127829.

(244) Morphy, R.; Kay, C.; Rankovic, Z. From Magic Bullets to Designed Multiple Ligands. *Drug Discov. Today* **2004**, *9* (15), 641–651. https://doi.org/10.1016/S1359-6446(04)03163-0.

(245) Fidanze, S. D.; Liu, D.; Mantei, R. A.; Hasvold, L. A.; Pratt, J. K.; Sheppard, G. S.; Wang, L.; Holms, J. H.; Dai, Y.; Aguirre, A.; Bogdan, A.; Dietrich, J. D.; Marjanovic, J.; Park, C. H.; Hutchins, C. W.; Lin, X.; Bui, M. H.; Huang, X.; Wilcox, D.; Li, L.; Wang, R.; Kovar, P.; Magoc, T. J.; Rajaraman, G.; Albert, D. H.; Shen, Y.; Kati, W. M.; McDaniel, K. F. Discovery and Optimization of Novel Constrained Pyrrolopyridone BET Family Inhibitors. *Bioorg. Med. Chem. Lett.* **2018**, *28* (10), 1804–1810. https://doi.org/10.1016/j.bmcl.2018.04.020.

(246) Hu, J.; Tian, C.-Q.; Damaneh, M. S.; Li, Y.; Cao, D.; Lv, K.; Yu, T.; Meng, T.; Chen, D.; Wang, X.; Chen, L.; Li, J.; Song, S.-S.; Huan, X.-J.; Qin, L.; Shen, J.; Wang, Y.-Q.; Miao, Z.-H.; Xiong, B. Structure-Based Discovery and Development of a Series of Potent and Selective Bromodomain and Extra-Terminal Protein Inhibitors. *J. Med. Chem.* **2019**, *62* (18), 8642–8663. https://doi.org/10.1021/acs.jmedchem.9b01094.

(247) Zhang, G.; Plotnikov, A. N.; Rusinova, E.; Shen, T.; Morohashi, K.; Joshua, J.; Zeng, L.; Mujtaba, S.; Ohlmeyer, M.; Zhou, M.-M. Structure-Guided Design of Potent Diazobenzene Inhibitors for the BET Bromodomains. *J. Med. Chem.* **2013**, *56* (22), 9251–9264. https://doi.org/10.1021/jm401334s.

(248) Němec, V.; Schwalm, M. P.; Müller, S.; Knapp, S. PROTAC Degraders as Chemical Probes for Studying Target Biology and Target Validation. *Chem. Soc. Rev.* **2022**, *51* (18), 7971–7993. https://doi.org/10.1039/D2CS00478J.

(249) Lu, J.; Qian, Y.; Altieri, M.; Dong, H.; Wang, J.; Raina, K.; Hines, J.; Winkler, J. D.; Crew, A. P.; Coleman, K.; Crews, C. M. Hijacking the E3 Ubiquitin Ligase Cereblon to Efficiently Target BRD4. *Chem. Biol.* **2015**, *22* (6), 755–763. https://doi.org/10.1016/j.chembiol.2015.05.009.

(250) Winter, G. E.; Buckley, D. L.; Paulk, J.; Roberts, J. M.; Souza, A.; Dhe-Paganon, S.; Bradner, J. E. Selective Target Protein Degradation via Phthalimide Conjugation. *Science* **2015**, *348* (6241), 1376–1381. https://doi.org/10.1126/science.aab1433.

(251) Bai, L.; Zhou, B.; Yang, C.-Y.; Ji, J.; McEachern, D.; Przybranowski, S.; Jiang, H.; Hu, J.; Xu, F.; Zhao, Y.; Liu, L.; Fernandez-Salas, E.; Xu, J.; Dou, Y.; Wen, B.; Sun, D.; Meagher, J.; Stuckey, J.; Hayes, D. F.; Li, S.; Ellis, M. J.; Wang, S. Targeted Degradation of BET Proteins in Triple-Negative Breast Cancer. *Cancer Res.* **2017**, *77* (9), 2476–2487. https://doi.org/10.1158/0008-5472.CAN-16-2622.

(252) Qin, C.; Hu, Y.; Zhou, B.; Fernandez-Salas, E.; Yang, C.-Y.; Liu, L.; McEachern, D.; Przybranowski, S.; Wang, M.; Stuckey, J.; Meagher, J.; Bai, L.; Chen, Z.; Lin, M.; Yang, J.; Xu, F.; Hu, J.; Xing, W.; Huang, L.; Li, S.; Wen, B.; Sun, D.; Wang, S. Discovery of QCA570 as an Exceptionally Potent and Efficacious Proteolysis Targeting Chimera (PROTAC) Degrader of the Bromodomain and Extra-Terminal (BET) Proteins Capable of Inducing Complete and Durable Tumor Regression. *J. Med. Chem.* **2018**, *61* (15), 6685–6704. https://doi.org/10.1021/acs.jmedchem.8b00506.

(253) Zhang, J.; Chen, P.; Zhu, P.; Zheng, P.; Wang, T.; Wang, L.; Xu, C.; Zhou, J.; Zhang, H. Development of Small-Molecule BRD4 Degraders Based on Pyrrolopyridone Derivative. *Bioorganic Chem.* **2020**, *99*, 103817. https://doi.org/10.1016/j.bioorg.2020.103817.

(254) Bemis, T. A.; La Clair, J. J.; Burkart, M. D. Traceless Staudinger Ligation Enabled Parallel Synthesis of Proteolysis Targeting Chimera Linker Variants. *Chem. Commun. Camb. Engl.* **2021**, *57* (8), 1026–1029. https://doi.org/10.1039/d0cc05395c.

(255) Hu, R.; Wang, W.-L.; Yang, Y.-Y.; Hu, X.-T.; Wang, Q.-W.; Zuo, W.-Q.; Xu, Y.; Feng, Q.; Wang, N.-Y. Identification of a Selective BRD4 PROTAC with Potent Antiproliferative Effects in AR-Positive Prostate Cancer Based on a Dual BET/PLK1 Inhibitor. *Eur. J. Med. Chem.* **2022**, *227*, 113922. https://doi.org/10.1016/j.ejmech.2021.113922.

(256) Min, J.; Mayasundari, A.; Keramatnia, F.; Jonchere, B.; Yang, S. W.; Jarusiewicz, J.; Actis, M.; Das, S.; Young, B.; Slavish, J.; Yang, L.; Li, Y.; Fu, X.; Garrett, S. H.; Yun, M.-K.; Li, Z.; Nithianantham, S.; Chai, S.; Chen, T.; Shelat, A.; Lee, R. E.; Nishiguchi, G.; White, S. W.; Roussel, M. F.; Potts, P. R.; Fischer, M.; Rankovic, Z. Phenyl-Glutarimides: Alternative Cereblon Binders for the Design of PROTACs. *Angew. Chem. Int. Ed Engl.* **2021**, 10.1002/anie.202108848. https://doi.org/10.1002/anie.202108848.

(257) Zengerle, M.; Chan, K.-H.; Ciulli, A. Selective Small Molecule Induced Degradation of the BET Bromodomain Protein BRD4. *ACS Chem. Biol.* **2015**, *10* (8), 1770–1777. https://doi.org/10.1021/acschembio.5b00216.

(258) Kounde, C. S.; Shchepinova, M. M.; Saunders, C. N.; Muelbaier, M.; Rackham, M. D.; Harling, J. D.; Tate, E. W. A Caged E3 Ligase Ligand for PROTAC-Mediated Protein Degradation with Light. *Chem. Commun. Camb. Engl.* **2020**, *56* (41), 5532–5535. https://doi.org/10.1039/d0cc00523a.

(259) He, S.; Gao, F.; Ma, J.; Ma, H.; Dong, G.; Sheng, C. Aptamer-PROTAC Conjugates (APCs) for Tumor-Specific Targeting in Breast Cancer. *Angew. Chem. Int. Ed.* **2021**, *60* (43), 23299–23305. https://doi.org/10.1002/anie.202107347.

(260) Raina, K.; Lu, J.; Qian, Y.; Altieri, M.; Gordon, D.; Rossi, A. M. K.; Wang, J.; Chen, X.; Dong, H.; Siu, K.; Winkler, J. D.; Crew, A. P.; Crews, C. M.; Coleman, K. G. PROTAC-Induced BET Protein Degradation as a Therapy for Castration-Resistant Prostate Cancer. *Proc. Natl. Acad. Sci. U. S. A.* **2016**, *113* (26), 7124–7129. https://doi.org/10.1073/pnas.1521738113.

(261) Liu, J.; Chen, H.; Liu, Y.; Shen, Y.; Meng, F.; Kaniskan, H. ümit; Jin, J.; Wei, W. Cancer Selective Target Degradation by Folate-Caged PROTACs. *J. Am. Chem. Soc.* **2021**, *143* (19), 7380–7387. https://doi.org/10.1021/jacs.1c00451.

(262) Gadd, M. S.; Testa, A.; Lucas, X.; Chan, K.-H.; Chen, W.; Lamont, D. J.; Zengerle, M.; Ciulli, A. Structural Basis of PROTAC Cooperative Recognition for Selective Protein Degradation. *Nat. Chem. Biol.* **2017**, *13* (5), 514–521. https://doi.org/10.1038/nchembio.2329.

(263) Xiong, Y.; Donovan, K. A.; Eleuteri, N. A.; Kirmani, N.; Yue, H.; Razov, A.; Krupnick, N. M.; Nowak, R. P.; Fischer, E. S. Chemo-Proteomics Exploration of HDAC Degradability by Small Molecule Degraders. *Cell Chem. Biol.* **2021**, *28* (10), 1514-1527.e4. https://doi.org/10.1016/j.chembiol.2021.07.002.

(264) Xiao, Y.; Wang, J.; Zhao, L. Y.; Chen, X.; Zheng, G.; Zhang, X.; Liao, D. Discovery of Histone Deacetylase 3 (HDAC3)-Specific PROTACs. *Chem. Commun.* **2020**, *56* (68), 9866–9869. https://doi.org/10.1039/D0CC03243C.

(265) Yang, K.; Zhao, Y.; Nie, X.; Wu, H.; Wang, B.; Almodovar-Rivera, C. M.; Xie, H.; Tang, W. A Cell-Based Target Engagement Assay for the Identification of Cereblon E3 Ubiquitin Ligase Ligands and Their Application in HDAC6 Degraders. *Cell Chem. Biol.* **2020**, *27* (7), 866-876.e8. https://doi.org/10.1016/j.chembiol.2020.04.008.

(266) Yang, K.; Wu, H.; Zhang, Z.; Leisten, E. D.; Nie, X.; Liu, B.; Wen, Z.; Zhang, J.; Cunningham, M. D.; Tang, W. Development of Selective Histone Deacetylase 6 (HDAC6) Degraders Recruiting Von Hippel–Lindau (VHL) E3 Ubiquitin Ligase. *ACS Med. Chem. Lett.* **2020**, *11* (4), 575–581. https://doi.org/10.1021/acsmedchemlett.0c00046.

(267) Yang, H.; Lv, W.; He, M.; Deng, H.; Li, H.; Wu, W.; Rao, Y. Plasticity in Designing PROTACs for Selective and Potent Degradation of HDAC6. *Chem. Commun.* **2019**, *55* (98), 14848–14851. https://doi.org/10.1039/C9CC08509B.

(268) Smalley, J. P.; Adams, G. E.; Millard, C. J.; Song, Y.; Norris, J. K. S.; Schwabe, J. W. R.; Cowley, S. M.; Hodgkinson, J. T. PROTAC-Mediated Degradation of Class I Histone Deacetylase Enzymes in Corepressor Complexes. *Chem. Commun.* **2020**, *56* (32), 4476–4479. https://doi.org/10.1039/D0CC01485K.

(269) Smalley, J. P.; Baker, I. M.; Pytel, W. A.; Lin, L.-Y.; Bowman, K. J.; Schwabe, J. W. R.; Cowley, S. M.; Hodgkinson, J. T. Optimization of Class I Histone Deacetylase PROTACs Reveals That HDAC1/2 Degradation Is Critical to Induce Apoptosis and Cell Arrest in Cancer Cells. *J. Med. Chem.* **2022**, *65* (7), 5642–5659. https://doi.org/10.1021/acs.jmedchem.1c02179.

(270) Nowak, R. P.; DeAngelo, S. L.; Buckley, D.; He, Z.; Donovan, K. A.; An, J.; Safaee, N.; Jedrychowski, M. P.; Ponthier, C. M.; Ishoey, M.; Zhang, T.; Mancias, J. D.; Gray, N. S.; Bradner, J. E.; Fischer, E. S. Plasticity in Binding Confers Selectivity in Ligand-Induced Protein Degradation. *Nat. Chem. Biol.* **2018**, *14* (7), 706–714. https://doi.org/10.1038/s41589-018-0055-y.

(271) Zibinsky, M.; Fokin, V. V. Reactivity of N-(1,2,4-Triazolyl)-Substituted 1,2,3-Triazoles. *Org. Lett.* **2011**, *13* (18), 4870–4872. https://doi.org/10.1021/ol201949h.

(272) Crawford, T. D.; Tsui, V.; Flynn, E. M.; Wang, S.; Taylor, A. M.; Côté, A.; Audia, J. E.; Beresini, M. H.; Burdick, D. J.; Cummings, R.; Dakin, L. A.; Duplessis, M.; Good, A. C.; Hewitt, M. C.; Huang, H.-R.; Jayaram, H.; Kiefer, J. R.; Jiang, Y.; Murray, J.; Nasveschuk, C. G.; Pardo, E.; Poy, F.; Romero, F. A.; Tang, Y.; Wang, J.; Xu, Z.; Zawadzke, L. E.; Zhu, X.; Albrecht, B. K.; Magnuson, S. R.; Bellon, S.; Cochran, A. G. Diving into the Water: Inducible Binding Conformations for BRD4, TAF1(2),

BRD9, and CECR2 Bromodomains. *J. Med. Chem.* **2016**, *59* (11), 5391–5402. https://doi.org/10.1021/acs.jmedchem.6b00264.

(273) Improvement in the Palladium-Catalyzed Miyaura Borylation Reaction by Optimization of the Base: Scope and Mechanistic Study. *J. Org. Chem.* **2020**, *86* (1), 103–109. https://doi.org/10.1021/acs.joc.0c01758.

(274) Lv, J.; Chen, X.; Xue, X.-S.; Zhao, B.; Liang, Y.; Wang, M.; Jin, L.; Yuan, Y.; Han, Y.; Zhao, Y.; Lu, Y.; Zhao, J.; Sun, W.-Y.; Houk, K. N.; Shi, Z. Metal-Free Directed Sp2-C–H Borylation. *Nature* **2019**, *575* (7782), 336–340. https://doi.org/10.1038/s41586-019-1640-2.

(275) Lv, J.; Zhao, B.; Yuan, Y.; Han, Y.; Shi, Z. Boron-Mediated Directed Aromatic C–H Hydroxylation. *Nat. Commun.* **2020**, *11* (1), 1316. https://doi.org/10.1038/s41467-020-15207-x.

(276) Wagner, F. F.; Lundh, M.; Kaya, T.; McCarren, P.; Zhang, Y.-L.; Chattopadhyay, S.; Gale, J. P.; Galbo, T.; Fisher, S. L.; Meier, B. C.; Vetere, A.; Richardson, S.; Morgan, N. G.; Christensen, D. P.; Gilbert, T. J.; Hooker, J. M.; Leroy, M.; Walpita, D.; Mandrup-Poulsen, T.; Wagner, B. K.; Holson, E. B. An Isochemogenic Set of Inhibitors To Define the Therapeutic Potential of Histone Deacetylases in β-Cell Protection. *ACS Chem. Biol.* **2016**, *11* (2), 363–374. https://doi.org/10.1021/acschembio.5b00640.

(277) Bauer, N.; Balourdas, D.-I.; Schneider, J. R.; Zhang, X.; Berger, L. M.; Berger, B.-T.; Schwalm, M. P.; Klopp, N. A.; Siveke, J. T.; Knapp, S.; Joerger, A. C. Development of Potent Dual BET/HDAC Inhibitors via 2 Pharmacophore Merging and Structure-Guided Optimization. *ACS Chem. Biol.* **2023**. https://doi.org/10.1021/acschembio.3c00427.

(278) Alekseyenko, A. A.; Walsh, E. M.; Wang, X.; Grayson, A. R.; Hsi, P. T.; Kharchenko, P. V.; Kuroda, M. I.; French, C. A. The Oncogenic BRD4-NUT Chromatin Regulator Drives Aberrant Transcription within Large Topological Domains. *Genes Dev.* **2015**, *29* (14), 1507–1523. https://doi.org/10.1101/gad.267583.115.

(279) Eaton, P. E.; Cole, T. W. Cubane. *J. Am. Chem. Soc.* **1964**, *86* (15), 3157–3158. https://doi.org/10.1021/ja01069a041.

(280) Eaton, P. E. Cubanes: Starting Materials for the Chemistry of the 1990s and the New Century. *Angew. Chem. Int. Ed. Engl.* **1992**, *31* (11), 1421–1436. https://doi.org/10.1002/anie.199214211.

(281) Eaton, P. E.; Cole, T. W. The Cubane System. *J. Am. Chem. Soc.* **1964**, *86* (5), 962–964. https://doi.org/10.1021/ja01059a072.

(282) Wlochal, J.; Davies, R. D. M.; Burton, J. Cubanes in Medicinal Chemistry: Synthesis of Functionalized Building Blocks. *Org. Lett.* **2014**, *16* (16), 4094–4097. https://doi.org/10.1021/ol501750k.

(283) Nicolaou, K. C.; Vourloumis, D.; Totokotsopoulos, S.; Papakyriakou, A.; Karsunky, H.; Fernando, H.; Gavrilyuk, J.; Webb, D.; Stepan, A. F. Synthesis and Biopharmaceutical Evaluation of Imatinib Analogues Featuring Unusual Structural Motifs. *ChemMedChem* **2016**, *11* (1), 31–37. https://doi.org/10.1002/cmdc.201500510.

(284) Chalmers, B. A.; Xing, H.; Houston, S.; Clark, C.; Ghassabian, S.; Kuo, A.; Cao, B.; Reitsma, A.; Murray, C.-E. P.; Stok, J. E.; Boyle, G. M.; Pierce, C. J.; Littler, S. W.; Winkler, D. A.; Bernhardt, P. V.; Pasay, C.; De Voss, J. J.; McCarthy, J.; Parsons, P. G.; Walter, G. H.; Smith, M. T.; Cooper, H. M.; Nilsson, S. K.; Tsanaktsidis, J.; Savage, G. P.; Williams, C. M. Validating Eaton's Hypothesis: Cubane as a Benzene Bioisostere. *Angew. Chem. Int. Ed.* **2016**, *55* (11), 3580–3585. https://doi.org/10.1002/anie.201510675.

(285) Houston, S. D.; Fahrenhorst-Jones, T.; Xing, H.; Chalmers, B. A.; Sykes, M. L.; Stok, J. E.; Soto, C. F.; Burns, J. M.; Bernhardt, P. V.; Voss, J. J. D.; Boyle, G. M.; Smith, M. T.; Tsanaktsidis, J.; Savage, G. P.; Avery, V. M.; Williams, C. M. The Cubane Paradigm in Bioactive Molecule Discovery: Further Scope, Limitations and the Cyclooctatetraene Complement. *Org. Biomol. Chem.* **2019**, *17* (28), 6790–6798. https://doi.org/10.1039/C9OB01238A.

(286) Reekie, T. A.; Williams, C. M.; Rendina, L. M.; Kassiou, M. Cubanes in Medicinal Chemistry. *J. Med. Chem.* **2019**, *62* (3), 1078–1095. https://doi.org/10.1021/acs.jmedchem.8b00888.

(287) Biegasiewicz, K. F.; Griffiths, J. R.; Savage, G. P.; Tsanaktsidis, J.; Priefer, R. Cubane: 50 Years Later. *Chem. Rev.* **2015**, *115* (14), 6719–6745. https://doi.org/10.1021/cr500523x.

(288) Yoshino, N.; Kato, Y.; Mabit, T.; Nagata, Y.; Williams, C. M.; Harada, M.; Muranaka, A.; Uchiyama, M.; Matsubara, S. Cubane Chirality via Substitution of a "Hidden" Regular Tetrahedron. *Org. Lett.* **2020**, *22* (11), 4083–4087. https://doi.org/10.1021/acs.orglett.0c01142.

(289) Collin, D. E.; Kovacic, K.; Light, M. E.; Linclau, B. Synthesis of Ortho-Functionalized 1,4-Cubanedicarboxylate Derivatives through Photochemical Chlorocarbonylation. *Org. Lett.* **2021**, *23* (13), 5164–5169. https://doi.org/10.1021/acs.orglett.1c01702.

(290) Okude, R.; Mori, G.; Yagi, A.; Itami, K. Programmable Synthesis of Multiply Arylated Cubanes through C–H Metalation and Arylation. *Chem. Sci.* **2020**, *11* (29), 7672–7675. https://doi.org/10.1039/D0SC01909G.

(291) Collin, D. E.; Jackman, E. H.; Jouandon, N.; Sun, W.; Light, M. E.; Harrowven, D. C.; Linclau, B. Decagram Synthesis of Dimethyl 1,4-Cubanedicarboxylate Using Continuous-Flow Photochemistry. *Synthesis* **2021**, *53* (7), 1307–1314. https://doi.org/10.1055/s-0040-1705964.

(292) Bernhard, S. S. R.; Locke, G. M.; Plunkett, S.; Meindl, A.; Flanagan, K. J.; Senge, M. O. Cubane Cross-Coupling and Cubane–Porphyrin Arrays. *Chem. − Eur. J.* **2018**, *24* (5), 1026–1030. https://doi.org/10.1002/chem.201704344.

(293) Wiesenfeldt, M. P.; Rossi-Ashton, J. A.; Perry, I. B.; Diesel, J.; Garry, O. L.; Bartels, F.; Coote, S. C.; Ma, X.; Yeung, C. S.; Bennett, D. J.; MacMillan, D. W. C. General Access to Cubanes as Benzene Bioisosteres. *Nature* **2023**, *618* (7965), 513–518. https://doi.org/10.1038/s41586-023-06021-8.

(294) Kazi, N.; C. Aublette, M.; L. Allinson, S.; C. Coote, S. A Practical Synthesis of 1,3-Disubstituted Cubane Derivatives. *Chem. Commun.* **2023**, *59* (51), 7971–7973. https://doi.org/10.1039/D3CC02164E.

(295) Falkiner, M. J.; Littler, S. W.; McRae, K. J.; Savage, G. P.; Tsanaktsidis, J. Pilot-Scale Production of Dimethyl 1,4-Cubanedicarboxylate. *Org. Process Res. Dev.* **2013**, *17* (12), 1503–1509. https://doi.org/10.1021/op400181g.

(296) Prentice, C.; Martin, A. E.; Morrison, J.; Smith, A. D.; Zysman-Colman, E. Benzophenone as a Cheap and Effective Photosensitizer for the Photocatalytic Synthesis of Dimethyl Cubane-1,4-Dicarboxylate. *Org. Biomol. Chem.* **2023**, *21* (16), 3307–3310. https://doi.org/10.1039/D3OB00231D.

(297) Zhang, M.-X.; Eaton, P. E.; Gilardi, R. Hepta- and Octanitrocubanes. *Angew. Chem. Int. Ed.* **2000**, *39* (2), 401–404. https://doi.org/10.1002/(SICI)1521-3773(20000117)39:2<401::AID-ANIE401>3.0.CO;2-P.

(298) Eaton, P. E.; Zhang, M.-X.; Gilardi, R.; Gelber, N.; Iyer, S.; Surapaneni, R. Octanitrocubane: A New Nitrocarbon. *Propellants Explos. Pyrotech.* **2002**, *27* (1), 1–6. https://doi.org/10.1002/1521-4087(200203)27:1<1::AID-PREP1>3.0.CO;2-6.

(299) Chapman, N. B.; Key, J. M.; Toyne, K. J. Preparations and Properties of Caged Polycyclic Systems. 1. Pentacyclo[5.3.0.02,5.03,9.04,8]Decane and Pentacyclo[4.3.0.02,5.03,8.04,7]Nonane Derivatives. *J. Org. Chem.* **1970**, *35* (11), 3860–3867. https://doi.org/10.1021/jo00836a062.

(300) Eremenko, L. T.; Romanova, L. B.; Ivanova, M. E.; Eremenko, I. L.; Nefedov, S. E.; Struchkov, Yu. T. Cubane Derivatives 1. Synthesis and Molecular Structures of the Esters of 1,4-Cubanedicarboxylic Acid. *Russ. Chem. Bull.* **1994**, *43* (4), 619–623. https://doi.org/10.1007/BF00699835.

(301) Barborak, J. C.; Watts, L.; Pettit, R. A Convenient Synthesis of the Cubane System. *J. Am. Chem. Soc.* **1966**, *88* (6), 1328–1329. https://doi.org/10.1021/ja00958a050.

(302) Eaton, P. E.; Xiong, Y.; Gilardi, R. Systematic Substitution on the Cubane Nucleus. Synthesis and Properties of 1,3,5-Trinitrocubane and 1,3,5,7-Tetranitrocubane. *J. Am. Chem. Soc.* **1993**, *115* (22), 10195–10202. https://doi.org/10.1021/ja00075a039.

(303) Doedens, R. J.; Eaton, P. E.; Fleischer, E. B. The Bent Bonds of Cubane. *Eur. J. Org. Chem.* **2017**, *2017* (18), 2627–2630. https://doi.org/10.1002/ejoc.201700427.

(304) Plunkett, S.; Flanagan, K. J.; Twamley, B.; Senge, M. O. Highly Strained Tertiary Sp3 Scaffolds: Synthesis of Functionalized Cubanes and Exploration of Their Reactivity under Pd(II) Catalysis. *Organometallics* **2015**, *34* (7), 1408–1414. https://doi.org/10.1021/acs.organomet.5b00151.

(305) Eaton, P. E.; Cassar, L.; Halpern, J. Silver(I)- and Palladium(II)-Catalyzed Isomerizations of Cubane. Synthesis and Characterization of Cuneane. *J. Am. Chem. Soc.* **1970**, *92* (21), 6366–6368. https://doi.org/10.1021/ja00724a061.

(306) Cassar, L.; Eaton, P. E.; Halpern, J. Catalysis of Symmetry-Restricted Reactions by Transition Metal Compounds. Valence Isomerization of Cubane. *J. Am. Chem. Soc.* **1970**, *92* (11), 3515–3518. https://doi.org/10.1021/ja00714a075.

(307) Toriyama, F.; Cornella, J.; Wimmer, L.; Chen, T.-G.; Dixon, D. D.; Creech, G.; Baran, P. S. Redox-Active Esters in Fe-Catalyzed C–C Coupling. *J. Am. Chem. Soc.* **2016**, *138* (35), 11132–11135. https://doi.org/10.1021/jacs.6b07172.

(308) Le, C.; Chen, T. Q.; Liang, T.; Zhang, P.; MacMillan, D. W. C. A Radical Approach to the Copper Oxidative Addition Problem: Trifluoromethylation of Bromoarenes. *Science* **2018**, *360* (6392), 1010–1014. https://doi.org/10.1126/science.aat4133.

(309) Sakai, H. A.; Liu, W.; Le, C. "Chip"; MacMillan, D. W. C. Cross-Electrophile Coupling of Unactivated Alkyl Chlorides. *J. Am. Chem. Soc.* **2020**, *142* (27), 11691–11697. https://doi.org/10.1021/jacs.0c04812.

(310) Levterov, V. V.; Panasiuk, Y.; Sahun, K.; Stashkevych, O.; Badlo, V.; Shablykin, O.; Sadkova, I.; Bortnichuk, L.; Klymenko-Ulianov, O.; Holota, Y.; Lachmann, L.; Borysko, P.; Horbatok, K.; Bodenchuk, I.; Bas, Y.; Dudenko, D.; Mykhailiuk, P. K. 2-Oxabicyclo[2.2.2]Octane as a New Bioisostere of the Phenyl Ring. *Nat. Commun.* **2023**, *14* (1), 5608. https://doi.org/10.1038/s41467-023-41298-3.

(311) Nicolaou, K. C.; Estrada, A. A.; Zak, M.; Lee, S. H.; Safina, B. S. A Mild and Selective Method for the Hydrolysis of Esters with Trimethyltin Hydroxide. *Angew. Chem. Int. Ed.* **2005**, *44* (9), 1378–1382. https://doi.org/10.1002/anie.200462207.

(312) Machleidt, T.; Woodroofe, C. C.; Schwinn, M. K.; Méndez, J.; Robers, M. B.; Zimmerman, K.; Otto, P.; Daniels, D. L.; Kirkland, T. A.; Wood, K. V. NanoBRET—A Novel BRET Platform for the Analysis of Protein–Protein Interactions. *ACS Chem. Biol.* **2015**, *10* (8), 1797–1804. https://doi.org/10.1021/acschembio.5b00143.

(313) Howitz, K. T. Screening and Profiling Assays for HDACs and Sirtuins. *Drug Discov. Today Technol.* **2015**, *18*, 38–48. https://doi.org/10.1016/j.ddtec.2015.10.008.

(314) Schwalm, M. P.; Krämer, A.; Dölle, A.; Weckesser, J.; Yu, X.; Jin, J.; Saxena, K.; Knapp, S. Tracking the PROTAC Degradation Pathway in Living Cells Highlights the Importance of Ternary Complex Measurement for PROTAC Optimization. *Cell Chem. Biol.* **2023**, *30* (7), 753-765.e8. https://doi.org/10.1016/j.chembiol.2023.06.002.

(315) Ito, H.; Abe, H.; Sato, A.; Tokishita, S.; Ohta, T. Synthesis of Fluorescence Pyriproxyfen Analogues as Juvenile Hormone Agonists. *HETEROCYCLES* **2011**, *83* (7), 1649. https://doi.org/10.3987/COM-11-12232.

(316) Xie, L.-Y.; Duan, Y.; Lu, L.-H.; Li, Y.-J.; Peng, S.; Wu, C.; Liu, K.-J.; Wang, Z.; He, W.-M. Fast, Base-Free and Aqueous Synthesis of Quinolin-2(1H)-Ones under Ambient Conditions. *ACS Sustain. Chem. Eng.* **2017**, *5* (11), 10407–10412. https://doi.org/10.1021/acssuschemeng.7b02442.

8   List of abbreviations

5mC	5-methylcytosine
A	alanine
acac	acetylacetone
ACN	acetonitrile
AcOH	acetic acid
ADP	adenosine diphosphate
ASN	asparagine
ATLL	adult T-cell leukemia-lymphoma
AUC	area under the curve
BCP	BD-containing protein
BD	bromodomain
BER	base excision repair
BET	bromodomain and extra-terminal
Boc	*tert*-butyloxycarbonyl
bpy	2,2'-bipyridine
CBRN	cereblon
CDK9	cyclin-dependent kinase 9
CGI	CpG islands
CoA	coenzyme A
CoREST	corepressor of REST
CpG	cytosine-phosphate-guanine
CTCL	cutaneous T-cell lymphoma
CTD	C-terminal domain
D	aspartic acid
DCE	1,2-dichloroethane
DCM	dichloromethane
DIAD	diisopropyl azodicarboxylate
DIPEA	*N*,*N*-diisopropylethylamine
DMAP	4-dimethylaminopyridine
DMF	*N*,*N*-dimethylformamide
DMF-DMA	*N*,*N*-dimethylformamide dimethyl acetal
DMP	Dess-Martin periodinane
DMSO	dimethyl sulfoxide
DNA	deoxyribonucleic acid
DNMT	DNA methyltransferase
DSF	differential scanning fluorimetry
EC_{50}	half maximal effective concentration
EDC	1-ethyl-3-(3-dimethylaminopropyl)carbodiimide
EMA	European Medicines Agency
ESI	electrospray ionization
ET	extra-terminal
et al.	and others
EtOH	ethanol
F	phenylalanine
FDA	United States Food and Drug Administration
Fmoc	fluorenylmethoxycarbonyl

FTO	fat mass and obesity-associated protein
H	histidine
H2A/2B/3/4	histone 2A/2B/3/4
HAT	histone acetyl transferase
HATU	*O*-(7-Azabenzotriazol-1-yl)-*N,N,N',N'*-tetramethyluronium-hexafluorphosphate
HDAC	histone deacetylase
HEPES	4-(2-hydroxyethyl)-1-piperazineethanesulfonic acid
HPLC	high-performance liquid chromatography
HRMS	high-resolution mass spectrometry
I	isoleucine
IC_{50}	half maximal inhibitory concentration
ip	intraperitoneal
*i*Pr	isopropyl
ITC	isothermal titration calorimetry
iv	intravenous
K	lysine
K_D	dissociation constant
LDA	lithium diisopropylamide
lncRNA	long non-coding RNA
m^6A	N^6-methyl adenosine
MALDI	matrix-assisted laser desorption/ionization
*m*CPBA	*meta*-chloroperoxybenzoic
MeOH	methanol
MeTHF	2-methyltetrahydrofuran
MiDAC	mitotic deacetylase complex
miRNA	microRNA
MM	multiple myeloma
mRNA	messenger RNA
MS	mass spectrometry
MsCl	mesyl chloride
N	asparagine
NAD	nicotinamide adenine dinucleotide
NaOAc	sodium acetate
NBS	*N*-bromosuccinimide
NCoR	nuclear receptor corepressor
NIS	*N*-iodosuccinimide
NMC	NUT midline carcinoma
NMPA	National Medical Products Administration
NMR	nuclear magnetic resonance
NuRD	nucleosome remodeling and deacetylase complex
NUT	nuclear protein in testis
P	proline
PDAC	pancreatic ductal adenocarcinoma
PDB	Protein Data Bank
pin	pinacol
Piv	pivaloyl
PK	pharmacokinetics
po	*per os*, by mouth

POI	protein of interest
PROTAC	proteolysis targeting chimera
PTCL	peripheral T-cell lymphoma
p-TEFb	positive transcription elongation factor b
PyAOP	(7-Azabenzotriazol-1-yloxy)tripyrrolidinophosphonium hexafluorophosphate
Q	glutamine
RNA	ribonucleic acid
RNAP II	RNA polymerase II
RT-PCR	reverse transcription polymerase chain reaction
SAHA	suberanilohydroxamic acid
SAR	structure-activity relationship
SEM	standard error of the mean
SMRT	silencing mediator of retinoic acid and thyroid hormone receptor
SUMO	small ubiquitin-related modifier
supersilane	tris(trimethylsilyl)silane
T3P	propanephosphonic acid anhydride
TCEP	tris(2-carboxyethyl)phosphine
TFA	trifluoroacetic acid
THF	tetrahydrofuran
THP	tetrahydropyranyl
T_m	melting temperature
TMS	trimethylsilyl
TRIM	tripartite motif-containing protein
tRNA	transfer RNA
Ts	tosyl
UPS	ubiquitin-proteasome system
UV	ultraviolet
V	valine
VHL	von Hippel-Lindau
vs.	*versus*, against, opposed to
W	tryptophan
WB	Western blot
Xphos	dicyclohexyl[2',4',6'-tris(propan-2-yl)[1,1'-biphenyl]-2-yl]phosphane
ZBG	zinc-binding group
ΔT_m	difference in melting temperature

9 List of Figures

10   List of Schemes

11 List of Tables

12 Appendix

12.1 Supporting Tables

Supporting Table S 1: Stabilization of BRD4 by different substituted phenols

Compound		DSF ΔT_m (K)	
		BRD4 BD1	**BRD4 BD2**
MS436 (**22**)		4.0	2.9
100		4.1	3.4
100a		1.5	1.2
100b		2.0	2.2
100c		0.2	0.2
100d		3.3	2.6
100e		2.2	1.9
100f		0.1	-0.4
100g		-0.8	-0.2
102a		5.2	3.0
106		4.0	2.0

Supporting Table S 2: NanoBRET data for BRD4-BD1/2 in intact and lysed cells

Compound	BRD4-BD1 EC$_{50}$ (µM)[1]		BRD4-BD2 EC$_{50}$ (µM)[1]	
	Lysed cells	Intact cells	Lysed cells	Intact cells
102a	> 50 (2)	40.2 ± 2.4 (2)	> 50 (2)	>50 (1)
107b	0.35 ± 0.06 (2)	0.19 ± 0.03 (2)	0.16 ± 0.02 (2)	0.05 ± 0.01 (2)
114a	0.30 ± 0.03 (3)	0.18 ± 0.03 (3)	0.20 ± 0.01 (3)	0.20 ± 0.03 (3)
123a	0.29 ± 0.01 (3)	0.25 ± 0.02 (3)	0.15 ± 0.01 (3)	0.19 ± 0.02 (3)
123b	2.34 ± 0.14 (3)	3.7 ± 0.5 (3)	1.32 ± 0.15 (3)	2.05 ± 0.37 (3)
123c	0.38 ± 0.05 (3)	0.39 ± 0.06 (3)	0.17 ± 0.02 (3)	0.23 ± 0.07 (3)
119	1.38 ± 0.09 (3)	2.55 ± 0.08 (3)	1.37 ± 0.30 (3)	2.94 ± 0.18 (3)
123d	0.24 ± 0.01 (3)	0.24 ± 0.02 (3)	0.10 ± 0.03 (3)	0.16 ± 0.04 (3)
123e	0.38 ± 0.01 (3)	0.39 ± 0.02 (3)	0.20 ± 0.02 (3)	0.29 ± 0.12 (3)
123f	0.35 ± 0.06 (3)	0.48 ± 0.14 (3)	0.19 ± 0.02 (3)	0.32 ± 0.13 (3)
132a	0.61 ± 0.19 (3)	0.42 ± 0.11 (3)	0.94 ± 0.34 (3)	0.52 ± 0.18 (3)
133	0.21 ± 0.01 (3)	0.34 ± 0.10 (3)	0.16 ± 0.03 (3)	0.10 ± 0.01 (3)
132b	0.32 ± 0.07 (3)	0.36 ± 0.13 (3)	0.13 ± 0.01 (3)	0.25 ± 0.12 (3)
132c	0.43 ± 0.06 (3)	0.37 ± 0.05 (3)	0.29 ± 0.05 (3)	0.31 ± 0.05 (3)
132d	0.33 ± 0.02 (3)	0.29 ± 0.05 (3)	0.22 ± 0.02 (3)	0.18 ± 0.04 (3)
MS436 (**22**)	3.61 ± 0.54 (2)	2.85 ± 0.40 (3)	> 50 (2)	61.7 ± 14.9 (3)
(+)-JQ1 (**13**)	0.043 ± 0.002 (2)	0.058 ± 0.015 (3)	0.13 ± 0.01 (2)	0.11 ± 0.01 (3)
CI-994 (**7**)	> 50 (3)	ND	> 50 (3)	ND

[1]Mean of n independent measurements with SEM. Number n of independent measurements (each performed in technical duplicates) is given in parentheses.

Supporting Table S 3: NanoBRET data for HDAC1/2 in intact and lysed cells

Compound	HDAC1 EC$_{50}$ (μM)[1]		HDAC2 EC$_{50}$ (μM)[1]	
	Lysed cells	Intact cells	Lysed cells	Intact cells
102a	2.58 ± 0.10 (3)	10.8 ± 5.1 (5)	0.85 ± 0.14 (2)	> 50 (2)
107b	0.70 ± 0.16 (2)	2.07 ± 0.73 (5)	0.51 ± 0.16 (2)	1.30 ± 0.86 (3)
114a	11.0 ± 1.8 (3)	23.2 ± 10.5 (5)	12.2 ± 5.9 (2)	24.8 ± 12.1 (3)
123a	0.46 ± 0.09 (3)	2.62 ± 1.08 (5)	0.48 ± 0.08 (2)	1.55 ± 0.73 (3)
123b	32.2 ± 7.1 (3)	34.4 ± 5.8 (5)	32.7 ± 8.9 (2)	39.7 ± 9.0 (3)
123c	> 50 (3)	> 50 (5)	43.3 ± 0.3 (2)	> 50 (3)
119	1.24 ± 0.13 (3)	2.26 ± 0.64 (5)	0.58 ± 0.01 (2)	3.73 ± 2.4 (3)
123d	1.09 ± 0.22 (3)	4.84 ± 2.28 (5)	0.62 ± 0.01 (2)	2.48 ± 0.66 (3)
123e	3.64 ± 0.32 (3)	16.8 ± 6.7 (5)	3.24 ± 0.30 (2)	4.56 ± 0.57 (3)
123f	3.25 ± 0.32 (3)	6.09 ± 0.96 (5)	2.58 ± 0.31 (2)	3.09 ± 0.13 (3)
132a	0.25 ± 0.10 (3)	0.19 ± 0.03 (5)	0.41 ± 0.05 (2)	0.36 ± 0.12 (3)
133	8.2 ± 2.1 (3)	36.3 ± 11.8 (5)	6.46 ± 1.50 (2)	14.2 ± 4.5 (3)
132b	0.027 ± 0.010 (3)	0.11 ± 0.03 (5)	0.037 ± 0.008 (2)	0.098 ± 0.016 (3)
132c	0.12 ± 0.06 (3)	1.32 ± 0.98 (5)	0.26 ± 0.05 (2)	2.87 ± 1.68 (3)
132d	0.022 ± 0.008 (3)	0.14 ± 0.05 (5)	0.064 ± 0.013 (2)	0.058 ± 0.014 (3)
MS436 (**22**)	> 50 (3)	18.8 ± 1.0 (4)	> 50 (2)	> 50 (2)
(+)-JQ1 (**13**)	> 50 (2)	> 50 (2)	> 50 (2)	> 50 (2)
CI-994 (**7**)	1.62 ± 0.36 (3)	4.95 ± 0.77 (8)	1.43 ± 0.14 (2)	2.02 ± 0.40 (3)

[1]Mean of n independent measurements with SEM. Number n of independent measurements (each performed in technical duplicates) is given in parentheses.

Supporting Table S 4: ITC thermodynamic data of inhibitors binding to BRD4 BD1

	Compound	
	123a	**123d**
K_d (M)	1.52E-07 ± 7.29E-08	4.58E-08 ± 3.51E-08
n	0.996 ± 0.029	1.003 ± 0.022
ΔH (kcal/mol)	-10.36 ± 0.501	-7.844 ± 0.360
ΔS (cal/mol·K)	-4.759	6.358
ΔG (kcal/mol)	-8.99	-9.676
-TΔS (kcal/mol)	1.371	-1.832
K_a (M^{-1})	6.58E+06	2.18E+07
Confidence Level (%)	95	95

Supporting Table S 5: Inhibition of zinc-dependent HDACs by compound 132b

Target	% Enzyme activity (no inhibitor control as 100% activity)[1]	
	1 μM **132b**	10 μM **132b**
HDAC1	20.6 ± 0.1	10.3 ± 0.6
HDAC2	50.3 ± 0.9	13.5 ± 0.3
HDAC3	95.5 ± 2.7	76.4 ± 1.0
HDAC4	91.5 ± 0.9	82.4 ± 0.5
HDAC5	89.3 ± 0.1	84.1 ± 5.7
HDAC6	100.3 ± 1.1	90.2 ± 2.8
HDAC7	100.6 ± 1.8	101.2 ± 3.0
HDAC8	96.4 ± 2.2	97.9 ± 1.8
HDAC9	96.2 ± 2.4	85.0 ± 1.6
HDAC10	98.1 ± 1.1	98.6 ± 0.3
HDAC11	97.7 ± 0.1	59.9 ± 2.5

[1] Average of duplicate measurements

Supporting Table S 6: Bromodomain panel selectivity data

Protein	Mean ΔT_m (K)[1]	
	123a	**132a**
ATAD2A	0.4 ± 0.2	-1.3 ± 0.1
BAZ2B	0.5 ± 0.0	1.4 ± 0.1
BRD1	0.2 ± 0.1	1.1 ± 0.1
BRD2 (1)	3.1 ± 0.5	3.2 ± 0.5
BRD2 (2)	5.3 ± 0.1	3.6 ± 0.4
BRD3 (1)	3.8 ± 0.3	3.8 ± 0.4
BRD3 (2)	6.1 ± 0.0	4.6 ± 0.7
BRD4 (1)	3.6 ± 0.1	5.5 ± 0.1
BRD4 (2)	4.6 ± 0.1	5.3 ± 0.2
BRD7	5.6 ± 0.3	1.1 ± 0.2
BRD9	5.2 ± 1.2	1.0 ± 0.8
BRDT(1)	3.0 ± 0.2	3.3 ± 0.1
BRDT(2)[2]	n.d.	n.d.
BRPF1B	0.8 ± 0.1	0.8 ± 0.3
BRPF3	-0.5 ± 0.1	1.2 ± 0.1
CREBBPA	1.8 ± 0.3	1.4 ± 0.3
EP300A	2.0 ± 0.3	1.0 ± 0.3
PB1A(3)	0.5 ± 0.2	0.0 ± 0.0
PB1A(4)	0.1 ± 0.1	1.0 ± 0.6
PB1A(5)	0.0 ± 0.1	1.1 ± 0.2
PB1A(6)	0.3 ± 0.1	1.3 ± 0.1
PCAFA	0.1 ± 0.4	1.9 ± 0.2
SMARCA2A	-0.1 ± 0.1	1.2 ± 0.5
SP100	-0.2 ± 0.1	0.4 ± 0.1
TAF1 (1)	0.4 ± 0.1	1.0 ± 0.2
TAF1 (2)	1.3 ± 0.0	1.7 ± 0.1
TAF1LA (1)	0.3 ± 0.1	0.6 ± 0.3
TAF1LA (2)	1.7 ± 0.1	1.2 ± 0.0
TRIM24[3]	0.6 ± 0.1	0.7 ± 0.5
TRIM28[3]	0.6 ± 0.4	0.0 ± 0.2
TRIM33B[3]	0.4 ± 0.1	0.5 ± 0.0
WDR9A(1)	-0.3 ± 0.2	0.0 ± 0.0

[1] Mean and SEM of an independent measurement performed in technical triplicates.
[2] Boltzmann fitting failed.
[3] Construct containing tandem PHD-BD.

Supporting Table S 7: Viability of PaTu8988t and HCC2429 cells upon treatment with dual BET/HDAC inhibitors for 3 days.

Compound	Cell viability (IC$_{50}$; µM)	
	PaTu8988t	HCC2429
CI-994 (**7**)	13.1 ± 2.4	1.8 ± 0.2
MS436 (**22**)	10.4 ± 1.2	0.81 ± 0.15
MS436 + CI-994	6.0 ± 0.5	0.96 ± 0.17
123a	2.7 ± 0.3	0.40 ± 0.03
123d	3.2 ± 0.4	0.22 ± 0.02
123e	8.5 ± 1.3	0.54 ± 0.06
123f	15.6 ± 2.4	0.93 ± 0.08
132a	2.8 ± 0.2	0.63 ± 0.08
133	5.2 ± 0.9	0.24 ± 0.02
132b	3.6 ± 0.4	0.42 ± 0.05
132c	2.6 ± 0.3	0.32 ± 0.04
132d	4.1 ± 0.7	0.55 ± 0.06

Supporting Table S 8: PK study data for compound 132a

NB512 (132a) @ 10 mg/kg po					
Time (h)	Mouse ID	Plasma conc. [ng/ml]	Mean [ng/ml]	SD [ng/ml]	CV%
0,25	#1	1395	1429	761	53,3
	#2	686			
	#3	2207			
0,5	#1	1159	1112	533	47,9
	#2	557			
	#3	1619			
1	#4	783	513	242	47,1
	#5	440			
	#6	316			
4	#1	49,0	39,2	9,6	24,5
	#2	29,7			
	#3	39,0			
8	#4	135	81,2	46,9	57,8
	#5	54,8			
	#6	53,4			
24	#4	91,1	32,6	50,7	156
	#5	5,5			
	#6	1,2			
NB512 (132a) @ 10 mg/kg iv					
Time (h)	Mouse ID	Plasma conc. [ng/ml]	Mean [ng/ml]	SD [ng/ml]	CV%

Time (h)	Mouse ID	Plasma conc. [ng/ml]	Mean [ng/ml]	SD [ng/ml]	CV%
0,083	#7*	4.2*	2613	102	3,9
	#8	2685			
	#9	2540			
0,25	#10	67,8	90,1	25,4	28,2
	#11	118			
	#12	84,7			
0,5	#7*	34.1*	663	644	97,1
	#8	208			
	#9	1119			
1	#10	28,6	47,3	27,4	57,9
	#11	78,7			
	#12	34,5			
4	#7*	14.4*	34,8	6,0	17,2
	#8	30,6			
	#9	39,0			
8	#10	8,8	13,7	5,0	36,7
	#11	18,9			
	#12	13,5			

NB512 (132a) @ 10 mg/kg ip					
Time (h)	Mouse ID	Plasma conc. [ng/ml]	Mean [ng/ml]	SD [ng/ml]	CV%
0,083	#13	2565	1651	1265	76,6
	#14	2182			
	#15	207			
0,25	#16	713	3519	2621	74,5
	#17	5903			
	#18	3940			
0,5	#13	2644	2140	882	41,2
	#14	2654			
	#15	1121			
1	#16	757	1434	922	64,3
	#17	2484			
	#18	1061			
4	#13	136	99,3	38,4	38,7
	#14	59,1			
	#15	103			
8	#16	98,3	52,3	41,2	78,7
	#17	40,0			
	#18	18,7			

Supporting Table S 9: PK study summary for compound 132b

Animal Species	Mouse		
Strain	CD1		
Gender	male		
BW range (g)	35-39	36-41	37-40
Dose route	po	iv	ip

Vehicle	5% DMSO/ 95% Cyclodextrin (10%)	5% DMSO/ 95% PBS	5% DMSO/ 95% Cyclodextrin (10%)
PK analysis software	Kinetica 5.0		
Dosage (mg/kg)	10	10	10
Application volume (ml/kg)	5	2	5
Test item	NB512 (**132b**)		
Mol. Weight (free base)	435,49		
Cmax (ng/ml)	1429	-	3519
C0 (ng/mL) [1]	-	354	-
tmax (h)	0,25	-	0,25
Cz (ng/ml)[2]	32,6	13,7	52,3
tz (h)[3]	24	8	8
t1/2z (h)[4]	6,1	3,8	1,4
AUC(0-tz) (ng*h/ml)[5]	2882	841	4704
AUC (0-inf) (ng*h/ml)[6]	3168	917	4807
%AUCextra	9,0	8,3	2,1
Vz/f (ml/kg)[7]	27721	-	4094
CL/f (ml/(h*kg))[8]	3156	-	2080
Vz (mL/kg)[9]	-	60583	-
CL(mL/(h*kg))[10]	-	10908	-

[1]extrapolated initial concentration. [2]last analytically quantifiable concentration. [3]time of the last sample which has an analytically quantifiable concentration. [4]half life of the terminal slope of a concentration-time curve. [5]area under the concentration-time curve up to the time t_z of the last sample. [6]area under the concentration-time curve extrapolated to infinity. [7]volume of distribution, in case of extravascular administration. [8]total body clearance, in case of extravascular administration. [9]volume of distribution. [10]total body clearance.

Compound	Cell viability (IC$_{50}$; µM)
	PaTu8988t
CI-994 (**7**)	13.7
JQ1 (**13**)	2.2
TW9 (**19**)	2.0
175e	0.8
175b	8.1
175c	17.5
177c	122.9

12.2 Supporting Figures
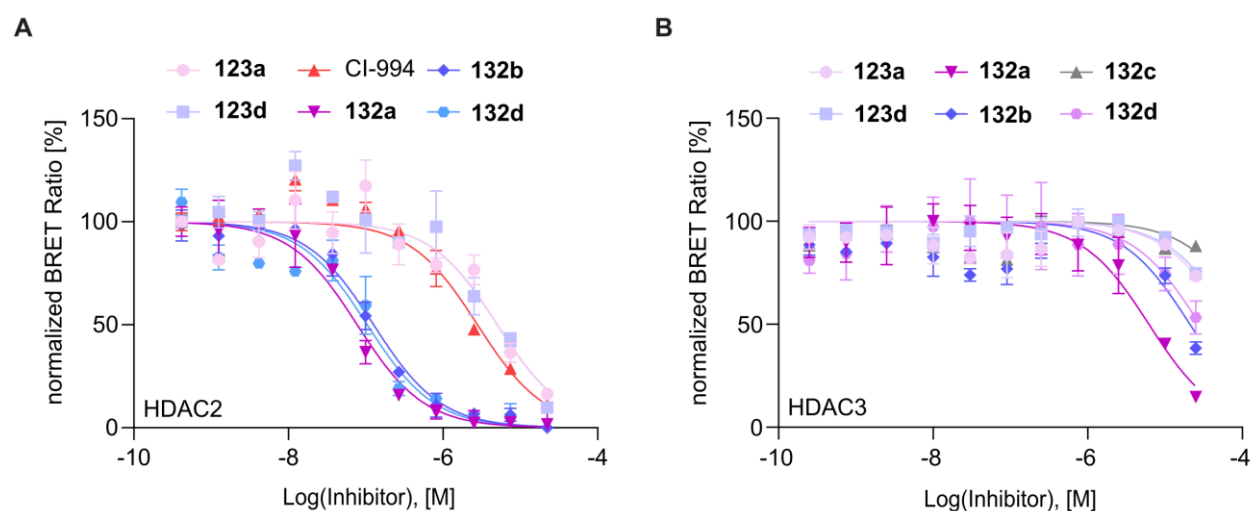
Supporting Figure S 1. NanoBRET data and fits of dual BET/HDAC inhibitors binding to HDAC2 (A) and HDAC3 (B) in intact cells.
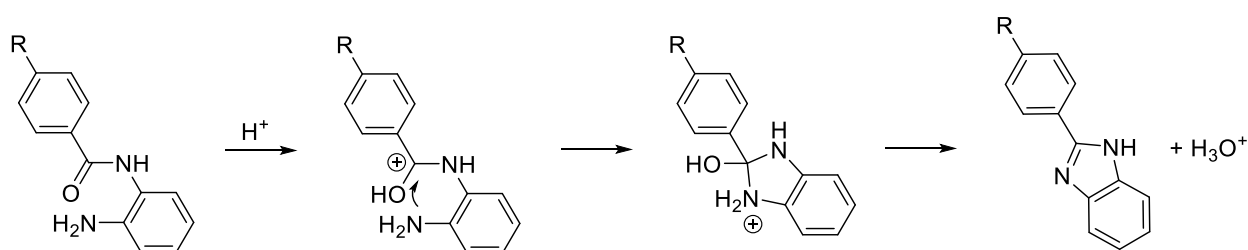
Supporting Figure S 2. Observed side reaction for the *Boc*-deprotection of PROTACs **174a**-**f** and **176a**-**e**.
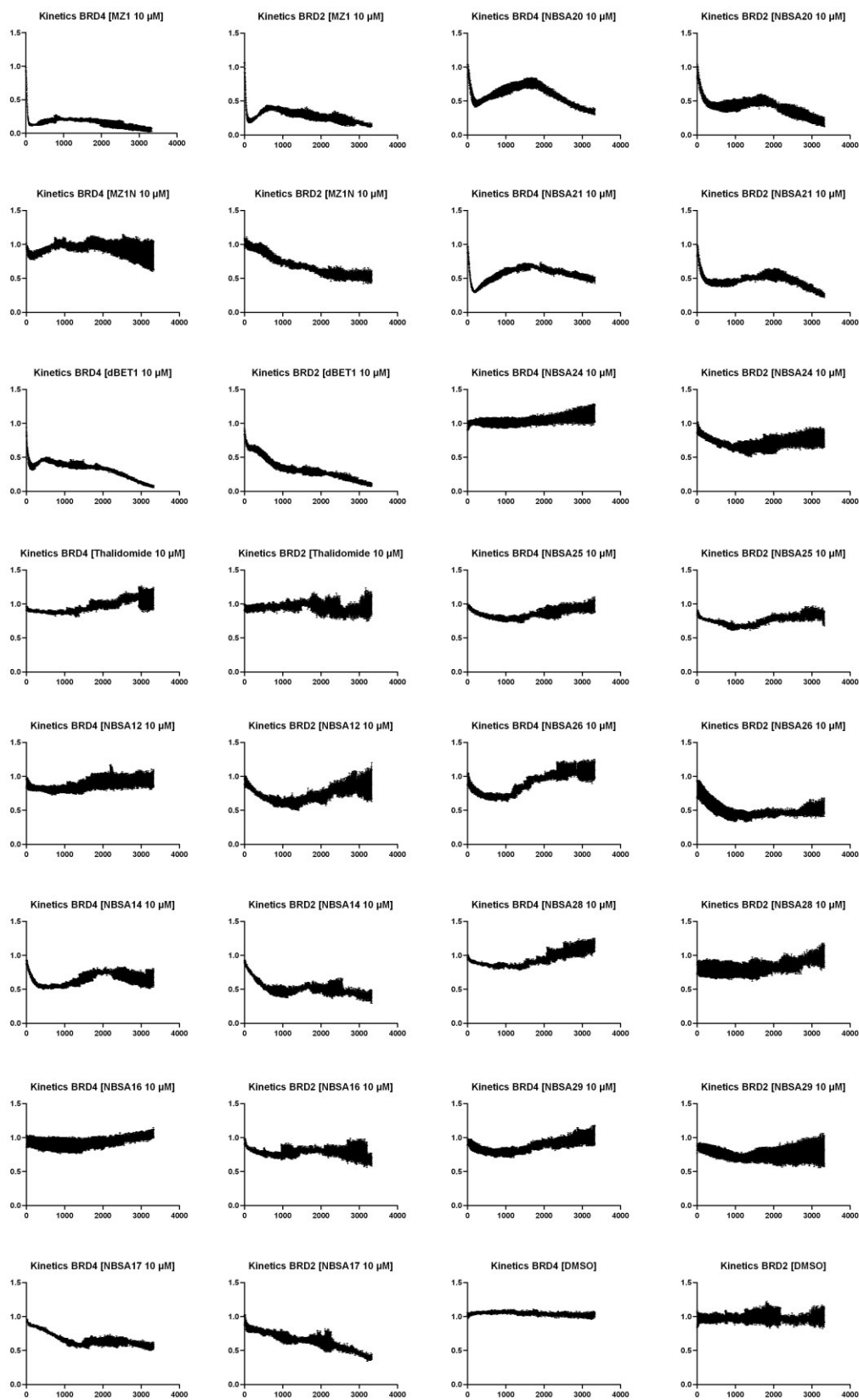
Supporting Figure S 3. Kinetics for the degradation of BRD2 and 4 measured *via* HiBiT.

12.3 HPLC

Blank measurement
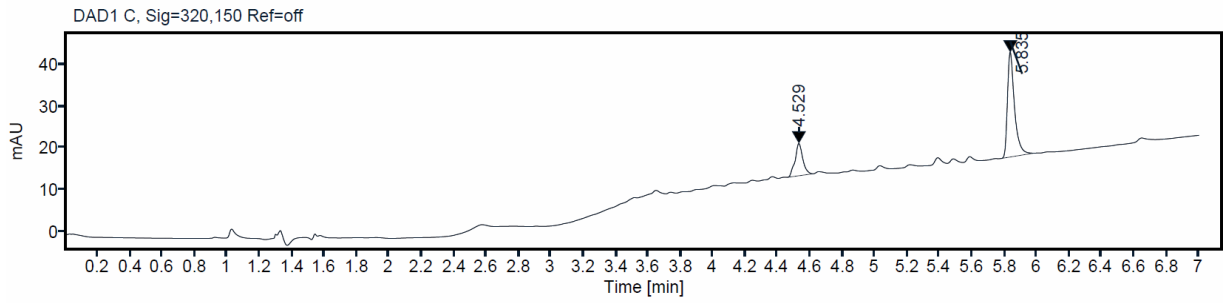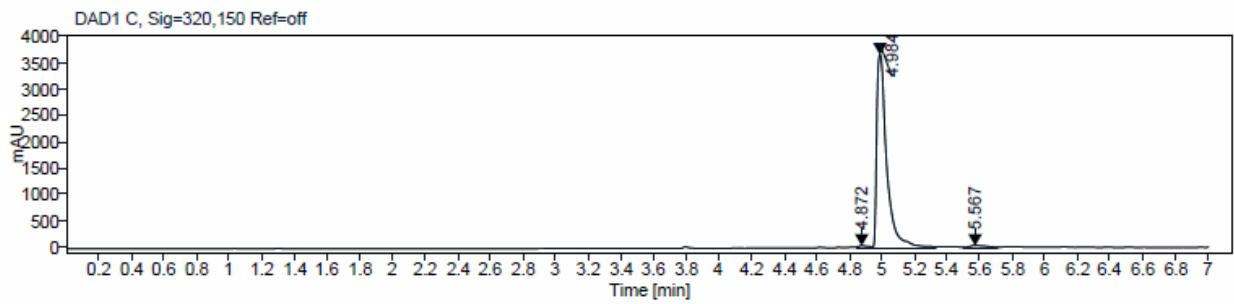
DAD1 C, Sig=320,150 Ref=off

NB102a

DAD1 C, Sig=320,150 Ref=off

Sample Purity

Signal Description   DAD1 C, Sig=320,150 Ref=off

Sample Name	Name	RT	Width	Area	Area%	Height
NB161		4.872	0.088	200.9542	1.24	46.0820
NB161		4.984	0.058	15612.1855	96.48	3644.0142
NB161		5.567	0.132	368.6589	2.28	45.0985

Max Area%   96.480

UV Signal Purity>95%   Pass

107b
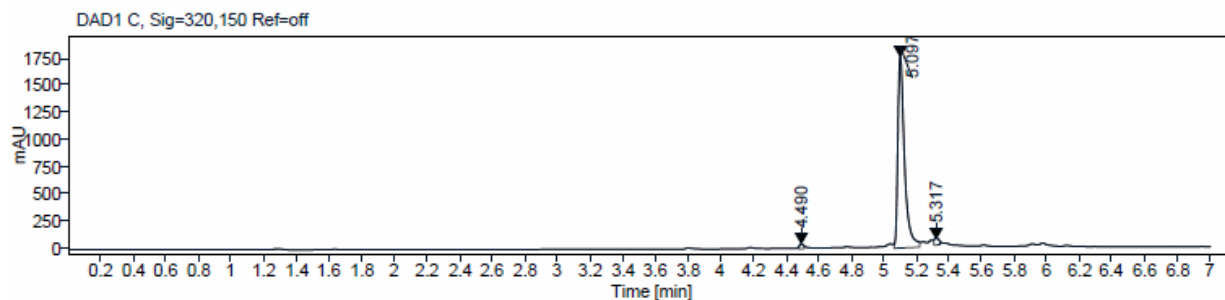
DAD1 C, Sig=320,150 Ref=off

Sample Purity

Signal Description   DAD1 C, Sig=320,150 Ref=off

Sample Name	Name	RT	Width	Area	Area%	Height
NB390		4.490	0.029	54.1471	1.10	36.5637
NB390		5.097	0.040	4800.5356	97.39	1741.9381
NB390		5.317	0.031	74.5046	1.51	45.1006

Max Area%   97.390

UV Signal Purity>95%   Pass

114a
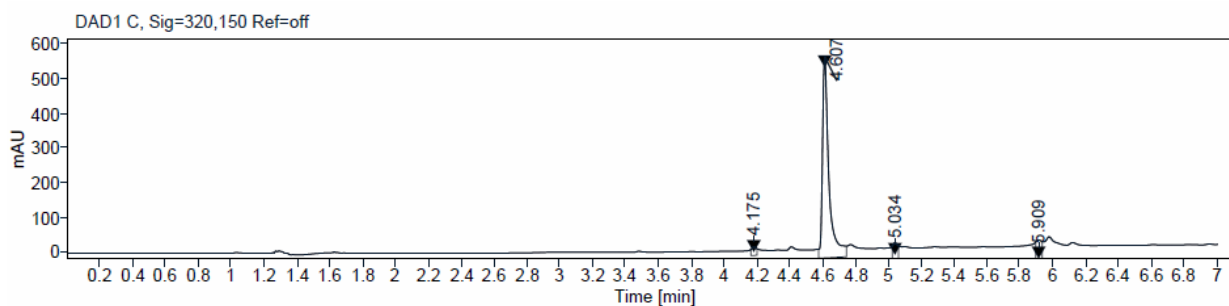
DAD1 C, Sig=320,150 Ref=off

Sample Purity

Signal Description   DAD1 C, Sig=320,150 Ref=off

Sample Name	Name	RT	Width	Area	Area%	Height
NB437		4.175	0.033	14.8471	1.11	8.6162
NB437		4.607	0.033	1286.3580	95.93	547.6205
NB437		5.034	0.026	14.7228	1.10	9.8781
NB437		5.909	0.038	25.0186	1.87	13.0276

Max Area%   95.929

UV Signal Purity>95%   Pass

119
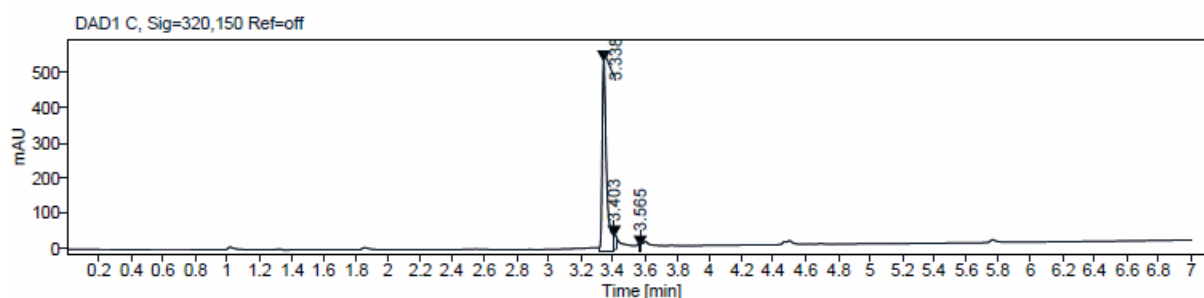
Sample Purity

Signal Description   DAD1 C, Sig=320,150 Ref=off

Sample Name	Name	RT	Width	Area	Area%	Height
NB480		3.338	0.024	948.8326	95.77	538.9740
NB480		3.403	0.020	34.6199	3.49	34.1772
NB480		3.565	0.015	7.3165	0.74	9.2308

Max Area%   95.767

UV Signal Purity>95%   Pass

123a
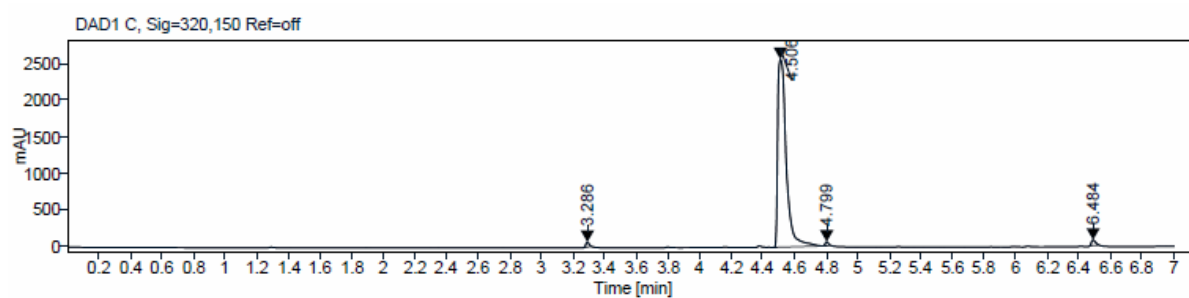
Sample Purity

Signal Description   DAD1 C, Sig=320,150 Ref=off

Sample Name	Name	RT	Width	Area	Area%	Height
NB462		3.286	0.024	91.5371	0.92	66.2465
NB462		4.506	0.053	9631.3271	97.13	2577.7595
NB462		4.799	0.023	65.2411	0.66	52.4126
NB462		6.484	0.030	127.9308	1.29	76.5870

Max Area%   97.129

UV Signal Purity>95%   Pass

123b
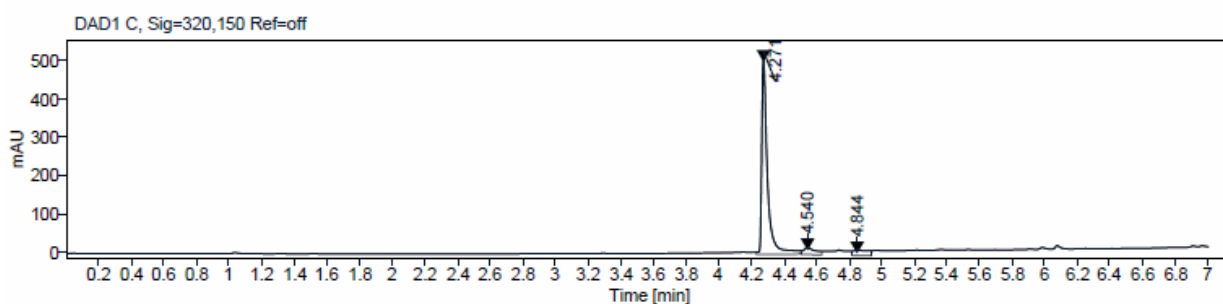
DAD1 C, Sig=320,150 Ref=off

Sample Purity

Signal Description   DAD1 C, Sig=320,150 Ref=off

Sample Name	Name	RT	Width	Area	Area%	Height
NB469		4.271	0.031	1119.2117	97.09	499.0727
NB469		4.540	0.034	23.7507	2.06	10.0126
NB469		4.844	0.029	9.8229	0.85	4.3816

Max Area%   97.088

UV Signal Purity>95%   Pass

123c
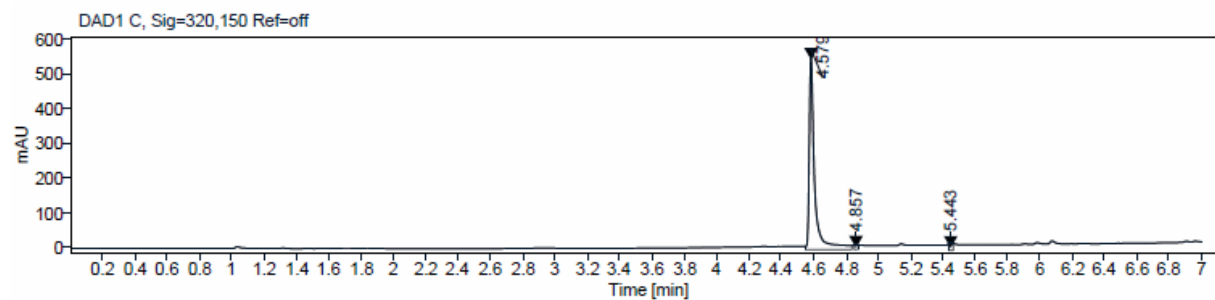
DAD1 C, Sig=320,150 Ref=off

Sample Purity

Signal Description   DAD1 C, Sig=320,150 Ref=off

Sample Name	Name	RT	Width	Area	Area%	Height
NB470		4.579	0.027	1101.4595	98.78	544.6414
NB470		4.857	0.024	5.1854	0.47	4.1291
NB470		5.443	0.026	8.4550	0.76	6.4661

Max Area%   98.777

UV Signal Purity>95%   Pass

123d
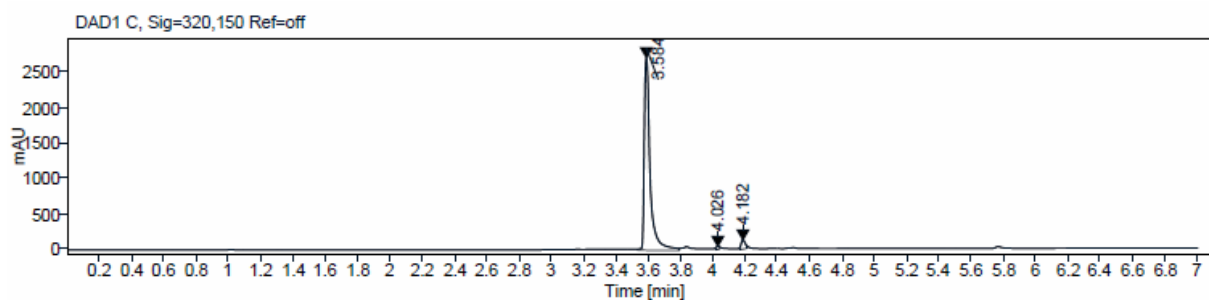
Sample Purity

Signal Description   DAD1 C, Sig=320,150 Ref=off

Sample Name	Name	RT	Width	Area	Area%	Height
NB500		3.584	0.033	6617.2954	97.23	2705.4158
NB500		4.026	0.020	24.7576	0.36	22.2138
NB500		4.182	0.026	163.5289	2.40	108.7853

Max Area%   97.233

UV Signal Purity>95%   <mark>Pass</mark>
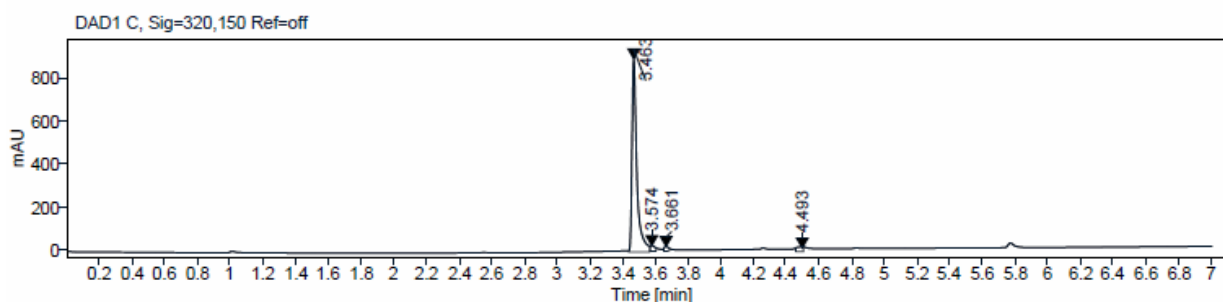
123e

Sample Purity

Signal Description   DAD1 C, Sig=320,150 Ref=off

Sample Name	Name	RT	Width	Area	Area%	Height
NB501		3.463	0.027	1781.5571	96.17	889.6945
NB501		3.574	0.029	30.4943	1.65	19.2803
NB501		3.661	0.023	18.5934	1.00	13.7266
NB501		4.493	0.047	21.9083	1.18	9.7645

Max Area%   96.168

UV Signal Purity>95%   <mark>Pass</mark>
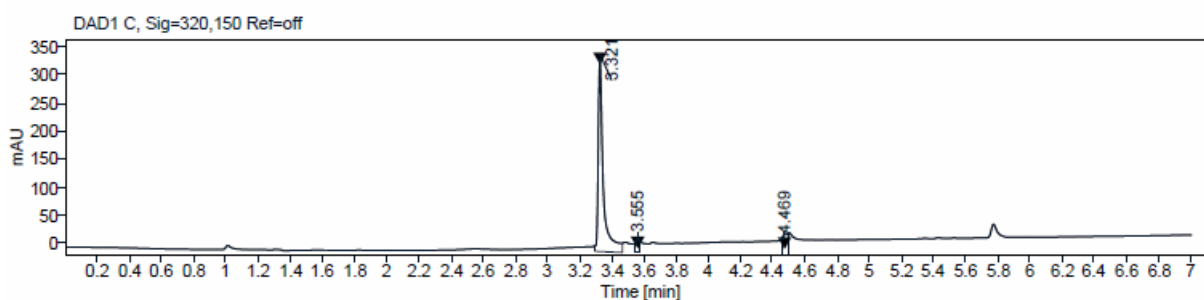
123e

Sample Purity

Signal Description   DAD1 C, Sig=320,150 Ref=off

Sample Name	Name	RT	Width	Area	Area%	Height
NB502		3.321	0.025	634.7424	95.96	334.3840
NB502		3.555	0.018	6.8211	1.03	6.7317
NB502		4.469	0.039	19.9128	3.01	9.8161

Max Area%   95.958
UV Signal Purity>95%   Pass

132a
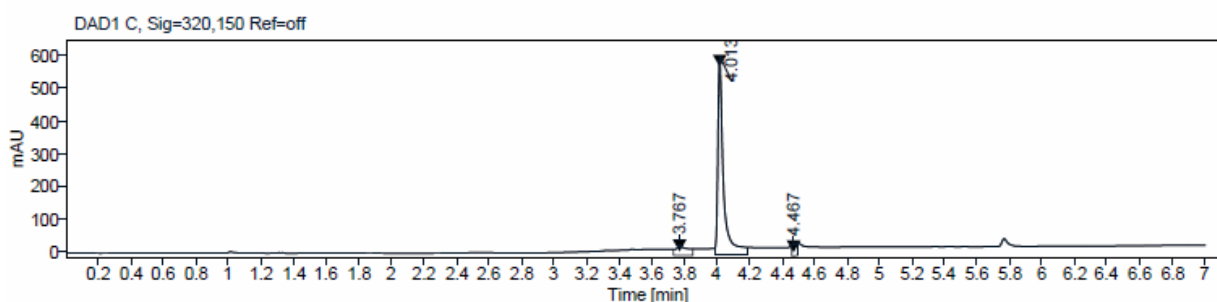
Sample Purity

Signal Description   DAD1 C, Sig=320,150 Ref=off

Sample Name	Name	RT	Width	Area	Area%	Height
NB503		3.767	0.031	25.0035	2.02	11.1851
NB503		4.013	0.028	1195.5093	96.53	574.0806
NB503		4.467	0.037	17.9701	1.45	9.6678

Max Area%   96.530
UV Signal Purity>95%   Pass

132b
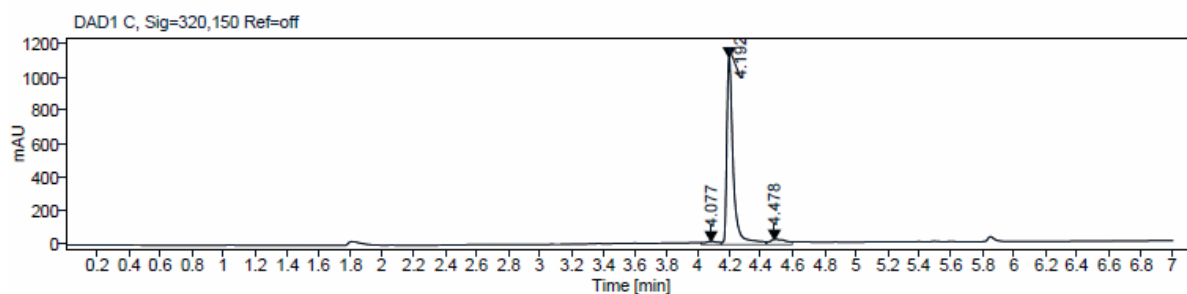
Sample Purity

Signal Description   DAD1 C, Sig=320,150 Ref=off

Sample Name	Name	RT	Width	Area	Area%	Height
NB533		4.077	0.047	33.9675	1.10	10.5429
NB533		4.192	0.038	2975.9663	96.45	1112.9037
NB533		4.478	0.055	75.6843	2.45	19.4026

Max Area%   96.446

UV Signal Purity>95%   Pass

132c
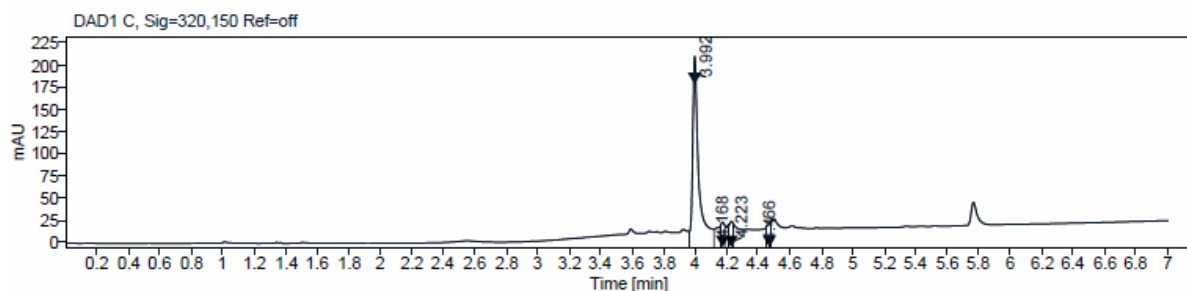
Sample Purity

Signal Description   DAD1 C, Sig=320,150 Ref=off

Sample Name	Name	RT	Width	Area	Area%	Height
NB513		3.992	0.031	527.8755	95.67	207.0565
NB513		4.168	0.023	7.1770	1.30	5.7963
NB513		4.223	0.024	6.6385	1.20	5.2439
NB513		4.466	0.026	10.0878	1.83	6.9494

Max Area%   95.668

UV Signal Purity>95%   Pass

132d
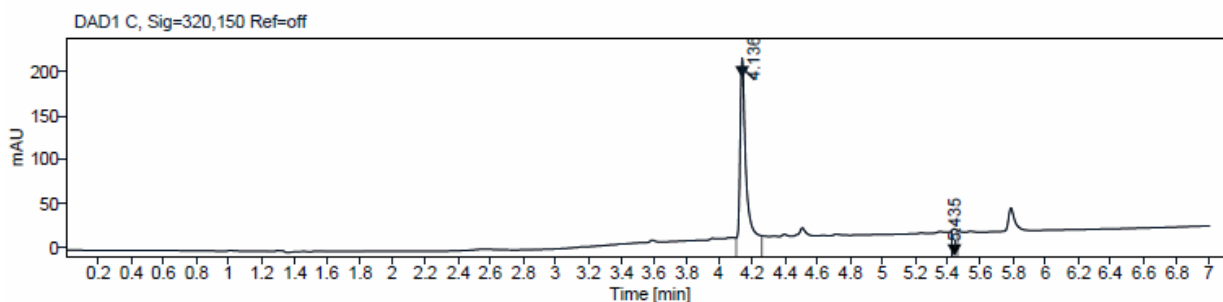
DAD1 C, Sig=320,150 Ref=off

Sample Purity

Signal Description   DAD1 C, Sig=320,150 Ref=off

Sample Name	Name	RT	Width	Area	Area%	Height
NB514		4.136	0.030	455.5850	97.95	203.8892
NB514		5.435	0.035	9.5244	2.05	5.4359

Max Area%   97.952

UV Signal Purity>95%   Pass

133
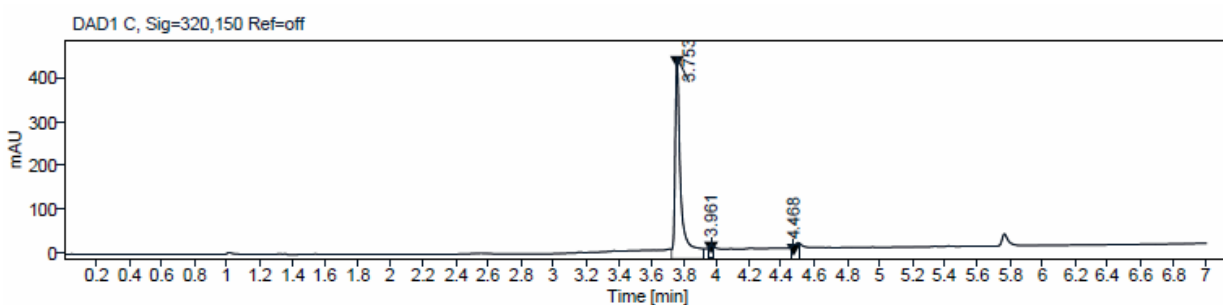
DAD1 C, Sig=320,150 Ref=off

Sample Purity

Signal Description   DAD1 C, Sig=320,150 Ref=off

Sample Name	Name	RT	Width	Area	Area%	Height
NB507		3.753	0.028	914.1124	97.29	433.9325
NB507		3.961	0.023	9.2851	0.99	7.2258
NB507		4.468	0.046	16.1563	1.72	6.7971

Max Area%   97.292

UV Signal Purity>95%   Pass

12.4   NMR and MS Spectra

MALDI HRMS Spectrum of **100** and simulated Spectrum

C14H14N4O3 +H: C14 H15 N4 O3 pa Chrg 1
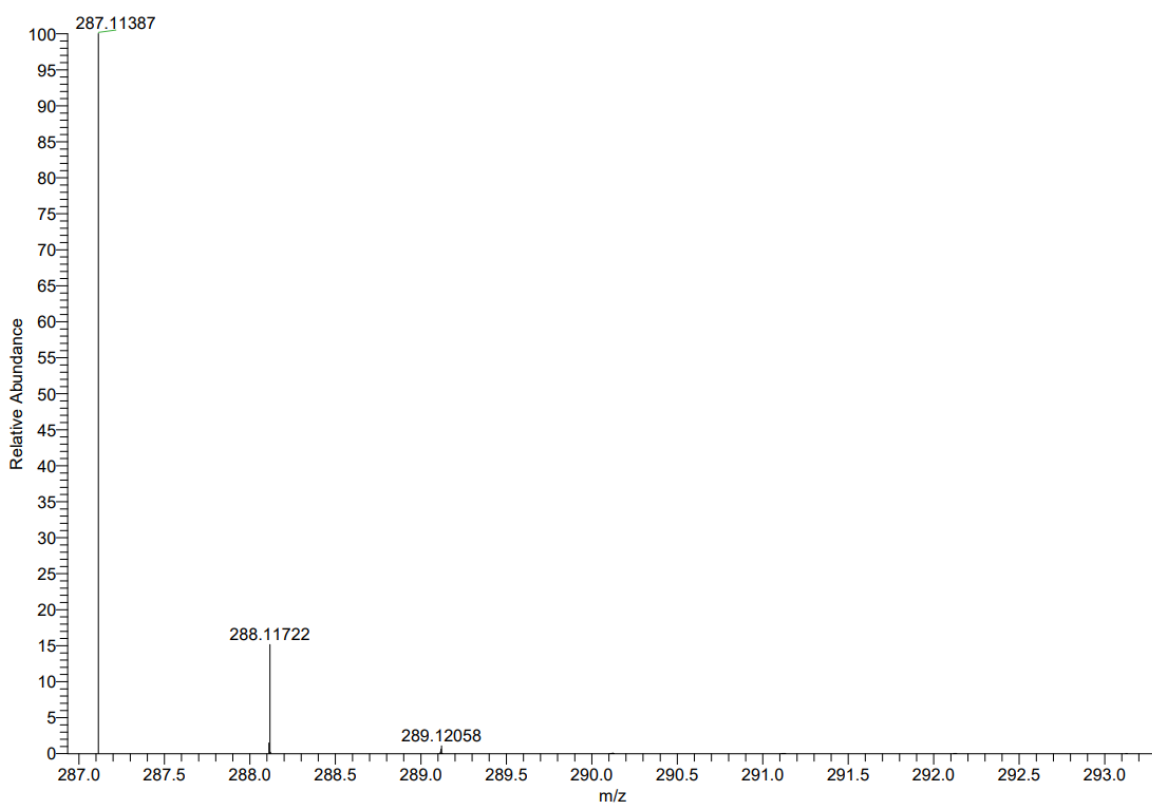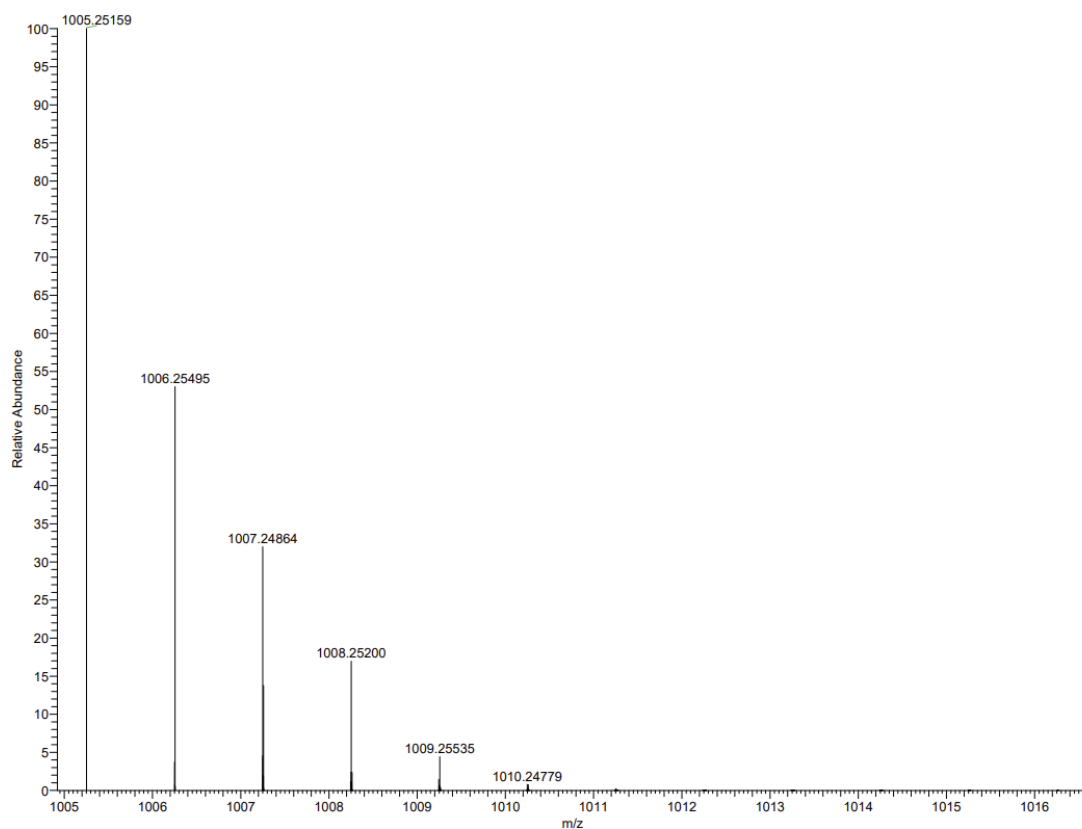

MALDI HRMS Spectrum of **102a** and simulated Spectrum

NB161_D9 #1-4 RT: 0.01-0.14 AV: 4 NL: 3.35E7
T: FTMS + p MALDI Full ms [200.00-700.00]
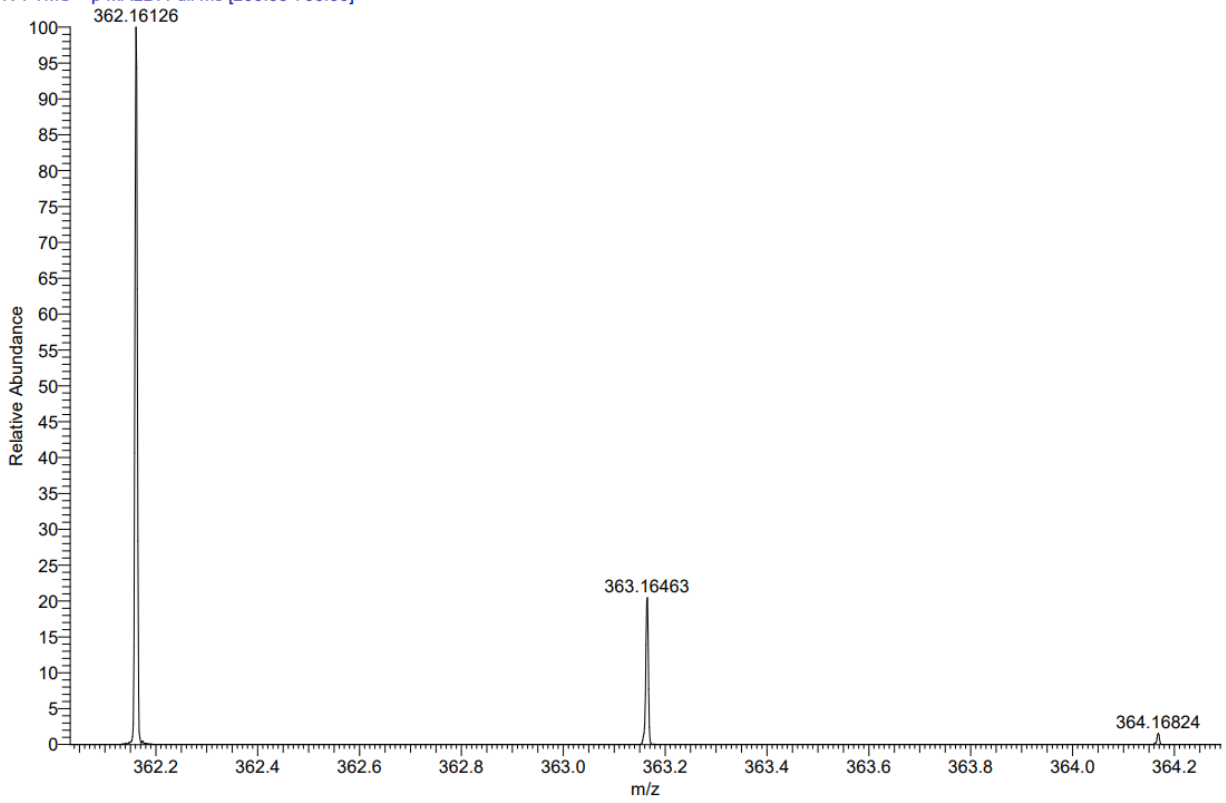
C20H19N5O2 +H: C20 H20 N5 O2 pa Chrg 1
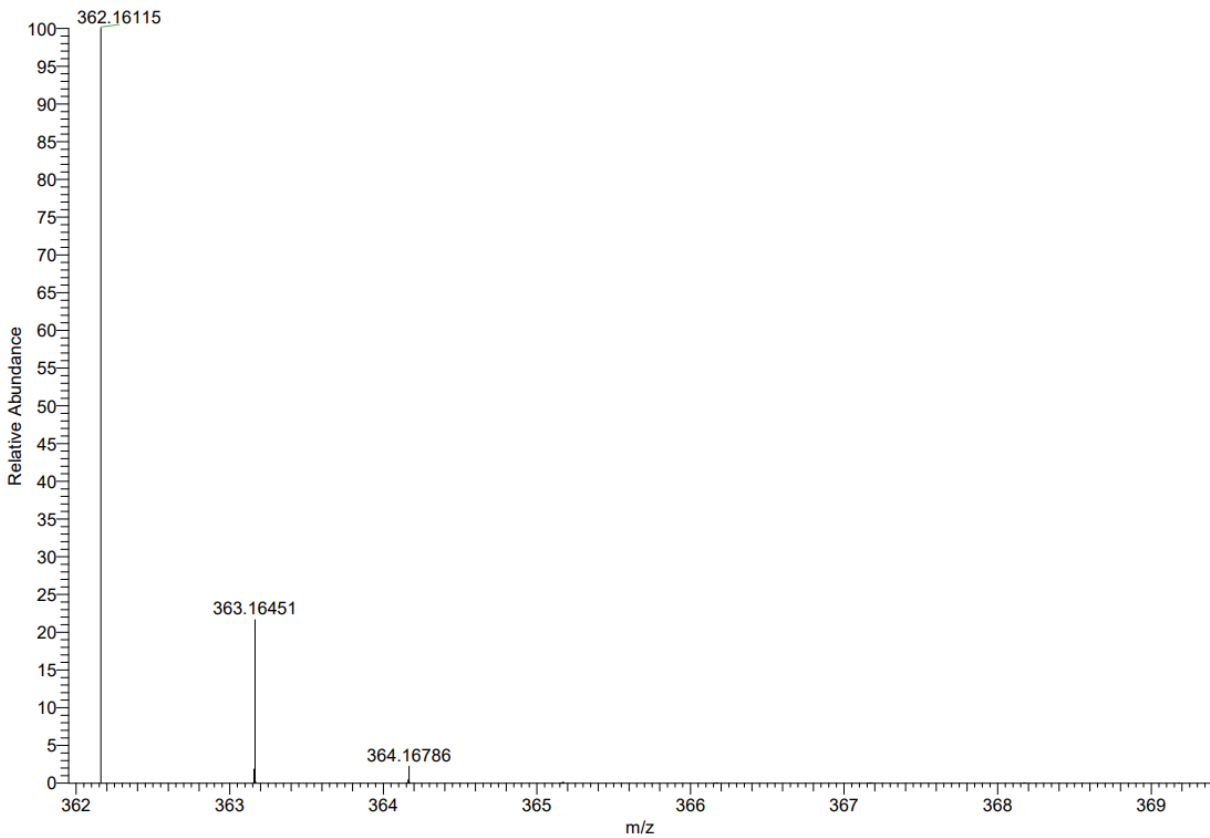
MALDI HRMS Spectrum of **102b** and simulated Spectrum

444.14802

445.15181

445.03826

446.14438

447.14729

m/z
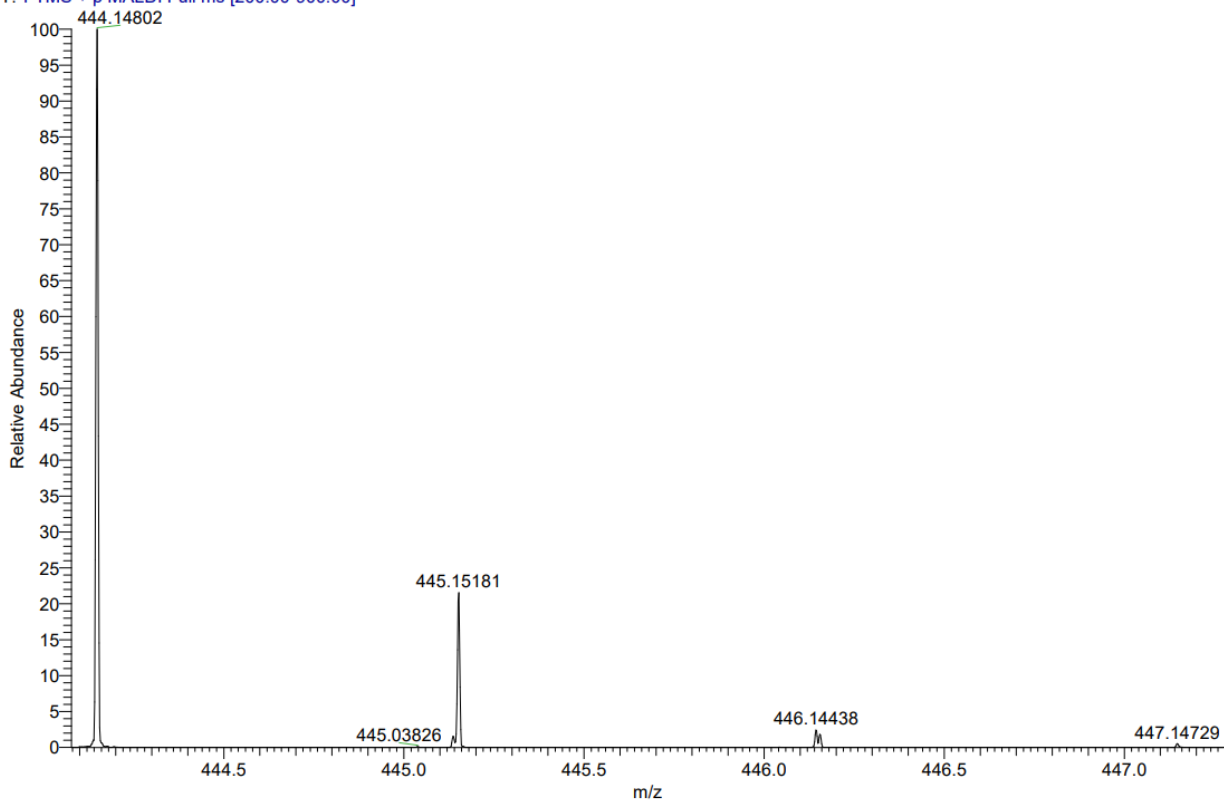
C24H21N5O2S1 +H: C24 H22 N5 O2 S1 pa Chrg 1

444.14887

445.15223

446.14467

447.14802

m/z
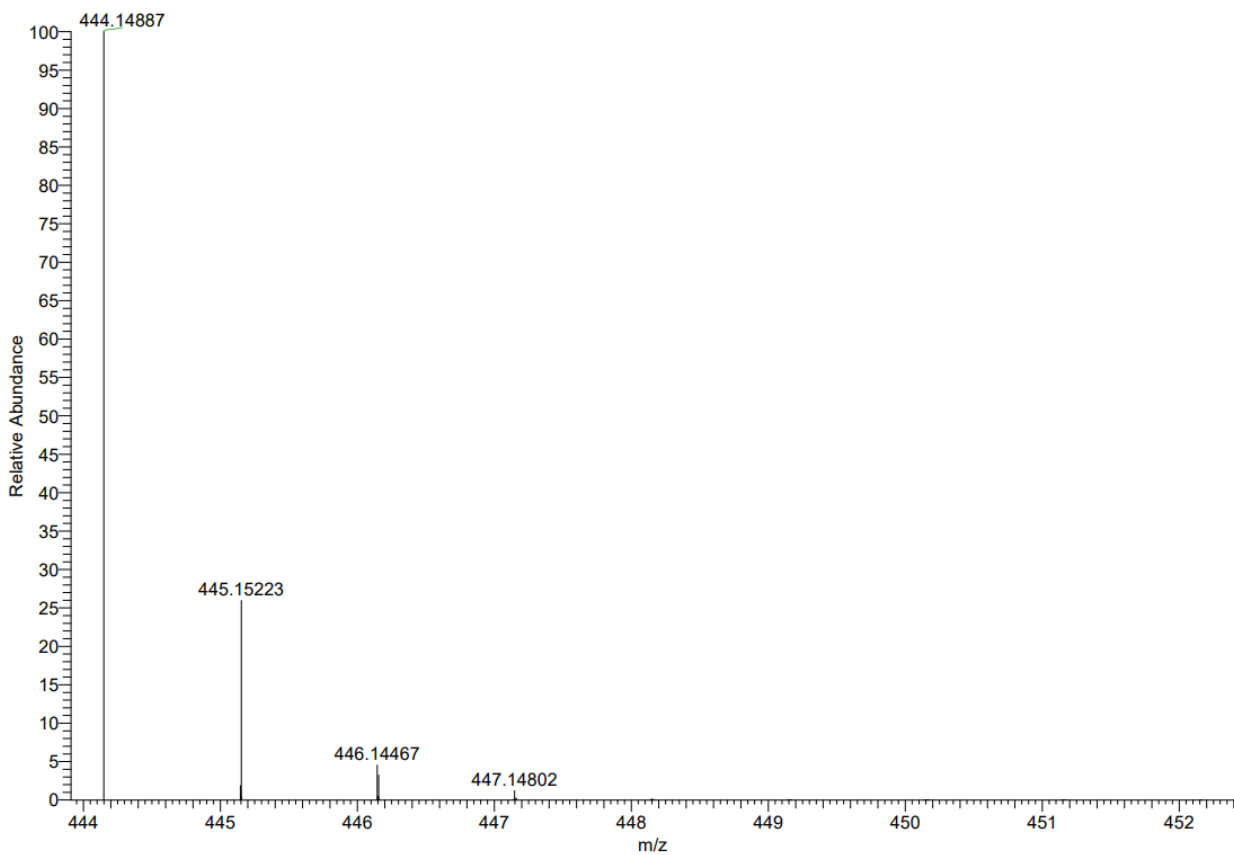
MALDI HRMS Spectrum of **102c** and simulated Spectrum

438.19179

439.19534

440.19865

Relative Abundance

m/z
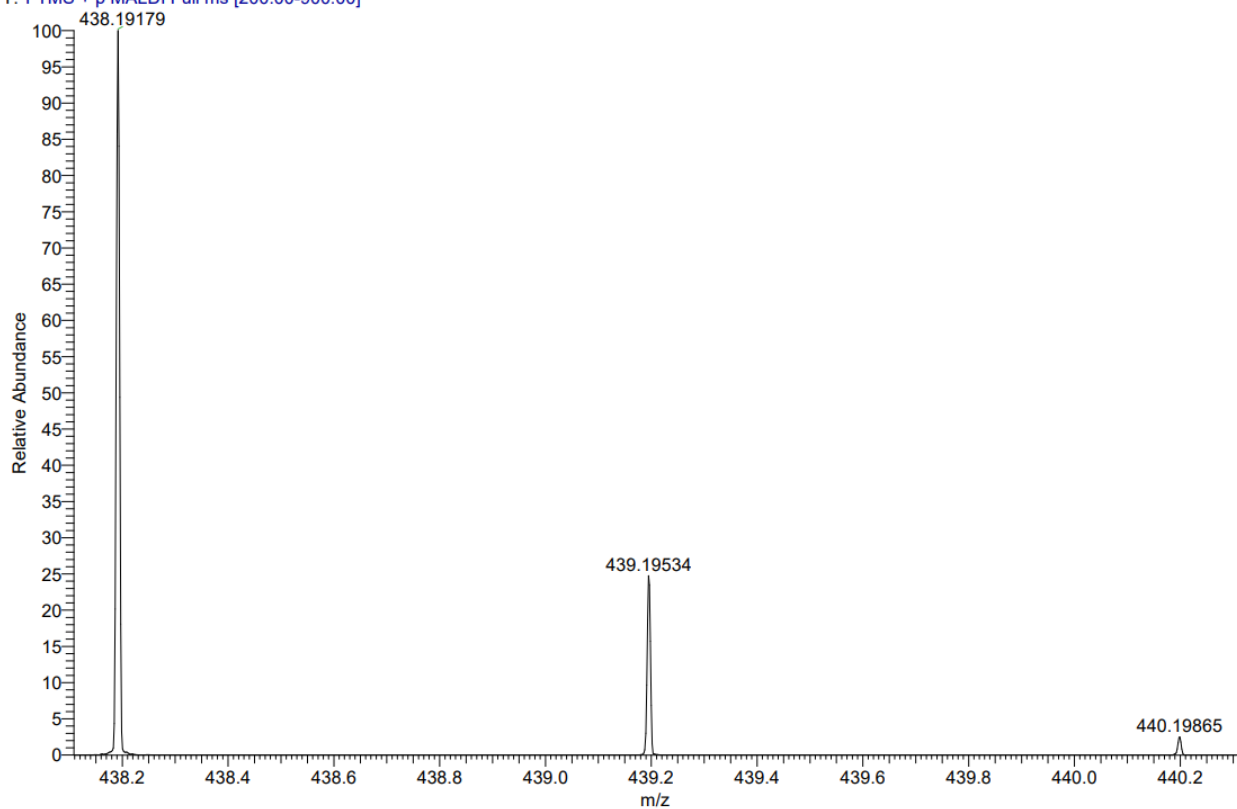
C26H23N5O2 +H: C26 H24 N5 O2 pa Chrg 1

438.19245

439.19581

440.19916

Relative Abundance

m/z
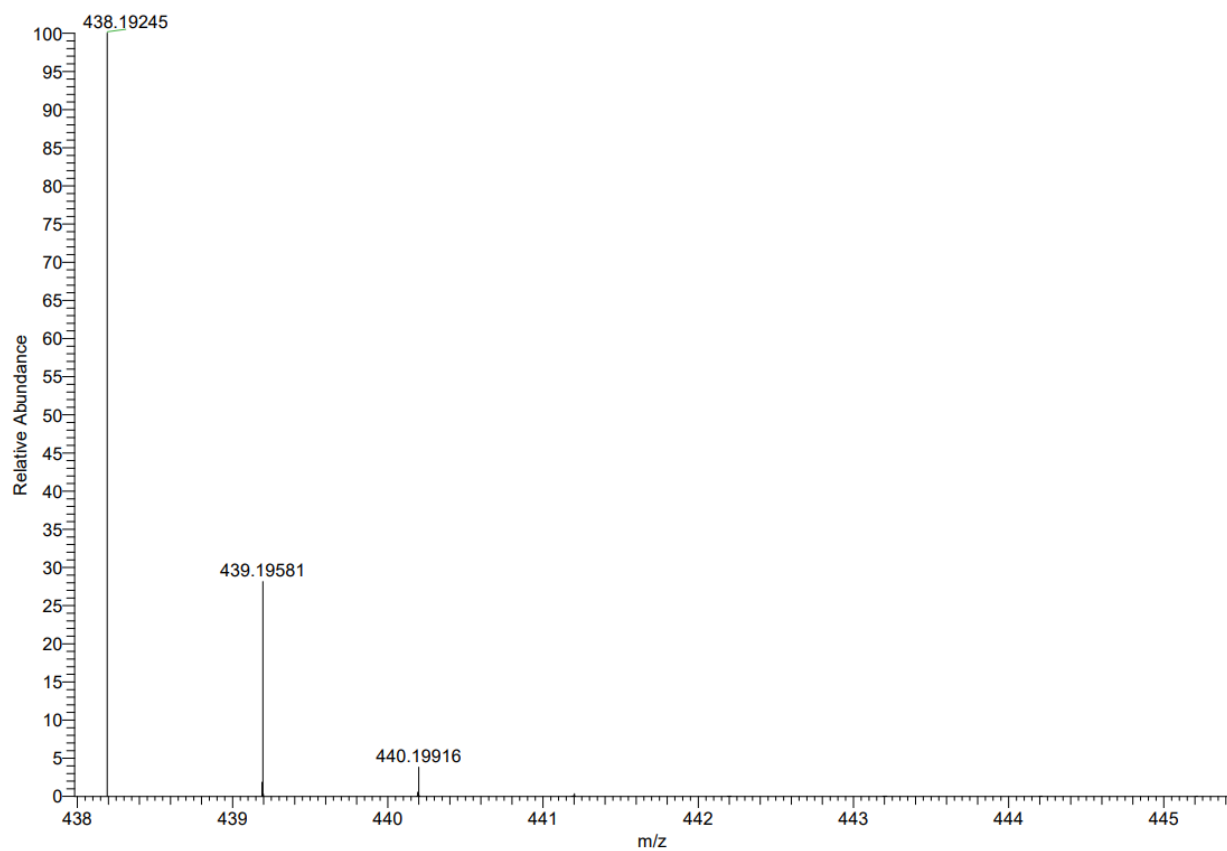
MALDI HRMS Spectrum of **107a** and simulated Spectrum
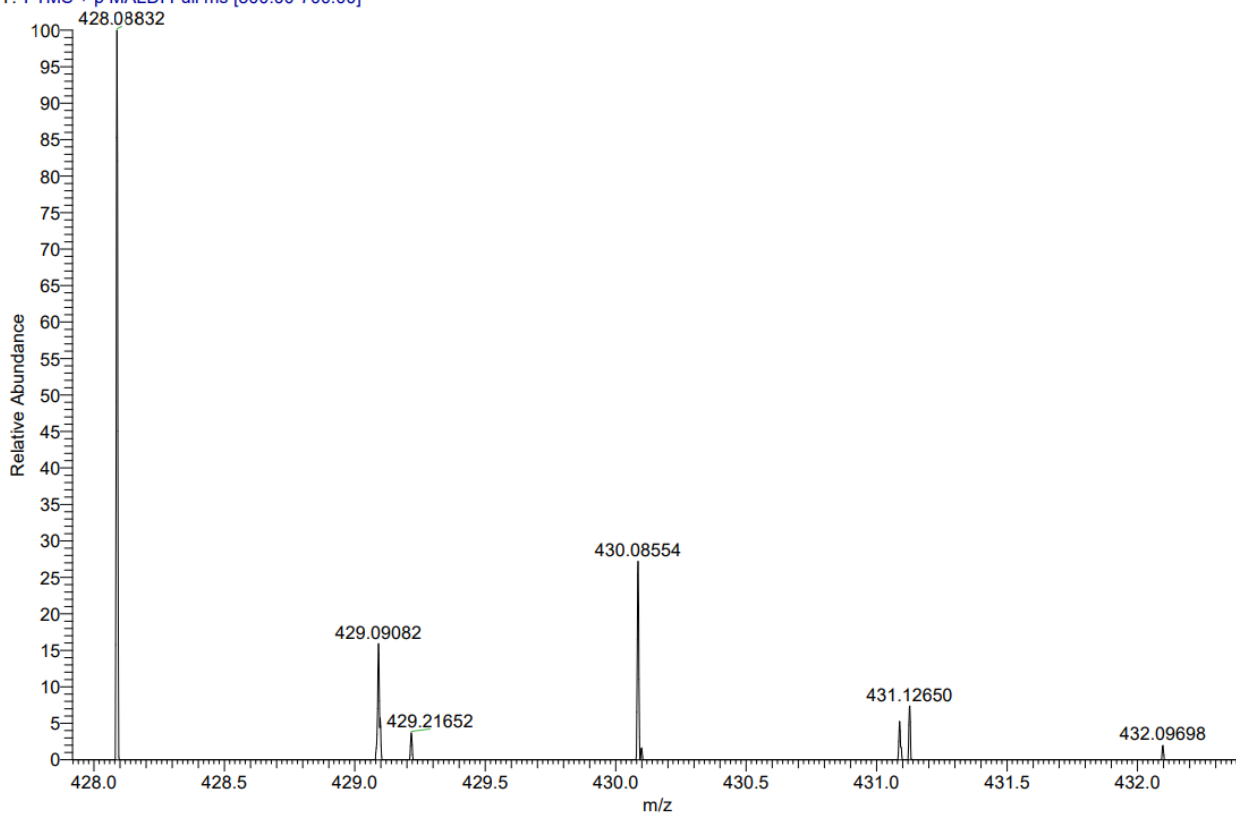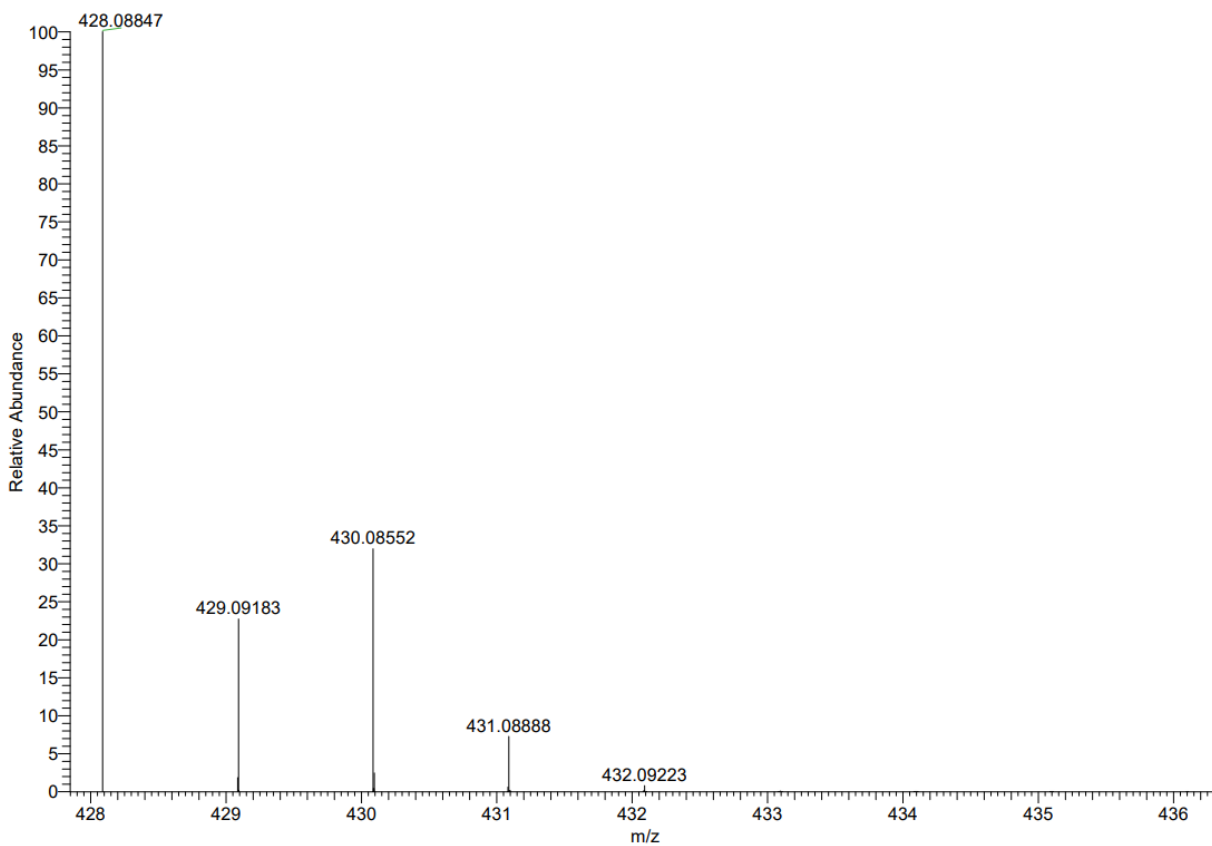
MALDI HRMS Spectrum of **107b** and simulated Spectrum

386.16108

387.16431

386.49929

388.16874
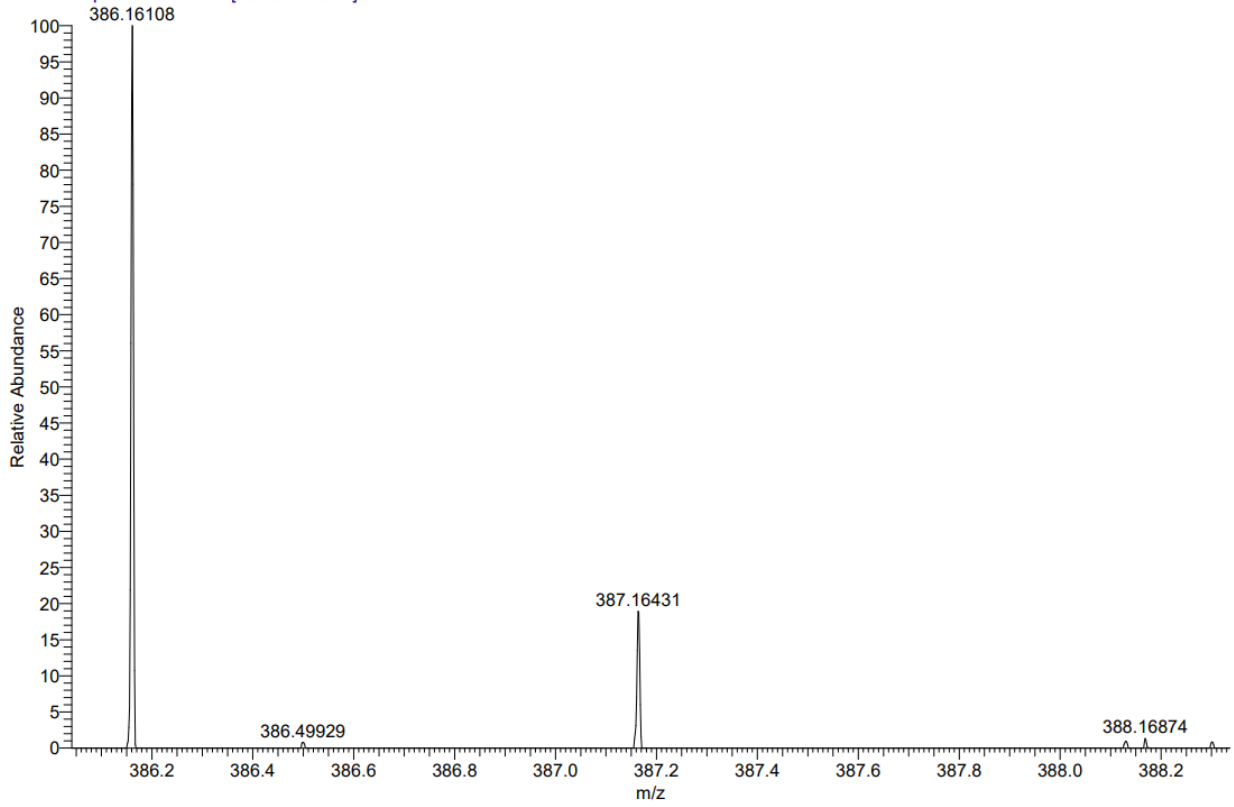
C22H19N5O2 +H: C22 H20 N5 O2 pa Chrg 1

386.16115

387.16451

388.16786
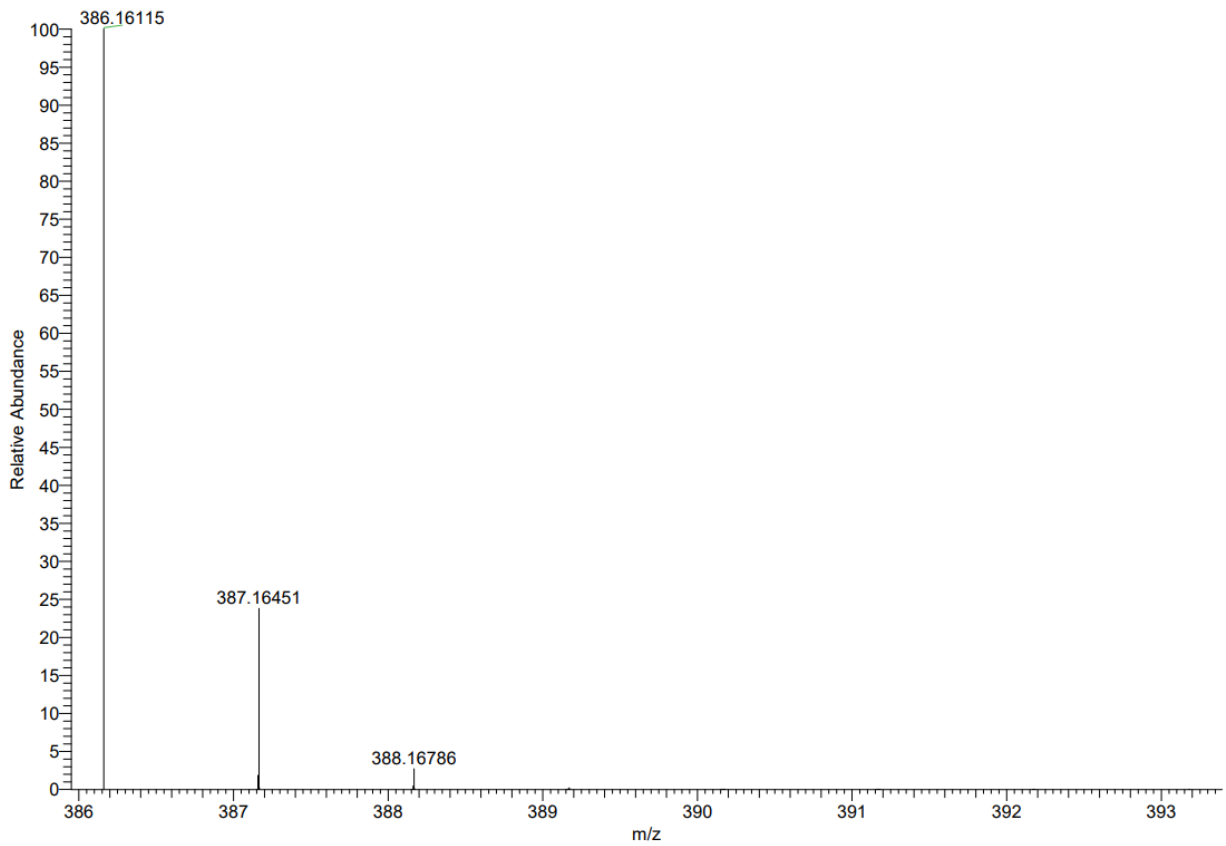
MALDI HRMS Spectrum of **114a** and simulated Spectrum

NB437_C2 #1-7   RT: 0.01-0.28   AV: 7   NL: 4.83E6
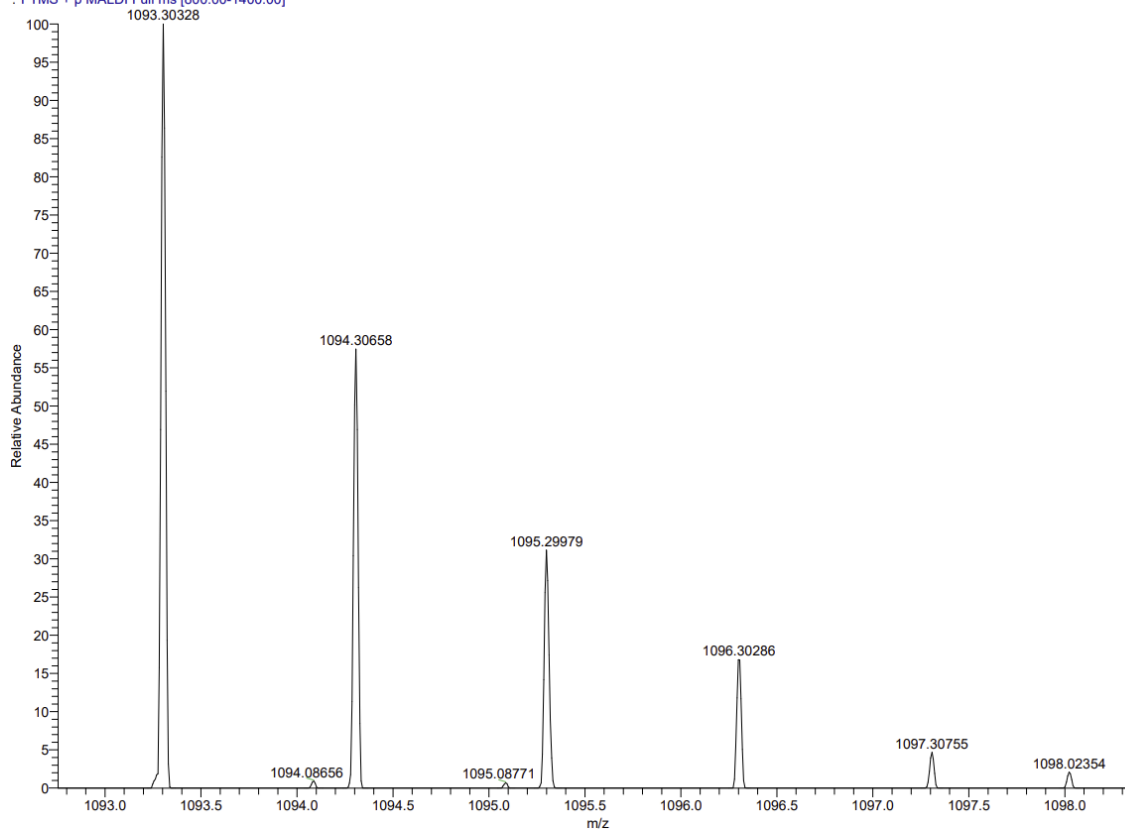T: FTMS + p MALDI Full ms [300.00-650.00]
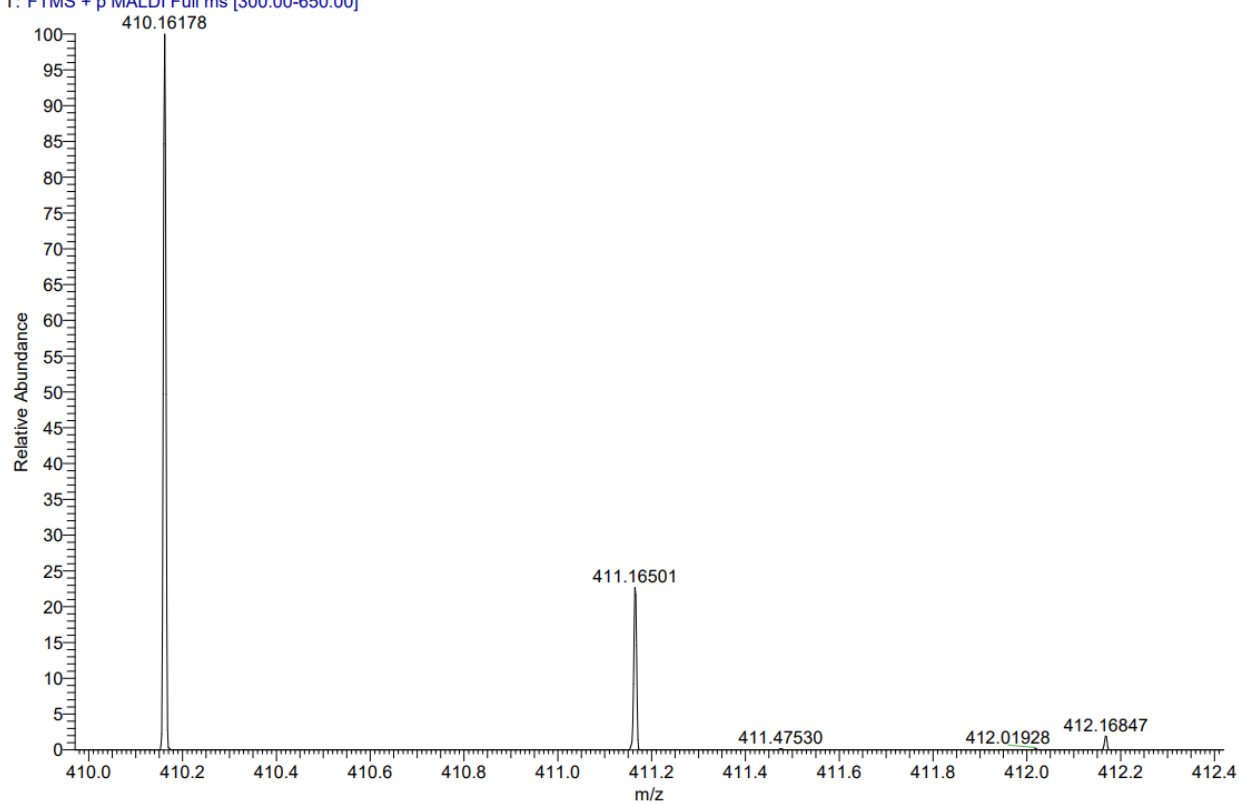
C24H19N5O2 +H: C24 H20 N5 O2 pa Chrg 1
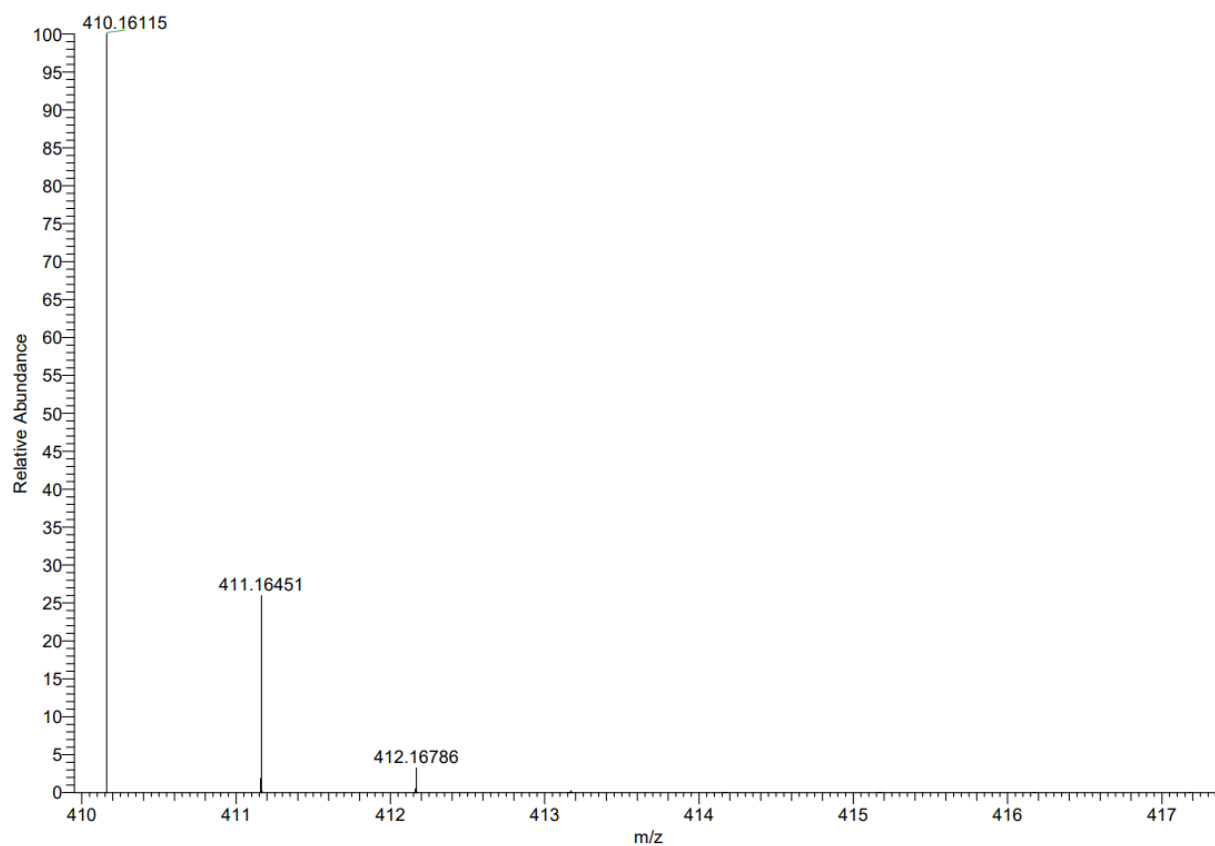
¹H and ¹³C Spectra of **119**
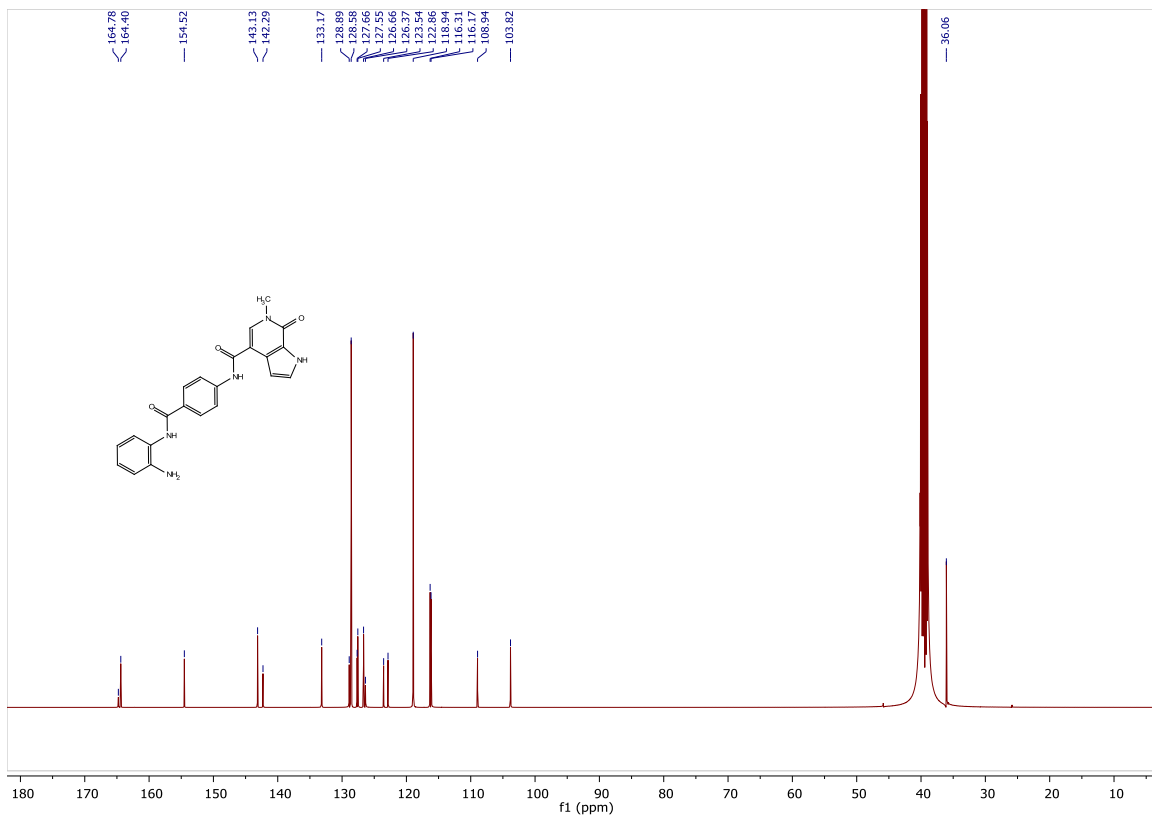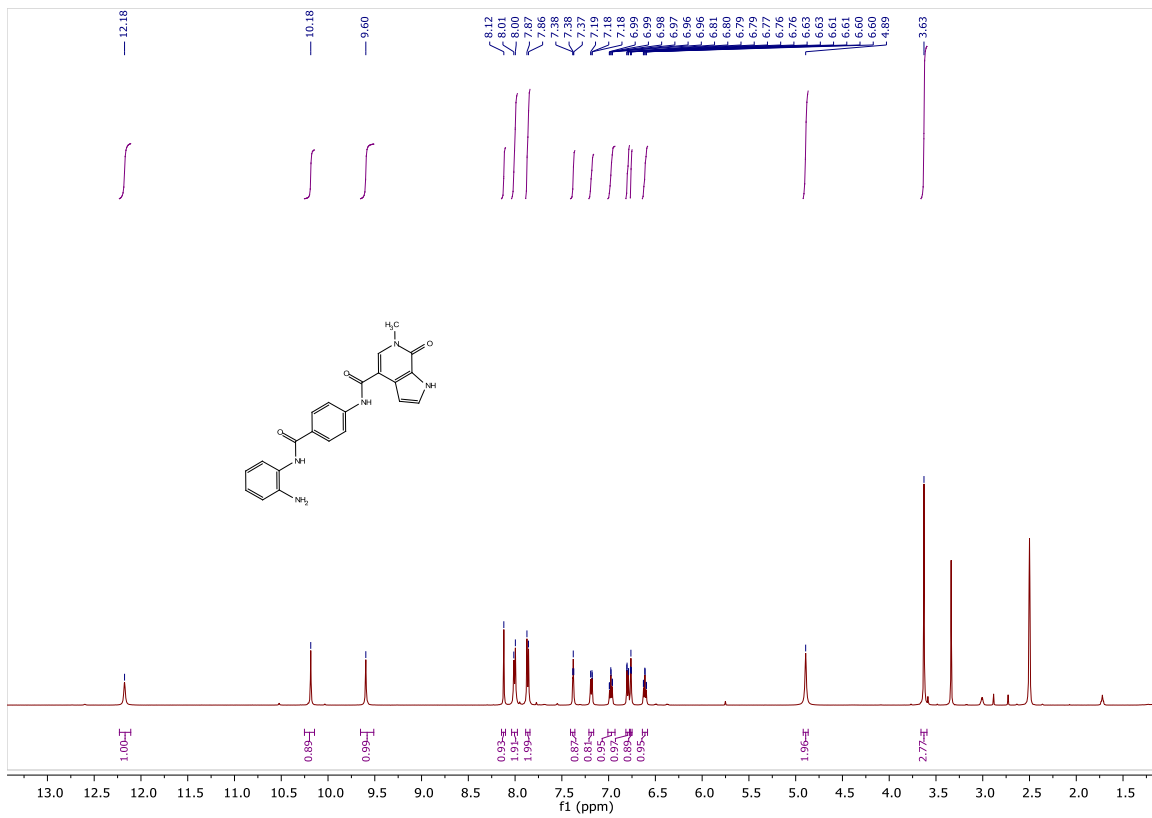
MALDI HRMS Spectrum of **119** and simulated Spectrum

NB480_C6 #1-6 RT: 0.00-0.23 AV: 6 NL: 8.70E6
T: FTMS + p MALDI Full ms [300.00-650.00]
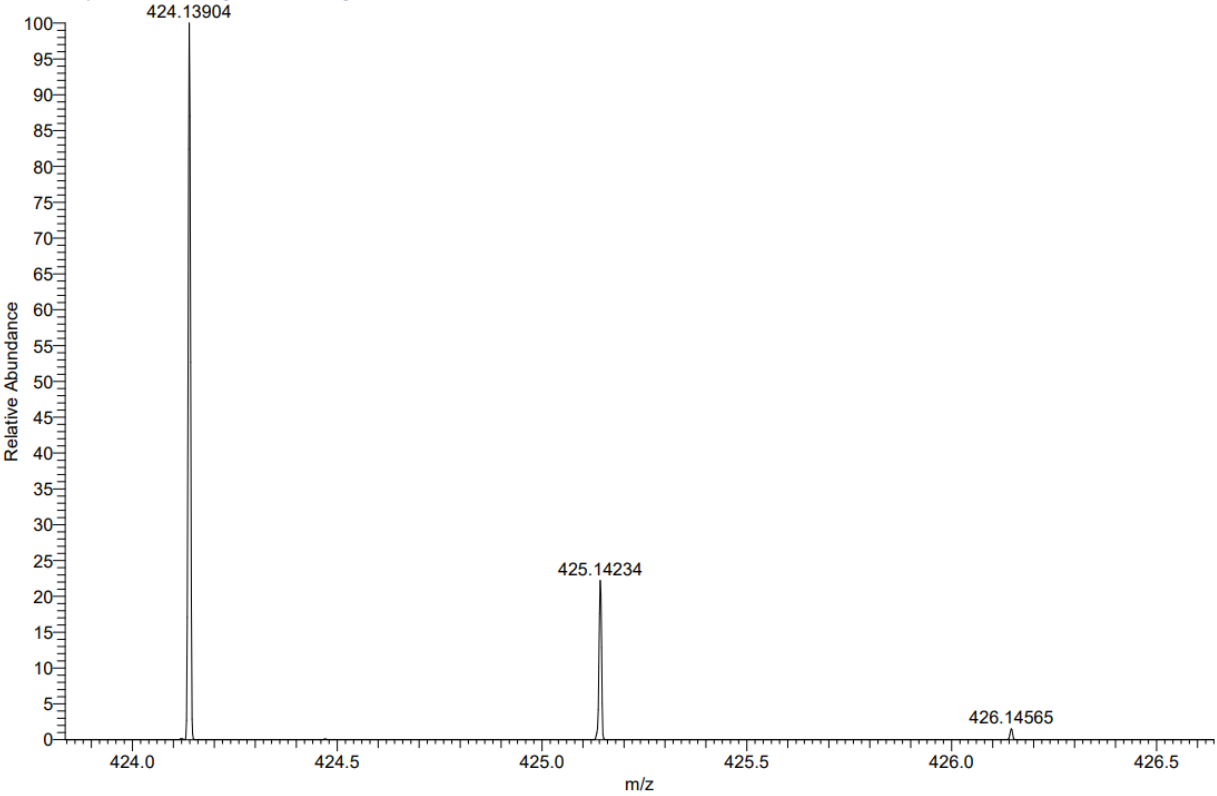
C22H19N5O3 +Na: C22 H19 N5 O3 Na1 pa Chrg 1
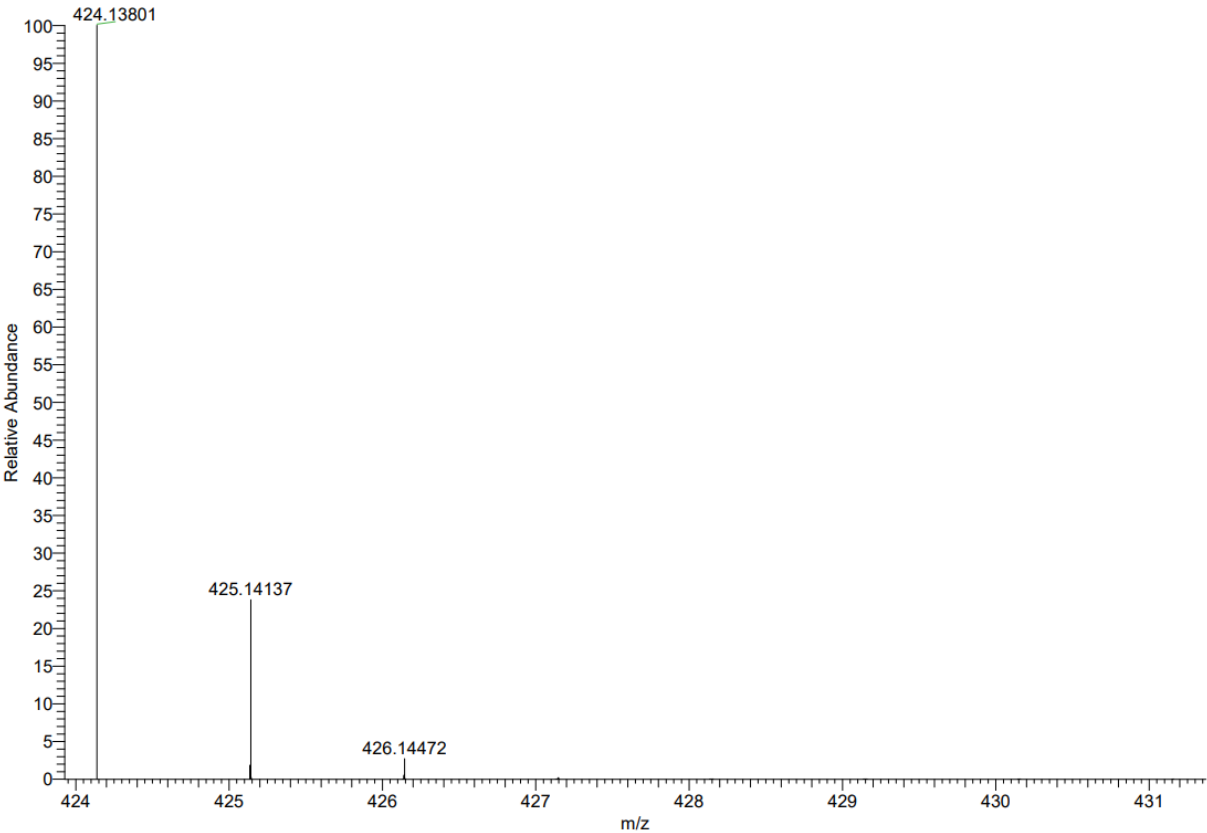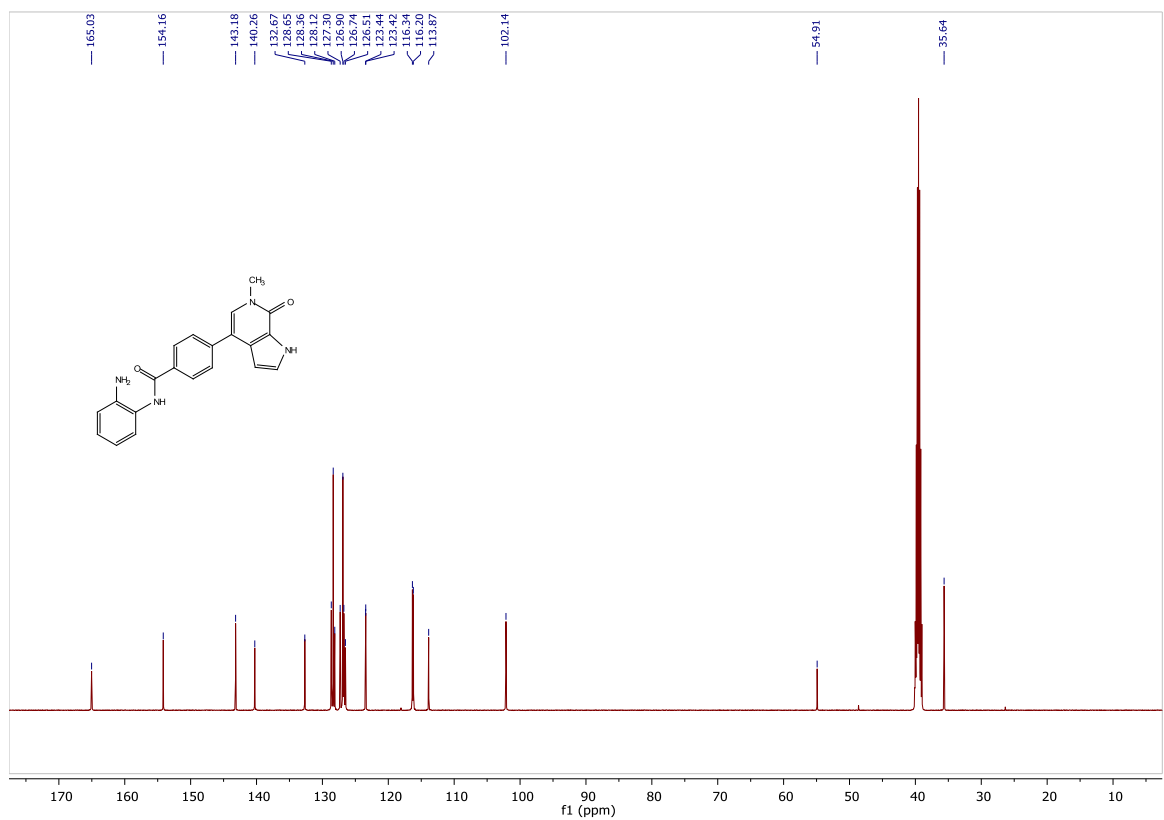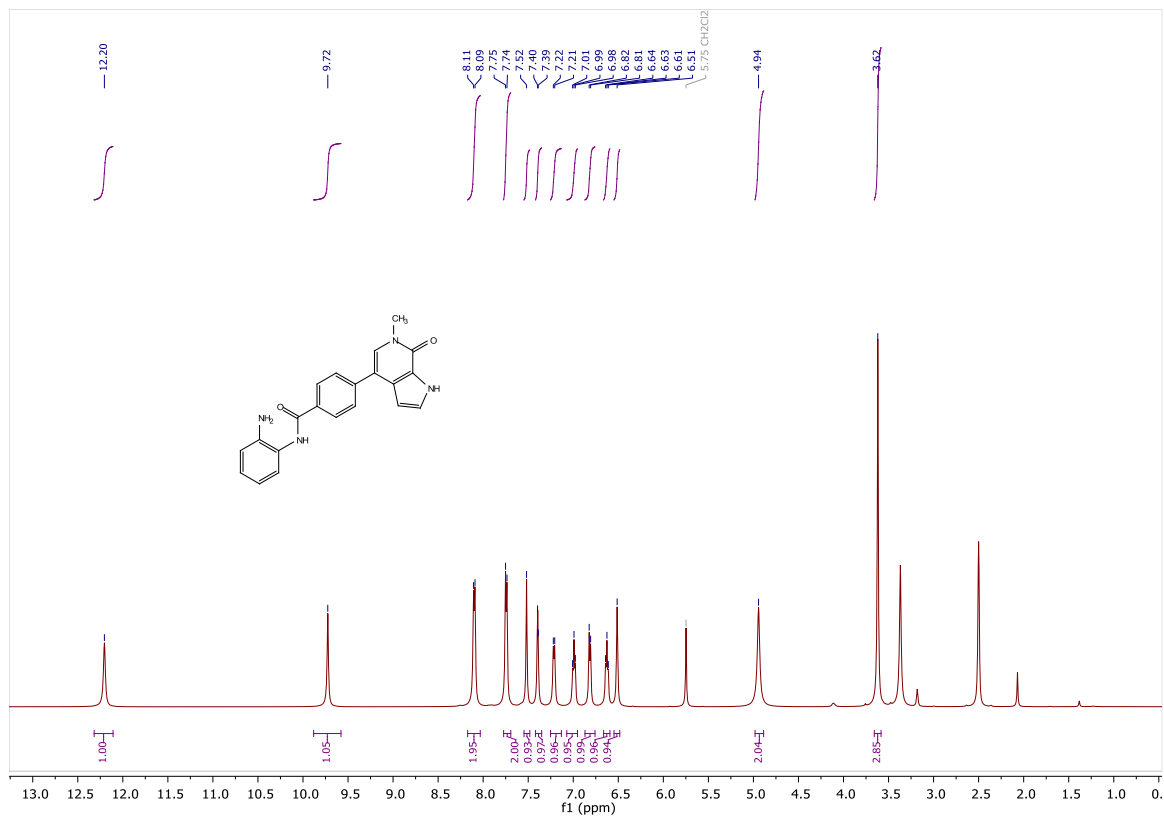
MALDI HRMS Spectrum of **123a** and simulated Spectrum

NB462_C3 #1-8 RT: 0.01-0.33 AV: 8 NL: 7.99E6
T: FTMS + p MALDI Full ms [300.00-650.00]
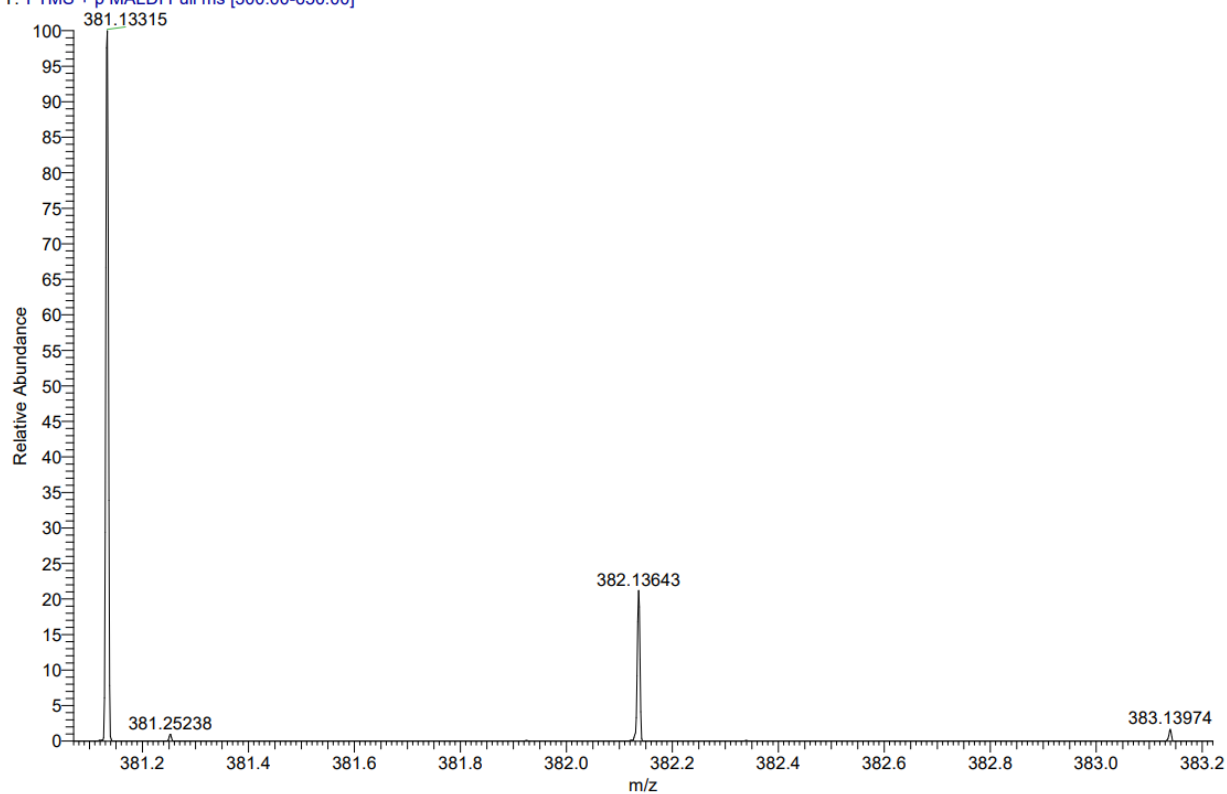
C21H18N4O2 +Na: C21 H18 N4 O2 Na1 pa Chrg 1
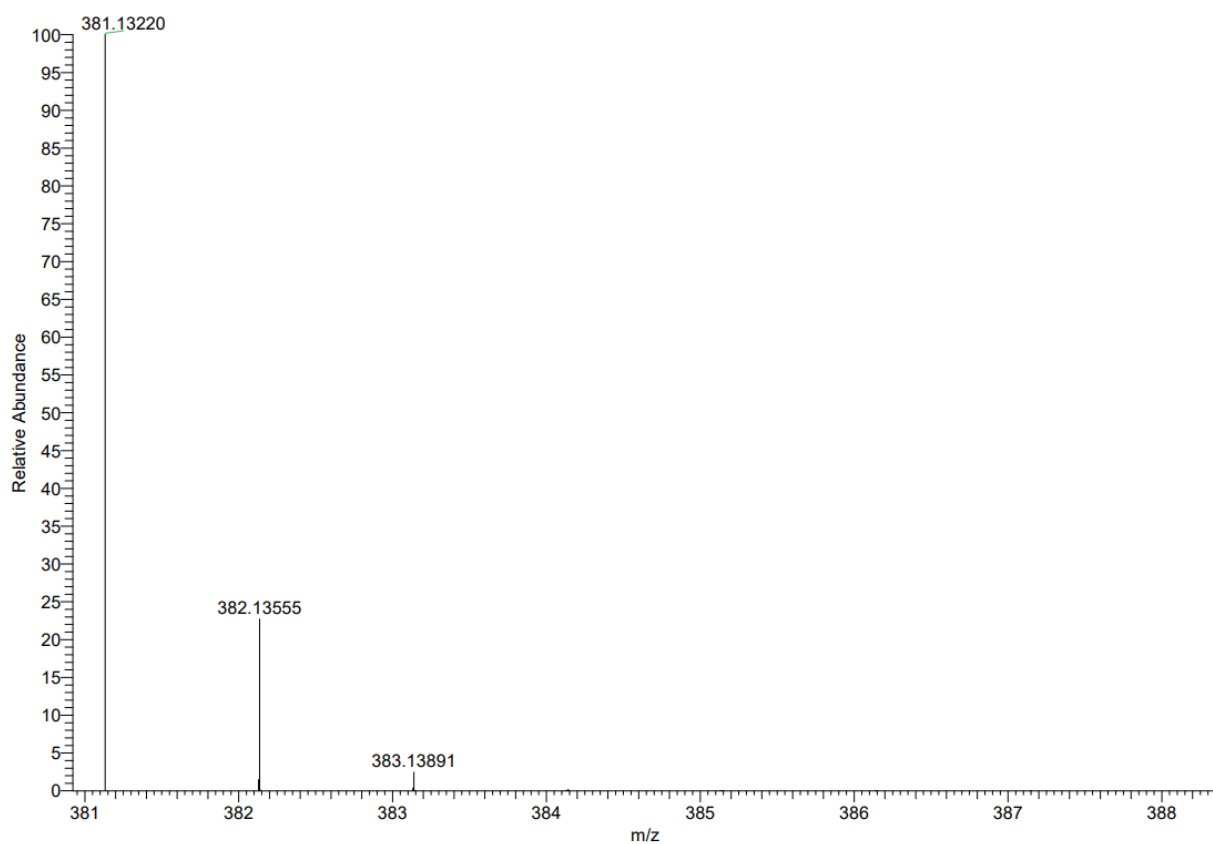
¹H and ¹³C Spectra of **123b**
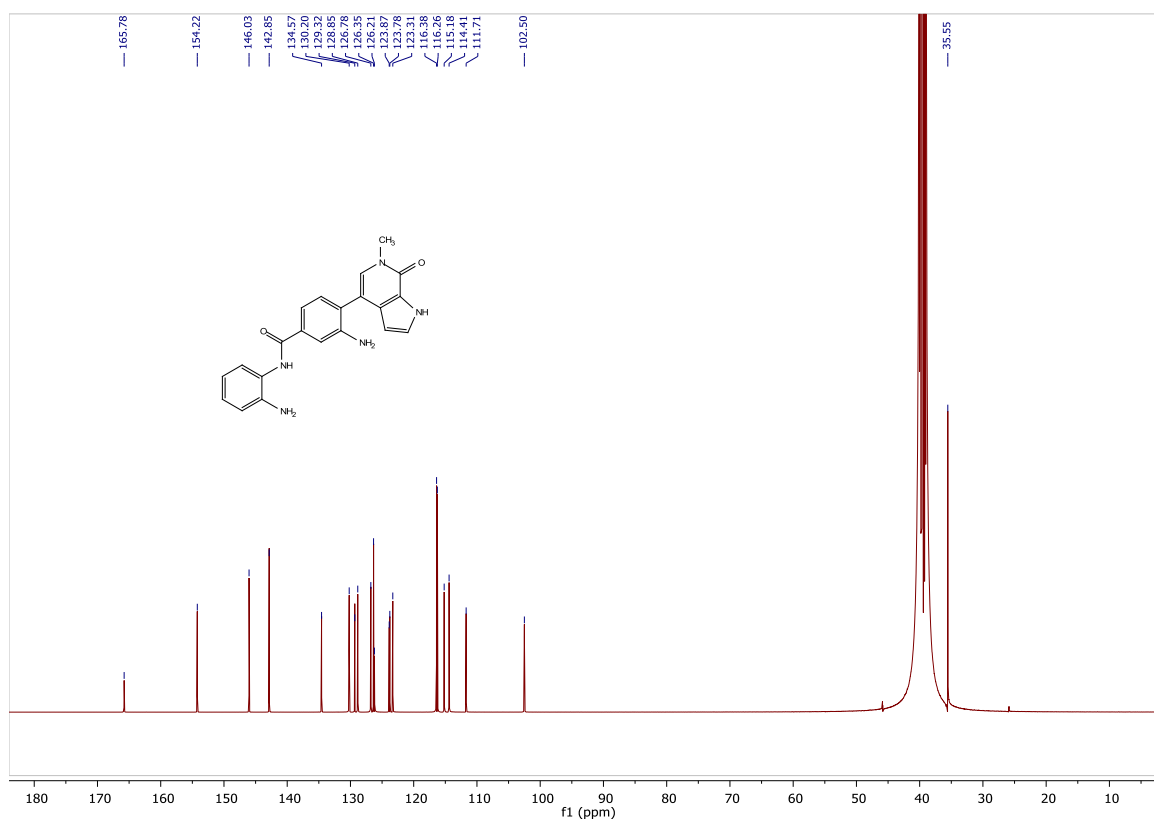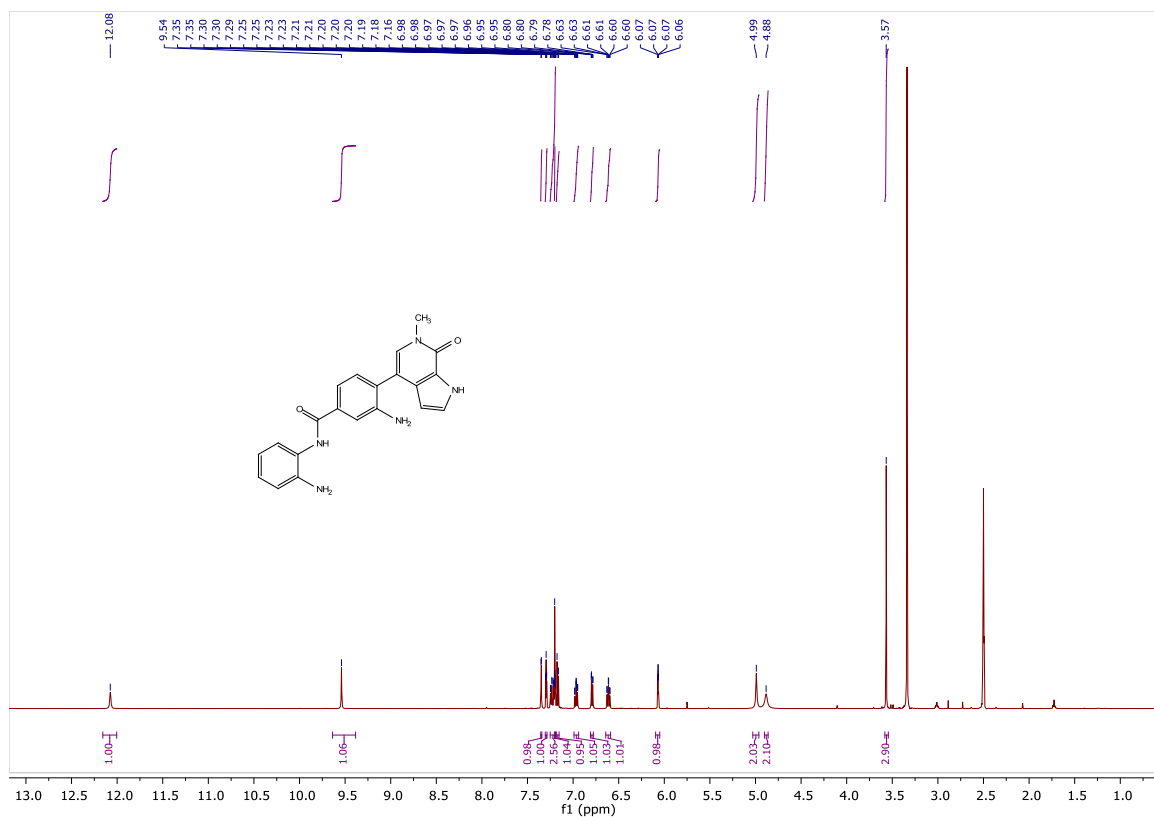
MALDI HRMS Spectrum of **123b** and simulated Spectrum

NB469_C4 #1-7   RT: 0.00-0.27   AV: 7   NL: 8.34E6
T: FTMS + p MALDI Full ms [300.00-650.00]
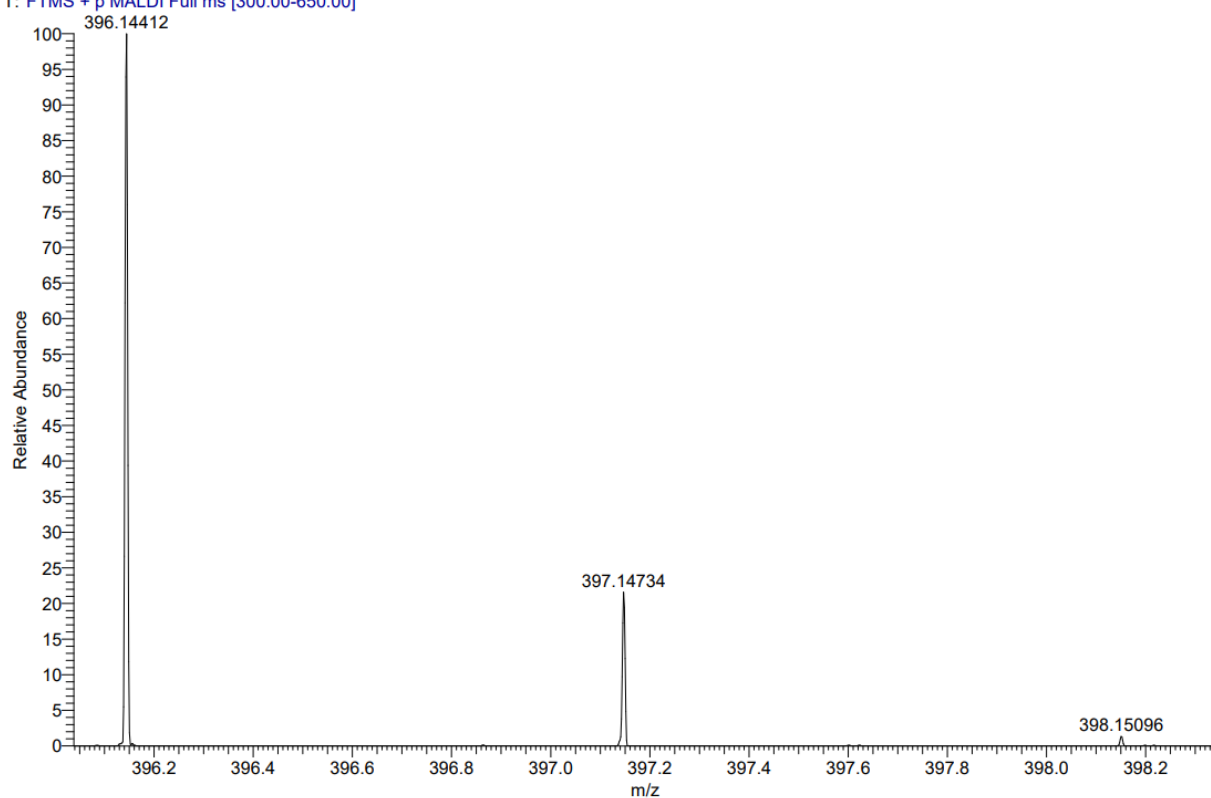
C21H19N5O2 +Na: C21 H19 N5 O2 Na1 pa Chrg 1
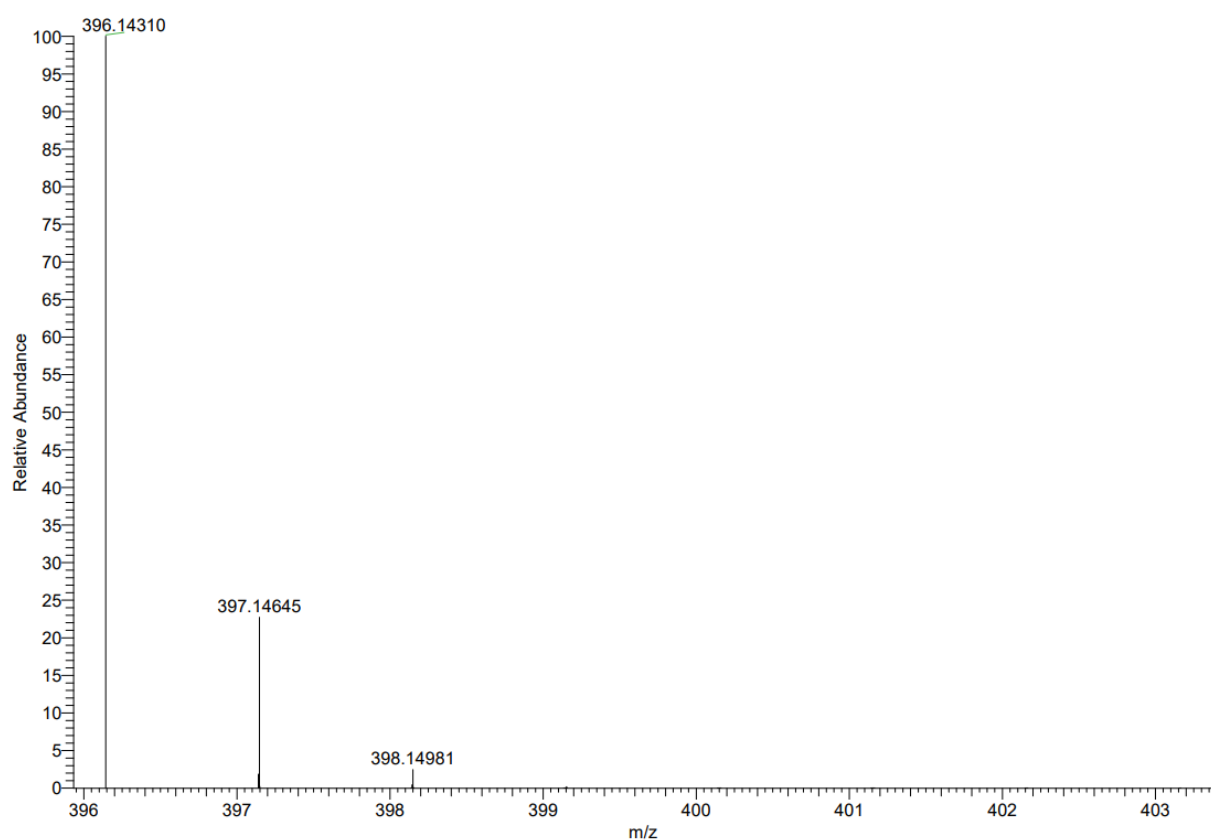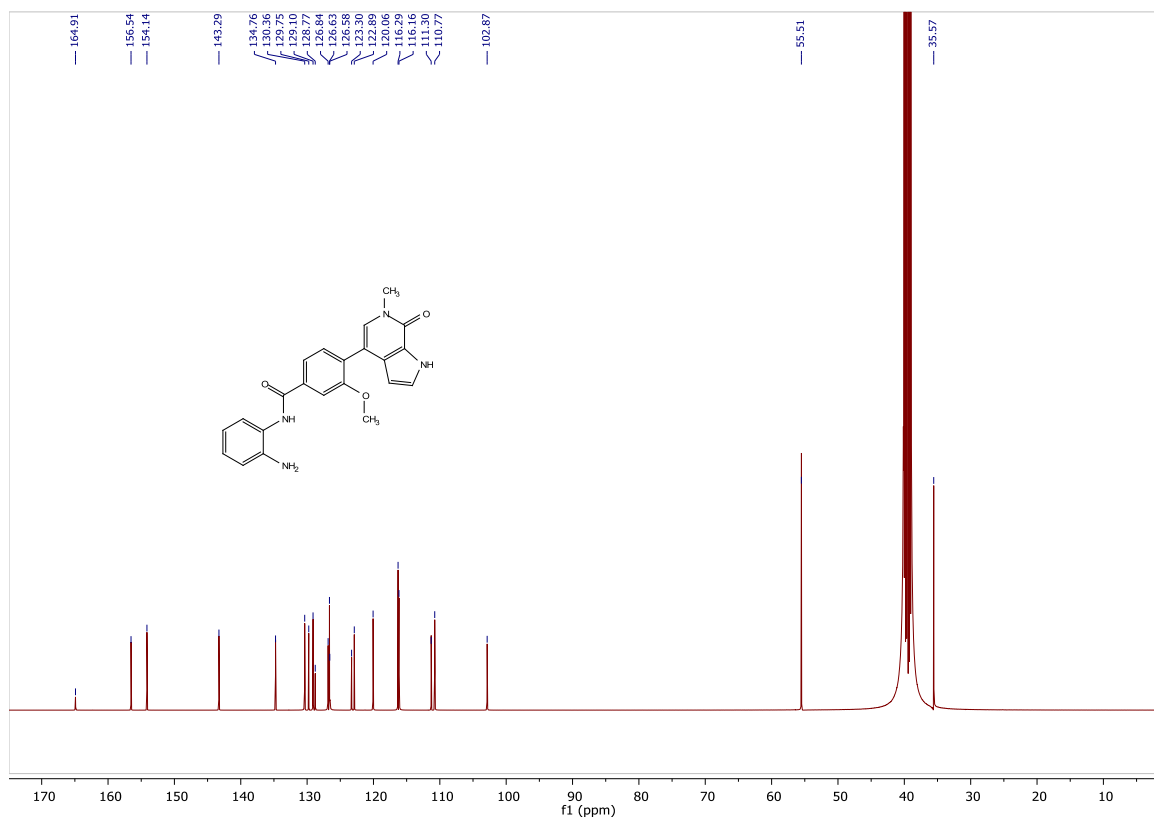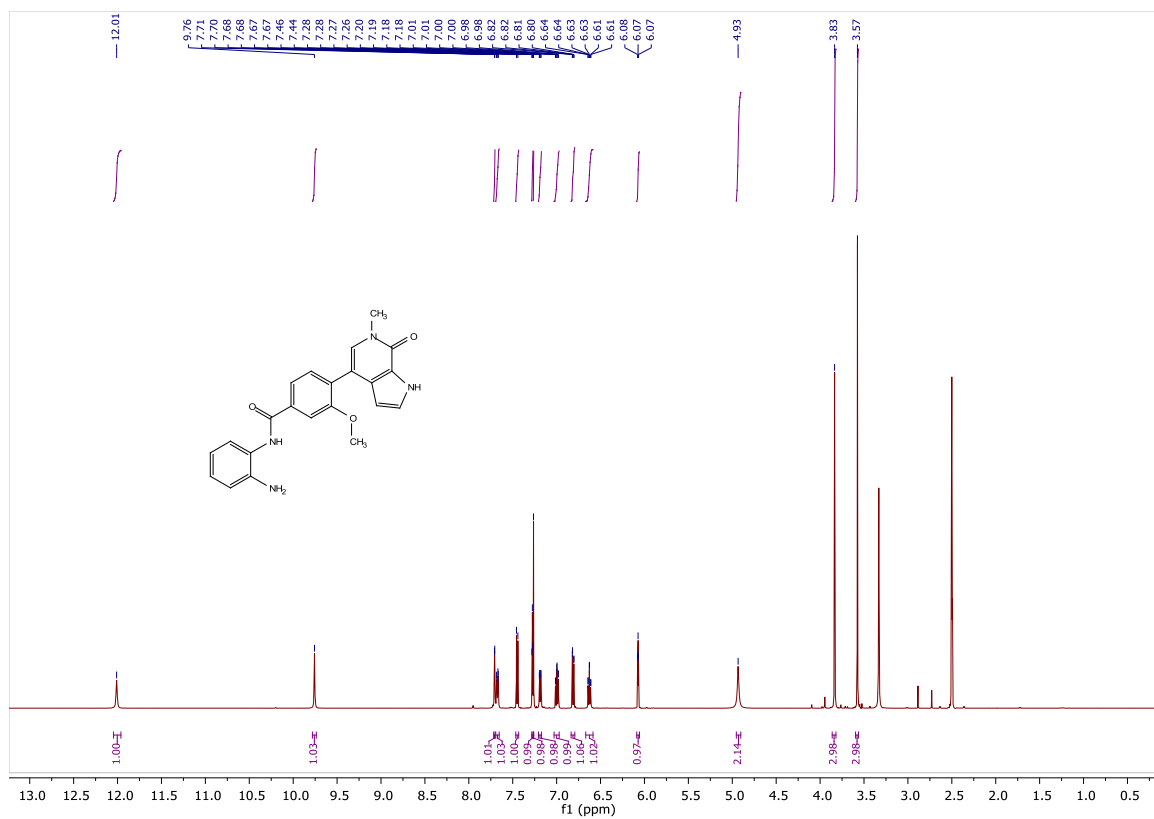
MALDI HRMS Spectrum of **123c** and simulated Spectrum

NB470_C5 #1-7 RT: 0.00-0.27 AV: 7 NL: 4.39E7
T: FTMS + p MALDI Full ms [300.00-650.00]

411.14341

412.14676

413.14998
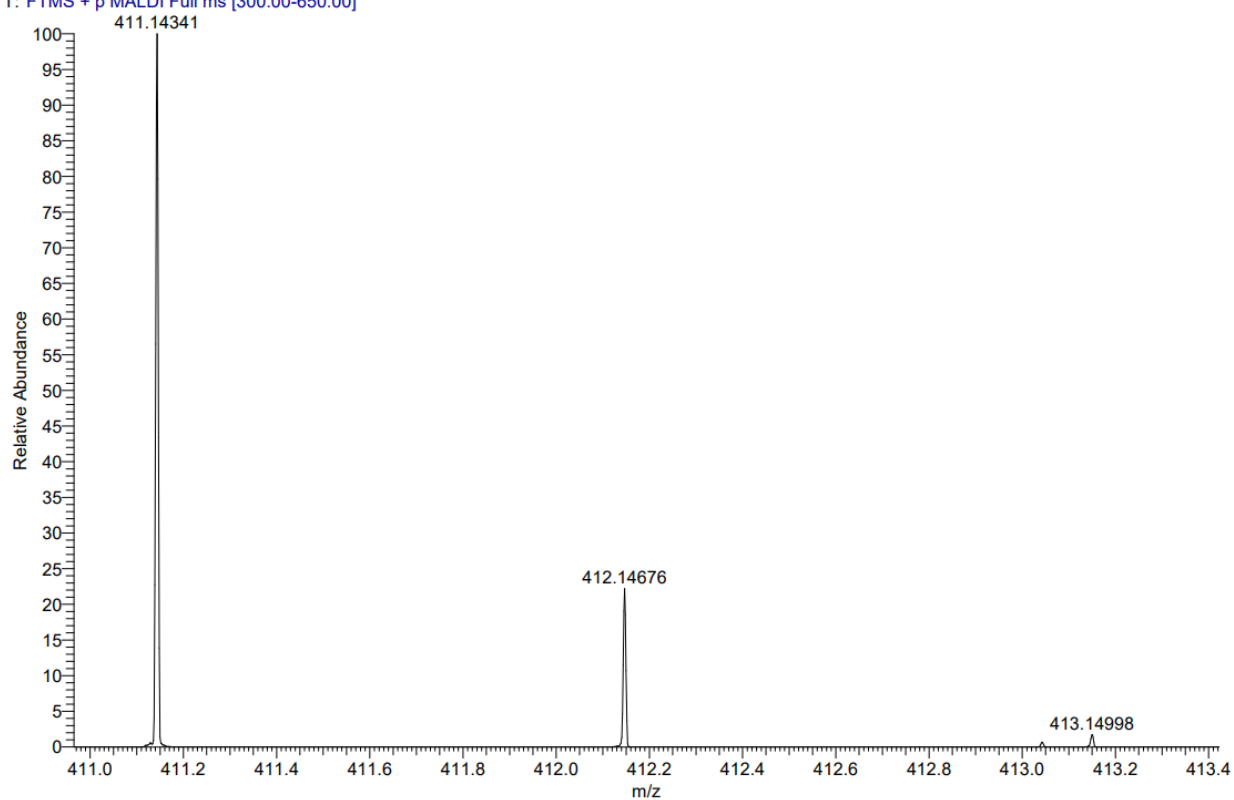
C22H20N4O3 +Na: C22 H20 N4 O3 Na1 pa Chrg 1

411.14276

412.14612

413.14947
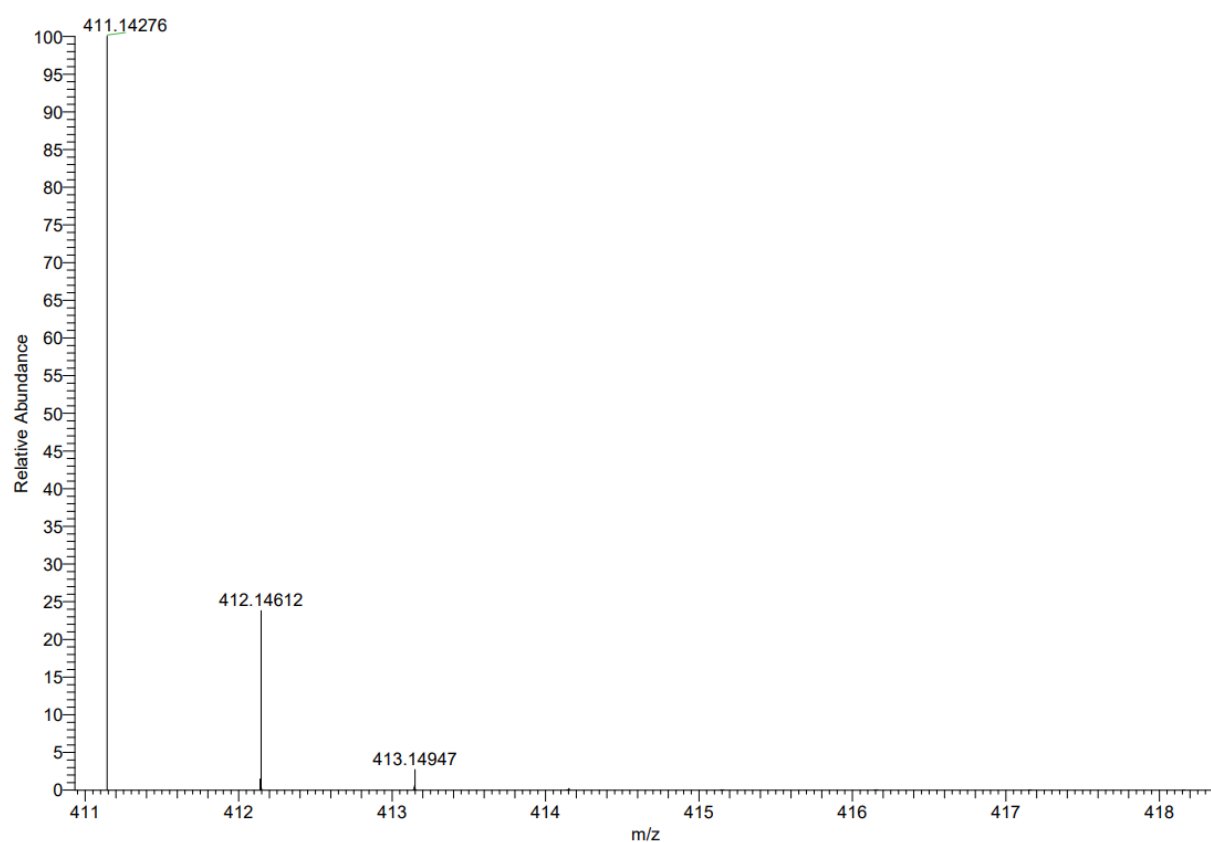
^{1}H and ^{13}C Spectra of **123d**
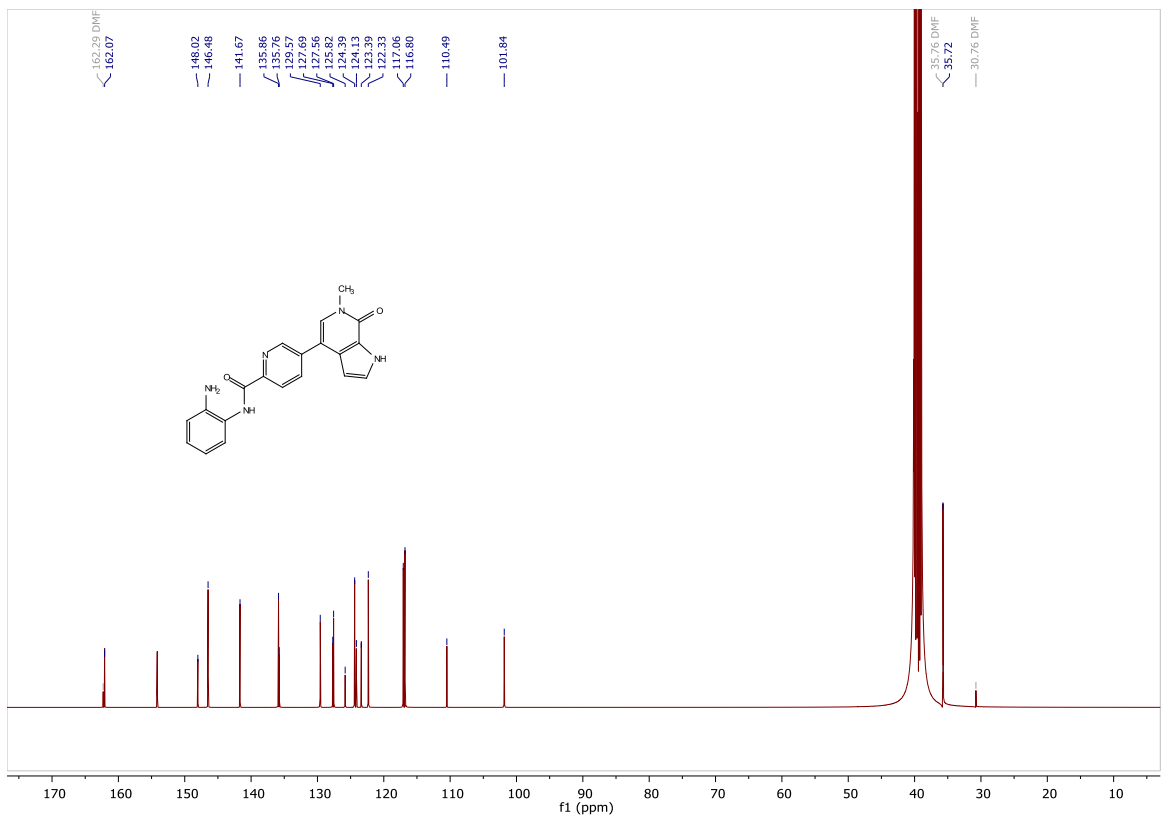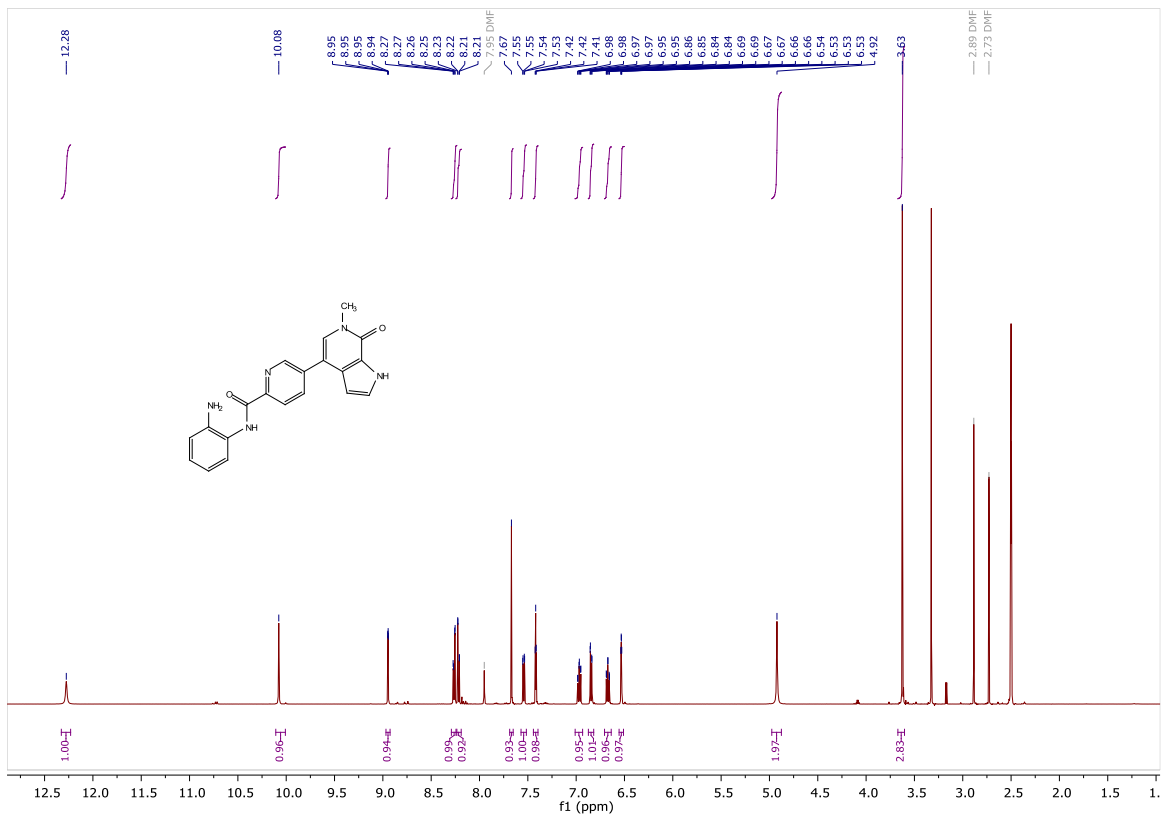
MALDI HRMS Spectrum of **123d** and simulated Spectrum

NB500_C7 #1-6   RT: 0.00-0.23   AV: 6   NL: 9.44E6
T: FTMS + p MALDI Full ms [300.00-650.00]

382.12858

383.13187

384.13520

C20H17N5O2 +Na: C20 H17 N5 O2 Na1 pa Chrg 1

382.12745

383.13080

384.13416
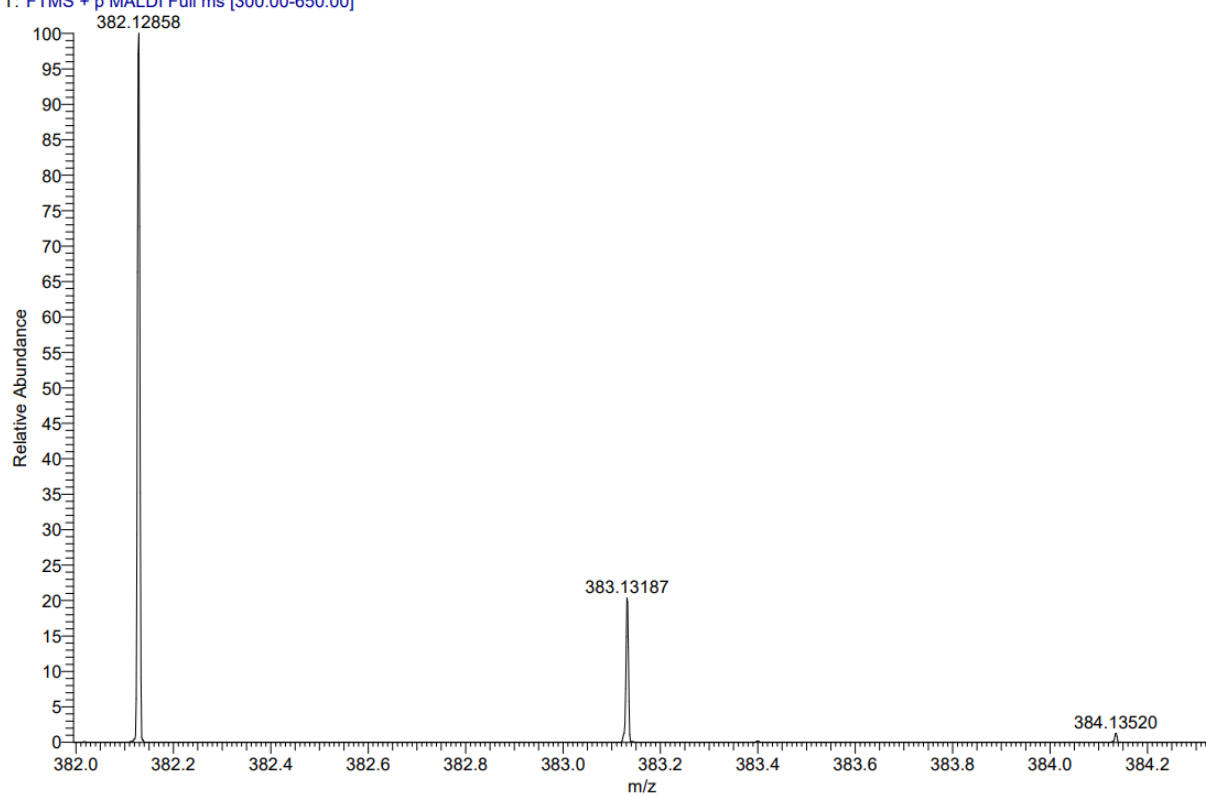
¹H and ¹³C Spectra of **123e**

MALDI HRMS Spectrum of **123e** and simulated Spectrum

NB501_C8 #1-4   RT: 0.01-0.14   AV: 4   NL: 1.34E7
T: FTMS + p MALDI Full ms [300.00-650.00]
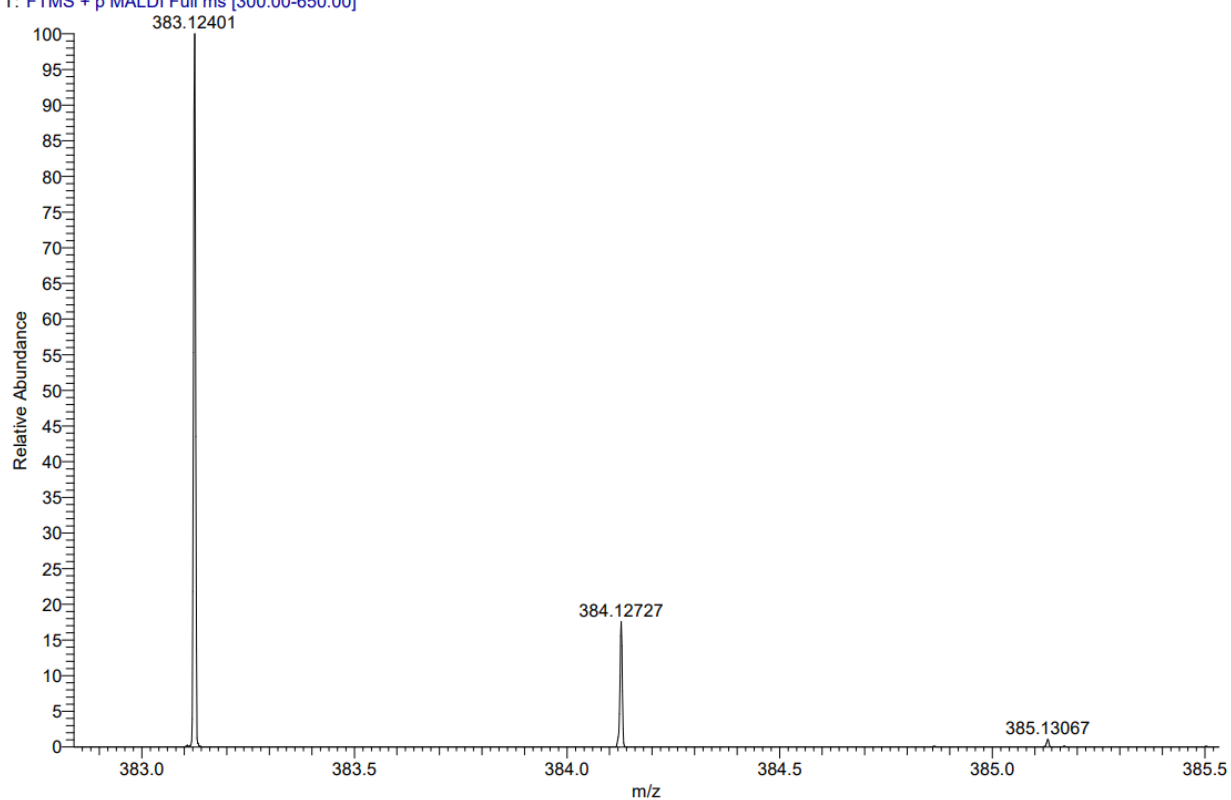
C19H16N6O2 +Na: C19 H16 N6 O2 Na1 pa Chrg 1
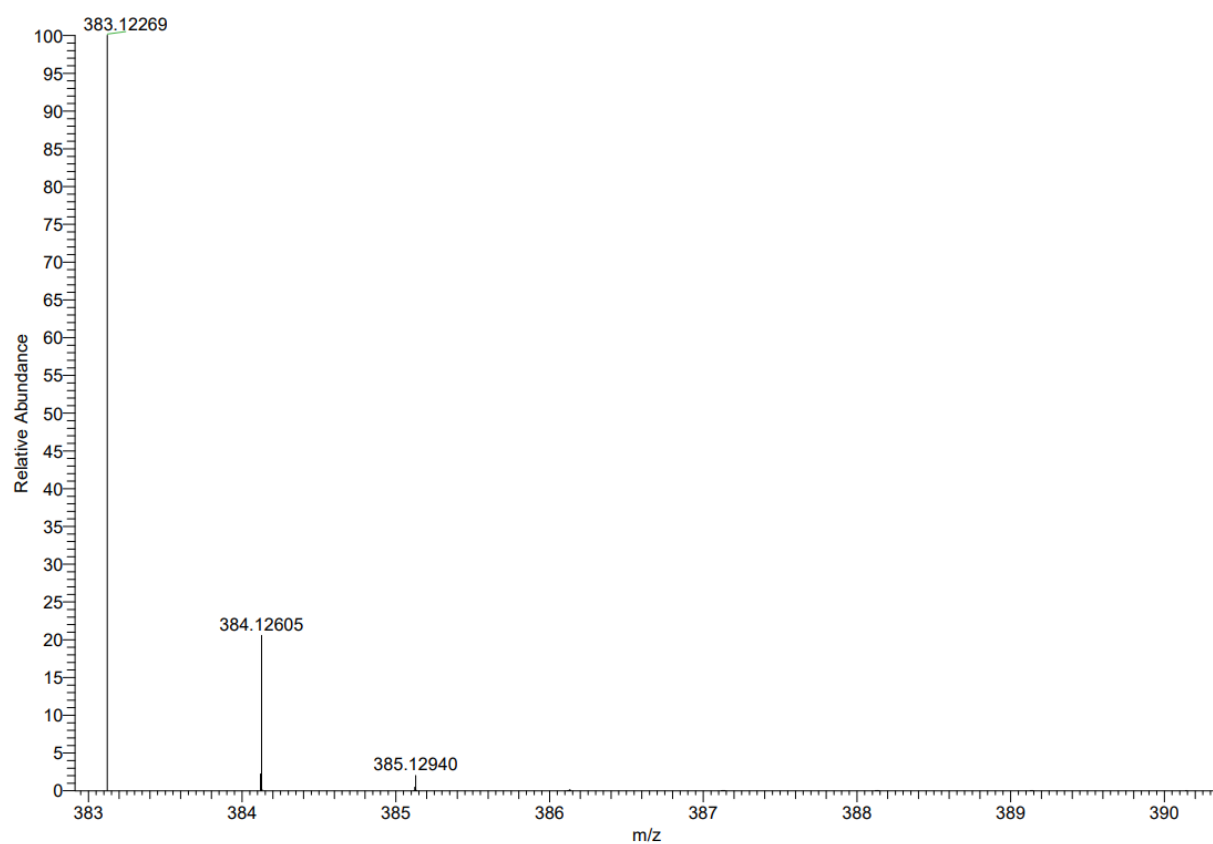
^{1}H and ^{13}C Spectra of **123f**
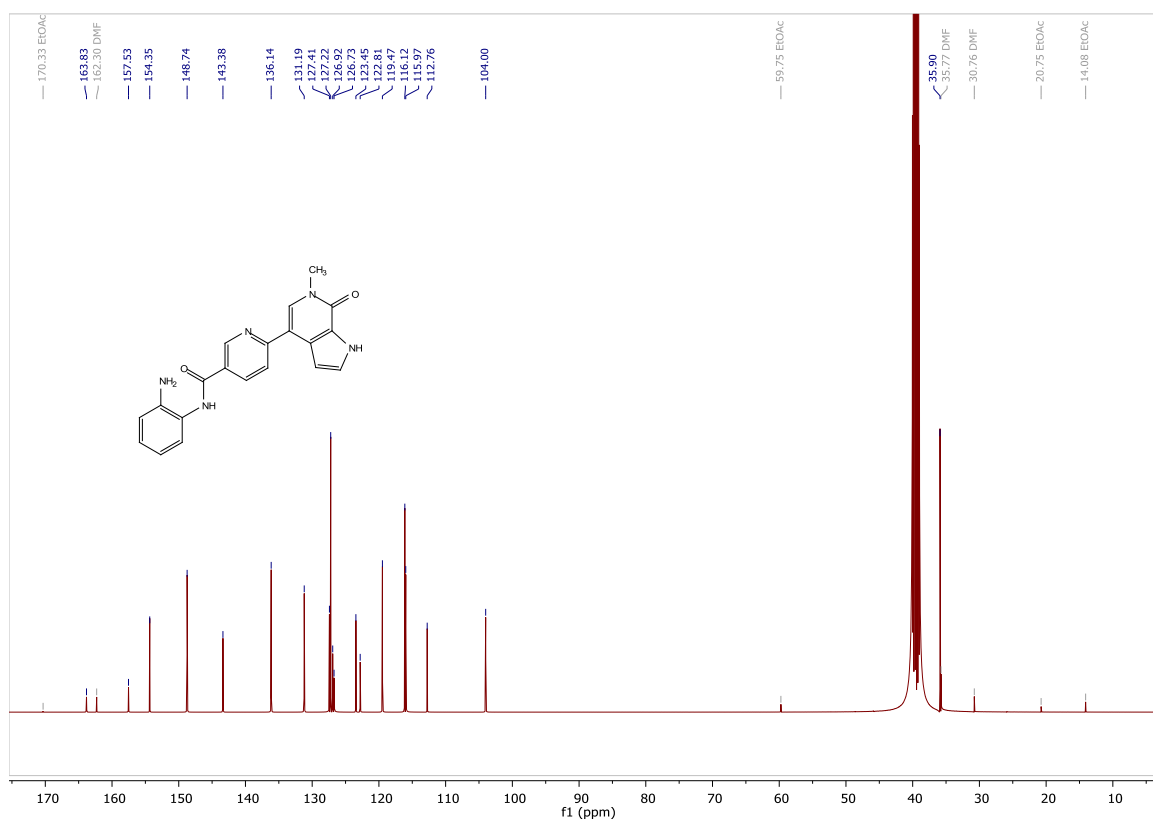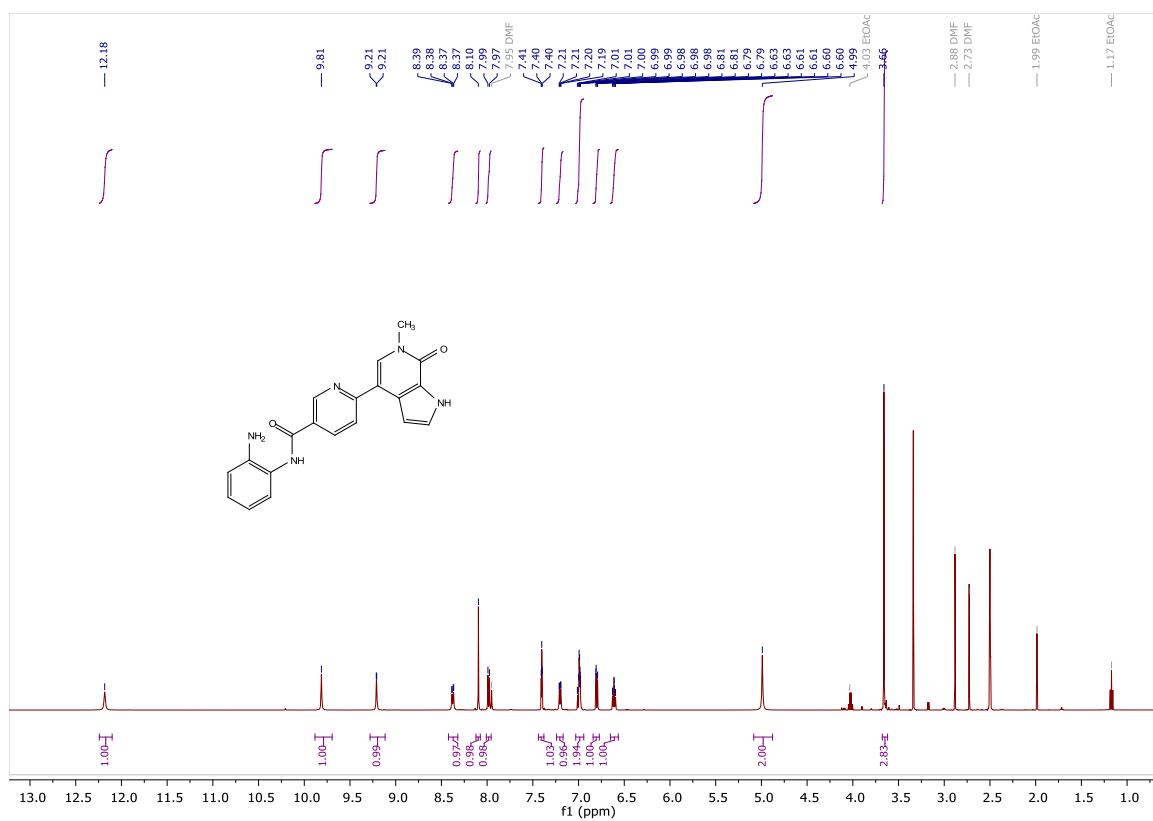
MALDI HRMS Spectrum of **123f** and simulated Spectrum

NB502_C9 #1-5   RT: 0.00-0.18   AV: 5   NL: 6.85E6
T: FTMS + p MALDI Full ms [300.00-650.00]
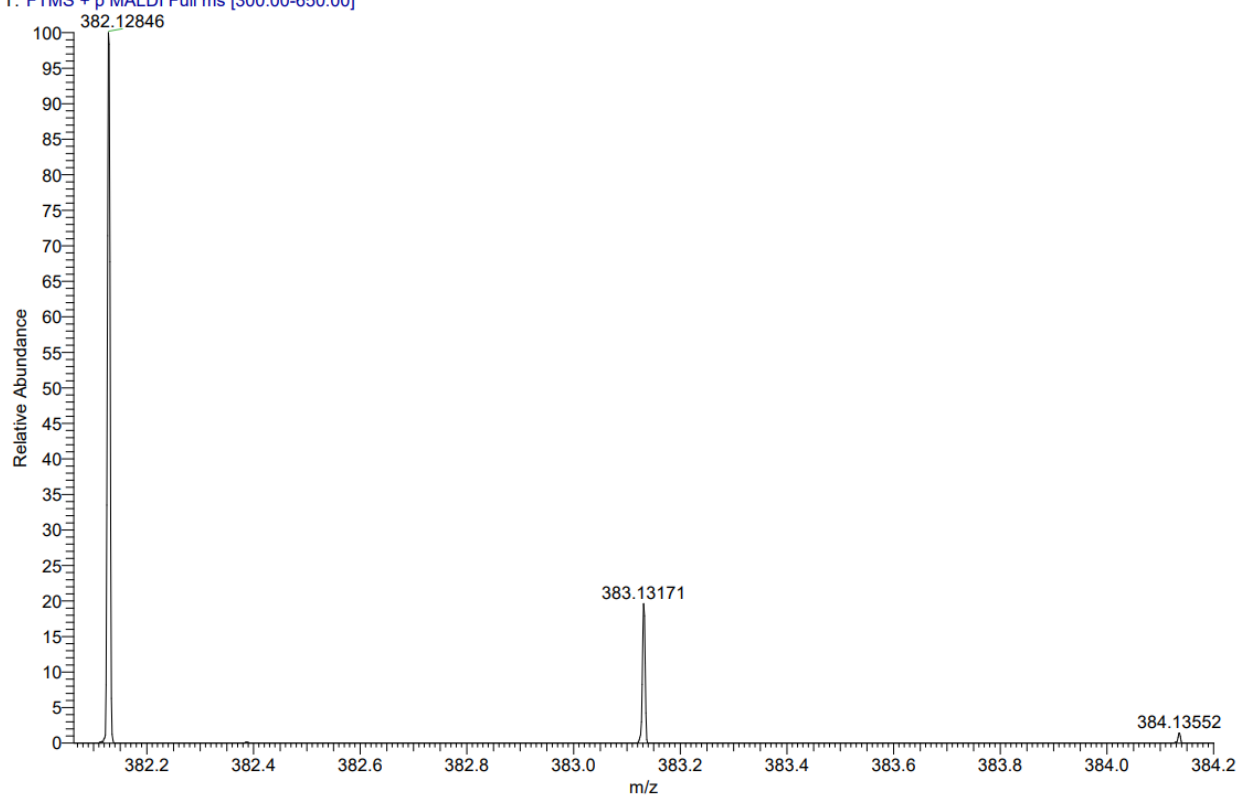
C20H17N5O2 +Na: C20 H17 N5 O2 Na1 pa Chrg 1
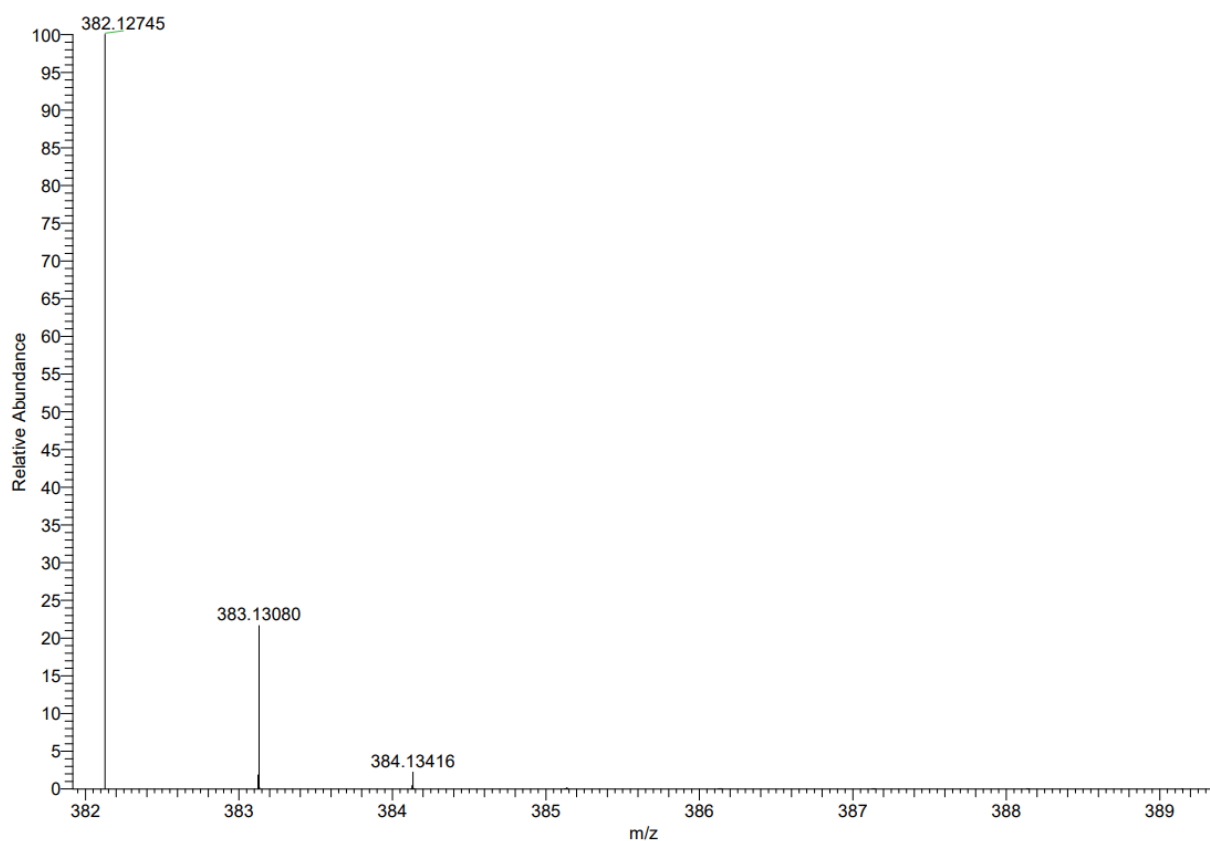
^{1}H and ^{13}C Spectra of **132a**
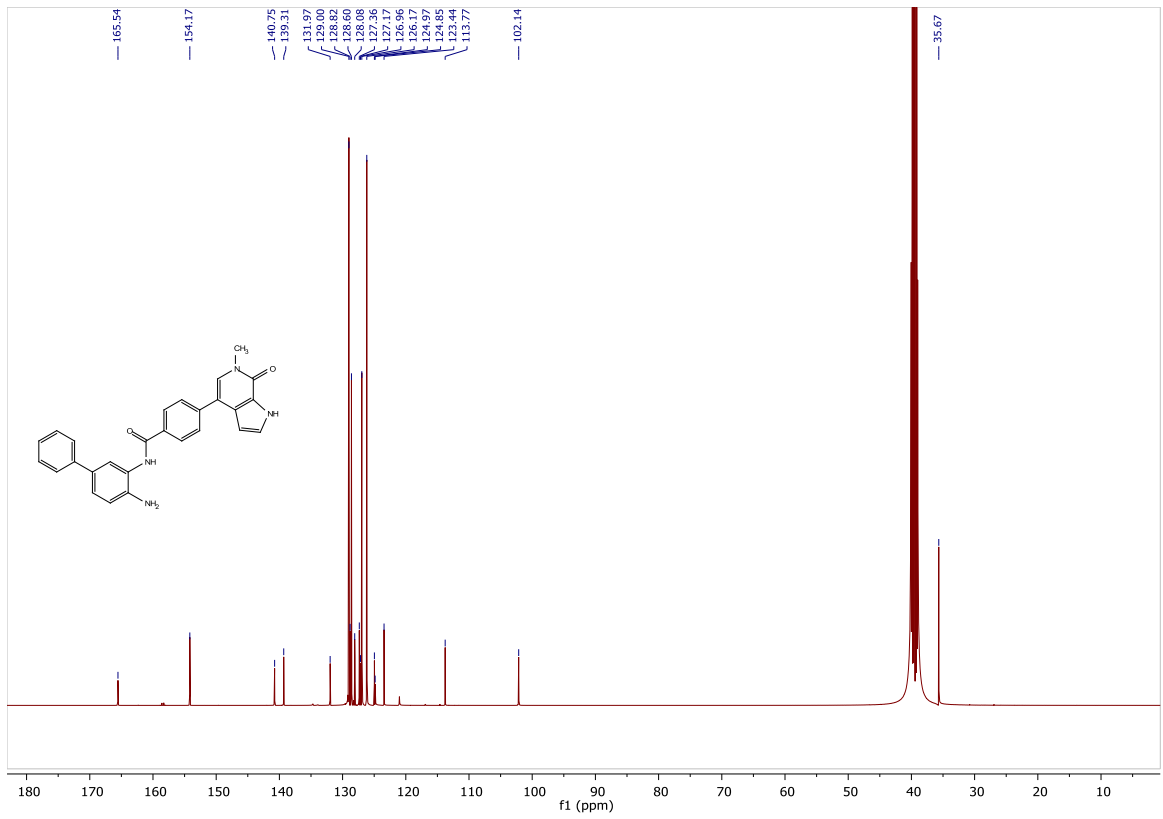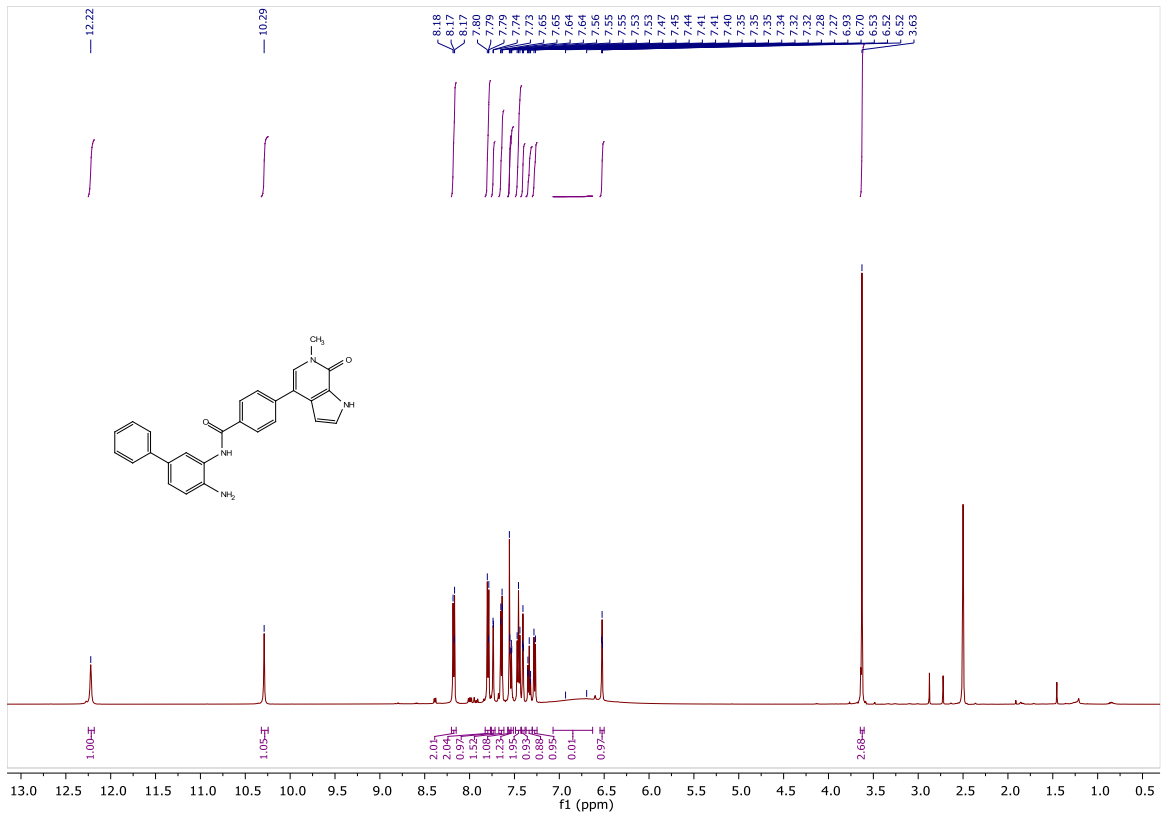
MALDI HRMS Spectrum of **132a** and simulated Spectrum

NB503_C10 #1-6 RT: 0.00-0.23 AV: 6 NL: 2.63E6
T: FTMS + p MALDI Full ms [300.00-650.00]
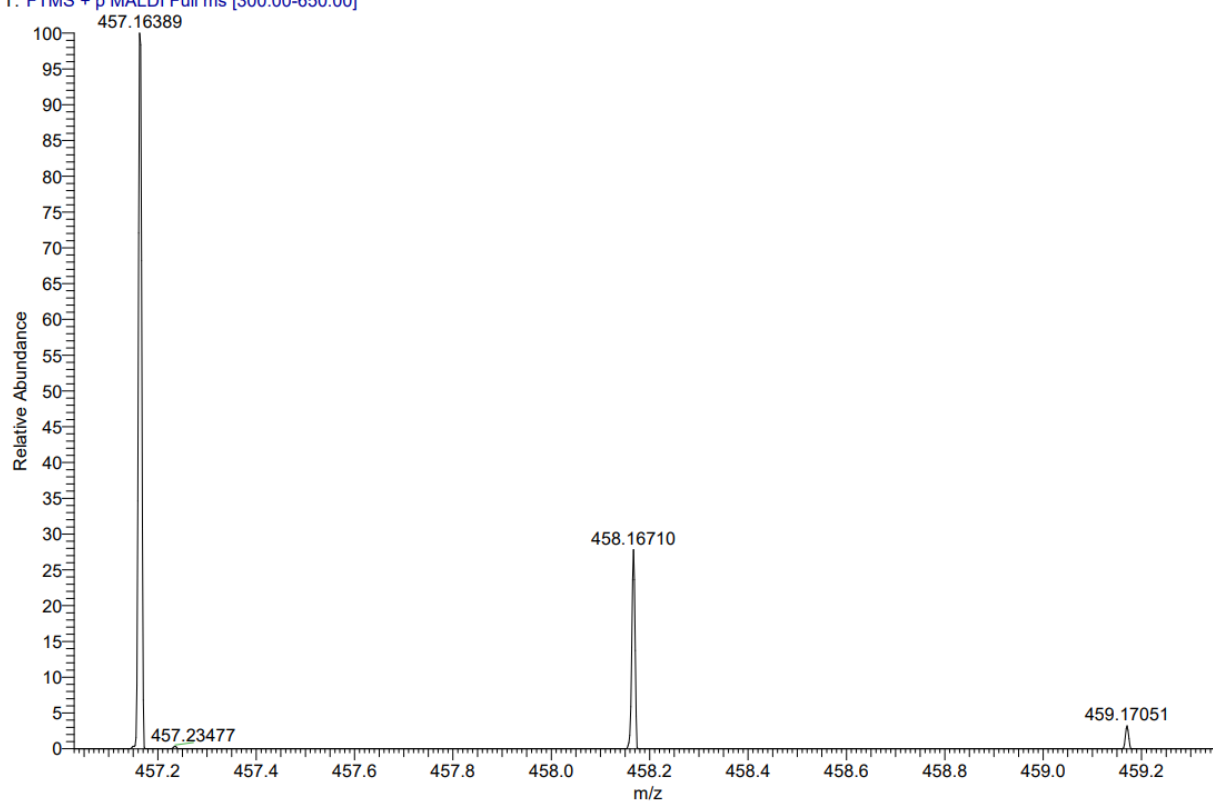
C27H22N4O2 +Na: C27 H22 N4 O2 Na1 pa Chrg 1
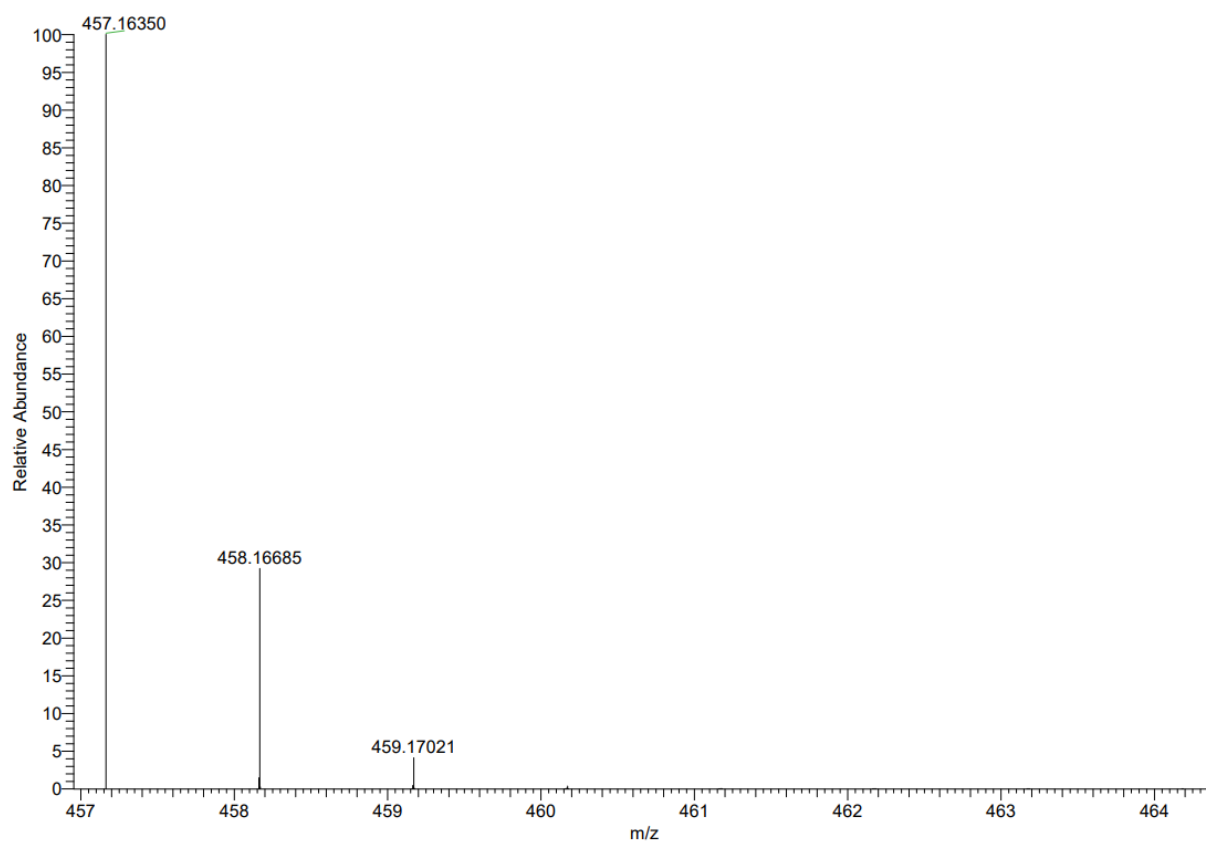
^{1}H and ^{13}C Spectra of **132b**
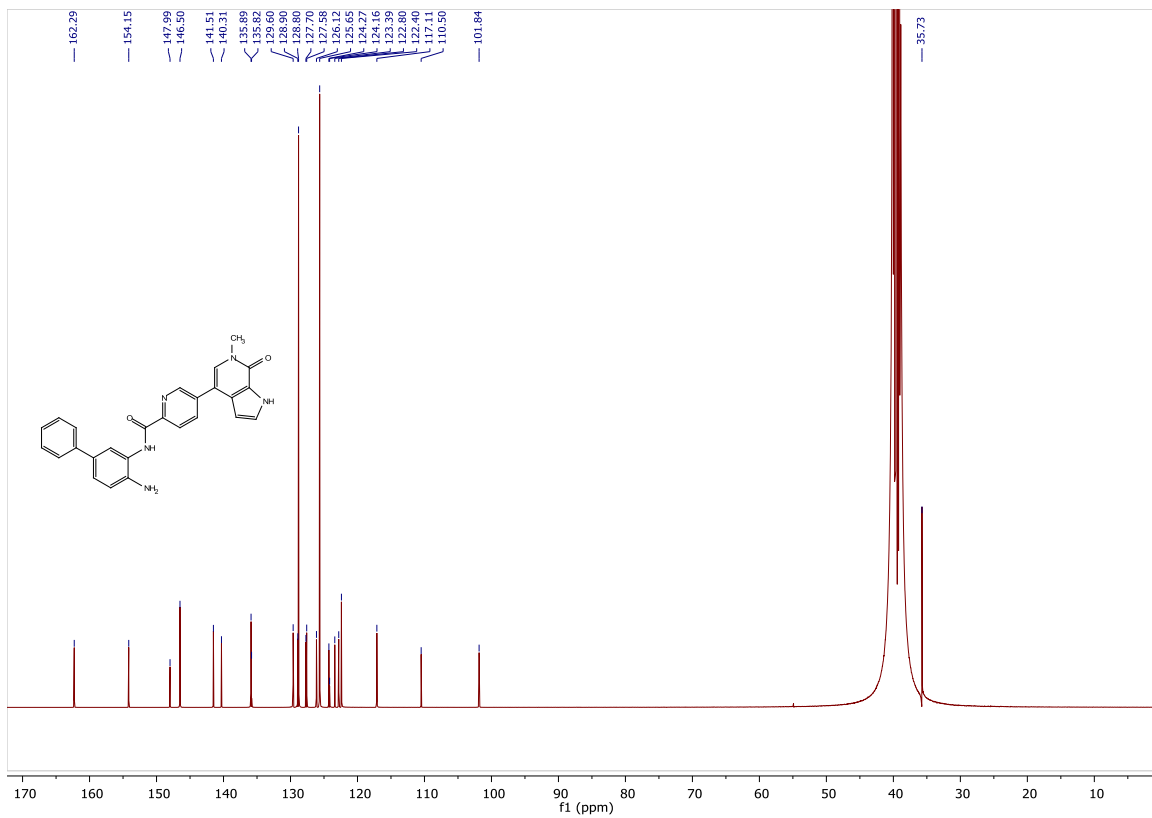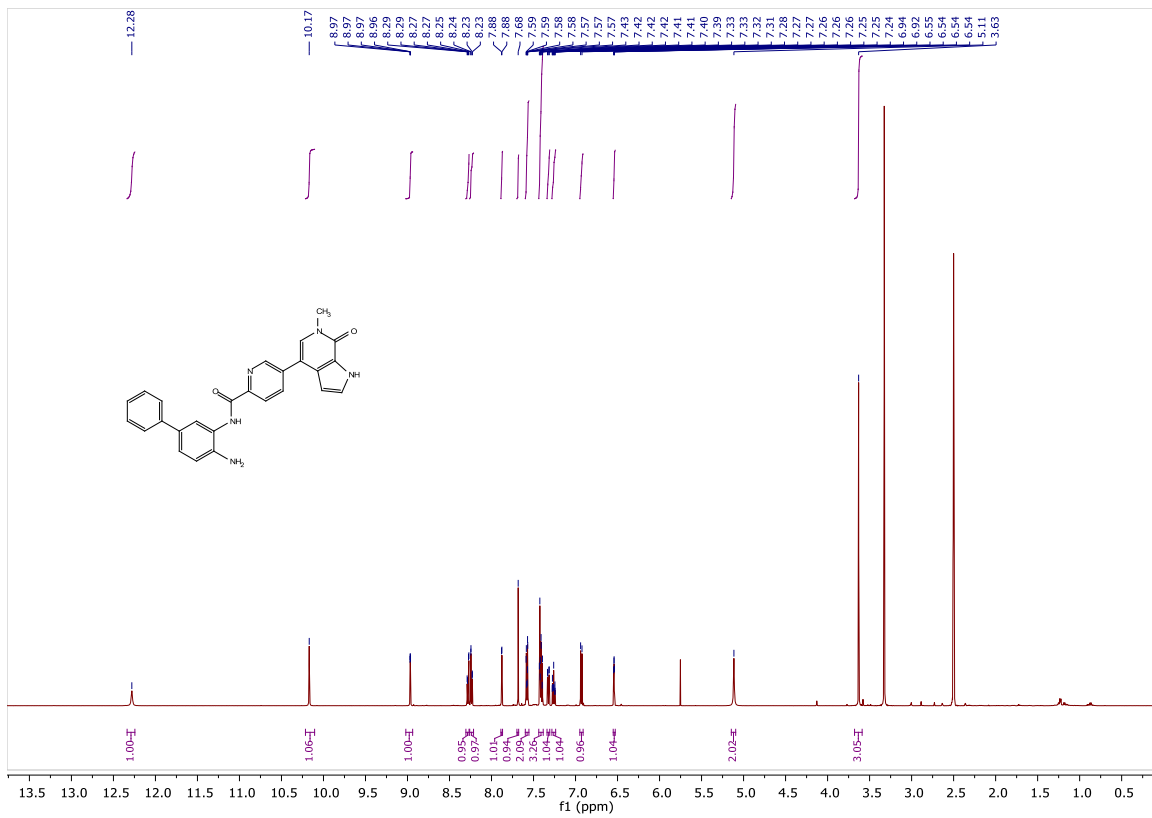
MALDI HRMS Spectrum of **132b** and simulated Spectrum

NB512_B10 #1-7 RT: 0.00-0.27 AV: 7 NL: 2.95E6
T: FTMS + p MALDI Full ms [300.00-600.00]
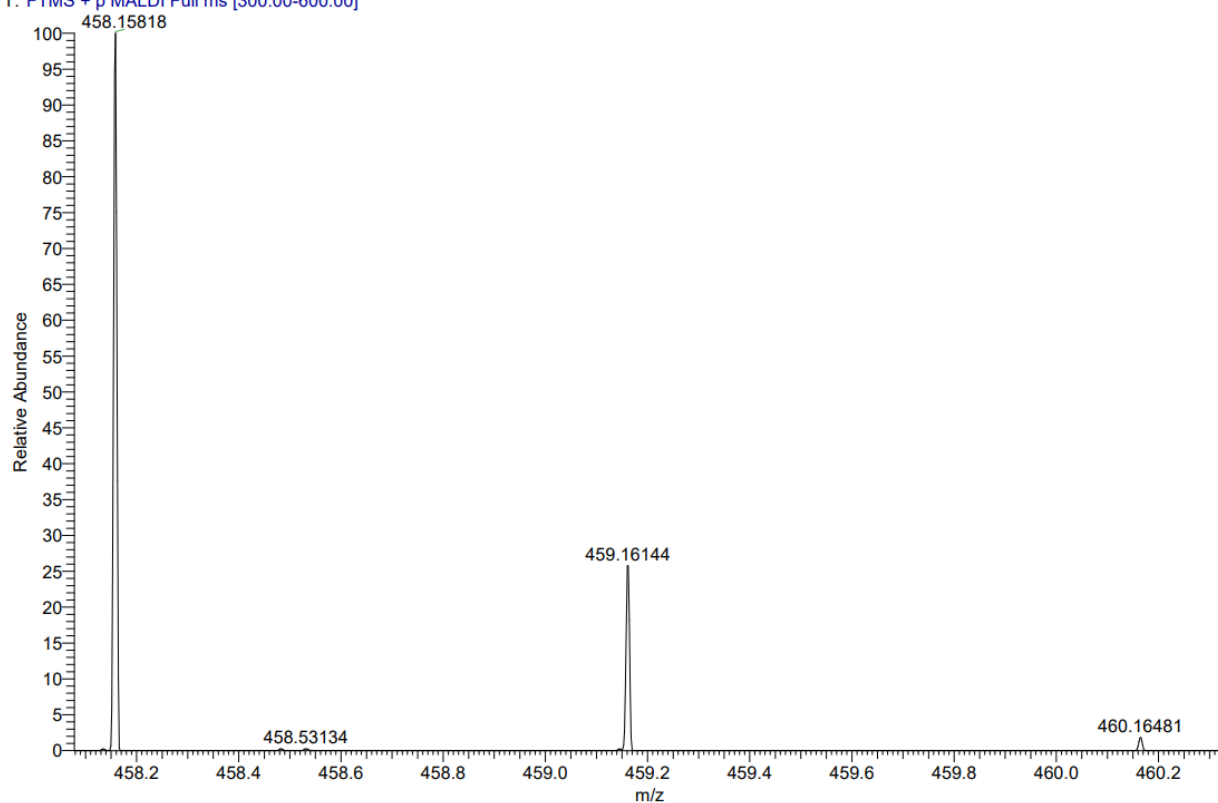
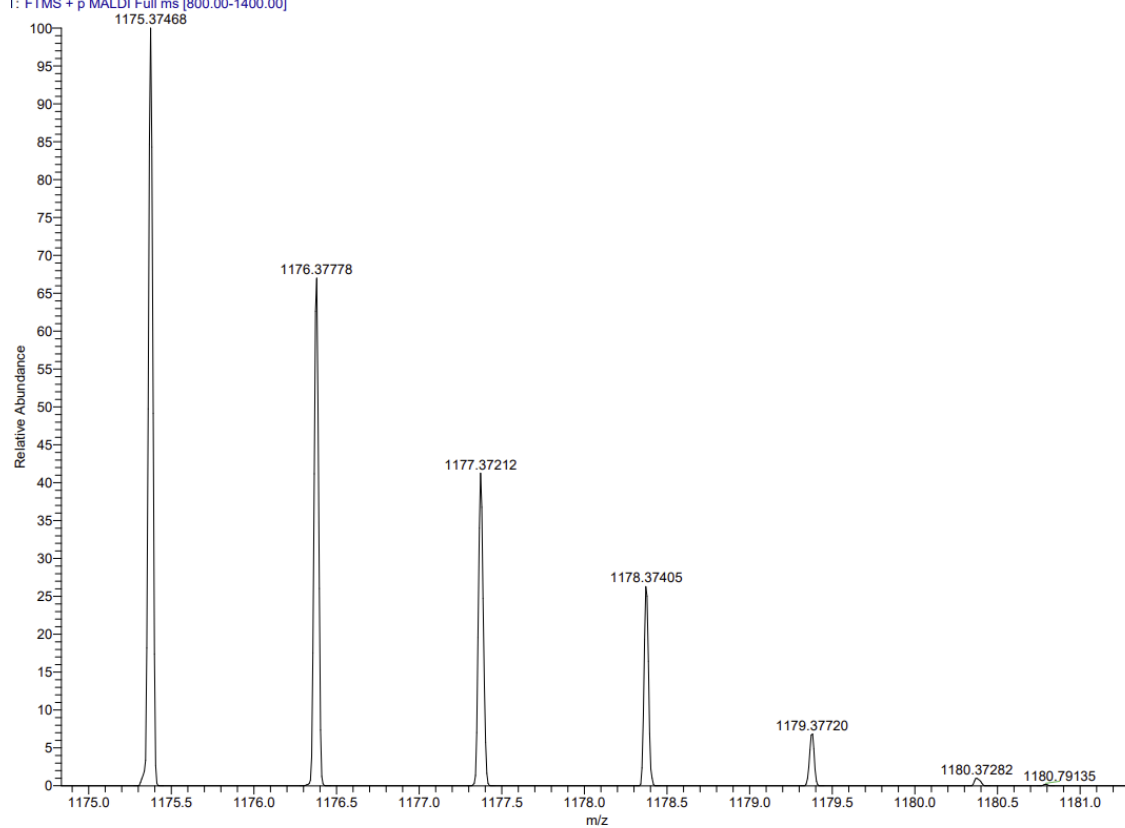C26H21N5O2 +Na: C26 H21 N5 O2 Na1 pa Chrg 1
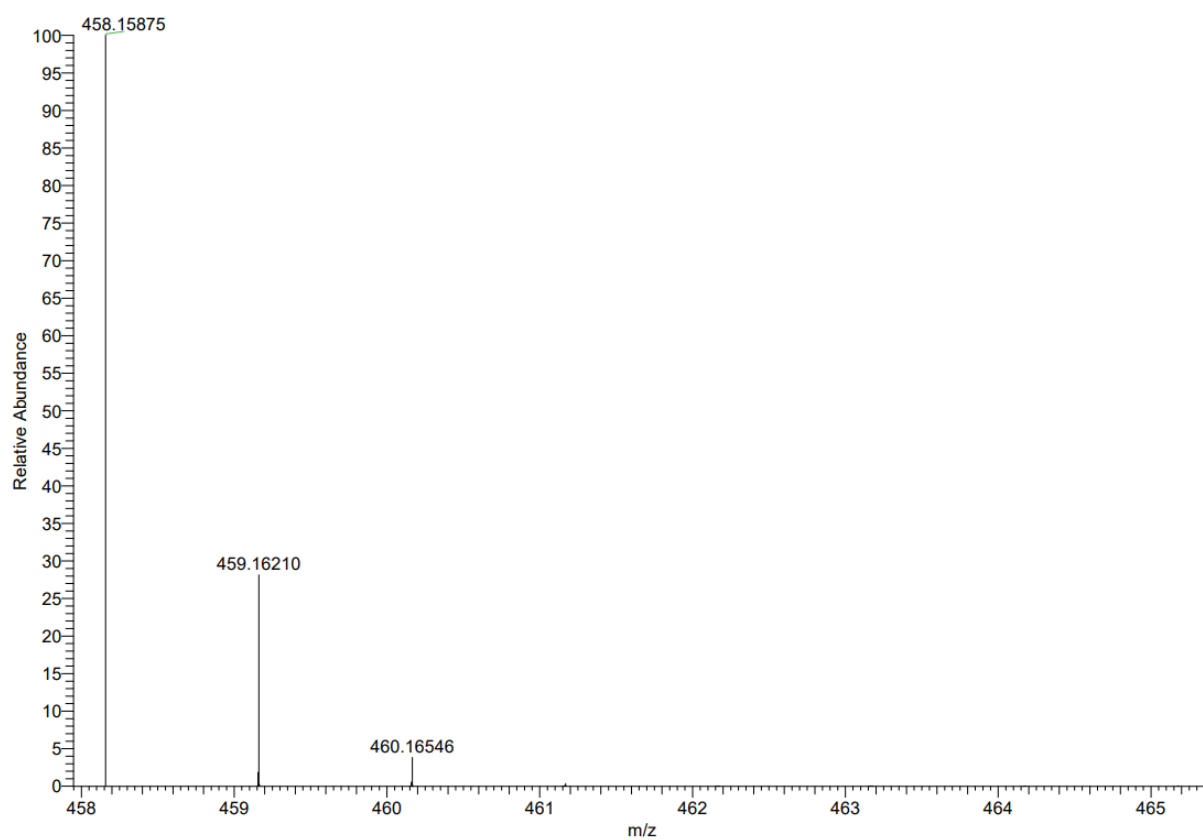
^{1}H and ^{13}C Spectra of **132c**
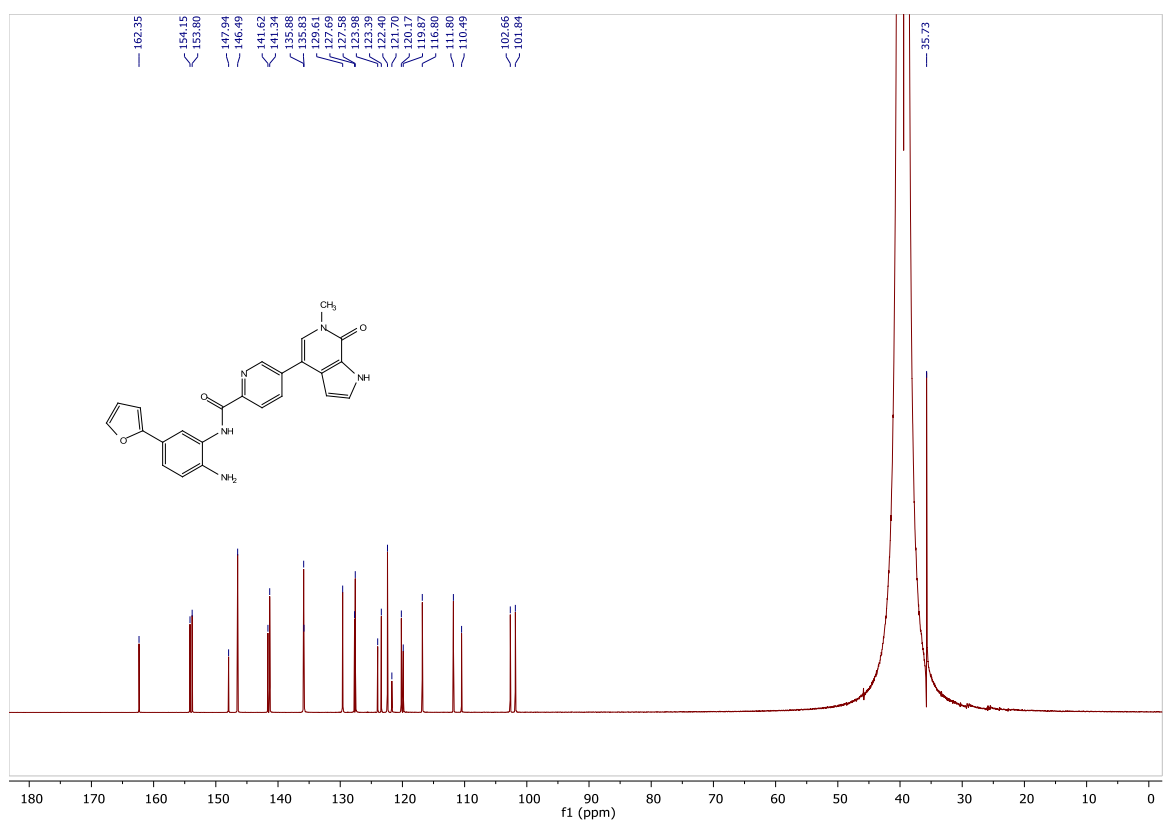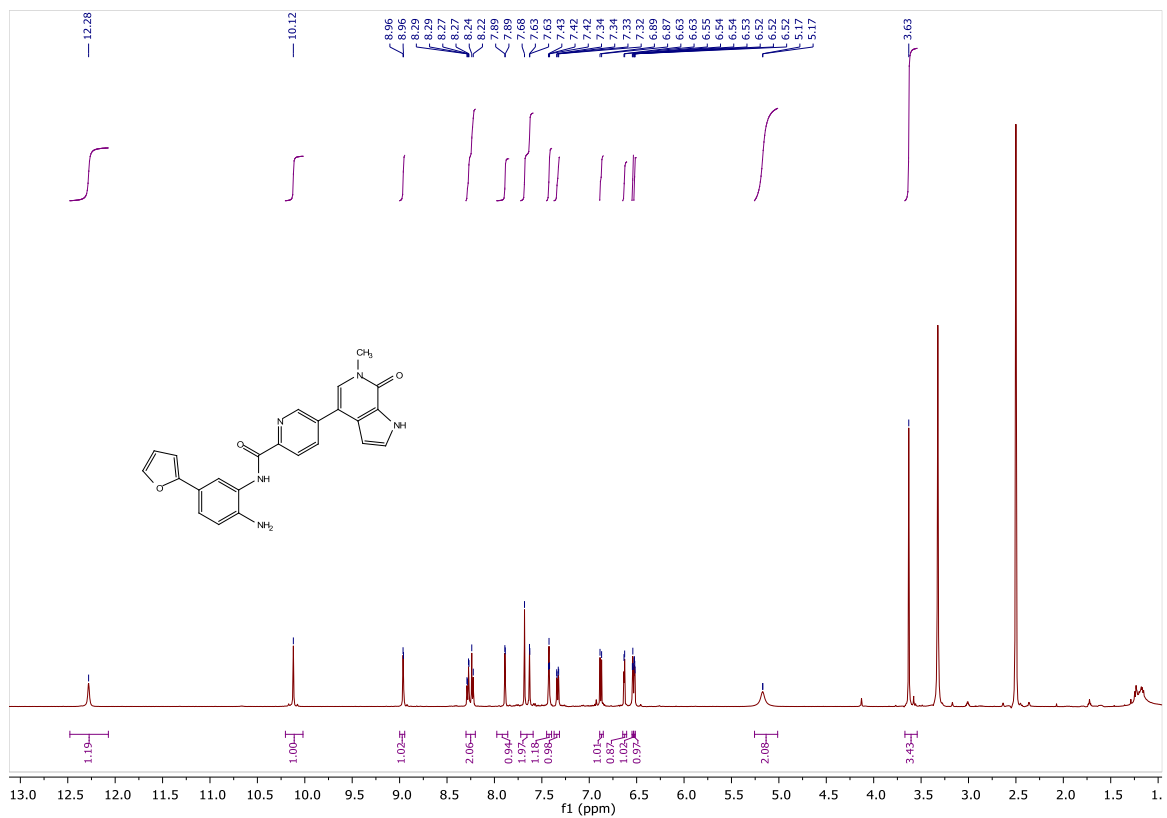
MALDI HRMS Spectrum of **132c** and simulated Spectrum

NB513_B11 #1-17   RT: 0.00-0.72   AV: 17   NL: 2.03E6
T: FTMS + p MALDI Full ms [300.00-600.00]
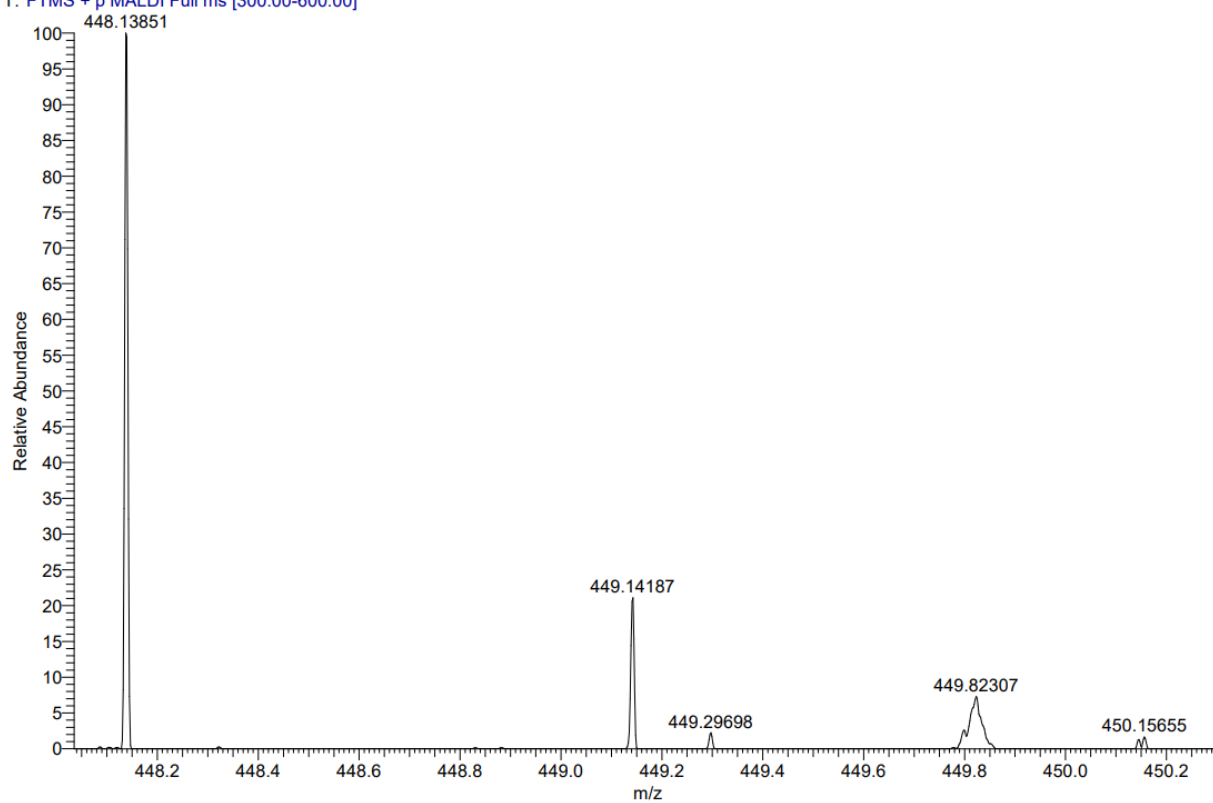
C24H19N5O3 +Na: C24 H19 N5 O3 Na1 pa Chrg 1
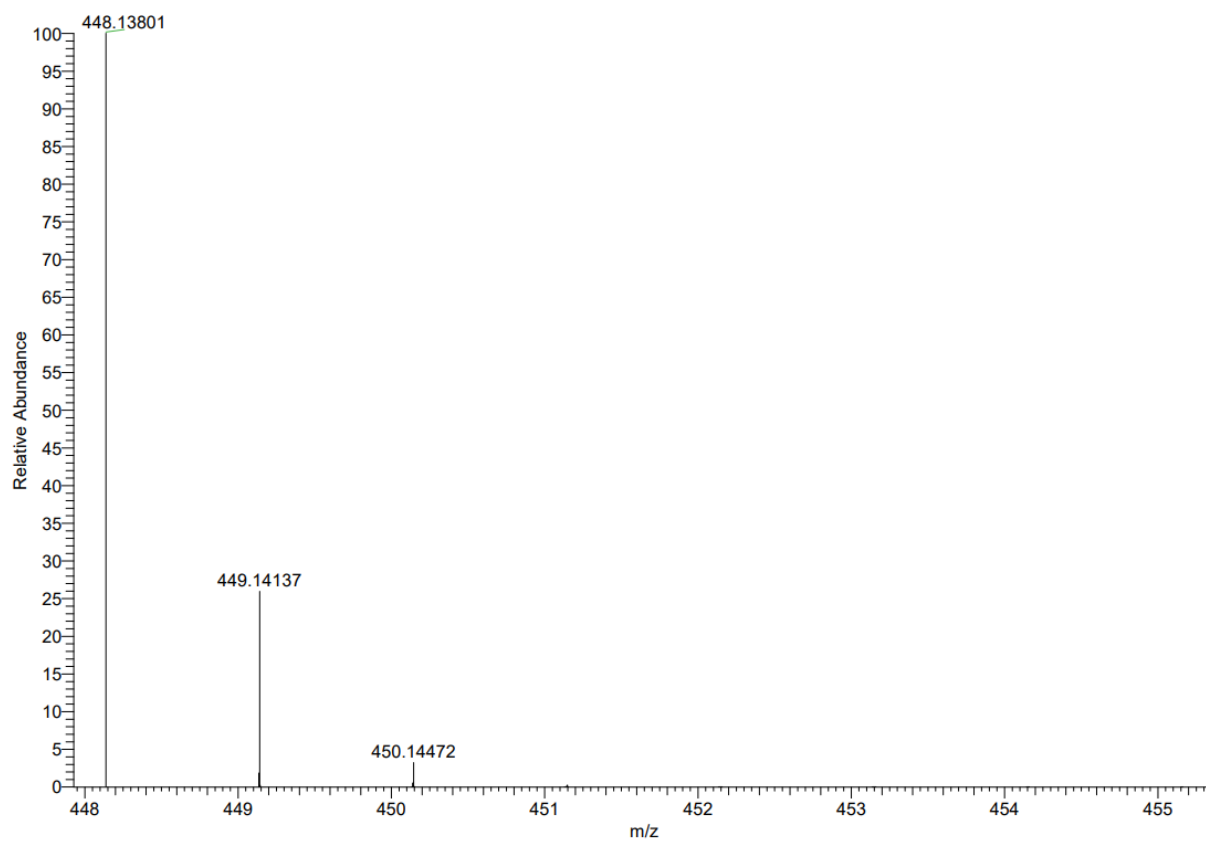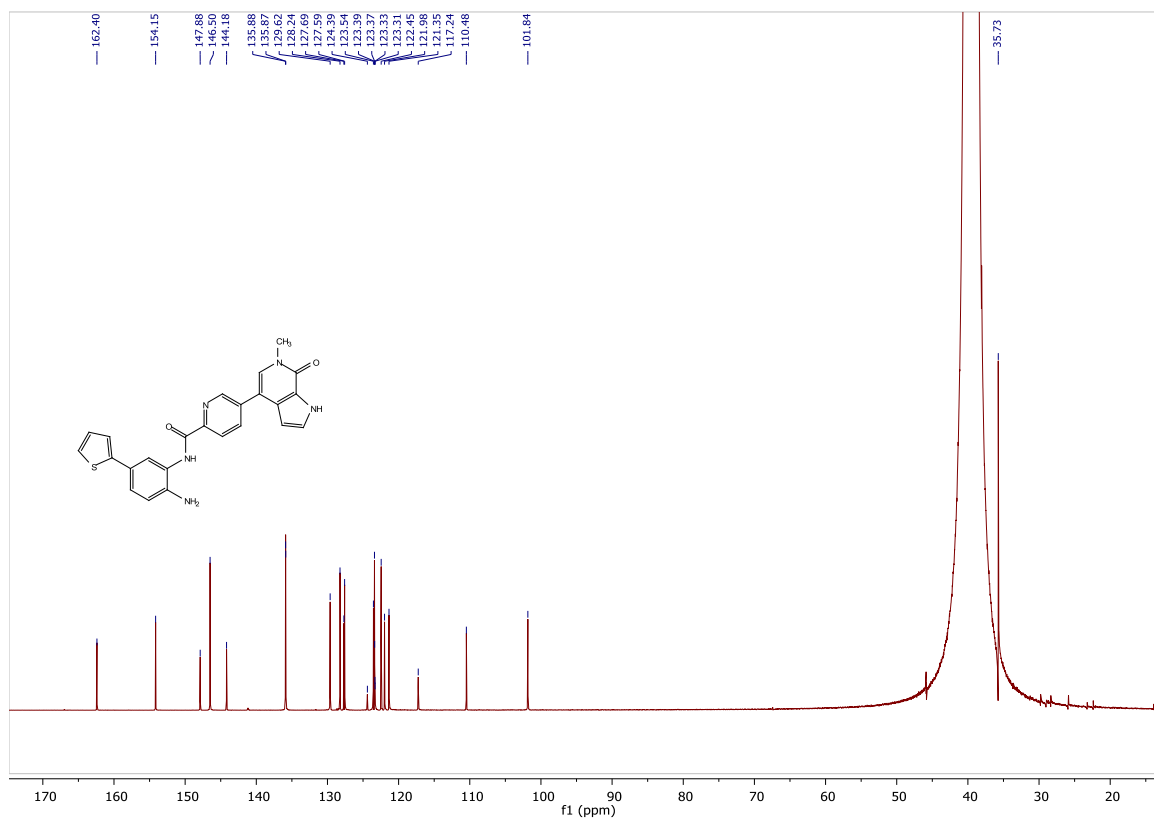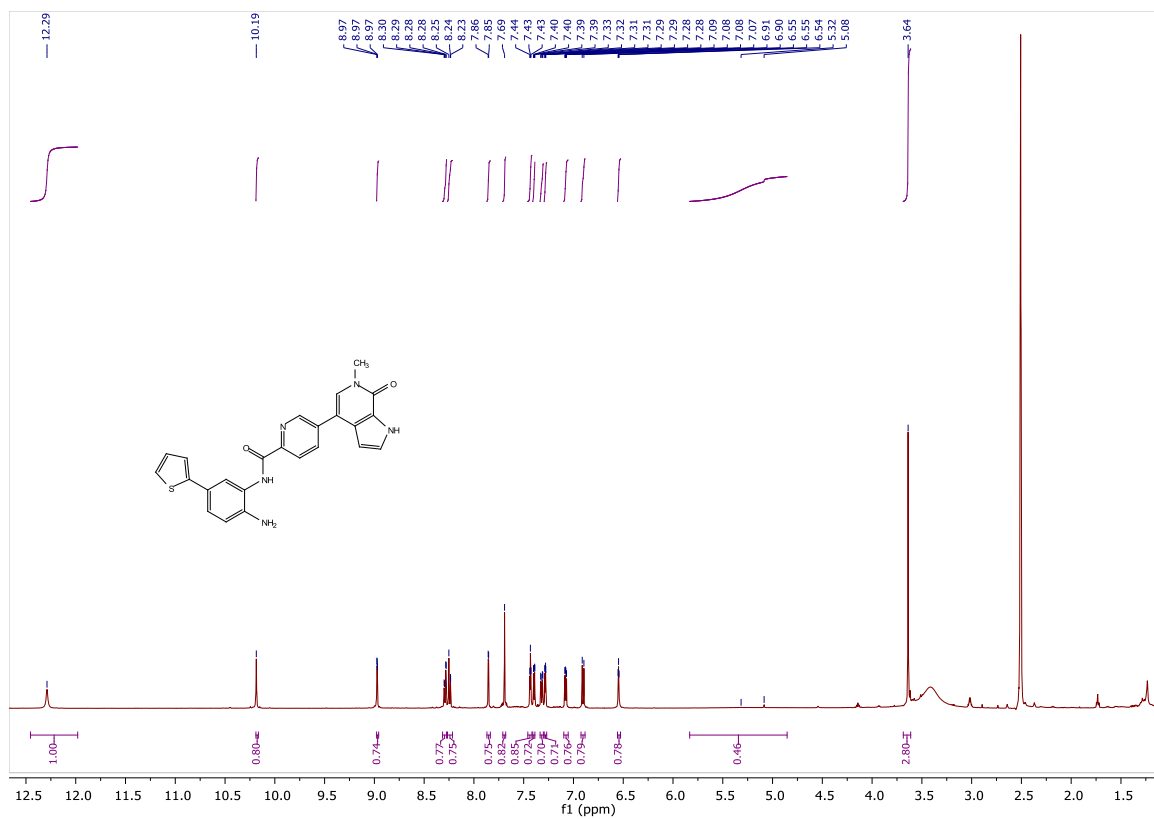
MALDI HRMS Spectrum of **132d** and simulated Spectrum

NB514_B12 #1-6   RT: 0.01-0.23   AV: 6   NL: 3.08E6
T: FTMS + p MALDI Full ms [300.00-600.00]
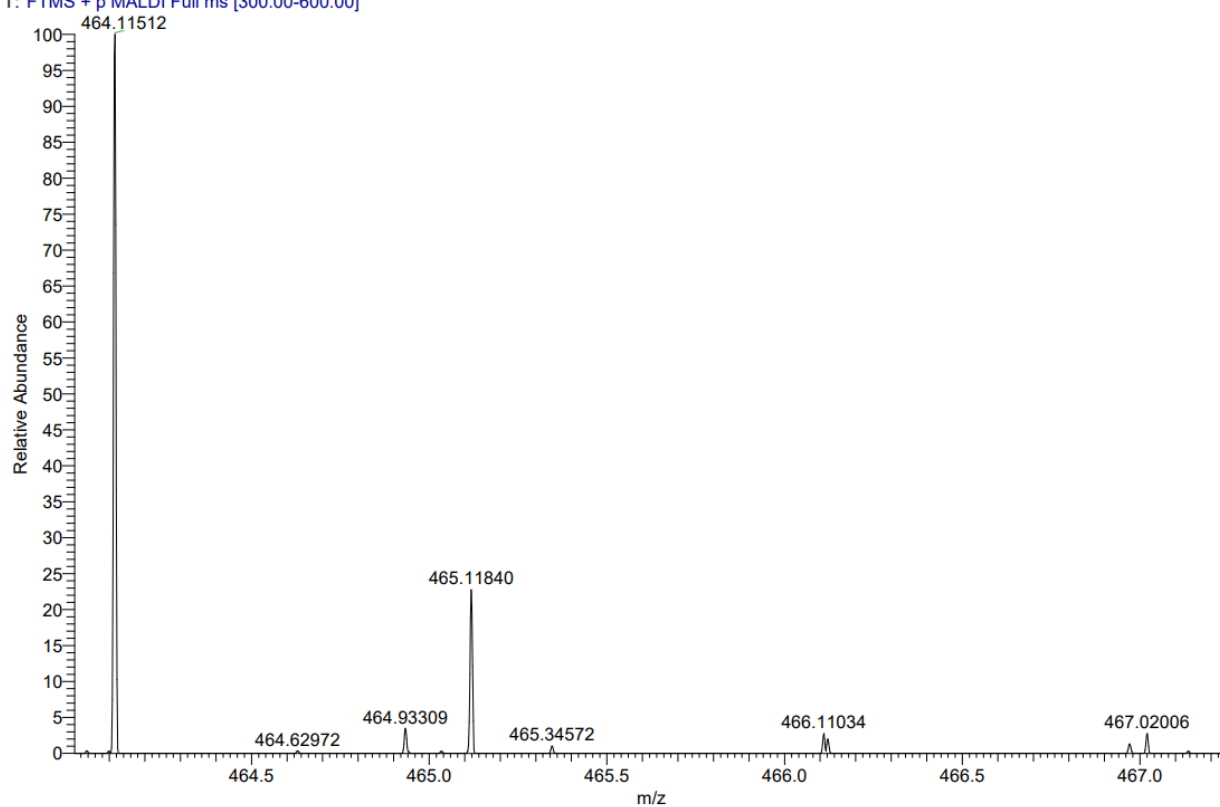
C24H19N5O2S1 +Na: C24 H19 N5 O2 S1 Na1 pa Chrg 1
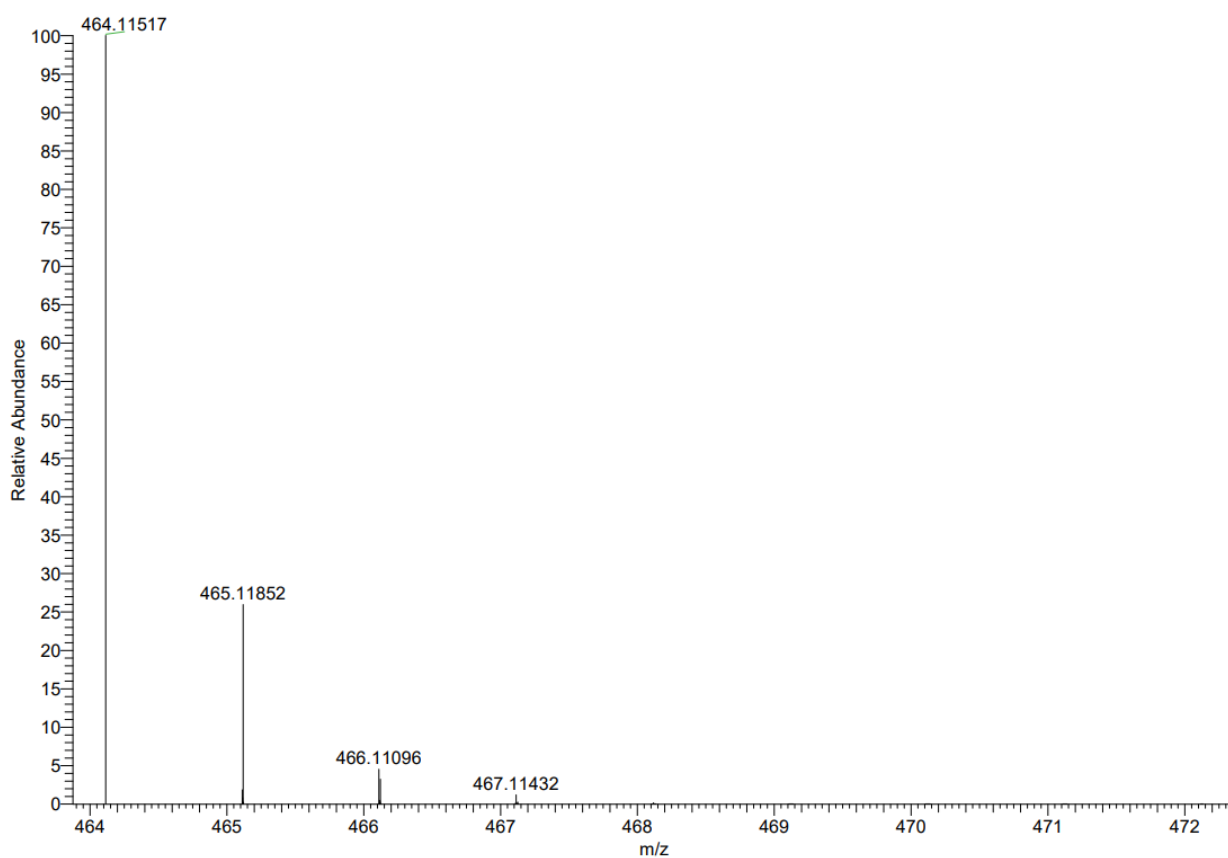
¹H and ¹³C Spectra of **133**
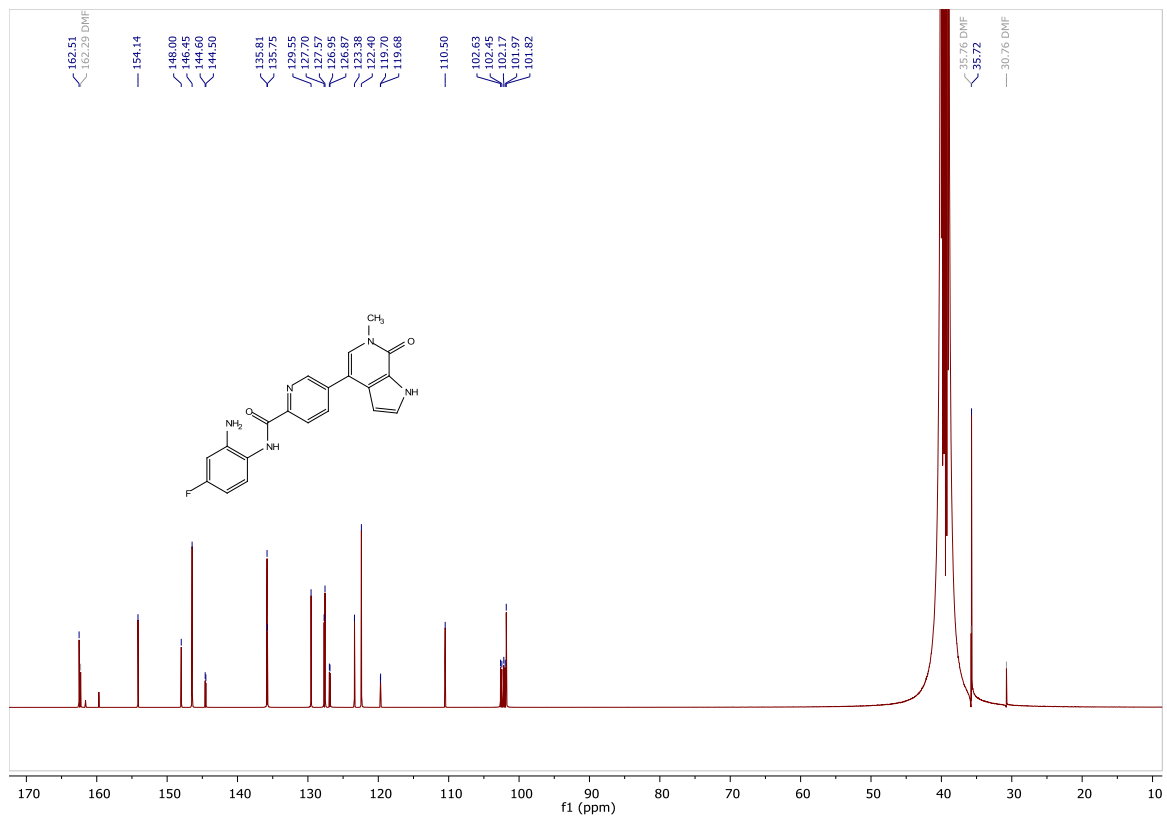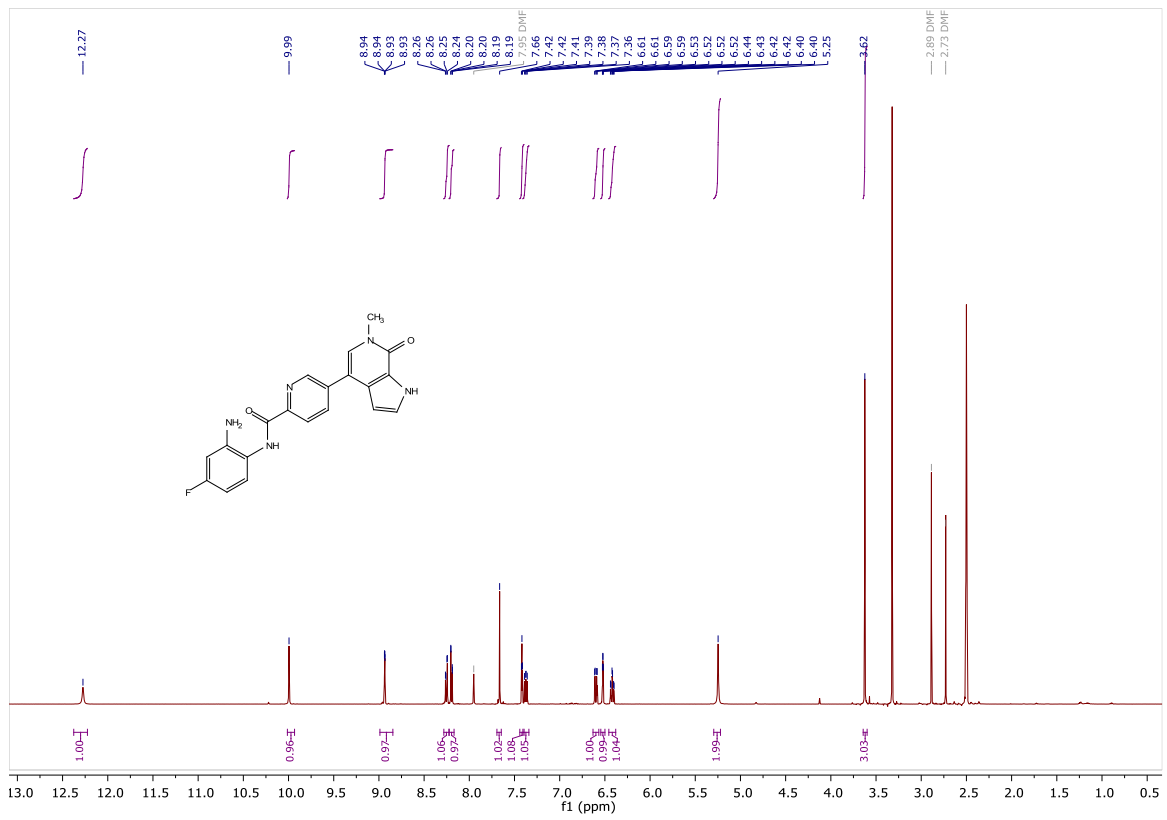
MALDI HRMS Spectrum of **132d** and simulated Spectrum

NB507_B9 #5 RT: 0.18 AV: 1 NL: 1.33E7
T: FTMS + p MALDI Full ms [300.00-600.00]

400.11829

401.12164

402.12512

m/z
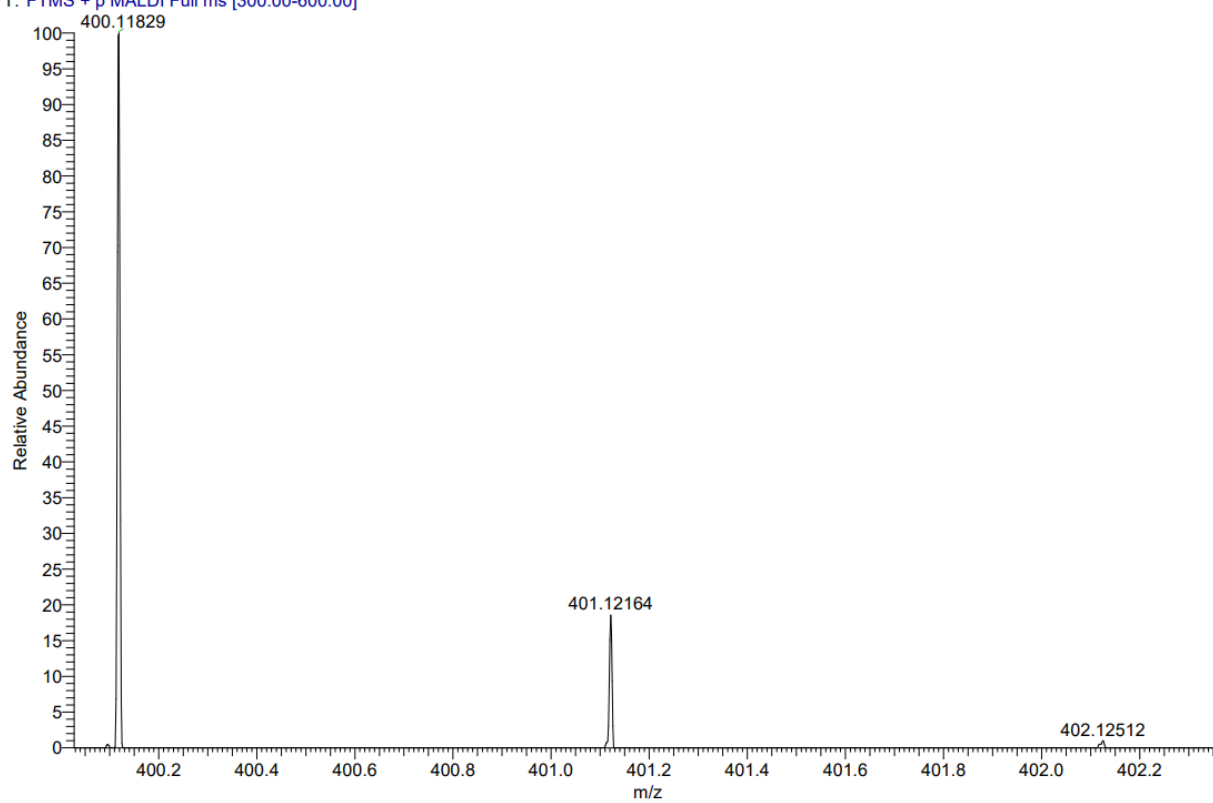
C20H16F1N5O2 +Na: C20 H16 F1 N5 O2 Na1 pa Chrg 1

400.11802

401.12138

402.12473

m/z
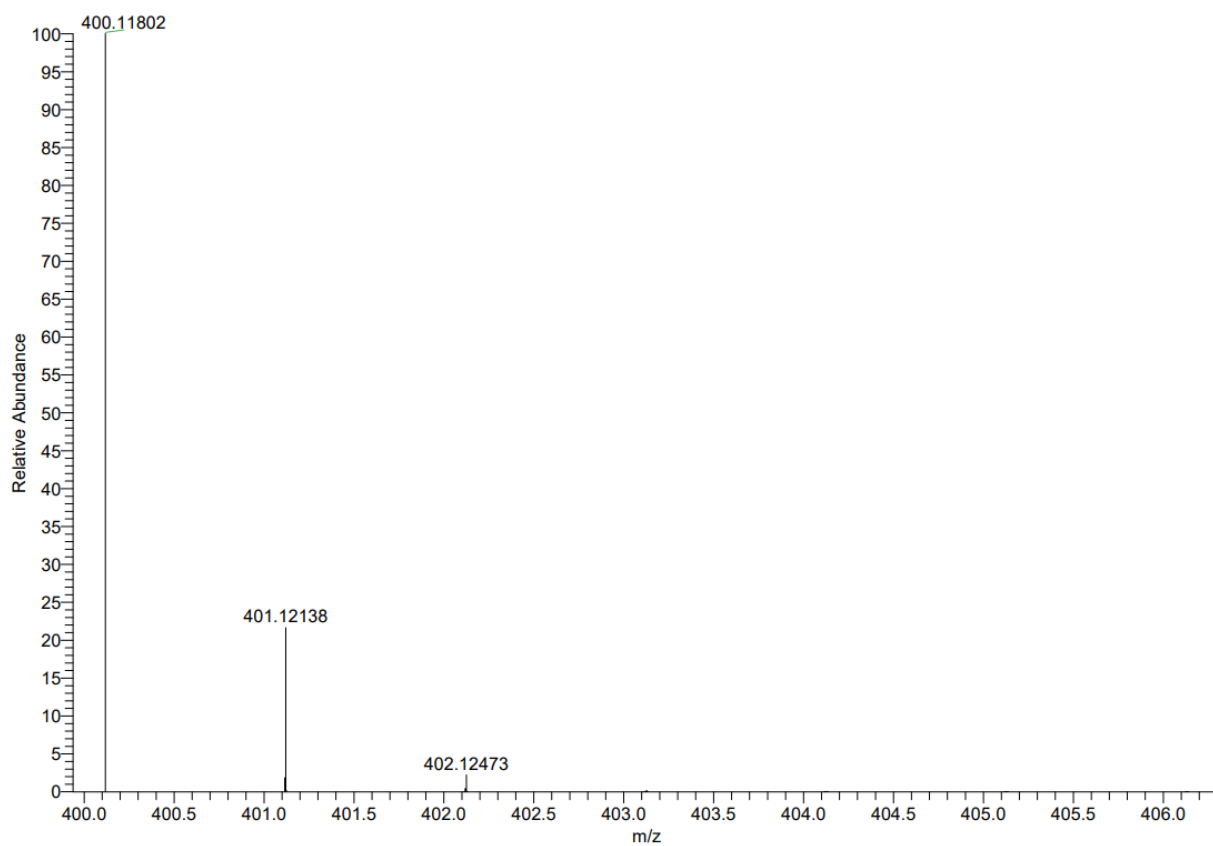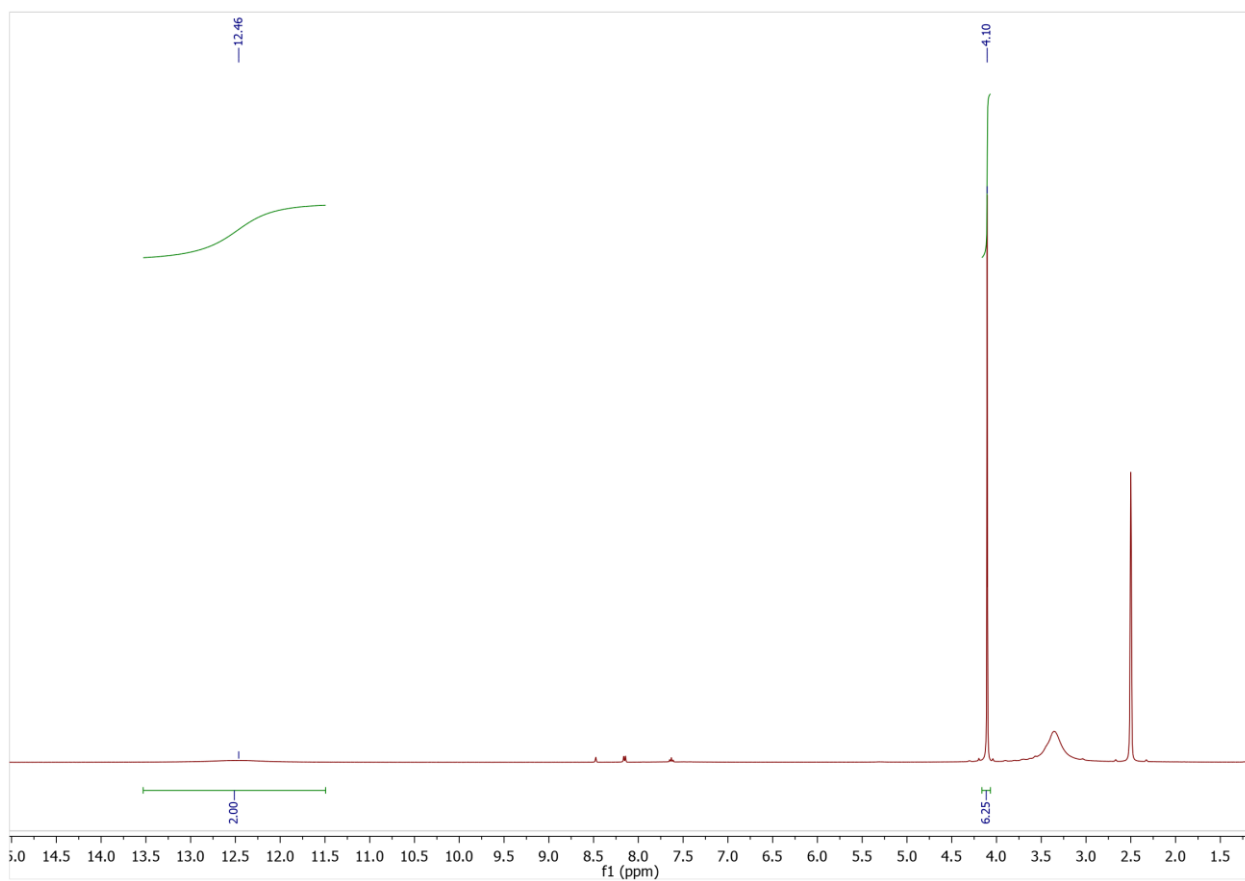
^{1}H Spectrum of **141**

MALDI HRMS Spectrum of **141** and simulated Spectrum

NN06_D10 #1-16 RT: 0.01-0.69   AV: 16   NL: 6.90E4
T: FTMS + p MALDI Full ms [150.00-350.00]
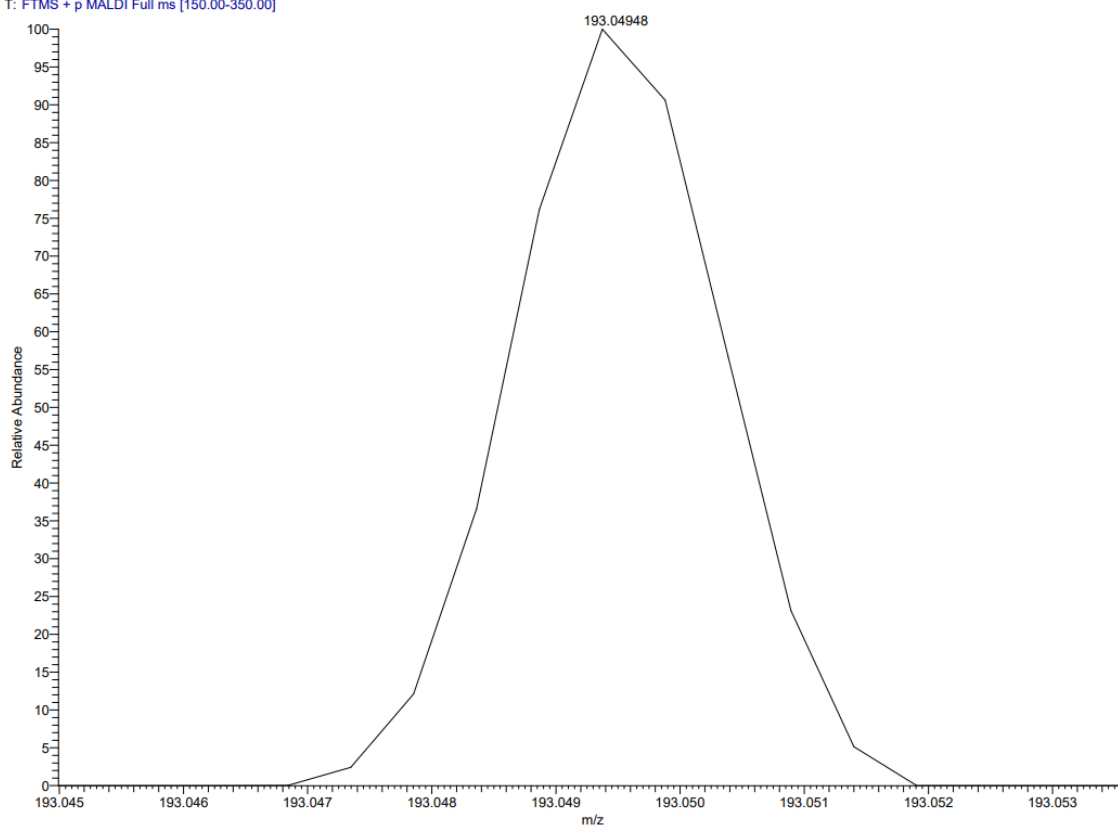
C10H8O4 +H: C10 H9 O4 pa Chrg 1
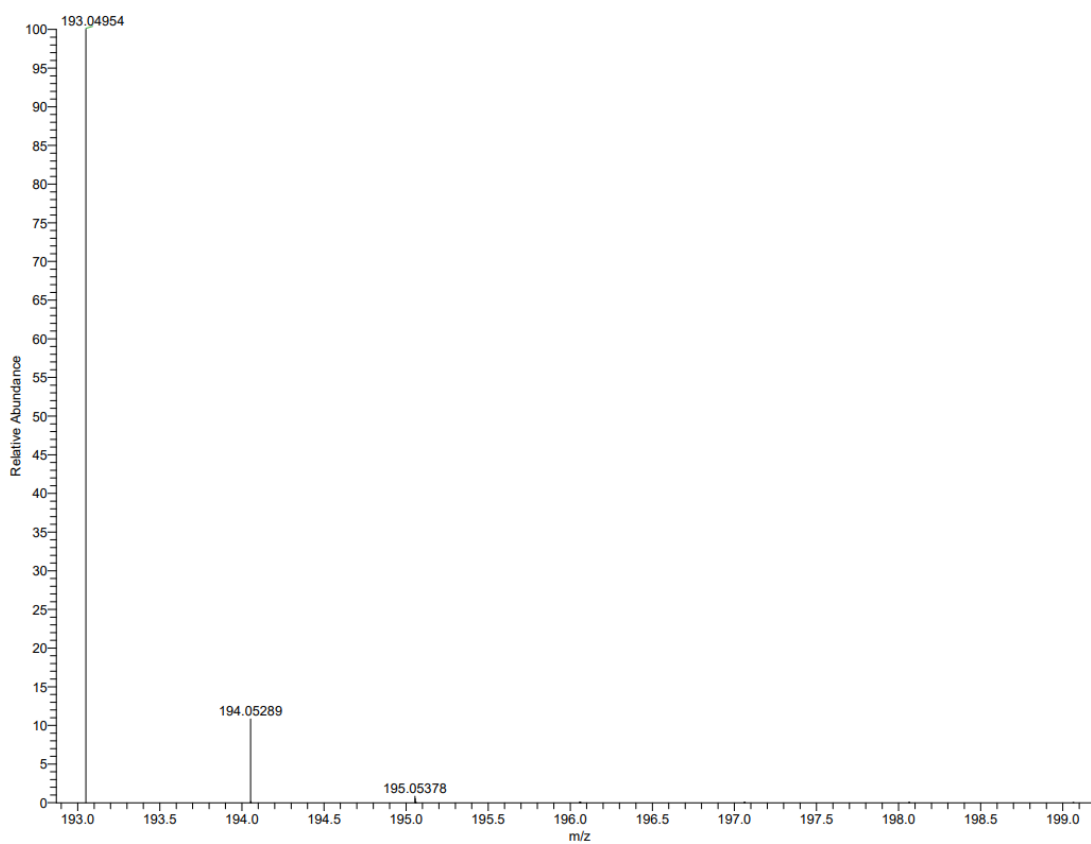
¹H and ¹³C Spectra of **161a**
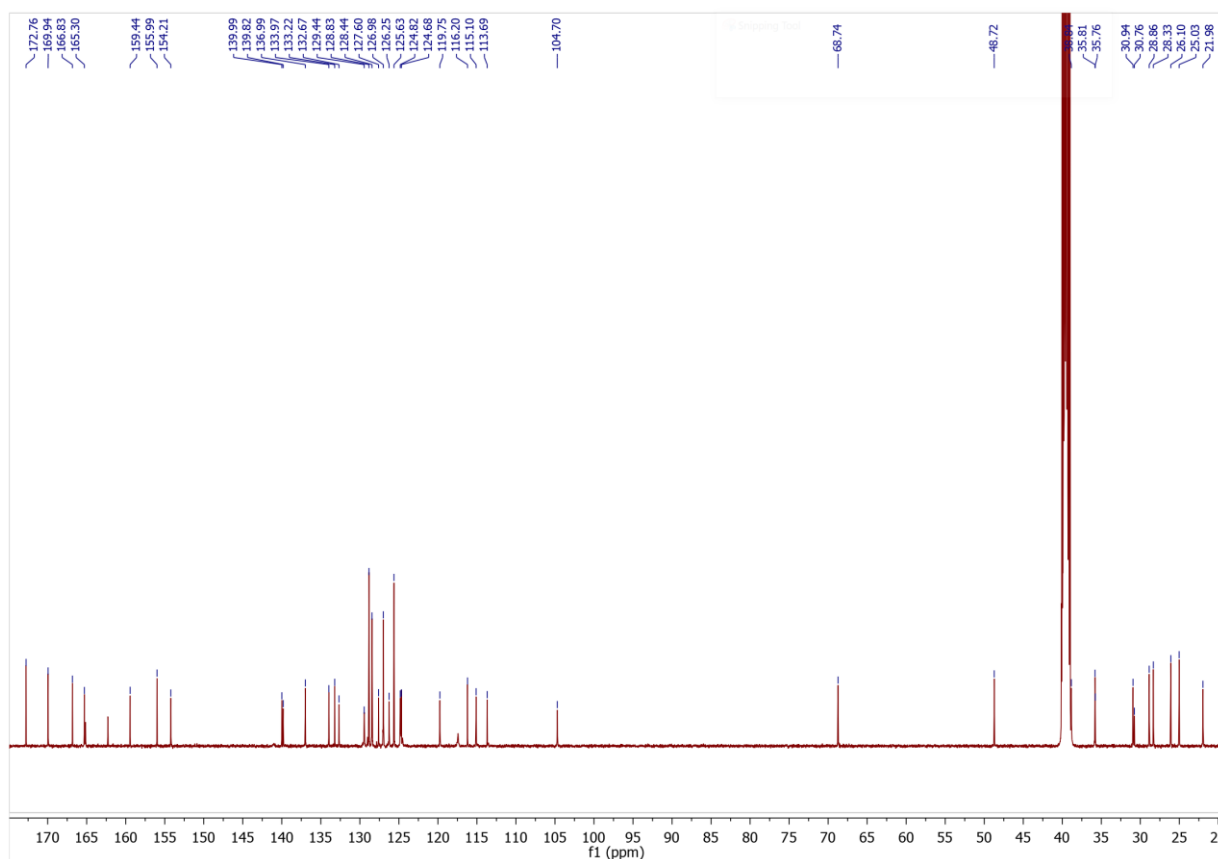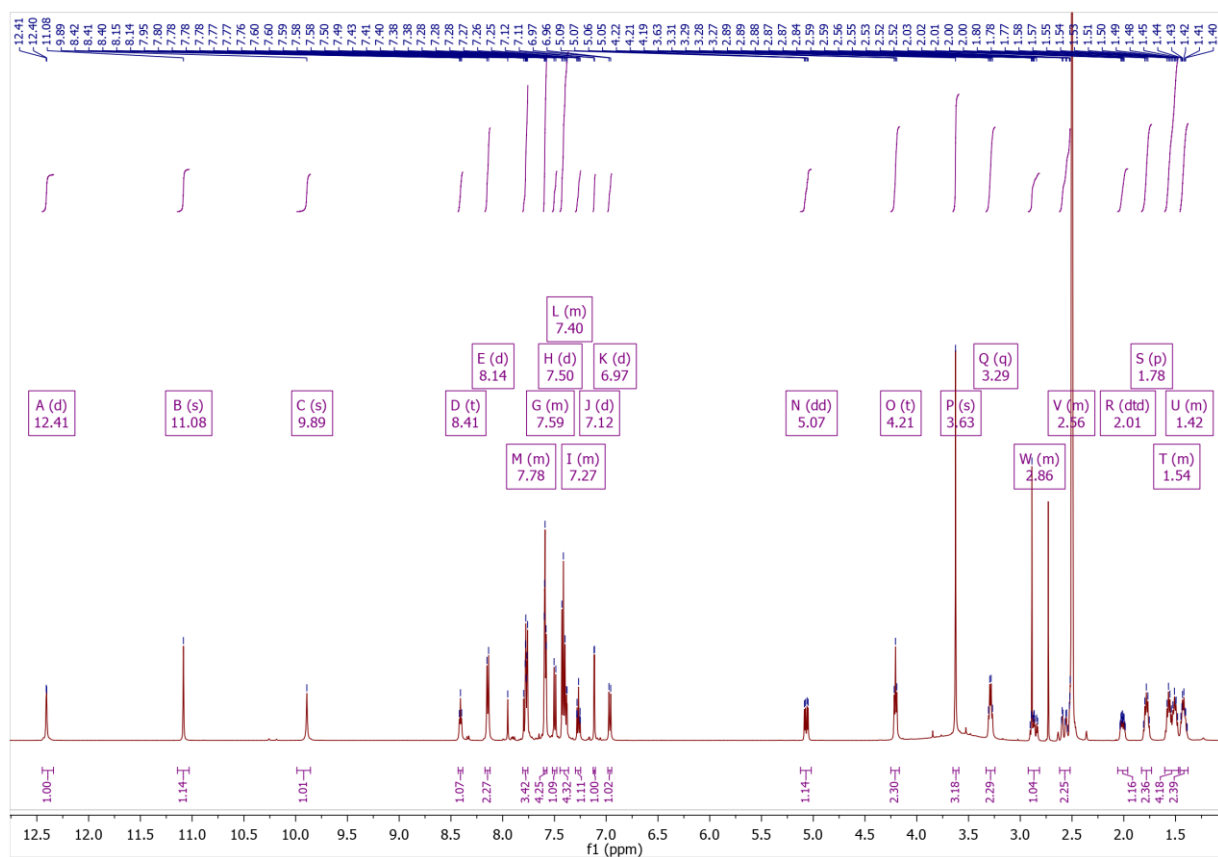
¹H and ¹³C Spectra of **161b**
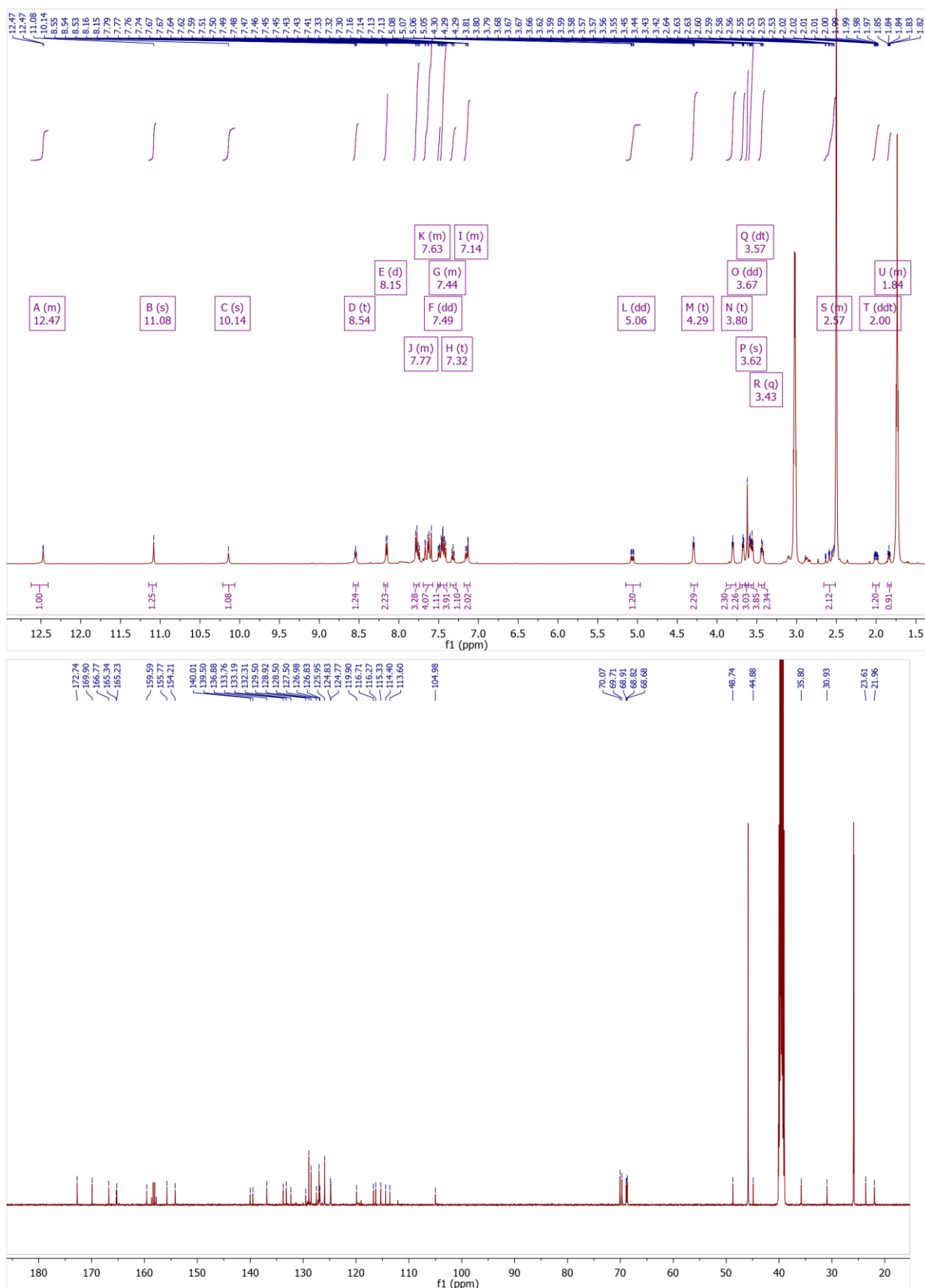
¹H and ¹³C Spectra of **161c**
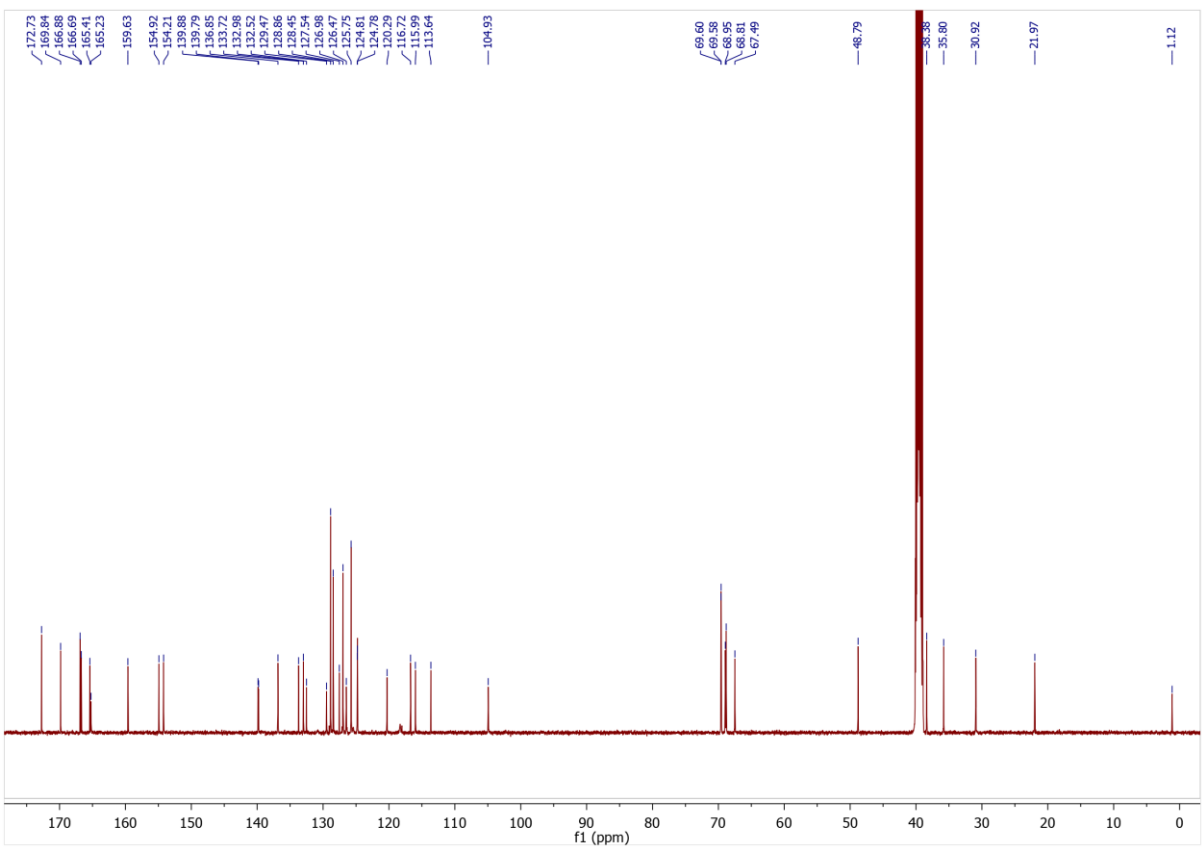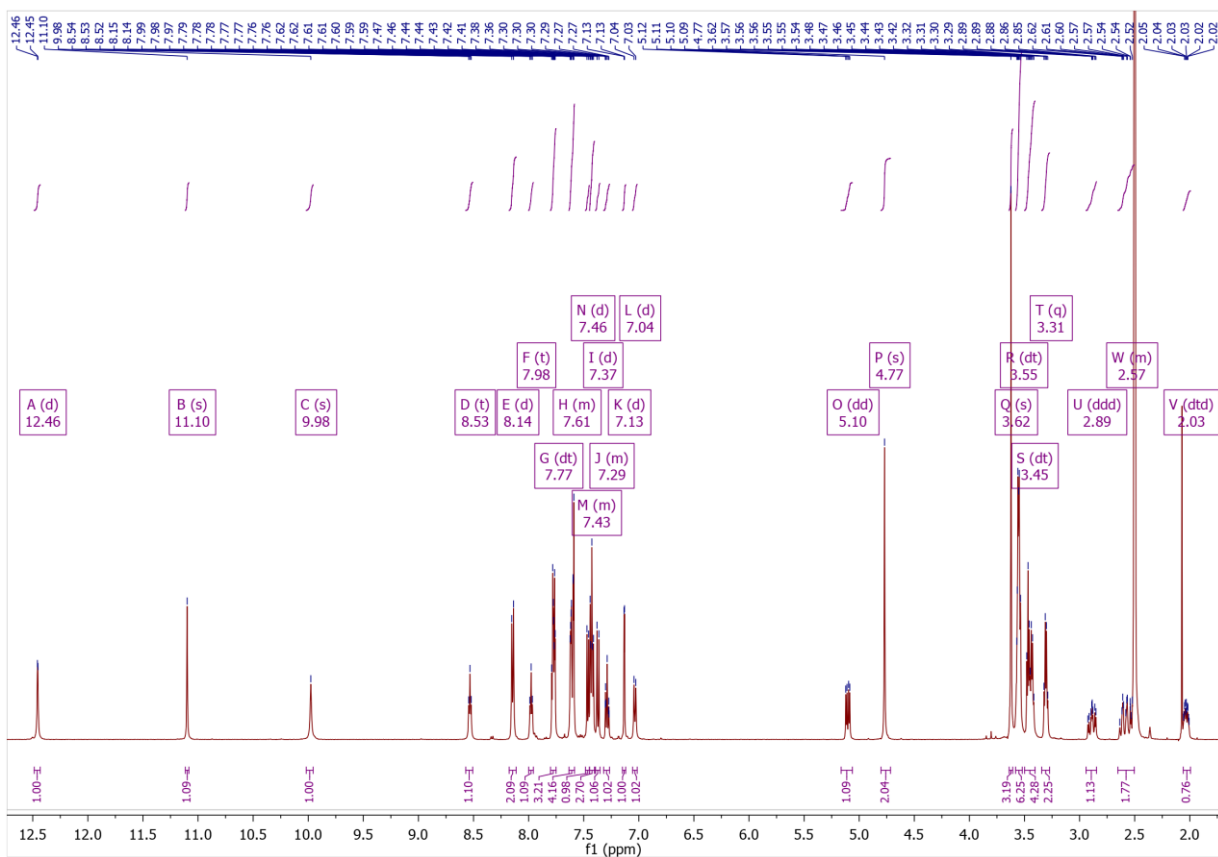
^{1}H and ^{13}C Spectra of **164a**
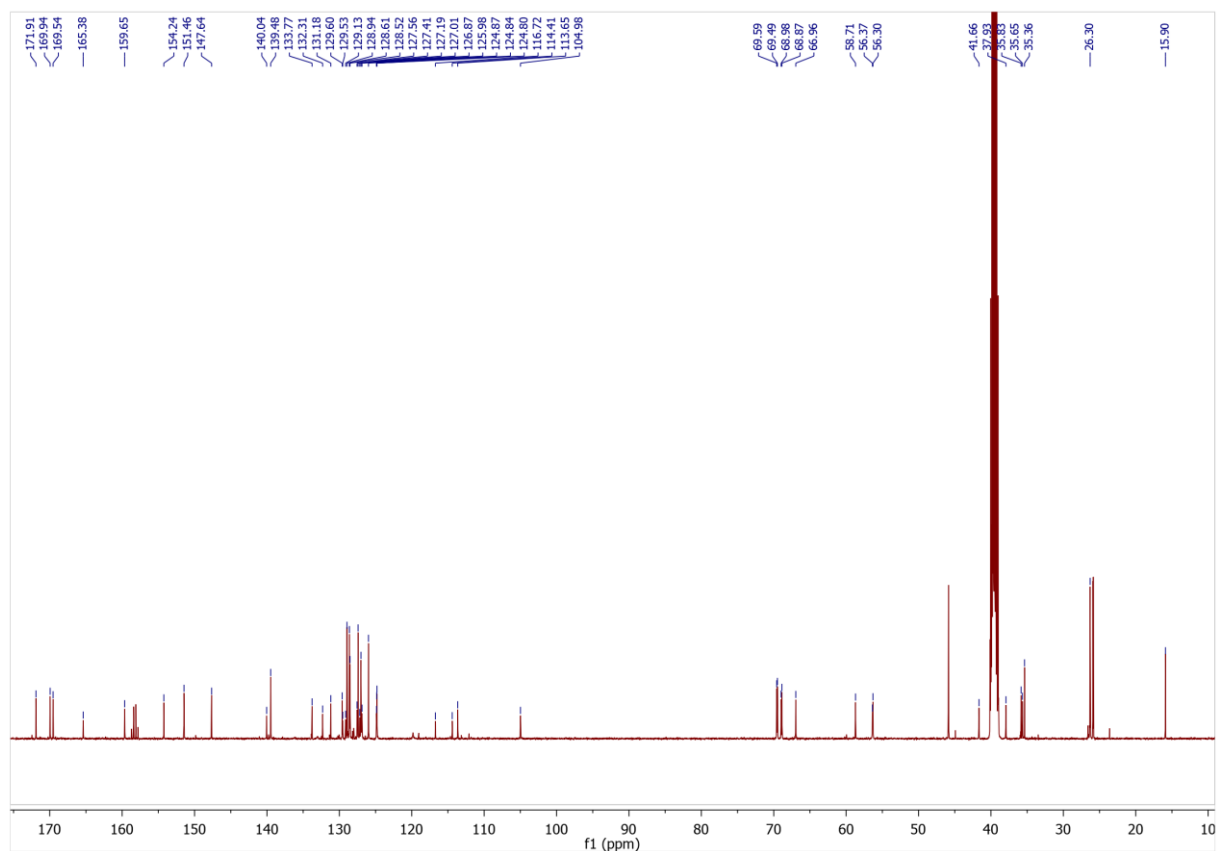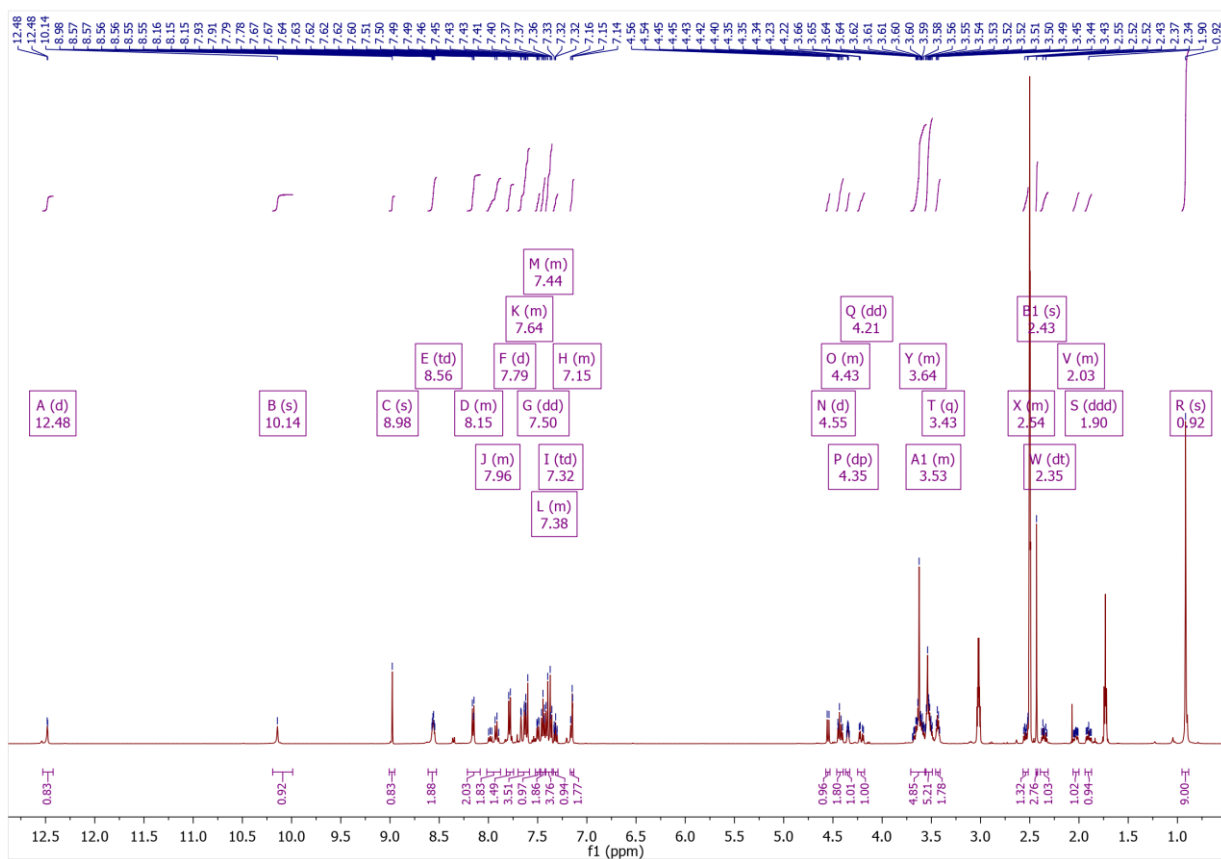
^{1}H and ^{13}C Spectra of **164b**
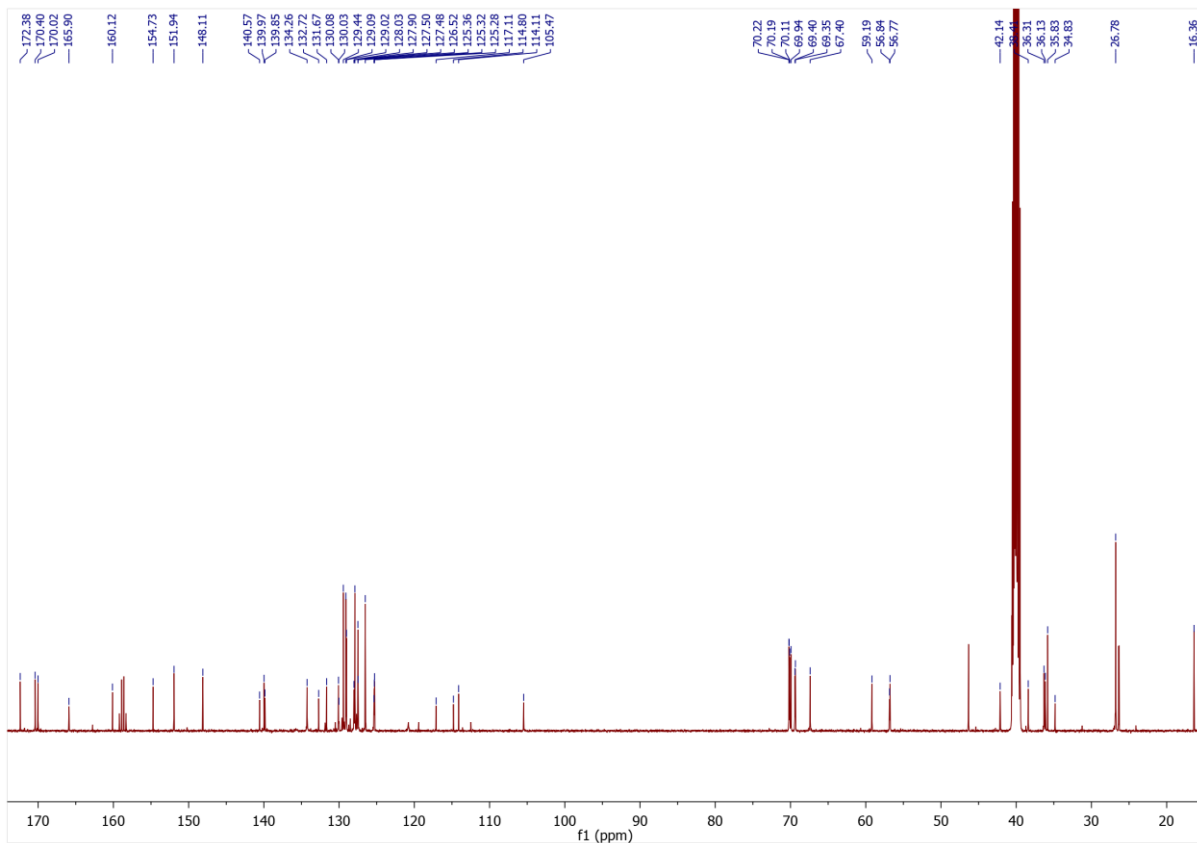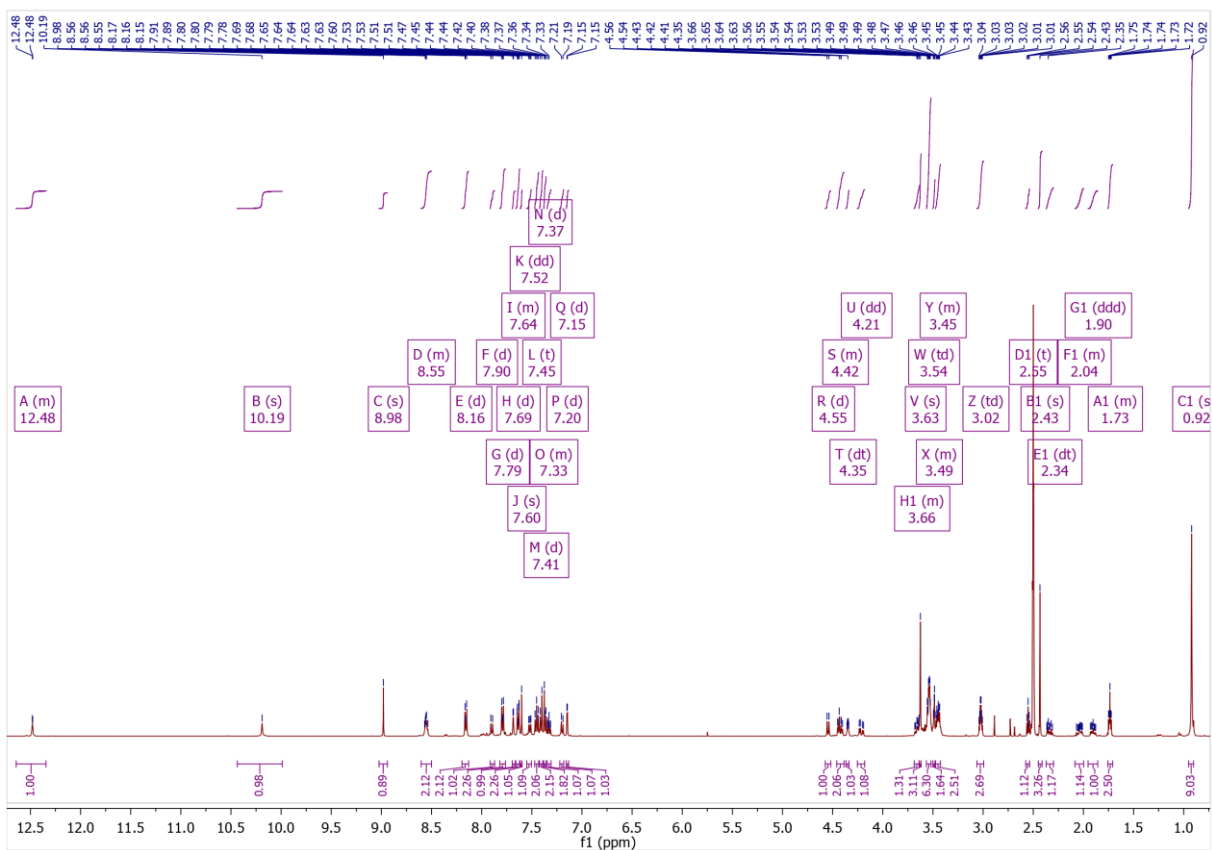
^{1}H and ^{13}C Spectra of **164c**
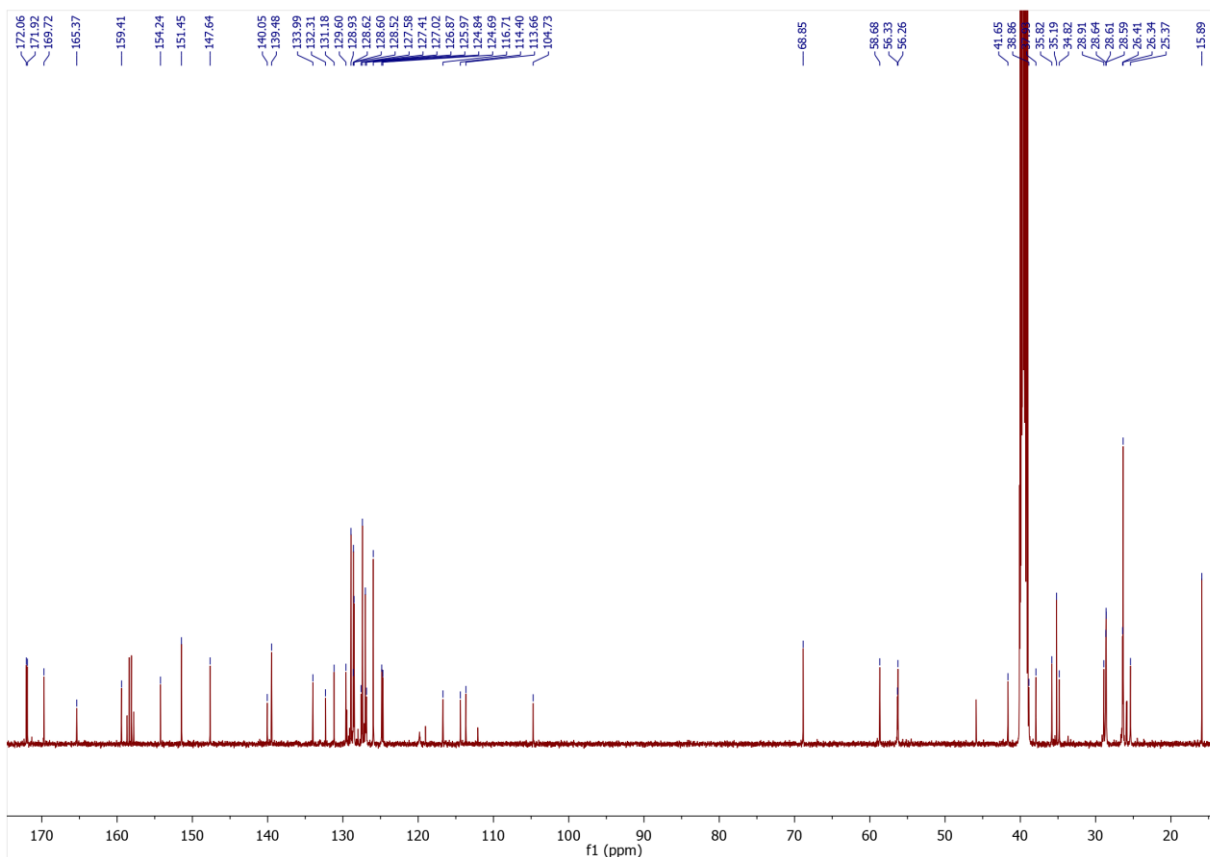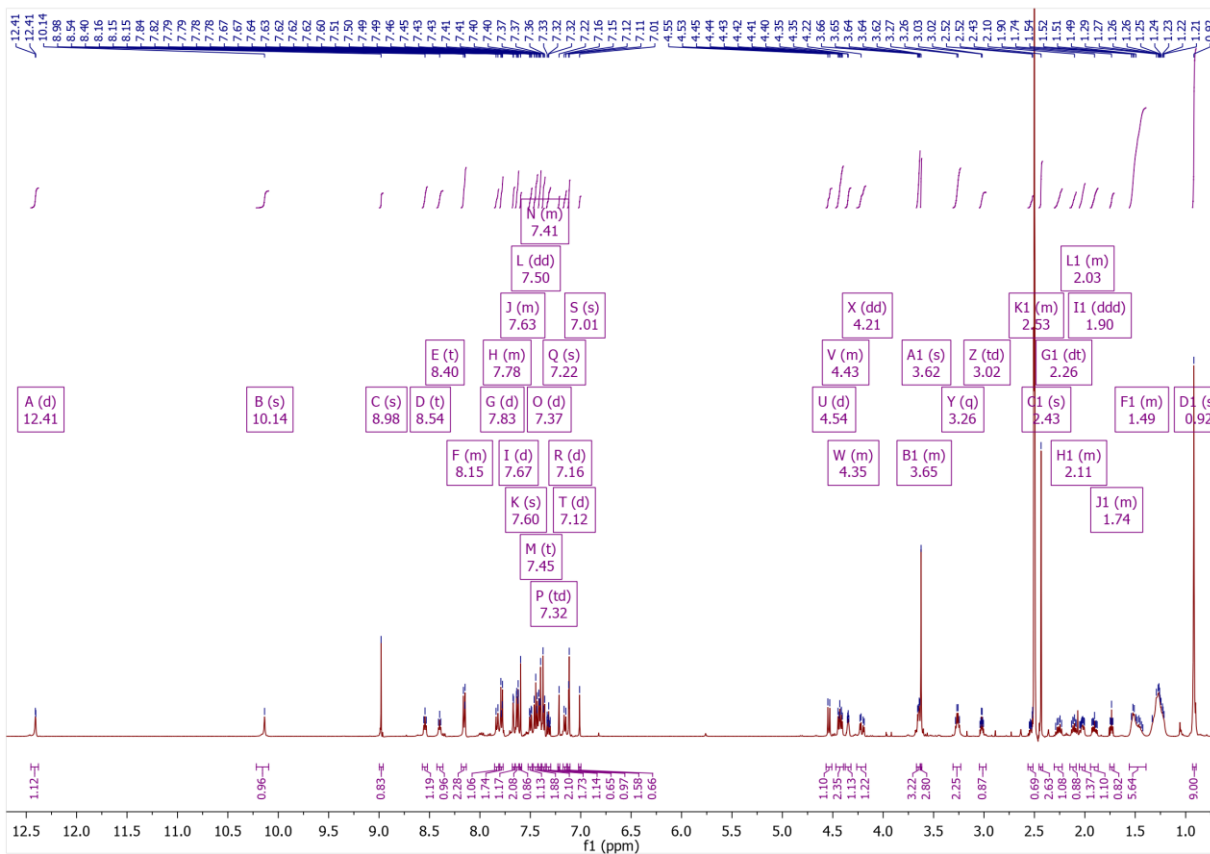
^{1}H NMR Spectra of **173** and **174**
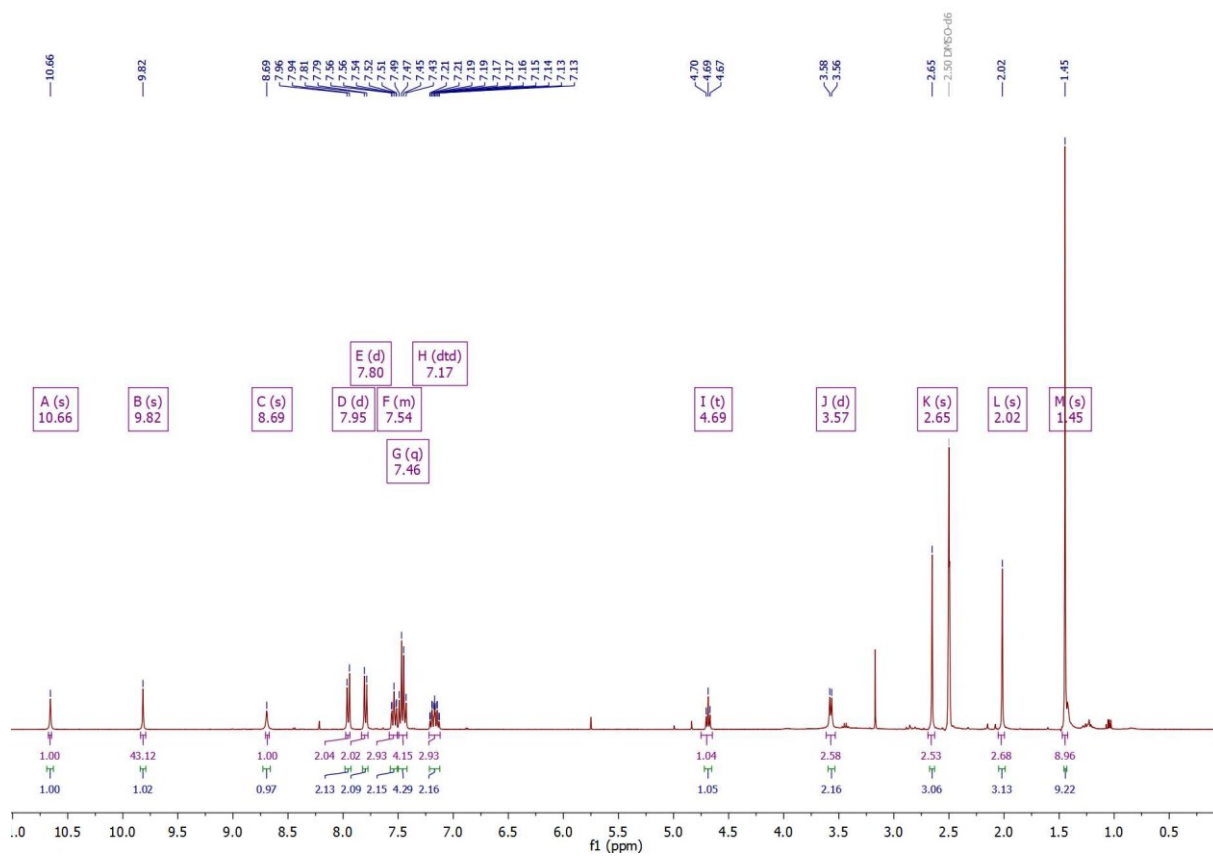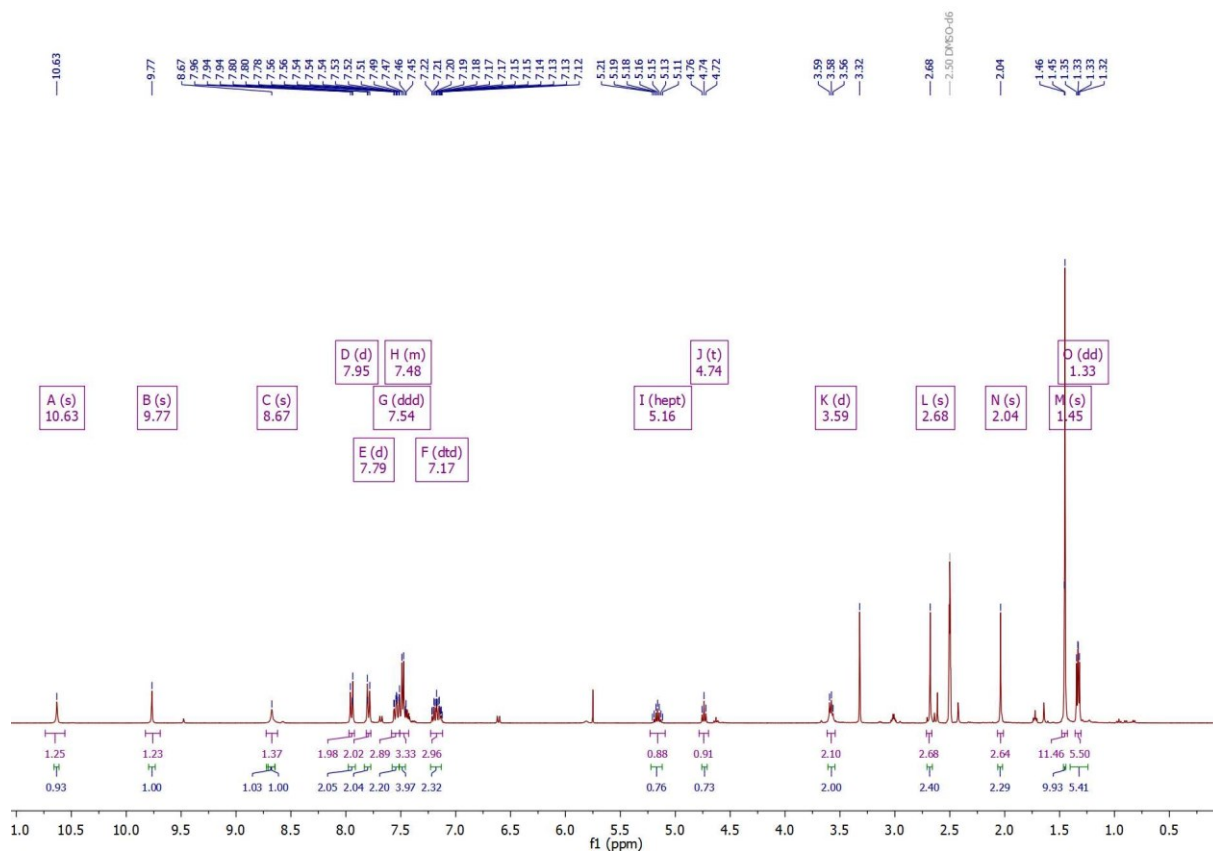
¹H and ¹³C Spectra of **175a**
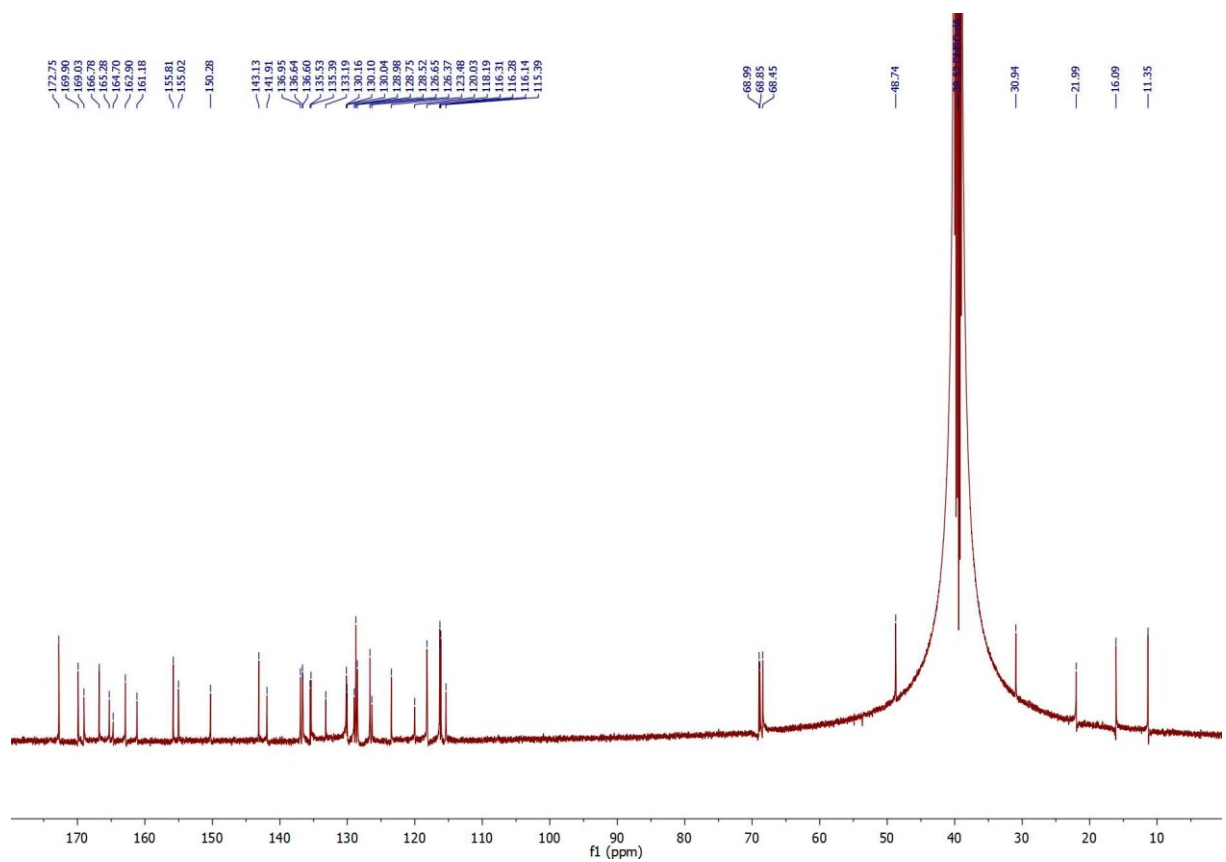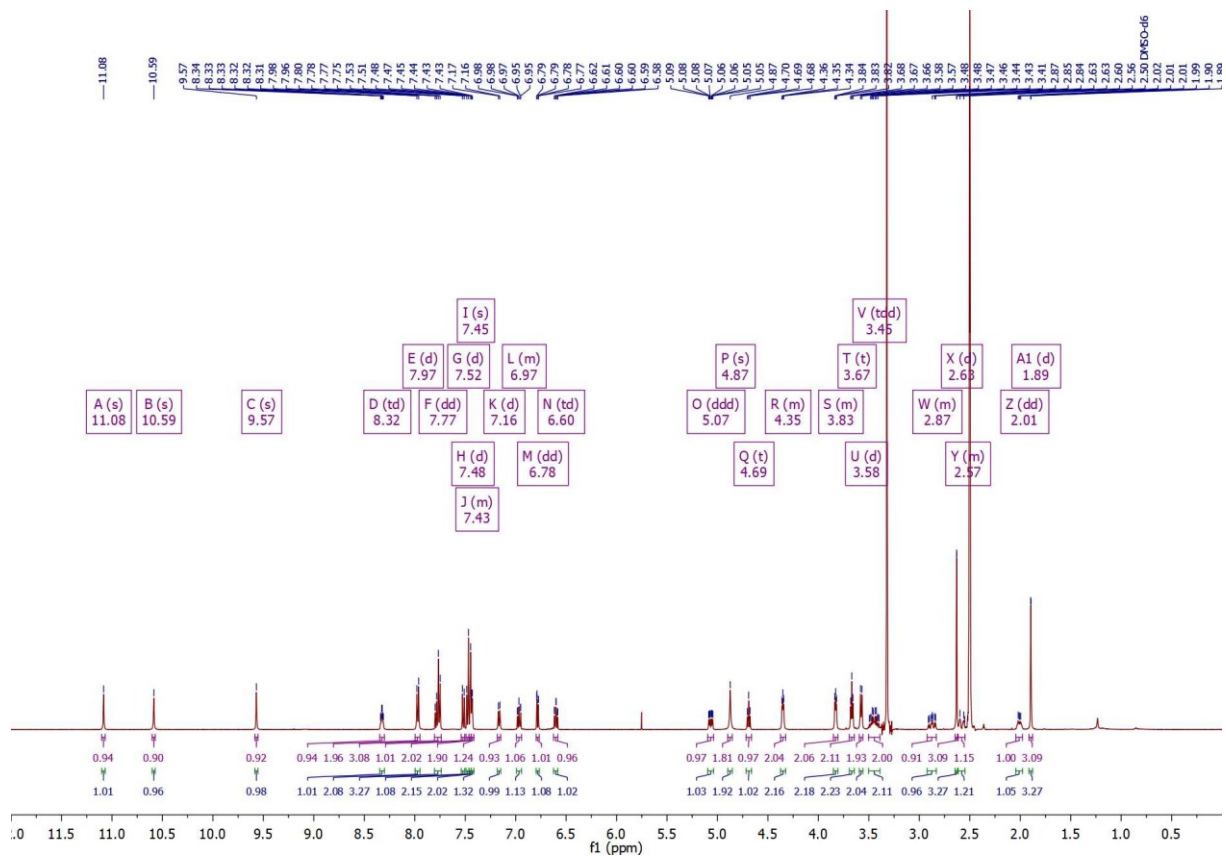
MALDI HRMS Spectrum of **175a** and simulated Spectrum

^{1}H and ^{13}C Spectra of **175b**

MALDI HRMS Spectrum of **175b** and simulated Spectrum

C5TH47CTTNT0OT6ST +Na: C5T H47 CTT N10 O16 ST NaT pa...

^{1}H and ^{13}C Spectra of **175c**

MALDI HRMS Spectrum of **175c** and simulated Spectrum

^{1}H and ^{13}C Spectra of **175d**

MALDI HRMS Spectrum of **175d** and simulated Spectrum

^{1}H and ^{13}C Spectra of **175e**

MALDI HRMS Spectrum of **175e** and simulated Spectrum

NBSA14_C12 #1-6 RT: 0.00-0.16 AV: 6 NL: 3.27E7
F: FTMS + p MALDI Full ms [800.00-1400.00]
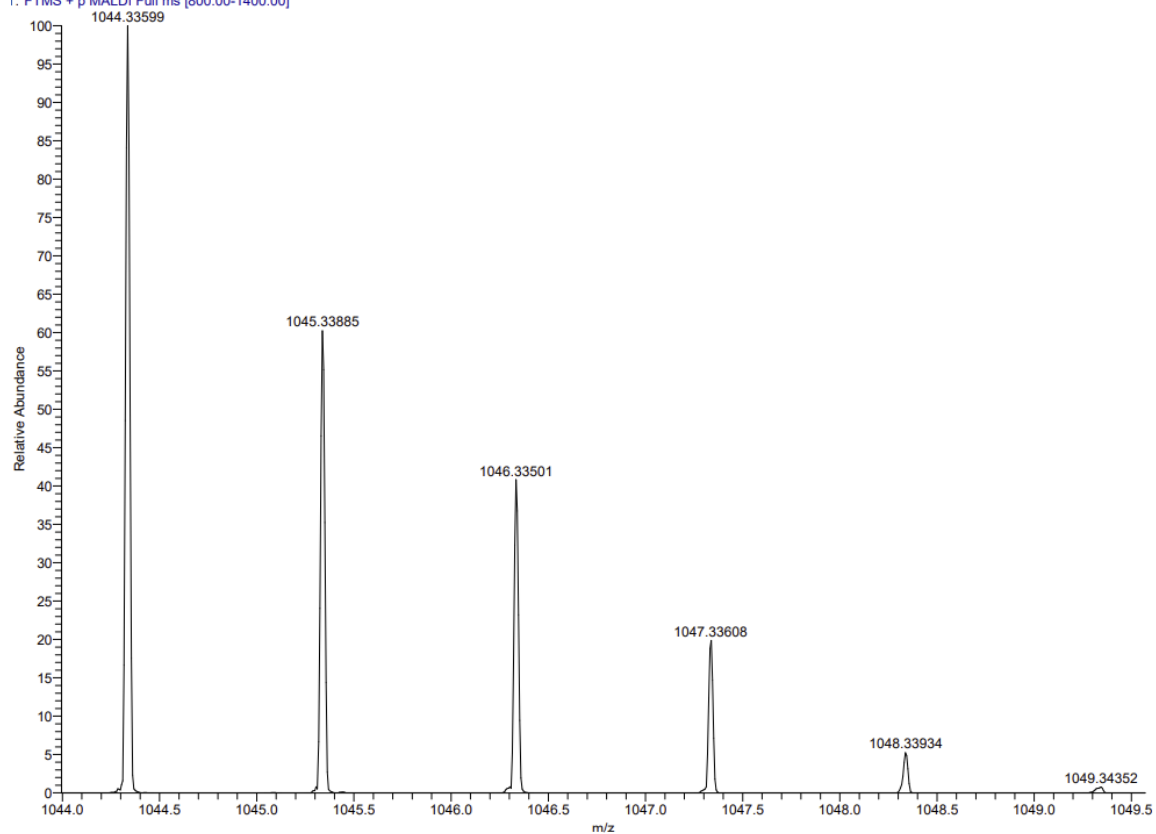
C53H52Cl1N11O7S1 +Na: C53 H52 Cl1 N11 O7 S1 Na1 pa C...
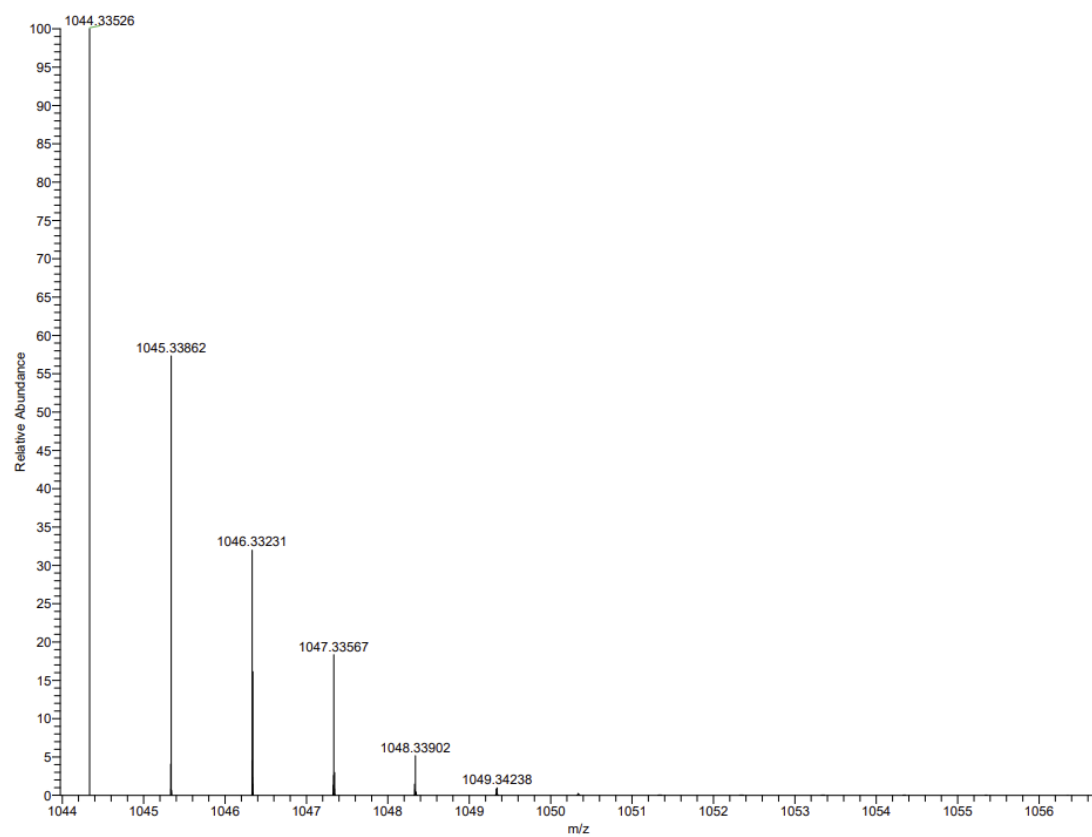
^{1}H and ^{13}C Spectra of **175f**
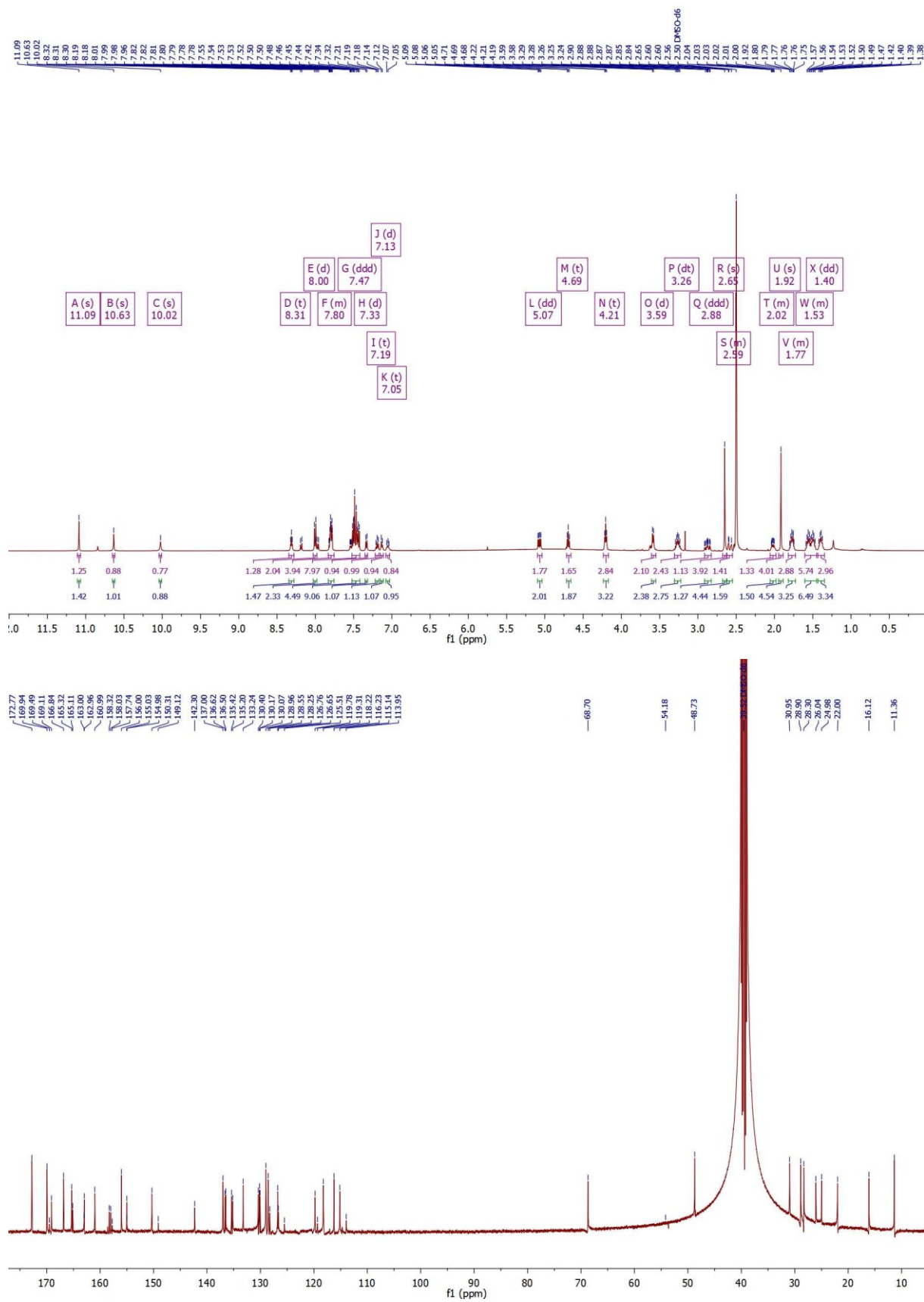
MALDI HRMS Spectrum of **175f** and simulated Spectrum
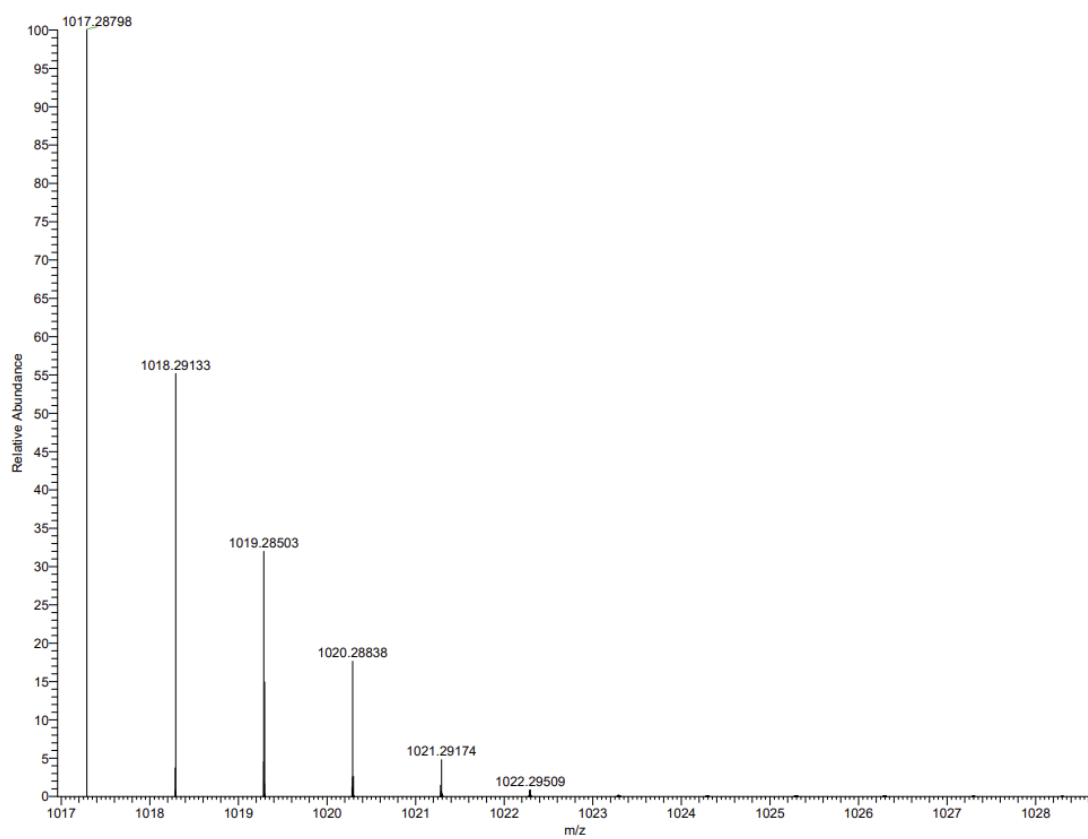
^{1}H and ^{13}C Spectra of **177a**
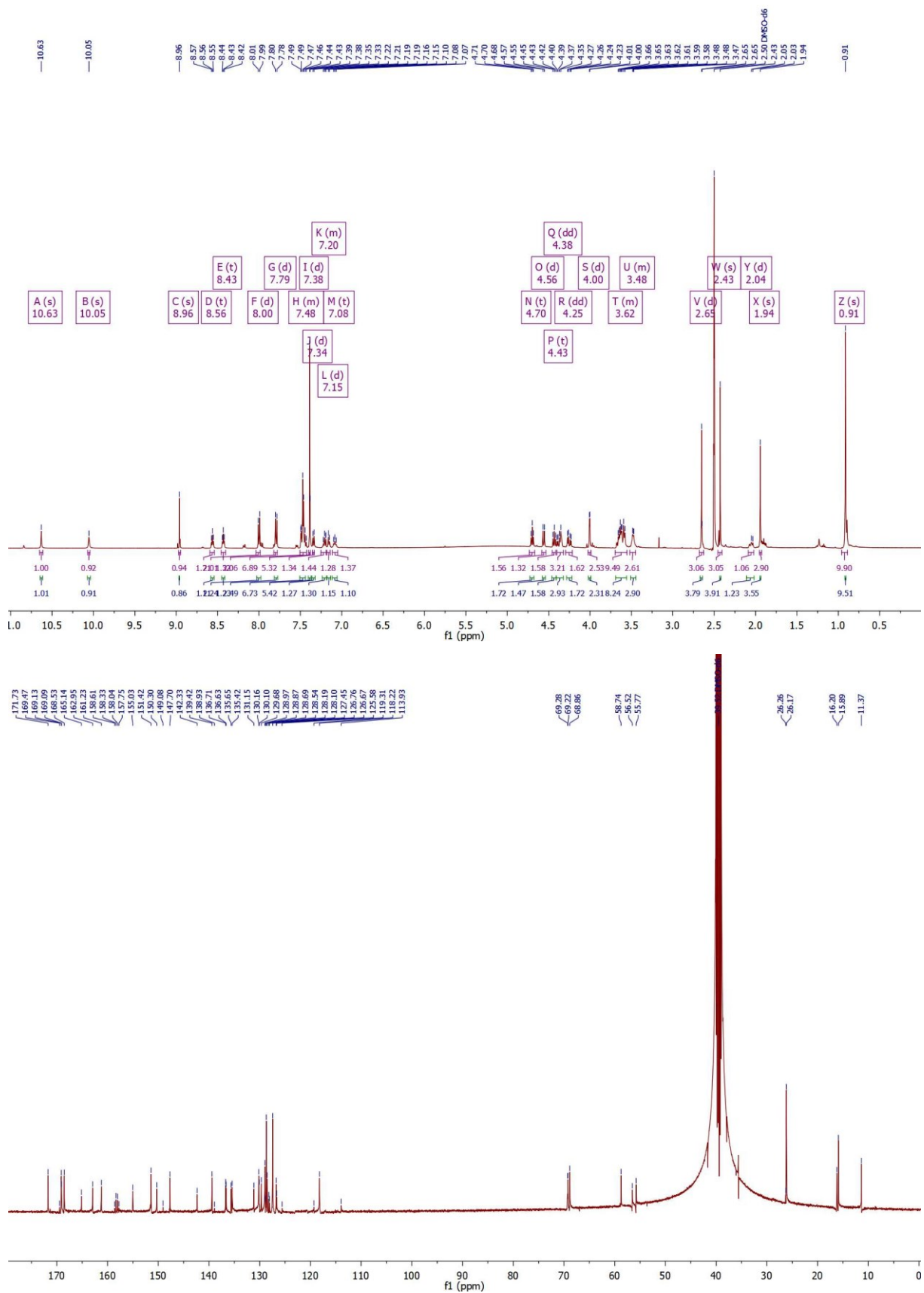
MALDI HRMS Spectrum of **177a** and simulated Spectrum
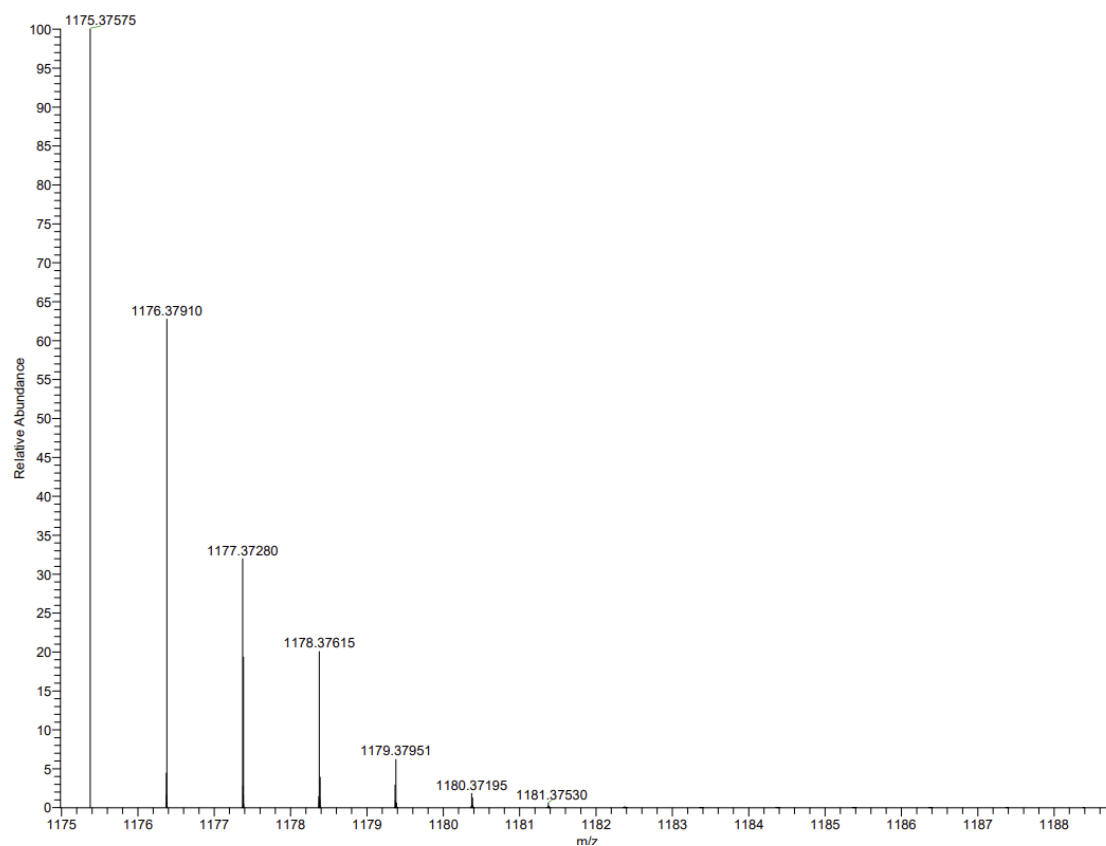
^{1}H and ^{13}C Spectra of **177b**
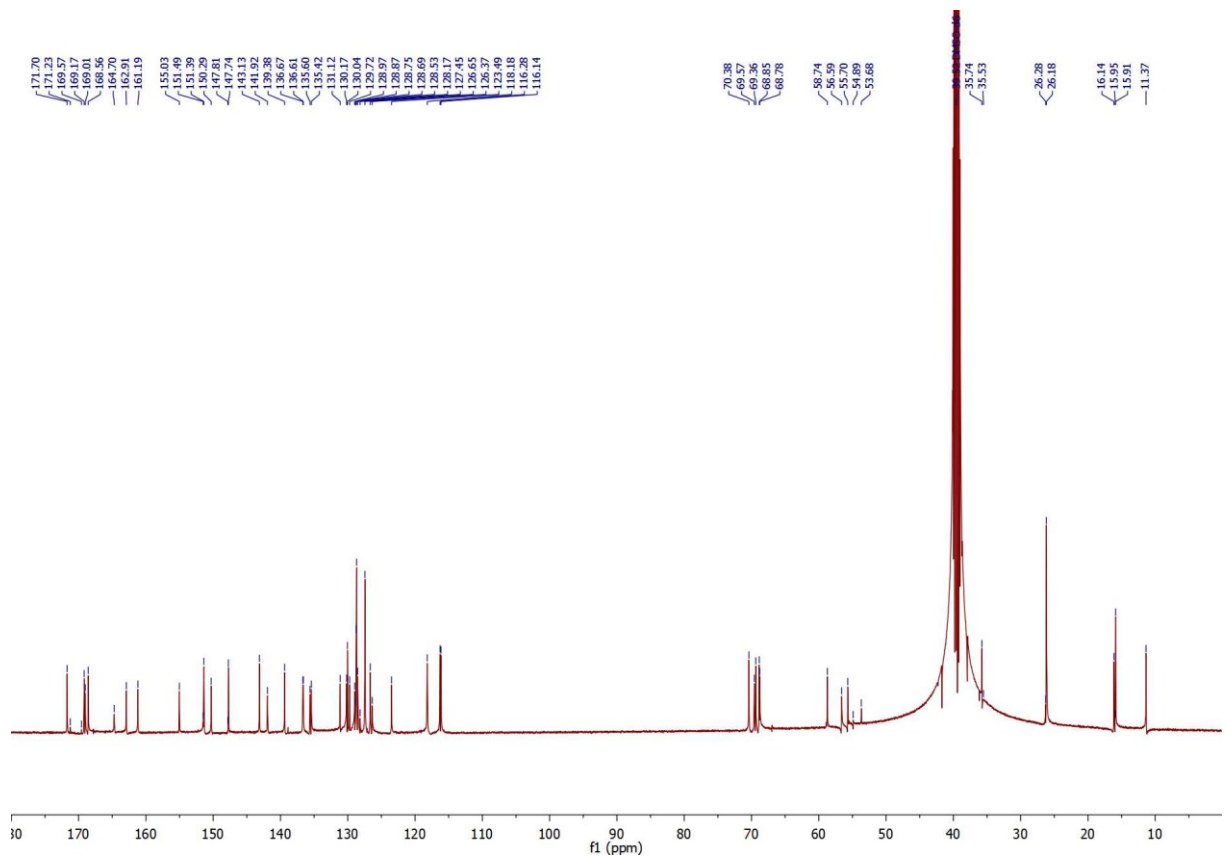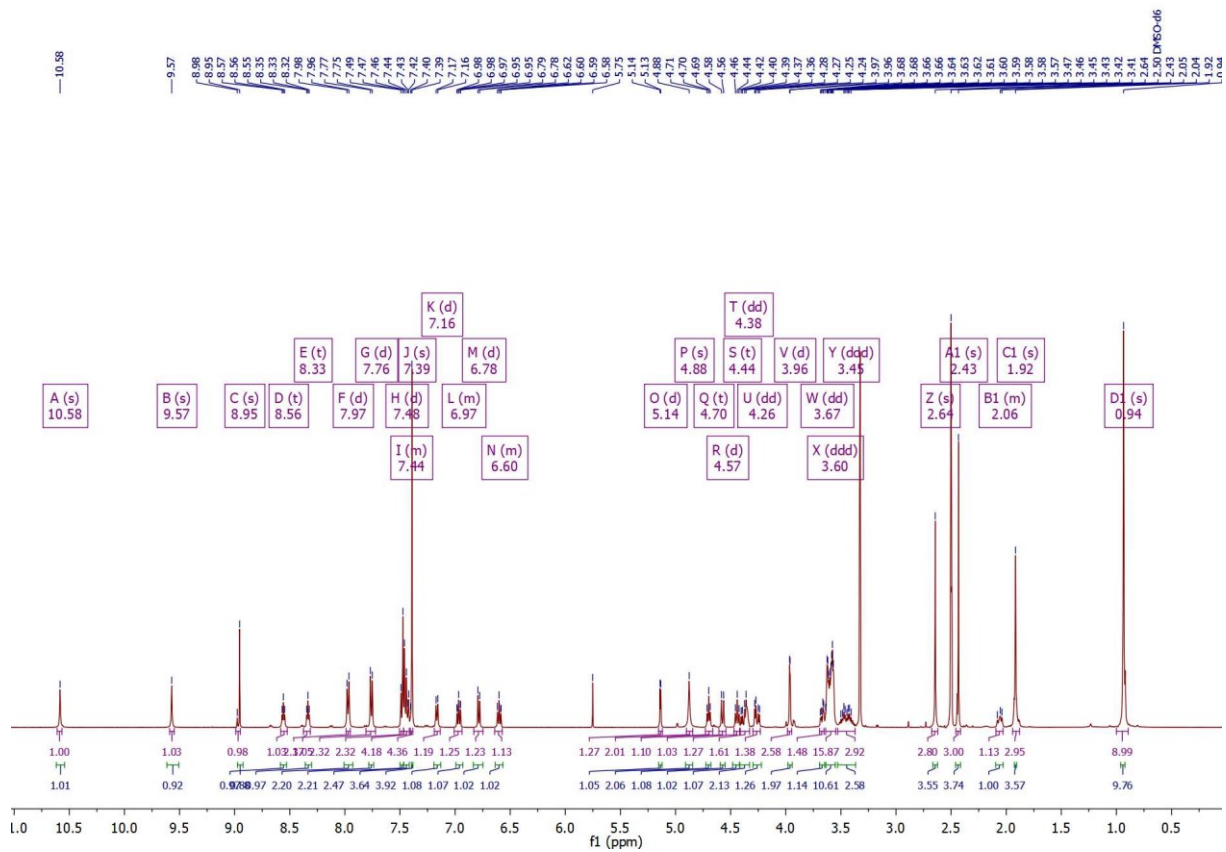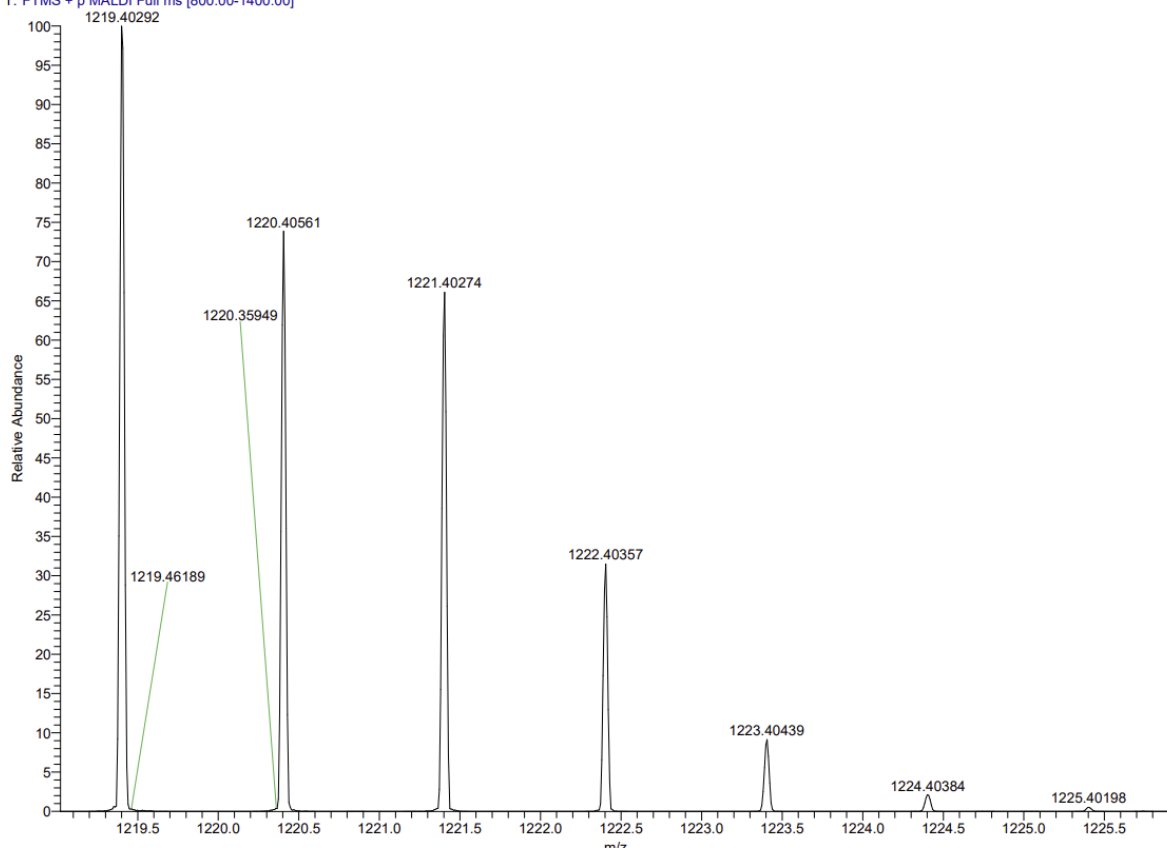
MALDI HRMS Spectrum of **177b** and simulated Spectrum
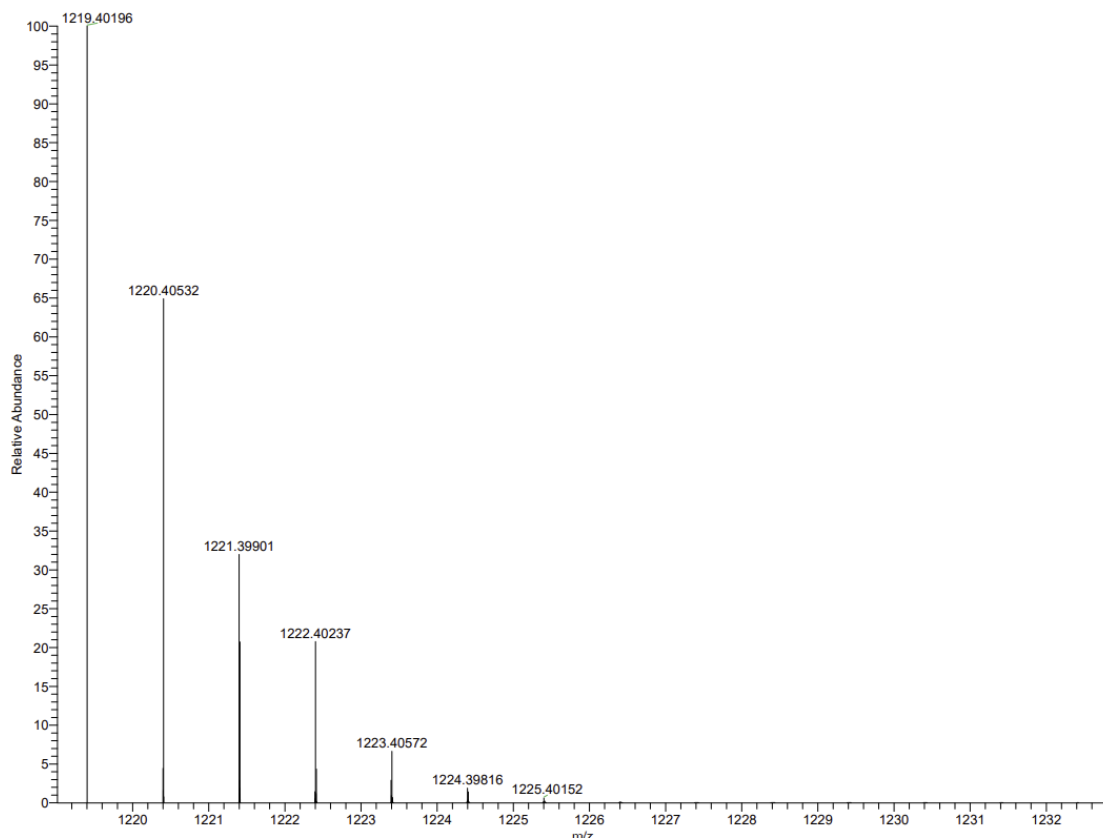
^{1}H and ^{13}C Spectra of **177c**
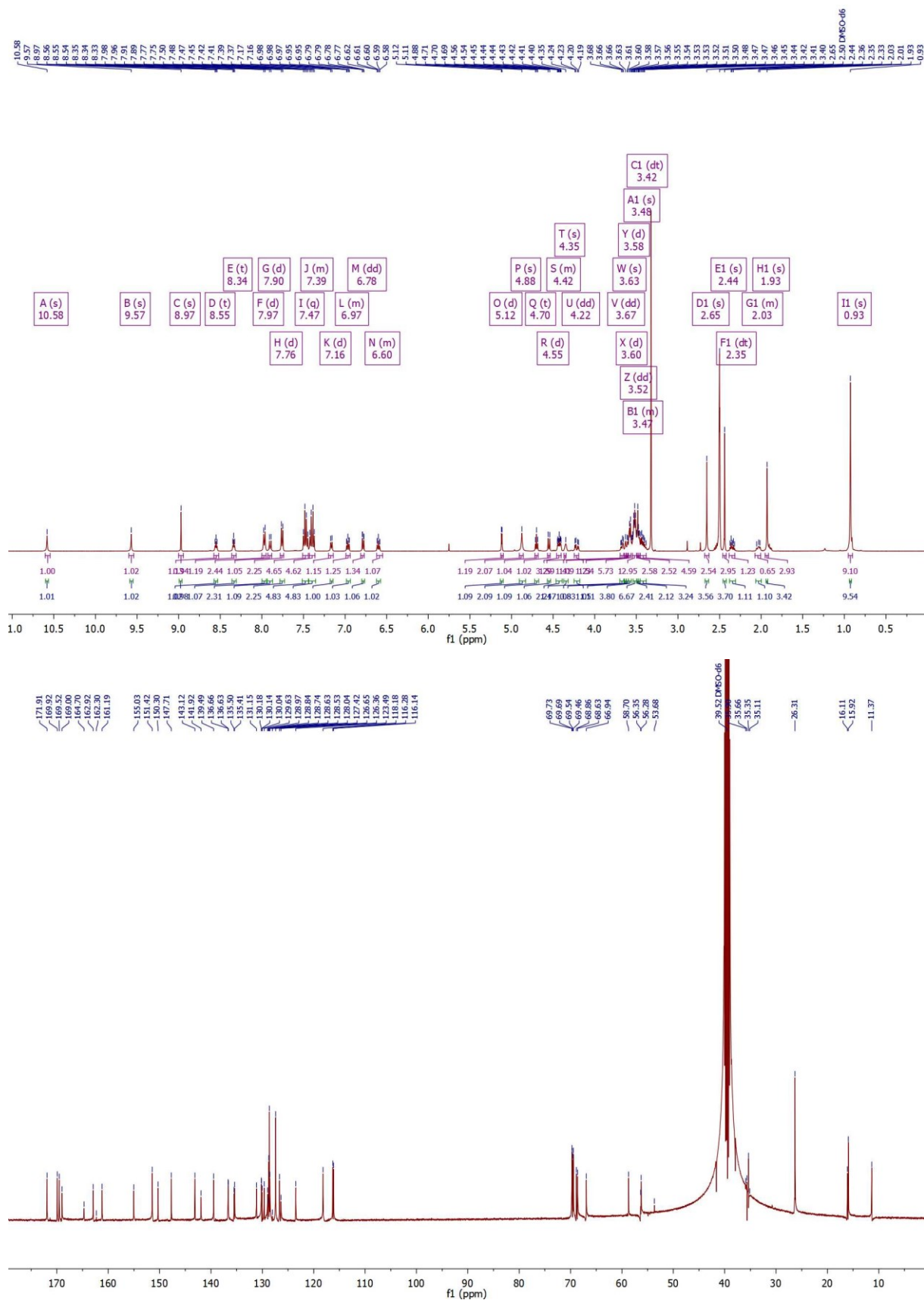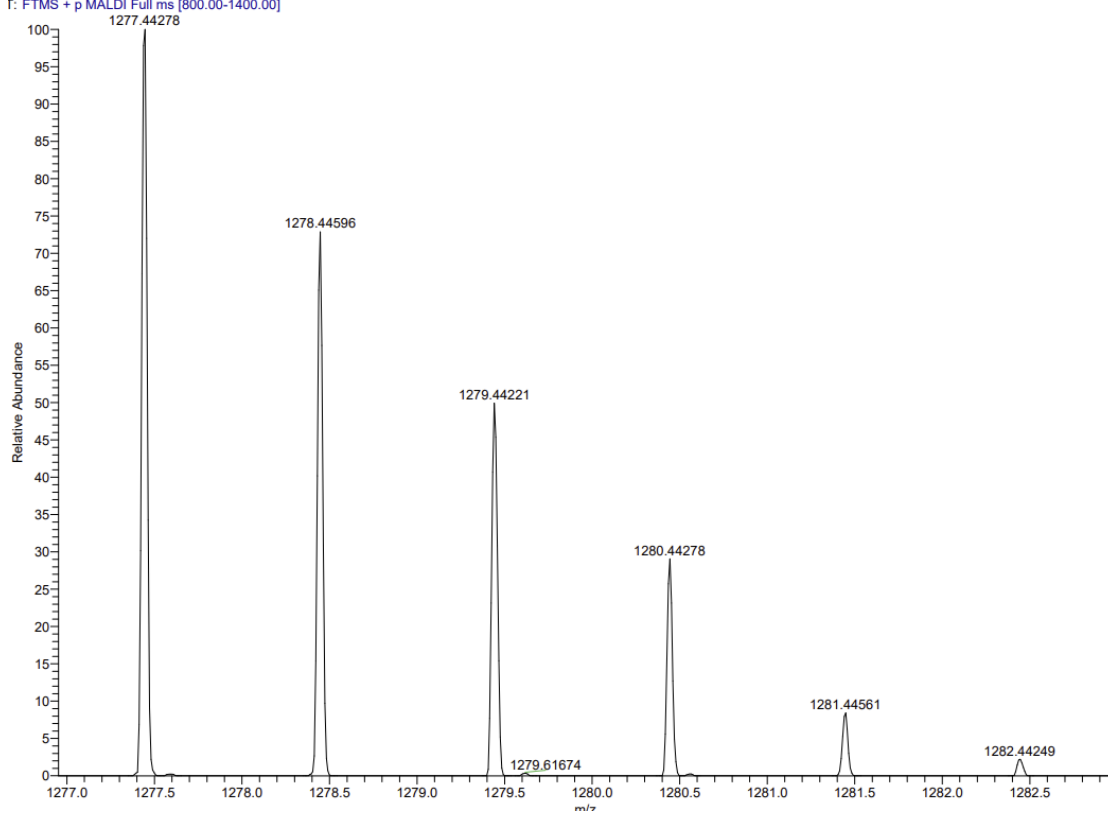
MALDI HRMS Spectrum of **177c** and simulated Spectrum

C63H71Cl1N12O10S2 +Na: C63 H71 Cl1 N12 O10 S2 Na1 pa...

¹H and ¹³C Spectra of **177d**

MALDI HRMS Spectrum of **177d** and simulated Spectrum

1201.42668
1202.42974
1203.42653
1204.42720
1205.42902
1206.42760
1207.42491

C61H67Cl1N12O7S2 +Na: C61 H67 Cl1 N12 O7 S2 Na1 pa C...

1201.42778
1202.43114
1203.42483
1204.42819
1205.43154
1206.42398
1207.42734
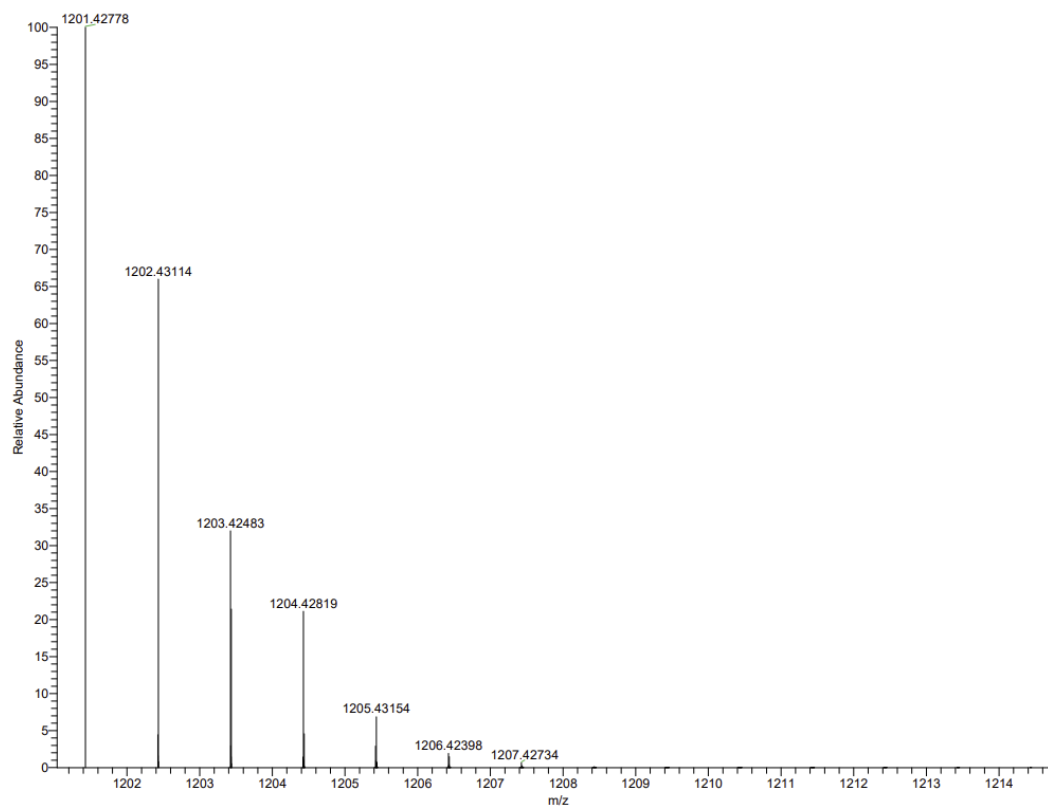
^{1}H and ^{13}C Spectra of **177e**

MALDI HRMS Spectrum of **177d** and simulated Spectrum

C62H69ClN12O7S2 +Na: C62 H69 Cl1 N12 O7 S2 Na1 pa C...